ELECTRIC TECHNOLOGY, U.S.S.R.

VOLUMES 1—4, 1959

Selected papers and abstracts from *Elektrichestvo*, Nos. 3—12, 1958

EDITORIAL BOARD

H. M. Barlow (London)
F. W. Bowden (San Luis Obispo)
F. Brailsford (London)
G. S. Brown (Cambridge, Mass.)
F. M. Bruce (Glasgow)
C. C. Carr (Brooklyn)
G. W. Carter (Leeds)
A. G. Conrad (New Haven, Conn.)
G. F. Corcoran (College Park, Md.)
J. D. Craggs (Liverpool)
A. L. Cullen (Sheffield)
G. E. Dreifke (St. Louis)
V. Easton (Birmingham)
A. R. Eckels (Vermont)
W. Fishwick (Swansea)
C. Froehlich (New York)
C. G. Garton (Leatherhead)
J. Greig (London)
L. D. Harris (Salt Lake City)
J. D. Horgan (Milwaukee)
E. C. Jones (Morgantown)
E. C. Jordan (Urbana)
I. H. Lovett (Rolla, Missouri)
J. M. Meek (Liverpool)
J. H. Mulligan Jnr. (N.Y.)
W. A. Murray (Blacksburg, Virginia)
J. E. Parton (Nottingham)
H. A. Peterson (Madison)
A. Porter (London)
J. C. Read (Rugby)
W. G. Shepherd (Minneapolis)
W. P. Smith (Lawrence, Kansas)
Philip Sporn (Chairman) (New York)
J. A. Strelzoff (East Lansing)
F. W. Tatum (Dallas, Texas)
C. V. O. Terwilliger (Monterey)
D. H. Tompsett (Stafford)
A. Tustin (London)
S. Reid Warren Jnr. (Philadelphia)
A. R. van C. Warrington (Stafford)
A. H. Waynick (Pa.)
E. M. Williams (Pittsburgh)
F. C. Williams (Manchester)
H. I. Wood (Manchester)
C. M. Zieman (Ohio)

PERGAMON PRESS LTD.

LONDON · NEW YORK · PARIS · LOS ANGELES

ELECTRIC TECHNOLOGY, U.S.S.R.

VOLUMES 1—4, 1959

Selected papers and abstracts from *Elektrichestvo*, Nos. 3—12, 1958

EDITORIAL BOARD

H. M. Barlow (London)
F. W. Bowden (San Luis Obispo)
F. Brailsford (London)
G. S. Brown (Cambridge, Mass.)
F. M. Bruce (Glasgow)
C. C. Carr (Brooklyn)
G. W. Carter (Leeds)
A. G. Conrad (New Haven, Conn.)
G. F. Corcoran (College Park, Md.)
J. D. Craggs (Liverpool)
A. L. Cullen (Sheffield)
G. E. Dreifke (St. Louis)
V. Easton (Birmingham)
A. R. Eckels (Vermont)
W. Fishwick (Swansea)
C. Froehlich (New York)
C. G. Garton (Leatherhead)
J. Greig (London)
L. D. Harris (Salt Lake City)
J. D. Horgan (Milwaukee)
E. C. Jones (Morgantown)
E. C. Jordan (Urbana)
I. H. Lovett (Rolla, Missouri)
J. M. Meek (Liverpool)
J. H. Mulligan Jnr. (N.Y.)
W. A. Murray (Blacksburg, Virginia)
J. E. Parton (Nottingham)
H. A. Peterson (Madison)
A. Porter (London)
J. C. Read (Rugby)
W. G. Shepherd (Minneapolis)
W. P. Smith (Lawrence, Kansas)
Philip Sporn (Chairman) (New York)
J. A. Strelzoff (East Lansing)
F. W. Tatum (Dallas, Texas)
C. V. O. Terwilliger (Monterey)
D. H. Tompsett (Stafford)
A. Tustin (London)
S. Reid Warren Jnr. (Philadelphia)
A. R. van C. Warrington (Stafford)
A. H. Waynick (Pa.)
E. M. Williams (Pittsburgh)
F. C. Williams (Manchester)
H. I. Wood (Manchester)
C. M. Zieman (Ohio)

PERGAMON PRESS LTD.

LONDON · NEW YORK · PARIS · LOS ANGELES

PERGAMON INSTITUTE

A DIVISION OF PERGAMON INTERNATIONAL CORPORATION,
OPERATED IN THE PUBLIC SERVICE FOR THE FURTHERANCE
AND DISSEMINATION OF SCIENTIFIC KNOWLEDGE

President of the Scientific Advisory Council:

Sir Robert Robinson, O.M., F.R.S.

Executive Director: Captain I. R. Maxwell, M.C.

Scientific Secretary: Dr. D. J. Hughes

1404 *New York Avenue, N.W. WASHINGTON, 5 D.C. (Telephone No. Metropole No. 8-5382)*
Headington Hill Hall, OXFORD (Telephone No. Oxford 64881)

Financial assistance has also been received from A.S.E.A., Sweden

1959

Elektrichestvo

Editor-in-Chief: N. G. DROZDOV

Deputy Editor-in-Chief: I. A. SYROMIATNIKOV

EDITORIAL BOARD

K. A. ANDRIANOV, N. I. BORISENKO, G. V. BUTKEVICH, M. G. CHILIKIN, A. A. GLAZUNOV, V. A. GOLUBTSOVA, E. G. KOMAR, M. P. KOSTENKO, L. R. NEIMAN, I. I. PETROV, V. I. POPKOV, A. M. FEDOSEEV, M. A. SHATELEN

ELECTRIC TECHNOLOGY, U.S.S.R.

CONTENTS OF VOLUMES 1–4, 1959

Vol. 1

PAGE

I. M. Postnikov: A method of calculating the performance of compound synchronous motors . 1

B. I. Nornevskii, V. F. Batko, V. E. Malishevskii, P. V. Kuropatkin and E. I. Rosin: Comparison of two-stage and three-stage rotary amplifiers with axial field . 18

V. D. Afanas'ev and Ivobotenko: Speed control of a d.c. motor fed from a magnetic amplifier . 28

Yu. E. Efroimovich: Model installation for remote control of electric parameters in arc furnaces . 39

L. Ia. Stanislavskii: Turbogenerators of 30 to 300 MV power built by Khetz factory . 50

V. G. Fastovskii and Iu. V. Petrovskii: On the possibility of intensification of cooling of turbo-generators . 61

A. P. Geppe: On the surface resistance of dielectrics . 68

K. F. Guba: The dependence of frequency of the rochelle salt piezo-electric vibrators on temperature 77

A. M. Kakhelnik: The use of electric locomotives with rectifiers—A review . 81

I. A. Glebov and S. F. Zonov: Service tests—Tests of the experimental installation of an ionic excited hydrogenerator . 89

T. A. Suetin: Ignition IVS-200/2 . 97

B. Konorskii: Discussion: Modification of the heaviside formula . 102

K. A. Andrianov: Synthetic compounds of high molecular weights as dielectrics . 110

P. V. Sakharov: Apparatus for low-voltage distribution gear . 127

G. V. Ostroumov: Investigation of transient processes in linear circuits by the method of loci . 137

I. G. Shubov: Determination of the level of magnetic noise of d.c. machines by the method of electromechanical analogy . 146

Yu. P. Petrov: Transient processes in an electric drive for an exponential variation of the magnetic flux . 156

T. A. Glazenko: The use of electromagnetic powder couplings for frequent reversals of a driven mechanism . 164

A. A. Sakovich: The increase of the reliability of conversion networks . 177

A. B. Oslon: Calculation of certain types of compound earthing devices . 187

A. G. Mirer: Service tests—A method of calculation of mechanical characteristics of asynchronous motors under conditions of dynamic braking . 198

S. Ia. Berezin: Experimental determination of parameters of elements of automatic control systems 201

Vol. 2

F. I. Butaev, N. S. Klimov, M. F. Kostrov and A. A. Sakovich: The high-power high-voltage rectifier . 209

B. L. Konstantinov: The problem of the approximate analytical solution of oscillations of a synchronous machine . 224

V. M. Matiukhin: The influence of the law of the excitation control on the damping of oscillations of a synchronous machine . 230

M. M. Akodis: Artificial methods of obtaining high power for the investigation of arc extinction devices . 240

O. G. Vegner: Increase of stability of a welding a.c. arc . 252

N. P. Bogoroditskii and I. D. Friberg: Physical processes in electrical ceramics and rational methods of development . 259

G. I. Poliuk: Automatically controlled series excitation for generators . 271

A. B. Vitanov: Negative sequence filters with independent arms . 284

1959

PAGE

V. V. ARTAMONOV: Calculation of the characteristics of an electric drive with frequency control by the equivalent resistance method 294

B. M. SHKOLNIKOV and I. I. SUD: Properties and design of a multi-motor drive system with a mechanical differential 302

Vol. 3

V. L. FABRIKANT: The utilization of semiconductors in relay protection 313

I. S. BRUK: Controlled reactors for long-distance transmission 322

I. K. KHRUSTALEV: New methods of connecting starter-control resistances of asynchronous motors. 334

R. A. LIPMAN and I. B. NEGNEVITSKII: Transient processes in a magnetic booster working in a relay system 337

Abstracts of papers published in *Elektrichestvo* No. 7, 1958 353

V. A. PREVEZENTSEV: Heat resistant winding conductors 358

IA. N. SHTRAFUN and M. S. ROSTOVTSEVA: An investigation for an automatic system of excitatiôn for large turbogenerators using semiconductor power rectifiers 373

N. S. SIUNOV, B. K. GAVRILOV and V. N. BREEV: The excitation of synchronous motors of normal construction by the application of mechanical rectifiers 384

T. V. STEPNOV: Directional protection from short-circuits to earth 392

Abstracts of papers published in *Elektrichestvo* No. 8, 1958 403

M. A. PANASENKOV: Surface effect in solid ferromagnetic bodies taking non-linearity into account . 408

L. IA. STANISLAVSKII: An experimental turbogenerator with internal hydrogen cooling of stator and rotor windings at a pressure of 3 atm 425

G. M. KASPRZHAK: Calculation of the reduction of voltage on the terminals of high-power current collectors with strong actuating currents 435

V. T. RENNE, N. N. KALIAZINA and M. N. MOROZOVA: Dielectric losses in condenser paper . . 445

Abstracts of papers published in *Elektrichestvo* No. 9, 1958 458

Vol. 4

I. M. POSTNIKOV: Eddy currents in synchronous and asynchronous machines with unlaminated rotors 463

E. D. SAPIR: Compensation of capacitive currents in differential phase carrier protection of transmission lines 480

V. A. GOLOVANOV: The problem of a circuit for a rectifying semiconductor set on electric rolling stock of a.c. single-phase—d.c. transmission 494

O. B. BRON and D. S. LIENBERG: Problems of liquid cooling in electrical equipment 503

Abstracts from papers published in *Elektrichestvo* No. 10, 1958 513

N. A. POLIAK: Short-circuits, asynchronous drive and turbogenerator resynchronization . . 519

V. V. KAPLAN, V. M. NASHATYR' and V. L. IVANOV: A synthetic method of testing high-voltage circuit-breakers 533

L. L. ROTKOP: The energy properties of an asynchronous motor with a system of impulse speed regulation 545

A. S. KURBASOV: On the conditions of the formation of flashover or arcing on to the framework of traction motors 556

Abstracts from papers published in *Elektrichestvo* No. 11, 1958 564

E. M. TSEIROV: The electrical properties of compressed air in an air-blast circuit-breaker . . 570

M. G. PORTNOI: The occurrence of sub-harmonic resonance in unbalanced line conditions . . 589

M. F. IUDOV: Experimental investigation of deformations and vibrations of the stator windings . 599

P. S. LIVSHITS: Calculation of losses in the sliding contacts of electric machinery 610

Abstracts from papers published in *Elektrichestvo* No. 12, 1958 619

A METHOD OF CALCULATING THE PERFORMANCE OF COMPOUND SYNCHRONOUS MOTORS*

I.M. POSTNIKOV

(Received 13 November 1956)

1959

General characteristics of motors and of methods of connexion

Excitation of synchronous motors through semiconductor rectifiers was first used in the U.S.S.R. in the DAG network [5]. This network was used for synchronization purposes, and the application of rectifiers fed from transformers was planned; or in the case of the low voltage grid, rectifiers had to be connected directly to the grid. It proved later that the DAG system cannot ensure satisfactory working characteristics of synchronous induction motors (small maximum torque in the case of increased load, low efficiency).

The situation changes radically if we make use of compounding. Synchronous induction compounded motors, with a d.c. exciter (Fig.1a) are widely used in foreign countries, particularly in England [3]. The use of synchronous induction compound motors without exciter but fed through a semiconductor rectifier was suggested by Iuditskii [1] and Tsiganek [6].

In 1954, Inosov [2] proposed exciting a network (Fig.1b) with rectifiers fed from current transformers. This system was tested on experimental synchronous salient-pole machines, and quite satisfactory working characteristics were recorded (constant $\cos\phi$, possibility of considerable overloading). Inosov and Krutikova gave a method of calculating the overload capacity and stability of these machines, as well as a method of calculating rectifying devices. At the same time, synchronous induction motors, constructed on this system, were investigated and calculations of synchronous motors, using the AK series, were performed by a method different from the method suggested by Inosov.

Calculations and tests showed that the use of rectifiers with a compounding device was expedient both for synchronous induction motors and for synchronous motors.

In the first case it is advisable to design these motors on the basis of AK series for powers above and below 100 kW. In the second case, for powers

* *Elektrichestvo*, No.3, 1-9, 1958.

less than 100 kW, it is advisable to design motors with mixed excitation on the basis of series generators ESG, SM and others; and for powers above 100 kW, on the basis of the unique series of big synchronous and asynchronous machines.

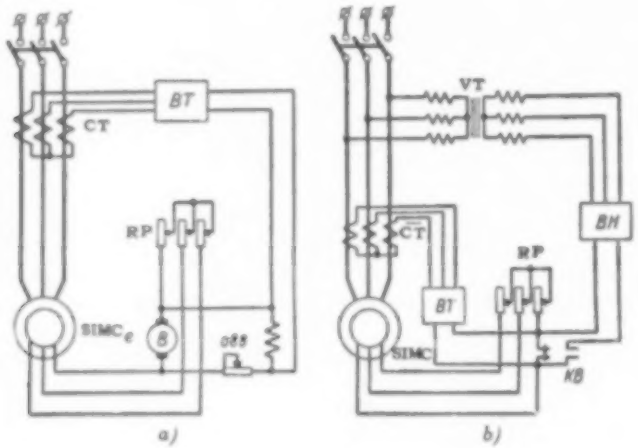

FIG.1. Basic networks for connecting a synchronous induction compounded motor with a d.c. exciter (SIMC$_e$) (a); and a synchronous induction compounded motor excited through 4 rectifiers (SIMC) (b).

The use of synchronous induction motors with compounding (abbreviated as SIMC; if the separate compounded exciter generator is used for excitation, it is convenient to introduce the notation SIMC$_e$)is economically justified in all cases when conditions of drive allow the use of synchronous motors. It is particularly desirable to use them when we have to start at heavy initial torques avoiding considerable current fluctuations; also where high reactances are present in the network, and consequently the increase of $\cos\phi$ is desired without introducing special compensating devices (condensers, synchronous condensers and others).

The use of the excitation compounded network (Fig.2) for a normal salient-pole synchronous motor (SMC) is also recommended. In this case the absence of exciters makes the motor cheaper.

Compounding permits us automatically to keep a high value of $\cos\phi$ when the load varies, and to obtain higher annual average efficiency and higher torques for rapidly varying loads. The use of compounded synchronous motors with separate exciters is recommended in the cases when the motor power is considerable and selenium rectifiers are less reliable than exciters. Nevertheless, with the improvement of semiconductor rectifiers, they may also be used for high-power motors.

The use of machines of SMC and SMC$_e$ types for powers less than 100 kW, based on the design of synchronous generators, needs an economic justification.

Lower cost of a set, due to the absence of an exciter, is partly offset by an increase in the cost of the motor itself, due to the introduction of an auxiliary winding on the poles and due to increased service costs in comparison with asynchronous motors. The use of SMC-type machines of power less than 100 kW is justified in cases when economy, due to the increase of $\cos\phi$, repays in two to five years their greater initial capital costs and additional operating costs compared with asynchronous motors.

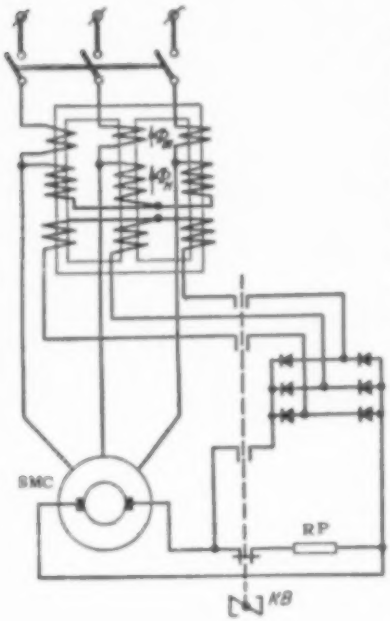

FIG.2. Basic network for connecting a compounded synchronous motor excited through rectifiers (SMC).

The use of SIMC-type motors of power less than 100 kW may also be advantageous in the following conditions. In certain cases it may be necessary to decrease the power of the motor of a given size by 15 - 20 per cent or to use a better rotor insulation of an increased thermal and electric strength. The main advantage of motors of SIMC type is that, without any change in the construction of series-made asynchronous machines, we may get synchronous motors by addition of compounding and rectifying devices. In the case of damage to these additional devices, the motors may continue working without interruption as asynchronous motors, until the defective rectifiers are repaired or replaced.

Methods of calculation for motors of SMC and SIMC type

In carrying out the calculations, it is advisable to begin with the existing types of synchronous and asynchronous machines.

The main problems in calculations are:

(a) to determine voltages and currents in the system of excitation;

(b) to determine parameters of current and voltage transformers and of rectifiers, that will ensure the required working characteristics of the motor and the necessary torques for overloads (with minimum dimensions of additional devices and sufficient service reliability);

(c) to obtain the required calculated working characteristics of the motor, and a good efficiency-load characteristic for the given rectifier and transformer parameters;

(d) to determine overloading;

(e) to verify stability;

(f) to calculate conditions in starting and in synchronizing;

(g) to determine whether overheating of the excitation winding and of the rectifying device takes place.

Inosov and Krutikova worked out methods for calculating the overload capacity of SMC motors, for calculating rectifying devices and for selecting current and voltage transformers. Nevertheless, so far as the overload capacity and motor characteristics are concerned, these methods give wrong results in certain cases.

The determination of the maximum torque, based on resistance, was given by Inosev by the formula: $M_{max} = U^2/4a - b$, where a represents the relative copper losses proportional to the square of the stator current at the rated current value, and b the relative losses in the stator steel.

This formula is only valid in the case when the compounding device ensures the constancy of $\cos\phi$ at limit loads, or, for low-power machines, when the overloading capacity is determined mainly by resistance.

Basic initial assumptions in choosing a practical

In order to simplify calculations for both synchronous induction (SIMC type) and synchronous (SMC type) motors, it is expedient to start from the theory of a motor with a cylindrical rotor, i.e. to assume that

$$x_d = x_q = x_g$$

In investigating general relationships it is advisable to neglect the influence of saturation on motor parameters, particularly in the determination of the limiting overload.

Saturation may be accounted for by constructing Potier diagrams and a series of auxiliary adjusting characteristics (Fig.3).

It is expedient to calculate motor operating conditions in the following way:

(1) to determine by ordinary methods, experimentally or by calculation, stator and rotor parameters: (a) leakage reactances of the stator x_s and of the rotor x_f, x_{kd}, x_{kq}; (b) synchronous reactance, neglecting saturation x_d and $x_{ad} = x_d - x_s$, (c) resistances of the stator r_1 and of the rotor r_f, r_{kd}, r_{kq};

(2) to calculate or to determine experimentally characteristics in no-load and short-circuit conditions;

(3) to choose a value of overload capacity (M_{max});

(4) to choose a value of $\cos\phi_N$ at the rated load;

(5) from the torque equation

$$M = \frac{UE_f}{z}\sin(\theta + \rho) - \frac{E_f^2 R}{z^2}$$

for $\theta + \rho = \frac{\pi}{2}$ to get:

$$M_{max} = \frac{UE_{f\,max}}{z} - \frac{E^2_{f\,max}}{z^2} R. \qquad (1)$$

For a given value of M_{max} from (1), the maximum value of the excitation e.m.f. is determined:

$$E_{f\,max} = \frac{Uz}{2R} - \sqrt{\left(\frac{Uz}{2R}\right)^2 - M_{max}\frac{z^2}{R}}, \qquad (2)$$

where $z = \sqrt{x^2 + R^2}$; $x = x_d + x_l$;

x_l is the reactance of the line; $rR = r_s + r_{cl} + r_r + r_f$, the sum of resistances of the stator winding, of the current transformer, of the rectifier and of the excitation winding, expressed in fractions of unity;

(6) to have current in fractions of unity at $M = M_{max}$

$$I_{max} = \sqrt{\frac{E^2_{f\,max} + U^2}{z^2}}. \qquad (3)$$

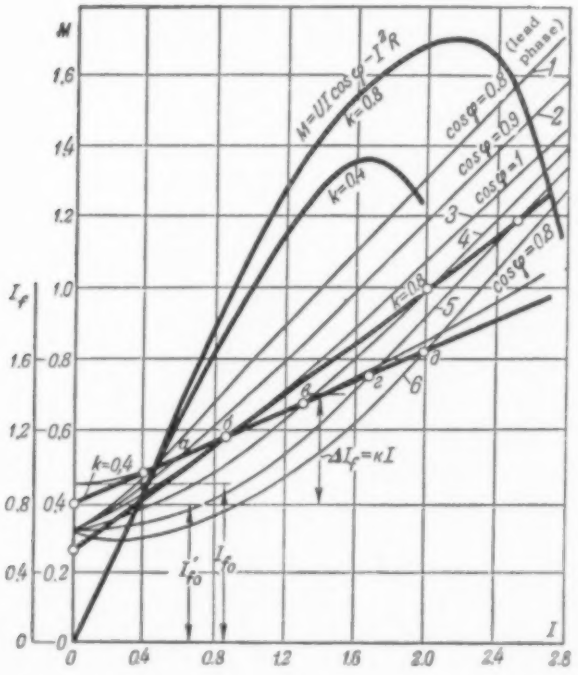

FIG.3. Determination of overloading and of working characteristics of motors SIMC and SMC, with saturation accounted for (1-6); characteristics in relative units constructed by Potier method.

(7) to have compounding factor

$$k = \frac{E_{f\,\max} - E_{fN}}{(I_{\max} - 1)\,x_{ad}}, \tag{4}$$

where, for $\cos\phi_N = 1$

$$E_{fN} = \sqrt{U^2 + (I_N x)^2}. \tag{5}$$

(8) to have e.m.f. E'_{fo} for the stator current equal to zero (Fig.3), (a conventional value),

$$E'_{fo} = E_{f\max} - \frac{E_{f\max} - E_{fN}}{I_{\max} - 1} I_{\max} \tag{6}$$

and the corresponding excitation current

$$I'_{fo} = \frac{E'_{fo}}{x_{ad}} \tag{7}$$

in fractions of the stator current;

(9) to have transformation ratio of the current transformer

$$k_{c.t} = \frac{w_1}{w_2} = k\,\frac{i_{f(1)}}{1.3 i_N}, \tag{8}$$

where $i_f(1) = i_{f\delta} X_{ad}$, the nominal excitation current from the rectilinear characteristics in amperes, corresponding to the e.m.f.

$$E_{f(1)} = I_N x_{ad}. \tag{9}$$

Factor 1.3 is the ratio of the rectified current to the alternating current (network in Fig.2);

(10) to show that the number of the parallel connected disks of the current

$$m_I = \frac{k i_{f(1)}}{i_1},$$

where $i_1 \approx 3.5$ - 4 A the current in one disk (d = 100 mm);

(11) to find the number of parallel connected disks of the voltage rectifier

$$m_U = \frac{i'_{fo} k_e}{i_1},$$

where i_1 is the permissible permanent current in one disc; $k_l \approx 1$ - 1.5 is the load factor; $i_{fo} = E_{fo}\, i_{f\delta}$;

(12) to show that the number of the series-connected disks of the voltage rectifier

$$n_U = \frac{i'_{fo} r_f}{U_1},$$

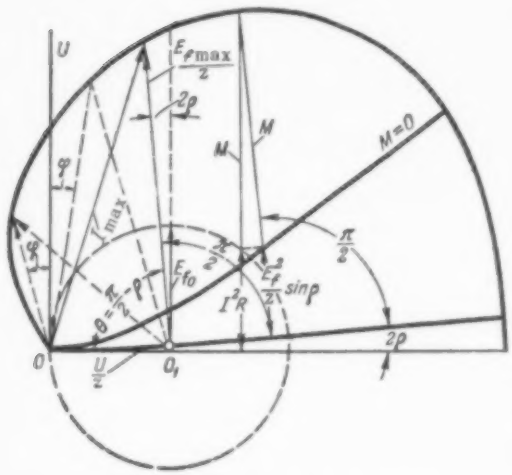

FIG.4. Hodograph of current of motors SMC and SIMC and determination of the maximum torque and of characteristics neglecting the influence of saturation.

where U_1 = 12-15 V, the permissible continuous back voltage across one disk; and r_f is to be expressed in ohms;

(13) to find the transformation ratio of the voltage transformer

$$k_{mn} = \frac{2.34U_p}{i'_{fo}r_f + \Delta U_v} \approx \frac{2.34U_p}{1.2i'_{fo}r_f}, \quad (11)$$

where U_p is given in volts, and r_f in ohms; $\Delta U_v \approx 2\ n_U$ is the voltage drop in the rectifier in volts; Factor 2.34 is the ratio of the rectified voltage to the alternating phase voltage (Fig.2); and

(14) to find the number of the series-connected disks in the network of Fig. 1 b

$$n_I = n_U$$

Construction of characteristics and determination of the overload capacity while taking into account saturation.

We construct a series of auxiliary adjusting characteristics for different values of $\cos\phi$, using the Potier diagrams (Fig.3). We draw the curve $I_f = f(1)$ and obtain the points of intersection a, b, c, d etc. Using the points of intersection we draw curves $\cos\phi = f(1)$ and $m = UI\cos\phi - I^2R$, whence we determine the value of the maximum torque taking into account saturation (in Fig.3 for $k = 0.4$ and $k = 0.8$).

Locus of points of the motor current while neglecting the influence of saturation and accounting for it.

Neglecting the influence of saturation from the diagram on Fig.4 we get:

$$E_f^2 + U^2 - 2E_fU\cos\theta = (Iz)^2. \quad (11a)$$

For $E_f = E'_{fo} + kx_{ad}I = E'_{fo} + k_1I$ we get:

$$I = \frac{k_1(E'_{fo} - U\cos\theta)}{z^2 - k_1^2} + \sqrt{\left[\frac{k_1(E'_{fo} - U\cos\theta)}{z^2 - k_1^2}\right]^2 + \frac{E'^2_{fo} + U^2 - 2UE'_{fo}\cos\theta}{z^2 - k_1^2}}. \quad (12)$$

In this case $E'_{fo} \leqslant U$.

From equation (12), it follows that for $k_1 = z$, $I = \infty$. Therefore, it is necessary to choose $k_1 < z$. Usually in this case $k \approx 0.8\text{-}0.9$.

The current hodograph may be easily constructed by points. For this purpose, on a curve $I_f = f(1)$ [or $E_f = f_1(I)$] we choose a series of values of I and the corresponding values of I_f. Striking from points 0 and 0_1 arcs of radius I and $I_f = E_f / z$ (Fig. 4), we find a point on the hodograph and the corresponding value of cos ϕ. Plotting current values and cos ϕ taken from Fig. 3, we may plot a hodograph taking the influence of saturation into account.

Angle - torque characteristic

Characteristics showing the dependence of torque on the power angle θ (angle between the rotor and stator fields) may be obtained from the hodograph in Fig.4, in a form shown in Fig.5. As may be seen, it differs slightly from the characteristic $M = M_{max} \sin \theta$, obtained at a constant excitation. If we assume a certain definite value of M_{max}, then for the motors of SMC or SIMC types we may, in many cases, use the equivalent sinusoid of the torque (moment) as a function of the angle.

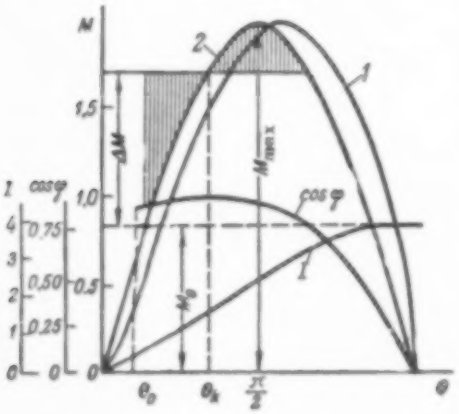

FIG.5. Comparison of angle characteristics for equal maximum torques. 1: for SMC and SIMC types; 2: for a synchronous motor with constant excitation.

Dynamic and static stability

To determine the dynamic loads for normal non-compounded synchronous motors we use the method of areas. Both static and dynamic angle characteristics (with regard to extra currents in the rotor) may be used. By constructing an angle characteristic for a motor with a mixed excitation (Fig.5), from Fig.4 we may approximately apply the method of areas in this case as well. The influence of extra currents is to be accounted for with quickly varying loads, lasting not more than the time constant T'_d of transient currents; this may be done in the ordinary way by replacing the synchronous reactance x_d by a transient reactance x'_d and the e.m.f. E_f by E'_{fd}.

For a shock load, not exceeding the limit of static stability and remaining afterwards constant during a period of time considerably greater than T'_d, we may disregard the extra currents and use a static angle characteristic. The additional limiting dynamic torque ΔM from the angle characteristic, which may be represented in a form of equivalent sinusoid in Fig.5, is the condition of equality of shaded areas, approximately determined by:

$$\Delta M \approx \frac{M_{max}}{\sqrt{2}} \left(1 - \frac{M_0}{M_{max}}\right). \tag{13}$$

The limit of static stability is determined by the curve $M = f(\theta)$. But in this case we disregard the possibility of self-excited rotor oscillations. The problem of permissible values of compounding factors, which are restricted to the possibility of oscillations, requires theoretical and experimental investigations. Investigations carried out by Inosov [7], are subject to criticism because they neglect the smoothing torque due to damping windings.

Starting and synchronizing a motor

If a motor with a mixed excitation is designed as an asynchronous motor with slip rings (for instance of AK type), then it starts as an asynchronous motor and usually has a sufficiently high subsynchronous torque. If in this case semiconductor rectifiers are used they should be disconnected during the start. When an exciter generator is present, starting may be done without commutation in the secondary winding; i.e. as if starting a short-circuited asynchronous motor.

If a motor with a mixed excitation is designed as a salient pole synchronous machine, it is necessary to include an additional winding for starting. In this case, if semiconductor rectifiers are used, the excitation winding should be connected to a suitable discharge resistance (in some cases it may be left open, if no danger exists of breakdown of the insulation of the excitation winding during the start).

1959

In practice, the idea of subsynchronous torque usually refers to the torque at the slip $s = 5$ per cent. It is usually accepted that for synchronization, it is necessary that subsynchronous torque should be greater than the shaft torque at subsynchronous speed. Experiments and calculations given below show that a motor may be synchronized at initial slips greater than subsynchronous slip, for example $s_0 = 10$ per cent and more, if the period of synchronization is correspondingly increased. Sometimes a slip, for which rotor windings are to be supplied with d.c., is determined from conditions of synchronization during the first hunting cycle by the Edgerton formula [4]:

$$s_{cr} = \frac{247}{n_s} \sqrt{\frac{P_{max}}{fGD^2}}. \tag{14}$$

This formula is not valid for determining self-synchronization conditions of synchronous motors with starting winding in cases of difficult starting, because it gives the value of a critical slip for synchronization during the first hunting cycle and does not allow the determination of the time for synchronization, in the case when s_0 is different from s_{cr} given by (14). We may obtain a formula for s_{cr} that approximately takes into account the influence of the asynchronous torque, of the external load torque and of the rotor position, by an approximate solution of the equation of rotor motion.

Attempts at a rigorous analysis of a synchronization process of a synchronous motor lead to very complicated non-linear equations. Nevertheless, a solution, sufficiently accurate in practice in most cases, may be obtained if we neglect the influence of idle currents and torques and consider electromagnetic moments as known functions of θ and $d\theta/dt$. In this case, only one equation of motion is to be considered.

The equation of the rotor motion may be written in this form:

$$H\frac{d^2\theta}{dt^2}+D\frac{d\theta}{dt}+M_c(\theta)=M_v, \tag{15}$$

where H is an inertial constant in radians. The angle characteristic $M_c(\theta)$ may be approximately represented, disregarding parametric moment (torque), in the form of an equivalent sinusoid:

$$M_c(\theta)\approx M_{\max}\sin\theta. \tag{16}$$

From the previous discussion (see Fig.5), we may assume this to be true for ordinary synchronous motors and for motors with mixed excitation, thus determining $M_{\max}$ by (1).

Damping torque per unit slip $s = d\theta/dt$ may be expressed, disregarding the salient pole motor properties, as in the case of symmetrical multiphase rotor winding*

$$D\approx\frac{U^2r_2'}{c_1^2(r_2'^2+s^2x_d''^2)}\approx\frac{U^2}{r_2'c_1^2(1+s^2T_d''^2)}. \tag{17}$$

Here U_* r_2' and x''_d are expressed in fractions of unity;

$$c_1=1+\frac{x_s}{x_{ad}}.$$

For small slips $s \ll 1/T''_d$, the value of D may be assumed to be constant, i.e. independent of the slip $D\approx\frac{U^2}{C_1^2 r_2}$, or its mean value within a given range of the slip may be taken.

Torque due to external load M_{ex}, generally speaking, is a function of slip, but during the synchronization process within narrow limits of speed variation, it may be taken as a constant.

For asynchronous starting, the torque $M_c(\theta) = 0$, and the established slip may be determined as a function of M_{ex} and D from the asynchronous characteristic (Fig.6):

$$s=\frac{M_{ex}}{D}=S_a,$$

* For synchronous salient-pole motors $D = M_{in}/0.05$, where M_{in} is an input torque.

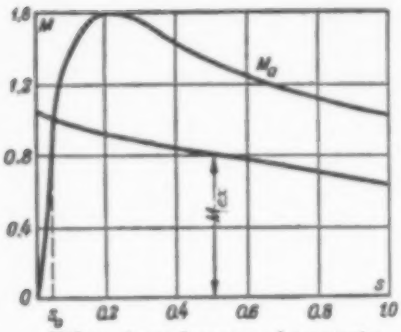

FIG.6. Asynchronous characteristics of motors SIMC or SMC and determination of the established slip S_0 before switching on a d.c.

whence

$$D = \frac{M_{ex}}{s} \tag{18}$$

At this slip, let us apply d.c. to the rotor. Let us consider conditions under which a motor will be pulled into step, and how long it will take. Conditions will differ according to the value of the initial slip $s_0 = s_a$ and the position of the axis of the rotor m.m.f. at the instant of switching on the current; i.e., according to the value of θ_0. The most unfavourable case will be when $\theta_0 = -\pi$. Therefore, if a motor is pulled into step in this case, then this will be so in all cases. To determine the conditions for synchronization we write equation (15) in the form:

$$\frac{d^2\theta}{dt^2} = f(\theta), \tag{19}$$

where

$$f(\theta) = \frac{1}{H}[M_{ex} - M_c(\theta) - D_s].$$

1959

Here $s = d\theta/dt$ is an unknown function of the angle θ. Equation (19) is solved by multiplying both sides by $2\,d\theta/dt$:

$$\frac{d}{dt}\left[\frac{d\theta}{dt}\right]^2 = 2f(\theta)\frac{d\theta}{dt},$$

where

$$s^2 - s_0^2 = 2\int_{\theta_0}^{\theta} f(\theta)\cdot d\theta = \tag{20}$$

$$= \frac{2}{H}\int_{\theta_0}^{\theta}[M_v - M_c(\theta) - Ds]\,d\theta.$$

Here s_0 is a slip when $t = 0$, i.e. at the instant when d.c. is switched on. This slip should be at least 1.5 - 2 times smaller, than pull-out slip, $S_k = r_2/x_d$. If switching-on takes place during established asynchronous running (characteristic in Fig.6), then

$$s_0 = s_a = \frac{M_{ex}}{D} \ll s_k.$$

From (20), slip s for $M_c(\theta) = M_{max}\sin\theta$ will be:

$$s = \sqrt{\frac{2}{H}\left[M_{max\,c}(\cos\theta - \cos\theta_0) + \int_{\theta_0}^{\theta}(M_{ex} - Ds)\,d\theta\right] + s_0^2}\,. \tag{21}$$

Synchronization will be assured if the slip s becomes equal to zero at a positive value of the synchronous torque, i.e. at the beginning or in the middle of any positive half-period of the sinusoid $M_{max}\sin\theta$, and this happens according to (21), when

$$s_0 = \sqrt{\frac{2}{H}\left[M_{max}\,(\cos\theta_0 - \cos\theta_c) + \int_{\theta_c}^{\theta}(Ds - M_{ex})\,d\theta\right]}\,. \tag{22}$$

We shall call angle $\theta = \theta_S$ the angle of synchronization. Obviously, it will be equal to

$$\theta_s = 2\pi X + \alpha, \tag{23}$$

where X is an integer;

$$\alpha = \frac{\pi}{2} \ldots\ldots \frac{\pi}{3}$$

Equation (22) enables us to find a criterion of pulling a synchronous motor into step.

Let us consider the case when d.c. is switched on at $\theta_0 = -\pi$. On condition that $\theta_0 = -\pi$, a motor will be syncronized if, for any value of the angle of synchronization $\theta_S = 2\pi X + \pi/2$, corresponding to a positive value of a half-cycle of the synchronous torque, slip s becomes zero. From (22) it follows that for this to happen it is necessary that s_0 should not exceed a certain value. Supposing $\theta_0 = -\pi$ and $\theta = \theta_S$, when $\theta_S = \pi/2 + 2\pi X$, we get:

$$s_0\sqrt{\frac{H}{2}} = \sqrt{\int_{-\pi}^{\theta_S} Ds\,d\theta - [M_{ex}(\theta_S + \pi) + M_{max}]}\,. \tag{24}$$

Introduce the average value of the asynchronous torque during the period of synchronization:

$$M_{aav} = Ds_{av} = \frac{1}{\theta_c + \pi}\int_{-\pi}^{\theta_S} Ds\,d\theta, \tag{25}$$

Pulling into step will be achieved if the work performed by this torque during the period of synchronization is greater than the sum of the work, performed by the external torque, by the synchronous torque and by the moment of inertia of the rotor, i.e.

$$(\vartheta_s+\pi)\,Ds_{av} \geqslant \frac{Hs_0^2}{2}+M_{\max}+M_{ex}(\vartheta_s+\pi)= \\ =A+M_{ex}(\vartheta_s+\pi),$$

where

$$A=\frac{1}{2}Hs_0^2+M_{\max}\,, \tag{25a}$$

or alternatively:

$$\left.\begin{aligned} Ds_{av} &\geqslant M_{ex}+\frac{A}{\vartheta_s+\pi}\,; \\ s_{av} &\geqslant s_0+\frac{A}{D(\vartheta_s+\pi)}\,, \end{aligned}\right\} \tag{26}$$

this means that the average asynchronous torque and the average slip should be greater than certain definite values.

It is seen from (26) that the longer the process of synchronization (large number of periods of oscillations κ), the smaller is the average synchronous torque required.

For example, let us verify the possibility of synchronizing a motor, if $H = 1000$ rad, $s_0 = 5$ per cent and $M_{\max} = 2$ for two periods of oscillations ($\chi = 2$) and the torque on the shaft $M_{sh} = 1$. In accordance with (26) $Ds_{av} = 1 + \frac{0.5\times 1000.0\times 0.05^2+2}{2\pi\times 2+3\pi/2}$ $= 1.2$ where $s_0 = 0.05$ and $M_{ex} = 1$, we get $D = M_{ex}S_0 = 1/0.05 = 20$. Therefore, the average slip should be not less than $s_{av} = 1.2/20 = 0.06$; i.e. about 6 per cent. Is it possible to get such a value?

The solution of equation (15) by the method of successive approximations, which is given below, suggests that the average slip during the period of synchronization varies within very narrow limits. In fact, the maximum possible slip occurs when $\theta_0 = -\pi$, and if we neglect the value of D from (21), when $\theta = 0$:

$$s_{\max}=\sqrt{\frac{4M_{\max}}{H}+s_0^2}. \tag{27}$$

The average value of the slip for a half-period under these conditions will be:

$$s_{av1}=\sqrt{\frac{2M_{\max}}{H}+s_0^2}. \tag{28}$$

For an infinite period of synchronization:

$$S_{av_2} = S_0. \tag{29}$$

Thus the value of s_{av} lies within the limits:

$$S_{av_1} > S_{av} > S_0 \tag{30}$$

A more accurate value of the average slip may be obtained from (21). In fact, for an interval from $-\pi$ to θ_s

$$(s^2)_{av} = \frac{2}{H}\left[M_{\max}\left(1+\frac{\sin\theta_s}{\pi+\theta_s}\right)+(M_{ex}-Ds_{av})\frac{\pi+\theta_s}{2}\right]+s_0^2. \qquad (31)$$

If we introduce the square of the shape factor of the curve $k^2_{sh}=\frac{(s^2)av}{s^2av}$, then from (31) we get:

$$s_{av} = -\frac{D(\theta_s+\pi)}{2Hk^2_{sh}} + \sqrt{\left[\frac{D(\theta_s+\pi)}{2Hk^2_{sh}}\right]^2+\frac{2M_{\max}}{Hk^2_{sh}}\left(1+\frac{\sin\theta_s}{\theta_s+\pi}\right)+\frac{s_0^2}{k^2_{sh}}+\frac{Ds_0}{Hk^2_{sh}}(\theta_s+\pi)}. \qquad (32)$$

In this case, we may assume $k^2_{sh} \approx 1.1\text{-}1.2$ according to Fig.7.

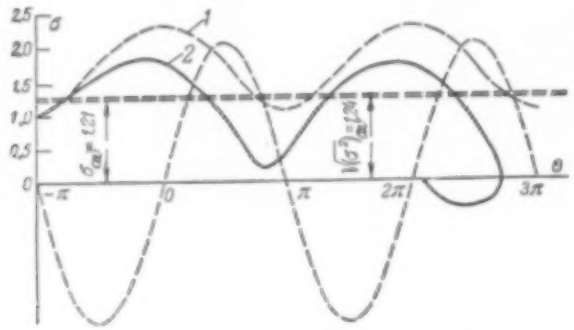

FIG.7. Curves of relative slip-angle θ (1) for $D = 0$; (2) for $D = 20$.

Above we have determined the value S_{ar} for which during the interval from $\theta = -\pi$ to $\theta = \theta_s$, the slip becomes zero (equation (26)). Equating (26) and (32), we find for given values of D,H and s_0, the number of rotor oscillations:

$$\gamma = \frac{A}{2\pi D\left[-\left(s_0-\frac{DM_{\max}}{HAk^2_{sh}}\right)+\sqrt{\left(s_0-\frac{DM_{\max}}{HAk^2_{sh}}\right)^2+\frac{1}{2}\left(\frac{2M_{\max}}{Hk^2_{sh}}-s_0^2\right)}\right]}-\frac{3}{4}, \qquad (33)$$

which is approximated to the nearest integer. From equation (33), it follows that the time of synchronization becomes infinite, if

$$s_0 = \sqrt{\frac{2M_{\max}}{Hk^2_{sh}}} = s_{cr}.$$

The last equation gives the limiting value of the slip for which synchronization of a motor is still possible. Inserting the value S_{cr} from (34) into (33) and rejecting the term - ¾, we get:

$$\varkappa = \frac{A}{2\pi D\left[-\left(s_0-\frac{D}{2A}s_{cr}^2\right)+\sqrt{\left(s_0-\frac{D}{2A}s_{cr}^2\right)^2+\frac{1}{2}\left(s_{cr}^2-s_0^2\right)}\right]} \quad (33a)$$

For the case, when

$$\frac{1}{2}\left(s_{cr}^2-s_0^2\right) \ll \left(s_0-\frac{D}{2A}s_{cr}^2\right)^2,$$

from (33a) we get

$$\varkappa = \frac{2}{\pi}\cdot\frac{A}{D}\left[\frac{s_0-\frac{D}{2A}s_{cr}^2}{s_{cr}^2-s_0^2}\right], \quad (34)$$

or

$$\varkappa = \frac{2}{\pi}\left[\frac{\varepsilon^2(1+\varepsilon^2)-0.5m}{(1-\varepsilon^2)m}\right], \quad (35)$$

where

$$\varepsilon = \frac{s_0}{s_{cr}}; \quad m = \frac{Ds_0}{M_{max}}.$$

The value of the slip from (26), (33), and (35):

$$s_{av} = s_0 + \frac{A}{D\left(2\pi\varkappa+\frac{3}{2}\pi\right)}. \quad (36)$$

The time of synchronization from (36) is:

$$t_s = \frac{2\pi\varkappa+1.5\pi}{\varepsilon_{av}2\pi f}\ [\text{sec}]. \quad (37)$$

In the above example we get, according to (26), (33), (36) and (37), when $k^2_{sh} \approx 1$:

$$A = \tfrac{1}{2}Hs_0^2 + M_{max} = \tfrac{1}{2}\,1000\times0.05^2 + 2 = 3.25;$$

$$D = 20; \quad s_0 = 0.05; \quad s_{cr} = 0{,}0632; \quad \chi = 2.1.$$

Using the approximate formula (35), we have

$$\varepsilon = 0.79; \quad m = 0.5; \quad \chi = 2.5.$$

The average slip for $\varkappa = 3$ will be $S_{av} = 0.0569$. Time of synchronization $t_s = 1.33$ sec. The approximate method given above was verified by solving equation (15), by the method of successive approximations. For this purpose it is convenient to decrease the number of equation constants by introducing the relative value of slip

$$\sigma = \frac{s}{\omega_{sw}} \quad (38)$$

where $\omega_{sw} = \sqrt{\frac{M_{max}}{H}}$, the angular speed of free oscillations of the rotor in a

magnetic field. The equation (15) assumes the form:

$$\frac{d\sigma}{d\theta}\sigma + k_A(\sigma - \sigma_0) + \sin\theta = 0, \tag{39}$$

where,

$$k_A = \frac{D\omega_{sw}}{M_{max}}; \quad \sigma_0 = \frac{s_0}{\omega_{sw}}; \quad k_A\sigma_0 = \frac{M_{ex}}{M_{max}} = m.$$

In the above example,

$$D = 20; \quad H = 1000; \quad M_{max} = 2; \quad s_0 = 0.05;$$

$$k_A = 0.5; \quad \sigma_0 \approx 1.$$

If $M_{sh} \neq Ds_0$ the equation (39) will have the form:

$$\frac{d\sigma}{d\theta}\sigma + k_A\sigma + \sin\theta = \frac{M_{ex}}{M_{max}} = m, \tag{40}$$

or

$$\frac{dw}{d\theta} + \sqrt{2}\,k_A\sqrt{w} + \sin\theta = m, \tag{41}$$

where, $w = \frac{1}{2}\sigma^2$.

Fig. 7 shows the curve of the relative slip σ. The solution for σ neglecting D, i.e. when $k_A\sigma = 0$, is also given in this figure (curve 1):

$$\sigma = \sqrt{-2\int_{\theta_0}^{\theta}\sin\theta d\theta + m} = \sqrt{2(\cos\theta - \cos\theta_0) + m}. \tag{42}$$

In this case, equation (21) will have, in relative units, the form:

$$\sigma = \sqrt{2\left[(\cos\theta - \cos\theta_0) + \int_{\theta_0}^{\theta}(m - k_A\sigma)\right] + \sigma_0^2}. \tag{43}$$

The analysis of equation (43) enables us to determine the criterion for entering into synchronization:

$$k_A\sqrt{2} > m, \quad \text{or} \quad D > m\sqrt{\frac{HM_{max}}{2}}. \tag{44}$$

Conditions for synchronization found above allow the solution of the inverse problem: to find the value of the relative resistance r_1' of the symmetrical starting winding for a motor with an inertial constant H, torques M_{max} and M_{ex} for the time of synchronizing t. For instance, let us take: $H = 500$ rad., $M_{sh} = 0.5$, $t_s =$ sec. We determine the critical slip by formula (34) for $k_{sh}^2 = 1.2$:

$$s_{cr} = \sqrt{\frac{2M_{max}}{1.2H}} = \sqrt{\frac{2 \cdot 2}{1.2 \cdot 500}} = 0.081.$$

The value of s_0 should be less than s_{cr}. Let s_0 = 7 per cent; in this case

$$D = \frac{M_{ex}}{s_0} = \frac{0.5}{0.07} = 7.1 \quad \text{and} \quad r_2' \approx \frac{1}{D} = \frac{1}{7.1} = 0.14.$$

Verification by formula (33) when $A = \frac{1}{2} \times 500 \times 0.07^2 + 2 = 3.25$; S_{cr} = 8.1 per cent, gives:

$$\kappa = 10.8.$$

By the approximate formula (35), for $\epsilon = 0.86$, $m = 0.25$, we find $\kappa = 11.4$. By formula (36), $s_{cr} = 0.76$, and by formula (37) for $\kappa = 11$ we have

$$t_s = \frac{\pi (2 \times 11 + 1.5)}{0.076 \times 314} = 3.1 \text{ sec},$$

i.e. a value greater than assumed. Therefore, it is necessary to diminish s_0 to the value s_0 = 6 per cent and the resistance of the starting winding r_2 in the ratio 6/7, i.e. to the value of 12 per cent.

The real conditions of synchronizing will be more favourable, since for switching on at $\theta_0 = -\pi$, the exciting current does not reach its full value instantaneously due to the winding reactance, and the work of braking from $-\pi$ to zero will be smaller.

The experimental verification of the conditions determined above agree with results obtained in practice using the calculated data; the use of the above methods may therefore be recommended.

Translated by S. Szymanski

REFERENCES

1. S.B. Iuditskii; *Sinkhronnye mashiny s poluprovodnikovymi vypriamiteliami (Synchronous machines with semi-conductor rectifiers)*, Gosenergoizdat (1954).
2. V.L. Inosov and V.E. Krutikova; *Electrichestvo*, No.6 (1956).
3. Griffin; *The synchronous induction motor*, London, MacDonald Co. Ltd. (1954).
4. *J. Inst. Elect. Engrs.* vol. 6, 1205 (1930).
5. O merakh povysheniia koeffitsients moshchnosti elektroustanovok promyshlennykh predpriiatii (Methods for increasing the power factor of electrical installations in industrial establishments), *Elektrichestvo*, No.2 (1953).
6. Ziganek; *Electricke stroje Praha, sixth edition* (1951).
7. V.L. Inosov; Sinkhronnyi dvigatel smeshannogo vozbuzhdeniia i teoriia ego raboty (Synchronous motor with mixed excitation and the theory of its action), in symposium, *Tr. inst. elektro-tekh, Akad Nauk Ukr. SSR* No.14 (1956).

1959

COMPARISON OF TWO-STAGE AND THREE-STAGE ROTARY AMPLIFIERS WITH AXIAL FIELD *

B.I. NORNEVSKII, V.F. BATKO, V.E. MALISHEVSKII, P.V. KUROPATKIN and E.I. ROSIN

Ulianov Lenin Institute of Electric Technology, Leningrad

(Received 21 May 1957)

Electric rotary amplifiers with a cross and axial field belong to the class of quick acting and highly sensitive regulators. The rate of voltage increase of these machines, at a control power of a few watts, reaches a value of 1000 - 2000 V/sec at the rated voltage of 230 V; the voltage amplification factor varies within limits of tens up to hundreds of units.

Investigations show that the amplifiers with an axial field have many important advantages in comparison with amplifiers with a cross field. Multistage amplifiers with an axial field have higher amplification factors and efficiencies and can act more quickly [2].

An additional advantage of these amplifiers is their wide range of power output, which makes possible their use in high power control systems as main exciters. It is known that the construction of high power amplifiers with a cross-field is limited by serious difficulties connected with commutation.

Amplifiers with an axial field may have one, two or more amplification stages according to the network and number of poles.

The work of the amplifier with an axial field is discussed in a series of articles by Soviet and foreign authors [1, 2, 4, 5, 6].

The three-stage rotary amplifier is at present the least investigated. Only a comparatively small number of works is devoted to its investigation [3, 7].

Recently in the laboratories of the LETI, LYIMU and LIIZhT, a series of investigations was carried out on a three-stage amplifier with an axial field. Some of the results obtained are discussed in the present article.

* *Elektrichestvo*, No. 3, 9-14, 1957.

The working principle of a three-stage amplifier

A three-stage rotary amplifier with an axial field is similar in its construction to an ordinary d.c. generator. Its magnetic system, like the system of the majority of other amplifiers, is usually unsaturated, since a satisfactory performance of an amplifier, from the point of view of the quality of regulation-amplification and quick action, is possible within the linear part of the magnetization curve. The armature winding of the amplifier is of the lap type without compensating windings.

Let us consider how the amplification stages are realized in a three-stage amplifier taking as an example a four-pole machine. Fig. 1 shows the network of this amplifier. *

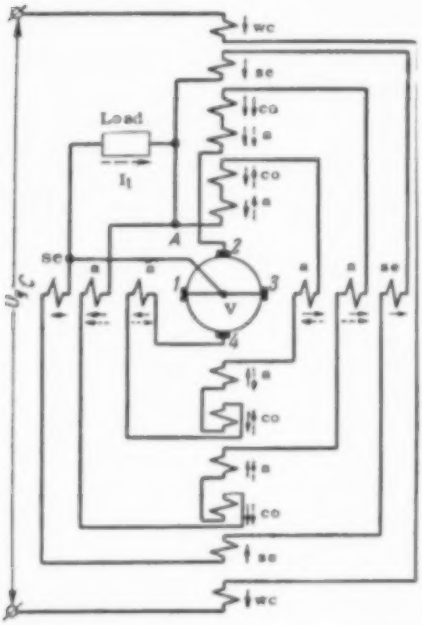

FIG. 1. Network of a three-stage amplifier

The basic four-pole flux Φ_3 in this amplifier is induced by a self-excitation winding $S\theta$ and an amplifying winding a. These windings are wound on four poles. Control windings are situated on the poles of the same polarity for a four-pole excitation system (for example 1-3).

Flux Φ_1, induced by m.m.f. of the control winding, induces a potential difference between brushes 1-3 when the armature rotates. The armature network between brushes 1-3 and the control winding constitute the first amplification stage, for which the input factor is the voltage, applied to the control winding, and the output is the e.m.f. E_{13}.

The second stage of amplification is produced by using the cross-reaction of the armature due to the compensating current i_{13}, which flows when the circuit of brushes 1-3 is completed. The armature reaction flux Φ_2, induced by the compensating current i_{13}, induces an e.m.f. $E24$ between brushes 2-4. The e.m.f. $E24$ is the output factor of the second amplification stage.

The third stage is achieved by connecting the four-pole amplifying winding to

* Interpoles are not shown on Fig. 1, 6 and 7. For a three-stage amplifier the number of sections of the interpole windings and the network of connections remain the same, as for a two-stage amplifier [1].

the brushes 2-4. The resultant output of this stage is the e.m.f. E_2 between the adjacent brushes.

When the compensating current I_{24} flows between brushes 2-4, a two-pole flux of the armature reaction is induced in the amplifier armature, this flux being directed against the flux of the control winding. To neutralize this reaction a compensating winding C, wound on poles 1-3, is connected in series with the amplifying winding.

The load and the parallel self-excitation winding are connected to the midpoints of the network of brushes 1-3 and 2-4. When the amplifier is on load, the load current and the current of the parallel winding of self-excitation flow in the networks of the amplifying and compensating windings.

To neutralize the influence of these currents on fluxes, set up by the compensating currents, windings a and c are arranged in such a way that for the compensating winding these sections are connected in series aidings and for the load current and the current of self-excitation they are connected in series opposing. The self-excitation winding of the amplifier is adjusted to a resistance near to the critical.

For $R_{se} = R_{se.c}$ we can assume <(cf. straight line, Fig. F), that the volt-ampere characteristic of the self-excitation winding coincides with the rectilinear portion of the magnetizing curve. For $R_{se} = R_{se.c.}$, n = const., and in the absence of an input signal, the amplifier is not self-excited, and its output voltage may assume any value within the limits of the rectilinear portion of the no-load characteristic in the case of idle running, or of the load characteristic, if the load is present. For open circuit conditions of the amplifier and with manual control, the voltage required on its terminals, for such an arrangement of the self-excitation winding, is obtained by voltage impulses applied to the control winding.

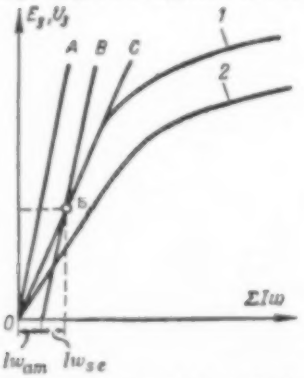

FIG. 2. Characteristics of idle running (1) and on-load (2) for R_e = const.

In the closed loop system the change of voltage is realized by means of a measuring device and a feedback coupling. An amplifier, working on load near the critical value, can be considered as an astatic regulator. Investigations which have been carried out [4] show that the work of the amplifier under these conditions is entirely stable, while, from the point of view of the stability of the amplifier itself, this occurrence is the limiting case.

An amplifier with an axial field can work with the resistance of the self-excitation winding se above the critical value, if the volt-ampere characteristic lies above the magnetization curve. Under these conditions it may be considered as a static regulator: for a definite value of the current in the control winding there corresponds a strictly determined value of the output voltage (lines A and B, Fig. 2).

A comparison of qualities of three- and two-stage amplifiers with an axial field

In comparing qualities of rotary amplifiers it is customary to consider their amplification factors and their ability to respond quickly. The notion of the static amplification factor may be applied to an axial amplifier; it has a theoretical meaning in the arrangement of the circuit of the self-excitation winding to a resistance larger than the critical one.

1959

Considering an amplifier as an unsaturated machine and using the well-known relationship between a.m.f. and e.m.f., we may establish the relationship between e.m.f. at the amplifier output E_3, and the voltage U_c, applied to the control winding. The equations of e.m.f. and m.m.f. of a three-stage amplifier, for the steady-state conditions, are:

(a) for the first stage

$$E_{13} = c\Phi_1 = \frac{c}{a} Iw_{13}; \tag{1}$$

$$Iw_{13} = 2w_c \frac{U_c}{r_c} + 2w_a \varepsilon \frac{E_{24}}{r_{24}}; \tag{2}$$

(b) for the second stage

$$E_{24} = c\Phi_2 = \frac{c}{a} Iw_{24}; \tag{3}$$

$$Iw_{24} = 2w_a i_{13} = 2w_a \frac{E_{13}}{r_{13}}; \tag{4}$$

(c) for the third stage

$$E_3 = c\Phi_3 = \frac{c}{a} Iw_3; \tag{5}$$

$$Iw_3 = 2w_a \frac{E_{24}}{r_{24}} + 2w_{se} \frac{E_3}{r_{se}}, \tag{6}$$

where Iw_{13}, Iw_{24} and Iw_3 are the m.m.f.'s of the first, second and third amplifying stages;

c factor of the proportionality between the e.m.f. and the flux;

a the factor of the proportionality between the m.m.f. and the flux;

i_c, i_{se}, i_{13}, i_{24} currents in the following windings: control, self-excitation and in the circuits of brushes 1-3 and 2-4;

r_c, r_{se}, r_{13}, r_{14} resistances of the following windings: control, self-excitation, and in the circuits of brushes 1-3 and 2-4;

w_c, w_a, w_{co}, w_{se} number of turns per pole of the following windings: control, amplifying, compensating and self-excitation;

$w_a = \frac{N}{16}$ equivalent number of turns of the armature winding per pole;

N number of active conductors of the armature winding,

$\epsilon = \frac{2w_{co} - 2w_a}{2w_a}$ degree of compensation of the armature reaction due to the compensating current i_{24}.

Solving equations (1–6) with respect to E_3 and dividing both sides of the formula so obtained by U_c, we have the following expression for the amplification factor of a three-stage amplifier.

$$K = \frac{E_3}{U_c} = \frac{K_c K_1 K_a}{(1 - T_{se})(1 - K_1 K_2 \epsilon)}, \tag{7}$$

where

$$K_c = \frac{2w_c c}{ar_c}; \quad K_1 = \frac{2w_a c}{ar_{13}}; \quad K_a = \frac{2w_c c}{ar_{24}};$$

$$K_{se} = \frac{2w_{se} c}{ar_{se}}; \quad K_2 = \frac{2w_a c}{ar_{24}}.$$

Similary we get the expression for the amplification factor of a two-stage amplifier

$$K' = \frac{K_c K'_a (1 + K_{op})}{(1 - K_{se})(1 + K_{op} + \epsilon_1 \epsilon_2 K'_1 K'_2)}, \tag{8}$$

where

$$K'_a = \frac{2w_c c}{ar'_{13}}; \quad K'_1 = \frac{2w_a c}{ar'_{13}}; \quad K'_2 = \frac{2w_a c}{ar'_{24}};$$

$$K_{op} = \frac{2w_{op} c}{ar_{24}};$$

$\epsilon_1 = \frac{2w_a - 2w_{co_{13}}}{2w_a}$; $\epsilon_2 = \frac{2w_a - 2w_{co_{24}}}{2w_a}$; degrees of compensation of the armature reaction due to the compensating currents i_{13} and i_{24}.

From the above formulae (7) and (8) we find the expression for the ratio of the amplification factors of two- and three-stage rotary amplifiers with an axial field:

$$\frac{K}{K'} = \frac{K_1(1 + K_{op} + \epsilon_1\epsilon_2 K_1' K_2')}{(1 - K_1 K_2 \epsilon)(1 + K_{op})}. \qquad (9)$$

In the case of total compensation of the armature reaction, when $\epsilon = \epsilon_1 = \epsilon_2 = 0$, ratio K/K' corresponds to the amplification factor K_1 of the second stage of a three-stage amplifier. The value of this factor is of the order of a few units or tens of units. This fact shows that it is possible, for a given set of conditions, to obtain a much greater voltage amplification in a three-stage amplifier than in a two-stage one, and consequently a much greater power amplification.

In the case of undercompensation of the armature reaction, $K/K' < K_1$. The nature of the influence of the degree of compensation on the amplification factors of the amplifiers in question is shown in Fig. 3, in the form of a curve $K/K' = f(\epsilon)$. This curve is plotted for the linear part of the magnetization curve by using the data from an experimental amplifier, assuming that $\epsilon = \epsilon_1 = \epsilon_2$. Usually the undercompensation of the armature reaction in the amplifier with an axial field does not exceed 1-6 per cent. For these values of E the amplification factor of a three-stage amplifier is 2.5-5 times greater than the a.f. of a two-stage amplifier.

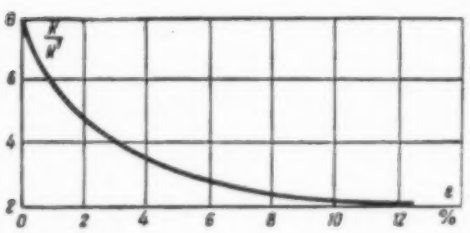

FIG. 3. The influence of the degree of compensation on the ratio of amplification factors of two-stage and three-stage amplifiers.

When the amplifier works as an astatic regulator, i.e. when the circuit of the self-excitation winding is arranged for a resistance equal to the critical one, the notion of the static amplification factor becomes meaningless, since under steady-state conditions the intermediate stages do no work. To evaluate the quality of an amplifier working under these conditions, we usually introduce the conception of the minimum control power and of the dynamic amplification factor. As a minimum control power we usually accept such a value, for which an amplifier begins to reverse its polarity. The value of the minimum control power characterizes a region of the amplifier insensibility and is determined by the width of the hysteresis loop. The minimum control power of existing amplifiers with an axial field is of the order of milliwatts.

The dynamic amplification factor is determined as a ratio of the rate of increase of e.m.f. at the output of the amplifier to the value of U_c of the voltage applied to the control winding; it characterizes the speed of the amplifier reaction to a unit disturbance.

Under conditions of total compensation of the armature reaction by the compensating current i_{24}, and neglecting the saturation and the reaction of commutation currents, we may write the expression for the dynamic amplification factor in the following form: (a) for the three amplification stages

$$K_{dyn} = \frac{\frac{dE_3}{dt}}{U_g} = \frac{K_c K_1 K_a}{T_a + T_{se}}, \tag{10}$$

where T_a and T_{se} are time constants of the amplifying winding and self-excitation winding;

(b) for the two amplification stages

$$K_{dyn} = \frac{\frac{dE_3'}{dt}}{U_g} = \frac{K_c K_a'}{T_a + T_{se}}. \tag{11}$$

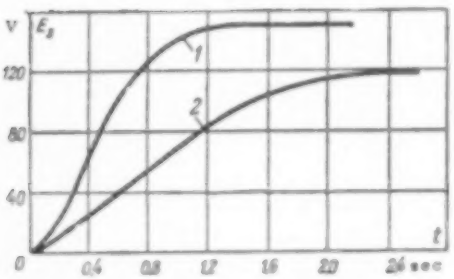

FIG. 4. Curves of a transient process for three (1) and two (2) amplification stages (i_{co} = 75 m A).

The ratio of these two factors and also the ratio of the amplification factors correspond to the amplification factor of the second stage of a three-stage amplifier;

$$\frac{K_{dyn}}{K'_{dyn}} = K_1 \tag{12}$$

The comparison of the quick operation of the two- and three-stage amplifiers with an axial field was carried out on the experimental model of 1.8 kW power, U_l = 60 V, I_l = 30 A, n = 1450 rev/min.

This amplifier, constructed in accordance with the design of the ordinary d.c. generator model PN, was made so that it was possible to arrange either two or three amplification stages by changing the winding connexions. This was done in order to carry out comparative tests under the same conditions. In both cases the resistance of the self-excitation winding was adjusted to its critical value. The same control winding was used (r_c = 30 Ω). The transient processes were recorded by an oscillograph at U_c = const.

The results of these comparative tests are shown in Fig. 4 and 5.

Fig. 4 shows the curves of the transient processes, plotted on the basis of oscillogram data, for two- and three-stage amplification, for the same degree of compensation of the armature reaction ϵ = 5.5 per cent, and the same control current equal to 75 m A. Fig. 5 shows the main values of the rate of increase of the

e.m.f. at the output for various values of currents in the control winding.

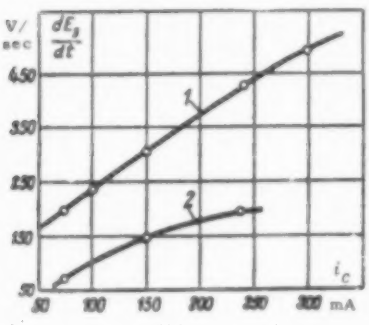

FIG. 5. Rate of increase of e.m.f. E_3 at the output for three (1) and two (2) amplification stages.

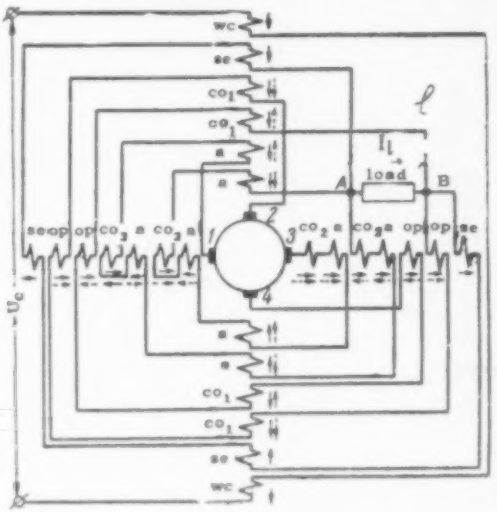

FIG. 6. The network of a two-stage amplifier with an oxide field.

1959

From the above experimental data it follows that, for the same magnetic system and for approximately the same weight of active materials and for the same values c and l_c the rate of increase of the e.m.f. at the output is approximately 2-2.5 times greater in a three stage amplifier than in a two-stage one.

Amplification and quick response are not the only criteria in the evaluation of amplifier qualities. It is necessary to consider such properties as the tendency to oscillate and the complexity of the networks.

A three-stage amplifier in comparison with a two-stage one has a greater tendency to oscillations and to self-excitation, which is due to the increase in the total amplification factor and the phase delay. However, experimental investigations showed that the working of a three-stage amplifier may be quite stable; possible causes of instability, which are common in the amplifiers and were compared (magnetic asymmetry, accelerated commutation and over-compensation of the armature reaction) may be entirely eliminated, or their influence reduced to a minimum.

The influence of magnetic asymmetry in an amplifier with an axial field may be compensated by varying the value of the resistance of the self-excitation winding, of the degree of compensation of the armature winding, and also by increasing the air gap [3]. For the adjustment of the required degree of compensation of the armature winding, we use a variable resistance, which is connected in parallel to

the compensating winding. The commutation adjustment is done in the same way as in an ordinary d.c. machine.

In comparing the networks of the two- and three-stage amplifiers (Fig. 6, 1) we may point out that a three-stage amplifier has a somewhat simplified network. In a two-stage amplifier the armature reaction, due to the equalizing current i_{11}, must be compensated rather accurately by the compensating winding co_2 and by the series opposing winding *op*, wound on poles 2-4, whereas in a three-stage amplifier this reaction is used for further amplification, and the additional windings co_2 and *op* on poles 2-4 are absent.

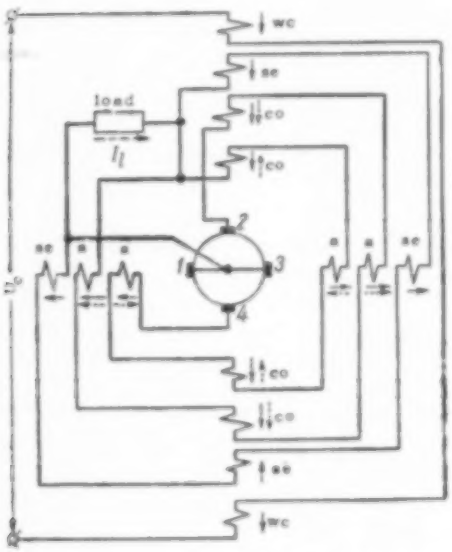

FIG. 7. Simplified network of a three-stage amplifier.

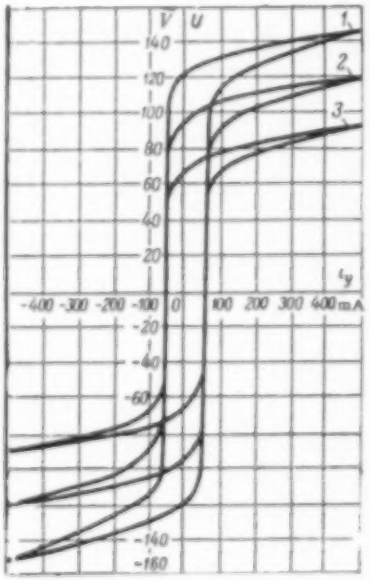

FIG. 8. Characteristics of an experimental three-stage amplifier of 5.5 kW power. 1 - characteristic idle running 2 – for R_e = 1.7 Ω; 3 – for R_e =0.83

This last feature permits a further simplification of the network of a three-stage amplifier as well as a reduction in the number of windings on poles 1-3; this is very desirable in order to improve the conditions of the distribution of control windings. The arrangement of the amplifying winding as shown in Fig. 7 may also be recommended.

As distinct from the network shown in Fig. 1 here the sections of the amplifying winding *a* are situated only on poles 2-4, but, since these windings are connected in series opposing, a four-pole excitation flux of the third stage is produced. This

method of connexions was used on two experimental models of 4 - 5.5 kW power, constructed basically according to the design of the machine model PN - 100.

Fig. 8 shows the characteristics of the idle and load working of one of these amplifiers of 5.5 kW power, running under conditions of astatic regulation.

Conclusions

(1) A three-stage amplifier has a number of advantages in comparison with a two-stage one. Its response is quicker for the same control power. For the same speed of response, a three-stage amplifier is controlled by a smaller power.

(2) A three-stage amplifier has a simpler network than an amplifier with two amplification stages.

Translated by S. Szymanski

REFERENCES

1. V.F. Baiko and A.A. Vavilov; Perekhodnye protsessy v dvukhstupenchatom usilitele s samovozbuzhdeniem (Transient processes in a two-stage rotary amplifier with self-excitation), *Elektrichestvo*, No. 10 (1956).
2. F.A. Goriainov and B.Ia.Gusev; Issledovanie dvukhstupenchatogo regulatora prodolnogo polia (Investigation of a two-stage regulator with an axial field), *Tr. Moscow Power Inst.*, XV (1955).
3. F.A. Goriainov and B.F. Tokarev; Vliianie magnitnoi nesimmetrii na rabotu trekhstupenchatogo elektro-machinnogo usilitelia (The influence of the magnetic asymmetry on the working of a three-stage rotary amplifier), *Elektrichestvo*, No. 8 (1949).
4. R.S. Piasetskii; Elektromachinnyi regulgator c kriticheskim samovozbuzhdeniem (Rotary regulator with a critical self-excitation), *Elektrichestvo*, No. 8 (1949).
5. W.R. Harris; The industrial application of regulators of the rototrol type. *Trans Amer. Inst. Elect. Engrs.* 118 - 123 (1945).
6. A.W. Kimbal; A two-stage rototrol for a low-power control system *Trans. Amer Inst. Elect. Engrs.* 66, 1507 (1947).
7. M. Liwshits, The multistage rototrol. *Trans Amer. Inst. Elect. Engrs.* 66, 564 - 568 (1947).

1959

SPEED CONTROL OF A D.C. MOTOR FED FROM A MAGNETIC AMPLIFIER *

V.D. AFANAS'EV and IVOBOTENKO

Central Scientific Research Institute for Machine Technology

(Received 18 October 1957)

In automatic control systems of electric drive, controlled small-power motors are being used more frequently; they constitute an integral part of control systems. The use of magnetic amplifiers for the feeding of these motors may ensure their speed control within large limits, and enables us to obtain rigid mechanical characteristics, similar to the characteristics of speed control in the generator-motor system. For this purpose it is necessary to choose an appropriate magnetic amplifier and a control system with a feed-back.

Simple methods for designing such systems are of considerable practical importance, provided they enable us to find characteristics with sufficient accuracy for practical use, and to determine the necessary parameters of the control networks.

The method described below is an approximate but very simple method of calculation; it permits the easy determination of the mechanical characteristics of the system amplifier-motor using the catalogue operational characteristic of an amplifier, which gives the dependence of the mean load current upon the magnetization current at the nominal load resistance.

$$I_1 = f(I_y) \text{ and } R = R_l.$$

For calculations of the static characteristics of a d.c. low-power motor, fed through a magnetic amplifier from a grid of line frequency, we may neglect the armature inductance and replace it by an equivalent resistance.

$$R_e = \frac{U_m}{I_m} = \frac{k_e \phi n}{I_m} + R_a \,, \tag{1}$$

* *Elektrichestvo*, No. 3, 14-19, 1958.

where U_m and I_m are the motor voltage and current,
R_a is the armature resistance,
n is the speed of rotation;
ϕ is the excitation flux;
k_e is the motor constant.

The equivalent resistance R_e may be easily determined from formula (1) for the given arbitrary operational conditions of the motor. If the amplifier characteristic, obtained for a load resistance $R = R_e$, is available, it is possible to determine the magnetization current corresponding to the given conditions (n, I_m) of work of the motor. Thus the problem is reduced to obtaining the artificial characteristics of the amplifier running at different load resistances, differeng from the nominal value of the load.

For calculating the necessary artificial characteristics of an amplifier we shall use the notion of its *universal characteristic* [1]. We shall construct the amplifier characteristic in relative units, but not as a function of the total magnetization current, [1], but as a function of the control current, i.e. taking into account a positive feed-back of the amplifier.

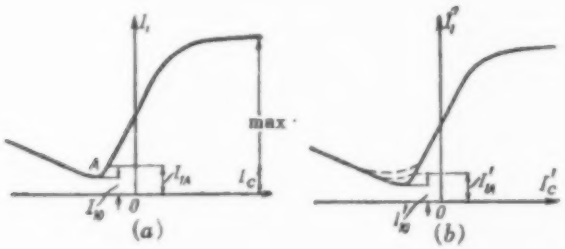

FIG. 1. Characteristics of a magnetic amplifier (a) in absolute units (b) in relative units.

Let the curve in Fig. 1a represent a catalogue or an experimentally obtained working characteristic of the amplifier in nominal conditions. We replot the amplifier characteristic in relative units (Fig. 1b),

$$I_1' = \frac{I_1}{I_{1u}}; \quad I_c' = \frac{I_c}{I_{c.u}}, \tag{2}$$

where I, I_c are the current values in absolute units
Unit values of currents are:

$$\left.\begin{aligned} I_{1u} &= \frac{U_\sim}{1,11R_{1u}}; \\ I_{c.u} &= \frac{I_{1u}}{k} \cdot \frac{w_1}{w_c}, \end{aligned}\right\} \tag{3}$$

where U is the effective value of the applied voltage;
R_{1u} is the total resistance of the load network, including the resistance of rectifiers and of amplifier windings;
W_1 is the number of turns of the a.c. winding;
W_c is the number of turns of the control winding;
$k = 1$ is for networks with a series connexion of windings w_1.
$k = 2$ is for networks with a parallel connexion of windings w_1 and networks with an internal feed-back.

With sufficient accuracy we may assume:

$$I_{1u} = I_{1\max}$$

where $I_{1\max}$ is the maximum value of the load current(according to the nominal amplifier characteristic, Fig. 1a).

We determine unit resistance of the load network where the amplifier saturation is:

$$R_{1u} = \frac{U_{\sim}}{1.11 I_{1u}}. \tag{4}$$

By changing the load resistance by ΔR, we determine the unit resistance, corresponding to another value of load resistance $R_{II} = R + \Delta R$.

$$(R_{1u})_{II} \approx R_{1u} + \Delta R, \tag{5}$$

whence the new unit values of current will be:

$$(I_{1u})_{II} = I_{1u} \frac{R_{1u}}{(R_{1u})_{II}}; \tag{6}$$

$$(I_{c.u})_{II} = I_{c.u} \frac{R_{1u}}{(R_{1u})_{II}}.$$

Choosing a certain value of the control current I_c, we determine its new value in relative units:

$$(I_c')_{II} = \frac{I_c}{(I_{c.u})_{II}}. \tag{7}$$

From the amplifier characteristic in relative units (Fig. 1b) we find the new relative expression for the load current $(I_1)_{II}$, corresponding to $(I_c)_{II}$, and then its absolute value.

$$(I_1)_{II} = (I_1')_{II}\,(I_{1u})_{II}. \tag{8}$$

Thus we have found the value of the load current for the new value of the resistance $(R)_{II}$, corresponding to the control current I_c. In this way we may construct artificial characteristics of an amplifier for different values of the load resistance R.

In determining $(R_{1u})_{II}$ in formula (5) we neglected the variation of value resistances with the variation of unit current, since usually it does not exceed a few per cent of the total resistance R_{1u}. For large variations of R it is necessary to take into consideration the variation of valve resistances from the curves valve resistance-load current. The minimum current I_{10} at the output of the amplifier is determined by its inductance x_{10}, which is considerably greater than the load resistance R. Therefore in varying R, current I_{10} remains practically unchanged.

The part of the artificial characteristic of an amplifier, in the region of minimum currents, has to be constructed while taking this fact into account. For every value of R, the universal characteristics of an amplifier in the region of minimum currents will be different (dotted curves on Fig. 1b).

If we assume, as is recommended [1] that the minimum current I_{1A} of the linear portion of the amplifier characteristic is equal to 1.55 I_{10}, then the portion of the characteristic in relative units between I_{10} and I_A can be approximately obtained by joining it smoothly with linear portions of the characteristic.

Fig. 2 shows experimental and calculated characteristics of the magnetic amplifier model PMU-1 for different values of the load resistance. The network of the amplifier connexions during the tests is also shown.

From Fig. 2 it follows that there are differences between the calculated and experimental values of characteristics of up to 10 per cent. Nevertheless, taking into account that the dispersion of characteristics is unavoidable, owing for example to the instability of rectifiers, we may assume that the method recommended for constructing artificial characteristics of an amplifier, while varying its load resistance, gives sufficiently accurate results in practice. Calculations for other amplifiers give similar results.

Construction of artificial characteristics of an amplifier, in varying resistance R, may also be carried out, as a first approximation, using as a basis the condition that, for a constant control current I_c, current I_1 at the amplifier output varies inversely as the unit load resistance R_{1u} of the load network, i.e.

$$(I_1)_{II} = I_1 \frac{R_{1u}}{(R_{1u})_{II}}. \tag{9}$$

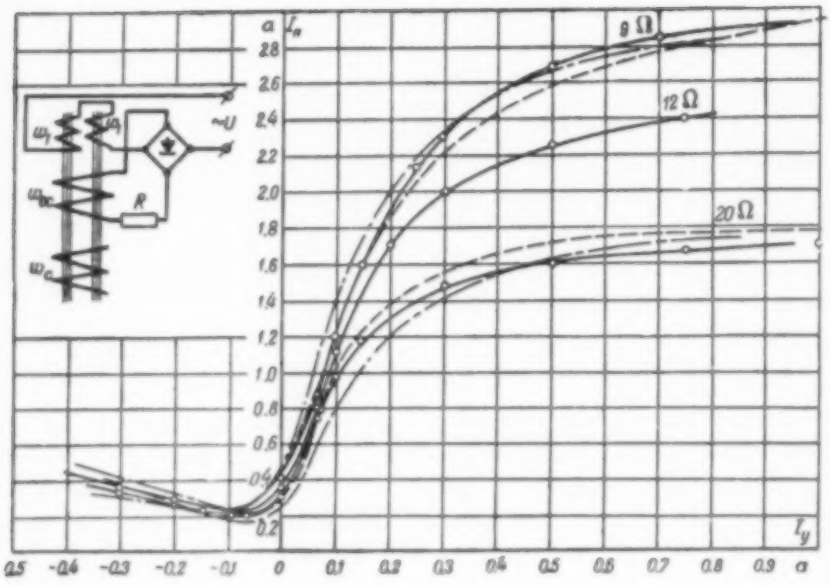

FIG. 2. Experimental and calculated characteristics of the amplifier PMU-1 ($U_\sim$ = 55 V, w_1 = 250; w_{bc} = 220; w_c = 450, selenium rectifier; into each leg of the rectifier two disks were series-connected, of d = 100 mm. —— – experimental characteristics; – – – calculated characteristics (calculations in relative units); – . – . – . calculated characteristics (calculations by formula (9).

This method of verifying calculations gives satisfactory results only for the working portion of the amplifier characteristics. Utilization of amplifier artificial characteristics, obtained by this method, in replacing an actual motor load by an equivalent resistance, calculated from equation (1), permits the easy determination of the mechanical characteristics of the amplifier-motor system as well.

Experimental verification of the possibility of replacing an actual motor load by an equivalent resistance was carried out in the following way.

The amplifier was assembled from three magnetic amplifiers, model BKN-1, in a three-phase bridge circuit. Characteristics were taken for different values of load resistances (dotted curves on Fig. 3). Then the armature of a d.c. motor (110 V, 9A, 4500 rev/min, was connected into the network instead of the load resistance (Fig. 4).

A rotary amplifier was used as the load, on the motor output shaft; the load was varied by using the resistance 9R.

TABLE 1.

I_c (mA)	– 5.0				0					5.0			10,0
I_1 (A)	2.5	5.0	5.3	5.95	3.0	5.0	5.5	6.0	8.0	6.5	6.9	7.5	8.0
n rev/min	1950	1250	1190	1040	2650	2130	2020	1885	1510	2620	2510	2400	2980
R_l (Ω)	17.5	7.0	6.0	5.0	20.0	10.0	9.0	8.0	5.0	10.0	9.0	8.0	9.0
R_e (Ω)	18.15	6.5	5.95	4.85	20.5	10.37	7.97	7.97	5.15	9.88	9.0	8.05	9.2

For control currents -10, -5, 0,5 and 10 mA, the load on the motor shaft was so chosen that the magnetic amplifier current was equal to the current corresponding to the load resistance.

The results of the measurements of the motor speed ($k_e \phi \approx 0.022$ V rev/min, $R_a = 1.0\ \Omega$) and of calculations of the equivalent resistance R_e from formula (1), shown in the table, confirm the possibility of replacing the motor by an equivalent resistance R_e. The error due to this lies within the limits 0-7 per cent. Experiments, which were carried out with other magnetic amplifiers and motors, gave similar results.

Thus, the replacing of a motor by equivalent resistances and constructing for these values artificial characteristics of the magnetic amplifier for different load resistances permit us to calculate the drive static characteristics.

The analysis of expression (1) shows, that the amplifier characteristics, obtained for a certain value of load resistance R_1 is the locus of points, for which the motor speed n is proportional to the load current I_1.

Amplifier characteristics for different values of R enable us to solve a series of other problems. Thus, for a constant magnetization current I_c, and choosing different load currents I_1, we may easily find by equation (1), putting $R = R_e$, corresponding values of the motor speed, i.e. we may easily construct the motor speed characteristic $n = f(I_m)$ for a given magnetization current I_c of the amplifier.

We may also solve the inverse problem: to determine the magnetization current, necessary to keep a constant speed n, when the load current of the motor varies.

The constant speed curves on Fig. 3 are shown as continuous lines.

Having obtained these relationships we may calculate the feed-back parameters, and the feed-back coupling will automatically maintain the desired speed of rotation. As follows from formula (1) and Fig. 3, the constant speed characteristic intersects the amplifier characteristic. This means that for a constant speed of rotation, a decrease in the equivalent resistance R_e corresponds to an

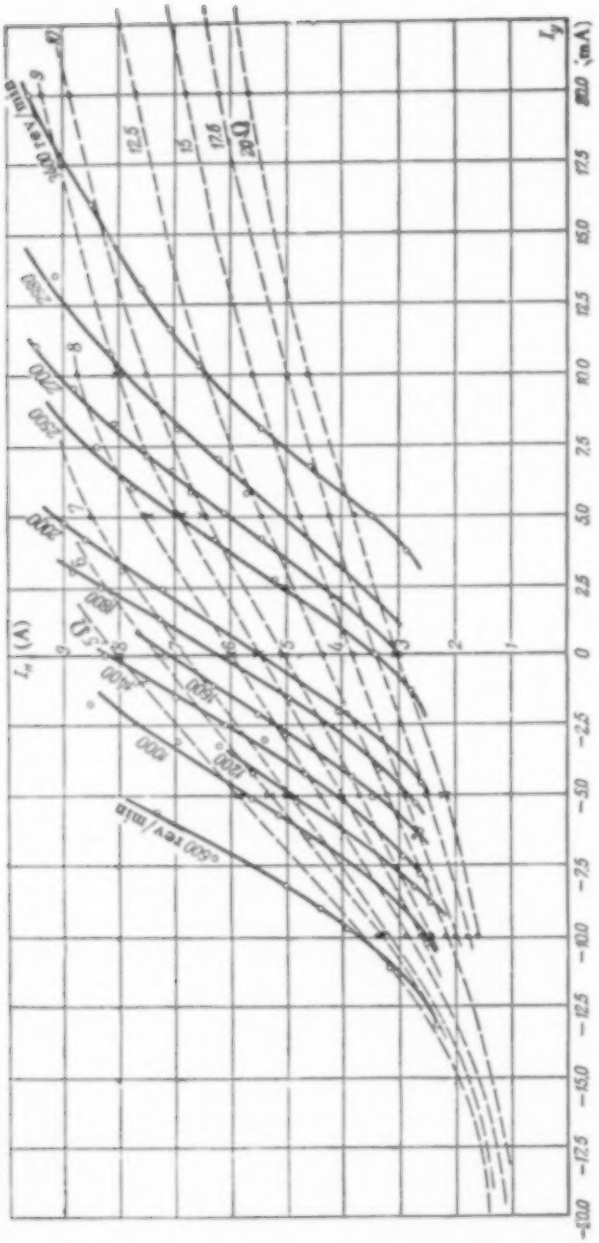

FIG. 3. Characteristics of an amplifier assembled in a three-phase bridge circuit from magnetic amplifiers BKN-1 ($U_{\sim}$ ph.i = 130 V; w_1 = 400; w_{OC} = 1500); – – – amplifier characteristic for load resistance; —— constant speed characteristics.

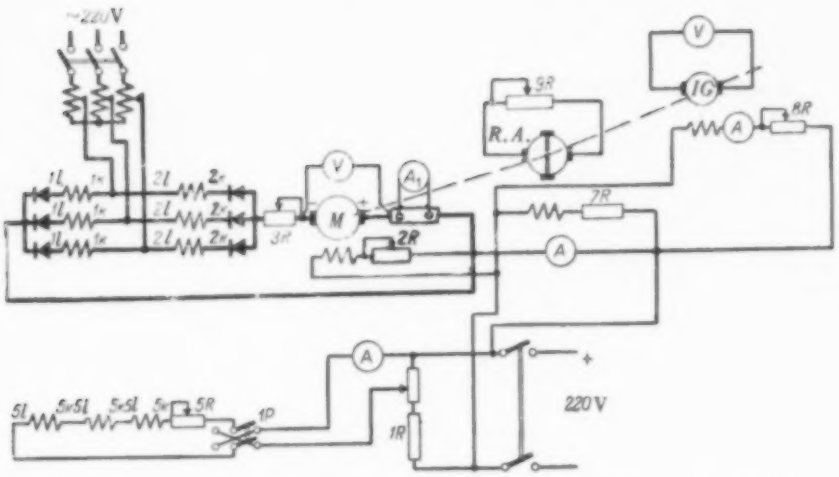

FIG. 4. Network for feeding a motor from magnetic amplifiers assembled in a three-phase bridge circuit.

increase in the motor current.

The constant speed characteristic may be considered as a straight line only in a restricted part of the curve. In the region of maximum and minimum currents this characteristic is obviously non-linear.

Comparison of the amplifier characteristic and the constant speed characteristic of the motor shows that by using linear feed-back in the amplifier-motor system we may obtain rigid motor speed characteristics, while varying the motor load within those limits of the amplifier characteristic, which are approximately rectilinear. Strictly determined values of the feed-back amplification coefficients correspond to this region.

From Fig. 3 we see that the constant speed characteristics have different slopes with respect to the coordinate axes: for greater speeds they are less steep. Hence, it follows that for the same range of load variation ($I_{min} - I_{max}$) to maintain a high constant speed we need a greater variation of the magnetization current than to maintain a smaller speed. Therefore, an invariable feed-back coupling in the amplifier-motor system does not ensure the constant characteristic rigidity of the motor at all speeds. If the feed-back network is designed to obtain rigid mechanical characteristics of the motor for certain mean speeds, then with the increase of speed the rigidity of mechanical characteristics will decrease, and with the decrease of speed will increase. In the latter case with the load (current) increase the motor speed may increase. Therefore, to ensure rigid mechanical characteristics of the motors a positive feed-back of current is not sufficient. Besides a positive feed-back of current, it is necessary to provide also for a negative feed-back from the motor voltage.

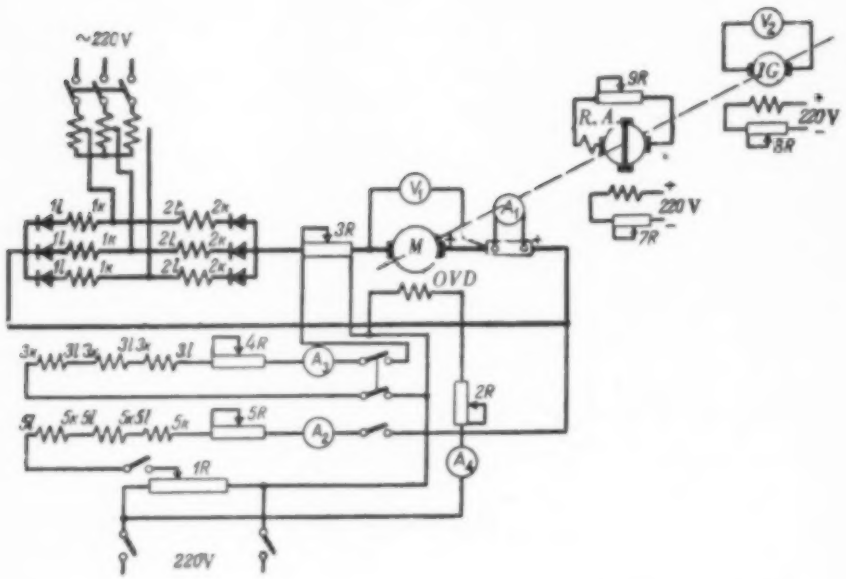

FIG. 5. Network for feeding a motor from magnetic amplifiers assembled in the three-phase bridge circuit with feed-back current and current couplings.

Experiments show that in networks with a magnetic amplifier, provided with an internal feed-back, it is necessary to use an additional small winding for external positive feed-back of the current in order to increase the coefficient of the positive feed-back of current by 3-5 per cent; in this way the realization of the negative feed-back from the motor voltage is facilitated.

Fig. 5 shows the network for feeding a d.c. motor in the amplifier-motor system with a positive feed-back of current and a negative feed-back from the motor-voltage (motor data: U= 110 V, I= 9A, n = 4500 min; magnetic amplifier model BKN-1).

The potential difference between the motor and the control potentiometer 1 R, was applied to windings 5 l – 5 k, ie. they were used simultaneously as control windings and as the feed-back windings from the motor voltage. As follows from Fig. 6, feeding of the motor in network 5 ensured the obtaining of rigid mechanical characteristics within the regulation limits 10: 1 (dotted curves).

In feeding the same motor from the amplifier BKN-1, connected in a single phase and with the use of similar feed-back couplings (for different values of feed-back amplification coefficients), rigid mechanical characteristics of the motor could not be obtained, for the same range of speeds and loads. This is due to the fact that the equivalent motor resistance R_e, under given conditions, cor-

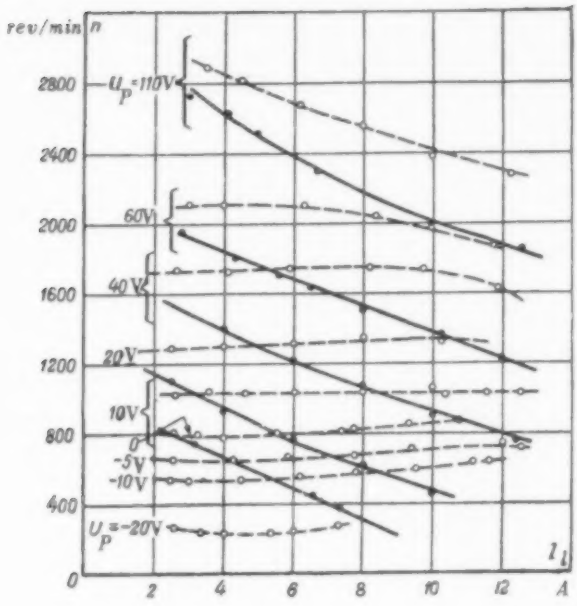

FIG. 6. Experimental characteristics of a motor connected in the network of Fig. 5. *Up* is the voltage of potentiometer 1*R*; 1 —— for coefficient of current feed-back equal 1; 2 – – – for coefficient of current feed-back equal 1.026.

responded to the work of the amplifier in the region of non-linear portions of the constant speed characteristics (Fig. 3).

Thus a proper choice of the amplifier is very important, to obtain the required characteristics of the drive to be controlled. Besides general considerations, the fundamental problem in choosing a magnetic amplifier for feeding a motor is a choice of an amplifier with a proper nominal load resistance. On the basis of the above discussion we may conclude that, if the nominal load resistance of the amplifier is equal or nearly equal to the equivalent resistance R_e of the motor, for its nominal current and a certain mean speed, then the conditions for obtaining rigid motor characteristics will be most favourable. Nominal amplifier resistance R_e should lie between the values of the equivalent motor resistance R_e for two sets of conditions: (a) I_{max}, n_{max} and (b) I_{min}, n_{min}. If R_l is considerably smaller than R_e, corresponding to I_{max} and n_{max}, or considerably greater than R_e corresponding to I_{min} and n_{min}, then obtaining rigid characteristics will be difficult: in the first case in the region I_{max}, n_{max}, and in the second case in the region I_{min}, n_{min}. According to concrete requirements the necessary value R_l may vary somewhat within specified limits.

Translated by S. Szymanski

REFERENCES

1. T.Kh. Stefanovich; Raschet magnitnykh usilitelei i magnitnykh rele pri pomoshchi universalnoi kharakteristiki (Calculation of data for magnetic amplifiers and magnetic relays by means of a universal characteristic) *VEP*, No. 6 (1956).

MODEL INSTALLATION FOR REMOTE CONTROL OF ELECTRIC PARAMETERS IN ARC FURNACES*

Yu.E. EFROIMOVICH

(Received 21 June 1957)

A system of automatic remote control of the parameters of the secondary winding of electric arc furnaces, of arc voltage and of useful power in each phase is necessary for the application of rational methods of regulating the complex technological processes of melting steel in these furnaces.

The solution of these problems is possible by using special model installations; a characteristic feature of these installations is the electrical relationship existing between the model and the object under investigation.

1959

The theory and principle of model installations

Fig. 1 shows two equivalent networks of a three-phase electric furnace installation. In Fig. 1 the e.m.f. of the mutual induction $e_{ik} = M_{ik}\, di_i/dt$ is taken into account by introducing two suitable generators with negligible impedances. In Fig. 1b, their influence is accounted for by a proper choice of the phase inductances of the secondary network [3]. According to Fig. 1b and [3], the arc voltage in any one phase will be:

$$e_{di} = u_{ti} - r_{kci} i_i - L_{kci} \frac{di_i}{dt} - (u_0'' - u_0') - u_0', \qquad (1)$$

where

$$u_0'' - u_0' = L_1' \frac{di_1}{dt} + L_2' \frac{di_2}{dt}; \quad L_1' = M_{12} - M_{23}; \quad L_2' = M_{12} - M_{13};$$

u_{ti} is the secondary voltage i th phase of the furnace transformer; u_0', u_0'' are respectively: potential difference between zero points O of the metal in the furnace, or O of the installation equivalent network and the zero voltage point of the secondary of the transformer.

Fig. 2 shows the basic network of the model installation for measuring resistances r_{kci} and inductances L_{kci} of the phases of the secondary network, voltages on arcs e_{ai} and differences between mutual phase inductances L_1' and L_2'. In the upper part of this figure the furnace transformer TF, the furnace itself and the secondary network, which feeds the powerful furnace arcs, are shown diagrammatically. The

* *Elektrichestvo*, No. 3, 22 – 27, 1958.

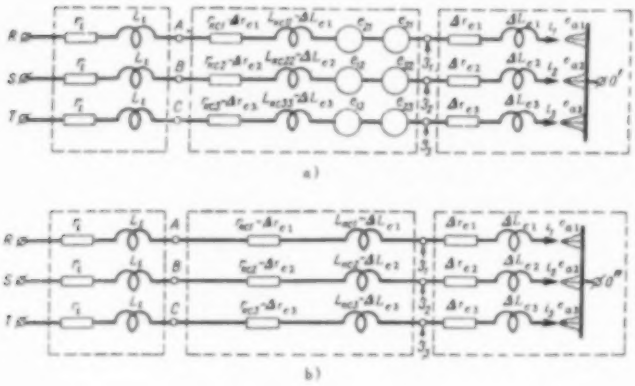

FIG. 1. Equivalent network of a three-phase arc furnace, r_i and l_i arc phase resistance and inductance of a furnace transformer; r_{kc} and L_{kci} the same but for a phase of the secondary; Δr_{ei} and ΔL_{ei} the same but for the electrode section situated inside the furnace; L_{kcii} the inductance of the i-phase; e_{ik} the e.m.f. of mutual induction, induced in phase k by current in phase i; e_{ai} and i_i the voltage and current of the ith phase.

equivalent model of the secondary network of the installation, corresponding to the network on Fig. 1b is shown below.

Let us assume that the values of the parameters r_{kci} and L_{kci} of the model are made equal to the instantaneous values of resistances and inductances of the furnace phases, and that real non-sinusoidal currents i_i of the corresponding furnace phases flow in them. Let us also assume that, between points O'' of the equivalent network and O' of the furnace, inductances L_1' and L_2' are connected, through which real furnace currents i_1 and i_2 flow. In this case potential differences, measured between the corresponding leads A, B, C of the secondary of the furnace transformer and the model leads A′, B′, C′, will, according to (1), exactly represent the non-sinusoidal arc voltages e_{a1}, e_{a2} and e_{a3} in the furnace.

In order to decrease electric losses in the model network k_m times in comparison with the losses in the secondary of the furnace and to obtain a proper scale for the model voltages, it is necessary to increase resistances and inductances in the model k_m times, and to decrease the values of the currents in the model networks k_m times.

Fig. 3 shows the basic network of a model installation for remote measurement of resistances $r_{kci} - \Delta r_{ei}$ and inductances $L_{kci} - \Delta L_{ei}$ and of differences of mutual inductances L_1'' and L_2'' of the sections of the secondary network, which are situated outside the furnace. On the left side of the figure networks of the furnace are shown; on the right side, networks of the model.

Contact-rods S_i are used to tap the potential of each electrode at the place where it emerges from the furnace. If the values of the model parameters correspond to the instantaneous values of the required parameter of the sections of the furnace secon-

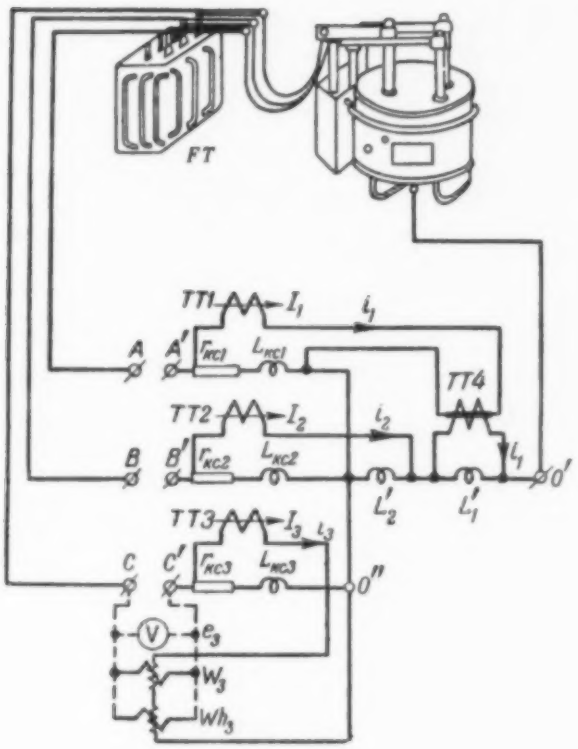

FIG. 2. Network of the model installation of the low-voltage part of an electrical melting furnace.

dary, and the currents in the network models correspond to the real non-sinusoidal currents in the furnace,* then the p.d. measured between points S_1 and E_1 will be equal to zero.

Introduction of contact-rods S_i enables us to measure directly the useful power of each phase of the furnace, equal to the sum of powers developed in the arc and on the portion of an electrode inside the furnace. If the parameters of the model shown in Fig. 3 are determined, the useful power say of Phase 1 may also be remote-controlled by means of a model by measuring p.d.s between points E_1 of the model and O' of the furnace.

Arranging models according to Figs. 2 and 3 on the furnace benchboard we have

* On Fig. 1 only networks for the phase current of Model 1 are shown.

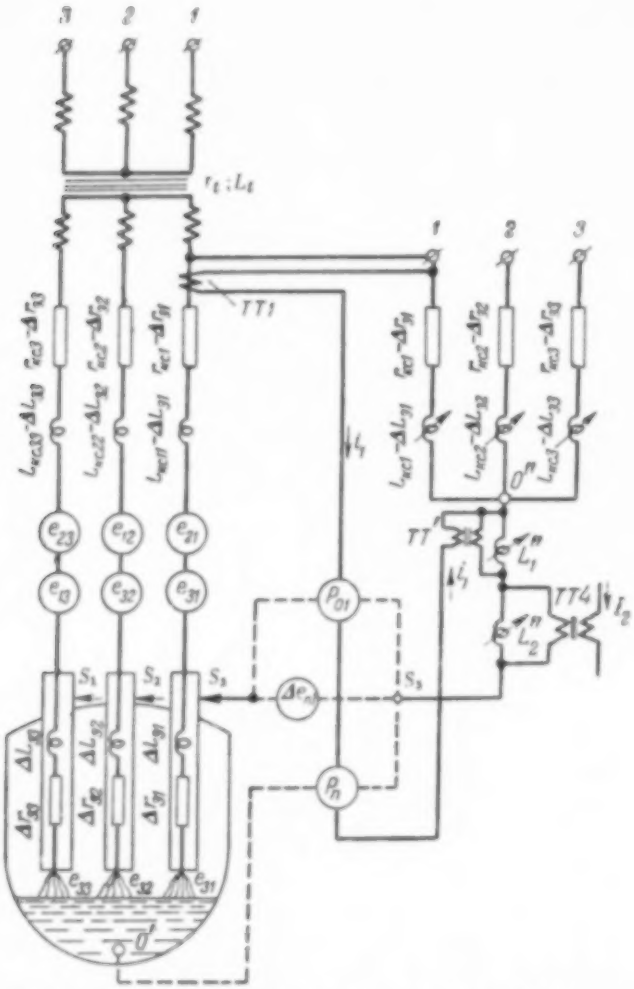

FIG. 3. Network of model installation of sections of the secondary, which are situated outside the furnace.

as 19 unknowns to be determined, L_{kci}, $L_{kci} - \Delta L_{ei}$, $r_{kci} - \Delta r_{ei}$, e_{ai}, r_{kci}, L_1', L_2', L_1'', L_2'', where $i = 1,2,3$.

Determination of the first 12 quantities may be made entirely automatic, since it can be performed under normal conditions when electrodes of all the three phases are arcing.

Experiments showed that, for the equal working lengths of the three electrodes: $L_1' = L_1''$, $L_2' = L_2''$ – this being due to the positioning of the electrodes in the furn-

ace at the apices of an equilateral triangle.

Values of L_1'', and L_2'', may be experimentally determined from a series of experiments by breaking one of the arcs, while the electrodes of two other phases are arcing under normal conditions. The order, in which these experiments are to be performed, is as follows.

We set $L_1'' = 0$ and break the arc in Phase 2. From the following equations:

$$(e_{d_2} + i_1 \Delta r_{e1}) - [u_{t1} - (L_{kc1} - \Delta L_{e1}) \frac{di_1}{dt} - L_1'' \frac{di_1}{dt} - \tag{3}$$

$$- L_2'' \frac{di_2}{dt} - i_1 (r_{kc1} - \Delta r_{e1})] = \Delta e_{n1} = 0; \tag{4}$$

$$i_1 = -i_3; \qquad i_2 = 0,$$

and varying either automatically or by hand the values of $L_{kc1} - \Delta L_{e1}$ and $r_{kci} - \Delta r_{e1}$ on the model, we may set and determine the values of $L_{kc1} - \Delta L_{e1} + L_1''$ and $r_{kc1} - \Delta r_{e1}$.

Striking the arc in Phase 2 and breaking it in phase 3($i_1 = -i_2$, $i_3 = 0$), and by condition (3), leaving the model parameters in Phase 1 unchanged, we may set up in Phase 2 the value L_2''.

After this, striking the arc in Phase 3 and breaking it in Phase 1, from the conditions required to satisfy equations

$$(e_{d2} + i_2 \Delta r_{e2}) - \left[u_{t2} - (L_{kc2} - \Delta L_{e2}) \frac{di_2}{dt} - L_1'' \frac{di_1}{dt} - \right. \tag{5}$$

$$\left. - L_2'' \frac{di_2}{dt} - i_2 (r_{kc2} - \Delta r_{e2})\right] = \Delta e_{n2} = 0; \tag{6}$$

$$i_2 = -i_3; \qquad i_1 = 0,$$

we may set up on the model, values of $L_{kc2} - \Delta L_{e2}$ and $r_{kc2} - \Delta r_{e2}$, and taking into account the equation

$$(e_{d2} + i_2 \Delta r_{e2}) - \left[u_{t3} - (L_{kc3} - \Delta L_{e3}) \frac{di_2}{dt} - L_1'' \frac{di_1}{dt} - \right. \tag{7}$$

$$\left. - L_2'' \frac{di_2}{dt} - i_3 (r_{kc3} - \Delta r_{e3})\right] = \Delta e_{n3} = 0$$

we may set up on the model values of $L_{kc3} - \Delta L_{e3}$ and $r_{ke3} - \Delta r_{e3}$. Further, by setting up the conditions satisfying equations (4), on the basis of equations (3), we may set up on the model values of $L_{kc1} - \Delta L_{e1}$ and L_1''.

Having determined by the above method values of L_1'' and L_2'' and keeping the electrodes arcing on all three phases in the furnace, we may determine values of $L_{kci} - \Delta L_{ei}$ and $r_{kci} - \Delta r_{ei}$, by equations (3), (5) and (7) and by measuring continuously these values on the model. The process of measuring may be made entirely automatic. For certain known values $L_1' = L_1''$ and $L_2'' = L_2''$, set on the model, we may, by touching the metal alternatively with each electrode, determine values L_{kci} and r_{kci} for every phase by means of the model (Fig. 2); after this, under normal conditions of electrode arcing in all three phases, we may measure p.d.s between leads A-A′, B-B′, C-C′ and the power in every phase of the furnace.

Inductances L_{kci} may be determined by means of the model under normal conditions of electrode arcing on all three phases of the furnace. The method in question is based on a known physical phenomenon, that in continuous arcing the instantaneous current values and arc voltages simultaneously change polarity, passing through zero values. Therefore, observing on Phase 1, say, the moments of passing through the zero value of the arc current and of the voltage between leads A - A of the model (Fig. 2), and adjusting the value of L_{kc1}, so as to obtain the simultaneous passing through zero both of current and voltage, we may find the value of L_{kc1}. Varying the values of currents in the furnace by ± 20 ... 30 per cent, while keeping all three electrodes arcing, or performing the series of experiments discussed above by breaking in turn one of the arcs, we may determine the values of L_1' and L_2' as well.

The values of resistances r_{kci} set up on the model and measured by this method may differ considerably from the true values, but this does not affect the accuracy of measurement of furnace inductances.

Instruments, constructed in the Central Automation Laboratory,* for automatic and manual measuring values of L_{kci}, are based on this principle.

We may investigate the influence of different factors on the parameters of the furnace secondary network by applying the above methods of measurements in various ways: we may feed the furnace by a three-phase and a single-phase current, or keep all electrodes arcing or short-circuit them by keeping them in contact with the metal, or vary currents at symmetrical and asymmetrical loads on phases.

Fig. 4 shows one of the oscillograms of arc voltages e_{1m} and e_{2m}, of Phases 1 and 2; these oscillograms were recorded by using a model installation on a furnace of 20 tons capacity.

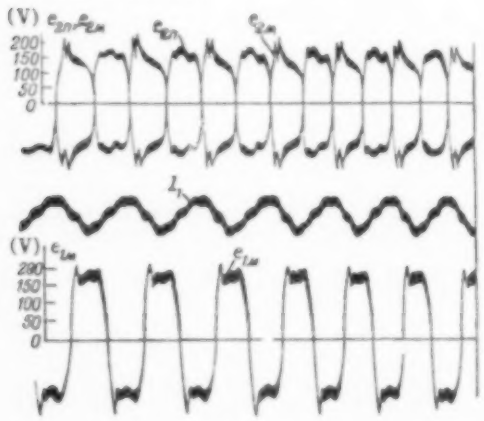

FIG. 4. Oscillograms of arc voltages.

In this figure, the oscillograms of true arc voltages e_{2n} of Phase 2 are shown for comparison; these voltages were directly measured by using two rods, introduced into the furnace: one rod was in contact with the electrode above the arc, the other in contact with the metal near to the arc and slightly below it.

Investigations of an industrial furnace carried out by using a model installation

A series of investigations was carried out by using an experimental specimen of a model installation on an industrial furnace of 20 tons capacity. By

* A.N. Kotikov, B.N. Znamenskii and V.B. Tikhmenev (Engineers of the Central Automation Laboratory) took part in the development of model installations and in carrying out investigations.

these investigations the character of variation of parameters of the furnace secondary network and of the useful power in phases during the melting was first studied; the influence of furnace currents and of the load asymmetry on the values of parameters of the secondary network was also determined, as were several other characteristics.

Some conclusions, which were made on the basis of the results obtained from these experiments, are given below.

(1) A comparison of many arc voltage oscillograms, obtained on the furnace and on the model, confirmed their complete identity, even in the case when disturbances occur in the arc voltage; these are characterized by a very steep slope on the oscillogram. The differences in voltage values were about 1 per cent of the measured value.

(2) During the process of melting and from one charge to another, the phase resistances $r_{kci} - \Delta r_{ei}$ may vary by more than 20 - 30 per cent; this is due to the contact instability, to the redistribution of currents among parallel branches of tubular conductors and so on.

For different phases these quantities, during weeks and months, may differ by more than 30 per cent.

The use of apparatus for the control of these quantities during service will contribute to the study of the causes of increased losses in the furnace secondary networks and will help in averting these losses.

Resistances of the electrode sections situated inside the furnace constitute more than 40 per cent of the total resistance of the secondary network. Thus, the true value of the electric efficiency of furnaces is considerably greater, and the real losses of electrical energy are 40 per cent smaller than those which are usually assumed, when only the total resistance of the secondary is measured.

(3) The difference in inductances of the extreme phases of the secondary network (for 20 ton furnace) usually does not exceed 4 per cent. The inductance of the middle phase of the secondary is smaller than inductances of extreme phase by approximately 30 per cent, and this is the cause of considerable difference in useful power of phases. The variation of the inductance of the section of the secondary, which is situated outside the furnace, $L_{kc1} - \Delta L_{e1}$, does not exceed 10 per cent, when an electrode is moved from its uppermost position into the lowest one; the variation of the value of inductance between one charge and another is of the same order. After the charge is melted, the values of inductances of the electrode portions situated inside the furnace are practically equal for all phases, do not vary with time and represent less than 15 per cent of the mean value of the inductance of the whole installation. Whilst the ferro-magnetic charge is still solid in the furnace, the inductance increases considerably.

(4) Values of the differences between the phase mutual inductances L_1' and L_2' are determined practically only by the influence of sections of the secondary, which are situated outside the furnace; they are approximately equal to 5 - 15 per cent of the mean value of the inductance of a phase. These values vary with time only during

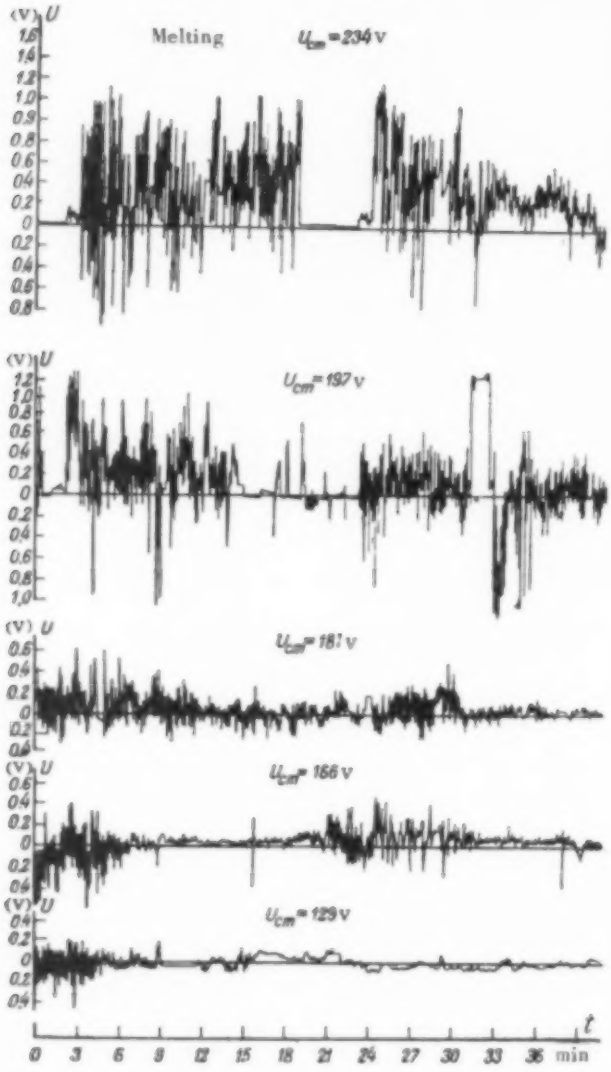

FIG. 5. Variation of voltage drop on the ohmic resistance of a section of the secondary, which is situated outside the furnace during the melting process.

the period when the electrodes are melting the cold charge.

(5) Only the reactance of the middle phase varies considerably with the current, and increases with an increase in current. Asymmetry in electric conditions has only slight influence on the variation in the reactances of a given furnace. Variation of phase resistances, caused by the influence of conditions of contact, is comparable to the influence of current variations and of the load asymmetry between phases.

This fact prevented an exact determination of the influence of each one of these factors.

(6) A d.c. component is present in the arc current; this component may be equal to 15 - 30 per cent of the current during the period of melting, while arcing occurs between an electrode and solid metal. The character of variation of currents during the process of melting is shown in Fig. 5. Directions and values of direct currents in the arc often vary.

The appearance of these currents is due to rectifier action of the arc [4, 5] and to the difference in the d.c. voltage components in arcs of different phases.

Fig. 6 shows the data which characterizes the real electric parameters of the work of an arc furnace of 20 tons capacity; these data were recorded during ten meltings at the higher value of the voltage (236 V).

For every melting, r.m.s values of the phase currents I_i, mean values of the furnace useful power ΣP_u, mean values of useful phase power P_{ui} and average values of the installation power factor cos ϕ are given.

Results of these investigations and of similar investigations carried out during meltings in another furnace of 20 tons capacity allow us to draw the following conclusions.

During melting the difference between mean values of phase useful power may exceed 20 per cent. This difference is still greater for various intervals of melting periods. Slightly small differences are observed during the process of metal refining. The results of this are: non-uniform rate of metal melting, delay in melting, the increase in energy consumption and non-uniform heating of the surface of the molten metal.

The mean value of the total useful phase power may vary from one charge to another by more than 10 per cent; this is due to different factors; delays in melting, increase in energy consumption because of electric conditions in the furnace, which differ from optimum conditions, and also because of abnormal melting conditions, which bring about the deterioration in the quality of the metal.

From one melting to another, power factors and electric efficiencies may vary within the limits 0.01 - 0.03.

Conclusions

1. The model installations, designed for non-sinusoidal currents and for electromagnetic transmissions of power from one phase to another, enable manual or automatic remote control of parameters in conductors carrying heavy currents, of voltages on arcs of useful powers in every phase of the installation.

2. During the normal work of installation, automatic and continuous control is possible of the following quantities: resistances and inductances of the low-voltage conductors, situated outside the furnace, total inductance of conductors, arc voltage and useful electric power. It is possible to control automatically conductor resist-

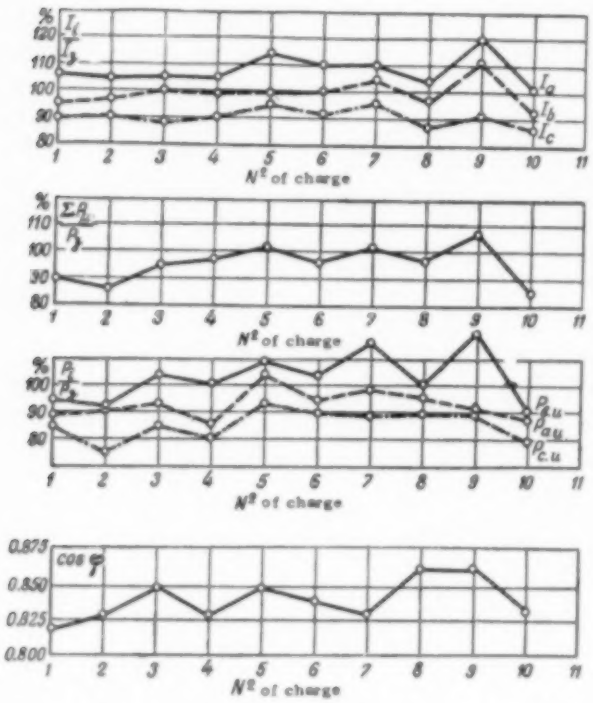

FIG. 6. Mean values for a period of melting of electric parameters in a furnace, recorded for ten charges; I_a, I_b and I_c are phase currents, P_{au}, P_{bu}, P_{cu} are useful phase powers, ΣP_u total useful electric power consumed by a furnace.

ances in each phase and the differences of coefficients of the phase mutual induction.

3. Experimental investigations carried out by using model installations show that there are considerable possibilities for decreasing electric losses and specific consumption of electric energy and for increasing power factors of arc furnaces, which are big consumers of electric energy.

The use of the installations described above offers prospects for the application of new methods of control of the useful power of the installation by computers [1].

4. The application of model installations may prove useful for the measurement of parameters of industrial sets and the control of technological processes which cannot be directly controlled.

Translated by S. Szymanski

REFERENCES

1. Yu. E. Efroimovich; *Kompleksnaia mekhanizatsiia i avtomatizatsiia protsessa vyplavki stali v dugovykh pechakh. Doklad na Vsesoiuznom soveshchanii po avtomatizatsii proizvodstvennykh protsessow (Complex mechanization and automation of processes of steel melting in arc furnaces. Report read at the All-Union Conference on automation of production processes)*, Metallurgizdat (1956).
2. *Avtomatizatsiia proizvodstvennykh protsessov, gl. IV. Elektrostaleplavilnye dugovye pechi. (Automation of production processes, Ch. IV. Electric arc furnaces for steel melting)*, Akademizdat (1956).
3. Iu.E. Efroimovich; *Elektrichestvo*, No. 1 (1951).
4. V.N. Nikolskii; *Elektrichestvo*, No. 11 (1951).
5. Iu.E. Efroimovich; *Elektrichestvo*, No. 3 (1954).

1959

TURBO-GENERATORS OF 30 TO 300 MW POWER BUILT BY KhETZ FACTORY *

L. Ia. STANISLAVSKII

Khar'khov Electrical Equipment Diesel Works

(Received 26 July 1957)

The production of turbo-generators in Khar'khov began in 1936 in the turbo-generator factory, (Khar'khov Turbo-generator Plant), built during the second five-year plan. During these years, the problem of organizing the production of turbo-generators of 50 MW at 1500 rev/min has been solved. In this factory, not only the problem of the output of these machines, which were unique at the time, was solved, but also in 1938 the first four-pole turbo-generator of 100 MW power was made in the Soviet Union; its rotor, weighing 100 tons, consisted of three parts [1]. In this factory, reconstructed after the war, a turbo-generator mark TGV-25, of 25 MW power and 3000 rev/min, was designed and production began.

In 1954 the production of turbo-generators was transferred to the Khar'khov factory of Dieselelectrical equipment, where the biggest generator unit in the world at that time was installed and fitted with first class nationally-made equipment. The production of large hydro-generators was also organized in these works.

In this article, the main topic is the description of new powerful turbo-generators with direct hydrogen cooling of the stator and rotor windings; a short account is also given of experience in building and using an experimental turbo-generator of 25-30 MW power.

In designing the construction of the turbo-generator mark TGV-25, of 25-30 MW at 3000 rev/min (Fig. 1) with hydrogen cooling at 0.04 a.t.g. (a.t.g = atmosphere gauge pressure) the following problems were posed. It was necessary to ensure the performance and service characteristics, required by G.O.S.T. standards; furthermore, an attempt was made to introduce several new constructive solutions, which might be useful in construction of turbo-generators of much greater power.

For the first time in the U.S.S.R. and to a certain extent for the first time in the world, welded stator shields with built-in bearings were used in this

* *Electrichestvo*, No. 3, 27-32, 1958.

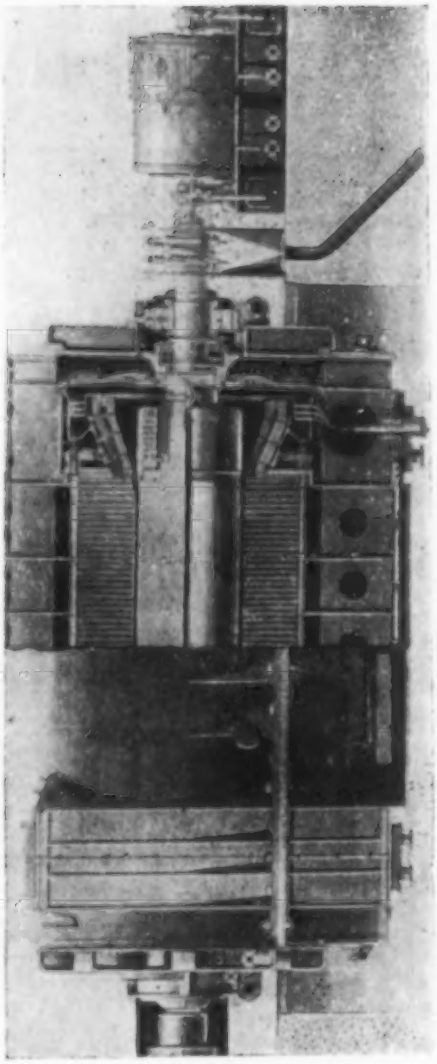

FIG. 1. Turbo-generator mark TGV-25, 25-30 MW, 6.3/10.5 kV, 3000 rev/min.

generator, as well as disk seals with small oil consumption and propeller ventilators. The vertical disposition of coolers and bracket fixing of retaining rotor rings was used. Moreover, at the author's suggestion, the stator cores and windings were produced in repetitive manufacture, and the stator winding was made for voltages of 6.3 and 10.5 kV by using a delta or star-connexion. The use of disk seals dispenses with a cumbersome and complicated vacuum purification of oil.

At present, since a large number of such generators has been made, and a considerable number of them has been in service for some years, we may draw certain conclusions.

Some apprehension, which was expressed concerning the ability of a generator with shield bearings to withstand vibration, did not materialize.

The results of measurements of double amplitudes of vibrations are given below; these vibrations were recorded on the covers of bearings built in the end shields of the generator type TGV-25. These measurements were taken on 50 turbo-generators, working on load and in normal service conditions. On 19 machines out of the total number, vibrations were measured in the transverse, vertical and axial directions; on the remaining machines only transverse vibrations were recorded.

No. of turbo-generators	Maximum double amplitude of vibrations (mm)
32	0.02
7	0.03
5	0.04
4	0.05
1	0.06
1	0.09*

* The generator was coupled to a foreign-made turbine, the critical speed of rotation of which was unknown.

The data show that the vibrations of turbo-generators are insignificant. In practice, the axial vibrations of the bearing from the exciter side are entirely eliminated, these vibrations being extremely undesirable, but unfortunately a common phenomenon in machines with the pedestal (external) bearings.

The experiment of making and using a turbo-generator mark TGV-25 gave an opportunity for improving the shield construction and for increasing the reliability of the electrical insulation of the shaft by protecting it from currents in the bearings; easier access in the assembly of stuffing boxes was achieved as well.

A disk seal permits the sealing of the rotor shaft, with the oil consumption inside the stator casing not exceeding 1 litre per minute. For this rate of consumption no necessity arises for separating oil from hydrogen.

The vertical arrangement of coolers is the most convenient with respect to conditions of assembly, working and inspection. The suppression of vibrations of the tubes of the cooler is achieved by fixing these tubes in appropriate places.

Because of this the vibrations of tubes decreased from 2 to 0.02 mm.

The use of propeller ventilators proved to be entirely justified; moreover, their cost was considerably reduced due to production by drop forging. Bracket fixing of retaining rings of the rotor prevents the breaking of the teeth of the rotor body or the wearing down of the places of setting, which happens, for instance, when a split set binding ring or elastic centring rings are used.

More than half the machines of mark TGV-25 already made are delta-connected. No extra overheating or other losses were recorded. The advantage of repetitive manufacture of stator cores and windings is obvious.

In 1956 the production of turbo-generators mark TVS-30, of 30 MW power at 3000 rev/min [2] began. In the design of this generator, the main problem was the creation of a unified machine based on the construction of turbo-generators marks TGV-25, TV2-30-2 and T2-25-2 produced in the Soviet Union. In this generator, all valuable improvements made in the generator TGV-25 were applied. The hydrogen pressure is 0.05 - 0.5 a.t.g. No doubt the hydrogen pressure will be raised in future up to 1 a.t.g., thus increasing the power of the generator by 10 - 15 per cent.

The generator mark TVS-30 is made with couplings of unified dimensions, so that it can be directly coupled with turbines, made in all turbine-making factories of the Soviet Union. The systems of oil distribution, of protection and of the generator voltage regulation are all standardized; a silicone insulation is used for the rotor winding; for insulating the retaining rings the compressed glass fabric is used, the aluminium saddles in the front part being absent.

1959

Due to difficulties encountered during the first period of service of generators of mark TGV-25, external bearings (on the outside pedestals) are used in generators TVS-30, this being, in the author's opinion, their disadvantage.

In the design of turbo-generators of 200-300 MW power the basic trends which appear in the development of the construction of generators were taken into account.

One of the most important problems in the construction of high power generators, while keeping their size within reasonable limits, is the increase of the hydrogen pressure inside the machine. On the basis of the tests carried out by the factory for turbo-generators mark TGV-25 [2], it was found that, by increasing the gas pressure from 0.05 to 0.5 a.t.g. and keeping the load constant, the rise in temperature of the generator is decreased in the ratio of 1.5 to 1, and by increasing the pressure up to 1 a.t.g. the corresponding decrease is more than two to one, i.e. instead of 32.6°C it becomes only 15° (taking into account the lowering of losses in the generator windings due to the drop in their temperature). Table 1 shows the results of the measurements of the temperature rise of generator windings as different hydrogen pressures.

For high-power generators the pressure of the cooling gas was fixed at 3a.t.g.

TABLE 1.

Hydrogen pressure (a.t.g.)	Temperature rise (°C)	
	Rotor winding	Stator winding
0.05	94.6	60.3
0.5	80.7	40.3
0.75	75.1	37.5
1.0	71.5	34.8

The values of the power, developed by a 200 MW generator in relation to the hydrogen pressure, are shown below:

Hydrogen pressure (a.t.g.)	Power of the generator (MW)
0.5	100
1	140
2	170
3	200

Nevertheless, by solely increasing the hydrogen pressure the problem of the construction of high-power generators cannot be solved. In the rotor windings and in the stator bars of ordinary design, the temperature distribution at the hydrogen atmospheric pressure is such, that 50-60 per cent of the temperature drop occurs in the insulation. The remaining part occurs in gaps, the surface gas layer and the steel of teeth, their thermal conductivity considerably increasing with the increases of the hydrogen pressure.

The thermal conductivity of the insulation, however, does not increase with increasing hydrogen pressure; therefore the use of external cooling does not permit an increase in the power of the generator by more than 30 per cent.

The use of direct internal cooling of the rotor and stator copper, permits the construction of the 200 MW generator (Fig. 2) of smaller dimensions than those of the turbo-generator TV2-150-2 of 150 MW.

This is due to the fact that direct cooling permits a more efficient use of the active materials of the machine. At present the next outstanding problem is the beginning of repetitive manufacture of turbo-generators, with direct cooling of the stator and rotor windings. This will result in an economy of up to 50 per cent in the materials required at present, and by slightly increasing the number of the working hours needed for production, the productive capacity of the turbo-generators factories will be nearly doubled, and the capital expenditure in building electric plants will be considerably lowered.

With metallurgy at the standard it is today, it is possible to make a rotor of 1,100 mm diameter and a body length of 6,500 mm for a generator rotating at a speed of 3000 rev/min. For this case, the limiting values of the power developed by generators with different methods of cooling are as follows:

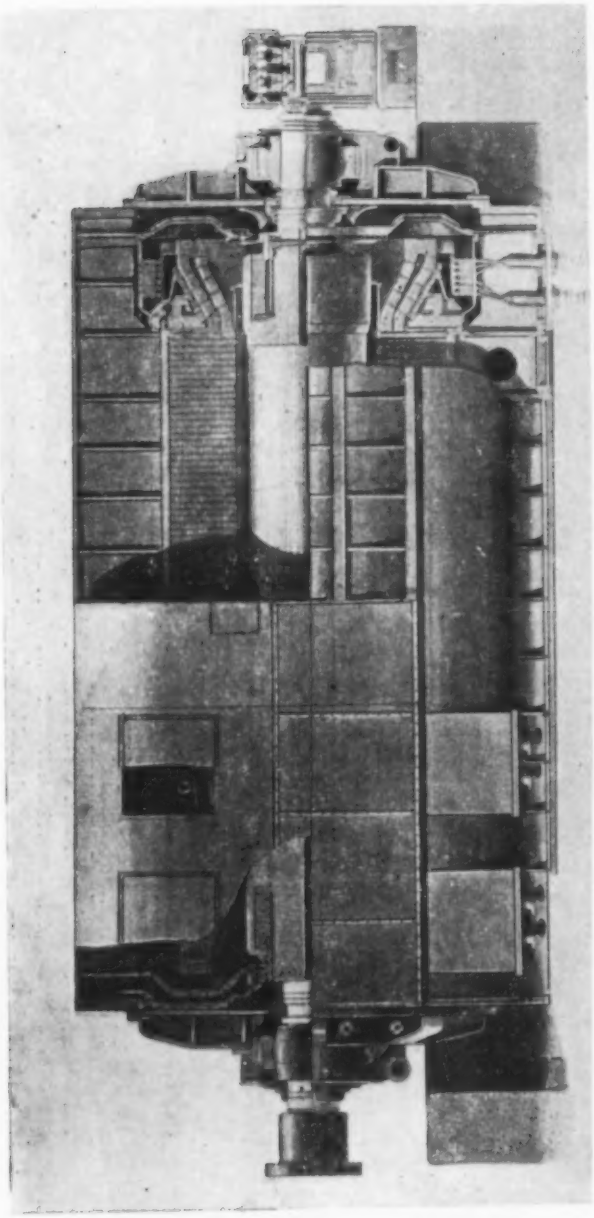

FIG. 2. Turbo-generator mark TGV-200, 200 MW, 15.75 kV, 3000 rev/min.

1959

Method of cooling	Power (MW)
Air cooling	140
Surface hydrogen cooling at the gas pressure 0.03 a.t.g.	210
Surface hydrogen at the gas pressure 3 a.t.g.	270
Internal hydrogen cooling at the gas pressure 3 a.t.g.	350-400

The considerable increase in power of generators with direct hydrogen cooling is possible due to the fact that the internal cooling of the rotor and stator windings permits a considerable increase of the current density in the windings. For comparison, in Table 2 the values of current densities are given for generators of different marks.

TABLE 2.

Generator mark	Nominal power (MW)	Nominal voltage (kV)	Current density (A/mm²)	
			Stator	Rotor
TGV-25	30	10.5	3.53	3.88
TV2-30-2	30	10.5	3.53	3.88
TV2-50-2	50	10.5	3.17	3.36
TV2-100-2	100	13.8	2.80	3.40
TV2-150-2	150	18.0	2.50	3.50
TGV-200	200	15.75	3.17	7.06

In the turbo-generator TGV-200 an axial-radial system of ventilation is used. A centrifugal pressure compressor, situated at the slip ring end of the rotor, delivers the gas at 3 a.t.g. into the hollow rotor windings and into the ventilating tubes situated in the stator windings. The hydrogen stream leaving the compressor is divided into three parts: one part flows into the ventilating tubes of the stator bar winding, the second part under the retaining ring from the side of rotor slip rings and further into the hollow rotor conductors, the third part also enters the hollow rotor conductors from the turbine side.

The gas, leaving the ventilating tubes of the stator bars, enters the axial ventilator, situated on the turbine side. The gas, which entered the gaps after leaving the hollow rotor conductors and hollow stator cores, comes into the same ventilator. The axial ventilator sends the hydrogen into a gas cooler; on leaving this cooler a part of the hydrogen stream cools the stator core and the stator and rotor surfaces, after which it passes into the gap and enters the axial ventilator. The second part of the gas stream comes into the centrifugal compressor.

The ventilating channels of the bar winding are made in the form of thin-walled non-magnetic steel tubes situated between the two rows of glass-insulated conductors. Investigations have shown that the temperature drop in the 0.3 mm thick insulation of such a bar is only 3°C, a rather small value.

At a gas speed in the bar channels of more than 30m/sec, the temperature drop between the channel walls and the gas is equal to 3°C. Thus the excess of the temperature of the stator copper winding over the gas temperature is only 6°C, hence the temperature of the copper depends mainly on the gas temperature.

The ventilating ducts of the rotor winding are formed by two conductors of channel sections. The investigations on the temperature distribution and on the flow of the gas in the ducts for internal cooling, which were carried out by ourselves together with the Scientific and Research Institute of the Electrical Industry and with the Chair of Blade Machines and Applied Gas Dynamics of the Khar'khov Aviation Institute, gave a result for the optimum cross-section of the windings and of their ventilating channels [3].

The shaft seals are the most important constructional details of a modern turbo-generator.

The study of the performance of these seals, which was carried out by this factory for many years, showed that a properly designed seal of the disk type may work safely at pressures up to 3 a.t.g. and more. The method of decreasing the load, carried by the packing of stuffing boxes which was designed by this factory, is very important, since it allows for a sharp decrease in overheating of the boxes and in the losses in packing.

Table 3 shows the experimental data of the work of one of these stuffing boxes.

TABLE 3.

Gas pressure in the chamber (kg/cm^2)	Oil pressure at the stuffing box inlet (kg/cm^2)	Oil temperature at the stuffing box inlet (°C)	Babbit temperature in the stuffing box (°C)	Oil consumption by the stuffing box (l/min)	
				Inside the stator body	On the outer side of the box
00	0.2	38	51	0.14	36
0.05	0.4	36	50	0141	36
0.5	0.9	35	49	0.64	38
1.0	1.4	36	48.5	0.43	46.5
2.0	2.4	36	47.0	0.21	53
3.0	3.4	36	46.5	0.15	58.5
3.0	3.6	36	46.0	0.5	62.5
3.0	3.8	36	44	1.9	72.0

The turbo-generators made by the factory have built-in bearings in the end shields; these bearings have many advantages in comparison with the external bearings.

This arrangement permits a large decrease in the distance between the centre lines of bearings; for example, in 200 MW turbo-generators this distance is cut by nearly 800 mm. In consequence the static sag of the rotor is considerably reduced, and this increases the critical speed of rotation. This reduction is very desirable, since both in the world at large and in home practice some cases of fracture of rotors of big generators are known. These accidents were caused by excessive sags, the second critical speed of rotation being smaller than the normal working speed.

The use of built-in shield bearings for turbo-generators weighing up to 250 tons

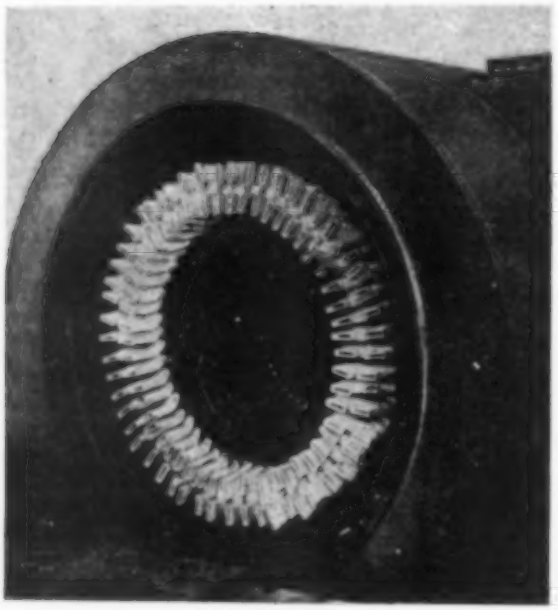

FIG. 3. Silicon rubber caps for the inlet and outlet of the cooling gas.

permits their transport in a completely assembled form (together with the rotor), and this fact permits assembling and sealing of the generator in the factory, thus shortening the time required for assembly 4-5 times.

By using built-in shield bearings we reduce the weight of a turbo-generator and its size, the amount of vibration and the resistance of bearings as well. Difficulties connected with the unavoidable axial vibrations of bearings situated on the exciter side disappear when these vibrations occur with the majority of big generators with external bearings.

The use of built-in shield bearings makes the accurate machining and assembling of the generator much easier, due to the presence of centring grooves in the shield and cover, in bushes and stuffing boxes; it also ensures a complete interchangeability of parts. The construction of front shields with built-in bearing bushes permits the examination of bushes without letting out hydrogen and examination of packing without dismantling the bearing. Shield bearings permit the examination of frontal parts without dismantling the bearings; for this purpose only the upper part of the shield is removed. By the use of "biscuits" for the insulation of the bush covers the suppression of currents in bearings is greatly simplified.

The turbo-generator of 200 MW power has the following nominal characteristics: voltage 15.75 kV, current 8.63 kV, the power factor $\cos \phi = 0.85$, 3000 rev/min.

For the same power factor for the 300 MW turbo-generators the stator winding voltage is taken as 20 kV. In both cases these generators have single-coil windings, thus permitting their use at 10 kV. The field winding of the generators, according to the design, will be fed from the generator terminals through gas rectifiers. The welded, gas-tight frame of the stator is calculated on the basis of long use at a gas pressure inside the stator of 3 a.t.g. The test pressure is 10 a.t.g. Two vertical gas coolers are situated at the side of the turbine. The stator core together with the winding is elastically attached to the stator body by means of flat springs, and this excludes the possibility of transmitting vibrations of double frequency to the stator body.

The stator winding is of the bar, basket type.

The inlet and outlet of the cooling gas into the ventilating tubes is made in the bar heads through the silicon-rubber caps (Fig. 3). For the bar insulation silicon plastic is used, a heat-resisting insulation of increased mechanical strength devised jointly with the All-Union Lenin Institute of Electrical Technology.

Bars with new insulation have been used in the stator of an experimental turbo-generator. Preliminary tests have shown that, so far as electrical strength and tangent of the loss angle are concerned, the new insulation is not inferior to the compound one and has a greater mechanical strength. There are, however, still some difficulties in the repetitive production of these windings.

1959

For the rotor winding, copper is used with the addition of some silver. This increases the mechanical strength of the copper, which is essential for securing reliable working of the rotor. In the system of ventilation adopted, teeth and slots of the rotors have no holes.

The rotor of the 200 MW turbo-generator is of smaller dimensions than the rotor of the 150 MW generator mark TV2-150-2, due to internal cooling of windings.

To solve a series of problems connected with the design and production of 200 and 300 MW turbo-generators, an experimental turbo-generator of 30 MW power was made. In the stator and rotor of this generator about 200 resistance thermometers, thermistors, tensometers and thermocouples were inserted, and valuable results were obtained.

Some parameters of the 200 MW turbo-generator mark TGV-200 are shown below.

Efficiency	98.87
Short circuit ratio	0.58
Subtransient reactance (%)	19
Transient reactance (%)	29.5
Synchronous reactance (%)	203.5
Mean temperature rise of the stator winding (°C)	38
Mean temperature rise of the rotor winding (°C)	38
Distance between bearings (mm)	8200
First critical speed of rotation (rev/min)	1340

Second critical speed of rotation (rev/min)	4380
Specific copper consumption (kg/kVA)	0.076
Specific active steel consumption (kg/kVA)	0.436
Total weight of the generator (tons)	287

Translated by S. Szymanski

REFERENCES

1. L. Ia. Stanislavskii; 100,000 Turbo-generator Khar'khov S.M. Kirova Turbo-generator Plant,*Vestnik elek. prom.*, No. 5 (1941).

2. L.Ia. Stanislavskii, Seriinyi turbo-generator s vodorodnym okhlazhdeniem tipa TVS-30 (Series-produced turbo-generator with hydrogen cooling, mark TVS-30) *Vestnik elek. prom.*, No. 2 (1956).

3. Raspredelenie temperatury i technik okhlazhdaiushchei sredy v provodnikakh vnutrennego okhlazhdenia.(Temperature distribution and flow of the cooling medium in a conductor with internal cooling) *Trud. Khar'khovskogo aviatsionnogo inst.* No. 2 (1957).

ON THE POSSIBILITY OF INTENSIFICATION OF COOLING OF TURBO-GENERATORS

V.G. FASTOVSKII and IU.V. PETROVSKII

Lenin All-Union Institute of Electrical Technology

(Received 1 April 1957)

The dimensions of modern turbo-generators, of 150-200 MW power with hydrogen cooling of the surface, reach limiting values (rotor diameter 1.10-1.15 m, rotor length 6.3 m), determined by the permissible stresses in the rotor material and by conditions, occuring when the machine passes through the critical speed of rotation at the start. It is well known that an increase in power of a turbo-generator, its dimensions being unchanged, is possible only by an intensification of the process of heat dissipation, the amount of heat developed increasing with the increase of current density in the machine windings.

In view of this fact, it follows that it is desirable to consider briefly some problems connected with methods of intensification of cooling of turbo-generators. Let us remember that the first important step in this direction was the use of hydrogen cooling, which permitted a decrease in the overheating of active parts of a machine and a reduction in the friction and windage losses in the rotor.

With surface cooling of the rotor, the increase of hydrogen pressure reduces the temperature difference between the rotor surface and the gas stream, this lowering constituting 17-22 per cent of the total temperature drop. In the limiting case, this permits an increase in the power of a turbo-generator by 20-25 per cent.

The system of internal hydrogen cooling of the active copper of the rotor and stator windings makes possible a considerable increase in power. Furthermore, the increase of hydrogen pressure is a very efficient method for the intensification of cooling, since the coefficient of thermal conductivity at a constant gas speed varies proportionally to $p^{0.8}$ (p is the gas pressure in abs atm). The permissible current density increases accordingly, and with it the power of a turbo-generator.

The problem of maximum output of a turbo-generator, with internal copper

* *Elektrichestvo*, No. 3, 32-35, 1958.

cooling, is of considerable interest. Calculations show that, at a hydrogen pressure of 5 abs atm and a speed in the channels of the excitation winding (where the major quantity of heat is developed) of the order of 80 m/sec, the coefficient of thermal conductivity from the copper surface to the gas is equal approximately to 1200 k cal/m²hr°C. At a current density of 10 A/mm² the increase of hydrogen temperature is about 31°C. For the hydrogen temperature at the channel inlet of 40°C, the maximum copper temperature is 85°C, which is considerably lower than the permissible temperature of 120°C. Under such conditions, which can certainly be realized, the power of a turbo-generator increases up to 350-400 MVA [1].

The actual importance of the problem of cooling gave rise to a series of new propositions for intensification of the process of internal cooling of excitation windings. Thus, evaporation cooling, based on the principle of using the latent heat of a volatile liquid, pumped directly into the channels of the excitation winding, is of considerable interest. With this method the rotor will rotate in the vapour of the cooling liquid, since a perfect sealing of the circulating system is rather difficult. To reduce the windage losses inside the body of a turbo-generator it is necessary to maintain a vacuum. For this purpose a powerful vacuum pump and surface condenser, to liquify the vapour and to return the liquid into the circulating system, will be needed. The liquid must have many specific properties: dielectric strength, large latent heat, a convenient boiling point, chemical inertness, non-inflammability etc. To find such a liquid, especially for cooling of the stator winding, is a difficult problem, and the cooling system becomes complicated.

The use of a liquid (for example of transformer oil) was also suggested for cooling the rotor; such a liquid must be a good dielectric and must not destroy the insulation, since hermetic sealing of the circulating system is impossible in practice, and a part of the liquid penetrates into the gap between the rotor and the stator. But in this case there is a danger of destroying the stator surface opposite the rotor, by the oil drops projected at a great speed from the rotating rotor.

Another suggestion was to use the so-called convection-evaporation cooling, which consists in injecting the liquid into the circulating hydrogen.

The result of the evaporation of the liquid is a drop in the hydrogen temperature, consequently the temperature difference between the copper to be cooled and hydrogen increases, thus increasing the process of heat dissipation. The condensation of the vapour of the liquid takes place at the surfaces of the gas coolers, from where the condensed liquid returns into the circulating system.

Obviously, we cannot expect a considerable increase in the rate of cooling from such a system since only a small proportion of the liquid will evaporate from the surface to be cooled.

The liquid cooling of a rotor is a complicated technical problem, the satisfactory solution of which would permit a considerable increase of the limiting power of turbo-generators, while keeping their dimensions unchanged.

Calculations show that particularly favourable conditions of heat dissipation can be achieved by using water for cooling of the rotor.

Liquid cooling of the stator is easier to solve and in this case the distilled water is very efficient; but during the process of circulation, the electric conductivity of water increases. By introducing into the circulation system an ion-exchange apparatus, it is possible to keep water resistivity at the level of 10^6 – 10^7 Ω cm [2].

The most serious attention should be paid to the technical design of water cooling systems for turbo-generators. Recently articles have appeared concerning the realization of the water cooling system of the stator winding of a turbo-generator at 11.8 kV [3].

Using a liquid system for cooling, power losses due to the circulating of the cooling agent are greatly reduced. Thus, for oil cooling of the stator winding of a 500 MW turbo-generator, in which the losses are approximately equal to 1.2 MW, a pump, driven by a 10 kW motor, will be required. The power needed for ventilation with hydrogen cooling is of the order of hundreds of kW.

Let us consider in greater detail the problem of the usefulness of forced hydrogen cooling [4].

If the temperature of the hydrogen after passing the water coolers is taken to be equal to 40°C under normal conditions, its temperature may be reduced considerably by the use of artificial cooling. In this case, however, it must be borne in mind that the power of the cooling devices increases rapidly as the cooling temperature is reduced.

The forced hydrogen cooling may be used to achieve one of two objects:
1. while keeping the dimensions of the active parts of a generator unchanged, to increase its output; in this case, the conditions of work of copper remain unchanged as regards temperature; the copper temperature remains at the previous limiting level, but heat dissipation increases due mainly to an increase in the temperature difference between copper and hydrogen;
2. while keeping the dimensions of the active parts of a turbo-generator and its power unchanged, to increase the efficiency of the machine by decreasing the copper temperature, which in turn decreases the copper resistivity; the advantage of this solution depends upon the relation between the decrease of losses in the windings and the power required for forced cooling.

The first problem is of greater interest. As an example, let us analyse the cooling conditions of a 200 MW generator. We assume that the hydrogen temperature at the inlet is 0°C; let the increase of the gas temperature be 40°C. The total losses of such a machine are estimated at 1.77 per cent of its nominal power [1], i.e. 3540 kW. Excluding losses in bearings (0.2 per cent), we find that the losses, to be dissipated by hydrogen, are 3240 kW, or in thermal units 2.7×10^6 kcal/h. – Assuming that the gas pressure inside the machine is equal to 4 abs atm and taking the specific heat of hydrogen, at the mean temperature of 20°C,

as equal to 3.4 kcal/kg °C, we find the total weight of the circulating hydrogen to be approximately equal to 20 t/hr, or 6 x 10^4 m³/hr. We have to design the ventilators for this output.

If the rotor winding has ventilating channels of rectangular cross-section, then the value I of the current in the winding conductors exceeds the value I_0 of the current in the conductor of the full section [1] by the ratio:

$$\frac{I}{I_0} = 12\alpha^{1/2}, \tag{1}$$

where α is the coefficient of thermal conductivity (W/cm². °C).

For the forced cooling of hydrogen the temperature difference between copper and hydrogen increases; for the same pressure and gas speed in channels, the value of the coefficient of thermal conductivity varies only slightly. Therefore, equation (1) may be written in such a form as

$$\frac{I}{I_0} = 12\left(\alpha \frac{\theta}{\theta'}\right)^{1/2}, \tag{2}$$

where θ is the temperature difference for the forced cooling of hydrogen, and θ' the temperature difference for the water cooling of hydrogen. Assuming the copper temperature is equal to 120°C, then θ = 100°C and θ' = 60°C. In this case

$$\frac{I}{I_0} \approx 15.5\alpha^{1/2}. \tag{3}$$

Thus, for the chosen set of parameters, the ratio I/I_0 increases approximately by 30 per cent.

By substituting external cooling of the rotor by internal cooling of the excitation winding, at the increased hydrogen pressure, we may increase the m.m.f of the excitation 2-3 times. In the case of forced cooling of hydrogen up to 0°C, we may further increase the m.m.f. of the excitation winding 2.5-4 times in comparison with its value, when the rotor slots remain without cooling.

Let us now consider the second problem – reducing the copper losses by decreasing the copper temperature. As a first approximation we may assume that the decrease of the mean hydrogen temperature by 40°C will bring about the same decrease of the copper temperature. Using the well-known relationship between the resistivity of copper and its temperature, it is easy to show that the decrease of the temperature by 40°C results in a decrease of copper losses by 17 per cent, thus increasing the effective power of a generator by 220 kW (the total copper losses in this machine are estimated at 1270 kW). It is quite obvious that the power required to drive the cooling system will be greater than the economy achieved.

Let us consider possible methods for the forced cooling of hydrogen up to 0°C: the use of a liquid evaporation and cooling installation with a compressor, an absorption cooling installation and a turbo-exhaust pump.

In a compressor cooling installation, working in vapour cycle, evaporation of the cooling agent takes place at a constant temperature and pressure. To cool hydrogen up to 0°C, the temperature of evaporation of the cooling medium should not exceed – 5°C, since, for smaller difference of temperature, the dimensions of gas coolers increase considerably.

Let us consider an installation working on freon-12 at an evaporation temperature 5.5°C, a pressure in the evaporator of 267 abs atm, a temperature of condensation 30°C, and a pressure in the condenser of 7.6 abs atm. For such an installation the effective specific cooling capacity is 37200 kcal/k Whr [5].

For the amount of heat to be dissipated, which we assumed above to be equal to 2.7×10^6 kcal/hr, the power of the cooling installation will be

$$P = \frac{2.7 \cdot 10^6}{3720} = 730 \text{ kW}.$$

This corresponds to a decrease in the efficiency of the turbo-generator of 0.4 per cent.

Taking into account the greater cooling capacity of a freon installation, it is advisable to use a turbo-compressor set.

Russian industry does not at present produce a cooling installation of this power but, according to published data [5], a turbo-compressor set of the cooling capacity 2.5×10^6 kcal/hr occupies an area 7-9 m², and the weight of the turbo-compressor is 4-7 tons. In the conditions of power stators driven by heat engines, where powerful turbo-generators are usually installed, we may use an absorption cooling system working on the exhaust steam at a pressure of 1.5-2.5 abs atm. Assuming that the amount of heat to be dispersed is equal (as above) to 2.7×10^6 kcal/hr, we find that the heat consumption in the absorption cooling installation, working in the water ammonia cycle, will be 5.3×10^6 kcal/hr, which corresponds to a steam consumption of 10 tons/hr [6].

This steam consumption at a pressure of 2.5 abs atm is equivalent to 1060 kW of power, if the steam condenses at a pressure of 0.04 abs atm, as happens in turbine condensers; the turbine efficiency is assumed to be 0.8, the generator efficiency 0.98 and the mechanical efficiency 0.98.

It is also necessary to take into account that the power of the circulating pump is about 100 kW.

The consumption of the cooling water is estimated at 515 m³/hr, i.e. approximately the same as the water consumption in the turbine compressor set.

From the above consideration it follows that from the point of view of power economy, the absorption cooling installation has no advantage whatsoever in

comparison with a compressor installation. The absence of machine equipment may be considered a certain advantage in the absorption installation (there is only one small circulating pump of rather small dimensions). The size of the absorption cooling installation is much bigger than the size of the compressor installation.

The lowering of the hydrogen temperature may be achieved by its expansion in a turbo-exhaust pump, after a preliminary compression. Let us assume that the hydrogen pressure inside the turbo-generator is 4 abs atm and the temperature of the compressed gas at the outlet of the cooler, situated after the turbo-compressor, is 30°C. In order that the hydrogen temperature be lowered to 0°C after expansion in the turbo-exhaust pump, the gas should be compressed to 6 abs atm, if the efficiency of the turbo-exhaust pump is 0.8.

The energy required to compress 1 kg of hydrogen from 4 abs atm to 6 abs atm is equal to 0.209 kWhr. Since, for the heat dissipation of a 200 MW generator, the total amount of hydrogen required is 20 tons/hr, then the total power required for the compression of hydrogen will be 4180 kW. It is necessary to point out that part of the work, performed by the gas expanding in the turbo-exhaust pump, may be usefully employed, but the amount so recovered does not exceed 10 to 12 per cent of the work spent in compressing the gas. Thus, the power required for the cooling of hydrogen in the turbo-exhaust pump will be 3700 kW, i.e. 5 times more than the power required to drive a compressor cooling installation. Moreover, the production of such a cooling system would require additional complicated equipment: a turbo-compressor to compress the hydrogen, coolers for the compressed gas and a turbo-exhaust pump for its expansion.

From the above discussion it follows that the development and realization of liquid cooling, first of the stator winding, and then of the rotor, offers the best prospects for increasing the power of a turbo-generator while keeping its dimensions unchanged.

The forced cooling of hydrogen by cooling installations does not produce the desired effect because of the great expense of running the installation and the necessary capital investment. It may prove advantageous in particular cases, for instance, when a considerable quantity of low temperature exhaust heat is available and when this heat may be used in an absorption installation.

Translated by S. Szymanski

REFERENCES

1. E.G. Kumar; *Voprosy proektirovaniia turbogeneratov (Problems concerning the design of turbo-generators)*, Gosenergoizdat (1955).
2. G.P. Monet; *Chemical Engineering Progress*, 52, No. 7, 299-302 (1956).
3. Water-cooled alternator windings. Successful system developed by Metropolitan-Vickers *Elect. Engng.*, 159, No. 24, 1089-1090 (1956).
4. Itogi raboty sektsii elektricheskikh mashin Tekhnicheskogo soveta MEP za 1955g

(Summary of the works of the section of electric machines of the Technical Council of MEP in 1955), *VEP*, No. 3, 76-78 (1956).

5. L.I. Rozenfeld and A.G. Tkachev; Kholodilnye mashiny i apparaty (Cooling machines and apparatus), Gostorgizdat, 426, 177-178 (1955).
6. Kaltetechnik, 8, No. 8, 1956, Arbeitsblatt.

1959

ON THE SURFACE RESISTANCE OF DIELECTRICS*

A.P. GEPPE

Moscow Power Institute

(Received 4 July 1957)

Although the specific surface resistance ρ_s is one of the five fundamental characteristic electrical properties of dielectrics along with ϵ, ρ_v, $\tan\delta$ and E_{b1}, it is not yet however fully characterized and the term "surface conductance" is not clearly defined.

The term "surface conductance" usually means the electric conductance of the surface layer of a substance, but the thickness of this layer remains undetermined in those cases where the dielectric is covered by a film of increased conductance. Consequently, the physical meaning of the surface conductance $\gamma_s = 1/\rho_s$ is not sufficiently clear. The fundamental equation, relating the value of the surface resistance R_s to the geometrical dimensions of a specimen (the length of electrodes l and the distance between them b)

$$R_s = \rho_s \frac{b}{l} \tag{1}$$

is often applied without sufficient physical foundation. For instance, on the basis of this equation the following definition is deduced: "The surface resistivity is numerically equal to the resistance of a square (of arbitrary dimensions), imagined to be constructed on the surface of a substance when the current flows through two opposite sides of this square" [1]. The second formal deduction is the "principle of similarity"; the meaning of this principle is that with geometrically similar configurations of electrodes (b/l = const.), the quantity R_s remains constant [2].

The nature of the conducting surface is usually connected with the presence of a film of moisture on the surface of the dielectric. The influence of moisture on the surface, usually enhanced by the presence of soluble ions, has been convincingly proved by many investigators of the phenomena of surface conductance [3-7]. Hydrophilic substances, however, do not always function in an atmosphere of increased humidity. Moreover, high quality hygrophobic dielectrics have recently been widely used, for example fluoroplastics, organic silicon compounds, polyethylene etc. The surface electric conductance of many of these substances deserves more detailed study.

* *Elektrichestvo*, No.3, 60 – 65, 1958.

A very important starting-point for theoretical research and for the measurement of surface electric conductance is the exact definition of such a term as the surface current (or the current surface leakage). The existing definition which defines a surface current as the current flowing on the surface of insulation (or in the surface layer) is not clear. It is necessary, however, to keep in mind that this current is of practical importance. The necessity for its determination has posed the problem of the study of the phenomenon of surface conductance. Consequently, the notion of surface current should be completely adapted to practical requirements. In practice it is necessary to know the current between the electrodes situated on one side of the insulator surface. This current should be considered as the surface current, without restricting the domain of its flow by a layer of any definite thickness. It is necessary that this definition should also include dimensions of the electrodes, i.e. their width and length, for determination of the surface current. At present we take into account only the length. This is the consequence of the formal character of the initial assumption.

The definition of the term "surface electric conductance" may be clearly deduced on the basis of the above definition of the term "surface current". This conductivity, therefore, means the conductance of the dielectric between the electrodes situated on the same side of its surface. In investigating the flow of the current between such electrodes we must distinguish two strictly different cases: the first, when electric conductances of the superficial and internal layers of the substances are equal, and the second, characterized by the presence on the surface of the dielectric of a layer with considerably increased conductance in comparison with the conductance of the internal region.

1959

Let us consider the first case and deduce the equation for the calculation of the value of the surface resistance R_S when a current is flowing between the flat electrodes A and B, of length l and width a, placed on the surface of the dielectric at a distance B apart (Fig. 1).

We assume that the volume resistance ρ_v has the same value on the surface layers and inside the dielectric.

Calculation can be carried out by an approximate method, assuming, for simplicity, that the boundary lines of the current tubes are semicircles.

In the absence of a strongly conducting layer on the surface, the resistance between the electrodes (surface resistance R_S) will be determined by the geometrical dimensions of the current tube (dimensions a, b and l), and by the value of $\rho_v = 1/\gamma_v$ of the dielectric.

The electric conductance dG of the elemental area $kstu$ will be:

$$dG = \frac{dF}{\rho_v d},$$

where $dF = l\,dr$;

$$d = r\,d\varphi.$$

The conductance of the portion $pqnm$,

$$G = \int dG = \int_{b/2}^{a+b/2} \frac{l\,dr}{\rho_v r\,d\varphi} = \frac{l}{\rho_v r\,d\varphi} \ln \frac{2a+b}{b},$$

and its resistance

$$dR = \frac{1}{G} = \frac{\rho_v}{l \ln \frac{2a+b}{b}}\,d\varphi.$$

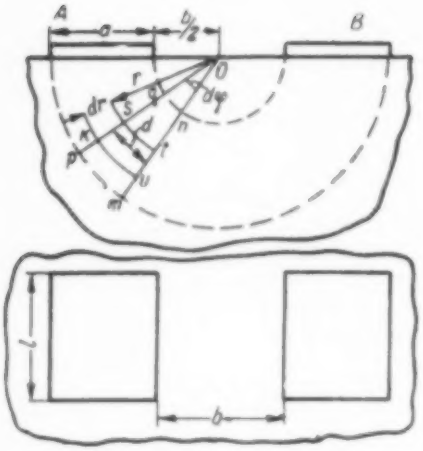

FIG. 1. Diagram for calculation of the surface resistance of a dielectric without surface film of increased conductance.

Now we can easily find the resistance encountered by the current between the electrodes A and B (i.e. R_s)

$$R_S = \int dR = \int_0^{\pi} \frac{\rho_v}{l \ln \frac{2a+b}{b}}\,d\varphi,$$

or

$$R_S = \frac{\pi \rho_v}{l \ln \frac{2a+b}{b}}. \qquad (2)$$

The comparison of equation (2) with equation (1), which at present is normally used, shows that only the electrode length l has the same influence in both cases on the value of R_s.

The dependence of R_S on the distance between the electrodes b, in equation (2), is, however, of a more complex nature than in equation (1). It should be particularly pointed out that in equation (2), as opposed to equation (1), the dependence of the electrode width a on R_s is taken into account.

The resistance R_s according to equation (2) does not increase linearly with the distance between the electrodes as it does in equation (1), but increases considerably less rapidly. Calculations show that, for instance, by increasing b from 1 to 20 mm, the value of R_S, according to equation (1), increases 20 times, and according to equation (2) only 3.3 times (the width of the electrodes a is taken as 20 mm) since its value enters into equation (2). Experimental investigations of specimens of genitax and textolite, performed with electrodes 80 mm long and 20 mm wide, show that, by increasing the inter-electrode distance b within the stated limits (from 1 to 20 mm), the resistance R_S in

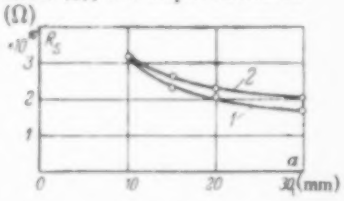

FIG. 2. Dependence of the surface resistance R_S on the electrode width a, for b = 5 mm and l = 80 mm; (1) experimental curve obtained by testing a specimen of getinax 10.4 mm thick, at 55 per cent relative humidity, (2) calculated (from equation (2)).

various experiments increased 1.75 - 4.25 times.

The experimental verification of the dependence of R_S on the electrode width shows a sufficiently close agreement between the experimental results and the values calculated by equation (2) (See Fig. 2).

Thus, despite certain simplifications, assumed in the deduction of equation (2), this equation correctly accounts for the influence of the geometric dimensions of the electrode and the distance between them on the value of the surface resistance of the dielectric, in the absence of the film of increased conductance on the surface. The current between electrodes situated on one side of the surface in this case flows through the bulk of the substance, and not only in a thin surface layer. The density of the current will be greater in the upper layers of the substance. In a sufficiently thick specimen, currents flowing in internal regions may be so small that we can neglect them. In consequence, we may consider the depth of penetration of the current into the specimen when the current flows between the electrodes situated at the surface. Experiments have shown that this depth is of the order of a few mm.

Calculating the value of R_S by equation (2), and afterwards finding the value of ρ_S by formula (1), we get

$$\rho_S = \frac{\pi}{b \ln \frac{2a+b}{b}} \rho_v \quad \text{or} \quad \rho_S = k\rho_v .$$

Hence, it follows that ρ_S is not a specific constant of a given substance (since the factor k depends on dimensions a and b), but this contradicts equation (1). Moreover, taking $a = 10$ mm and $b = 2$ mm, these being the usual dimensions of ordinary electrodes, we have $k = 6.55$ cm^{-1}. For other values of a and b found in practice, the factor k will be within the limits 1 - 10 cm^{-1}. Hence, we may conclude that, in the absence on the surface of the dielectric of a conductive film, the value of ρ_S determined by the above method should be expressed by a number of the same order as the value of ρ_v (for instance, for various types of getinax, $\rho_v = 10^{11} - 10^{12}$ ohm.cm, $\rho_S = 10^{11} - 10^{12}$ ohm., etc.).

In fact, it is well known that many hydrophilic dielectrics in a comparatively low relative humidity (60 - 70 per cent), and hydrophobic dielectrics in a high relative humidity have the values of ρ_v and ρ_S expressed by approximately the same number, although given in different units; consequently this coincidence of numerical values is not accidental, but caused by the flow of the surface current through the internal region of the substance.

For the above case, the surface resistance R_S is determined, not only by the geometric dimensions, but also by the value ρ_S of the substance. The influence of these factors is quite satisfactorily accounted for by equation (2). The investigation described above leads to the conclusion that formula (1) is not valid for this case; and its modification for widely used round electrodes is also invalid. In the absence from the surface of the insulation of the film with the increased conductance (or when the thickness of the film is very small), such a characteristic of the substance as ρ_S proves to be superfluous.

Although the surface conductance of dielectrics in presence of the layer with the increased conductance has been investigated very thoroughly, nevertheless it is desirable to consider some aspects of this phenomenon. Fig. 3 shows a diagrammatic cross-section of a portion of a dielectric, on the surface of which is a film with a thickness of δ; the volume conductance γ_{vf} is much greater than the conductance of the internal regions of the substance ($\gamma_{vf} \gg \gamma_v$).

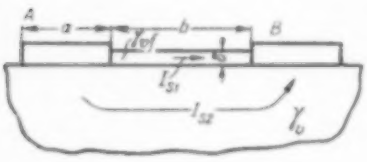

FIG. 3. Diagram for determining the value of the surface resistance R_s of a dielectric in the presence on its surface of the film of increased conductance.

Let us determine for this case the value of the surface resistance R_s, when a current flows between the flat electrodes A and B of length l and width a, situated at a distance b apart. The current between the electrodes, which is a surface current, can be considered as a sum of the currents, one flowing in the surface layer and the other inside the dielectric $I_s = I_{s1} + I_{s2}$. In this case, for a film of a sufficient thickness, δ $I_{s1} \gg I_{s2}$, so we may assume that $I_s = I_{s1}$. Then $R_s = R_f$, (R_f is the resistance of the film). Obviously, $R_f = \rho_{vf} b/F$, where $\rho_{vf} = 1/\gamma_{vf}$, and $F = l\delta$ (the area of transverse section of the film).

Hence
$$R_s = \frac{\rho_{vf}}{\delta} \frac{b}{l}. \tag{3}$$

If the thickness of the film is uniform, the ratio ρ_{vf}/δ is a constant.

If we denote this ratio
$$\rho_s = \rho_{vf}/\delta\,(\Omega) \tag{4}$$
then equation (3) transforms into equation (1). Thus, the realm of applicability of equation (1) is made clear. Using this equation we may determine the surface resistance; but this is possible only when on the surface of the dielectric there is a film of increased conductance γ_{vf}, and of a sufficient thickness δ, i.e. when we may neglect the current I_{s2}. Such conditions occur in the case of hydrophilic dielectrics in an atmosphere of increased humidity, when the thickness of the humid layer on the surface sharply increases. The presence of the soluble ions in the substance, of various gases in the surrounding air and of surface impurities, giving soluble ions, decreases the value of R_s still more, since the volume resistance of the film γ_{vf} decreases.

For the case in question, the physical meaning of the surface conductance $\gamma_s = 1/\rho_s$ becomes clear. From equation (4) it follows that $\gamma_s = \delta/\rho_{vf}$, or
$$\gamma_s = \delta \cdot \gamma_{vf}. \tag{5}$$

The volume electric conductance of the film
$$\gamma_{vf} = nKq, \tag{6}$$

where n is the number of ions in 1 cm³, q the ion electric charge, K the ion mobility. Equation (6) is given for the case when the film contains ions of the same polarity and mobility. After substitution of (6), equation (5) becomes

$$\gamma_S = \delta \cdot n \; K \cdot q. \tag{5a}$$

The product $\delta.n = n_{sur}$ represents the number of ions in a portion of the surface layer with an area of 1 cm² (ion surface density). Taking this into consideration, we obtain the expression for γ_s in its final form:

$$\gamma_S = n_{sur} \cdot K \cdot q. \tag{7}$$

If the film thickness δ is comparatively small (for instance in the presence of slightly though not excessively increased air humidity), we cannot neglect the current I_{s2}. In determining the surface conductance G_S it is necessary to consider the conductance of the upper layer $G_1 = 1/(\rho_S b/l)$, on which the current I_{s1} depends, and the conductance of the internal region of substance $G_2 = \dfrac{1}{\dfrac{\pi\rho_v}{l \cdot \ln\dfrac{2a+b}{b}}}$, which determine the value of the current I_{s2}:

$$G_S = G_1 + G_2 = l\left(\frac{1}{\rho_S b} + \frac{\ln\dfrac{2a+b}{b}}{\pi\rho_v}\right).$$

For the case in question, the surface resistance is

$$R_S = \frac{1}{G_S}$$

or

$$R_S = \frac{1}{l\left(\dfrac{1}{\rho_S b} + \dfrac{\ln\dfrac{2a+b}{b}}{\pi\rho_v}\right)} \tag{8}$$

Equation (8), for the determination of R_s, is of a more general character, and equations (1) and (2) are its particular cases.

The surface resistance of substances with an open porous surface will decrease very sharply in an atmosphere of high humidity, since in this case the volume resistance ρ_v considerably decreases. As follows from the previous discussion, the surface resistance is determined by the value of ρ_S only in the presence on the surface of the substance of a film of increased conductance. Moreover, if the thickness of the film is small, then R_s, according to equation (8), also depends on the value of ρ_v of the substance. As has already been stated, for a very thin film or in the absence of a film, we do not need to know the property ρ_S at all. In cases when it is important to a certain extent, it is necessary to bear in mind, that the value of ρ_S depends on properties of the surface film. Certainly, the film thickness δ and its volume resistivity ρ_{vf} depend to a considerable degree on the properties of the dielectric,

but we also have to reckon with the possible influence of various objective factors. All this leads to the conclusion that the existing cautious opinion about the factor ρ_s, as a characteristic of insulating materials is sufficiently justified.

Since the surface resistance of dielectrics is important in practice, we can find its value not from the value of ρ_s, but by measuring the surface resistance of specimens of dielectrics by using round electrodes of strictly specified dimensions, thus ensuring the attainment of comparable results.

The methods of determining R_s (ρ_s), recommended by standards GOST 6433-52, are basically incorrect and therefore subject to criticism.

The tendency to measure not the total current, flowing between the electrodes A and B situated on the surface (Fig. 4), but only the part of it I_{s1} which flows in the surface layer of the specimen, and which is considered by GOST authors as the surface current, has resulted in a natural tendency to lead away the current I_{s2} so that it is not recorded by a galvanometer G. For this purpose, an electrode C is fixed to the lower surface of the specimen and the earthing of this should ensure the desired result. At a first glance everything seems to be correct: first, the galvanometer measures only the current required; secondly, such an arrangement of electrodes permits the use of the same specimen for the determination of ρ_v and ρ_s, this being convenient.

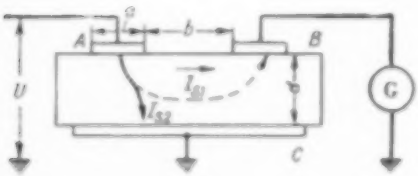

FIG. 4. Diagrammatic lay-out of electrodes for determination of the surface resistance by the standard method.

In fact, however, the presence of the electrode C and still more the fact that it is earthed are not only undesirable, but often quite inadmissible. If we accept the definition of the surface current which is recommended in this article, then the uselessness of the electrode C becomes obvious. Still more, this electrode cannot perform its function in the actual method of measurement of the surface current. In fact, why should the electrode C lead away the total so-called "volume current" I_{s2}? It is quite clear that for the same substance the value of the current I_{s1} will vary with the specimen thickness d, other things being equal (equal voltages U and dimensions a and b). For sufficiently thick specimens (8-10 mm and more) and for the recommended standard distance between the electrodes $b = 2$ mm, a very considerable part of the "volume current" will nevertheless flow towards the electrode B. Thus, both the thickness of the layer, in which the current flows between electrodes A and B, and the current I_{s1} itself are determined, and this corresponds to the vagueness of the existing definition of the term "surface current".

When a film of considerably increased conductance is present on the surface of the dielectric, the electrode C will be superfluous, since in this case we can neglect the current I_{s2} in comparison with I_{s1}.

The experimental determination of R_s for thin fabrics should be particularly considered (i.e. for lacquered fabrics and substances in the form of a thin film).

In this case $b >> d$, and this is very important as the electrode B is far away from the electrode A, while the electrode C is very close to the electrode A along the whole length of the latter.

Taking into account that the potentials of B and C, the latter being earthed, are almost equal ($\phi_B = \phi_C = 0$), it becomes clear that the electrode C entirely screens the electrode B, which finds itself practically outside the electric field. When a voltage is applied to the specimen, the total current from the electrode A in fact flows towards the electrode C, by-passing the electrode B. As a result, the use of the standard method creates the false impression that thin insulation fabric has a very high surface resistance. For instance, in tests on specimens of various cotton lacquered fabrics, carried out according to the above method, no surface current could be detected even when these specimens were heated up to 120°.

Yet the test on the same specimens carried out without the electrode C resulted in the measurement of R_s even at room temperature; and this resistance was far from infinity (10^{10} - 10^{11} Ω), decreasing at 120° approximately to 10^4 Ω.

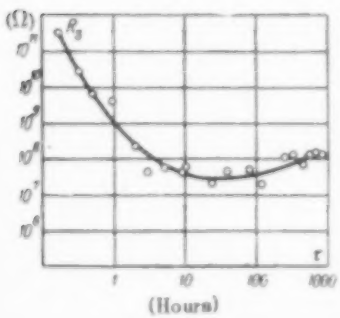

FIG. 5. Relationship between the surface resistance R_s of the lacquered fabric LKh - 2, 0.17 mm thick, and the time of keeping specimens in water. Tests carried out by the standard method.

A paradoxical result also was obtained in finding the relationship between the surface resistance of the lacquered fabric LK_h - 2 0.17 mm thick, and the time of keeping the specimens in water, when carrying out this experiment by the standard method. The graph of this dependence (see Fig. 5) shows that at the beginning the resistance R_s sharply decreases and after passing through a minimum, increases slowly, a result which is entirely unexpected.

This behaviour is also due to the experimental method. The sharp decrease in R_s for the initial stages when the specimens were kept in water is caused by the moistening of the substance. Further, the difference in conductance of outer and inner layers begins to decrease, and this is due to the penetration of moisture inside the specimen, this penetration being helped by the tissue structure of the material. In consequence, the current flowing towards the electrode C sharply increases, and the screening action of this electrode becomes effective. This, in turn, brings about the decrease of the current I_{s1}, and the apparent increase of the value of R_s.

Hence it is advisable to carry out the measurement of the surface resistance without the lower electrode C, because only in this case is it possible in fact to measure the current between the electrodes situated on the same side of the specimen surface, i.e. the surface current. The specimen under test should be placed on an insulated base avoiding any metal supports, even non-earthed, when the current between the

electrodes A and B (Fig. 4) will flow not directly but by a path A C B.

Translated by S. Szymanski

REFERENCES

1. N.P. Bogoroditskii; V.V. Pasynkov and B.M. Tareev; *Elektrotekhnicheskie materialy (Electrotechnical materials)* Gosenergoizdat (1955).
2. B.M. Tareev; Osnovy fiziki dielektrikov (Principles of the physics of dielectrics), *Izd. Vses.Zauch. energ. inst.* (1954).
3. P.A. Florenskii; Dielektriki i ikh tekhnicheskoe primenenie (Dielectrics and their technical applications), *Red.-izd. otd. Glovelektro Vys. Sov. narod. khoz.* (1924).
4. N.N. Semenov and N.M. Chirkov; O poverkhnostnoi elektroprovodnosti dielektrikov (On the surface conductance of dielectrics), *Dokl. Akad. Nauk SSSR*, 51, No.1 (1946).
5. N.P. Bogoroditskii and I.D. Fridberg; *Vysokochastotnye neorganicheskie dielektriki (High frequency inorganic dielectrics)*, Izd. "Sovetskoe radio" (1948).
6. M.M. Mikhailov; *Elektromaterialovedenie (Electrical materials reference book)* Gosenergoizdat (1953).
7. Le Clerc; Variation with time of the surface electrical conductivity of glasses in a conditioned atmosphere, *Silicates industr.*, 19, No. 6/7 (1954).

THE DEPENDENCE OF FREQUENCY OF THE ROCHELLE SALT PIEZOELECTRIC VIBRATORS ON TEMPERATURE*

K.F. GUBA

Lvov Institute of Forest Technology

(Received 30 October 1957)

We have investigated twelve orientations of the Rochelle salt piezo-plates with respect to X, Y, Z co-ordinate axes; nine orientations were investigated on metallized plates, and three orientations were tested under the influence of electric field, with metallized as well as non-metallized plate surfaces.

1959

The experimental investigation of the dependence of the frequency of vibrations of a piezoelectric plate on temperature at different orientations led to the exact determination of temperature frequency coefficients of different cuts, and this is of practical industrial importance.

Fig. 1 shows temperature-frequency characteristics of the Rochelle salt piezoelectric vibrators with the basic surface perpendicular to the X-axis. The curves are: (1) for a metallized vibrator of length $l = 2.073$ cm, width $b = 0.253$ cm and thickness $d = 0.08$, its long side being inclined to the Y-axes at an angle $\theta = 22° 30'$; (2) for a metallized vibrator of dimensions $l = 1.60$ cm, $b = 0.20$ cm, $d = 0.09$ cm and $\theta = 45°$; (3) for metallized vibrator of dimensions $l = 2.17$ cm, $b = 0.194$ cm, $d = 0.071$ cm, and $\theta = 67° 30'$; (4) for non-metallized vibrator of dimensions $l = 2.59$ cm, $b = 0.449$ cm, and $d = 0.11$ cm its long side being parallel to the Z-axis; (5) this vibrator differs from 4 only in that it is non-metallized.

Plates characterized by curves 1-3 are excited by a longitudinal force, therefore their frequency is determined by their longitudinal dimensions (length). [1]. The frequency of the plate, characterized by curves 4 and 5 (Fig. 1) is determined by its linear dimensions along the crystallographic "b"-axis of a Rochelle salt monocrystal [2].

Curves 1-3 (Fig. 2) correspond to the three metallized vibrators with their basic surface perpendicular to the Y-axis; the vibrators are inclined to the X-axis at angles $\theta = 22° 30'$, 45° and $67° 30'$.

* *Electrichestvo*, No. 3, 71-72, 1958.

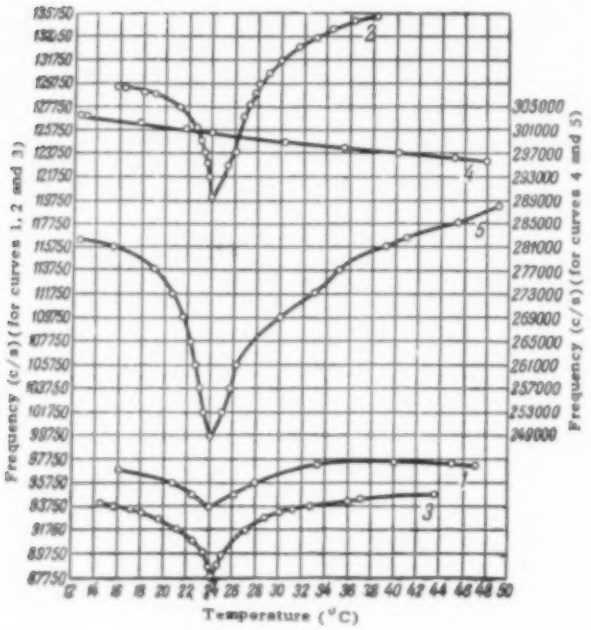

FIG. 1.

Linear dimensions of the specimens are respectively equal to: length, 2.795, 2.266 and 2.655 cm; width, 0.21, 0.235 and 0.24 cm; thickness, 0.096, 0.091 and 0.09 cm. The frequency of plates characterized by curves 1-3 is a function of their length. Curves 4 and 5 (Fig. 2) are temperature-frequency characteristics of the same vibrator; non-metallized (curve 5) with its basic surface perpendicular to the Y-axis. The linear dimensions of the specimen are $l = 2.51$ cm, $b = 0.46$ cm, $d = 0.345$ cm. The length of the plate is parallel to the Z-axis. The frequency of the plate, characterized by curves 4 and 5 (Fig. 2), is a function of its dimensions along the crystallographic "a" axis of a Rochelle salt monocrystal.

Curves 1-3 (Fig. 3) show the influence of temperature on the frequency of vibrations of the three Rochelle salt piezoelectric vibrators, cut with their lengths at angles $\theta = 22° 30'$, 45° and $67° 30'$, respectively, to the X-axis; the basic surface of plates is perpendicular to the Z-axis. The linear dimensions of specimens are respectively: length, 2.469, 2,512 and 3.13 cm; width, 0.282, 0.328 and 0.348 cm; thickness, 0.082, 0.131 and 0.158 cm. The frequency of vibrations is a function of the plate length.

The last result (curves 4 and 5, Fig. 3) is related to investigations of the frequency of the same Rochelle salt plate in the absence of metallization (curve

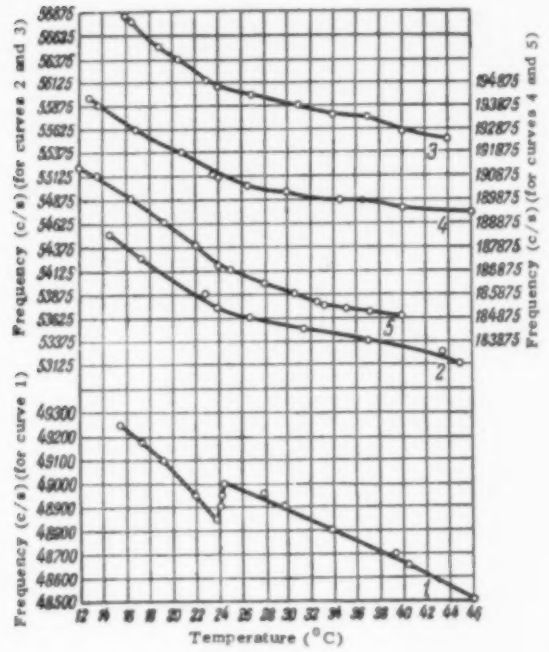
Frequency (c/s) (for curves 2 and 3)
Frequency (c/s) (for curves 4 and 5)
Frequency (c/s) (for curve 1)
Temperature (°C)

FIG. 2.

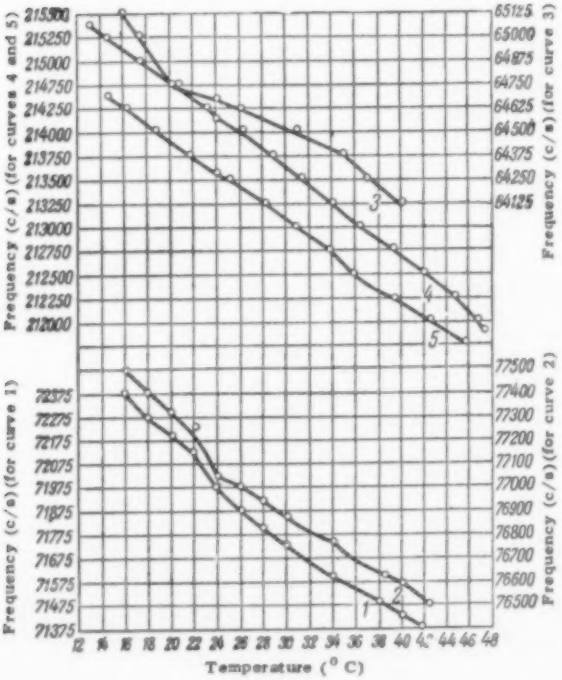
Frequency (c/s) (for curves 4 and 5)
Frequency (c/s) (for curve 3)
Frequency (c/s) (for curve 1)
Frequency (c/s) (for curve 2)
Temperature (° C)

FIG. 3.

4) and in the presence of metallizations, (curve 5). The length of the specimen is parallel to the X-axis and its basic surface is perpendicular to the Z-axis. The dimensions of the plate are: $l = 4.13$ cm, $b = 0.569$ cm, $d = 0.17$ cm. The frequency of the plate is determined by its dimensions along the crystallographic "b"-axis of a Rochelle salt monocrystal.

In recording the temperature frequency characteristics, the crystal temperature was varied at the rate of 0.1°C in 5-10 min. In the vicinity of the Curie-point the rate of variation did not exceed 0.05°C in 10-12 min [3].

Translated by S. Szymanski

REFERENCES

1. W.P. Mason; *Phys. Rev.*, 55, 775 (1939).
2. G.P. Mikhailov; *Zh. tekh. fiz.* VI, 7 (1936).
3. K.F. Guba; K voprosu opredelenia dielektricheskoi pronitsaemosti p'ezokristalla segnetovoi soli (Problem of determination of the permittivity of a Rochelle salt piezocrystal). *Tr. Vses. zaoch. lesotekhnicheskogo inst.* II Leningrad, (1956).

THE USE OF ELECTRIC LOCOMOTIVES WITH RECTIFIERS – A REVIEW *

A.M. KAKHELNIK

(Received 15 October 1957)

The beginning of the use of electric traction may be ascribed to the year 1837, when the Russian Academy of Science considered a scheme of the Russian scientist B.S. Iakobi, "The application of electric power for ship propulsion," It is known that in 1838-39 an electrically propelled ship navigated on the Neva river with 14 passengers on board. F.A. Pirotskii, in September 1880, after some preliminary experiments, set in motion the first electric carriage in the world with 40 passengers. Later, with a centralized production of electrical energy, electric traction using a d.c. current found wide application in many countries.

1959

With the development of the electric d.c. traction and of public electric grids the idea of using a.c. current for the railway traction arose.

The first attempts abroad to use a.c. current for electric traction relate to the last decade of the nineteenth century, when Werner Siemens in 1892 tried to use three-phase a.c. current for this purpose; in 1895 a Swiss firm Brown-Boveri opened the first electric railway (of the urban type) in Lugano using three-phase current.

In 1899 the main-line electric a.c. locomotive – the first in Europe – was built for the Burgdorf – Thun line (Switzerland). It was fed by a three-phase current of the frequency 40 c/s. Simultaneously with this, electric traction of lower frequency was developed: in Europe at 15 and 16 2/3 c/s, in the U.S.A. at 25 c/s. This is a short and very incomplete summary of the development of a.c. electric traction; this period preceded the appearance of an electric locomotive with devices for converting a.c. energy into d.c. energy. Such a conversion may be realized either by means of a rotary convertor (motor-generator), or by using a static converter. By this method we may have both the advantages of an a.c. supply system and the good traction qualities of a d.c. motor.

In 1904 in Switzerland on the Seebach-Vettingen section the Oerlikon firm was the first in the world to attempt to use a single-phase current of normal

* *Elektrichestvo*, No. 3, 73-76, 1958

frequency 50 c/s, by converting it, on the electric locomotive, by means of a synchronous motor-generator.

This 400 h.p. locomotive, type Bo - Bo, underwent successful tests on the above mentioned section. But further development of this construction was abandoned since the electric machine industry at that time was unable to produce an electric locomotive, with a rotary a.c.-d.c. convertor, within reasonable weight limits. Later, with the improvement of production methods and with the weight reduction of the motor-generator set, electric locomotives of this type were used.

In the search for reducing the convertor weight, attention was drawn to the mercury rectifier.

First experiments in the use of a static convertor were carried out by the Westinghouse firm, which in 1914 built a motor coach, with a multi-anode exhaust-type mercury rectifier, for the New-Kanaon branch of the New York - New Haven railway. These tests proved unsuccessful, since at that time technical ability was insufficient to produce rectifier tanks with sufficiently strong and tight seams to withstand travel shocks. Moreover, this system caused disturbances in the telephone network. This carriage was withdrawn after a 35,000 km run.

Tests which were carried out by the same firm with mercury rectifiers with welded tanks did not give more successful results because of the lack of effective protection of the tanks from vibrations.

Thus, more than 20 years elapsed from the first attempts to use a.c. for railway traction up to the first application of a static a.c. - d.c. convertor on the locomotive itself.

It is necessary to add that besides the single-phase a.c. - d.c. system, other systems were investigated such as: a three-phase single-phase, electric locomotives with single-phase commutator motors and others.

After unsuccessful attempts in 1914, the problem of using mercury rectifiers on electric locomotives did not arise until 1925, when Reichel (Germany) presented the plan of such a locomotive. This plan was never realized since it was based on the three-phase method of feeding, and such a system offered no advantage.

The progress in making welded seams in metallic tanks and the experience accumulated in production and exploitation of mercury rectifiers in the traction substations brought about the renewal, by the Brown-Boveri firm in 1930, of work on the application of mercury rectifiers for the system of traction using a single-phase a.c.

For this purpose an old electric locomotive type 1-C_o-1 of the Simplon line was provided with a multi-anode rectifier, capable of working on frequencies from 15 to 60 c/s.

In the same year, 1930, Siemens-Schuckert built a contact-accumulator electric locomotive, which was fed from a single-phase grid at 15 kV, 16 2/3 c/s

through two glass mercury rectifiers. This locomotive was destined for repair, for inspection of the grid and for shuntling work.

In 1932 Reichel renewed his proposal, but this time he suggested single-phase a.c. feeding with control-grid rectifiers. However, this system with a low frequency (16 2/3 c/s) does not offer any particular advantages in comparison with electric locomotives, equiped with single-phase commutator traction motors.

In June 1932, the first All-Union Conference on railway electrification decided to press for work concerning the practical use of electric traction, based on a single-phase normal frequency current.

In this year "Elektrosila" ("Electric power") factory mastered the production of mercury rectifiers with control grids. As a further step, such a rectifier was used for the equipment of an electric locomotive, built by the "Dinamo" factory; it was fed by the single-phase industrial frequency current.

In 1933 the Directorate of the German railways decided to begin trials on traction using a single-phase, 50 c/s, 20 kV current; the trials were to be carried out on the Hollentall line in Schwarzwald. Work on the project for electrification of this line started in 1930, but the initial intention was to use a current of 16 2/3 c/s frequency.

In 1936, of the four electric locomotives which were put in service on this line for trial, two locomotives were fitted with the multi-anode exhaust type mercury rectifiers, with water cooling. Locomotive E 244.01 was built by the A.E.G. Co., and locomotive E 24411 by Brown-Boveri.

Simultaneously with this, in the U.S.S.R., both research and design were carried out with a view to building a similar electric locomotive. In September 1938 the Kirov "Dinamo" works jointly with the V.V. Kuibyshev locomotive factory at Kolomna, built the first Soviet electric locomotive mark OR-22-01, for the single-phase a.c.-d.c., fitted with the 12-anode mercury rectifier model RV-20, which is used on traction substations.

During the period between the two World Wars, electric high-power grids were developed on a large scale, and feeding of a railway single-phase grid from a three-phase grid was made much easier. In 1942 the construction of the ignitron rectifiers was greatly improved; these improvements greatly contributed to the wide use of ignitrons in the metallurgy of non-ferrous metals during the Second World War, particularly in aluminium and magnesium production. These two circumstances gave a new impetus to the development of the single-phase-d.c. system of electric traction with the use of static convertors.

The results of trials, carried out on the Hollental line, which after the War was placed under French occupation, drew the attention of French Railways. A few weeks after the occupation of Germany the Society appointed a commission to carry out tests on this line. The conclusions of the commission led to electrification in 1950 of the 78 km line Aix-les-Bains – La-Roche-sur-Fauron in Savoy

(France), in view of the final investigation of problems, arising with the single-phase 50 c/s system.

Positive results of the experiment with exploitation of this line led to the large-scale electrification of the north-eastern French Railways region, which carries much goods traffic; a single-phase current of line frequency is used throughout.

In 1948, in the U.S.A., trials were undertaken: first on a stand, and later on an experimental el-motor coach built by the Westinghouse Company, with a mercury rectifier. This carriage started its running tests on 15 July 1949, and after completing 4000 km was assigned for the normal service on the Pennsylvania railway (25 c/s). The results of this trial led to the conclusion that rolling stock of the single-phase d.c. system with mercury rectifiers had passed the stage of laboratory tests.

The outcome of these experiments was the order of the New York-New Haven railway of the Westinghouse Co. for 100 such el-motor coaches.

On the trial section of French Railways in Savoy a motor coach, mark Z-9055, with the single-anode ignitron rectifiers of American construction was tested; these rectifiers were made in France on licence. In July 1955, the Alstom firm delivered for this line an electric locomotive mark VV-8051 with mercury rectifiers of the same type.

In November 1957 the first of the two electric locomotives with rectifiers built for the Pennsylvania railway was delivered for use. In 1957 the A.E.G. Co. equipped electric locomotives, fed by 50 c/s. a.c., with a bridge circuit system; and the Brown-Boveri Co. performed an experiment for the first time with two single-anode air-cooled rectifiers, installed on the locomotive E-244.11 of the Hollental line.

At the beginning of 1952, two double-section electric locomotives, built by the Westinghouse Co., were delivered for the Pennsylvania railway; they were fitted with ignitron rectifiers 2/VVV/ and 2/SS/, their power was 6000 h.p.

In December 1952, on the Lancaster-Morecambe-Heysham line, a motor-coach, with a mercury rectifier fed by a single-phase, 50 c/s current at 6.6 kV, was sent on experimental runs. A regular passenger service began in August 1953. For this purpose three three-coach sets were equipped with a d.c. installation fed through mercury rectifiers.

In 1953, the Administration of Peat Transport of the Shatur Administration of the Ministry of Electric Stations in the U.S.S.R. electrified the ten-kilometer Baksheevo-Lidino section, and at the end of 1956 the length of the electrified line run by the Shatur Administration was more than 20 km. For this line an electric locomotive, with a six-anode, controlled, non-exhaust mercury rectifier mark P-KO-1 was built by the S.M. Budennyi electric locomotive factory in Novocherkassk; this locomotive was fed by a single-phase, 50 c/s current at 6 kV. This locomotive is still in service at the present time.

On 1 April 1954 a ten-motor-coach train with mercury rectifiers was delivered for the New York - New Haven line. It was equipped by the Westinghouse Co. and worked on a multi-unit system. In 1955 this line received a hundred more coaches.

In December 1954 the delivery of ten high-speed electric passenger locomotives, of rectifier power 4000 h.p., began for this railway; delivery by the General Electric Co. was finished in March 1955. These motor - coaches and locomotives work equally well on the 25 c/s a.c. or on d.c. at 650 V. In 1954, in the U.S.S.R., the Novocherkask electric locomotive factory built two electric locomotives of the NO series, which were equipped with the ignitron single-anode rectifiers. These rectifiers were designed and constructed by the All-Union V.I. Lenin Institute of Electric Technology and were tested on the experimental ring of the All-Union Railways Scientific and Research Institute. These locomotives are fed by a single-phase 50 c/s a.c. and have the same power as the Soviet main line d.c. locomotives VL 22m.

In June 1955 the Virginia Railway ordered 12 electric locomotives of the type supplied by the General Electric Co. for the New York-New Haven line. These locomotives will replace the 36 old electric locomotives with asynchronous motors, since these locomotives are already 30 years old.

It is necessary to point out that an ionic convertor usually works as a rectifier, converting a.c. into d.c. At present, the work of an ionic convertor acting as an inverter i.e. as a device for converting the a.c. energy into the d.c. energy, is explained theoretically and verified in practice. This opens up the possibility of the use in practice of the regenerative braking of electric locomotives with mercury rectifiers. In this case an appreciable amount of energy is returned to the grid and the specific consumption of energy decreased.

At the beginning of 1955 only one out of the 17 electric locomotives, which were ordered from the Brown-Boveri Co. for open-cast brown coal mines in the Rhineland, was to be fitted with a mercury rectifier with regeneration; at the end of 1955, locomotives for the same purpose were in production, and these were equipped with pumpless air-cooled valves, capable of regenerating the energy.

M. Tessier, in his lecture delivered at the conference in Lille (France) on problems of electric single-phase traction at line frequency, stated that nearly half the rolling stock of the north-eastern French Railways will consist of electric locomotives with mercury rectifiers.

In October 1955 tests began on the Japanese State railways, on two electric locomotives of type Bo - Bo, of the ED 451 series, with mercury rectifiers to be fed from the 20 kV, 50 c/s grid.

On 1 December 1955, for the first time in the world, a motor-coach with a semiconductor germanium 750 kW rectifier was put into service on the Lancaster-Heysham line. The rectifier was made by the British Thomson-Houston Co.; it is of the two half-period system and is air-cooled.

In the U.S.S.R. from the beginning of 1956 electric locomotives of the NO

series, produced by the locomotive factory in Novocherkassk, have been in service on the Ozherel'e-Mikhailov section, and since the end of 1956 they have been used on the Ozherel'e-Mikhailov-Pavelets section of the Moscow-Kursk-Donbas railway.

In 1956, the British Transport Commission recommended, for the electrification of British railways, a single-phase line frequency current at 25 kV, and decided to accept in principle electric locomotives with rectifiers.

The good characteristics of the locomotives fitted with rectifiers, their ability to cope with different traction conditions, as well as experience in service with electric locomotives of other systems led to the decision of French National Railways to suspend completely orders for locomotives with motor-generator sets or with single-phase commutator traction motors. The table given below clearly proves the accuracy of this statement and gives a picture of trends in the distribution of orders for the north-eastern French railways.

For the Lisbon-Oporto line of the Portugese railways, which was electrified at the end of 1956 on an industrial frequency a.c., 15 ignitron electric locomotives Bo-Bo were ordered together with other items of rolling stock.

Year of order	Number of electric locomotives			
	Motor generator type with electric traction motors		With a.c. commutator traction motors	With rectifiers feeding d.c. series traction motors
	on d.c.	on three-phase a.c.		
1952	20	65	15	5
1954	–	37	9	9
1955, first half	–	–	29	38
1955, second half	–	–	–	75
1956	–	–	–	130

As early as 1932 in Hungary, the Budapest-Hodieshalom section was electrified on a single-phase line frequency current; electric locomotives of the Kando system were used on this line. But, because of defects which were recorded during service, construction of these locomotives was abandoned.

Taking into account progress achieved during recent years, the Hungarian State Railways intend in future to buy single-phase locomotives, fitted with rectifiers and d.c. motors.

On 27 May 1957 in Munich a six-axle shunting electric locomotive came into service; on this locomotive, instead of two mercury rectifiers, a silicon semiconductor rectifier made by the Siemens-Schuckert Co. was fitted. With air-cooling and a continuous power $P_{\infty} = 800$ kW, this rectifier is remarkable for its small dimensions. It is necessary to point out the advantages which silicon rectifiers offer in electric traction, because of their greater reliability in service,

under difficult temperature conditions, in comparison with germanium rectifiers.

At present British Railways have ordered 35 complete germanium semiconductor rectifiers from the British Thomson-Houston Co. for some sections of the Manchester-Crewe line.

On 1 October 1957 in Japan an electric locomotive with rectifiers of the series ED 70 at 20 kV, 60 c/s came into service.

At the end of 1957 in the U.S.S.R. the first model of the main-line series electric locomotives was delivered; it works on a single-phase line frequency current and is fitted with ignitron rectifiers, series N 60. This locomotive with an axle formula Ho-Ho, a power 4000 kW and with six-pole traction motors is one of the best locomotives of this type in the world.

Thus we may draw the conclusion that during recent years electric locomotives, fed by a.c. and fitted with static rectifiers, are more widely used than other types. This is due to great improvements, which were made in the production of rectifiers during the last 15-20 years, and also to the good traction qualities of electric locomotives fitted with rectifiers.

Translated by S. Szymanski

REFERENCES

1. E.S. Avatkov and A.S. Avatkov; *Elektricheskaia tiaga na odnofoznom toke normalnoi chastoty (Electric traction on a single-phase industrial frequency current)*, Transzheldorizdat (1934).
2. A.E. Alekseev; *K voprosu ob elektrifikatsii zheleznykh dorog v SSSR na odnofaznom toke promyshlennoi chastoty. Materialy nauchno-tekhnicheskogo soveshchaniia po tiagovonu elektrochorudo-vaniiu (The problem of electrification of railways in the U.S.S.R. on a single-phase industrial frequency current. Proceedings of the Scientific and Technical Conference on electrical traction equipment)*, Riga (1955).
3. B.R. Bondarenko, N. Kh. Sitnik and V.A. Stekolshchikov; *Zhelez. Trans.* No. 11, 8, (1955).
4. L.A. Visloukh, *Elektrichestvo*, No. 5, 85 (1952).
5. L.A. Visloukh; Elektrifikatsia zheleznykh dorog Anglii (Electrification of English railways), *Biulleten tekhniko-ekonomicheskoi informatsii*, No. 11, 3 (1956).
6. L.A. Visloukh; *Elektrichestvo*, No. 9, 85 (1953).
7. D.I. Gordeen; *Elektrooborudovanie elektrovozow peremennogo toka (Electrical equipment of a.c. locomotives)*, Transzheldorizdat (1938).
8. S.S. Kalinin; *Zhelez. trans.* No. 10, 84 (1956).
9. *M.P.S. Biulleten tekhniko-ekonomicheskoi informatsii (Bulletin of technical and economic information)* No. 4, p.20 (1957).
10. Novye vidy tiagi na transporte (New aspects of transport traction), *Izd. Akad. Nauk SSSR* (1956).
11. Opytnii motornyi vagon rtutnym wyprianitelem (Experimental motor-coach with a mercury rectifie *Elektrichestvo*, No. 2, p.71 (1951).
12. F.Ia. Slavgorods ; *Opytnye lokomotivy (Experimental locomotives)*, Tranzheldorizdat (1949).

13. V.N. Stasuk; *Gornyi zh.* No. 4, p. 26 (1956).
14. B.M. Shliaposhnikov; *Zhelez. trans.* No. 9, 59 (1952).
15. *Elektricheskaia i teplovaia tiaga (Electric and thermal traction)*, No. 5, p. 35 (1957).
16. *Elektrichestvo*, No. 3, 84; No. 6, 86 (1957).
17. *Elektrovozy odnofaznogo toka promyshlemnoi chastoty (Electric locomotives fed by a single-phase industrial frequency current)*, Transzheldorizdat (1956).
18. S.B. Iuditskii and S.E. Nemchin; Vypriamitel dla elektrovoza uzkoi kolei (Rectifier for electric locomotives for a narrow-gauge railway),*Elektrichestvo*, No. 5, p.55 (1956).
19. *AEG Mitteilungen*, No. 9/10, 442 (1955).
20. *Trans. Amer. Inst. Elect. Engrs.*, II, p.107 (1954).
21. *Brown-Boveri Mitteilungen* No. 4/5, 167 (1955).
22. La traction electric dans les chemin de fer, *Bull. Ass. Int. Congr. Chem.de-fer.* No. 3, 165 (1956).
23. *Bull. SFE*, No. 9, 544 (1951).
24. *Elect. Engr.* No. 5, 408 (1955).
25. *Elect. Rev.* 158, No. 1, 19 (1956); No. 26, 1159.
26. *Elect. Traction on the Railways* No. 3, 149 (1957).
27. *Elekt. Bahnen*, V, 1 (1956); No.5, 116 (1957).
28. *Genie Civ.* No. 19, 367 (1951).
29. *Gen. Elect. Rev.* 59, No.1, 41-43, 45 (1956).
30. *Rly. Age, N.Y.*, 132, No. 10, 68 (1952).
31. *Rly. Gaz.* 104, No.1, 2 (1956); 107, No. 21 (1957).
32. *Rly. Mech. and Elect. Engr.*, 124 No. 3, 141 (1950).
33. *Rev. Gen. Chem.de-fer*, 7, 595 (1955).
34. Paper, American Society of Mechanical Engineers, No. 55-A-187 (1955).
35. *Tract. Elect. Chem. de-fer* No.6, 228 (1956).

SERVICE TESTS

TESTS OF THE EXPERIMENTAL INSTALLATION OF AN IONIC EXCITED HYDROGENERATOR*

I.A. GLEBOV

Institute of Electromechanics of the U.S.S.R. Academy of Sciences

S.F. ZONOV

Lenergo

(Received 1 November 1957)

Ionic systems of excitation act very quickly and owing to this they are very effective means for increasing the stability of synchronous generators. These systems are also very efficient economically.

1959

In 1951-1955 an installation for independent ionic excitation was designed and made for the Hydro Electric Power Station (H.E.P.S.) in Nizhnii Svirsk.† In this installation sealed single-anode rectifiers were used.

Description of the installation

In order to ensure the highest possible service reliability of the installation a six-phase converter system was chosen; the same potential was applied to all cathodes. This system may work with a reduced number of rectifiers, whilst the rectified voltage decreases less than in other systems. It is to be pointed out that the converter may work with or without the ground equalizer.

The system of ionic excitation of Nizhnii Svirsk H.E.P.S. consists of an auxiliary synchronous generator, an ionic converter, a control device, a protection and a signalling device.

Since it was impossible to drive an auxiliary generator directly by the shaft of the main set, a synchronous motor, fed from the station local grid, was used. Nevertheless, this arrangement does not change the principle character of the system, which is a system of independent ionic excitation. As an auxiliary synchronous

* *Elektrichestvo*, No. 3, 77–80, 1958.

† In different stages of work there participated: "Elektrosila" Factory, OKB Ministry of the Electrotechnical Industry, LIAP, Institute of Electromechanics of the U.S.S.R. Academy of Sciences, Lenergo, Central Electrical Research Laboratory.

generator, a synchronous machine type S-15-12-6 of 950 kVA power was used; the stator winding of this machine was rewound for this purpose.

The parameters of the auxiliary generator, which were determined experimentally, are given below.

The auxiliary generator

U_{ph} (V)	490	x_s (ohm)	0.312
I_{ph} (A)	490	r_g (ohm)	0.021
$S = 6U_{ph}.I_{ph}$ (kVA)	1440	x_l (ohm)	0.17
I_{ex} (A)	87		
x_d (ohm)	3.02	**Main generator**	
x_q (ohm)	2.02	U_l (kV)	11
x''_d (ohm)	0.276	I_l (A)	1730
x_2 (ohm)	0.037	S (MVA)	33
x_3 (ohm)	0.205	I_{rn} (A)	900
x_4 (ohm)	0.037	U_{rn} (V)	300

Remarks:

1. Excitation current I_{ex} is given under no-load conditions.
2. Phase resistance of the stator winding r_g is shown together with cable resistance.
3. Excitation voltage U_{rn} is shown when rotor is warm.
4. Leakage inductance of the stator winding x_l was determined by calculation.

In the case of six-phase construction of the generator, we have to deal with parameters of the first (forward or positive), second, third, fourth and fifth sequences. The stator winding of the generator is designed in such a way as to ensure the sustained action of the excitation system with one rectifier idle and to get a three-fold over-excitation while working with the total number of rectifiers.

The effective value of the phase current under nominal conditions is

$$I_{pn} = g\frac{I_{rn}}{\sqrt{6}} = 0.96\,\frac{900}{\sqrt{6}} = 350 \text{ A}$$

where g is the shape factor of the curve of phase current.

In the case of working with an incomplete number of rectifiers $I_{pn} = \sqrt{2} \times 350 = 490$ A, i.e. it is equal to the nominal current of the auxiliary generator.

To increase the reliability of the action of the set, feeding of control networks, including gas-filled rectifiers and thyratrons, is done by an auxiliary generator. A carbon-pile regulator of excitation is used for stabilizing the generator voltage. The ionic converter consists of six ignitrons of VET type I-200 with an average value of rectified current 200 A and a back voltage of 1300 V. Therefore, under nominal conditions of the generator work, ignitron current is 900/6 = 150 A, i.e. about 75 per cent

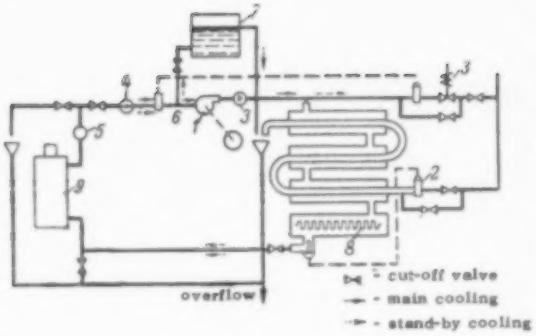

FIG. 1. Diagram of the ignitron cooling: (1) pump; (2) thermo-regulator; (3) return valve; (4) stream relay; (5) water stream indicator; (6) thermo-signalling device; (7) water-tank; (8) water heating resistance; and (9) ignitron.

of its nominal value. Ignitrons are situated in a cabinet divided into six cells; this arrangement allows a quick replacement of the faulty rectifier during the working of the set.

Ignitrons are water-cooled in a closed cycle (Fig. 1). For water heating before the start and for its cooling during the work, a heat exchanger is used with automatic regulation of the water temperature. The cooling system is provided with a stand-by device working in an open cycle. Action of a stream relay or of a thermo-signal device sends an impulse through an auxiliary relay to a contactor, which turns on a solenoidal valve 3; after this the ignitron cooling continues by the flowing water, whilst the temperature of the water leaving the ignitrons is automatically regulated.

1959

Since ignitron ignition requires a considerable pulse power, an independent ignition system is used with a charge-discharge circuit. Control of the instant of the ignition of a thyratron and, consequently, of an ignitron, is made by a magneto-peak system, of which windings for magnetizing peak-transformers are connected to an automatic voltage regulator. The installation is provided with an electro-magnetic compounding system with voltage correction and with an electronic excitation regulator, the so-called "strong action" regulator. In order to force an intensive excitation and to cut it short when the electro-magnetic system is saturated, the magnetizing windings are connected to the operative current grid by the action of the minimum and maximum voltage relay. Besides the automatic regulation of excitation there is a manual control of the generator excitation, which is exerted either by means of phase regulators, or from the station benchboard, or from the machine hall. Elements of the control system are situated in a cabinet divided into six cells in the same way as the ignitron cabinet.

The voltage phase of the igniter with respect to the main anode voltage is so chosen, by means of phase regulators, as to ensure forcing of excitation and cutting off by bringing the converter into inverter action.

The auxiliary generator is provided with axial differential protection. Moreover, to protect its stator windings from overvoltages six dischargers of PVVM-3 type are set up. The protection of ignitrons from flash-back is ensured by the use of quick-acting breakers type VAB-2. To protect the rotor of the main generator from overvoltages a discharger P-100 with a limiting resistance of 1 Ω for 200 A current is provided.

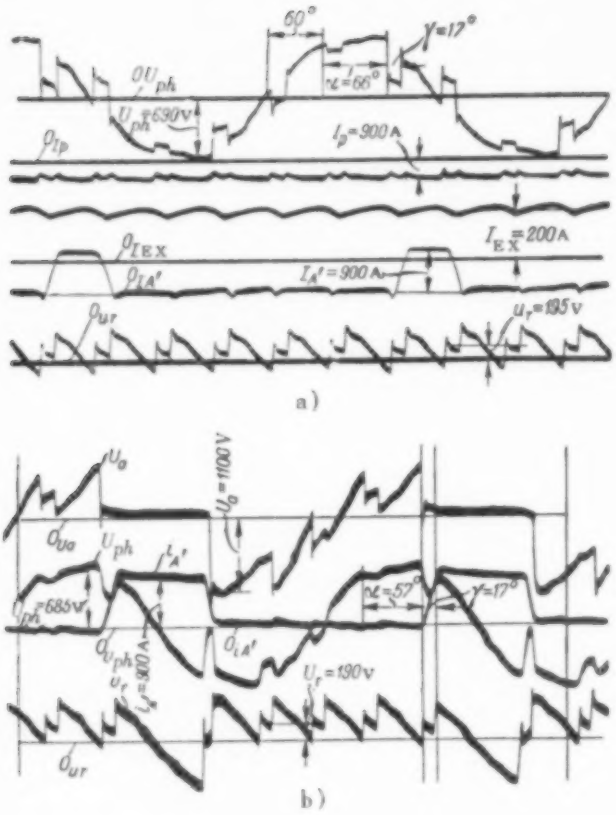

FIG. 2. Nominal condition of the installation: (a) with complete number of the rectifiers; (b) with incomplete number of the rectifiers.

On the benchboard of the station there is a signalling installation that indicates the following undesirable events: flashback in ignitrons, repeated omissions in ignitron firing, stopping of water flow or an excessive water temperature, stoppage of excitation of the main generators and so on. Moreover, an electronic indicator of the voltage on the rotor slip-rings of the hydrogenerator facilitates the control of the performance of the set.

Tests of the installation

Tests were first carried out on an equivalent load with a stalled rotor, and then with a generator running on no-load and on load. The tests showed that the installation ensures forcing of quick excitation and quick braking of exciting current. It may work with an incomplete number of rectifiers, thus permitting the replacement of a faulty rectifier without cutting off the converter. During these tests, the performance

of the ignitrons was checked under passing overloads (Table 1). Despite the fact that the amplitude of the p.d. between the rectifier anodes and cathodes in the ionic excitation installation was near to the nominal, forcing of the excitation during one min with a full number of rectifiers and with five rectifiers only, was not accompanied by a flash-back. In certain cases flash-backs were recorded when two adjacent rectifiers were cut off.

TABLE 1.

Conditions	Mean current of the most heavily loaded rectifier (A)	Duration (min)
Forcing with six ignitrons working	330	11
Work with five ignitrons	300	30
Forcing with five ignitrons working	660	1
Work with four ignitrons	450	15
Forcing with four ignitrons working	900	1

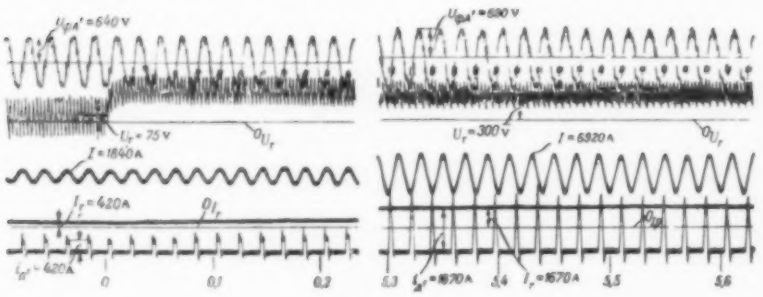

FIG. 3. Forcing of the excitation with the three phases of the main generator short circuited.

Oscillograms were taken at the nominal value of the rotor current of the main generator with a complete (Fig. 2a) and incomplete (Fig. 2b) number of rectifiers. In a converter without a ground equalizer, the normal instant of rectifier igniting was shifted by 60° from the point of passing of the phase voltage through the zero value. Therefore counting of the regulation angle is made from this moment.

In order to show the quickness of response of the system, oscillograms of the forced excitation, with the three phases of the hydrogenerator short-circuited, are shown in (Fig. 3). The minimum regulation angle was limited in such a way as to have the stator current, at the end of the transition period, not exceeding the fourfold normal value. The time necessary to obtain a full value of the voltage, with the forced excitation started and cut off, is approximately equal to 0.01 sec. These oscillograms were recorded during the work without the ground equalizer.

Thermal tests of the auxiliary synchronous generator were carried under two loads with a complete number of ignitrons. Results of these tests are shown in Table 2.

TABLE 2.

I_r (A)	U_l (V)	I_{ex} (A)	Temperature of incoming air (°C)	Increase of temperature (°C)			
				of incoming air	of stator steel	of rotor winding	of stator winding
650	845	163	30	11	44	38	37
800	840	182	29.5	16	56	50.5	46

Temperature of stator and rotor winding was measured by the resistance method. Increase of temperature of the stator steel was measured by a few thermocouples situated on the stator outer surface. Table 2 shows the maximum temperature which was recorded in the middle part of the stator. The maximum increase of temperature occurs in the stator steel.

Experimentally obtained values of voltages and currents and of angles of regulation and commutation were compared with calculated values. For this purpose relationships were determined for various converter networks. For the network without the ground equalizer they are:

$$U_r = \frac{3\sqrt{2}}{\pi} E \cos\alpha - \frac{3}{\pi}\left[x_g + \left(\frac{\pi}{3} - \frac{\gamma}{2}\right) r_g\right] I_d - \Delta U;$$

$$\cos(\alpha + \gamma) = \cos\alpha - \frac{\sqrt{2}\, x_g I_r}{E},$$

where x_g and r_g are the inductance and resistance of a generator phase; E is the effective value of the e.m.f. not distorted by the commutation process; ΔU is the voltage drop in the arc. Inductance x_g may be represented [1] in this form:

$$x_g = \frac{x_d'' + 3x_2 + 4x_3 + 3x_4 + x_5}{12}.$$

Taking into consideration that inductances of the second, third and fourth sequences are determined by the stator leakage fluxes and by the higher harmonic components of the flux in the gap, it is convenient to represent reactance x_2 as a sum of two terms:

$$x_g \approx \frac{x_d'' + x_5 - 2xl}{12} + \frac{3x_2 + 4x_3 + 3x_4 + 2xl}{12}.$$

The second term determines that part of x_g which is caused by leakage fluxes of the stator winding and by higher harmonics of the flux in the gap.

Fig. 4 shows a vector diagram of the auxiliary salient pole synchronous generator.

On this diagram the fundamental harmonic of the stator current is

$$I_1 \approx \frac{I_r}{\sqrt{2\pi}},$$

and the angle $$\varphi_1 = \tan^{-1} \frac{\gamma - \sin\gamma\cos(2\alpha+\gamma)}{\sin\gamma\cdot\sin(2\alpha+\gamma)}$$

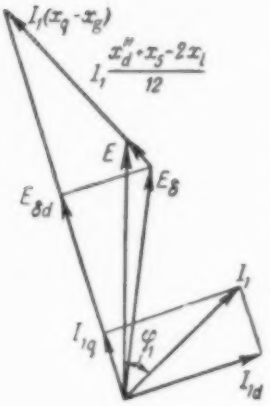

FIG. 4. Vector diagram of an auxiliary generator.

To determine ϕ_1 we may also use a simplified formula. Thus, on the condition of forcing with $\alpha = 0$; $\phi = \frac{3}{4}\gamma$; when working with high values of α, $\phi_1 = \alpha + \gamma/2$

Knowing the longitudinal component of the e.m.f. in the air gap, $E_{\delta d}$, the current in the machine longitudinal axis, and the load characteristic for this current at cos $\phi = 0$, we may determine the exciting current in the auxiliary synchronous generator.

As a certain approximation we may use instead of the load characteristic the no-load characteristic.

Comparison of data calculated by formulae and experimental data (see Table 3) shows that they agree rather well.

TABLE 3.

Quantity	U_r (V)	I_r (A)	α (°C)	γ (°C)	I_{ex} (A)
Experimental value	180	900	65	17	200
Calculated value	180	900	64	17.5	205

Conclusions

The tests showed that the ionic excitation system using sealed single-anode rectifiers ensures a good performance in all service conditions (forcing and cutting off excitation, working with an incomplete number of rectifiers and so on). These tests also showed that the ionic excitation installation acts very quickly (time of growth of the total voltage is of the order of 0.01 sec). The validity of the above method of calculating the currents and voltages of the excitation system is confirmed by experimental results, obtained during tests of installation.

The installation of ionic excitation in the Nizhnii-Svirsk HEPS may be used as an experimental basis for designing new and simpler control systems without gas-discharge devices, with simpler methods of the rectifier protection (grid instead of cumbersome quick-acting breakers), for trial of the new types of rectifier in different service conditions, processes of excitation control and so on.

Translated by S. Szymanski

REFERENCES

1. D.A. Zavalishin and A.Ia. Glebov; Ustanovivshiisia rezhim sinkhronnogo shestifaznogo generatora, rabotaiushchego v skheme ionnogo vozbuzhdeniia (Steady state conditions of

REFERENCES (cont.)

1. a synchronous six-phase generator working in a network with ionic excitation) in symposium "*Elektrosila*", No. 10 (1951).

IGNITRON IVS-200/2*

T.A. SUETIN

All-Union Lenin Institute of Electric Technology

(Received 5 November 1957)

Sealed rectifiers compare favourably with demountable (pump) rectifiers in their electric strength, load capacity, reliability in work, simple construction and smaller size. The use of sealed rectifiers instead of demountable ones permits a considerable cut in working expenses and capital expenses in converter substations. Ignitron IVS-200/2 is now widely used in converter design. At present it is used to equip converter sets of substations for electric urban traction, for ion excitation, electric drive etc.

1959

In the sealed mercury rectifier laboratory of the All-Union Lenin Institute of Electric Technology (V E T), a few types of ignitron IVS-200/2 were developed for mean current 200 A and back-voltage 2500 V. A description is given below of a construction, that is distinguished for its good working qualities and is now widely used.

Fig. 1 shows a general view in section of the ignitron IVS-200/2. The body of the ignitron is made as a welded cylinder with a water jacket. Anode and grid leads of the rectifier are made of glass and metal. Hermetical sealing of lead inlets is achieved by welding molybdenum glass with kovar (fernico) alloy. The anode lead is of high thermal strength and may work for a long time carrying heavy currents. The junction of the rectifier anode is made by using a flexible copper conductor fitted with a terminal, which is screwed into the anode rod. The flexible conductor allows the removal of the mechanical loads, due to the joining of the anode cable, from the glass insulator.

Anode and control grids are made of high quality graphite pressed in closed dies.

Ignitron IVS-200/2 has two igniters and an auxiliary (pick-up) anode. Addition in the ignitron of an auxiliary (pick-up) anode not only facilitates striking of the main arc, or in certain systems unloading the igniter, but also allows for control of the rectified voltage in these ignitrons by a grid, instead of by varying the moment of ignition of a cathode spot by the igniter.

* *Elektrichestvo*, No. 3, 80-82, 1958.

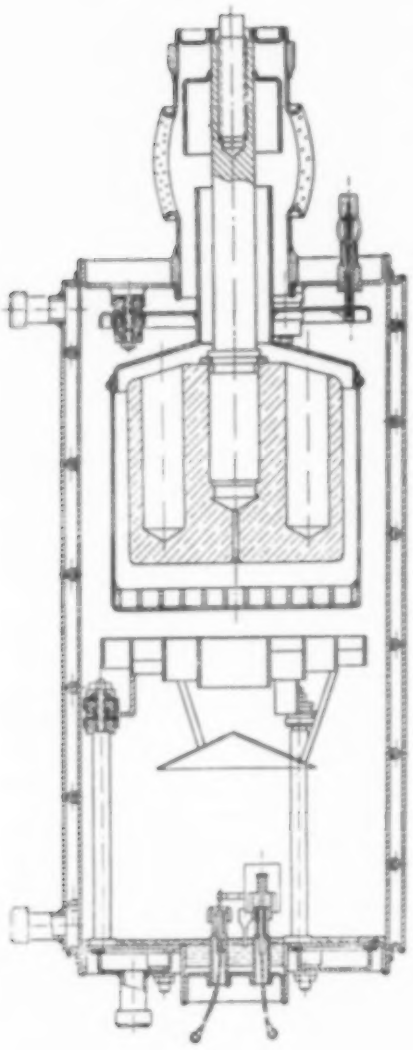

FIG. 1. Cross-section of ignitron IVS-200/2.

In the case when the auxiliary anode is fed by a sinusoidal voltage in phase with the main anode voltage, it is easy to obtain arcing of the auxiliary anode during almost the whole half-cycle of positive anode voltage. The moment of striking of the arc on the main anode depends in this case only on the moment of application to the grid of a positive trigger pulse. Thus, by varying the phase of a positive grid pulse we obtain the control of the rectified voltage in the same way

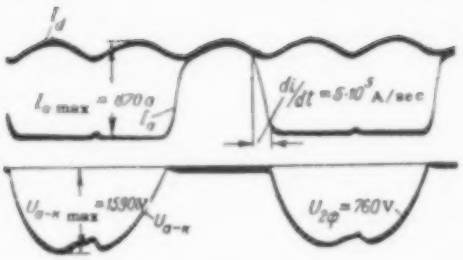

FIG. 2. Oscillograms of rectified current I_d, anode current I_a and p.d. between the anode and the cathode, U_{a-c}, during tests of an ignitron IVS-200/2 under rheostat load (mean rectifier current 240 A.

as is done in rectifiers with a permanent exciting arc (excitron).

A steel wafer base with igniters and a pick-up anode is welded together with a steel sleeve of a cathode flange. The presence of the steel sleeve permits quick replacement, when necessary, of igniters in a rectifier without cutting off a whole cathode flange. The cathode of the ignitron IVS-200/2 is water-cooled; during use, water flows around the cathode and the rectifier body.

To prevent hydrogen diffusion from the water jacket into the cylinder, which is inadmissible in sealed (pumpless) rectifiers because of vacuum deterioration, water-cooled rectifiers (i.e. the body and the cathode flange) are made from stainless steel or, in cases when low carbon steel is used, they should be enamelled. Both methods were tested under laboratory conditions and during long periods of normal service and gave equally good results.

In the first samples of ignitrons, igniters were made from silicon carbide. Experience showed that most of these igniters have a short period of service – 1500 - 2000 hr.

At present, in VET ignitrons, igniters are used made from boron carbide. Their electric characteristics are: ignition current not more than 12A, ignition voltage not more than 350 V. The period of service of the boron carbide igniters is estimated as not less than 20,000 hr, as may be assumed from the data obtained at present.

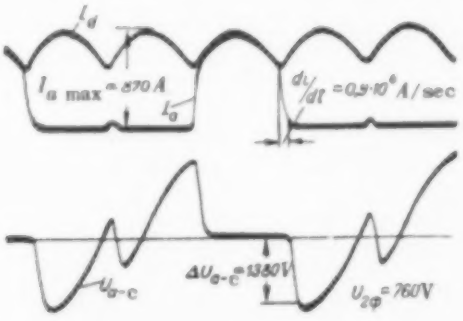

FIG. 3. Oscillograms I_a, I_d and U_{a-c} during the tests of rectifiers under short-circuit conditions (mean rectifier current 240 A).

We may point out that all igniters, even after working 15,000-20,000 hr, continue to work normally and do not require any alterations (forcing) in ignition circuits.

The period of service of sealed ignitrons is determined in practice by the period of service of igniters. Due to the presence of two igniters in ignitrons IVS-200/2 it may be safely assumed that the period of service of these ignitrons will be not less than five years. Technological processes developed by the VET laboratories in production of sealed metallic mercury rectifiers allow a high degree of degassing (exhaustion) of details and of the rectifier as a whole; this ensures stability of its properties during long storage, after which, as experiments have shown, rectifiers may be immediately used for work at the nominal current and voltage without preliminary electrical forming at a low voltage. The weight of the ignitron is 26 kg.

To determine electric parameters of ignitrons and to verify that they satisfy technical specifications, bench tests were carried out in VET. These tests were carried out in a three-phase zero wire network at the nominal phase voltage 760 V under two sets of conditions: using a rheostat as a load and in a short-circuit (Figs. 2 and 3).

Nominal anode currents were drawn for a long time and overloads up to 130 per cent of the nominal current were applied.

As can be seen from these oscillograms tests under short circuit conditions are the hardest ones, since at a high rate of decrease of the anode current ($dI_a/dt = 10^6$ A/sec) the anode back voltage jumps nearly up to the maximum value.

Bench tests were carried out with water-cooled rectifiers; water temperature was within the limits of 20 to 35°C.

On the basis of bench and service tests it has been found that ignitron IVS-200/2 has the following electric parameters

Mean anode current		200 A
Current overload:		
during 10 min		265 A
during 2 min		320 A
during 30 sec		450 A
Maximum back voltage		2500 V
Voltage drop in the arc not more than		16 V
Negative grid bias		150 V
Grid current (amplitude)		150mA
Current of the pick-up anode		1.5-2 A
Igniter parameters		
(a) ignition current	not more than	12 A
(b) ignition voltage	not more than	350 V
Cooling	forced water cooling	
Temperature of cooling water	+ 20 – + 35°C	

Water consumption at $\Delta t = 8°C$ 6 l/min.

During the bench tests ignitrons IVS-200/2 worked smoothly for long periods under nominal currents and under all overloads; grid control worked without failure, direct breaks and back ignitions did not occur.

Translated by S. Szymanski

1959

DISCUSSION

"MODIFICATION OF THE HEAVISIDE FORMULA"* **

B. KONORSKI
Lodz Polytechnic Institute, Poland

The method and formula (12) given by the author of the article are well known; they may be found even in textbooks on operational calculus. The Russian reader may find this formula in the book by Gardner & Burns (translated from English and published in 1951 by Gosizdat. This formula is by no means so universal; it deals only with one particular case, when the denominator $H(p)$ has only one zero root.

It is easy to obtain a more general formula assuming

$$pH(p) = \prod_{k=0}^{n} (p - p_k)^{m_k},$$

where $P_0 = 0$

$$\frac{G}{pH(p)} = \sum_{k=0}^{n} \sum_{s=1}^{m_k} \frac{A_{ks}}{(p - p_k)^{m_k - s + 1}}.$$

With these assumptions we get:

$$L^{-1} \frac{G(p)}{H(p)} = \sum_{k=0}^{n} \sum_{s=1}^{m_k} \frac{A_{ks}}{(m_k - s)!} t^{m_k - s} e^{p_k t},$$

in this case

$$A_{ks} = \frac{1}{(s-1)!} \left\{ \frac{d^{s-1}}{dp^{s-1}} \left[\frac{(p - p_k)^{m_k}}{p} \frac{G(p)}{H(p)} \right] \right\}_{p = p_k};$$

$k = 0, 1 \ldots n;$
$s = 1, 2 \ldots m_k.$

B. SAVIUK Kraiova, Rumania

* *Elektrichestvo*, No. 3, 86-89, 1958.
** Cf. O.M. Bogatyrev, *Elektrichestvo*, No. 2 (1957).

The "modification" of the Heaviside formula, proposed by Bogatyrev, has for a long time been in textbooks on Electric Technology (for example, I. Fallon, *Lecons d'electrotechnique*, Paris Gauthier-Villars, 865 (1948); I.S. Antoniu, *Chestine speciale de electrotehnica*, Bucuresti, Ed. Acad. R.P.R. (1956). Bogatyrev's article contains nothing new.

F. CSAKY
Budapest, Hungary.

The article contains a modification of the Heaviside expansion theorem in the case when the denominator of the fraction representing a function has multiple roots. The author uses the following method. The fractional operational equation, the solution of which we want to find, is expanded into partial fractions; coefficients of these fractions are determined, and from tables we find time solutions, corresponding to every fraction.

To determine the coefficients the author recommends expression (12) (Cf. also (1)).

In connexion with the article, I would like to say this. The time solution may be obtained by means of a single universal expression, avoiding the expansion into partial fractions and the use of tables. In different publications (see for example [2], we may find the following expression:

1959

$$F(t) = L^{-1}\{\varphi(p)\} = \sum_{k=1}^{m} \left\{ \frac{1}{(n_k-1)!} \frac{d^{(n_k-1)}}{dp^{(n_k-1)}} [(p-p_k)^{n_k} \varphi(p) e^{pt}] \right\}_{p \to p_k}. \quad (1)$$

where m is the number of different roots of the denominator of the function ϕ (p), and n_k the order of the kth root p_k. Function ϕ (p) is a Laplace transformation of the function F (t), i.e.

$$\varphi(p) = L\{F(t)\} = \int_0^\infty F(t) e^{-pt}\, dt.$$

If all roots of the denominator are unequal ($n_k = 1$, $k = 1,2 \ldots m$), then expression (1) assumes the form:

$$F(t) = L^{-1}\{\varphi(p)\} = \sum_{k=1}^{m} \{(p-p_k)\varphi(p) e^{pt}\}_{p \to p_k}. \quad (2)$$

Let us remark that expression (1) is only slightly more complicated than formula (12). Moreover, formula (12) gives only coefficients of partial fractions, but by expression (1) we may determine directly the required time function. The last property constitutes an advantage from a theoretical point of view, and the use

of the expression (1) for solving practical problems does not increase the amount of work in comparison with the method based on the expansion theorem.

The correctness of expression (1) may be easily proved by using a theorem on functions of a complex variable:
(a) by the Riemann-Mellin theorem [3],

$$F(t) = L^{-1}\{\varphi(p)\} = \frac{1}{2\pi j}\int_{c-j\infty}^{c+j\infty} \varphi(p)\, e^{pt}\, dp. \tag{3}$$

(b) by the theorem of residues [3, 4],

$$\frac{1}{2\pi j}\int_{c-j\infty}^{c+j\infty} \varphi(p)\, e^{pt}\, dp = \sum_{k=1}^{m} \operatorname{Res}_{p=p_k} \{\varphi(p)\, e^{pt}\}. \tag{4}$$

We assume that the number of poles ϕ (p) to the left of the straight line p-c is equal to m (c is a real number);
(c) If any function ψ (p) at a point $p = p_k$ has a pole of the order n_k, then the residue of the function (p) may be determined by the relationship:

$$\operatorname*{Res}_{p=p_k}\{\psi(p)\} = \left\{\frac{1}{(n_k-1)!}\frac{d^{(n_k-1)}}{dp^{(n_k-1)}}[(p-p_k)^{n_k}\psi(p)]\right\}_{p\to p_k} \tag{5}$$

Let

$$\psi(p) = \varphi(p)\, e^{pt};$$

then, on the basis of (5), (4) and (3), we get expression (1).

Finally, two further remarks:
(1) Expression (1) is nothing other than a generalization of the Heaviside expansion theorem. In fact let

$$\varphi(p) = \frac{G(p)}{pH(p)} \tag{6}$$

and let the equation $H(p) = 0$ have only m unequal roots p_k equal to zero. From expression (1a) we get:

$$\left\{(p-p_k)\frac{G(p)}{pH(p)}\, e^{pt}\right\}_{p\to p_k} = \frac{G(p_k)}{p_k H'(p_k)}\, e^{p_k t}. \tag{7}$$

The term corresponding to the zero root of the denominator will be:

$$\left\{(p-0)\frac{G(p)}{pH(p)}e^{pt}\right\}_{p\to 0}=\frac{G(0)}{H(0)}\,. \tag{8}$$

In this case, expression (1) leads to the inverse Heaviside expansion theorem:

$$F(t)=\frac{G(0)}{H(0)}+\sum_{k=1}^{m}\frac{G(p_k)}{p_kH'(p_k)}\,. \tag{9}$$

If the function $H(p)$ has multiple roots[or if $p = 0$ is also a root of the equation $H(p) = 0$], then on the basis of expression (1) we may also get the expression similar to expression (9) (see for instance [1,5, 6]. But in this case the expression becomes complicated; therefore it is more convenient to use expression (1).

(2) If instead of the Laplace transformation we use the Carson [7] and Wagner [6] transformations:

$$f(p)=\mathfrak{F}\left\{F(t)\right\}=w\left\{F(t)\right\}=p\int_0^\infty F(t)e^{-pt}dt, \tag{10}$$

then, in using expression (1), we have instead of $\phi(p)$ to write everywhere

$$\mathfrak{F}(p)=\frac{f(p)}{p}\,.$$

1959

REFERENCES

1. M.F. Gardner and J.L. Burns; *Perekhodnye protsessy v lineinykh sistemakh (Transient processes in linear systems)*, Gostekhizdat (1951).
2. J. Millmann; Laplacian Transform Analysis of Circuits with Linear Lumped Parameters, *Elect. Engrg.* (1942).
3. M.I. Kontorovich; *Operatsionnoe ischislenie i nestatsionarnye iavleniia v elektricheskikh tsepiakh (Operational calculus and transient processes in electric networks)*, Gostekhizdat (1949).
4. V.I. Smirnov; *Kurs vysshei matematiki (Textbook of advanced Mathematics)* VIII, part 2, Gostekhizdat (1951).
5. I.I. Teumin; *Spratochnik po perekhodnym elektricheskim protsessam* (Reference book on transient electric processes), Gosizdat literatury po voprosam sviazi i radio (1951).
6. K.W. Wagner *Operatorenrechnung und Laplacesche Transformation. (Operational calculus and Laplace transformation)*, J.A. Bart Verlag, Leipzig (1950).
7. J.R. Carson *Electric Circuit Theory and the Operational Calculus*, New York (1958).

V.M. GRESHNIAKOV and A.A. MODEROV
Kalinin Polytechnic Institute, Leningrad

Formula (12), recommended in Bogatyrev's article is well known and may be found in books, for instance in the book *Transient processes in linear circuits* by Gardner and Burns. The derivation of formula (12) given by Bogatyrev corres-

ponds to the derivation given by Gardner and Burns. The difference consists in that Bogatyrev derives the formula on a simple particular example, whilst Gardner and Burns deduce the formula for a general case.

The latter deduction is made in a rigorous mathematical way and is distinguished by its clarity; it takes nearly as much or a little more space than Bogatyrev's deduction.

Moreover, as Bogatyrev points out himself, formula (12) gives only the last coefficient $A_k^{(n-1)}$ in the fraction $\frac{A_k^{(n-1)}}{p-p_k}$

for the n-fold multiple root. The usefulness of this formula for determination of remaining coefficients is connected with an artificial method of notation used by the author.

Indeed, it is quite unusual in mathematical literature to ascribe to the same index in the same formula different meanings, as was done by Bogatyrev (index n) Thus, in an example given in the Bogatyrev article, he puts in evaluating index A_1, $n = 3$ in one place of the formula (12) [in expression $(p-p_k)^n$], and in other places of the same formula (12) he puts $n = 2$.

It is quite natural that the Gardner and Burns formula, which gives any arbitrary coefficient of expansion, contains, instead of a single index n in formula (12), two indices: m_k, the order of the kth root, and the ordinal index j, taking all integral values from unity to m_k.

Thus, formula (12) in Bogatyrev's article is not new and has the above defects.

P.A. SAPOZHNIKOV and N.D. SAPERSHTEIN
Leningrad Military Mechanical Institute

In dealing with transient processes by operational methods it is necessary to solve the problem of transformation of operational solution of the form $G(p)/H(p)$. It is done by expanding the operational solution into partial fractions, transforms of which are either known or easily found. Bogatyrev considers the expansion of fractional rational expressions of the type $G_k(p)/H_m(p)$ (in the case of the Laplace transformation $K < m$, and in the Carson transformation $K \leq m$) in the presence of single and multiple poles. Having written, as an example, about the expansion of a non-reducible fraction (1), the author of the article makes use of a well-known method of consecutive multiplication of both sides of the identity

$$\frac{G(p)}{H(p)} = \frac{A_0}{p} + \frac{A_1}{(p-p_1)} + \frac{A_2}{(p-p_2)} + \frac{A_2'}{(p-p_2)^2}$$

by denominators of the right hand side terms, i.e. cancels out poles 0, p_1, p_2; and, from the identities so obtained, he determines coefficients A_0, A_1, A_2 A_2'. In the case of absence in the numerator of the Carson expression of the factor p, the author of the article also recommends a well-known method of introducing this

factor into the numerator and denominator. But he does not show that expressions (4) and (5) for the coefficients A_0 and A_1 so obtained may be reduced to a more general and more convenient form, namely

$$A_1 = \left[\frac{G(p)}{\frac{H(p)}{p-p_1}}\right]_{p=p_1} = \left[\frac{G(p)}{\frac{H(p)-H(p_1)}{p-p_1}}\right]_{p=p_1} =$$

$$= \left[\frac{G(p)}{H'(p)}\right]_{p=p_1} = \frac{G(p_1)}{H'(p_1)}$$

and similarly

$$A_0 = \frac{G(O)}{H'(O)}.$$

This makes the expression for A_0 and A_1 more similar to the usual form of the Heaviside formula and also allows for the determination of coefficients of partial fractions (for single poles, they are residues as well) in the case when $G(p)$ and $H(p)$ are not polynomials, but arbitrary functions having no common roots. Thence it follows that the transformation of meromorphic forms is possible.

In the last case it often happens that it is easier to evaluate $G(p_1)/H(p_1)$ than

$$\frac{G(p_1)}{\left[\frac{H(p)}{p-p_1}\right]_{p=p_1}}$$

For example, in transforming the operational solution (by the Laplace method)

$$\frac{1}{p}\tanh\frac{p}{2} = \frac{\frac{1}{p}\sinh\frac{p}{2}}{\cosh\frac{p}{2}},$$

$$G(p) = \frac{1}{p}\sinh\frac{p}{2};\ H(p) = \operatorname{ch}\frac{p}{2},$$

it is much easier to evaluate

$$\frac{G(p_k)}{H'(p_k)} = \frac{\frac{1}{p_k}\sinh\frac{p_k}{2}}{\frac{1}{2}\sinh\frac{p_k}{2}} = \frac{2}{p_k}$$

[$p_k = (2_k + 1)\ \pi i$ – single roots $\cosh p/2$] than "merely to cancel out" in the denominator the factor $(p - p_k)$.

O.M. BOGATYREV
Moscow

Formula (12) is known in different forms in scientific literature, but in textbooks in our country not much attention has been paid to it. For solution of transient processes many various formulae are derived according to the nature of roots and for different applied voltages. These formulae depend upon the kind of transformation, whether Laplace or Carson. The aim of my article is to suggest the use in all cases of the only one and unique universal formula [formula (12)] that is easy to deduce in an elementary way and does not depend upon the type of transformation.

With Konorski's remark that formula (12) "is not as universal as that" I cannot agree. It may seem so if we disregard the fact that the number n in different places in formula (12) has different meanings. Thus, in the expression $(n\text{-}p_k)/n$ index n shows that the root p_k is the nth root, i.e. the number n coincides with the number m_k in the formula given by Konorski and in Gardner and Burns. In other parts of formula (12) n takes all integral values from unity to the number equal to the order of the root p_k; i.e. n coincides with the current index s in the Konorski formula or with the index j in the Gardner and Burns formula.

I have seen two editions of the Gardner and Burns book. The formula in question is encumbered there by indices. The formula given by Konorski, being more general, does not differ in principle from my formula (12), except for the expression for A_{ks} in Konorski's article, where the factor p is inserted in the denominator, probably by mistake.

References given by Saviuk contain nothing new, since the formula in question is not derived there, it is only quoted besides other similar formulae; there is no suggestion whatsoever about the universal use of this formula.

The main point in F. Csaky's comment is this: its author thinks that expression (1) "from the theoretical point of view" has certain advantages and practically does not require more labour than the universal method and the formula recommended in my article. F. Csaky considers that the universal formula gives "only coefficients" of partial fractions, whilst formula (1) gives directly the time solution. This is correct, but the author ignores the fact that the evaluation of coefficients constitutes 95 per cent of the whole problem.

The defects of the formula and of its deduction that are criticized by V.M. Greshniakov and A.A. Moderov, in my opinion are advantages. In fact, what could be simpler than substituting into the binomial $(n\text{-}1)$ (and only into the binomial) of formula (12) the values from unity to n, where n is the order of a given root p_k, and so on for every root. The deduction of the formula is elementary, easy to understand and not tiresome.

The authors write that my notations are artificial. In my opinion they are very convenient, since in the formula there are only two indices, k and n, whilst in the Gardner and Burns notations there are many indices in double sums. It

seems to me that their formula is not widely used just because it looks so cumbersome.

I derived formula (12) by a generalization of operations shown in one particular example. I never wrote that this formula is essentially a new one, but I want this formula, that was known in this or another form, to become universal and indispensable in the form that is given in my article.

P.A. Sapozhnikov and N.D. Sapershtein wrongly use the example of evaluation of meromorphic functions, while the theory applies to fractional rational functions (and this point, it follows from their remark, is known to them).

Translated by S. Szymanski

1959

SYNTHETIC COMPOUNDS OF HIGH MOLECULAR WEIGHT AS DIELECTRICS*

K.A. ANDRIANOV

All-Union Lenin Institute of Electric Technology

(Received 28 November 1957)

The progress of modern chemistry of compounds of high molecular weight has reached such a level that the possibility now exists of considerably improving the polymers already known and of producing new ones, not yet obtained, with properties specified in advance. To build the chains of polymer molecules, chemists now make use not only of carbon and silicon but also of other elements: titanium, aluminium etc. All this offers wide opportunities for obtaining many diverse polymers which differ basically in the structure of their molecules and their technical properties. The use of carbon compounds only led to polymers with organic molecular chains. Such polymers have a rather low thermal stability and can be used for a long time at temperatures up to 130°C.

With the use of silicon in combination with organic groups the possibility appeared of building polymers with mineral molecular chains, consisting of atoms of silicon and oxygen surrounded by organic groups.

This development has already resulted in the production of a large group of polymers, polyorganosiloxanes, and in the production of electro-insulating materials with high thermal stability, which can work for a long time at a temperature of 180°C. The use of other inorganic elements, aluminium, titanium, boron and others, greatly increases the prospects of the synthesis of polymers with mineral molecular chains, consisting, for example, of: silicon, oxygen and aluminium; silicon, oxygen and titanium; silicon, carbon, oxygen and aluminium, etc., which are surrounded by organic or silico-organic groups.

This offers good prospects for obtaining new polymers which are similar in their molecular chain structure to silicates but are surrounded by organic or silico-organic groups. Such polymers should combine properties of both kinds; the high thermal stability proper to silicates, and elasticity, which is a characteristic property of the organic part of the molecule.

Along with the above discussed trends in the synthesis of high polymer sub-

* *Elektrichestvo*, No.4, 1-10, 1958.

stances, during recent years new methods of polymerization have been widely developed; these methods make use of new catalysts and they enable us to obtain polymers of a strictly regular structure with great molecular weight and better physical-technical properties than those of the same polymers obtained by the old methods.

Thus, for example, polyethylene obtained by the old methods melts at 125°C, but that obtained by new methods at 170°C. The use of mechanical chemical methods for production of block- and kraft-polymers on the basis of many very varied polymers enables us to change very considerably the properties of the existing polymers in a desired way.

The use of high-energy particles (γ - rays and others) for changing polymers also enables us to change properties of the known polymers according to our requirements.

Synthetic compounds of high-molecular weight play an important role in electric technology, and their use for the insulation of electric machines, apparatus, cables and other electrical and radio devices increases each year. This is explained by their good electrical and physical-technical properties (particularly their thermal stability and resistance to moisture) compared with natural polymeric substances.

Thus their use enables designers to construct machines and apparatus and to solve problems the solution of which would be impossible using only natural polymers.

1959

Polymeric hydrocarbons

Polymeric hydrocarbons proved themselves as good dielectrics, particularly in the production of high-frequency cables and various types of radio apparatus.

Nevertheless, these polymers which were produced by ordinary methods of polymerization had a low melting point. In consequence, the region of their application, in spite of good electric properties, was limited to temperatures up to 85°C.

Recently new catalysts for polymerization have been obtained, the use of which leads to the production of polymeric hydrocarbons and other polymers with a strictly regular structure; they are now known as "isotactic polymers".

Isotactic polymers possess a regular molecular chain structure; this is due to regular alternation of the carbon atoms with the same space configuration in the main chain. These polymers are characterized by their high melting point and high mechanical strength in the aligned direction in comparison with polymers, produced by the polymerization of monomers by the widely used radical mechanism of polymerization.

Isotactic polymers are produced by the polymerization of monomers in the presence of special catalysts: triethyl aluminium and titanium tetrachloride. The mechanism of polymerization is ionic in nature and, in comparison with the radical

one, which is characterized by the branching of molecular chains and the formation of amorphous products, leads to the formation of polymers with strictly regular molecular structure and a high degree of crystallinity. At present the isotactic polyethylene, polypropylene, polybutene, polystyrene and other polymers are synthesized. They are all polymeric hydrocarbons and at ordinary temperature are solid crystalline substances, with small dielectric losses for various frequencies of an electric field.

As opposed to the polymers of the same class, but produced by the ordinary methods, they have a higher melting point and are not soluble in the majority of solvents (Cf. Table 1).

TABLE 1

Polymer	Temperature of the transition of the first kind (softening point) (°C)	Density (g/cm^3)
Polyethylene:		
isotactic	170...175	
ordinary	110...125	0.92
Polypropylene:		
isotactic	158...170	0.92
ordinary	75	0.85
Polystyrene		
isotactic	230	1.08
ordinary	70...100	1.04

The properties of isotactic polymers permit a very great extension of the use of polymeric hydrocarbons for electric insulation. Due to the increase of temperature of their melting point they can be used in the form of plastic masses, as cable sheaths and as fibres for working temperatures of 105°C and more.

The regular structure of the isotactic polymer hydrocarbons ensures a high degree of crystallinity and makes them suitable for preparing fibres [2]. The properties of the fibres of the isotactic polymers are shown in Table 2.

TABLE 2

Polymer	Limiting tensile strength (kg/mm^2)	Specific strength (g/denier)	Total elongation at breaking (%)	Work of breaking (g/denier)	Density (g/cm^3)
Isotactic polypropylene ..	77	9.3	31	1.6	0.92
Nylon	54	5.3	26	0.9	1.14
High strength nylon	78	7.7	14	0.7	1.14
Steel	210	3.0	8	0.2	7.8

Fibres made of such substances as polypropylene or polystyrene do not absorb moisture at all. They posses high electric resistivity greatly exceeding that of other fibres. These fibres have a wide range of application in the insulation of

magnetic wires and in the production of different electric insulating materials. The disadvantage of these fibres is their low melting temperature, which prevents their use in insulation above class A.

Table 3 shows the electric properties of the pure polymeric hydrocarbons, which were recorded at a temperature of 20 ± 2°C. Electric strength is shown for a specimen 1.5 mm thick.

TABLE 3

Polymer	ρ_v (Ω cm)	$\tan\delta \times 10^4$	E_{str} (kV/mm)	ϵ
Polyethylene:				
isotactic	$10^{17}\ldots10^{15}$	3...6	20...25	2.2...2,3
ordinary	$10^{17}\ldots10^{15}$	2...5	24...26	2.25...2,35
Polypropylene:				
isotactic	$10^{16}\ldots10^{14}$	4...8	18...24	2.15...2,3
Polystyrene:				
isotactic	$10^{16}\ldots10^{14}$	2...5	20...22	2.5...2,55
block	$10^{17}\ldots10^{14}$	1...2	24...28	2.5

1959

Polytetrafluoroethylene

Among the heat resistant polymers polytetrafluoroethylene is of the greatest interest. It has a regular linear structure of molecules, which ensures its crystalline structure, and possesses a high thermal stability and softening temperature (about 400°C) [12].

Polytetrafluoroethylene is a non-polar polymer; its permittivity within the frequency range 50-10^6 c/s, is equal to 2.0-2.2; its tangent of the loss angle, equal to 2×10^{-4}, does not depend upon the field frequency up to 10^8 c/s and varies little with temperature within wide limits. It possesses a high resistivity (up to 10^{17} Ω cm) and its electric properties vary little with temperature and under the influence of moisture.

It is necessary to point out that the electric strength of polytetrafluoroethylene greatly depends on the time of the voltage application. For short periods of application for specimens 1.5 mm thick it is 15-20 kV/mm, for long periods it decreases to 6-8 kV/mm. Difficult working and ability to creep at low temperature limit its use.

Nevertheless, the high thermal stability of the polymer, which permits its use at temperatures of 250°C and even 280°C, together with its small dielectric losses and high electric resistance, permit its use in the production of high frequency cables, where its tendency to creep at low temperature and its lower electric strength under a long-lasting applied voltage are of no serious importance.

Polyester resins

Polyesters as dielectrics are of great interest; they are known under the name "unsaturated polyester resins" [3-6]. They are produced in the form of liquids, which are solutions of linear unsaturated polyesters in unsaturated compounds stabilized by inhibitors. Such liquid products, when heated in the presence of initiators of the peroxide type, become solid infusible polymers, which possess valuable properties. Polyesters are obtained from diatomic alcohols, glycols and unsaturated dibasic acids, for example, maleic acid.

In order to decrease the polyreactivity of a polyester and to increase its elasticity, the mean distance between double bonds is increased by replacing a part of the unsaturated acid by an equivalent quantity of a saturated dibasic acid: phthalic, adipic, sebacic and others.

Unsaturated polyesters are also modified by monobasic acids and oils (castor oil and others) to obtain less viscous polymers. Such polyesters are usually dissolved in unsaturated compounds, especially in styrene, which acts as a solvent and reacts with the unsaturated ester, thus producing a three-dimensional infusible polymer. This is due to the linking of unsaturated linear ester molecules by styrene. Quinones and amines are used as inhibitors. Peroxides are used as accelerators for solidification.

Industry produces various polyesters, among which KGMS-1 and KGMS-2 are used as dielectrics. Table 4 gives the properties of liquid and solid polyester resins according to the data supplied by the VEI. From the data given in Table 4, it is seen that polymers possess high electric strength and high volume resistivity; the insignificant variation in dielectric characteristics of specimens, after they have remained in a humid atmosphere, proves their rather high moisture stability. This is confirmed by tests of specimens which are kept in an atmosphere with a relative humidity of 98 per cent at temperatures 20°C + 40°C [Fig.1].

The introduction into polymers of fillers decreases shrinking, the coefficient of thermal expansion of the sealing compound and the exothermal heat of the reaction of copolymerization. Therefore, the possibility of cracking decreases and the thermal conductivity of compounds increases.

Table 5 shows dielectric characteristics of polymers with fillers. In electric insulation a polyester made from terephthalic acid and ethylene glycol plays an important role; it is known under the names of lavsan, mylar and Terylene. This polymer, obtained in INEOS of the U.S.S.R. Academy of Sciences, has a comparatively straight linear chain; it crystallizes and forms strong fibres and mechanically strong films. The melting point of lavsan is 220-240°C and breaking stress 400-500 kg/cm². The aligned fibres and films have a greatly increased strength, and breaking stress lies within the limits 350-4500 kg/cm². Electric properties of lavsan are high; for example, the tangent of the loss angle for lavsan films at a frequency of the electric field 50 c/s and temperature 20°C is 0.005-0.01 and

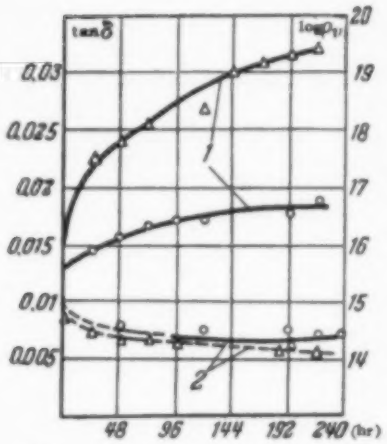

FIG.1. Curves of tan δ (curve 1) and ρ_v (curve 2) as functions of the time of wetting.

varies little up to 100°C in a humid atmosphere. Its volume resistivity is 10^{14}-10^{15} Ω cm. Its permittivity is 3-4. Lavsan is easily made into fibres, films, laminae etc. Lavsan fibres are of great interest since they can be successfully used for the insulation of conductors, and lavsan films, owing to their great mechanical and electrical strength (100 kV/mm for films 0.11 mm thick), can be widely used for insulation of slots in electric machines instead of lacquered fabrics, micanite etc. This results in a much better filling of the slot by copper.

Polyester resins made from terephthalic acid and a mixture of alcohols, glycerine and glycol, have a branched molecular structure. Therefore they cannot crystallize and dissolve in solvents with the formation of lacquers. Such lacquers form mechanically strong films, and, by coating copper conductors with these lacquers, we get enamelled conductors of greater mechanical strength than that of vinyflex enamelled conductors.

TABLE 4. Properties of solid polymers

Characteristics		KGMS-1	KGMS-2
In the initial state	tan $\delta \times 10^4$ at frequency 50 c/s	142...250	168...190
	Permittivity	3.7...4.3	3.7...4.0
	Volume resistivity (Ω cm)		
	at 20°C	$1.1\cdot10^{14}$...$4.0\cdot10^{15}$	$1.7\cdot10^{14}$...$1.5\cdot10^{15}$
	at 120°C	$1.2\cdot10^{11}$...$8.9\cdot10^{12}$	$1.8\cdot10^{11}$...$5.8\cdot10^{12}$
	Electric strength (kV/mm)	21.8...29.2	21.1...27.1
After remaining 48 hr in an atmosphere of tropical humidity at+ 50°C	tan $\delta \times 10^4$ at frequency 50 c/s	191...292	199...290
	Volume resistivity at 20°C	$1.0\cdot10^{13}$...$3.1\cdot10^{14}$	$5.4\cdot10^{13}$...$7.7\cdot10^{13}$
	Electric strength (kV/mm)	23.2...28.3	25.4...27.5
	Frost resistance	-60°C	-60°C
	Shrinkage at solidification (%)	9.2	9.5

N.B. All properties are shown after heating the specimen for 6 hr at 120°C; thickness of the specimen 0.9 ± 0.1 mm.

IA polyester 124 and a lacquer, modified by the addition of substances binding linear molecules, have been produced in the VEI; this lacquer is used for the production of mechanically strong enamelled conductors which are stable in solvents, and which can work for a long time at a temperature of 130°C in machines with Class B insulation.

TABLE 5

Composition of the sealing compound	Parts by weight	In the initial state			After remaining 48 hr in an atmosphere with relative humidity 97 ± 2 per cent	
		$\tan\delta \times 10^4$	ρ_v (Ω cm)	E_{str} (kV/mm)	$\tan\delta \times 10^4$	ρ_v (Ω cm)
KGMS-2 . . .	100					
Quartz sand .	60	272	$2.8 \cdot 10^{13}$	29.0	1380	$2.8 \cdot 10^{11}$
KGMS-1 . . .	100					
Quartz sand .	60	370	$3.4 \cdot 10^{13}$	30.0	1080	$1.0 \cdot 10^{13}$
KGMS-2 . . .	100					
Mica	60	308	$8.0 \cdot 10^{14}$	31.4	1350	$3.0 \cdot 10^{12}$
Titanium dioxide . .	3					

In electric technology, moreover, polyester resins are used as impregnating and casting compositions for the production of textolite. The high impregnating capacity of polyester resins ensures good impregnation of products: on heating a uniform insulation is formed. The use of these resins enables us to avoid the difficulties connected with the porosity of an insulation obtained by impregnation with ordinary lacquers [10]. Articles joined by polyester compounds are distinguished by their good cementation, high electrical and mechanical properties, high vibration stability, frost resistance, increased moisture resistance and operational reliability.

Hermetic sealing of electrical apparatus by filling with polyester resins gives protection from vibration, mechanical damage and atmospheric influence [7].

Epoxide resins

Epoxide resins are obtained by the reaction of different diphenyls with epichlorohydrin and usually have a softening temperature of 40-120°C. By treatment with amines they solidify at room temperature and become infusible and insoluble. Anhydrides of phthalic, maleic and other acids cause the epoxide resins to solidify when heated up to temperatures of 120°C and higher. In industry, the epoxide resins made from diphenylpropane are used; they are issued under trade marks E-40, E-37, ED-6.

At temperatures 90-100°C epoxide resins become liquid and at these temperatures they can remain unchanged during a rather considerable time [9]. They show good adhesion to metals and non-metallic materials. Electric properties of epoxide resins are high:

$\rho_v = 10^{15} - 10^{17}$ Ω cm; $\tan\delta = 0.006 - 0.01$; $\epsilon = 3.7 - 4.2$; $E_{str} = 20 - 24$ kV/cm for a specimen 1.2 mm thick.

In the electrical industry the epoxide resins are mainly used as glues in laminated insulation and as a cast insulation. For filling up current transformers, epoxide-polyester compound E-37 has been developed and is in use; for protection of semiconductor apparatus, epoxide-polyester compounds K-168 and K-239 are used. Compound E-37 consists of epoxide resin E-37 with addition of a polyester as a plasticizer component. Quartz powder serves as a filler. Phthalic anhydride with a small addition of maleic anhydride is used as a solidifying agent.

After the introduction of the anhydrides of acids into an epoxide resin, heated up to 80-100°C, the mixture at first becomes more liquid; after further heating it becomes more viscous, and gradually a solid infusible polymer is formed. The electric properties of Compound E-37 (20 per cent polyester) are given in Table 6.

Compound E-37 with a filler is used as a sealing insulation of current transformers for voltages up to 10 kV.

TABLE 6

Conditions of test	Volume resistivity (Ω cm)	Tangent of the loss angle	Electric strength (kV/mm)
At 20°C	$2.6 \cdot 10^{13}$	0.004	24.5
At 100°C	$7.2 \cdot 10^{11}$	0.083	23.0
After remaining 48 hr in a humid atmosphere	$7.9\ 10^{14}$	0.003	–

Fig.2 shows the dependence of the tangent of the loss angle of a sealing insulation on voltage, and Fig.3 the dependence of insulation resistance on temperature.

Fig.4 shows the electric strength as a function of the thickness of the specimen of the compound E-37.

Tan δ somewhat increases with temperature, but within the range of temperatures 20 ± 80°C it remains within the range 0.02-0.08. Under the continuous influence of a temperature of 120°C, the impact strength of the cast insulation preserves its initial value and even slightly increases, from 5 to 7 kg/cm/cm². The compound is easily cast in moulds and easily machined.

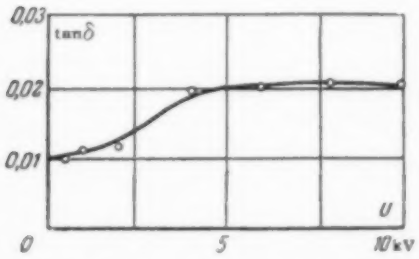

FIG.2. Tan δ as a function of voltage for an epoxide-polyester compound.

Current transformers filled with the fused cast epoxide-polyester compound E-37 with a filler (quartz powder) were tested under short-circuit conditions. These tests showed that they can withstand an electro-dynamic load at short-circuit for a current 500 times above the nominal current, and a thermal load of 1 sec for a current 100 times greater than the rated one. Examination of the sealing insulation of transformers after the short-circuit tests shows a good stability of all characteristics and the absence of any deformations.

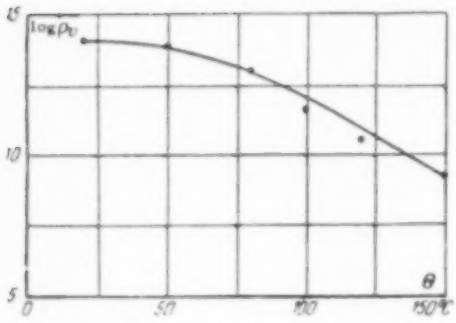

FIG.3. Volume resistivity of an epoxide-polyester compound as a function of temperature.

Epoxide-polyester compounds K-168 and K-293, which are used for hermetic sealing of apparatus, consist of epoxide resin E-37 or ED-6, plasticized by the polyester MGF-9. Compound K-293 contains moreover a filler (quartz powder) and a plasticizer (dybutyl phthalate). As solidifying agents for these compounds hexamethylenediamine or polyethylenepolyamine are used.

Compounds K-168 and K-293 may be used as sealing cold solidifying compounds. They possess the following characteristics: $\rho_V = 10^{12}$-10^{13} Ω cm at 20°C, and 10^{11}-10^{12} Ω cm after reamining 24 hr at + 40°C in a medium of the relative humidity 95 ± 3 per cent; for a frequency 10^6 c/s at 20°C and also after remaining 24 hr at + 10°C in a medium of the relative humidity 95 ± 3 per cent, their tan $\delta < 0.1$ and their resistance to frost is - 60°C.

Polymers based on acrylic and metacrylic esters

Compounds MBK-2 and MBK-3 were developed and are produced on the industrial scale by the All-Union Instrument Scientific Research Institute, Ministry of the Electric Technology Industry; they are based on acrylic and metacrylic esters; they differ from one another in their degree of elasticity, which depends upon the content of plasticizers.

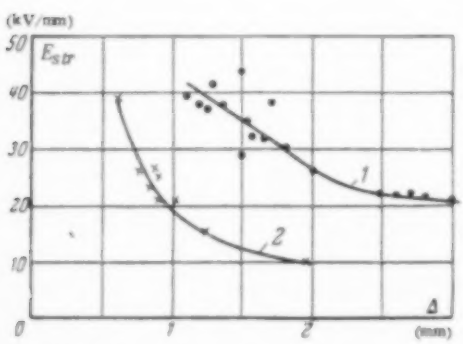

FIG.4. Electric strength of an epoxide compound as a function of its thickness: (1) θ = 20°C; (2) θ = 100°C (puncture in the transformer oil).

Compounds MBK are used in the electrical industry, particularly for insulation in electric motors immersed in water, and also in the radio industry. These compounds are liquids, which polymerize and become solid at temperatures of 100-110°C. By introducing appropriate initiators of polymerization, the MBK compound can be made to solidify even at 20°C.

The principal properties of Compounds MBK, after their polymerization at 70-75°C for 8 hr and after subsequent heating at 100-105°C for 8 hr, are shown in Table 8. The high water-resistance of the compounds MBK permitted their use for the protection of windings of the electric motors

immersed in water, which are used for driving water pumps. The windings of these motors successfully withstand a test under hydraulic pressure of 3 atm for 6 hr and the short-circuit conditions in a wet state at - 25°C. After intermittent work in water over more than 1500 hr the insulation resistance of these motors remains at the level of 500 MΩ.

TABLE 7

Characteristics	Epoxide resin	Epoxide polyester compound	Epoxide polyester compound with a filler (quartz powder)
Tangent of the loss angle multiplied by 10^4			
at 20°C	10 ... 20	20 ... 40	100 ... 300
at 80°C	300 ... 500	400 ... 800	600 ... 800
after remaining in water 48 hr	10 ... 30	40 ... 50	—
Volume resistivity, (Ω cm)			
at 20°C	10^{15}	10^{15}	10^{14} ... 10^{15}
at 80°C	10^{11}	10^{11}	10^{11}
after remaining in water 48 hr	10^{14}	10^{14}	—
Electric strength (kV/mm)	25 ... 30	25 ... 30	25 ... 30
Permittivity	4.0 ... 4.5	—	5.0 ... 6.0
Impact strength (kg cm/cm²)	4.0 ... 6.5	6.0 ... 8.0	4.0 ... 6.0
Temporary compression strength (kg/cm²)	900	—	900
Temporary bending strength (kg/cm²)	750 ... 1 000	600 ... 750	800 ... 900
Temporary tensile strength (kg/cm²)	—	—	550
Thermal stability according to Marten's method (°C)	60 ... 70	55 ... 60	60 ... 70

The apparatus coils, which remained for 20 days under conditions of tropical humidity with a periodical dew-fall, show an insulation resistance above 100 MΩ. It has been found that the use of the MBK compounds, which eliminate all cavities in windings, brings about a considerable decrease in overheating of the apparatus coils.

Polyurethane resins

Polyurethane resins recently have found wide practical application in different branches of technology, particularly as adhesive substances. For the manufacture of electric insulation polyurethanes are of great interest; they are compounds of high molecular weight and are based on polyesters and diazocynate. These

TABLE 8

Characteristics	Type of compound		
	MBK-1	MBK-2	MBK-3
Specific gravity	1,06	1,09	1,04
Breaking tensile strength (kg/cm²)	85...130	–	–
Elongation at fracture (%)	200...250	–	–
Moisture absorption during 24 hr (%)	0.07...0.08	0.07...0.08	0.06...0.08
Moisture absorption during 20 days (%)	0.16...0.17	0.15...0.19	0.10...0.11
Volume resistivity (Ω cm)			
at 20°C	10^{14}	$10^{13}...10^{15}$	$10^{13}...10^{15}$
at 100°C	$10^{12}...10^{13}$	10^{10}	$10^{10}...10^{11}$
after remaining in water for 10 days	$10^{12}...10^{13}$	$10^{11}...10^{12}$	$10^{12}...10^{13}$
Tangent of the loss angle at 50 c/s			
at 20°C	0.06...0.062	0.036...0.042	0.002...0.009
at 100°C	0.005	0.19...0.34	0.010...0.017
after remaining in water for 10 days	0.07...0.08	0.04...0.06	0.007...0.010
for frequency 10^6 - 10^7 c/s			
at 20°C	0.01	–	–
Permittivity at 50 c/s			
at 20°C	2.9...3.1	4.0...5.6	4.0...4.7
at 100°C	4.1...4.3	4.5...5.4	3.6...4.2
after remaining in water for 10 days	3.6...3.7	4.2...5.8	4.1...4.9
Electric strength (for a specimen about 1 mm thick) (kV/mm)	20...28	18...21	18...21

polymers can be obtained in the form of films, resistant to the action of solvents, of rubberlike materials, porous materials etc.

They are of great interest in the production of conductors with an enamel insulation. The high adhesive capacity of polyesteruretanes to copper, good stability in the presence of solvents and comparatively high mechanical strength of the lacquer film ensure the good qualities of enamelled conductors.

Enamelled conductors with polyesteruretane insulation are similar in their properties to conductors insulated by polyvinylacetate resins of the type vinyflex or formex, and they can be used for windings of electric machines and apparatus for a continuous working temperature of up to 120°C.

Silico-organic polymers

Silico-organic polymers – polyorganosiloxanes as opposed to high molecular weight substances discussed above – are compounds in which molecular chains are built not from carbon atoms, but from silicon and oxygen surrounded by organic

groups. Such a structure of molecules determines a series of properties which differs from those of the organic polymers already discussed.

In the first place, the non-organic framework of the molecules gives rise to their high thermal stability, photo-stability, and resistance to atmospheric influences. The ratio of organic groups to silicon atoms in polyorganosiloxane resins exerts a great influence on the properties of polymers. In polyorganosiloxane resins the ratio of organic groups to silicon atoms is smaller than in polyorganosiloxane rubbers. This enables us to obtain thermo-setting resins forming lacquer films, which have a considerable number of cross-links between the basic chains of molecules. In consequence these films, as a rule, possess rather low thermoplasticity at high temperatures.

Polyorganosiloxane resins are copolymers, containing alkyl and aryl groups on silicon atoms. By varying the relative proportion of these groups and also the ratio between all organic groups to silicon atoms it is possible to obtain polymers with different degrees of elasticity, starting with an elasticity typical of a rubber, up to a brittleness approaching that of glass. Polyorganosiloxane resins are easily dissolved in ordinary solvents and mix together; in this way we may also give them the properties that we want.

Industry produces various polyorganosiloxane resins and lacquers based on them and also polydimethylsiloxane rubber. All types of materials for working temperatures of 180°C (Class CB) are produced by electrical insulation factories on the basis of polyorganosiloxane resins; these materials are used for insulation of electric machines and transformers [11].

Among new polyorganosiloxanes it is necessary to mention types K-55 and K-43, which are already used in practice. Some properties of polymers are shown below; they were recorded in the All-Union Institute of Electric Technology. Fig.5 shows the electric strength and volume resistivity of polymer films as functions of temperature within a range of 20-350°C; Fig.6 shows some characteristics of pigmented films of a polymer. Non-pigmented films have a volume resistivity more than 10^{12} Ω cm and electric strength about 40 kV/mm at 350°C.

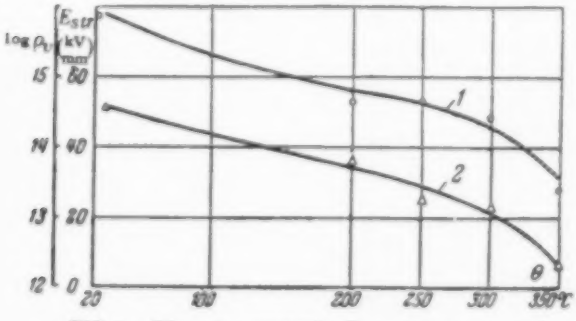

FIG.5. Electric strength E_{str} (curve 1) and volume resistivity ρ_v (curve 2) for films of the polyphenyldimethylsiloxane polymer K-55, as functions of temperature.

Data related to thermal ageing of films of polymers (K-55 and K-43) in a pure state and pigmented bimetal oxides (PKE-14 and

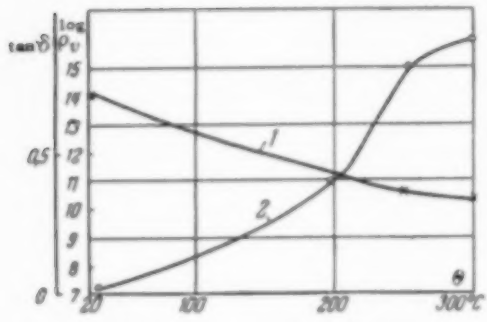

FIG.6. ρ_v (curve 1) and tan δ (curve 2) of films of the polyphenyldimethylsiloxane with a mineral pigment (enamel PKE-19), as functions of temperature.

PKE-19) are shown in Table 9. Films were heated to a fixed temperature, and their cracking after ageing was observed. The variation in the electric strength of films on a copper underlayer after ageing at temperatures 250°C and 300°C is shown in Table 10.

By using the polyphenylmethylsiloxane resin as a bonding substance we obtain heat-resistant plastic substances. Table 11 shows certain properties of plastic substances with an asbestos filler and a glass-cloth filler. Curves of tan δ, E_{str} and ρ_v as functions of temperatures are shown in Fig.7. Dependence of electrical properties of the polyphenylmethylsiloxane resin with an asbestos filler on temperature is shown in Fig.8; Fig.9 shows the electrical properties of a polymethylsiloxane rubber, deposited on a glass-cloth.

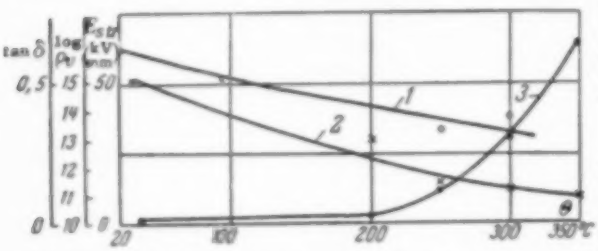

FIG.7. E_{str} (curve 1), ρ_v (curve 2) and tan δ (curve 3) as functions of temperature for polyphenyldimethylsiloxane on a glass cloth (glasslactocloth LSK-7).

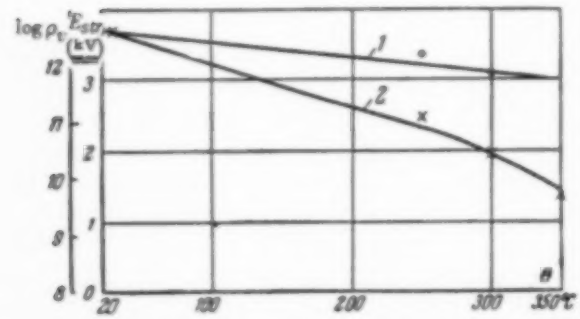

FIG.8. E_{str} (curve 1) and ρ_v (curve 2) as functions of temperature for polyphenylmethylsiloxane with an asbestos filler (plastic material K-41-5).

Among heat-resistant materials which can be used as electrical insulators, it is necessary to mention the blockcopolymer, which is obtained from polydimethylsiloxane elastomer and polytetrafluorethylene. Fig.10 shows the mechanical properties of a resin based on a blockcopolymer, containing 70 per cent of a metal oxide as a filler, as functions of temperature; Fig.11 shows the variation of its mechanical properties during the process of ageing; tan δ and ρ_v as functions of temperature are shown in Fig. 12.

As can be seen from

these data, polyorganosilaxone polymers and blockcopolymers of a polydimethylsiloxane rubber with polytetrafluorethylene possess high electrical properties even at temperatures 250-300°C and a considerable thermal stability at high temperatures. These properties permit their use in conjunction with asbestos, glass, mica and other inorganic substances for the production of insulation which can work for a short time at temperatures above 200°C.

TABLE 9

Type of the polymer	Underlayer	Time (hr) after which cracks appear on films for temperature of heating shown (°C)		
		250	300	350
K-55	Copper	(more) 240	100	120
	Steel	" 1800	1800	1000
K-43a	Copper	340	100	
	Steel	—	768	120
PKE-14	Copper	240	50	
	Steel	—	—	1200
PKE-19	Steel	2880	1800	840

1959

TABLE 10

Characteristics	Time (hr)				
	0	200	500	10	30
	Temperature (°C)				
	250	250	250	300	300
E_{str} (kV/mm) at 20°C	74.8	59.3	46.6	10 . . 15	7 . . 10
at 250°C	57.6	50.6	25 . . 30	—	—

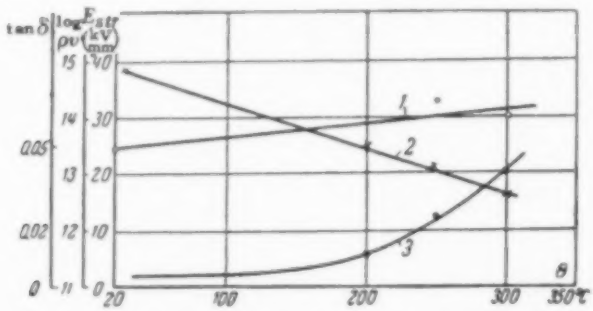

FIG.9. E_{str} (curve 1), ρ_v (curve 2) and tan δ (curve 3), as functions of temperature of resinglass-cloth RSLT.

TABLE 11

	Characteristics	Initial state	At 250 °C	At 350 °C	Temperature (°C) 250	300	350	420
					Time of ageing (hr) 500	30	20	30
Polyphenylmethylsiloxane with an asbestos filler (plastic material)	E_{str} (kV/mm)	5.2		5.0	4.2	4.4	3.8	2.8
	Static bending stress (kg/cm²)	320		—	264	220	218	257
	Impact strength, (kg.cm/cm²)	5.6		—	4.5	4.3	4.1	2.7
	Thermal stability, according to Marten's method	400		—	—	—	—	—
Polyphenylmethylsiloxane with a glass-cloth filler (glass-textolite)	E_{str} (kV/mm)	17.8	13.0	9.4	3.3	3.0	—	—
	ρ_v (ohm.cm)	$1.6 \cdot 10^{14}$	$8 \cdot 10^{11}$	$1.6 \cdot 10^{11}$	$1.7 \cdot 10^{14}$	$3.9 \cdot 10^{14}$	—	—
	$\tan \delta$	0.004	0.12	0.8	0.002	0.002	—	—
	Static bending stress (kg/cm²)	1 360	—	—	1 280	1 325	—	—

N.B. Thickness of specimens during tests, 2 mm.

Conclusion

Synthetic polymers discussed in this article cannot satisfy all requirements of modern electrical technology. It is necessary to work on the synthesis of new polymers possessing high mechanical strength, good electrical properties and moisture resistance; this should be done by pursuing investigations in order to obtain new organic polymers, and also polymers containing non-organic elements in molecular chains. Non-organic molecular chains of polymers will make them more similar in their properties to non-organic substances, and surrounding groups, containing carbon, will make them similar to organic polymers.

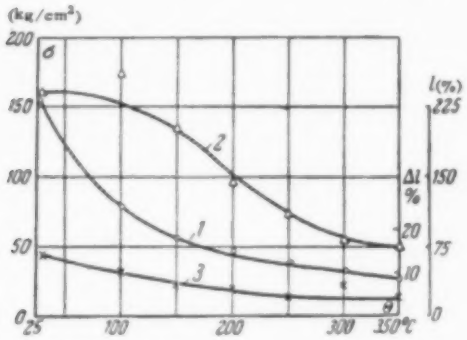

FIG.10. Mechanical properties of a thermostable polymethylpolytetrafluorethylene blockcopolymer with zinc oxide filler as functions of temperature (1) tensile strength σ; (2) of relative elongation l; (3) of total elongation Δl.

1959

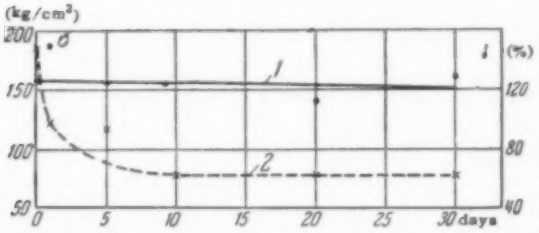

FIG.11. Tensile strength σ (curve 1) and relative elongation l (curve 2) as functions of the time of heating at 350°C.

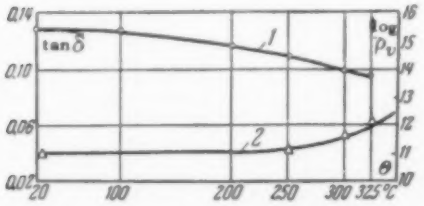

FIG.12. ρ_v (curve 1) and tan δ (curve 2) as functions of temperature.

It is important to work on the development of such polymers, which will decrease the big difference in quality which exists between organic and inorganic polymers in such important properties as thermal stability, elasticity and mechanical properties. Organic polymers, with their exceptionally valuable elastic properties and mechanical strength, do not possess the desired thermal stability; inorganic polymers lack elastic properties.

One of the most important problems which research workers should solve as soon as possible is the synthesis of available polymers, which will possess both a set of properties indispensable for dielectrics and such a thermal

stability as would exclude the necessity of limiting the operation of a machine or apparatus by temperatures of Class A, B and even (in many cases) CB.

Such a solution of the problems of insulation would not only facilitate the work of designers, but would also permit the construction of improved and operationally reliable machines, apparatus and other electrical devices.

Translated by S. Szymanski

REFERENCES

1. G. Nata; *Makromol Chem*, No.3, 213 (1955).
2. I. Nearli and W.S. Skinners; *Silk Rayon Record*, 30, No.4, 354 (1956).
3. E. P. Muller; *Kunststoffe*, 41, No.13 (1951).
4. B.S. Parkyns; *British plastics*, 24, No.264, 479 (1951).
5. C.M. Zaffon; *Trans. Amer. Inst. Elect. Engrs.*, 70, 421 (1951).
6. K.A. Andrianov, M.S. Rakitskaia and A.G. Prelkova; Elektroizoliatsionnye kompounndy na osnovye polie' firnykh smol. (Electrical insulating compounds based on polyester resins), *VEP*, No.2 (1956).
7. B. Tolentino; *Moderic plastiche*, 20, No.9, 623 (1954).
8. R. Weller; *Paint Technol.*, 18, No.207, 151 (1954).
9. K.A. Andrianov, L.N. Iukina, A.V. Koval' skaia and M.S. Rakitskaia; Litaia izoliatsia na osnovye epoksidnoi smoly (Sealing insulation based on epoxid resins), *VEP*, No.11 (1956).
10. *Modern Plastics* No.11, 147 (1955).
11. K.A. Andrianov; *Kremniiorganicheskiye teplostoikiye dielektriki (Silico-organic thermostable dielectrics)*, Gosenergoizdat (1957).
12. M.I. Garber (Editor); *Ftoroplasty (Fluoroplastics)*, Goskhimizdat, Leningrad (1954).

APPARATUS FOR LOW-VOLTAGE DISTRIBUTION GEAR*

P.V. SAKHAROV

All-Union Correspondence Institute of Power Engineering

Uninterrupted and rapid growth of the Russian national economy and steadily increasing production and service requirements pose new problems to our apparatus-making industry; better apparatus for low-tension distribution gear is needed and production should be sharply increased.

During recent years considerable progress has been made in the design and production of this type of apparatus.

In this article, the present situation and the technical level of the design of the basic series of industrial apparatus for low-tension distribution installations made by industry in the Soviet Union are discussed, and comparison is made with the best foreign apparatus. Problems and tendencies in the further development of the design of this apparatus are also discussed with reference to catching up with capitalist countries and overtaking them in the field of production of electrical apparatus.

1959

Basic trends in the development of design

Besides general modern requirements, such as decrease of weight and of dimensions, unification and normalization of details, the use of high protective technological methods and the lowering of cost, basic tendencies in development in the design of distribution installations in the U.S.S.R. and in foreign countries as well are:

(a) increase of the limit switching capacity in connexion with the increased installed power of electric gear;

(b) development of design of separate apparatus with a view to fitting them into complete sets and to quick exchange of the apparatus for inspection and repair; i.e. providing the apparatus with contact connectors and devices, which allow the apparatus to be withdrawn from complete sets;

(c) development and increase of production of the complete low-voltage distribution sets, the major part of all apparatus being produced in the assembled form;

(d) development and manufacture of series additional to the basic series of apparatus, for example in order to increase the range of nominal permissible currents; production of dust- and water-proof apparatus and others; all this should be done in order to satisfy fully the needs of the different branches of the national economy.

* *Elektrichestvo*, No. 4, 10–15, 1958.

It is also necessary to mention the tendency in many installations to replace knife switches and protectors by automatic breakers. Such a replacement is desirable in important switchgear, where a rapid restoration of feeding or automatic breaking under abnormal conditions (and not only at over-currents) is necessary, or where remote control is to be used. Moreover, the dimensions of automatic breakers are smaller than those of knife-switches with fuses.

For protection of networks with very large short-circuit currents, fuses are much simpler and more reliable than automatic circuit-breakers. Moreover, the limit breaking-capacity of widely used automatic circuit breakers is considerably smaller than the capacity of breakers with a fusible link and filling for the same rated current. Because of this, in the U.S.A. during recent years automatic breakers with H.R.C. fuses have been widely used. They ensure a reliable protection of networks, by automatic devices, from overloads, and by fuses from short-circuits.

Automatic circuit-breakers for switchgear

Our national industry produces two series of automatic circuit-breakers for switchgear in general industrial use:

(a) automatic breakers, Series A 3100, for currents 15-600 A and voltages up to 500 V a.c. or 220 V d.c. with a limit breaking-capacity up to 50 kA a.c. (shock current), or up to 25 kA d.c.;

(b) automatic breakers, AP 25, for currents 1-25 A and voltages up to 3.80 V a.c. or 220 V d.c. with limit breaking capacity 3 kA a.c. (shock current) and 2 kA d.c.

These automatic devices up to this time were not inferior, so far as their basic technical characteristics are concerned, and particularly in their limit breaking-capacity, to the best foreign constructions. Nevertheless, we have to add that similar apparatus of foreign make is manufactured in a greater variety of models. For instance the Westinghouse Co. (U.S.A.) makes switchgear automatic breakers, Series AB, for rated currents 400 and 800 A – double-pole and four-pole ones with an electrodrive, voltage-reducing relays, distance tripping, block contacts, plug-contacts, and types filled with oil, dust-proof and water-proof, and others. Moreover, in 1956 the I.T.E. Co. (U.S.A.) designed an attachment for switchgear automatic apparatus, containing a fusible link (protector), with a spring mechanism. If the fusible link melts in any of the poles, the trigger is released. This attachment, owing to the current limiting action of fusible links, ensures protection by the automatic breakers of networks in which the short-circuit currents may reach the value of 80 kA (effective value of a symmetrical component), i.e. for a shock current up to 160-190 kA.

Establishments of the electrical industry in the U.S.S.R. are working on the improvement and development of new automatic devices for switchgear. The Khar'khov Electro-mechanical Factory (KhEMZ) has designed new automatic apparatus, Series A 3100, with distance triggers, with block and plug contacts and so on. The Kursk Electrical Apparatus Factory (KEAZ) is now preparing the production of a small single-pole automatic breaker type A 015 for current up to 15 A for industrial in-

stallations and big buildings; this model was designed by the Science and Research Institute of the Electrical Industry (Fig. 1).

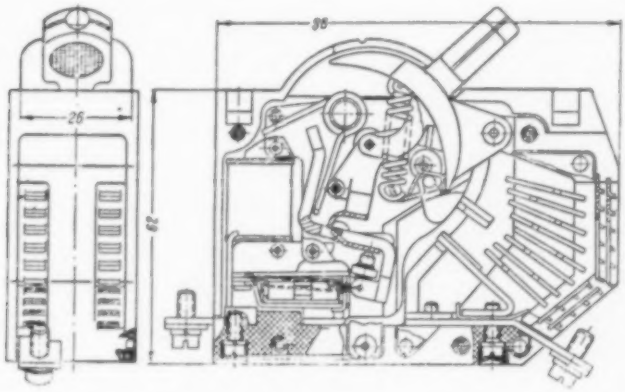

FIG. 1. Automatic single-pole circuit-breaker for currents up to 15 A, Type AO 15.

It is necessary to continue the work in order to increase the breaking-capacity and to develop several additional types of automatic apparatus of Series A 3100. Moreover, it is necessary to develop a small automatic apparatus for currents up to 15 A of a simple construction and to organize its mass production in order to replace the screw fuses in communal and other networks.

1959

Universal automatic circuit breakers

The universal automatic circuit-breakers Series A-2000 for currents 200-1500 A, which were made until recently, are considerably inferior in their basic performance characteristics to the leading foreign constructions and do not satisfy altogether the increased modern requirements for electric supply.

Ul'ianov Apparatus Factory redesigned the construction of automatic apparatus Series A-2000, and started series production of universal-selective automatic breakers Series A 15, A 20 and A 25 for currents 100-1800 A and voltages up to 380 V a.c., 50 c/s with a limit breaking capacity up to 50 kA (shock current) and for voltages up to 440 V d.c., up to 30 kA. Nevertheless, we have to add that this series does not yet satisfy all modern requirements, in particular as regards limit breaking capacity and variety of types, and is inferior to leading foreign constructions.

Among foreign automatic apparatus, the Series AK-1 of the General Electric Co. (U.S.A.) deserves the greatest attention. Apparatus of this series is made for nominal currents of 600, 1600, 3000 and 4000 A, 250 V d.c. and for 600 V a.c., 60 c/s. This equipment has a limit breaking capacity of 25, 50, 75 and 100 kA respectively (effective value with a constant component included), or approximately 40, 80, 120 and 160 kA (shock current).

Greater compactness, in comparison with other similar constructions, has been achieved by using in every pole a few parallel connected contacts, separated by partitions of the arc extinction chamber. In this case, the high limit breaking-capacity of the apparatus was achieved by establishing a current loop by fixed spring contacts; this current loop produces a compensating effect for electrodynamic forces, which rejects the contacts in the case of large short-circuit currents. The apparatus is provided with a spring drive, which is wound by a small electric motor, selective tripping devices for maximum current with various time lags and is capable of instantaneous action.

Fig. 2 shows the protective characteristics of the three automatic breakers of this series. This automatic apparatus may be fitted into the complete gear, and the automatic breakers made for different rated currents are of the same height and depth, owing to the use of unified component parts. Flexible current leads are absent; instead, silvered cylindrical rods are used which conduct the current through the joints of mobile parts equally well.

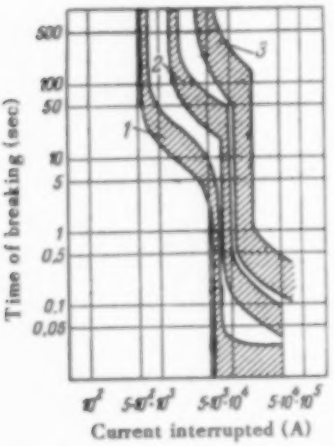

FIG. 2. Protection characteristics of automatic breakers of Series AK-1. (1) AK-1-25, I_{nom} = 600 A; (2) AK-1-75, I_{nom} = 1600 A; (3) AK-1-100, I_{nom} = 3000 A.

The basic constructional solutions mentioned above, such as the parallel contact connexion and the use of the current loop, are applied in other series of foreign automatic breakers, for instance in the automatic apparatus Series R 913/R 914 of the Siemens Co. (Federal German Republic).

It is interesting to mention the use of electromagnetic contactors instead of automatic breakers in low-voltage distribution systems. Telemechanique Electrique Co. (France) make contactors of two types: contactors for currents of 125-2750 A and voltages up to 500 V for work with fusible links, and automatic contactors for currents 800-2750 A and voltages up to 500 V, with limit breaking capacity 30-65 kA, respectively (effective value of a symmetrical component), or approximately 60-130 kA (shock current).

On the basis of the above discussion we come to the conclusion that it is necessary to develop a new series of home built universal selective automatic breakers for currents up to 4000 A. Their design should allow for fitting into the complete distribution gear.

Fusible link protectors

Fusible link protectors are a simple, reliable and cheap means of protecting electrical gear from short-circuits and considerable overloads.

At present in the Soviet Union and in foreign countries three basic kinds of low-voltage fuses are widely used: a tube fuse without a filler, a tube fuse with a filler

and a screw fuse. Fig. 3 shows diagrams of the weights of these kinds of fuse, made by our national factories.

Tube fuses without a filler of PR-1 series, made by the Electrical Apparatus Factory, Ufa, have been improved during recent years. A modernized series called PR-2 has ratings, including the limit breaking capacity, not inferior to the best foreign fuses of similar construction.

The factory continues its work for further increase of the limit breaking-capacity by increasing the strength of the tube cartridges.

Substantial disadvantages of tube fuses without a filler – and this also applies to Series PR-2 – are their large size and weight, the considerable amount of labour needed for their manufacture due to the lathe turning and threading operations, and the large amount of non-ferrous metals required. The use of Series PR-2 fuses should be restricted to installations where it is not expedient to use fuses with a filler due to conditions of fuse refilling, for example in mobile installations.

Tube fuses with a filler have, in comparison with fuses without a filler, a considerably higher limit breaking-capacity; they occupy less space, require less labour for their production and are approximately twice as cheap.

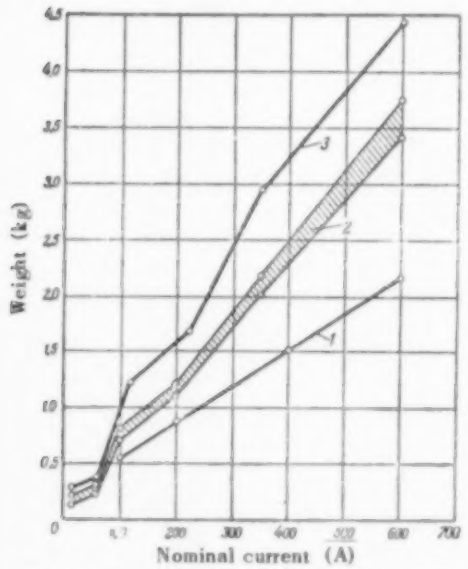

FIG. 3. Weight of protectors. (1) Series PN2; (2) Series PR2 (short and long, with a front-and-back leads connexion); (3) Series PD5.

In the U.S.S.R. until recently fuses with a quartz filler were made of Types NPN, NPR, PNR, A and KP; in these fuses the fusible link is made of copper and not of silver, as in the European constructions. At present the construction of these fuses is already obsolete.

The Factory of Electrical Apparatus, Kursk, has developed demountable fuses with quartz filler of a new series, PN-2, for currents 100, 250, 400 and 600 A and voltages up to 380 V. For putting the cartridges in the contact rack frames and for repair, a plastic detachable handle is provided.

Series PN-2 fuses, according to their basic ratings, are up to the modern technical level, but their limit breaking-capacity is not yet determined. Moreover, fuses of this series are rated only for use on a.c.; the cartridges give no indication that a fuse has "blown". There is no fuse for 1000 A. No construction allows for the back connexion of leads.

Among the best foreign low-voltage fuses with quartz filling, fuses made by

Siemens and A.E.G. (Federal German Republic) deserve the greatest attention. A distinctive feature of these fuses is the use of a fusible wafer link, made of thin copper metal sheet and soldered in the middle by easily melting metal (Fig. 4). The link consists of strips joining all longitudinal bands; when the arc is struck, all longitudinal bands melt. The limit breaking-currents for these fuses, at nominal currents 200, 350, 600 and 1000 A and voltages 380 V a.c. and 440 V d.c., are equal to 70, 50, 50 and 50 kA, respectively (effective value of a symmetrical component), i.e., approximately 140, 100, 100 and 100kA (shock currents). Cartridges are easily taken to pieces and are provided with an indicator for when the fuse has "blown".

The basic problem in the further development of national cartridge fuses with filling is to redesign PN-2 series in order to eliminate the above defects.

Fuses with a threaded cartridge, which is screwed into a base ("plug"), for currents of 6-20A and a voltage of 250V, with a limit breaking capacity of 600 A, are widely used in the Soviet Union for lighting purposes and also in control networks and in low-power installations. During recent years, these fuses have been considerably improved: dimensions of the porcelain base are considerably reduced, and the porcelain cover is replaced by a plastic one. But the most important detail of the fuse – the cartridge itself – was not improved, and the limit breaking-capacity of these protectors is still low; moreover, there is no indicator in the cartridge that the fuse has "blown".

In Western European countries, screw fuses in general use are usually made for currents up to 60A. The fuses have a removable steatite cylindrical cartridge, inside which are inserted fusible links with a quartz filling; the cartridges are provided with an indicator showing whether the fuse has "blown". These fuses are similar to the fuses type PD and PDS which are made by our factories. The limit breaking capacity of Western European fuses is several times greater than that of general fuses made by our national factories.

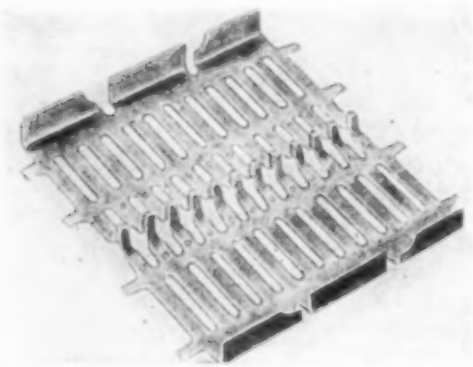

FIG. 4. Fusible link of a protector with fillings, of the Siemens Co. (Federal German Republic).

Since screw fuses, which are manufactured in the U.S.S.R. in tens of millions, are widely used and play an important role in the protection of electric networks and against fires, it is urgent that a new series of general purpose fuses should be developed for currents 6, 10, 15, 25, 40 and 60A.

In foreign countries, particularly in the U.S.A., inertial fuses are widely used, mainly for the protection of synchronous motors from overloads. In these fuses, we may use conductors of smaller cross-section than in ordinary high-speed fuses. Inertial fuses have two elements:

one which melts at overloads, and another which melts at short-circuits; this construction allows us to dispense with a starter with a thermal relay and to replace it by a non-automatic circuit-breaker with such fuses. This brings down the total cost of the apparatus, although inertial fuses are more expensive than ordinary ones.

Non-automatic power circuit-breakers and switches

Among different constructions of power circuit-breakers used in the U.S.S.R. and abroad we may distinguish three basic types: packet-type breakers and switches, knife-breakers and switches, and breaker-protectors.

Packet-type breakers and switches are more and more widely used because of their smaller overall dimensions in comparison with the other power breakers and switches. The smaller dimensions are due to two-stage current-breaking and to arc extinction in a closed chamber with fibre disks.

Tashkent Electrotechnical Factory has recently modernized a series of breakers and switches. The new type, which received the series name PV, is designed for nominal currents 10/6, 15/10, 25/15, 40/25, 60/40, 100/60, 150/100, 250/150 and 400/250 A and voltage 220 V d.c. (the value of the current is shown in the numerator), or for 380 V a.c., (the value of the current is shown in the denominator). In this series three new sizes were included, and in the three other sizes the rated current values were increased.

1959

In switches with complicated circuits, sizes and weights are decreased due to the change in the contact shapes. The technical performance of the new series is not inferior to the performance of the best foreign packet-type breakers and switches.

Among the new foreign constructions the three-pole breakers of the Westinghouse Co. (U.S.A.) and of the Arrow Co. (England) deserve attention. The mobile contact system of these breakers is similar to the construction of the packet-type Series PV breakers, but fixed contacts are situated on a plastic or ceramic flat rectangular base. The advantage of this construction is the use of the easily removable cover which offers access for inspection and repair of the contacts; this is absent in the packet-type breakers of the PV series.

Knife circuit-breakers and switches made by our home factories may be divided into two series. The Electric Apparatus Factory, Ufa, finished the development and started the production of a new series for currents of 100, 250, 400 and 600 A and voltages up to 500 V. Breakers and switches of this series are provided with a side handle with side and central lever drives. The use of arc extinction chambers has greatly increased the breaking capacity of this apparatus.

The second multiampere series for nominal currents up to 30 kA was developed and put into production during the last few years by the Khar'khov Electromechanical Factory. Both series of knife breakers and switches are not inferior to the best similar foreign-made devices.

Breaker-protectors are devices that perform the functions both of cut-outs and protectors, and of knife-breakers and protectors. Such a unification of the two separate

pieces of apparatus into a single one permits a decrease in overall dimensions and allows a reduction in the size of complete switchgear. Moreover, an economy in copper is achieved, because the blades of knife-switches or of cut-outs are replaced in such an apparatus by the fuse cartridges. Moreover, in an unified apparatus total circuit-breaking occurs in two stages, and this contributes to the arc extinction. The number of contact junctions is also reduced, and the energy losses due to contact heating are cut. Nevertheless, the complication in contact and kinematic nodes is an obstacle to the wider use of this apparatus.

In the U.S.S.R. only the Saratov factory makes small quantities of breaker-protectors. Because of defects in the design of this apparatus, constructions of a new type are being developed.

In foreign countries in recent years, the use of breaker-protectors has been spreading. The English firm, Lancashire Dynamo, makes breaker-protectors which can be fitted into switchgear. This equipment is made for currents 30-400 A and voltages 660 V a.c. and 250 V d.c. The English firm of Dorman and Smith makes similar apparatus for currents up to 300 A and 500 V with butt-joint contacts (not wedge joint as is usual).

American firms, for example the General Electric Co, also make breaker-protectors. In the German Democratic Republic disconnector-protectors are made.

Taking into account the advantages of breaker-protectors, it is necessary to speed up their development and to organize their production in our national factories.

Complete distribution gear

During recent years, low-voltage apparatus for distribution gear has been made in the form of complete devices, which may be divided into five types.

Complete distribution gear with universal selective automatic apparatus was made by the Moscow Transformer Factory for individual orders as component parts of complete transformer substations. Such complete distribution devices without transformers are needed for the secondary distribution points in industrial plants. Moreover, the existing construction of these devices is already obsolete, and it is necessary to develop new designs of complete distribution gear.

Complete distribution gear with automatic apparatus Series A-3100 are made by the Khar'khov Electromechanical Factory in the form of cubicles Type SU, which are situated in the walls of buildings. Distribution devices of this type, in dust- and water-proof casings, were recently developed by this factory. This apparatus is not inferior to the best foreign-made equipment.

The development of complete distribution gear of a new design, fitted with plug contacts, is required to permit quick exchange of an automatic apparatus which needs inspection or repair.

Boxes, cubicles, cells with fuses, knife switches, knife-switch-protectors, packet-type breakers, all assembled in one complete distribution gear, dust- and

water-proof, are needed for many branches of the national economy. In the first place, these branches are: agriculture, building trade, forest, coal, textile, light industry, food and other branches of industry.

At present, boxes and cubicles are made only in limited quantities and only by special order. Their construction does not satisfy the requirements of mass production and use.

At present the building industry trade "Elektromontazhkonstruktsiaa" has developed a series of boxes, which are assembled into complete gear. It is important that their mass production should be organized and that the development of new types of this series should be continued.

Distribution boards for small electric power stations of Type ShUP, developed by the "Armelektrozavod" factory, are now produced in great quantities in connexion with the intensive building of small agricultural and industrial hydraulic power plants and of small electric power stations, driven by steam engines or by gas generators. Distribution boards of Type ShUP are used for the control of synchronous generators of outputs up to 150 kVA, 400/230 V, and for the power distribution in a few feeders.

The construction of these boards satisfies modern requirements and is not inferior to the best foreign-made apparatus of this kind. Control boards of two types for electric stations and substations are made by our home factories.

1959

The Leningrad factory "Elektropult" has produced control boards for many years. Control boards of the same design are also made by the Khar'khov Electromechanical Factory. During the last few years in the TsKB "Elektroprivod", control and protection boards of a new design have been developed, and their production is carried out by Novosibirsk Turbo-generator Factory and Minsk Electro-technical Factory. These boards differ from those made by "Elektropult"; they are of block construction. In every block the control and protection devices are collected separately for every individual object, generator, transformer, line etc. In the most widely used two-row type on the front panel are placed measuring instruments, control keys and buttons, signalling apparatus and circuit diagram. Protection and automatic relays are located on the back panel.

A passage is provided inside the block. In the single-row construction, the apparatus of the single block is placed on one or two closely situated panels. In comparison with the board designed by "Elektropult", the weight of the board of KU type is on the average 20-30 per cent less, the length is smaller by 15-20 per cent, and the depth in comparison with a two-row board, consisting of two separate panels, control and protection panel assembled together, is smaller by 700 mm. These control boards are not inferior to the best foreign-made boards.

Among the newest solutions in the design of complete distribution boards in foreign countries we have to mention the use of frontal panels made from transparent insulation materials, which enables the operator to watch the apparatus from his place (firms in the Federal German Republic), and also the use of luminous elements in circuit diagrams, including straps representing busbars, (A.S.E.S., Belgium).

Conclusion

During recent years our home factories have developed and put into production a series of apparatus of low-voltage distribution gear. The output of this apparatus has been greatly increased.

Nevertheless, so far as technical characteristics and performances of some series, particularly of automatic breakers, are concerned, this apparatus does not satisfy modern requirements and is inferior to the best foreign-made apparatus.

In order to ensure the further development of the designs under consideration and to organize the production of apparatus for low-voltage distribution gear along the lines discussed in this article, it is necessary, besides the enlargement of the production basis, to take several measures, of which the most important are:

(a) development of the scientific research and laboratory establishments, in particular the setting up of laboratories for the investigation of breaking capacity in the Science and Research Institute of Electrical Industry, and in certain factories, designing and producing apparatus for low-voltage distribution gear, for instance in the Ul'ianov, Ufa and Kursk factories;

(b) the carrying-out of all scientific and research work in accordance with a unified plan; these tasks are to be carried out by all establishments developing low-voltage apparatus, by the research institutes and by the universities; investigations should deal with problems concerning contacts, arc extinction, kinematics and dynamics of the apparatus, and the use of new materials;

(c) the unification, normalization, standardization and development of All-Union series of apparatus for low-voltage distribution gear;

(d) development and production of the new improved electrical insulating, conductive and magnetic material.

Translated by S. Szymanski

INVESTIGATION OF TRANSIENT PROCESSES IN LINEAR CIRCUITS BY THE METHOD OF LOCI*

G.V. OSTROUMOV
Khar'khov Lenin Polytechnic Institute

Received 21 May 1957

The loci method is generally used in the theory of automatic control for the analysis of transient processes in linear networks (the separation of the stability regions with the help of the D-division method [1]. In the present article the method of loci is extended to the problem of finding the roots of the characteristic equation for linear oscillating systems.

The proposed method is the most effective when it is applied to the investigation of the effect exerted by a certain circuit parameter on the transient process. The method is based on a construction on the complex plane which gives the locus of the roots for the characteristic equation of the circuit, when the locus corresponds to all possible (i.e. real) values of the circuit parameters. A general method of finding the analytical equation of the locus is given in the article. The construction of the locus according to its equation avoids the necessity for a numerical solution and considerably reduces the volume of calculation.

Consider the practical application of this method to an example, of the calculation of the transient process in the two-frequency circuit shown in Fig. 1.

The circuit is one of the phases in a three-phase system with a circuit-breaker B, the contacts of which are opened. At the moment when the arc is extinguished, the process of voltage recovery u_B across the contacts of the breaker begins. As usual, a shunt resistor is applied in order to ease the operation of the circuit-breaker, which leads to the reduction of the speed with which the voltage builds up. Now we set out the problem of investigating the influence of the shunt resistor value on the process of building up the voltage u_B. This problem directly arises at the selection of the shunt resistor value.

In the majority of cases the process is so quickly attenuated that we can disregard the variation of the mains voltage during the build-up time of the voltage.

* *Elektrichestvo*, No. 4, 22-26, 1958.

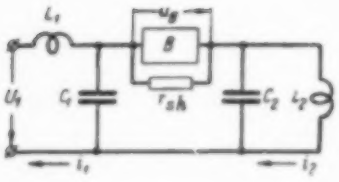

FiG. 1. The calculated circuit.

In addition, after the extinction of the arc the remaining admittance of the gap becomes vanishingly small very quickly. Therefore, we shall assume (as usual in the calculation of a voltage-recovery [2]) that during this process the e.m.f. of the source, and consequently the input voltage U, remains constant and that the residual admittance of the gap is zero. We shall assume furthermore that the extinction of the arc takes place when the arc current goes through zero and that the voltage across the gap at the moment of extinction is zero [2, 3]. Then the initial conditions of the process are expressed by the equations:

$$i_1(0)=i_2(0)=0;\ u_{C1}(0)=u_{C2}(0)=U_1\frac{L_2}{L_1+L_2}. \tag{1}$$

For convenience, we introduce the dimensionless independent variable

$$\tau=\frac{1}{\sqrt{L_1C_1}}t=\omega_{01}t. \tag{2}$$

The form of the voltage recovery $u_B(\tau)$ with the initial conditions (1) has the following form:

$$u_B(p)=U_1\frac{p^2\frac{1+k_C}{1+k_L}+\frac{k_C}{k_L}}{p^4+\varepsilon b_3p^3+a_2p^2+\varepsilon b_1p+a_0}. \tag{3}$$

The coefficients occurring in (3) are the following:

$$k_C=\frac{C_1}{C_2}\qquad k_L=\frac{L_2}{L_1};\quad \varepsilon=\frac{\omega_{01}L_1}{r_{sh}};\quad a_0=\frac{k_C}{k_L};$$

$$b_1=\frac{k_C}{k_L}(1+k_L);\quad a_2=1+\frac{k_C}{k_L};\quad b_3=1+k_C.$$

Equating the denominator of (3) with zero, we obtain a characteristic equation of the fourth order:

$$p^4+\varepsilon b_3p^3+a_2p^2+\varepsilon b_1p+a_0=0. \tag{4}$$

The value of the shunt resistor occurs only in coefficient ε, which is itself a variable parameter in this particular case. The locus corresponding to the various values of parameter ε can be found in the following way.

We solve equation (4) relative to ε:

$$\varepsilon=-\frac{p^4+a_2p^2+a_0}{b_3p^3+b_1p}. \tag{5}$$

Assuming that ϵ is a function of $p = x + jy$ (in relative units x is the attenuation factor, y the angular frequency), we separate the real and imaginary parts of (5), for which we multiply the numerator and denominator of the fraction by a polynomial which is the conjugate of the denominator

$$b_3(x - jy)^3 + b_1(x - jy).$$

The result of the multiplication can be represented in the following general form

$$\epsilon = \frac{M(x, y)}{S(x, y)} + j\frac{N(x, y)}{S(x, y)}, \tag{6}$$

where M, N and S are polynomials and are functions of x and y.

Since parameter ϵ, in effect, is a real number, the imaginary part of (6) must be zero. Therefore equation

$$N(x, y) = 0 \tag{7}$$

establishes such a functional relationship between x and y, at which to each pair of x and y values, satisfying equation (7), corresponds a certain real value of parameter ϵ. Consequently equation (7) is the required locus.

1959

Equation (7) is obtained in the form of a polynomial of the sixth order relative to x and y. However, introducing the new variable

$$z = \sqrt{x^2 + y^2} \tag{8}$$

and eliminating one of the independent variables, we can convert the equation of the locus into a form which can be easily solved relative to the other independent variable.

Eliminating y, we find:

$$x^2 = -\frac{b_3}{4b_1} \cdot \frac{z^6 - \left(a_2 + \frac{b_1}{b_3}\right) z^4 + \left(a_0 + a_2\frac{b_1}{b_3}\right) z_2 - a_0\frac{b_1}{b_3}}{z^2 - a_0\frac{b_3}{b_1}}. \tag{9}$$

Thus the co-ordinates of the points on the complex plane are the distance from the imaginary axis (x) and the distance from the origin (z). It is convenient to take z as the independent variable and x as a function of Z. Selecting various values for Z and calculating the corresponding values of x according to (9), we can construct the locus point by point.

Now we note some general properties of the locus.

Since the roots of the characteristic equation are complex conjugate values, therefore the locus is always symmetrical to the real axis and we can confine

ourselves to its construction on the upper half-plane. In addition, if the investigated oscillating system is stable, then the real components of the roots are negative or zero. In this case, that part of the locus which is in the right-hand half-plane has no physical meaning and it is sufficient to examine the locus in the second quadrant of the complex plane.

If the investigated system has n degrees of freedom then the characteristic equation has n roots and to each value of parameter ϵ correspond n points on the complex plane. Hence it follows that the locus must have n branches. Each branch, placed in the upper half-plane, corresponds to a conjugate branch in the lower half-plane. If n is an even number then half the branches are placed in the upper half-plane and the other half in the lower half-plane. If n is an odd number then, in the limiting case, one of the roots will be real at any ϵ and the corresponding branch will fall into the real axis.

The locus constructed according to (9) when $k_L = 2$ and $k_C = 0.2$ is shown in Fig. 2. Out of the four branches, numbers 1 and 2 are on the upper half-plane. Both branches start from the imaginary axis at the points for which $\epsilon = 0$. When ϵ increases from zero to infinity, the points representing the roots of the characteristic equation will move along the branches.

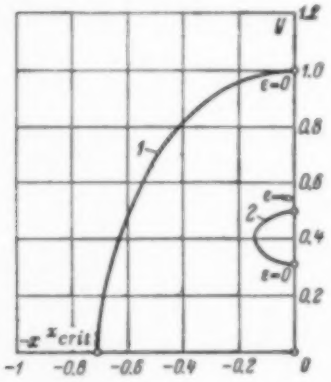

FIG. 2. The locus of the roots of the characteristic equation when $k_C = 0.2$; $k_L = 2$, $z_4 > z_3$; (1) mixed branch; (2) complex branch, $z_1 = 1$; $z_2 = 0.316$; $z_3 = 0.5$; $z_4 = 0.633$; $x_{crit} = 0.707$.

Branch 1 reaches the real axis at the point x_{crit} which corresponds to the critical operating condition for one of the oscillating components of the investigated process (at the critical value of ϵ). At a further increase in ϵ the two conjugated branches meeting at the point x_{crit} (i.e. the branches placed in the upper and lower half-planes) are directed along the real axis in opposite directions.

Branch 2 does not reach the real axis. Consequently, the second pair of roots at all values of ϵ remain complex. This means that with the change in the value of the shunt resistor it is impossible to reach the damping of the second oscillating component of the process; i.e. it is impossible to bring it into the aperiodic condition.

For the complete solution of this problem it is necessary to calculate the ϵ parameter value corresponding to the various points of the locus. Selecting a number of arbitrarily positioned points and substituting the co-ordinates of these points into (5) or (6), we find the value of ϵ for

each pair of x and y values.

It is convenient to represent the result of this calculation in the form of $x(\epsilon)$ and $y(\epsilon)$ curves. Such curves, corresponding to the locus given in Fig. 2, are shown in Fig. 2. (To branch 1 in Fig. 2 correspond curves x_1 and y_1 in Fig. 3. To branch 2 correspond curves x_2 and y_2). Since the imaginary components of the conjugate roots differ only in sign and the real components of the roots in this particular case are not positive, in Fig. 3 the curves for the moduli of x and y are constructed. At the critical value of ϵ, branch y_1 is zero and branch x_1 is doubled.

Some problems can be solved by qualitative analysis of the locus without the point-by-point construction of its branches. One such problem, for example, is the question of damping the oscillations and the conditions necessary for damping.

We shall examine the qualitative analysis in an example.

According to the position of the branches, the place of the characteristic points can be estimated. To the characteristic points belong those points which correspond to the limiting values of ϵ; i.e. $\epsilon=0$ and $\epsilon=\infty$, also the intersection points with the axes. In some cases the first and second types of these special points are coincident.

1959

Now we shall find the characteristic points for the locus defined by (9). Assuming $\epsilon=0$ in formula (4), we obtain two pairs of imaginary conjugated roots:

$$p_1=\pm j;\quad p_2=\pm j\sqrt{\frac{k_C}{k_L}}.$$

When $\epsilon=\infty$ the characteristic equation, in addition to the zero root, has a pair of conjugated imaginary roots:

$$p_3=\pm j\sqrt{\frac{k_C(1+k_L)}{k_L(1+k_C)}}.$$

Thus, in this particular case, the points for which $\epsilon=0$ and $\epsilon=\infty$ are simultaneously the intersection points with the axes.

Since the roots p_1, p_2 and p_3 are imaginary and the corresponding points are on the imaginary axis, the moduli of these roots, z_1, z_2 and z_3 must satisfy equation (9). Consequently, the numerator of the right hand side of (9) has the roots $\pm z_1$ $\pm z_2$ and $\pm z_3$, and it can be represented in the following, more convenient, form:

$$x^2=-\frac{b_3}{4b_1}\cdot\frac{(z^2-z_1^2)(z^2-z_2^2)(z^2-z_3^2)}{z^2-z_4^2}, \tag{10}$$

where

$$z_1 = 1,\quad z_2 = \sqrt{\frac{k_C}{k_L}};\quad z_3 = \sqrt{\frac{k_C(1+k_L)}{k_L(1+k_C)}};$$

$$z_4 = \sqrt{a_0\frac{b_2}{b_1}} = \sqrt{\frac{1+k_C}{1+k_L}}.$$

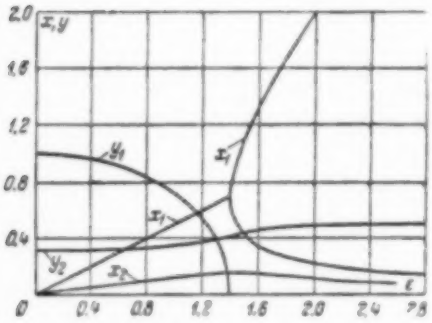

FIG. 3. The real and imaginary parts of the characteristic equation as functions of the variable parameter ϵ.

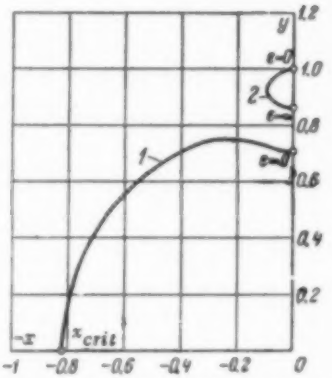

FIG. 4. The locus of the roots of the characteristic equation when $k_C = 1$; $k_L = 2$; $z_4 < z_3$
(1) mixed branch; (2) complex branch;
$z_3 = 0.866$; $z_4 = 0.817$; $|x_{crit}| = 0.814$

For those values of z to which a real value of x corresponds, the right hand side of (10) must be positive. Consequently, the real values of z, i.e. those values which satisfy the physical conditions of this problem, fall into a certain region which is divided into intervals. The region of the real z values can be determined from the conditions that on the boundary of each region one of the four differences $(z^2 - z_k^2)$ is zero, and inside the region the right hand side of (10) is positive.

It can be seen from (10) that to each z value, taken in the region of its real values, corresponds only one negative x value. Therefore to each region of real z values corresponds one branch of the locus.

The comparison of the z_1, z_2, z_3 and z_4 values shows that the two latter values are always between the first two. Two variants of the mutual position of the branches are possible, depending on whether z_3 or z_4 is larger. The branch with the final point p_3 does not reach the real axis. We shall call it complex. The other branch reaches the real axis at the critical point and we shall call it mixed.

To be specific, we assume that $z_1 > z_3$ i.e. $k_C < k_L$. Then the variants of the positions for the complex and mixed branches can be represented as follows.

Variant	Complex branch	Mixed branch
I	$z_3 < z < z_3$	$z_4 < z < z_1$
II	$z_1 > z > z_3$	$z_4 > z > z_2$

In the case when $z_1 < z_3$ ($k_C > k_L$), it is necessary to interchange the position of z_1 and z_2 in these inequalities.

To the two variants of the branch positions correspond two types of loci, shown in Figs. 2 and 4.

When $z_3 = z_4$, the locus consists of the arc 1:

$$z = z_3 = z_4$$

and curve 2:

$$x^2 = -\frac{b_3}{4b_1}(z^2 - z_1^2)(z^2 - z_2^2).$$

This case is represented by Fig. 5.

The abscissa of point x_{crit} can be found by solving (10) when $|x| = z$. This will be an equation of the third order relative to z^2. For the numerical data, by which Fig. 2 was constructed, we find:

$$x_{crit} = -\frac{1}{\sqrt{2}}; \quad \epsilon_{crit} = \sqrt{2}.$$

The regions of the z values will be:

$0.316 \leqslant z \leqslant 0.5$, Complex branch;
$0.633 \leqslant z \leqslant 1$ Mixed branch.

In effect, the complex part of the mixed branch ends at $z = |x_{crit}| = 1\sqrt{2} > z_4$ instead of $z = z_4 = 0.633$; i.e. the region of the real values for the complex part of the mixed branch will be somewhat narrower than that established before.

Now we shall generalize the procedure for finding the analytical expression of the locus to the case of a characteristic equation having an arbitrary form, with the single limitation that the coefficients of the characteristic equation linearly depend on the variable circuit parameter. We denote the variable by ϵ. The characteristic equation in the general case is of the following form:

$$\sum_{k=0}^{n} (a_k + \varepsilon b_k) p^k = 0, \tag{11}$$

where

$$p = x + jy.$$

Solving equation (11) relative to ϵ, we obtain

$$\varepsilon = -\frac{\sum_{k=0}^{n} a_k p^k}{\sum_{k=0}^{n} b_k p^k} \tag{12}$$

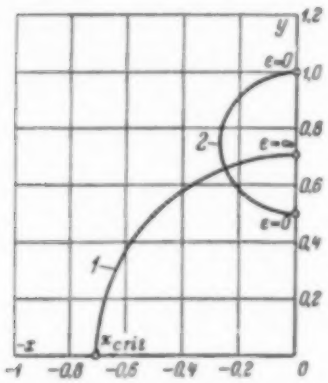

FIG. 5. The locus of the roots of the characteristic equation when $k_C = 0.5$; $k_L = 2$; $z_4 = z_5$ $z_1 = 1$; $z_2 = 0.5$; $z_3 = z_4 = |x_{crit}| = 0.707$

Converting (12) in a similar way, as was done before with (5), we obtain an equation of the form of (6). In this case equation

$$N(x, y) = 0$$

is also the required locus. Introducing the new variable z, we find that the locus will be a polynomial, the order of which is one degree lower than that of the characteristic equation, relative to x. In many cases, however, the coefficients of the higher powers of x are zero and the degree of the locus, relative to x, is two units smaller than that of the characteristic equation. This is especially true in the above case.

We represent the locus in the form of a polynomial relative to x:

$$\sum_{k=0}^{n-1} A_k x^k = 0.$$

Then, for example, for $n = 6$ coefficients A_k will be the following:

$$A_0 = c_{65}z^{10} + (c_{54} - c_{63})\,z^8 + (c_{43} - c_{52} + c_{61})\,z^6 + \\ + (c_{32} - c_{41} + c_{50})\,z^4 + (c_{21} - c_{30})\,z^2 + c_{10};$$

$$A_1 = 2\,[c_{64}z^8 + (c_{53} - 2c_{62})\,z^6 + (c_{42} - 2c_{51} + \\ + 3c_{60})\,z^4 + (c_{31} - 2c_{40})\,z^2 + c_{20}];$$

$$A_2 = 4\,[c_{63}z^6 + (c_{52} - 3c_{61})\,z^4 + (c_{41} - \\ - 3c_{50})\,z^2 + c_{30}];$$

$$A_3 = 8\,[c_{62}z^4 + (c_{51} - 4c_{60})\,z^2 + c_{40}];$$

$$A_4 = 16\,[c_{61}z^2 + c_{50}];$$

$$A_5 = 32c_{60}.$$

To reduce the amount of writing, the following notation was introduced

$$c_{ik} = a_i b_k - a_k b_i.$$

The equation of the locus when $n < 6$ will be obtained as a special case of the examined equation, when zero is substituted for the corresponding C_{ik} coefficients.

Finally we note that (12) can be examined as a function of the complex variable p, which gives a conformal transformation of the p plane on the plane of the complex parameter ϵ, while the locus determined in the p plane is transformed into the positive part of the real axis on the ϵ plane.

1959

REFERENCES

1. *Fundamentals of automatic regulation. Theory.* V.V. Solodovnokov (Editor); Mashgiz (1954).
2. L.E. Mashkilleison; *Determining the speed of the voltage recovery on the contacts of a circuit-breaker at the extinction of the arc. In symposium, "High voltage apparatus design"*, United Scientific and Technical Press (1935).
3. P. Hammarlund; *Voltage recovery on the contacts of a circuit-breaker*, Gosenergoizdat (1956).

DETERMINATION OF THE LEVEL OF MAGNETIC NOISE OF D.C. MACHINES BY THE METHOD OF ELECTROMECHANICAL ANALOGY*

I.G. SHUBOV

S.M. Kirov Factory "Elektrosila"

(Received 7 May 1957)

Magnetic noise produced by d.c. machines in many cases prevails over noise of non-magnetic origin and thus determines the general noise level of the machine.

One of the fundamental problems in calculating magnetic noise is the determination of the space forms of the frame vibrations and of magnetic forces appearing in the machine air gap. Therefore, in this article, before the discussion of determination of magnetic noise by the method of electromechanical analogy, basic formulae for calculation of various types of vibrations and of periodic magnetic forces are given; basic assumptions, used for deducing these formulae, are stated.

The space forms of frame vibrations

The frame of a d.c. machine, being an elastic ring, has an infinite number of degrees of freedom, but due to the nature of exciting forces acting on the frame, only certain definite forms of vibrations are produced. These vibrations may appear in the form of a symmetrical tension – compression, bending or torsion of the ring.

In designing a d.c. machine it is necessary to pay particular attention to the possibility of coincidence of the frequency of exciting forces f_e with the frequency of natural vibrations f_n of the system, consisting of the frame with main and auxiliary poles:

$$f_e = Zn/60 \tag{1a}$$

$$f_n = 1/(2\pi\sqrt{m_e\lambda_e}) \tag{1b}$$

where m_e is the equivalent mass of the system; λ_e is the equivalent compliance of the system for various kinds of vibrations; Z is the number of slots in the armature; n is the speed of rotation of the armature. The coincidence of frequencies f_e and f_n results in a sharp increase of machine vibration, i.e. leads to a resonance of vibrations, which is highly undesirable. Let us note the similarity of formula (1b) with the formula for the frequency of natural oscillations of an electric circuit consisting of

* *Elektrichestvo*, No. 4, 30–35, 1958.

inductance L and capacitance C:

$$f = \frac{1}{2\pi\sqrt{LC}} \tag{2}$$

In calculating the vibrations of a frame at resonance or at frequencies near to resonance it is necessary to take into account the damping resistance of vibrations in the frame:

$$r_{mf} = 2\pi f_c m_f D, \tag{3}$$

where D is the damping factor, equal for steel to 0.0525; m_f is the mass of frame.

The action of this resistance is analogous to the action of an electric resistance in a circuit r_E, L, C, to which an oscillating voltage is applied.

According to the nature of exciting forces, the space vibrations of frames are possible with the number of deformation waves equal to $\nu = 0$ and $\nu \geq 1$.

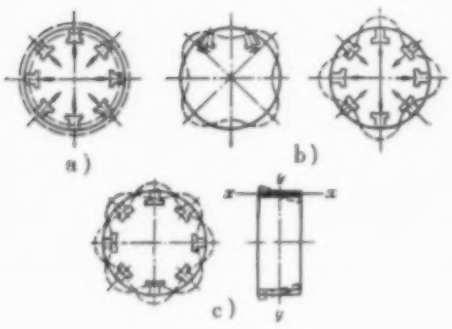

FIG. 1. Space forms of frame vibrations; (a) vibrations of the zero kind, (b) vibrations of the first kind, (c) vibrations of the second kind.

Vibrations of the zero kind ($\nu = 0$)

The frame undergoes deformations of extension and compression (Fig. 1a). Radial compliance of the frame is:

$$\lambda_{f0} = \frac{R}{2\pi ES} [cm/kg], \tag{4}$$

where R is the radius of the mean line of the frame (cm); E is Young's modulus of elasticity (kg/cm²); S is the area of the transverse section of the frame (cm²).

Vibrations of the first kind ($\nu \geq 1$)

The frame undergoes bending deformations (Fig. 1b). Here we have to distinguish two cases:

First case ($\nu = 1$)

The frame is clamped at two points. In this case the radial compliance of the frame is:

$$\lambda_{f1} = \frac{R^3}{2\pi E J_x \xi_1^2} [\text{cm/kg}], \tag{5}$$

where factor ξ_1 depends on the angle ψ of the frame clamping and may be found from Fig. 2; and J_k is the moment of inertia of the frame cross-section with respect to the x - x axis (cm⁴).

Second case ($\nu \geq 2$)

Vibration nodes are situated at places where main poles are fixed or between them. The radial compliance of the frame in this case is given by the formula (5):

$$\xi_1 = \frac{\nu(\nu^2 - 1)}{\sqrt{\nu^2 + 1}}. \tag{6}$$

1959

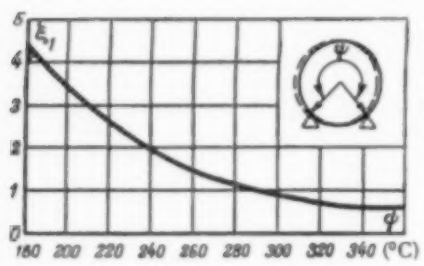

FIG. 2. Dependence of ξ_1 on ψ.

Vibrations of the second kind (Fig. 1c)

Such vibrations occur in machines with wedge-shaped armature slots or wedge-shaped pole shoes. In this case the frame executes bending and torsional vibrations.

Radial compliance of the frame is:

$$\lambda_{f2} = \frac{R l_f^3 \xi_2}{4\pi E J_y} \text{ [cm/kg]}, \qquad (7)$$

where l_f is the length of the frame (cm);
J_y is the moment of inertia of the frame transverse section with respect to the y-y axis (cm⁴);

$$\xi_2 = \frac{1+\sigma}{1+\sigma+2\nu^2}; \qquad (8)$$

σ Poisson's ratio, equal for steel to 0.3.

The action of periodic magnetic forces caused by the armature teeth

All periodic magnetic forces, so far as their action on main poles and frame is concerned, can be subdivided into three groups:

(a) radial forces F_r producing radial displacements of poles and the frame vibrations of the first and second kind;

(b) bending moments M_r producing angular displacements of poles in the transverse plane of the machine and frame vibrations of first kind;

(c) torsional moments M_p producing angular displacements of poles in the longitudinal plane of the machine and frame vibrations of the second kind.

TABLE 1.

Number of teeth in a pole division and in a pole arc	Kind of the exciting force	Vibrations of the adjacent poles	Number of deformation waves on the frame circumference and the kind of vibration
$\frac{Z}{2p} = n; \quad \alpha = \frac{b_p}{t_1} = n$	Bending moment M_r	In phase	$\nu = 2p$ (first kind)
$\frac{Z}{2p} = n, \quad \alpha = \frac{b_p}{t_1} = n + \frac{1}{2}$	Radial force F_r	In phase	$\nu = 0$ (zero kind)
$\frac{Z}{2p} = n + \frac{1}{2}; \quad \alpha = \frac{b_p}{t_1} = n$	Bending moment M_r	In antiphase	$\nu = p$ (first kind)
$\frac{Z}{2p} = n + \frac{1}{2}; \quad \alpha = \frac{b_p}{t_1} = n + \frac{1}{2}$	Radial force F_r	In antiphase	$\nu = p$ (first kind)
Thoughout, n is an integer			

The conditions for the appearance of radial forces and bending moments for the idle run of the machine are given in Table 1.

So far as torsional moments M_p are concerned, they are due to the wedge shape of the armature slots or pole shoes, this shape being used in d.c. machines to weaken the action of radial forces and bending moments.

During the run of an electric machine, superposition of different kinds of vibrations takes place, and this complicates the problem of determination of the vibration level of the frame. Nevertheless, as investigations show, for practical calculations in most cases we may only consider the influence of these forces that excite oscillations of the first kind. Nevertheless, we may only neglect the action of radial forces producing oscillations of the zero kind, and of torsional moments due to these forces, in the absence of the resonance of vibrations. Such an assumption is permissible owing to the following considerations:

(1) Radial forces producing oscillations of the zero kind are to a considerable extent attenuated by the damping action of the excitation winding.

(2) The torsional moments produce only insignificant vibrations of the frame, owing to its small torsional compliance.

Considering that radial forces and bending moments can produce only vibrations of the first kind, it is convenient in designing an electromechanical analogy to replace the action of bending moments by the action of equivalent radial forces (so far as values of deformations, which are produced by them, are concerned).

Thus a bending moment M_r applied to a pole may be replaced by an equivalent force F_{eq} applied between the poles:

$$F_{eq} = \frac{\gamma M_r}{R}, \tag{9}$$

where the value of γ for various ν may be taken from Table 2.

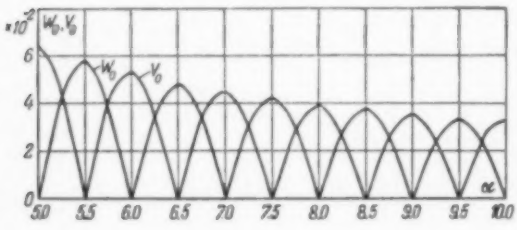

FIG. 3. Dependence of W_0 and V_0 on α.

Moreover, to simplify calculations we may neglect the action of tangential forces, since they are always smaller than radial ones.

The magnitude of periodic magnetic forces may be determined by formulae given in Table 3 for machines having rectangular or wedge-shaped armature slots, or an uniform or eccentric gap, this is often done in practice.

Formulae given in Table 3 are derived for the no-load and on-load run of the machine, on the basis of the following assumptions:

(a) the alternating magnetic field in the armature slots varies sinusoidally;

TABLE 2.

ν	2	3	4	5	6
γ	9.3	54	140	262	486

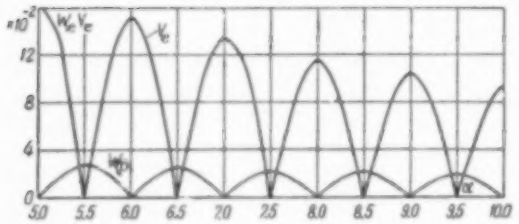

FIG. 4. Dependence of W_e and V_e on a.

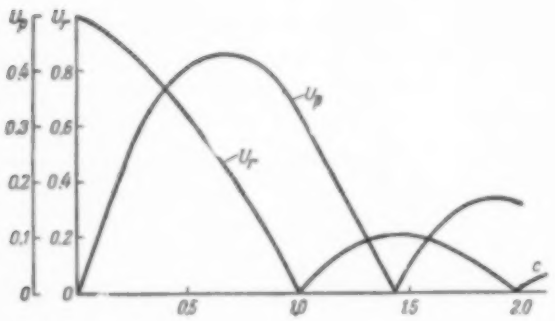

FIG. 5. Dependence of U_p and U_r on c.

(b) the magnetic system is unsaturated;

(c) the stepped shape of the curve of armature reaction is neglected.

$$F_0 = \left(\frac{B_\delta}{5\,000}\right)^2 b_p l_n \text{ [kg]},$$

where $\epsilon = k_c - 1$;

$x = \frac{Asb_p}{1{,}6\alpha B_\delta}$, the load factor; W_e, V_e, W_e, V_e are functions of $a = b_p/t_1$ (Fig. 3 and 4); U_r and U_p are functions of the slope of wedge shaped slots, c (Fig. 5); B_δ is magnetic induction in the air gap (G); b_p is width of the pole shoe (cm); l_n is the length of the pole (cm); k_c is Carter's coefficient; As is linear load of the armature (A/cm); δ is thickness of the air gap (in the case of an eccentric gap the thickness of an equivalent uniform air gap is used) (cm).

Noise due to yoke

The yoke of an electric machine may be considered as a cylindrical radiator of sound waves; its radiation power N is determined by the vibration speed of the yoke x_0 and by the acoustical resistance of the yoke in air r_a [4]:

$$N = \frac{1}{2} r x_0^2. \tag{10}$$

Acoustical resistance r_a may be calculated approximately by the formula [4]:

$$r_a = \pi R l_c \rho v_s \phi_1, \tag{11}$$

TABLE 3.

Shape of the armature slot or of the pole shoe	Kind of excitation	Value of the amplitude of forces and moments		Kind of forced vibrations
		Uniform gap	Eccentric gap	
Rectangular	Radial force	$F_r = 2F_{0\epsilon}\sqrt{W_0^2 + x^2V_0^2}$	$F_r = 0.36F_{0\epsilon}\sqrt{W_e^2 + 1.7x_e^2}$	Vibrations of the zero or first kind
	Bending moment	$M_r = F_{0\epsilon}b_p\sqrt{V_0^2 + x^2W_0^2}$	$M_r = 0.18F_{0\epsilon}b_p\sqrt{V_e + 1.7x^2W_e^2}$	Vibrations of the first kind
Wedge-shaped	Radial force	$F_r = 2F_{0\epsilon}U_r\sqrt{W_0^2 + x^2V_0^2}$	$F_r = 0.36F_{0\epsilon}U_r\sqrt{W_e^2 + 1.7x^2V_e^2}$	Vibrations of the zero or first kind
	Bending moment	$M_r = F_{0\epsilon}b_pU_r\sqrt{V_0^2 + xW_0^2}$	$M_r = 0.18F_{0\epsilon}b_pU_r\sqrt{V_e + 1.7x^2W_e^2}$	Vibrations of the first kind
	Torsional moment	$M_p = F_{0\epsilon}l_nU_p\sqrt{W_0^2 + x^2V_0^2}$	$M_p = 0.18F_{0\epsilon}l_nU_p\sqrt{W_e^2 + 1.7x^2V_e^2}$	Vibrations of the second kind

where $\rho v_s = 41.3$, the specific acoustic resistance of the air. Function ϕ_1 depends on the effective radius of the cylinder $2\pi R/\lambda$ where λ is the length of the sound wave for the frequency f_w (Fig. 6).

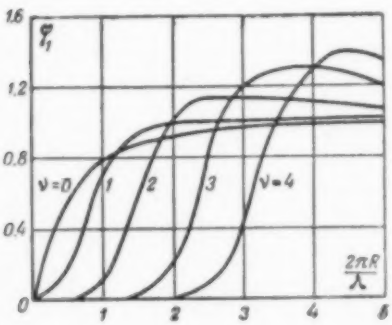

FIG. 6. Dependence of ϕ_1 on $2\pi R/\Lambda$ for different V.

Acoustical pressure of a distance d from the machine yoke in the case of open space is:

$$q = 408\sqrt{\frac{N}{4\pi(R+d)^2}} \text{ [bar]}. \tag{12}$$

The level of the machine noise with respect to the level of the acoustical pressure $q_0 = 2 \times 10^{-4}$ bar, which is arbitrarily chosen as a zero level, will be:

$$T = 20\log\frac{q}{q_0} \text{ [dB]}. \tag{13}$$

Electromechanical analogy

It is known that for calculating complicated mechanical and acoustical oscillating systems we often replace them by better-known systems. Such systems are elec-

tric circuits whose equations are analogous to the basic equations of motion in mechanics and acoustics.

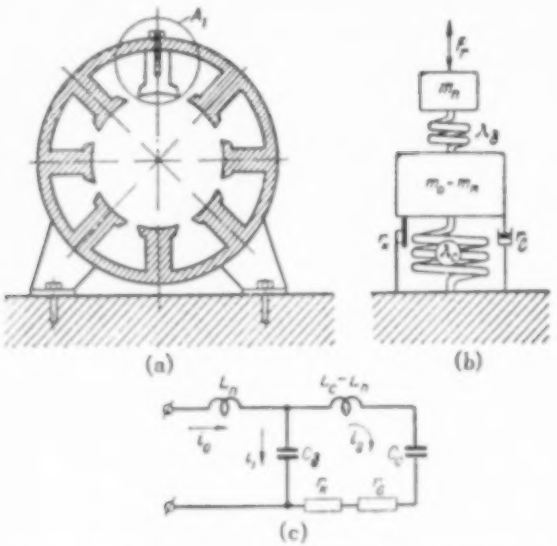

FIG. 7. Equivalent circuit of the node A_1 of a vibrating d.c. machine: (a) machine; (b) mechanical system; (c) equivalent electric circuit.

In comparing these equations we see that as friction r_m, mass m and compliance λ of a mechanical system determine its motion, so resistance r_E, inductance L and capacitance C determine current in an electric circuit.

In calculating the magnetic noise produced by an electric machine, we may replace the system under investigation by a simple translational mechanical system, which in turn may be represented by an equivalent electric circuit (Fig. 7).

In designing an analogy we may neglect the compliance of poles and the mass of bolts attaching the poles to the frame. Table 4 gives the conventional symbols of mechanical and electrical systems and formulae for their calculation.

The knowledge of parameters of a mechanical system and frequency of exciting ω enables us to determine the total impedance z_m of the mechanical system by analogy with an electric circuit (Table 5). It is customary to call the units of resistance of a mechanical system "mechanical ohms"; their dimension is kg sec/cm.

For the electric circuit (Fig. 7c), we may determine the current i_2 and in consequence the speed of vibrations of the machine frame x_1.

After having performed calculations using the circuit in Fig. 7, it is interesting to find the level of magnetic noise under the condition of absolutely rigid attachment of the poles to the frame. In this case the equivalent circuit becomes a simple cir-

cuit with elements r_1, L, C connected in series; solution of this problem is quite easy.

TABLE 4.

Element of a mechanical system	Conventional symbols adopted and mathematical formulae.	
	in a mechanical system	in an electric circuit
Mass of a pole	m_p	L_p
Compliance of bolts, attaching a pole to the frame, for tension: for a radial force for an equivalent force	λ_δ $\lambda_\delta = \frac{l_\delta}{kEs}$ [cm/kg]; $\lambda_\delta = \frac{2Rl_\delta}{\gamma akEs}$ [cm/kg], where l_δ is length of a bolt in a smooth part (cm); k – number of bolts; a – width of the core of the main pole (cm) s – area of a section of one bolt (cm²)	C_δ
Mass of the magnetic system without one main pole	$m_s - m_p$	$L_s - L_p$
Radial compliance of the frame for tension compression (zero kind of vibrations)	λ_{f0} [formula (4)]	C_{f0}
Radial compliance of the frame for bending (first kind of vibrations)	λ_{f1} [formula (5)]	C_{f1}
Radial compliance of the frame for tension (second type of vibrations)	λ_{f2} [formula (7)]	C_{f2}
Damping resistance of the frame vibrations	r_{mf} [formula (3)]	E_f
Mechanical resistance of the machine frame in air	r_{ma} $r_{ma} = \frac{r_a}{g}$ [formula (11)]	r_{Ea}

TABLE 5.

Electric circuit	Mechanical system
$z_{1E} = j\omega L_p$	$z_{1m} = j\omega m_p$
$z_{2E} = \frac{1}{j\omega C_\delta}$	$z_{2m} = \frac{1}{j\omega \lambda_\delta}$
$z_{3E} = r_E + j\omega (L_a - L_p) + \frac{1}{j\omega C_f}$	$z_{3m} = r_m + j\omega (m_a - m_p) + \frac{1}{j\omega \lambda_f}$

Example

Calculation of magnetic noise of a d.c. machine. 1. Initial data: $n = 1600$ rev/min, $2p = 4$; $B_\delta = 5680$ G; $As = 187$ A/cm; $Z = 42$; $t_1 = 1.72$ cm; $b_p = 12$ cm; $a = 6.8$ cm; $l_a = 14.5$ cm; $k_c = 1.23$; $c = 0$; $\delta = 0.25$ cm (uniform); $J_x = 16.6$ cm^4; $R = 20$ cm; $S = 50$ cm^2.

Weights of: pole, $G_p = 13.2$ kg; magnetic system, $G_a = 135$; frame, $G_f = 63$ kg.

Bolts: $k = 2$; $l_\delta = 1.8$ cm; $s = 1.13$ cm^2.

Calculations

1. $f_a = 42 \times 1600/60 = 1120$ c/s; $\omega = 7030$ 1/sec; $\Lambda = 29.4$ cm.

2. $\frac{Z}{2p} = 10.5$; $a = \frac{12}{1.72} = 7.0$; $c = 0$.

For these ratios vibrations of the first kind are excited by bending moments M_r with the number of waves in the circumference of the frame $\nu = 2$ (Fig. 1).

3. $$x = \frac{187 \cdot 12}{1.6 \cdot 0.25 \cdot 5680} = 1.0.$$

4. $M_r = \frac{1}{\sqrt{2}} \left(\frac{5680}{5000}\right)^2 12^2 \cdot 14.5 \cdot 0.23 \cdot 4.5 \cdot 10^{-3} = 19.8$ kg/cm; $F_{equ} = \frac{9.3 \cdot 19.8}{20} = 9.2$ kg.

5. $$\lambda_\delta = \frac{2 \cdot 20 \cdot 1.8}{9.3 \cdot 6.8 \cdot 2 \cdot 2.1 \cdot 10^6 \cdot 1.13} = 0.24 \cdot 10^{-4} \text{ cm/kg};$$

$$\lambda_{c1} = \frac{20^2}{2\pi \cdot 2.1 \cdot 10^6 \cdot 16.6 \cdot 2.69^2} = 5.1 \cdot 10^{-4} \text{ cm/kg};$$

$$\xi_1 = \frac{2(2^2 - 1)}{\sqrt{2^2 + 1}} = 2.69; \quad \omega_f = 1\,200 \text{ 1/sec}.$$

6. $$z_{1m} = j7030 \frac{13.2}{981} = j0.094 \cdot 10^3 \text{ mech } \Omega;$$

$$z_{1m} = \frac{1}{j7\,030 \cdot 0.24 \cdot 10^{-6}} = -j0.595 \cdot 10^{3} \text{ mech } \Omega;$$

$$z_{2m} = 0.0525 \cdot 1\,200\,\frac{63}{981} + j7\,030\,\frac{135 - 13.2}{981} +$$

$$+ \frac{1}{j7\,030 \cdot 5.1 \cdot 10^{-6}} = 0.0040 \cdot 10^{3} + j0.842 \cdot 10^{3} \text{ mech } \Omega;$$

$$r_a = \pi \cdot 20 \cdot 25 \cdot 41.3 \cdot 1.0 = 6.5 \cdot 10^{4} \text{ g/cm}.$$

7. Total mechanical impedance of the machine from the circuit in Fig. 7.

$$z_m \approx 2.1 \cdot 10^{3} \text{ mech } \Omega$$

8. $$\dot{x}_0 = \frac{9.2}{2.1 \cdot 10^{3}} = 4.4 \cdot 10^{-3} \text{ cm/sec} \quad \dot{x}_2 = 10.4 \cdot 10^{-3} \text{ cm/sec}.$$

9. $$N = \frac{1}{2}\, 6.5 \cdot 10^{4} \cdot 108 \cdot 10^{-6} \cdot 10^{-4} = 350 \cdot 10^{-6} \text{ W}.$$

10. $$q = 408 \sqrt{\frac{350 \cdot 10^{-6}}{4\pi (0.2 + 1.0)^2}} = 1.8 \text{ bar}.$$

11. Magnetic noise $$T = 20 \log \frac{1,8}{2 \cdot 10^{-6}} = 79 \text{ dB}.$$

1959

The analysis of the noise spectrum of the machine shows that the level of magnetic noise for the frequency of magnetic forces 1120 c/s is equal to 76 *dB*.

Translated by S. Szymanski

REFERENCES

1. G. Olson; Dinamicheskie analogii (Dynamical analogies), *Izd. inostrannoi lit.* (1947).
2. V.V. Furduev; *Elektroakustika (Electro-acoustics)* United State Press (1948).
3. W.P. Ermolin; Shum mashin pastiannogo toka (Noise in d.c. machines), *Izv. Lengingradskoge elektrotekhnicheskogo inst. im. Lenina* 24, (1951); 28, (1955).
4. K. Schmidt; Gehäuseschwingungen von Gleichstrom-Mashinen als Ursache magnetischen Geräusches (Frame vibrations of d.c. machines as a cause of magnetic noise), *A.F.E.* (1938).
5. Mikina; Effect of skewing and pole spacing on magnetic noise in electric machinery, *Trans. Amer. Soc. Mech. Engrs.*, 5, No. 10 (1934).
6. K. Gamata; Magnitnyi shum mashin postoiannogo toka (Magnetic noise of d.c. machines). *Elektrotechnicky obzor*, No. 6 (1954).
7. V.K. Iofe and A.A. Iasnopolskii; *Raschetnye grafiki i tablitsky po elektroakustike (Graphs and tables for electro-acoustical calculations)*, Gosenergoizdat (1954).

TRANSIENT PROCESSES IN AN ELECTRIC DRIVE FOR AN EXPONENTIAL VARIATION OF THE MAGNETIC FLUX *

Yu. P. PETROV Leningrad

(Received 11 July 1957)

In many d.c. drives transient processes occur when the magnetic flux varies exponentially: the starting of a motor when the excitation winding was not connected before the start, the control of the motor speed by varying the magnetic flux, and others, are examples of such processes. In spite of the importance of these transient processes, no convenient methods for their calculation are available. The method proposed by Kuznetsov, [1] which consists in integrating the differential equations of the motor by means of power series, requires tedious calculations. Nikitin and Kunitskii in 1943 suggested a description of the transient processes in an electric drive, for the exponential variation of the magnetic flux, by means of new, non-elementary functions [2]. The realization of this idea proved to be difficult because these non-elementary functions depend on many parameters. Consequently, their evaluation and use was not easy.

In this article the functions of one parameter (and of time) are discussed; they permit an easy calculation of transient processes.

Let us make the following assumptions:

(a) the magnetic flux in the motor increases and decreases as a strictly exponential function;
(b) the armature reaction is absent;
(c) the armature inductance is zero;
(d) the torque due to the load resistance of the drive is constant.

With these assumptions the differential equations of the drive, when the motor is started without the excitation winding being energized in advance, are:

$$\left.\begin{aligned} U &= ir_a + C\Phi\left(1 - e^{-\frac{t}{T_w}}\right)\omega; \\ Ci\Phi\left(1 - e^{-\frac{t}{T_w}}\right) &= J\frac{d\omega}{dt} + M_r, \end{aligned}\right\} \qquad (1)$$

* *Elektrichestvo*, No. 4, 35-38, 1958.

where U is the grid voltage
r_a is the armature circuit resistance
Φ is the steady state value of the magnetic flux;
ω is the angular speed of the armature rotation;
J is the moment of inertia reduced to the motor shaft;
M_r is the torque due to the load resistance of the drive;
T_w is the time constant of the excitation winding.

We introduce the relative values for current $i_k = \frac{i}{I_{st}}$; angular speed $\omega_k = \omega/\omega_{nl}$; time $x = t/T_\omega$ and the torque $\lambda = M_r/M_{max}$, where I_{st} is the current for for the stalled armature of the motor, ω_{nl} angular speed of an ideal no-load running and $M_{max} = CI_{st}\Phi$ the maximum torque of the motor.

Dividing the first of the equations (1) by $U = r_a I_{st} = C\Phi \cdot \omega_{nl}$ and the second by $M_{max} = CI_{st}\Phi$, we get:

$$\begin{aligned} 1 &= i_k + (1 - e^{-x})\omega_k; \\ i_k(1 - e^{-x}) &= \frac{1}{k}\frac{d\omega_k}{dx} + \lambda, \end{aligned} \tag{2}$$

where $K = T_w/T_m$; $T_m = I\omega_{nl}/M_{max}$, the electromechanical time constant. Eliminating i_k from the system (2) we get:

$$\frac{d\omega_k}{dx} + k(1 - e^{-x})^2\omega - k(1 - e^{-x}) + k\lambda = 0. \tag{3}$$

Equation (3) reduces to quadratures: $\omega_k = e^{-k(x-0,5e^{-2x}+2e^{-x}-1,5)} \times$

$$\times \left[f_0 + k\int_0^x (1 - e^{-x} - \lambda)\, e^{k(x-0,5e^{-2x}+2e^{-x}-1,5)}dx \right], \tag{4}$$

where f_0 is the initial condition value ω_k for $x = 0$.

The integral in equation (1) cannot be evaluated in a finite form and is inconvenient for an approximate calculation. Expression (4) can be represented as a sum of three terms:

$$\omega_k = f_1(x, k) + f_0 \cdot f_2(x, k) + \lambda \cdot f_3(x, k),$$

where

$$f_1(x, k) = f_2(x, k) \cdot k \times$$

$$\times \int_0^x (1 - e^{-x}) e^{k(x-0.5e^{-2x}+2e^{-x}-1,5)}dx;$$

$$f_2(x, k) = e^{-k(x-0,5e^{-2x}+2e^{-x}-1,5)};$$

$$f_3(x, k) = -f_2(x, k)\, k \int_0^x e^{k(x-0.5e^{-2x}+2e^{-x}-1,5)}dx.$$

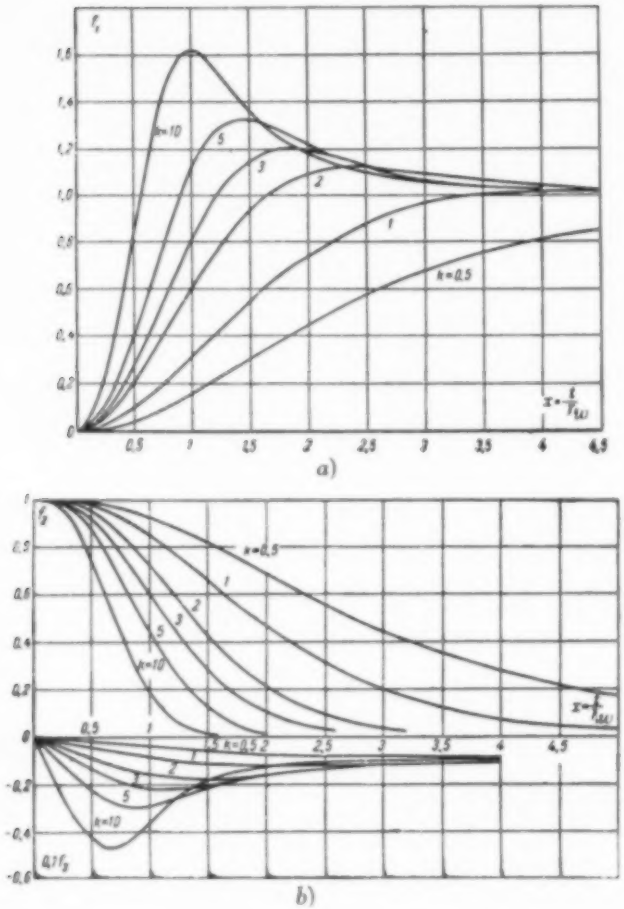

FIG. 1. Graphs of f_1, f_2 and $0.1f_3$ as functions of $x = t/T_w$.

Since f_1, f_2 and f_3 depend only on two parameters, x and k they can be represented as a family of curves.

Fig. 1 shows curves f_1, f_2 and $0.1\ f_3$. Values of $k = 0.2 - 1$ are characteristic for low power electric drives; values $k = 0.5 - 5$ are characteristic for the medium power drives.

Curves in Fig. 1 may be used for the calculation of transient processes not only for the case when $\Phi = 0$, but also for any value of the initial magnetic flux. From the expression:

$$1 - (1 - a)\, e^{-x} = 1 - e^{-(x + x_0)},$$

where $x_0 = ln/1{-}a$, it follows that, after the change of variable $x_1 = x_0 + x$, the calculation of the transient process for an initial magnetic flux not equal to zero also reduces the use of the curves in Fig. 1.

The application of the method of calculation discussed is illustrated by the following examples.

Example 1.

The start of a motor, for which $k = 1$ and $\lambda = 0.2$, is made without previous switching-on of the excitation winding.

It is required to find the current and speed.

The process of accelerating the motor begins when its driving torque becomes greater than the torque due to the load-resistance; i.e. when $1 - e^{-x} = 0.2$. Hence we find $x = -ln\ (1\text{-}0.2) = 0.222$. Hence we have:

$$\omega_x = f_1(k=1,\ x=0.222) + f_0 \cdot f_2(k=1).\ x=0.222) + \\ + 0.2 \cdot f_3(k=1,\ x=0.222) = 0. \tag{6}$$

Since the values of f_1, f_2 and f_3 are known from Fig. 1, we find from equation (6) $f_0 = -0.06$.
Finally, for $0 < x \leq 0.222$, we have

$$[\omega_k = 0;]$$

for $x \geq 0.222$

$$\omega_x = f_1(k=1,\ x) - 0.06 \cdot f_2(k=1,\ x) + \\ + 0.2 \cdot f_3(k=1,\ x).$$

Having found ω_k, we use the equation $i_k = 1 - (1 - e^{-x})\omega_k$, and calculate the armature current.

Example 2.

In a motor ($k = 2$ and $\lambda = 0.1$), after shunting the resistance in the circuit of its excitation winding, the magnetic flux increases from $\Phi_0 = 0.5\ \Phi$ *to* Φ.

The initial angular speed $\omega_0 = 1.6\ \omega_{nl}$, the initial current $i_0 = 0.2\ I_{sl}$. It is required to calculate the transient process, which takes place after shunting the resistance.
From (5) we find:

$$x = -\ln\ (1 - 0.5) = 0.696$$

Therefore, when $x = 0.696$ we have $\omega_k = \omega_0 = 1.6$.
On the other hand, at the same moment of time:

$$\omega_x = f_1(k=2,\ x=0.696) + f_0 \cdot f_2(k=2,\ x=0.696) + \\ + 0.1 \cdot f_3(k=2,\ x=0.696). \tag{7}$$

1959

Having found the values of f_1, f_2 and f_3 from Fig. 1 on the basis of (7) we find $f_0 = 1.58$.

Finally we have:

$$\omega_x = f_1(k=2,\ x-0.696) + 1.58 \cdot f_2(k=2,\ x-0.696) + \\ + 0.1 \cdot f_3(k=2,\ x-0.696).$$

The results of calculations are given in Table 1.

TABLE 1.

$x_1 = x - 0.696$	0	0.3	1.3	2.3
ω_k	1.6	1.57	1.36	1.03
i_k	0.2	0	−0.18	0.03

Example 3.

Start of the motor PN – 28.5, 110V, 2.2 kW, 1500 rev/min is made without previous connexion of its excitation winding to the generator PN-85, 115 V, 6.5 kW, 56.5 A, 1460 rev/min.

The armature resistance of the motor 0.443 ohm; armature resistance of the generator 0.141 ohm; resistance of connected leads 0.167 ohm. The magnetic flux of the motor 0.328 x 10^6 maxwell; the number of turns of the excitation winding per pole 1400. The time constant of the excitation winding, the dissipation factor being accounted for T_w = 0.184 sec; the electro-mechanical time constant T_m = 0.31 sec.; k = 0.184/0.31 = 0.594. The values of i_k and ω_k are calculated as in Example 1.

Table 2 gives the results of calculations and the experimental data, recorded by means of oscillograms.

TABLE 2.

x	t, (sec)	ω_k		i_k	
		calculated	experimental	calculated	experimental
0	0	0	0	1	0
1	0.184	0.183	0.177	0.885	0.880
2	0.368	0.44	0.450	0.620	0.670
3	0.552	0.68	0.700	0.350	0.400
4	0.736	0.8	0.850	0.220	0.205

TABLE 2.

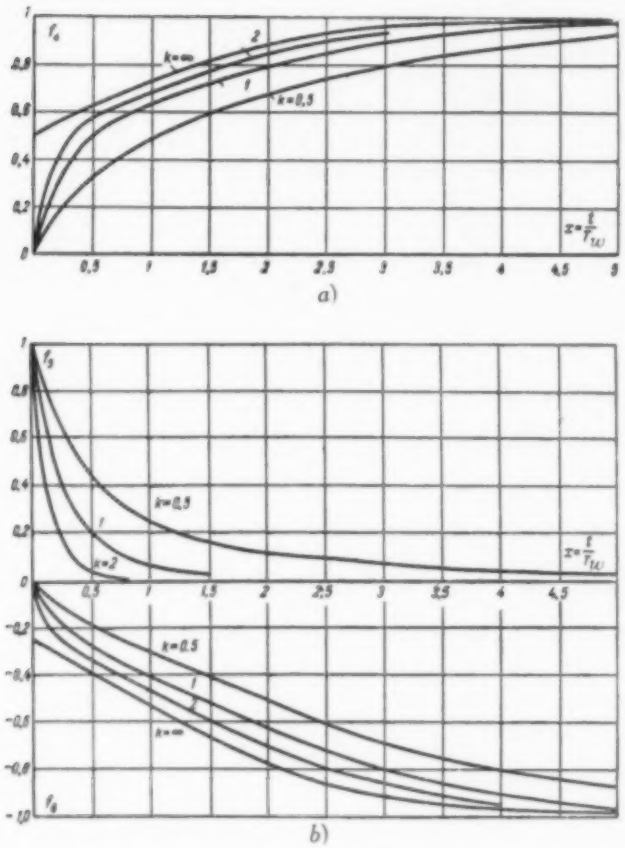

FIG. 2. Graphs of f_3, f_4, f_5 and f_6 as functions of $x = t/T_W$.

For calculation of transient processes with an exponentially decreasing flux it is necessary to introduce new functions f_4, f_5 and f_6 corresponding to functions f_1, f_2 and f_3 for the case of an increasing magnetic flux. Fig. 2 shows these functions, calculated for the case when the magnetic flux decreases according to the law:

$$\Phi = \Phi_{fin}(1 + e^{-x}).$$

As in the case of the increasing magnetic flux, on the basis of the equality

$$ae^{-x} + 1 = e^{-(x + x_0)} + 1,$$

where $x_0 = \ln a$,

by the change of the variable $x_1 = x + x_0$, we reduce the calculation of a transient

process, for any initial value of the magnetic flux (less than twice the value of the final flux) to the use of the curves in Fig. 2.

Example 4.

A resistance stage is introduced into the excitation circuit. The initial magnetic flux is 1.5 Φ; the initial speed is 0.6 of the steady state speed (after the end of the transient process). The time constant of the excitation winding, calculated with the introduced resistance accounted for, is $T_w = 0.2$ sec. The electromechanical time constant of the drive, calculated for the final value of the magnetic flux Φ_{fin}, $T_m = 0.15$ sec; $\lambda = 0.1$. We find $T_w/T_m = 1.33$ and $x_0 = -\ln 0.5 = 0.696$. For $x = 0.696$ the following equation is valid:

$$\omega_x = f_4(k = 1.33,\ x = 0.696) + f_0 \cdot f_5(k = 1.33,\ x = 0.696) + \\ + 0.1 \cdot f_6(k = 1.33,\ x = 0.696) = 0{,}6.$$

Having found from curves in Fig. 2 f_4, f_5 and f_6, we find $f_0 = 6.7$ and finally we get:

$$\omega_x = f_4(k = 1.33,\ x - 0.696) + 6.7 \cdot f_5(k = 1.33,\ x - 0.696) + \\ + 0.1 \cdot f_6(k = 1.33,\ x).$$

Accounting for the armature inductance

The comparison of the results obtained by using curves in Fig. 1 and 2 with the experimental data shows that neglecting the armature inductance leads to an appreciable error only at the beginning of the transient process. In particular, at the start of the motor the maximum value of the current due to the armature inductance is always smaller than that for the armature stalled ($i_{k\ max} < 1$), whereas by calculating by means of the curves in Fig. 1 and 2, we get $i_{k\ max} = 1$. To introduce corrections into the calculation of currents at the start, appropriate curves are constructed in Fig. 3; they give the values of the maximum current at the start as functions of the factor $k = T_w/T_m$ and of the ratio T_a/T_m, where $T_a = L_a/r_a$, time constant of the armature circuit (sec).

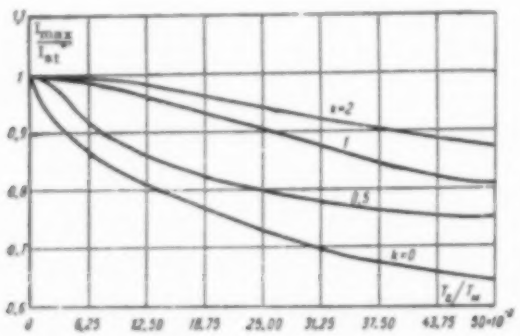

FIG. 3. Graphs of I_{max}/I_{st} as functions of T_a/T_m.

For the drive discussed in example 3, the armature inductance of the motor is 0.00357 H, of the generator armature – 0.00136 H. Hence the time constant of the armature circuit $T_a = 0.0066$ sec.

For this case, according to Fig. 3 we have $i_{k\ max} = 0.98$, and the experimental value of $i_{k\ max} = 0.96$.

The lower curve in Fig. 3 ($k = 0$) is constructed for the infinite rate of increase of the current, which is equivalent to the previous connexion of the excitation winding. From Fig. 3 it follows that the influence of the armature inductance in the case, when the excitation winding was not energized before the start, is less pronounced than in the case when the excitation winding was switched on before the start.

Conclusions

The above method, based on the use of special functions given by the graphs of Fig. 1 and 2 allows both quick and sufficiently accurate calculation in practice of the transient processes for the exponentially varying magnetic flux.

Translated by S. Szymanski

REFERENCES

1. P.I. Kuznetsov; Transient processes in an electric motor when the armature and excitation voltages vary simultaneously, *Avtomatika i telemekhanika*, No. 5 (1951).
2. V.P. Nikitin, V.K. Turkin and N.P. Kunitskii; An analytical method for the investigation of the operation of a shunt motor for speed control, by the excitation flux, *Izv. Akad. Nauk SSSR (Otd. tekh. nauk)*, No. 9-10 (1943).

1959

THE USE OF ELECTROMAGNETIC POWDER COUPLINGS FOR FREQUENT REVERSALS OF A DRIVEN MECHANISM*

T.A. GLAZENKO

Leningrad

(Received 13 June 1957)

Many types of electric drives operate under conditions of frequent reversals of the direction of motion of a driven mechanism, the frequency of reversals varying within the limits 0.1 - 10 / sec. Very often in this case a quite definite graph of motion is prescribed; to comply with the specified requirements sufficiently large accelerations for starting and braking should be applied. The use of electric machines, working with a reclosing feedback, usually does not satisfy all the requirements of the drive. Owing to difficult thermal conditions and a large value of the dynamic

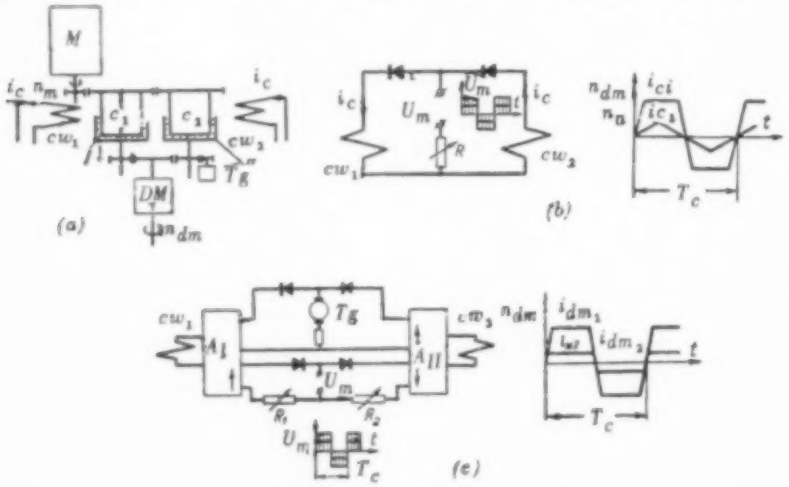

FIG. 1. Diagrams of a drive with the use of powder couplings to control a driven mechanism: M is the motor of the drive; I, II the couplings; CW_1 and CW_{11} excitation windings of the couplings; DM the driven mechanism; TG a d.c. tachogenerator; and A_1 and A_{11} amplifiers.

* *Elektrichestvo*, No. 4, 38 - 43, 1958.

torque, necessary for quick accelerating and braking, the power of a motor should be greatly increased, and special arrangements for its cooling are needed.

The use for this purpose of two powder couplings together with a mechanical reductor (Fig. 1) enables us:

(a) to decrease the power and facilitate operation of the driving motor;
(b) to use, for accelerating and braking, the kinetic energy accumulated by the rotating masses of the non-reversible part of the drive;
(c) to shorten the duration of transient processes and to decrease thermal losses in the drive;
(d) to realize the specified graph of motion and to vary the mean speed of rotation of the driven mechanism.

Transient processes in an electric drive at reversals of a driven mechanism.

The analysis of the reversal process has been carried out according to the method and assumptions which are stated in [1].

Let us adopt the following notation:

M_1, M_{11} are torques transmitted by couplings 1 and 11 to the shaft of the driven mechanism;

ω_I, ω_{II} and s_I, s_{II}: angular speeds and slips of non-reversible and reversible parts of the drive;

T_{eI}, T_{eII}, T'_{eI} and T'_{eII}: equivalent time constants of the couplings I and II during the period of connecting and dis-connecting from the grid and switching in a discharge resistance;

$T_I = J_I \omega_0 / B$ and $T_{II} = J_{II} \omega_0 / B$: electromechanical constants of the driving and driven parts of the drive.

The torque of the motor Bs_1, torques of both parts of the drive for no-load run M_{0I}, M_{0II}, torque due to the static resistance of the load, M_S, and moments of inertia on non-reversible and reversible parts of the drive, J_I, J_{II}, are all considered to be reduced to the shaft of the couplings.

Equations of motion of the driving and driven parts of the drive are:

$$Bs_1 = -J_1\omega_0 \frac{ds_1}{dt} + M_1 + M_{II} + M_{0I}; \tag{1}$$

$$M_1 + M_{II} = J_{II} \frac{d\omega_{II}}{dt} + M_{0II} + M_s. \tag{2}$$

The reversal begins at the instant of disconnecting the winding of the coupling I from the grid and closing it through the discharge resistance.

In this case

$$M_1 = M_{s\,s}\, e^{-\frac{t}{T'_{e1}}},$$

where $M_{s\,s}$ is the moment of the coupling corresponding to the steady state value of the excitation current. Let us split up the process under consideration into four periods.

In the first period, slowing down begins at the instant of time

$$t = t_0 = T'_{e1} \ln \frac{M_{s\,s}}{M_s + M_{0II}},$$

when the decreasing torque of the coupling I becomes equal to $M_s + M_{0}II$, and lasts until the instant of switching of the winding of coupling II ($t = t_0 + t_1$). The length of this period is equal to the time t_1, of operation of the switching device. Denoting $t - t_0 = t'$, $(M_1)_{t_0} = M_{s\,s\,1} + \exp(-t_0/T_{e\,1})$ and taking into account the initial conditions, for $t' = 0$, we get

$$s_1 = s_{II} = \frac{M_{01} + M_s + M_{0II}}{B} = \frac{M_{01} + M'_s}{B}$$

integrating equations (1) and (2) we get:

$$s_1 = \frac{M_{01}}{B} + \frac{M'_s}{B} e^{-\frac{t'}{T_1}} + \\ + \frac{(M_1)_{t_0} T'_{e1}}{B(T_1 - T'_{e1})} \left(e^{-\frac{t'}{T_1}} - e^{-\frac{t'}{T'_{e1}}} \right); \tag{3}$$

$$\omega_{II} = \omega_0 \left(1 - \frac{M_{01} + M'_s}{B} \right) - \frac{M'_s}{J_{II}} t' + \\ + \frac{(M_1)_{t_0} T'_{e1}}{J_{II}} \left(1 - e^{-\frac{t'}{T'_{e1}}} \right). \tag{4}$$

Usually the electromagnetic constant of the process of disconnexion of couplings is so small that at the end of the first period of the reversal the torque of the coupling I becomes zero. Substituting into formulae (3) and (4) the value $t' = t_1$, we shall find the values of speeds and slips at the beginning of the second period: s_{1b}, s_{IIb}, ω_{1b}, ω_{IIb}.

The second period, of reversal-braking, lasts during the time t_2 from the moment of connecting the second coupling ($t = t_0 + t_1$) till the moment of stand-

still if the driven mechanism ($t = t_0 + t_1 + t_2$). The increasing torque of the coupling II brakes the reversible part, and we have to substitute into equation (2):

$$M_{II} = -M_{ssII}\left(1 - e^{-\frac{t'''}{T_{eII}}}\right) \tag{5}$$

Choosing the instant when $t = t_1 + t_0$ as a zero moment for time-counting, and denoting $t - t_0 - t_1 = t,''$ we solve equations (3) and (4) with regard to the initial conditions ($t'' = 0$; $s_I = s_{Ii}$ and $\omega_{II} = \omega_{IIi}$)

$$s_I = \frac{M_{0I} + M_{ssII}}{B} + \frac{M_{ssII}T_{eII}}{B(T_I - T_{eII})}e^{-\frac{t''}{T_{eII}}} + \tag{6}$$

$$+\left[s_{Ii} - \frac{M_{0I}}{B} - \frac{M_{ssII}T_I}{B(T_I - T_{eII})}\right]e^{-\frac{t'''}{T_I}};$$

$$\omega_{II} = \omega_{IIi} + \frac{M_{ssII}T_{eII}}{J_{II}}\left(1 - e^{-\frac{t'''}{T_{eII}}}\right) - \tag{7}$$

$$-\frac{M_{ssII} + M_s'}{J_{II}}t''.$$

1959

The last equation is valid up to the moment of time, when ω_{II} becomes zero.

The third period of the acceleration of the driven part in the opposite direction (t_3), lasts till the moment, when the slip between the driving and driven part of the coupling vanishes.

For $t = t_0 + t_1 + t_2 + t_3$,

$\omega_I = \omega_{II} = \omega_{eng}$. Equations and formulae, given in [1] for the acceleration of the driven mechanism are also valid in this case.

In the fourth period, that of reversal, the acceleration of the driven and driving parts of the drive reaches the steady-state speed under conditions of rigid engagement (t_4).

The motion of the system is characterized by a single general equation [1]. with initial conditions: for

$t'''' = t - (t_0 + t_1 + t_2 + t_3) = 0$,

$s_I = s_{II} = s_{eng}$.

The total time of the reversal will be $t_{rev} = t_0 + t_1 + t_2 + t_3 + t_4$.

Calculations of the transient process and construction of the graph of the motion of the load are greatly simplified if $T_{II} > 3\ T_e$.

In this case we may assume that the decrease and increase in the torques of couplings occur instantaneously and in the equations of motion (1) and (2):

$$M_{\mathrm{I}} = M_{ss\mathrm{I}} = \text{constant}; \quad M_{\mathrm{II}} = M_{ss\mathrm{II}} = \text{constant}.$$

Then the formulae for speed of the reversible parts are reduced to the form:
(a) during the period of braking:

$$\omega_{\mathrm{II}} = 1 - \left(s_{ss} + \frac{M_{ss\mathrm{II}} + M_s}{J_{\mathrm{II}}\omega_0} t'' \right) \omega_0 = \omega_{ss} - \frac{M_{ss\mathrm{II}} + M'_s}{J_{\mathrm{II}}} t'' \tag{8}$$

and

$$t_2 = \frac{J_{\mathrm{II}}\omega_{ss}}{M'_s + M_{ss\mathrm{II}}}; \tag{9}$$

(b) during the period of accelerating

$$\omega_{\mathrm{II}} = \frac{M_{ss\mathrm{II}} - M_s}{J_{\mathrm{II}}} t'' \quad \text{и} \quad t_2 = \frac{J_{\mathrm{II}}\omega_{ss}}{M_{ss\mathrm{II}} - M'_s}, \tag{10}$$

where s_{ss} and ω_{ss} are steady state values of the slip and angular speed of the coupling.

Fig. 2 shows curves s_{I} and $s_{\mathrm{II}} = f(t)$ and $M_{\mathrm{I}}, M_{\mathrm{II}} = f(t)$ calculated by the above equations.

On comparing these curves with the reversal oscillograms (Fig. 3) recorded on a certain installation, we may note the analogy in the shape of the theoretical and experimental curves $\omega_{\mathrm{II}} = f(t)$. The oscillogram of the change of the motor current (Fig. 3) shows that in this system the motor works under a nearly constant load; braking and accelerating of the driven mechanism is done at the expense of the kinetic energy of the rotating masses of the non-reversible part of the drive (in this installation $J_{\mathrm{I}} \approx 3\ J_{\mathrm{II}}$). It is easy to show that the mean speed of the driven mechanism and the torque of the powder coupling are related by the following equations:
(a) in the case when the curve (Fig. 3) has a horizontal portion;

$$\omega_{cp\mathrm{II}} = \omega_{ss} - \frac{2J_{\mathrm{II}}\omega_y^2}{T_q} \frac{M_{ss}}{M_{ss}^2 - M_s'^2}; \tag{11}$$

(b) for a triangular shape of the curve $n_{II} = f(t)$:

$$\omega_{mell} = \frac{T_c}{8J_{II}} \cdot \frac{M_{ss}^2 - M_s'^2}{M_{ss}}, \tag{12}$$

where T_c is a period of the curve $\omega_{II} = f(t)$.

Thus, varying the excitation current in the couplings, we control the mean speed of the output shaft of the installation by decreasing the steady-state torque of the coupling ($M_{ss} = ki_{sh}$). Speed control of installations has been realized by means of magnetic amplifiers connected in the excitation circuit of the couplings. To obtain a steady-speed control of the mechanism for a constant period of reversal in the circuit in Fig. 1b, a feedback coupling is necessary in systems with a variable torque of the load resistance.

If the shaft of the driven mechanism is to rotate at a constant angular speed for all values of the angle of rotation, i.e. if for all angles we want to preserve the trapezoidal shape of the curve $n_{II} = f(t)$, then a negative speed feedback has to be introduced in the system (Fig. 1c). Experimental and theoretical investigation of such a system will be the subject of another work of the author.

1959

We may also control the speed n_{II} for a constant excitation current of the coupling by varying the speed of rotation of the driving motor. In this case the trapezoidal shape of the curve $n_{II} = f(t)$ is preserved for all the values of the speed, and the period of the reversal process decreases with the decrease of n_m [The speed of the motor].

Thermal conditions of the couplings

The heat developed during the reversal of the driven mechanism should be dissipated by the couplings, without overheating them to a temperature dangerous for winding insulation. Therefore, the dimensions and construction of the couplings should be so chosen as to ensure an adequate dissipation of heat. Losses of energy in couplings consist of losses due to slip A_{sl}, copper losses in windings A_w and friction losses during no-load running A_{nl}. Losses due to slip play the most important part in the development of heat in couplings controlling a reversible mechanism. These losses are taken as a basis for calculations.

Fig. 4 shows diagrams of power losses in couplings I and II in relation to the graph of the output shaft speed. In calculating losses due to slip we assume that the change of the torque of the coupling takes place instantaneously and the speed of rotation of the driving part of the system remains constant during the reversal process:

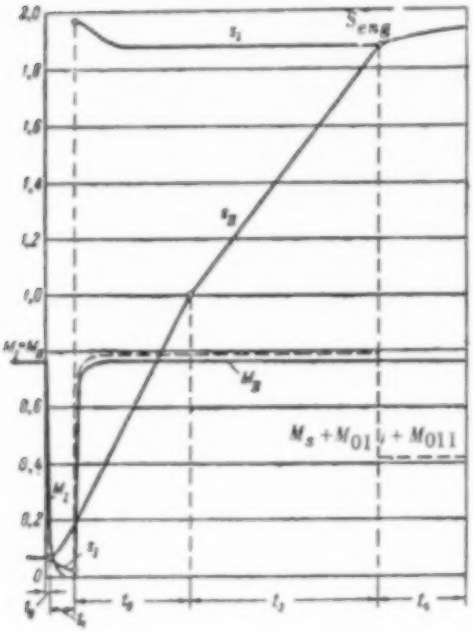

FIG. 2. Graphs for calculation of reversal parameters $S_{I}, S_{II} = f(t)$ and $M_{I}, M_{II} = f(t)$.

$\omega_I = \omega_{ss}$ = constant.

The loss of energy due to the slip in a powder coupling during the braking and accelerating processes is determined by:

$$A_{sl}\ A_b + A_a = \int_0^{t_3} M_y\ (w_1 + w_2)\ dt'' + \int_0^{t_3} M_y\ (w_1 - w_2)\ dt'' \tag{13}$$

Integrating this equation and taking into consideration relationships (8) - (10) we get:

$$A_{ca} = \frac{3}{2} J_{II} \omega_{ss}^2 \frac{M_{ss}}{M_{ss} + M'_s} + \frac{1}{2} J_{II} \omega_{ss}^2 \frac{M_{ss}}{M_{ss} - M'_s} \tag{14}$$

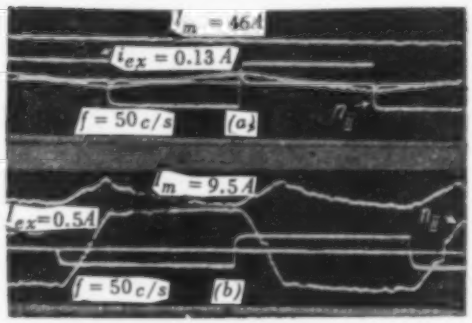

FIG. 3. Reversal oscillograms of the driven mechanism for the constant angular rotation of the motor n_m = 8000 rev/min (Fig. 1b): (a) I_m motor current; i_{ex} excitation current in the coupling; n_{II} mean = 16 rev/min, the mean angular velocity of the output shaft; angle of rotation of the shaft for ½ T_c α = 120°; reversal frequency f = 0.4 c/s; (b) $n_{II\,mean}$ = 1.67 rev/min; α = 10°; f = 0.5 c/s.

Introducing the notation for the security factor of the coupling $K = M_{ss}/M_s$ and rearranging the formula (14), we get the expression for energy losses due to slip for one cycle.

$$A_{sl} = \frac{1}{2} J_{II} \omega_{ss}^2 \frac{2k(2k-1)}{k^2-1} = A_0 \cdot f(k). \tag{15}$$

The relative loss of energy due to slip

$$a_{sl} = \frac{A_{sl}}{A_0} = \frac{2k(2k-1)}{k^2-1}$$

as a function of the security factor of the coupling, k is given in Fig. 5.

It is advisable to choose a value of k greater than 2. It is remarkable that within the range of values of the coupling security factor from 1.8 to ∞, the value of energy losses due to slip for the period of braking and accelerating remains nearly constant (Fig. 5) and may be considered equal to that for no-load running

$$A_{sl} = 4 \frac{I_{II} \omega_{ss}^2}{2}. \tag{16}$$

Mean power losses in the coupling for a cycle are:

$$P_{me} = \frac{A_{sl} + A_w + A_{n.l}}{T_c}, \tag{17}$$

where

$$A_w = i_e^2 r_w \; t_{su}; \quad A_{n.l.} = M_{n.l} \Delta\omega \cdot t_{off};$$
$$\Delta\omega = 2\omega_y; \quad M_{n.l} \approx M_y \cdot (0{,}03 \ldots 0{,}08).$$

Having determined P_{mean} and chosen the method of cooling of the coupling, we may calculate the area of the external surface of the coupling, which is required for heat dissipation, from the relationship:

$$P_{me} \leqslant k_t S (t_e^\circ - t_0^\circ), \tag{18}$$

where k_t is the coefficient of thermal dissipation of the coupling surface;

$S = \pi D_{ex} \; 1 + 2 \; \frac{\pi D_{ex}^2}{4} \sim (1.7 - 2.04) \; D^2 + 2.08 \; D^2 = (3.78 - 4.12) \; D^2$, the area of the external surface of the coupling, which dissipates heat (cm^2);

t_e° the permissible limiting temperature of the coupling frame;

t_0 the temperature of the ambient medium;

D mean diameter of the working layer.

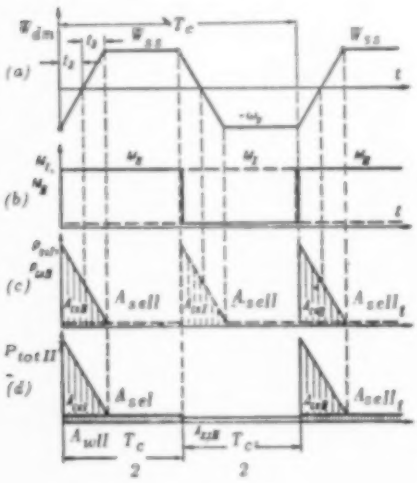

FIG. 4. Graph of the speed of the driven mechanism $w_{dm} = f(t)$, coupling torques M_1, $M_{11} = f(t)$ and power losses P_{sell}; $P_{sell} = f(t)$ and $P_{tot} = f(t)$.

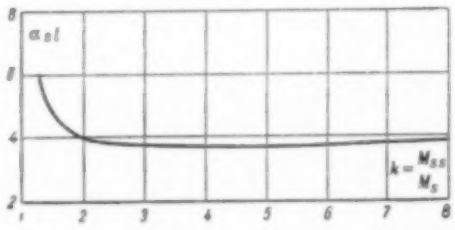

FIG. 5. Graph of the variation of relative energy losses in the coupling due to slip, during the period of braking and accelerating, as a function of the coupling safety factor $K = M_{ss}/M_s$.

The limiting temperature of overheating of the powder couplings, t_e° is determined by the type of insulation of its excitation winding and varies within the limits

70 - 130°C (The last figure applies to the couplings with a glass-mica insulation on a silicone-organic base).

Values of k_t, determined experimentally for various speeds of motion of the external surface of the coupling, are given in Fig. 6. The curve $k_t = f(v)$ is obtained from experiments with a single-gap cylindrical coupling with a smooth, zinc-plated external surface [δ_g = 0.35 mm; filler carbonyl iron-talc (10:1)].

The value of the coefficient of thermal dissipation may be increased several times by blowing on the coupling surface (Fig. 6).

In installations in which the dimensions and weight of the coupling play a decisive role, it is necessary to provide the heat dissipating surface with fins and to use forced ventilation. In this case the maximum value of k_t should be taken for calculations.

In the class of drives which are discussed here, the reduction ratio from the motor shaft to the driven mechanism is rather large. In designing the drive we have to choose a place for fixing the couplings and determine the reduction ratio i_3. For this purpose we may be guided by the following considerations.

The magnitude of the area of the heat dissipating surface ,S, of the coupling, which was found by formula 18, determines the dimensions (external diameter D_{ex} and the diameter of the layer) and, consequently, the torque of the powder coupling M_{ss}.

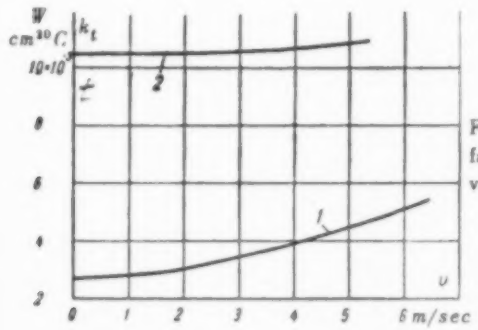

FIG. 6. Dependence of the coefficient of surface cooling of the coupling on the linear velocity of its external surface: (1) for natural cooling; (2) for forced cooling.

Knowing the torque due to the static resistance of the load, we may determine the dynamic torque on the output shaft M_{dyn}, which ensures the required acceleration of the driven mechanism during the specified period of time t_a. The ratio of these two moments determines the appropriate value of i_3.

From the above considerations we can recommend the following order for the calculation of similar electrodrive systems:

(1) Determination of the energy losses due to slip for a cycle and of the mean

power losses in the coupling;

$$A_{sl} = 2 \cdot 1.1 \cdot J_{d.m.} \omega_{d.m.}$$

$$P_{sl} = \frac{1.05 A_{sl}}{T_c}.$$

Coefficient 1.1 takes into account the moment of inertia of the driven part of the coupling and toothed gears of the reductor. Coefficient 1.05 is introduced to account for losses of the no-load run of the coupling and thermal losses in the winding.

(2) The choice of the method of cooling the coupling and of the coefficient of thermal dissipation (Fig. 6) [3].

(3) Determination of the external area of the coupling surface, which is needed for the heat dissipation:

$$S = \frac{P_{me}}{k_t (t^\circ_e - t^\circ_0)} [cM^2].$$

(4) The choice of the number of gaps and a preliminary calculation of the driving torque of the coupling:

(a) a single-gap coupling

$$M_{ss} \approx \frac{(V\overline{S})^3}{48} [kg\ cm];$$

(b) a double gap coupling

$$M_{ss} \approx \frac{(V\overline{S})^3}{35} [kg\ cm].$$

(5) Calculation of the dynamic torque of the coupling, required to achieve the acceleration of the driven mechanism during a specified period of time t_a:

$$M_{\text{dyn}} = \frac{J_{d.m.} \omega_{d.m.}}{t_a}.$$

(6) Determination of the transmission reduction ratio from the coupling shaft to the load shaft (i_2):

$$i_2 = \frac{(1{,}1 \ldots 1{,}25) M_{\text{dyn}} + M_s}{\eta M_{ss}},$$

where η is the efficiency of the reductor. Coefficient 1-1 is used in the case of a double-gap coupling, 1.25 for a single-gap one.

(7) Calculation of the basic dimensions of powder couplings and of their windings. The known data in this case are: the driving torque transmitted by the coupling to the driven shaft and operational conditions of the coupling. Comprehensive discussion of methods of calculation is given in [2-4].

(8) Checking of thermal calculations of the coupling on the basis of data obtained (moment of inertia of the reversible part of the drive, geometrical dimensions of the coupling, security factor and winding losses).
(9) Calculation of transient processes in the system and construction of the graph of motion of the driven mechanism by the above methods.

Recommendations for designing powder couplings

For the class of drives discussed above it is advisable to use powder couplings of the cylindrical type. In order to decrease dimensions and weight of the installation, high speed (n = 1000 - 2000 rev/min) double-gap couplings are constructed. Their driven part is made in a form of a hollow thin-walled shell to obtain a small moment of inertia. Labyrinth glands in the axial direction together with ordinary felt packing keep the powder mixture quite safely in the working gap.

In order to decrease the torque of the no-load running in the high speed couplings, it is necessary to decrease the volume of the frontal gaps and to separate them from the working chambers by the strip labyrinth glands, and to avoid relative speeds of rotation of the coupling componenta greater than 10 - 12 ,m/sec.

As a filler for the coupling gap, dry mixtures of the carbonyl iron R-8 with silicon dioxide may be recommended, the coefficient of volume filling being

$$K_{Fe} = \frac{G_{Fe}}{\gamma_{Fe} V} \approx 0.34 - 0.4$$

where G_{Fe} is the weight of the carbonyl iron in the mixture, which occupies volume V (cm^3) (g);
γ_{Fe} is iron density (g/cm^3).

The mixture of carbonyl iron with ground mica, which was proposed by Pugovkin, has also a high general and thermal stability.

The specific tangential stress, which is transmitted by dry fillers for a given value of magnetic induction in the coupling gap, and also the permeability of the mixture, are determined mainly by the properties of the ferromagnetic powder and the coefficient of its volume filling.

The values of the specific tangential stress τ, which is steadily transmitted by the dry fillers containing carbonyl iron R-8, and also the values of the relative permeability $\mu/\mu 0$ have been determined experimentally ; Fig. 7 shows them as functions of the mean value of magnetic induction in the coupling gap B_g

Within the range of induction values 0.2 - 1.2 $V.\ sec/m^2$, the value of τ for powder mixtures during slip is practically independent of the relative speed of the working surfaces of the coupling. Experiments have shown that, due to the redistribution of

the mixture in the coupling gap, the torque of a powder coupling with a dry filler varies during the first 2-3hr of its running-in. After that the torque remains constant.

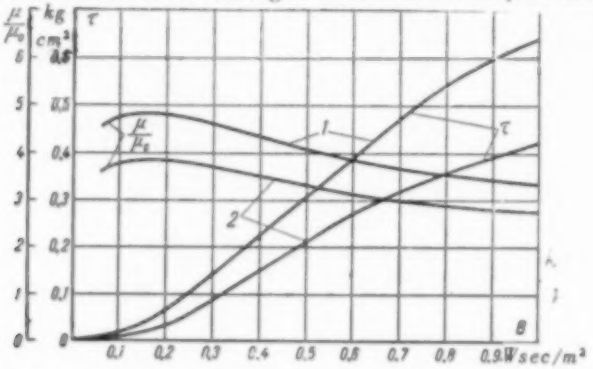

FIG. 7. Variation of the specific tangential stress τ in a layer and the relative permeability μ/μ_0 of dry fillers as functions of the inductance B in the coupling gap. (1) $k_{Fe} = 0.4$; (2) $k_{Fe} = 0.3$.

Tests of powder couplings were carried out under conditions of frequent reversal at a steady winding temperature of about 110°C. The mechanical characteristics of these couplings $M_m = f/i_{sh}$/were again recorded after 400 hr running. No decrease in the value of the torque was found.

Control characteristics of some individual couplings $M_m = f(i_{sh})$ were taken eighteen months after their filling (average working time of a coupling was 800 hr). Maximum variation of the torque did not exceed 5 per cent.

The above discussion leads to the conclusion that powder couplings with dry fillers are quite reliable elements of electric drive systems; they offer wide possibilities in the field of automatic control and regulation.

Translated by S. Szymanski.

REFERENCES

1. T.A. Glazenko; Transient processes in an electric drive equipped with an electromagnetic coupling with a ferromagnetic filler, *Elektrichestvo*, No. 12 (1954).
2. V.G. Zusman and O.N. Tatur; Electromagnetic couplings and their use in machine construction, *Elektrichestvo*, No. 3 (1956).
3. G.M. Petukhin; Characteristics and calculation of electromagnetic couplings with a ferromagnetic filler, *Elektrichestvo*, No. 3 (1956).
4. O.N. Tatur; Electromagnetic powder couplings, *Eksp. nauch.-issled. inst. metallor. stankor, tsen-byro tond. norm.* 1 (1956).

THE INCREASE OF THE RELIABILITY OF CONVERSION NETWORKS*

A.A. SAKOVICH

All-Union Lenin Institute of Electric Technology

(Received 10 October 1957)

In a conversion network there are elements which introduce lumped or distributed capacitances and inductances, thus forming additional oscillating circuits. In networks electrically connected with rectifiers, we have to take into account:

(1) capacitances with respect to the earth of the transformer and reactor windings, of cables, wall bushes, current transformers, anode dividers, auxiliary insulating transformers, transformers and conductors of the auxiliary circuits;

(2) dissipation reactances of the power transformer and of the anode dividers, inductances of the feeding busbars, of the blocking and smoothing reactors.

In the circuits comprising the above-mentioned reactive elements oscillations arise; harmful effects of these oscillations increase with the increase in power and voltage of the conversion installations. Oscillations arise at the beginning and at the end of commutation, when a sharp change of conditions occurs in the network; they become more prominent with the increase of the control angle, when the commutation voltage increases. As an example we may mention interference in wire communications, which arose during the transition into the inversion operation of the traction substations of the electrified railways; these disturbances were so strong that it was necessary to abandon the regeneration of energy. One of the power conversion installations, which worked quite satisfactorily during the process of adjustment, at a low voltage, could not be put into operation at a high voltage; investigations have shown a strong influence of the commutation processes on the control networks, which made the normal working of the rectifiers impossible. In many cases intermittent currents, resulting from heavy overvoltages, were observed.

Investigations, carried out directly on installations and using modern and specially designed instruments (cathode oscillographs, dividers, shunts, electronic incicators) gave a satisfactory explanation of the character of these phenomena, and their analysis helped, in the development of practical improvements to secure the normal operation of the high-voltage conversion networks and to remove or to reduce

* *Elektrichestvo*, No. 4, 53 – 57, 1958.

considerably disturbances caused by the operation of these networks. These results may be useful in normalizing the work of invertors on railway transport substations, in installations for methane electrocracking and in other high-voltage converting networks, working separately or in parallel with other networks.

Problems connected with overvoltages arising in the case of parallel connected converting networks (for example on converting substations of d.c. transmission lines) are not discussed in this article.

Processes at the end of commutation

Let us consider a three-face bridge network, which is normally used for power conversion installations for voltages from 10 kV upwards. Taking into account complementary capacitances and inductances of the elements of the installation, we obtain a network as shown in Fig. 1a. Assume that, at the given instant, rectifier 6 is working and that current commutation takes place from rectifier 1 to rectifier 2 (Fig. 1b). At the end of the commutation period, current in rectifier 1 ceases to flow and the voltage across it becomes:

$$u_c = \sqrt{2}\cdot\sqrt{3}\,u_{ph}\sin(\alpha+\gamma). \tag{1}$$

Owing to the presence in the network of reactive elements, this voltage does not appear instantaneously, but increases gradually. Since this system consists of a complicated network, divided into branches comprising capacitances and inductances, oscillations of two or more frequencies arise; the losses in the links of the system bring about rather rapid damping of these oscillations. In the general case, the shape of the curve of the recovery voltage is determined by the equation:

$$u_{rec} = \sqrt{2}\cdot\sqrt{3}\,U_{ph}\Big\{\sin(\alpha+\gamma+\omega t) - \sin(\alpha+\gamma)\Big[A_1\sin(\omega_1 t+\psi_1)\,e^{-\frac{t}{\tau_1}} + \tag{2}$$
$$+ A_2\sin(\omega_2 t+\psi_2)\,e^{-\frac{t}{\tau_2}} + \ldots + A_c\sin(\omega_c t+\psi_c)\,e^{\frac{t}{\tau_K}}\Big]\Big\},$$

where A_1 and A_2 are coefficients which determine the relative value of a harmonic* ω_1 and ω_2 appropriate angular frequencies of the harmonics; ψ_1 and ψ_2 phase angles; τ_1 and τ_2 time constants, characterizing the damping of oscillations.

From formula (2) it is seen that the amplitude of the reverse voltage cannot attain the double value of the amplitude of the commutation voltage, which could happen in the simplified equivalent network (Fig. 1b) free from losses. On a real installation the reverse voltage amplitude does not exceed 140–160 per cent of the commutation voltage amplitude. This is due to the loss of energy in the links of the installation and also to the fact that the maxima of the individual harmonics do not coincide.

The usual method of decreasing the first amplitude of the reverse voltage and of slowing down its rate of increase is damping by additional circuits comprising capacitances and resistances (Fig. 1c). The methods of calculating damping circuits are discussed in the literature [1–3]. However, it is necessary to point out that we

* The value of the coefficients $A_1, A_2 \ldots A_k$ is subject to the condition $\sum_{n=1}^{n=k} A_n\cdot\sin\psi_n = 1$.

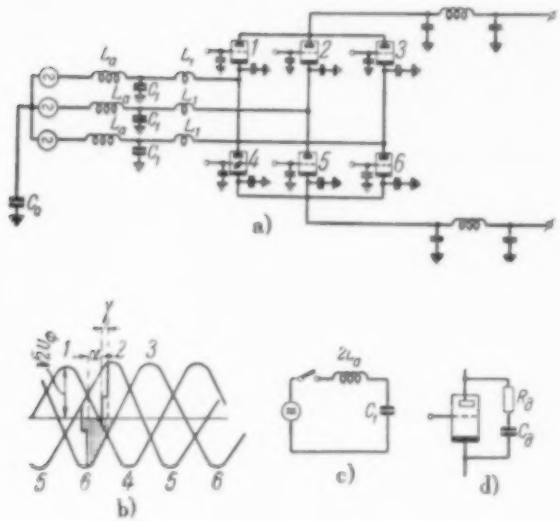

FIG. 1. Circuit showing starting-up of oscillations at the end of commutation.

1959

cannot choose the value of the damping resistance solely on the basis of decreasing the first amplitude of the reverse voltage (the "optimum value of the damping resistance"). The value of the resistance of the damping circuit is chosen on the basis of the relationship between the rate of increase of the reverse voltage and the amplitude of its first rise, which is given by the characteristics of the rectifiers and the circuits; the condition of the ignition process should also be taken into account, and this will be discussed later. The practical value of the damping resistance is taken to be much less than that following from the conditions of the optimum damping of oscillations of the recovery voltage.

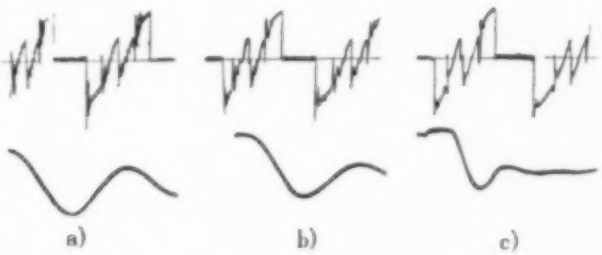

FIG. 2. Oscillogram of the recovery voltage curves for various values of the damping resistance.

Fig. 2 shows the oscillograms of the curves of the anode-cathode voltage (upper series) and the shapes of the initial rise of the recovery voltage for the same curves

(lower series), recorded on a high power installation (1600 A, 10 kV).

In Fig. 2a) we see a very small value of the damping resistance-oscillations of the recovery voltage are considerable and slowly die away. Fig. 2b shows a slightly greater value of the resistance: the oscillation amplitude is decreased and damping is stronger. Finally, in Fig. 2c the resistance is near to the value for conditions of optimum damping; considerable damping takes place, but the slope of increase of the recovery voltage has increased sharply.

Taking into account the characteristics of mercury rectifiers for high voltages we may remark that the shape of the curve of the reverse voltage in the case of the optimum value of the damping resistance (Fig. 2c) is less favourable, since the slope of the voltage increase is considerably greater than that of the curve in Fig. 2b.

Processes during the ignition of rectifiers

During the ignition of the rectifiers, the discharge occurs of the capacitances connected with the rectifier anode and cathode; these capacitances are charged to the potential $u_i = \sqrt{2}\ \sqrt{3}\ U_{ph} \sin \alpha$. Fig. 3a shows an approximate circuit diagram. In this figure the distributed inductances of the anode busbars and also the capacitances of the busbars and the connected elements of the installation are shown in the form of a chain of lumped inductances and capacitances. The capacitances, which take part in this process, have approximately the same value as those in the oscillating circuit for the recovery voltage, but inductances are considerably lower (inductances of the feeding busbars are of the order of 10^{-4} H/m.)

Owing to this fact frequencies become much higher, of the order of 10^5 - 10^6 c/s, and because of the distributive character of the capacitances and the inductances a nearly continuous spectrum of oscillations appears with individual peaks of resonant frequencies. Let us consider a simplified equivalent circuit for the dominating frequency (Fig. 3b).

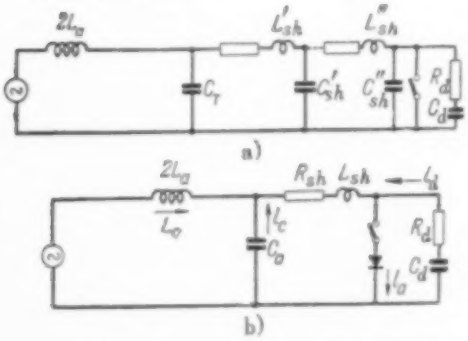

FIG. 3. Circuits showing starting-up of oscillations during the ignition process of rectifiers.

On closing of the knife switch, which is equivalent to the ignition of rectifier, the value of the current flowing in the circuit is:

$$i_a = \sqrt{3} \cdot \sqrt{2} U_{ph} \left\{ \int_0^t \left[\frac{1}{2L_a + L_{sh}} \sin(\alpha + \omega t) - \right.\right.$$

$$- \frac{1}{2L_a} \sin \alpha \cdot \sin(\omega_1 t + \psi_1) e^{-\frac{t}{\tau_1}} \Big] dt + \quad (3)$$

$$\left. + \frac{\sin \alpha}{\omega_1 L_1} \cdot \sin \omega_1 t \cdot e^{-\frac{t}{\tau_1}} + \frac{\sin \alpha}{R_0} e^{-\frac{t}{\tau_2}} \right\},$$

where L_a is a lumped dissipation inductance of one phase of the power transformer with the reactance of the feeding-grid added; L_1 the inductance of the network supplying the rectifier; ω the angular fre-

quency of the feeding voltage; ω_1 the angular frequency of oscillations; C_d the capacitance of the damping circuit; τ_1 the time constant characterizing the damping of high-frequency oscillations; ψ the phase angle of the voltage of high-frequency oscillations. Moreover, if

$$\int_0^{\frac{3\pi}{2\omega_1}} \left[\frac{1}{2L_a + L_{sh}} \sin(\alpha + \omega t) - \frac{1}{2L_a} \sin\alpha \cdot \sin(\omega_1 t + \right.$$
$$\left. + \psi_1) e^{-\frac{t}{\tau_1}} \right] dt + \frac{\sin\alpha}{R_d} e^{-\frac{3\pi}{2\omega_1\tau_2}} < -\frac{\sin\alpha}{\omega_1 L_1} e^{-\frac{3\pi}{2\omega_1\tau_1}}, \quad (4)$$

then the current in the rectifier circuit will pass through the zero value and will change direction. If a rectifier is connected in the circuit, which conducts currents only in one direction, the current in the network will be intermittent, and anode peaks of the reverse voltage will appear on the rectifier. Fig. 4 shows the oscillogram of the intermittent ignition process. Such a character of ignition is harmful to the rectifier because of increased sputtering of the anode material. Also, frequent extinctions of the excitation anode in the excitrons or of the arc of the igniter in the ignitrons take place; this is due to the high rate of voltage decrease and to the growth of reverse voltage on the main anode during the ignition process. This results in failure of operation of rectifiers and produces strong overvoltages in the control circuits, which is very dangerous for the auxiliary equipment. In the case when, during the ignition process, high frequency oscillations of a great amplitude arise, they cause strong radio interference.

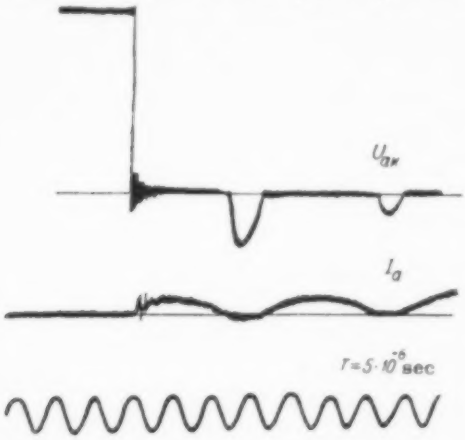

FIG. 4. Oscillogram of current and voltage oscillations during the ignition process.

To eliminate harmful effects during the ignition periods, blocking reactors are used in the anode circuits and the appropriate resistances are chosen in the damping circuit.

By connecting the reactor we decrease the oscillation frequency and the current amplitude during the ignition process. By a careful choice of the value of the damping circuit resistance, we may increase the current component of the aperiodic discharge and achieve a situation in which the anode current at ignition will decrease to zero and pass through the zero value. Fig. 5 shows the components of the anode current during the ignition process: in presence of oscillations and intermittent ignition (a), and for the normal ignition process (b).

A right choice of the parameters of the damping circuit and the blocking reactor is rather difficult. The available methods of calculation are complicated and not

sufficiently tested.

Experiments with an electrical model, with an enlarged time scale, or direct detailed investigations on the installation are the proper methods for choosing the parameters. The values of inductances of the blocking reactors lie within the limits of 10^{-3} - 10^{-4} H; in the case of high power installations, reactors become rather cumbersome. The value of the capacitance of the damping capacitors of each phase is of the same order as that of all secondary windings of the transformer with respect to earth. The value of the damping resistances chosen to obtain the current, overlapping the current of high oscillations, is usually smaller than the value of resistances, that ensure the aperiodic damping of the oscillations of the recovery voltage. In choosing the value of damping resistances it is necessary to bear in mind that losses in the resistances may be heavy and may reach 0.5 - 2 per cent of the power of a conversion installation. The losses increase considerably with the increase of the ignition angle.

The influence of processes in the power network on the control network

For considerable values of the ignition angle, the rectifier ignition is accompanied by an abrupt variation of the potential of its electrodes. Abrupt variation of the cathode voltage can influence the control network and disturb the operation of the conversion circuit. Premature ignitions or ignition failures may occur in the individual rectifiers. One of the causes occurring in practice and producing these failures is

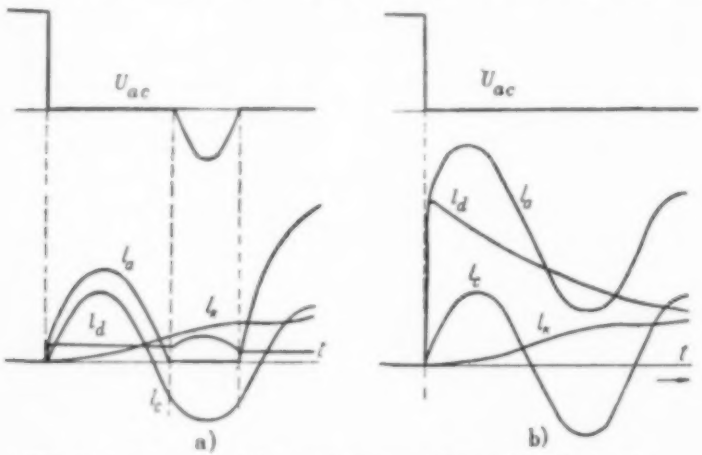

FIG. 5. Components of the anode current of a rectifier during the ignition process.

shown in Fig. 6a. It can be seen from the circuit that with the ignition of the rectifier of the anode group (for example, 2), its cathode potential sharply increases and becomes equal to the anode potential. If the control networks have a considerable capacitance with respect to earth (for example, if the feeding leads are not sufficiently screened or screening is badly executed), then the change of the potential values on the corresponding conductors will be delayed (owing to the influence of

capacitance). This will lead to the appearance on the grids of impulses of negative polarity. In consequence, of the two parallel connected rectifiers only one will work, namely that which fired first.

In the case of the oscillating growth of the anode current, the working rectifier may also be extinguished.

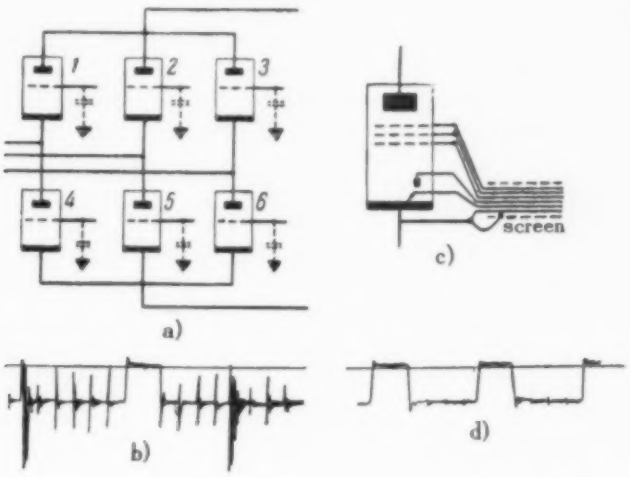

FIG. 6. The influence of processes in the power networks on the control networks of a rectifier.

Fig. 6b shows an oscillogram of the grid voltage in the above case. On the other hand, the induced voltage on the grids may cause premature ignition, for example, of the rectifier 2 when the commutation of rectifiers 3 and 4 takes place. The presence of similar induced voltages in the ignition circuit of the ignitron may also cause ignition failures and lead to the early damage of the semiconductor igniters. From the above discussion it follows that the method of construction of feeding leads of the control networks plays a very important part in high-voltage conversion networks. The screening of all in-leads is recommended, and the screen should be connected to the cathode of the corresponding rectifier, as shown in Fig. 6c. Fig. 6d, shows the voltage oscillograms of the grid circuits of the same installation (in Fig. 6a), but after alteration of its network. There is a possibility of overvoltages arising in the grid circuits due to the capacitance between the grid and the main anode. Nevertheless, for voltages on the main anode of the order of 10 kV these overvoltages are easily suppressed by connecting a small capacitor between the grid and the cathode.

Very dangerous voltages arise in the case of intermittent currents. Under such conditions, rectifiers of the anode and cathode groups fire each in turn for a short period; current impulses flow in the circuit, which is formed by the capacitance with respect to earth of all secondary windings of the transformer and the lumped dissipation inductance of the secondary windings of the transformer. With every ignition of

the rectifier the periodical recharging of this capacitance takes place. Overvoltages with respect to earth are 5–8 times greater than the working voltage on the secondary windings; this is very dangerous for the equipment and causes breakdowns and backfires in the rectifiers. The elimination of these harmful effects, under the conditions of intermittent currents, may be achieved by one of the following methods:

(1) Earthing of the star point of the transformer and of the star point of the load through resistances, or connecting these two points through a resistance. In the case when transformer windings are delta-connected and there is no star point, artificial zero points are formed by resistances, which are either interconnected or earthed. Thus a leakage path is provided for the capacitance charges of the secondary windings of the power transformer.

(2) Wide control impulses (width 60–90 el deg) are used to establish conditions for re-ignition of rectifiers after their extinction by the oscillating anode current.

(3) A special control circuit is used to apply trigger pulses on the rectifiers, when the anode voltage on a given rectifier exceeds a predetermined value.

These methods have been tested on real installations and on models; positive results have been obtained in suppressing overvoltages caused by intermittent currents.

Increase of operational stability of an invertor

Recently the use of inversion installations has increased; bridge circuits controlled by various methods are also widely used; in these systems one group of rectifiers works as convertors, and another is controlled to act as invertors.

The output voltage in these networks may vary within wide limits, with a better power factor on the d.c. side than in the usual networks.

Nevertheless, ignition failures hamper the invertor operation; the occurrence of failures increases with increasing voltage.

To prevent the harmful effects of ignition failures and to increase the operational stability of the invertor, we may use the following method. Consider a three-phase network working under inversion conditions, a voltage diagram of which is shown in Fig. 7a. If the ignition of a consecutive rectifier (voltage diagram 2) fails, this causes the "reversal" of the invertor, which is not spontaneously suppressed, since the increase of current at the "reversal" leads to the increase of the commutation angle, and the transition of the current to another rectifier cannot be accomplished.

Fig. 7b shows the action of the technique of "advanced ignition". In this technique, in the case of ignition failure in a consecutive rectifier (for example 2), a trigger pulse is applied to the grid of the next rectifier, 3, with a lead of about 60 el deg. This produces a switching of the current from rectifier 1 to rectifier 3, and the invertor continues operating even in the case of a long delay in ignition. This method was tested in practice and gave positive results. The circuit for applying a trigger pulse is comparatively simple and may be realized in different ways [4].

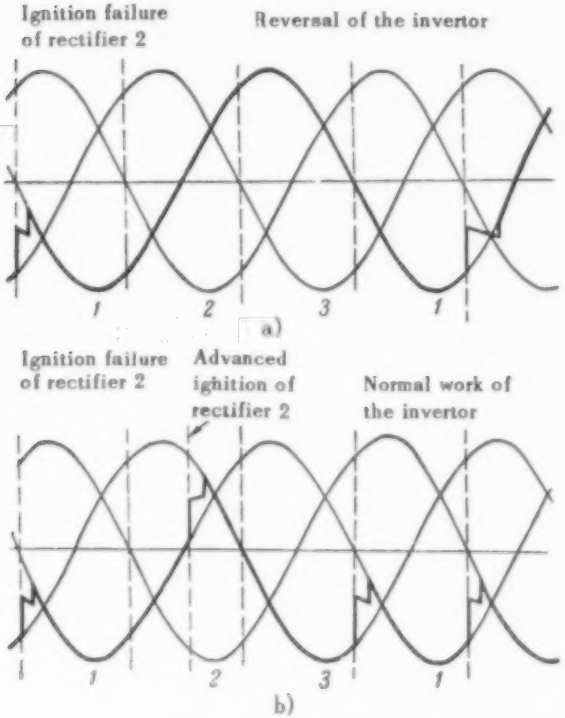

FIG. 7. Method of increasing the operational reliability of an invertor.

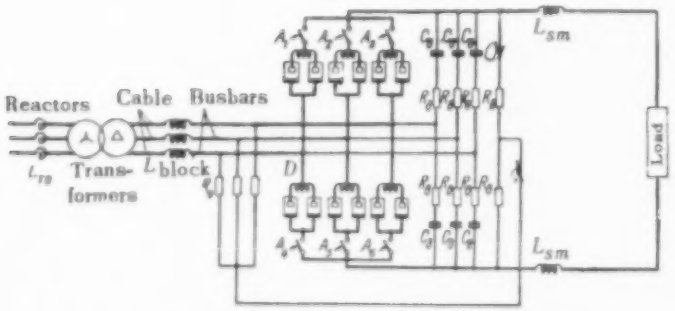

FIG. 8. Network of a high-voltage inversion installation.

Conclusion

The measures discussed above were developed as a result of research, and they were applied and tested on one of the conversion installations of about 15 MW power working at 10 kV. The result was such that this installation, which previously could

not be put into operation, began to work normally. On the basis of these experiments similar measures have been undertaken on more powerful installations, where they also produced positive results. The system of advanced ignition was tested by the Direct Current Scientific Research Institute employees on the invertor substation of the transmission line from Kashira to Moscow.

Fig. 8 shows a complete network of a conversion installation with blocking reactors and damping circuits, which – as experience proves – should be regarded as an indispensable attribute of a powerful conversion network.

In carrying out the experimental part of this work the following persons participated: N.M. Maslennikov, S.M. Luzhanskii, V.P. Nadgornyi, E.P. Shmarina. L.I. Luzhanskaia and I.V. Blond.

Translated by S. Szymanski

REFERENCES

1. M.M. Akodis; Narastanie obratnogo napryazheniia pri kommutatsii v ionnykh ventiliakh (Increase of a back voltage during the commutation period in ionic rectifiers) *Elektrichestvo*, No. 6 (1950).
2. V.B. Samodelkin; O roischete vossstanavlivaiushchegosia napriazheniia na ventiliakh v trekhfaznoi mostovoi skheme (Calculation of the recovery voltage on rectifiers in a three-phase bridge circuit), *Elektrichestvo*, No. 12 (1952).
3. V.B. Samodelkin; Dempfirovanie kolebanii vosstanavlivaiushchegosia napriazheniia v trekhfaznoi mostovi skheme (Damping of oscillations of the recovery voltage in a three-phase bridge circuit) *Elektrichestvo*, No. 4 (1954).
4. A.A. Sakovich; *Ustroistvo dla setochnogo upravleniia ventiliami inventora (Device for a grid control of rectifiers of an invertor)*, Author's Patent 84681.

CALCULATION OF CERTAIN TYPES OF COMPOUND EARTHING DEVICES *

A.B. OSLON

(Received 18 April 1957)

For calculation of compound earthing devices it is customary to make use of utilization factors, which take into account the increase of the earthing resistance due to the mutual screening of elements of an earthing device. These factors depend on many parameters (length, depth of earthing of the individual elements, their mutual position etc). Nevertheless, in many cases, we may carry out calculations of earthing devices by using simple formulae, without regard to utilization factors.

Consider a compound earthing device comprising n elements. Using the electrostatic analogy we derive a system of equations with coefficients of potential:

$$\left.\begin{aligned} \varphi_1 &= \alpha_{11}I_1 + \alpha_{12}I_2 + \ldots + \alpha_{1n}I_n; \\ \varphi_2 &= \alpha_{21}I_1 + \alpha_{22}I_2 + \ldots + \alpha_{2n}I_n; \\ &\ldots\ldots\ldots\ldots\ldots \\ \varphi_n &= \alpha_{n1}I_1 + \alpha_{n2}I_2 + \ldots + \alpha_{nn}I_n, \end{aligned}\right\} \qquad (1)$$

where $I_1 \ldots_n$ are currents leaking to the earth from each element of the earthing device;

α is coefficient of self and mutual potential;

$\phi_1 \ldots \phi_n$ are potentials of the elements of the earthing device.

For the parallel connexion of the elements of the earthing device $\phi_1 = \phi_2 = \ldots = \phi_n = \phi$. Solving the system of equations (1) with respect to currents, we get:

$$\left.\begin{aligned} I_1 &= \varphi(\beta_{11} + \beta_{12} + \ldots + \beta_{1n}); \\ I_2 &= \varphi(\beta_{21} + \beta_{22} + \ldots + \beta_{2n}); \\ &\ldots\ldots\ldots\ldots\ldots \\ I_n &= \varphi(\beta_{n1} + \beta_{n2} + \ldots + \beta_{nn}). \end{aligned}\right\} \qquad (2)$$

* *Elektrichestvo*, No. 4, 58-61, 1958

Earthing resistance of the compound earthing device is:

$$R = \frac{\varphi}{\Sigma I} = \frac{1}{\Sigma \beta_i}. \tag{3}$$

The determination of the coefficients of conductance is complicated in a general case, and, consequently, the calculation of resistance R by the formula is also complicated. This resistance is much more easily found if the currents in all elements of the earthing device are equal:

$$I_1 = I_2 = \ldots = I_n = I.$$

Then

$$R = \frac{\varphi}{\Sigma I} = \frac{\varphi}{nI} = \frac{\alpha_{k1} + \alpha_{k2} + \ldots + \alpha_{kk} + \ldots + \alpha_{kn}}{n}, \tag{4}$$

i.e. in this case resistance R can be found by dividing the sum of the coefficients of any of the equations (1) by the number of elements n.

If the currents of the elements of the earthing device are not equal to one another, but their corresponding ratios are known, for example

$$\frac{I_1}{I_k} = A; \quad \frac{I_2}{I_k} = B; \quad \ldots \quad \frac{I_n}{I_k} = N,$$

then

$$R = \frac{\varphi}{\Sigma I} = \frac{\alpha_{k1} A + \alpha_{k2} B + \ldots + \alpha_{kk} + \ldots + \alpha_{kn} N}{A + B + \ldots + 1 + \ldots + N}. \tag{5}$$

Thus, the problem of the calculation of compound earthing devices is reduced to the problem of finding the coefficients of self and mutual potential and the current distribution in the elements of the earthing device. Coefficients of self potential are usually much larger than of mutual potential, therefore there is no need for particularly exact determination of the latter.

In the case of linear earthing electrodes, whose transverse dimensions are small in comparison with the longitudinal, the simplest way for calculation coefficient α is to use the method of mean potentials [1].

The determination of potentials by this method is carried out on the basis of two assumptions:
(1) the current density is everywhere constant along the length of the conductors;
(2) the potential, acquired by the conductor l_2 in the field of the conductor l_1, is equal to the arithmetic mean of the potentials, produced by the field of the conductor l_1 at all points of the conductor l_2.

From the first assumption it follows that in a conducting medium of the resistivity ρ the potential of a point in the field of the linear conductor l_1 is:

$$\varphi = \frac{I_1 \rho}{4\pi l_1} \int_{l_1} \frac{dl_1}{r}, \tag{6}$$

where I_1 is the current in the conductor l_1;

r is the distance from the element dl_1 to the point where the potential is to be found.

According to the second assumption the potential of the conductor l_2 in the field of the conductor l_1 is equal to:

$$\varphi_{21} = \frac{1}{l_2}\int_{l_2}\varphi dl_2 = \frac{I_1\rho}{4\pi l_1 l_2}\int_{l_2}\int_{l_1}\frac{dl_2 dl_1}{r}. \tag{7}$$

The potential of the point A in the field of a rectilinear conductor (Fig. 1) is found in the following way:

$$\varphi = \frac{I_1\rho}{4\pi l_1}\int_{l_1}\frac{dl_1}{r} = \frac{I_1\rho}{4\pi l_1}\int_{x_1}^{x_2}\frac{dx}{\sqrt{x^2+y^2}} = \frac{I_1\rho}{4\pi l_1}\ln\frac{x_2+r_2}{x_1+r_1}, \tag{8}$$

where x_1 and x_2 are to be taken with their corresponding signs.

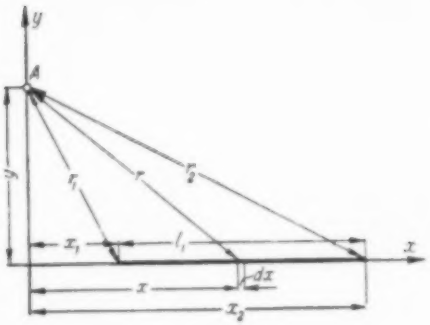

FIG. 1.

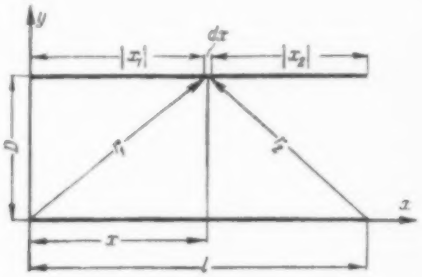

FIG. 2.

Since $$x_1 = \frac{r_2^2 - r_1^2 - l_1^2}{2l_1}, \qquad \text{and} \qquad x_2 = x_1 + l_1,$$

we get

$$\varphi = \frac{I_1\rho}{4\pi l_1}\ln\frac{2a+l_1}{2a-l_1}, \tag{9}$$

where $2a = r_1 + r_2$, the sum of distances from the point to the ends of the conductor l_1.

For the electrostatic field this expression has been derived [2].
From expressions (7), (8) and (9) we have:

$$\alpha_{12}=\alpha_{21}=\frac{\varphi_{21}}{I_1}=\frac{\rho}{4\pi l_1 l_2}\int_{l_2}\ln\frac{x_2+r_2}{x_1+r_1}\,dl_2 \tag{10}$$

or

$$\alpha_{12}=\alpha_{21}=\frac{\rho}{4\pi l_1 l_2}\int_{l_2}\ln\frac{2a+l_1}{2a-l_1}\,dl_2. \tag{11}$$

The use of this or other formulae is only a matter of convenience for calculations.

By using formula (2), let us calculate α_{12} between two parallel conductors of equal length (Fig. 2). In this case:

$$l_1=l_2=l;\quad x_1=-x;\quad x_2=l-x;$$
$$r_1=\sqrt{x_1^2+D^2};\quad r_2=\sqrt{x_2^2+D^2};$$
$$\alpha_{12}=\frac{\rho}{4\pi l^2}\int_0^l\ln\frac{x_2+\sqrt{x_2^2+D^2}}{x_1+\sqrt{x_1^2+D^2}}\,dx=$$
$$=\frac{\rho}{4\pi l^2}\int_0^l\ln\frac{\frac{x_2}{D}+\sqrt{\left(\frac{x_2}{D}\right)^2+1}}{\frac{x_1}{D}+\sqrt{\left(\frac{x_1}{D}\right)^2+1}}\,dx=$$
$$=\frac{\rho}{4\pi l^2}\cdot 2D\int_0^l\operatorname{sinh}^{-1}\left(\frac{x}{D}\right)d\left(\frac{x}{D}\right).$$

Hence

$$\alpha_{12}=\frac{\rho}{2\pi l}\left(\operatorname{sinh}\frac{l}{D}-\sqrt{\left(\frac{D}{l}\right)^2+1}+\frac{D}{l}\right). \tag{12}$$

For $\frac{l}{D}<1$

$$\alpha_{12}=\frac{\rho}{4\pi D}, \tag{12a}$$

and for $\frac{l}{D}>3$ we may assume, as a good approximation, that:

$$\alpha_{12}=\frac{\rho}{2\pi l}\ln\frac{l}{D}. \tag{12b}$$

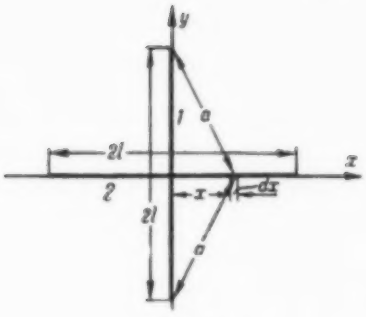

FIG. 3.

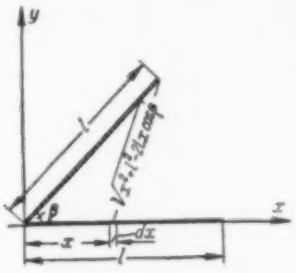

FIG. 4.

Let us apply formula (11) to find α_{12} in the case of the two conductors of the length $2l$, situated in the same plane and intersecting at right angles in the middle of their length (Fig. 3). In this case

$$l_1 = l_2 = 2l; \quad 2a = 2\sqrt{l^2 + x^2};$$

$$\alpha_{12} = \frac{\rho}{4\pi 4l^2} \int_{-l}^{l} \ln \frac{2\sqrt{l^2+x^2} + 2l}{2\sqrt{l^2+x^2} - 2l}\, dx =$$

$$= \frac{\rho}{16\pi l^2} \int_{-l}^{l} \ln \frac{\sqrt{l^2+x^2} + l}{\sqrt{l^2+x^2} - l}\, dx.$$

Assuming

$$\sqrt{l^2+x^2} = lz,$$

we obtain:

$$\alpha_{12} = \frac{\rho}{2\pi l} \ln (\sqrt{2} + 1) = \frac{\rho}{2\pi l} 0{,}88. \tag{13}$$

In many cases it is required to determine the coefficient of mutual potential α_{12} for two rays of equal length, diverging from a common point at an angle β (Fig. 4). In this case:

$$\alpha_{12} = \frac{\rho}{2\pi l} \ln \frac{2 + \sqrt{2 - 2\cos\beta}}{\sqrt{2 - 2\cos\beta}}. \tag{14}$$

In the case of two rays of different length diverging from a common point at a right angle (Fig. 5):

$$\alpha_{12} = \frac{\rho}{4\pi l_1 l_2} \left(l_2 \sinh^{-1} \frac{l_1}{l_2} + l_1 \sinh^{-1} \frac{l_2}{l_1} \right). \tag{15}$$

The derivation of formulae (14) and (15) is given in the appendices.

The coefficient of self potential of a rectilinear conductor in a conductive

medium is:

$$a_{11} = \frac{\rho}{2\pi l} \ln \frac{2l}{d}, \tag{16}$$

where d is the diameter of the conductor [2, p.99].

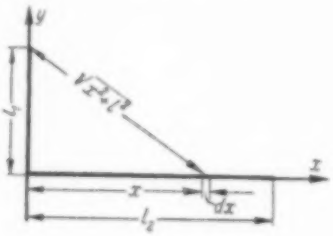

FIG. 5.

In calculating earthing devices, which are earthed to the depth t, the method of images is used, which differs from the analogous method in electrostatics in that images are of the same sign (direction of current flow) as conductors. The earthing resistance of the earthing device is twice as large as the value of the resistance, calculated by formulae (4) or (5) for a system of conductors and their images, since the current, flowing down the conductors of the earthing device, is equal only to a half of the current of this system. In future, symbols of quantities relating to images will be primed.

The above considerations enable us to calculate earthing resistance of the following earthing devices:

A four ray star (Fig. 3) By expression (4) and taking into consideration the above discussion, we get:

$$R = 2\frac{a_{11} + a'_{11} + a_{12} + a'_{12}}{4} = \frac{a_{11} + a'_{11} + a_{12} + a'_{12}}{2}.$$

Here a_{11}, a'_{11} and a_{12} are determined on the basis of expressions (16), (12b) and (13). Hence also assuming $a'_{12} = a_{12}$, we get:

$$R = \frac{a_{11} + a'_{11} + 2a_{12}}{2} = \frac{\rho}{8\pi l} \ln \frac{4(\sqrt{2}+1)^4 l^2}{dt} =$$

$$= \frac{\rho}{8\pi l} \ln \frac{135 l^2}{dt}.$$

The exact calculation of a'_{12} gives:

$$a'_{12} = \frac{\rho}{2\pi l} \ln \frac{\sqrt{2l^2+4t^2}+l}{\sqrt{l^2+4t^2}} \frac{\rho t}{4\pi l^2} \tan^{-1} \frac{l^2}{2t\sqrt{2l^2+4t^2}}.$$

For $\frac{l}{t}=10$

$$\alpha'_{12}=\frac{\rho}{2\pi l}\,0.85,$$

i.e. the difference between α_{12} and α'_{12} is about 3 per cent.

Denote the sum of the lengths of the earthing conductors by L. Then $L = 4l$, and

$$R=\frac{\rho}{2\pi L}\ln\frac{8.45L^2}{dt}. \tag{17}$$

A right-angle For a right angle consisting of two horizontal rays, each of length l, the earthing resistance is:

$$R=\frac{\alpha_{11}+\alpha'_{11}+\alpha_{12}+\alpha'_{12}}{2},$$

where

$$\alpha_{11}=\frac{\rho}{2\pi l}\ln\frac{2l}{d}\;;\;\alpha'_{11}=\frac{\rho}{2\pi l}\ln\frac{l}{2t}.$$

For $\beta = 90°$ from the expression (14) we get:

$$\alpha_{12}=\frac{\rho}{2\pi l}\ln(\sqrt{2}+1).$$

Assuming $\alpha'_{12} = \alpha_{12}$, we get:

$$R=\frac{\rho}{4\pi l}\ln\frac{(\sqrt{2}+1)^2l^2}{dt}=\frac{\rho}{2\pi L}\ln\frac{1.46L^2}{dt}. \tag{18}$$

A three ray star In this case

$$R=\frac{\alpha_{11}+\alpha'_{11}+2\alpha_{12}+2\alpha'_{12}}{3}.$$

For $\beta = 120°$ formula (14) gives

$$\alpha_{12}=\alpha'_{12}=\frac{\rho}{2\pi l}\ln\left(\frac{2+\sqrt{3}}{\sqrt{3}}\right)=\frac{\rho}{2\pi l}\ln 2.15.$$

As a result we get

$$R=\frac{\rho}{6\pi l}\ln\frac{2.154l^2}{dt}=\frac{\rho}{2\pi L}\ln\frac{2.38L^2}{dt}. \tag{19}$$

For a six-ray star similarly we get:

$$R=\frac{\rho}{2\pi L}\ln\frac{192L^2}{dt}. \tag{20}$$

For a square:

$$R=\frac{\rho}{2\pi L}\ln\frac{5.53L^2}{dt}. \tag{21}$$

For a rectangle: Denoting the long side of the rectangle l_1 and the short one l_2 and assuming

$$\frac{l_1}{l_2}=\frac{l_1}{l_2},$$

by formula (5) we get:

$$R=\frac{1}{2+2\frac{l_2}{l_1}}\left[\frac{\rho}{2\pi l_1}\ln\frac{2l_1}{d}+\frac{\rho}{2\pi l_1}\ln\frac{l_1}{2t}+\right.$$
$$+4\frac{\rho}{4\pi l_1 l_2}\left(l_2\,\operatorname{sinh}^{-1}\frac{l_1}{l_2}+l_1\,\operatorname{sinh}^{-1}\frac{l_2}{l_1}\right)\frac{l_2}{l_1}+$$
$$\left.+2\frac{\rho}{2\pi l_1}\left(\operatorname{sinh}^{-1}\frac{l_1}{l_2}-\sqrt{\left(\frac{l_2}{l_1}\right)^2+1}+\frac{l_2}{l_1}\right)\right]= \qquad (22)$$
$$=\frac{\rho}{2\pi L}\left[\ln\frac{l_1^2}{dt}+2\frac{l_2}{l_1}\left(\operatorname{sinh}^{-1}\frac{l_1}{l_2}+\frac{l_1}{l_2}\operatorname{sinh}^{-1}\frac{l_2}{l_1}\right)+\right.$$
$$\left.+2\left(\operatorname{sinh}^{-1}\frac{l_1}{l_2}-\sqrt{\left(\frac{l_2}{l_1}\right)^2+1}+\frac{l_2}{l_1}\right)\right].$$

Expressions (17) -(22) can be represented in a general case by the formula

$$R=\frac{\rho}{2\pi L}\ln\frac{KL^2}{dt}. \qquad (23)$$

In formula (23) the value of K depends only on the configuration of the earthing device.

For different types of earthing devices the values of K is given in Table 1.

TABLE 1.

Earthing device	K	Earthing device	K	Earthing device	$\frac{l_1}{l_2}$	K
—	1	+	8.45		1.5	5.81
○	1.27*	✳	192		2	6.42
L	1.46		$\frac{l^2}{4D^2}$**		3	8.17
Y	2.38	□	5.53		4	10.4

* $R=\frac{\rho}{2\pi^2 D}\ln\frac{4\pi D^2}{dt}$, where D is the diameter of the circle [4].
** For $D\geqslant 5l$.

The error, due to the assumption $a_{12} = a'_{12}$, is significant only for $l/t < 10$. The values of earthing resistances calculated by formula (23) are 3-5 per cent greater than those calculated by means of utilization factors. This is due to the fact that in calculating utilization factors we used less exact methods for determining the mutual influences of the elements of the earthing device [3].

Appendix

(1) *Derivation of formula (14).*

We make use of formula (11). In our case (Fig. 4).

$$2a = x + \sqrt{x^2 + l^2 - 2xl\cos\beta}.$$

We denote:

$$x^2 + l^2 - 2xl\cos\beta = X.$$

Then

$$a_{12} = \frac{\rho}{4\pi l^2}\int_0^l \ln\frac{x + \sqrt{X} + l}{x + \sqrt{X} - l}\,dx =$$

$$= \frac{\rho}{4\pi l^2}\left[\int_0^l \ln(x + \sqrt{X} + l)\,dx - \int_0^l \ln(x + \sqrt{X} - l)\,dx\right].$$

Putting:

$$du = dx,\quad v = \ln(x + \sqrt{X} \pm l),$$

we evaluate each integral by parts:

$$\int_0^l \ln(x + \sqrt{X} + l)\,dx = [x\ln(x + \sqrt{X} + l)]_0^l -$$

$$-\int_0^l x\frac{x + \sqrt{X} - l\cos\beta}{\sqrt{X}(x + \sqrt{X} + l)}\,dx = l\ln[l(2 + \sqrt{2 - 2\cos\beta})] -$$

$$-\frac{1}{2}\int_0^l \frac{x\,dx}{\sqrt{X}} + \frac{l}{2}\int_0^l \frac{dx}{\sqrt{X}} - \frac{1}{2}\int_0^l dx;$$

$$\int_0^l \ln(x + \sqrt{X} - l)\,dx = l\ln(l\sqrt{2 - 2\cos\beta}) -$$

$$-\frac{1}{2}\int_0^l \frac{x\,dx}{\sqrt{X}} - \frac{l}{2}\int_0^l \frac{dx}{\sqrt{X}} - \frac{1}{2}\int_0^l dx.$$

Subtracting the second integral from the first we get:

$$\int_0^l \ln\frac{x+\sqrt{X}+l}{x+\sqrt{X}-l}\,dx = l\ln\frac{2+\sqrt{2-2\cos\beta}}{\sqrt{2-2\cos\beta}} + l\int_0^l \frac{dx}{\sqrt{X}} =$$

$$= l\left(\ln\frac{2+\sqrt{2-2\cos\beta}}{\sqrt{2-2\cos\beta}} + \ln\frac{\sqrt{2-2\cos\beta}+1-\cos\beta}{1-\cos\beta}\right) =$$

$$= 2l\ln\frac{2+\sqrt{2-2\cos\beta}}{\sqrt{2-2\cos\beta}}$$

Substituting the expression obtained into formula (11), we get formula (14).

(2) *Derivation of formula (15)*. For this case (Fig. 5).

$$2a = x + \sqrt{x^2+l_1^2};$$

$$a_{12} = \frac{\rho}{4\pi l_1 l_2}\int_0^{l_2} \ln\frac{x+\sqrt{x^2+l_1^2}+l_1}{x+\sqrt{x^2+l_1^2}-l_1}\,dx = \frac{\rho}{4\pi l_1 l_2}\left[\int_0^{l_2}\ln(x+\right.$$

$$\left.+\sqrt{x^2+l_1^2}+l_1)\,dx - \int_0^{l_2}\ln(x+\sqrt{x^2+l_1^2}-l_1)\,dx\right].$$

As in the previous case, putting $du = dx$; $v = \ln(x+\sqrt{x^2+l_1^2}\pm l_1)$ and evaluating each integral separately, we get:

$$\int_0^{l_2}\ln\frac{x+\sqrt{x^2+l_1^2}+l_1}{x+\sqrt{x^2+l_1^2}-l_1}\,dx = l_2\ln\frac{l_2+l_1+\sqrt{l_2^2+l_1^2}}{l_2-l_1+\sqrt{l_2^2+l_1^2}} +$$

$$+ l_1\int_0^{l_2}\frac{dx}{\sqrt{x^2+l_1^2}} = l_2\sinh^{-1}\frac{l_1}{l_2} + l_1\sinh^{-1}\frac{l_2}{l_1}.$$

Translated by S. Szymanski

REFERENCES

1. L.R. Neiman and P.L. Kalantarov; *Teoreticheskie osnovy elektrotekniki (Theoretical principles of electric technology)* part 3, Gosenergoizdat (1948).
2. K.A. Krug; *Osnovy elektrotekhniki (Principles of electrical technology)* vol. 1, Gosenergoizdat (1946).
3. A.P. Beliakov; *Osnovaniia dlia proektirovaniia zazemlenii elektricheskikh ustanovok (Principles of earthing design of electrical installations)*, State United Scientific and

Technical Publishing House, People's Commissariat of Heavy Industry (1938).

4. I.S. Stekolnikov (Editor); Grozozashchita promyshlennykh sooruzheni i zdanii pod redaktsiei *(Lightning protection of industrial constructions and buildings)*, Izv. Akad. Nauk SSSR (1951).

1959

SERVICE TESTS

A METHOD OF CALCULATION OF MECHANICAL CHARACTERISTICS OF ASYNCHRONOUS MOTORS UNDER CONDITIONS OF DYNAMIC BRAKING*

A.G. MIRER

Central Scientific Research Institute for Machine Technology

Generally accepted methods of calculation of mechanical characteristics of dynamic braking do not give a clear idea how the characteristics vary when the excitation current varies (direct current in the stator winding).

In this article a method of calculation of a family of mechanical characteristics for dynamic braking is given; these characteristics allow a proper choice of the excitation current, corresponding to the required characteristic.

Certain relationships which determine the operation of an asynchronous motor under conditions of dynamic braking form the basis for the calculations:

$$E_2' = I_\mu \cdot x_\mu; \tag{1}$$

$$I_2' = \frac{E_2' s}{\sqrt{R_2'^2 + x_2'^2 s^2}}; \tag{2}$$

$$I_e^2 = I_\mu^2 + I_2'^2 + 2 I_\mu I_2' \sin \varphi_2; \tag{3}$$

$$\sin \varphi_2 = \frac{x_2' s}{\sqrt{R_2'^2 + x_2'^2 s^2}}; \tag{4}$$

$$M = 2.92 \frac{I_2'^2 R_2'}{n_s s}, \tag{5}$$

where E_2' is the e.m.f. of the rotor phase, reduced to the stator winding; I_2' is the current of the rotor phase reduced to the stator winding; I_μ is the magnetizing current; x_μ is the reactance of the magnetizing circuit; I_e is the alternating current of the stator phase, equivalent to a direct current inducing in the stator winding the same m.m.f; n_s is the synchronous speed; s is the slip; x_2' is the reactance of the rotor phase reduced to a stator winding; $R_2' = r_2' + R_a'$ is the total resistance of the rotor phase, comprising the winding resistance r_2' and additional resistance r_a', all reduced to the stator winding.

* *Elektrichestvo*, No. 4, 65 – 66, 1958.

Under conditions of dynamic braking, the magnetic flux of the machine depends to a considerable extent on the speed of rotation, in consequence the calculation of dynamic characteristics neglecting the influence of saturation, leads to inadmissible errors. For calculation, the magnetization curve of the machine $E_1' = f(I_\mu)$ or the relationship $x_\mu = f(I_\mu)$ must be known. If these data are not available we can make use of universal curves [1, 2]. In contrast to the generally accepted methods of calculation, which consists of the solution of the simultaneous equations (1)-(5), we shall choose a set of values of the magnetizing current $I_{\mu 1}$, $I_{\mu 2}$, . . . , $I_{\mu n}$ and calculate for each chosen value the values of I_1', M and I_e for different values of slip s_1, s_2 . . . s_m.

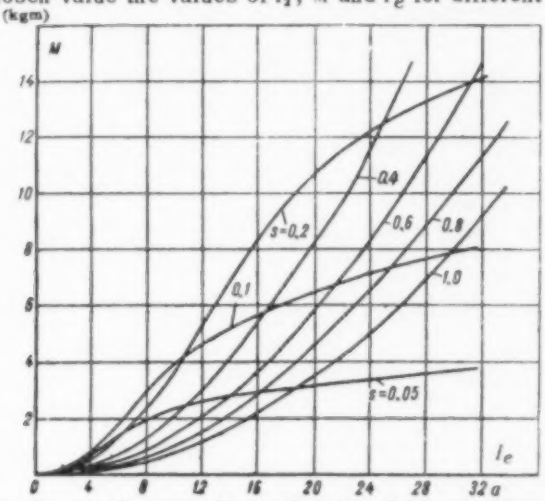

FIG. 1. Curves showing the torque M as a function of the equivalent current I_e.

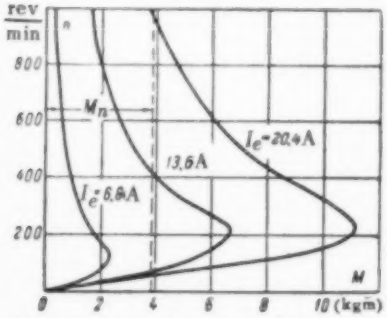

FIG. 2. Mechanical chracteristics of the dynamic braking of a motor of the MTK-12-6 type.

Using these data we may plot the relationship $M = f(I_e)$ for every value of slip s_1, s_2, . . . , s_m Fig. 1 shows such graphs calculated for a short-circuited motor of type MTK-12-6. The graphs so obtained give a clear idea of the family of mechanical characteristics of dynamic braking, and they enable us easily to construct characteristics corresponding to any equivalent current, since the ordinates of these curves, for given values of I_e, give the values of torques for slips s_1, s_2, . . . , s_m (Fig. 2).

For motors with a phase rotor we have to construct curves $M = f(I_e)$ for short-circuited rotor rings ($r_a' = 0$), from which it is easy to find corresponding natural mechanical characteristics of dynamic braking. The artificial characteristics for $r_a' \neq 0$ are determined from natural ones by simple recalculation: $s' = s$. R_2'/r_2' for M = constant and I_e = constant, where s' and s are the values of slip

for the required artificial and given natural characteristics respectively.

Relationships $M = f(I_e)$, when once calculated for a certain given type of motor, may be introduced as the catalogue data, in a similar way as for working characteristics, so as to be used for calculation of mechanical characteristics of dynamic braking.

Translated by S. Szymanski

REFERENCES

1. A.T. Golovan; *Elektroprivod (Electric drive)* Gosenergoizdat (1948).
2. S.N. Veshenevskii; *Raschet kharakteristik i soprotivlenii dlia elektrodvigotelei (Calculation of characteristics and resistances for electric motors)*, Gosenergoizdat (1955).

EXPERIMENTAL DETERMINATION OF PARAMETERS OF ELEMENTS OF AUTOMATIC CONTROL SYSTEMS*

S.Ia. BEREZIN

Leningrad

(Received 11 December 1957)

For theoretical investigation of automatic control systems it is necessary to know the parameters of the individual elements of these systems. At present many methods for the determination of the parameters of automatic control systems exist [1, 2].

The majority of these methods are cumbersome, and do not permit the determination of the parameters of elements which are characterized by differential equations of an order greater than the second. In finding these parameters we also assume that the order of the differential equation of the element is known.

1959

The most widely used method of experimental investigation of automatic control systems is the frequency method, owing to its many advantages, which are described in [3]. In using frequency characteristics for finding the parameters of an individual element of automatic control systems it is very convenient to make use of inverse amplitude-phase characteristics, because this permits a considerable reduction of the time required for calculations. The inverse amplitude-phase characteristics of the elements under investigation can be obtained by one of the known methods, for example, those discussed in [3].

The inverse transfer function of an aperiodic link of the first order is of the form:

$$Y(p) = \frac{1}{K_0}(1 + Tp), \tag{1}$$

where K_0 is the amplification factor of the link; T is the time constant of the link. For a sinusoidal disturbance at the link input

$$Y(j\omega) = \frac{1}{K_0}(1 + Tj\omega)$$

the inverse amplitude-phase characteristic of the first order aperiodic link is a straight line parallel to the imaginary axis and passing it at a distance $1/K_0$ (Fig.1).

To find the time constant of the first order aperiodic link it is sufficient to find

* *Elektrichestvo*, No. 4, 66 – 69, 1958.

experimentally the phase of the vector of the inverse amplitude-phase characteristic for one frequency, say ω_i.

From Fig. 1 it follows that

$$\frac{AB}{OB} = \tan \phi = T\omega_i$$

hence

$$T = \frac{\tan \phi}{\omega_i} \tag{2}$$

The amplification factor of the link can be determined by meters or from the experimentally found amplitude and phase of the vector of the inverse amplitude-phase characteristic for the same frequency:

$$OB = \frac{1}{K_0} = OA \cos \phi$$

hence

$$K_0 = \frac{1}{OA \cos \phi} \tag{3}$$

where OA is the amplitude (modulus) of the vector of the inverse amplitude-phase characteristic ω_i.

To check the accuracy of the parameters so found it is recommended that calculations should be repeated for other frequencies.

If the parameters found for various frequencies differ considerably one from another, and points A_i of the inverse amplitude-phase characteristic do not lie in the straight line, this will prove that the link in question is not a link of the first order.

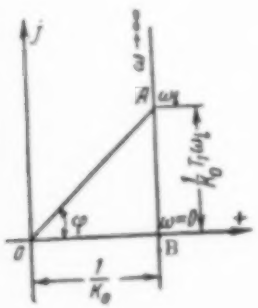

FIG. 1. The inverse amplitude-phase characteristic of an aperiodic link of the first order.

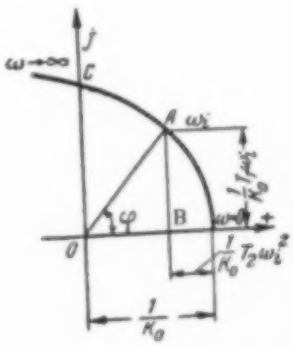

FIG. 2. The inverse amplitude-phase characteristic of a link of the second order.

The inverse complex transfer function for the second order link (aperiodic or oscillatory) is of the form:

$$Y(j\omega) = \frac{1}{K_0}(1 + T_1 j\omega - T_2\omega^2). \tag{4}$$

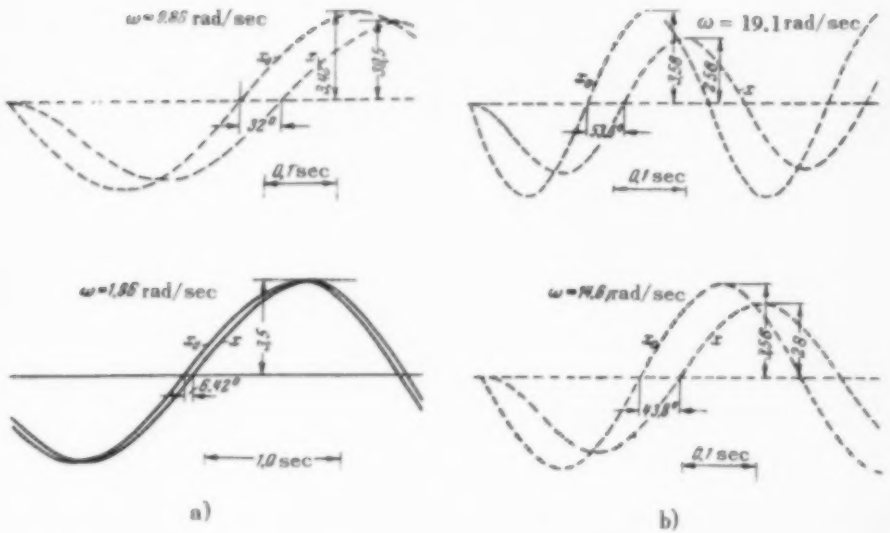

FIG. 3. Curves of the variation of the input and output signals in the presence of sinusoidal disturbances at the input to the element under investigation.

The inverse amplitude-phase characteristic for this link is shown in Fig. 2. This characteristic lies in two quadrants.

From Fig. 2:
$$\sin\phi = \frac{AB}{OA} = \frac{T_1\omega_i}{K_0 OA}\ ;\quad T_1 = \frac{OA.K_0}{\omega_i}\sin\phi. \tag{5}$$

The amplitude OA and phase ϕ are found from the inverse amplitude-phase characteristics, which were experimentally determined for the frequency ω_i.

$$\cos\phi = \frac{(1 - T_2\omega_i^2)}{K_0.OA}, \tag{6}$$

hence
$$T_2 = \frac{1}{\omega_i^2}(1 - K_0.OA\cos\phi). \tag{7}$$

The calculation of the constant T_2 can be carried out in a different way. From the triangle OAB (Fig. 2):
$$\frac{AB}{OB} = \frac{T_1\omega_i}{1 - T_2\omega_i^2} = \tan\phi, \tag{8}$$

hence

$$T_2 = \frac{1}{\omega_i^2} - \frac{T_1}{\omega_i \tan \phi} \tag{9}$$

The calculation of T_2 can be considerably simplified, if we determine experimentally the frequency for which the inverse amplitude-phase characteristic intersects the imaginary axis ($\phi = 90°$) (the real part of the characteristic is zero):

$$\frac{1}{K_0}(1 - T_2\omega_i^2) = 0; \quad T_2 = \frac{1}{\omega_i^2} \tag{10}$$

In this case, for a known modulus we have:

$$T_1 = \frac{OA \cdot K_0}{\omega_i}. \tag{11}$$

If the amplitude-phase characteristics are recorded at low frequencies, then, with an accuracy sufficient in practice, we may assume that

$$OA = \frac{1}{K_0}$$

and then:

$$T_1 = \frac{\sin \phi}{\omega_i}; \tag{12}$$

$$T_2 = \frac{1}{\omega_i^2}(1 - \cos \phi). \tag{13}$$

But in this case, the accurate determination of the phase value is rather difficult.

In certain cases the preliminary determination of the amplification factor of the element in question is connected with many difficulties. Therefore, the determination of the parameters of this element from two points of the inverse amplitude-phase characteristic, obtained experimentally, may be recommended.

For example, if ϕ_1, ϕ_2, OA_1 and OA_2 are determined experimentally, then from (6) we find:

$$K_0 = \frac{1}{\cos \varphi_1 OA_1} - T_2 \frac{\omega_1^2}{\cos \varphi_1 OA_1} = \frac{1}{\cos \varphi_2 OA_2} - T_2 \frac{\omega_2^2}{\cos \varphi_2 OA_2},$$

hence

$$T_2 = \frac{\cos \varphi_1 OA_1 - \cos \varphi_2 OA_2}{\omega_2^2 \cos \varphi_1 OA_1 - \omega_1^2 \cos \varphi_2 OA_2} \tag{14}$$

or

$$T_2 = \frac{B_1 - B_2}{\omega_2^2 B_1 - \omega_1^2 B_2}, \tag{14a}$$

where $B_1 = OA_1 \cos \phi_1$; $B_2 = OA_2 \cos \phi_2$, the real parts of the vector of the inverse amplitude-phase characteristic for frequencies ω_1 and ω_2.

The calculation of the constant T_1 can be made by formula (8):

$$T_1 = \frac{\tan \phi_i}{\omega_i}(1 - T_2\omega_i^2). \tag{15}$$

The amplification factor of the link is most easily found by expression (5):

$$K_0 = \frac{T_1\omega_i}{OA_i \sin \phi_i}. \tag{16}$$

To check the accuracy of the values of the parameters thus found it is advisable, as in the first case, to repeat the calculations for certain other frequencies.

If from experimental determination of the amplitude-phase characteristic it follows that the phase is near to 180°, it then proves that the order of the link in question is higher than two, and the inverse amplitude-phase characteristic for high frequencies will lie in the third quadrant. The electric integrator MPT-9 was used to verify the accuracy of the above method for determining the parameters of the elements of an automatic control system. By means of the integrator several points of the amplitude-phase characteristic were obtained for a given element characterized by the equation:

$$\frac{1}{10}(1 + Tip + P_2 p^2)x = x_0$$

Fig. 3 shows the curves of variation of input and output signals in the presence of sinusoidal disturbances at the input to the element under investigation for frequencies 1.96, 9.86, 14.6, 19.1 rad/sec. The results of the analysis of the oscillograms and of the performed calculations are shown in Table 1.

1959

TABLE 1.

ω_i (rad/sec)	$\varphi_{i\cdot}(^\circ)$	$\frac{A_1}{A_2}$	T_{1i} (sec)	T_{2i} (sec^2)
1.96	6.42	0.1	0.057	$1.56 \cdot 10^{-3}$
9.86	32	0.112	0.0603	$5.14 \cdot 10^{-4}$
14.6	43.8	0.127	0.06	$4.7 \cdot 10^{-4}$
19.1	53.6	0.142	0.06	$4.7 \cdot 10^{-4}$

Note. Calculations of T_1 and T_2 were carried out by the approximate formulae (12) and (13).

The results of these calculations prove the high precision of the method proposed for determining the parameters of the linear elements of automatic control systems.

The error in determining the parameters is smallest for sufficiently large values of ϕ and A_1/A_2; i.e. in the region of high frequencies. Therefore, the determination of parameters should be carried out from the amplitude-phase characteristics recorded for high disturbing frequencies.

Translated by S. Szymanski

REFERENCES

1. G.L. Rabkin, B.A. Mitrofanov and Iu.D. Steinberg; *Avtomatika i telemekhanika*, No. 5 (1955).
2. E.L. Ettinger and Iu.R. Reingold; *Elektrichestvo* No. 3, (1956).
3. Iu.R. Reingold; *Elektrichestvo*, No. 4 (1954).

THE HIGH-POWER HIGH-VOLTAGE RECTIFIER*

F.I. BUTAEV, N.S. KLIMOV, M.F. KOSTROV and A.A. SAKOVICH

All-Union Lenin Electrotechnical Institute

(Received 5 November 1957)

Directives of the XXth congress of the Communist Party of the Soviet Union envisage power transmission at high direct voltage; for this purpose during the next five years the d.c. transmission line between Stalingrad Hydro-Electric Station and the Donbas should be put into operation. The electrical industry should develop and manufacture the equipment for this line. Putting into effect this decision of the Party, the Board of the All-Union Lenin Electrotechnical Institute (VEI) has developed a high-power high-voltage rectifier for the converter substations of the d.c. transmission line.

1959

Work on the development of high-voltage rectifiers began long ago in the U.S.S.R. and abroad.

In Sweden, work on the development of high-voltage rectifiers has been carried out since 1929. A rectifier with two parallel-working anodes, each anode designed for a maximum current of 100 A and a voltage of 65 kV, has been constructed.

In Germany the AEG and Siemens Cos. have been working for a long time on the development of high-voltage rectifiers. The AEG Co. has developed a rectifier for a voltage of 120 kV and a maximum current of 150 A, and the Siemens Co. has developed rectifiers for a still higher voltage but for the same current. The former rectifiers were to be connected, three in series, into an arm of a 220 kV bridge and the latter were to be connected two-in series into an arm of a bridge of the same type.

High-voltage rectifiers of a multianode construction have been designed by the B.B.C. but the work of this firm resulted in no practical solution.

In other foreign countries the achievements in the development of high-voltage rectifiers are even less significant.

In the Soviet Union before the war, work was carried out on these rectifiers

* *Elektrichestvo* No. 5, 1-7, 1958.

in the VEI laboratories (Larionov and Krauz in 1937, Klimov in 1938-39 and Galdin in 1940). The result of this work led to the development and testing of the following devices: a rotary d.c. machine for 80 kV, 5 kW, an ionic-mechanical convertor for 10 kV, 100 kW and a six-anode mercury rectifier for 25 kV, 100 A, with an intermediate electrode, a shield in the anode assembly and also aluminium seals.

Large scale work on the development of high-power high-voltage rectifiers began in our country after the war.

During the first years after the war, high-voltage rectifiers and control gears were developed for the first experimental d.c. transmission line from Kashira HEPS* to Moscow. This work started and to a considerable extent was accomplished by the scientific and technical office of the former Ministry of the Electrical Industry, with the co-operation of prominent German experts (Dobke, Chelters and others). In addition, the following investigations on models were performed in this office: a system of control from the earth potential of all rectifiers of the substation with the use of a double impulse; a d.c. transformer; substation protection with a pick-up device and the use of a shunting rectifier. Investigations were also carried out on the method of damping spurious oscillation processes.

Numerous investigations and tests of rectifiers were performed on various test benches and installations of the VEI.

As a result of this work a batch of 30 rectifiers of the VR-1 (which passed the tests) and their control panels were made by the scientific and technical office, and partly by the experimental factory of the VEI; in the second half of 1950 they were delivered to the Ministry of Power Stations for the substation equipment of the experimental transmission line.

During the adjustment of the experimental d.c. transmission line, the VEI jointly with the Institute of Direct Current carried out tests on rectifiers under normal service conditions.

On an equivalent circuit in the VEI, where normal conditions for rectifiers are produced, the probability of backfires was determined: on the average one backfire in 24 hours occurred. The recovery time of the controlling capacity of the grid was equal to 2 el deg. at a cooling-oil temperature of 16°, and a rise in the anode voltage of 70 kV.

The investigation of the flashover and the anode insulator showed, that the distribution of the potential along the external part of the insulator was uniform: In the case of flashover between the intermediate electrodes (between all or a part of them) the distribution of the potential outside becomes very irregular, and this brings about an increase in the field intensity which causes flashover along

* Hydro-electric Power Station.

the insulator. This probably happens owing to the fact that the speed of discharge formation in vacuum is considerably smaller than the corresponding speed in air.

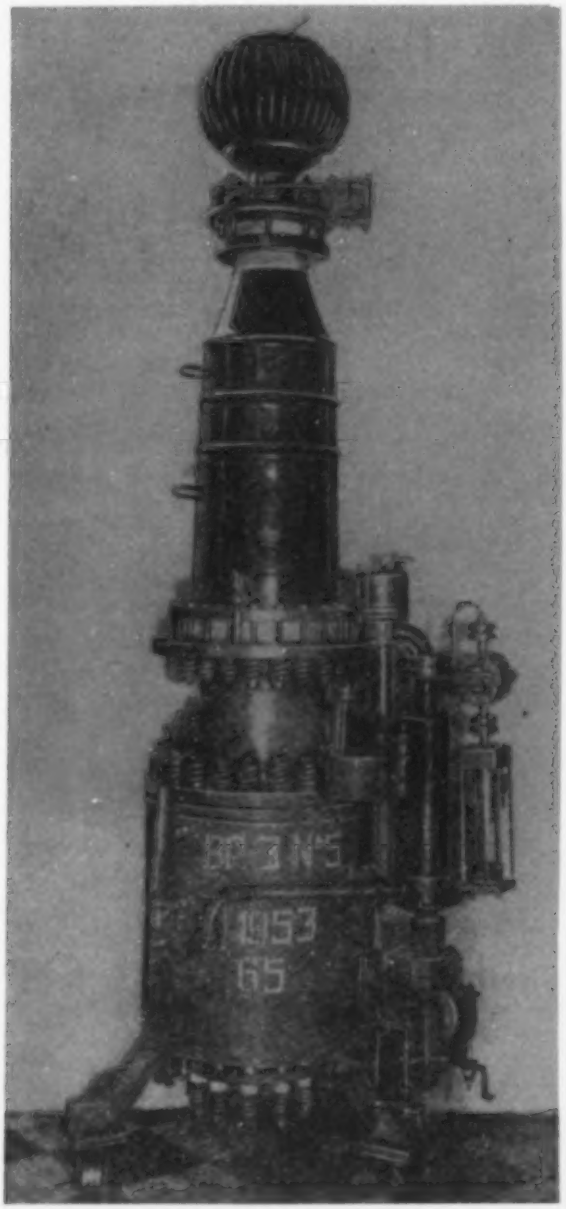

FIG. 1.

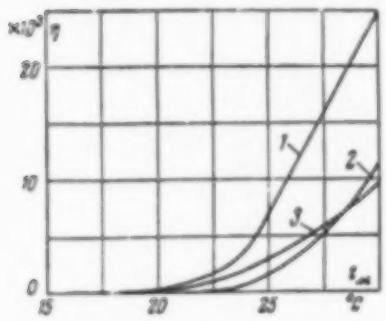

FIG. 2. The relationship between the arcing back frequency and the valve cooling temperature, revealed by the pulse counter (Gorev and Kingdon-Lawton circuit).
1 – valve VR-1 ($\frac{di}{dt} = 2.10^8$ A/sec, U_{pr} 150 kV);
2 – valve VR-3 ($\frac{di}{dt} = 1.27.10^7$ A/sec, $U_{pr} = 160$ kV);
valve VR-9.

In the case of ignition failure, when one of the intermediate electrodes begins acting as a grid, a violent distortion of the potential distribution takes place on the insulator, which may cause the insulator flashover.

The problem of the possibility of breaking a small anode current (up to 0.5 A) by a grid was investigated and it was found that such a possibility existed.

In 1950-51 work was performed in the VEI in order to increase the power of rectifiers for the experimental transmission line.

The rectifier (Type VR-3) for maximum current 300 A and maximum voltage 130 kV was developed (Fig. 1). Twelve of these rectifiers were constructed.

Investigations and tests showed that these rectifiers have a considerably greater electric strength than the first rectifiers for the experimental transmission line, with ratings: maximum current 150 A and maximum voltage 120 kV. Thus a static electric strength of this rectifier without ageing was 160 kV of the effective value, and in the case when the external ohmic potential divider was connected, this voltage was increased to 205 kV, which corresponds to a maximum voltage of 290 kV. High peak inverse anode voltage of this rectifier can be seen from curve (2) in Fig. 2.

Operation of high power rectifiers in the experimental transmission line network showed that sputtering in the anode assembly is insignificant.

In 1952 work was begun in the VEI on the development of high-power high-voltage rectifiers with a maximum voltage of 130 kV and a maximum current of

rectifier), 5, 4, 3, 2 and 1 (Andree's design) intermediate electrodes were built and tested under varying conditions.

These investigations have shown that with an increased number of intermediate electrodes, the peak inverse anode voltage and the electric strength increase; the sputtering and poisoning of the anode decrease, but the losses also increase and arcing is hampered. With a decreased number of intermediate

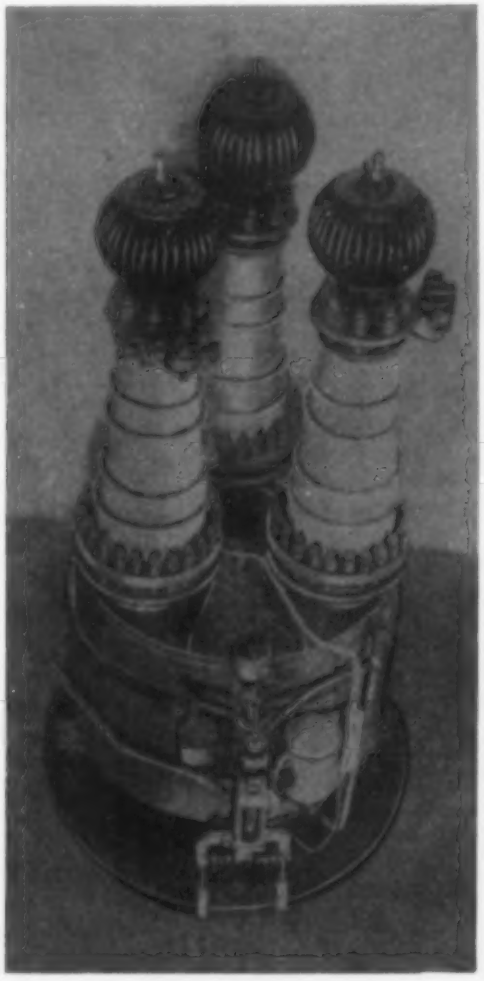

FIG. 8.

900 A, which had to be connected in series into an arm of a bridge circuit. To develop such a rectifier, suitable for industrial transmission, it was necessary to perform exhaustive research work and to answer many major problems.

It was necessary to decide whether the rectifier had to be a single-anode or multi-anode one. Many experts in our country and abroad denied the possibility of obtaining high power in a single anode because of a danger of concentrating a discharge on a small section, which may disturb the working of the rectifier. It was difficult to give a single well-founded answer to this question solely on a theoretical basis. Therefore, work was carried out in the VEI on the development of single-anode and multi-anode rectifiers, and experimental models were made.

Fig. 3 shows a three-anode rectifier for maximum voltage of 130 kV and a maximum current of 750 A made in 1952. A current divider between the three parallel working anodes was developed and made for this rectifier. The rectifier proved to be very cumbersome, unwieldy in assembling, handling and rather unreliable.

The comparison of the designs of three-anode and single-anode rectifiers showed the incontestable superiority of the latter. Nevertheless, it remained to be proved that the difficulties connected with the concentration of discharge on a small section could be overcome.

For this purpose, the current distribution on the anode and grid surfaces was investigated.

The current distribution proved relatively uniform on an anode with a diameter of a few hundred millimetres. Edges of the anode were less loaded.

Fig. 4 shows a typical curve of the mean distribution of the current on the anode (ion current on probe, measured by a magneto-electric device). The distribution of the instantaneous current (Fig. 5) shows that the arc column moves from place to place with a considerable speed. This speed increases with the increase of current. At every given point the current varies within wide limits, and these oscillations increase from the centre of the anode towards its periphery.

Investigations on the current distribution have shown that:

(a) the whole end surface of the anode works, although not quite uniformly;
(b) the whole surface of the anode is heated;
(c) the drop in the current density is smaller in the anode of a larger diameter than in the smaller one. Therefore, if it is desirable to increase the rectifier current, it is advisable to increase the anode diameter.

On the basis of these investigations a single-anode rectifier was adopted.

It was decided to determine the optimum number of intermediate electrodes for the anode assembly. Experimental models of rectifiers with 15 (Kesaev's

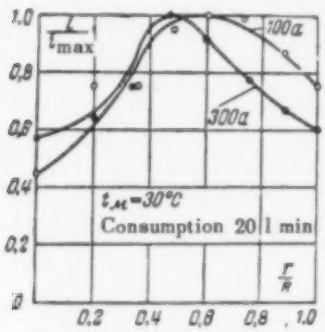

FIG. 4

electrodes, the inverse phenomena are observed. The number of intermediate electrodes was chosen to obtain the maximum advantage and the fewest possible defects.

The next important problem was the choice of the geometrical shape and the distribution of intermediate electrodes. The ring-shaped, shutter-type, conical, overlapping, radial, grid and other electrodes were considered. On the basis of the experiments performed, the electrodes that showed the best results were used on the majority of rectifiers.

1959

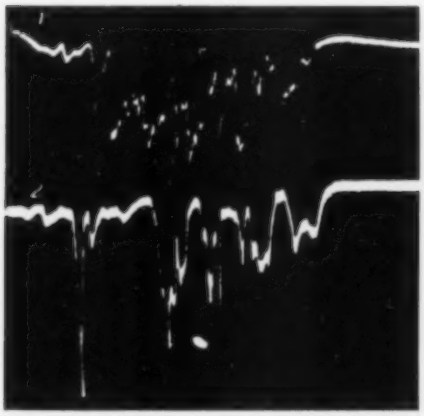

FIG. 5. Oscillograms of current distribution over the anode (ionic current on a sonde) 1—in the centre (R = 0); 2—at the edge (R = 1).

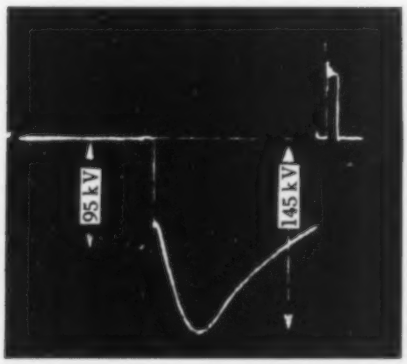

FIG. 6

Operational experience will enable us to choose the best geometrical shape of the intermediate electrodes.

Extensive work was performed in testing the materials used in the manufacture of high-voltage rectifiers, and particularly materials for the main and control electrodes, and for other components situated in the discharge zone. Materials were tested with regard to backfires, gassing, sputtering and other properties. As a result of these tests, materials were chosen for the various rectifier components.

Special vacuum technical installations were developed, constructed and put into operation in 1951-52; namely vacuum ovens of large capacity, benches for technical finishing and vacuum testing of the individual assembles of the rectifier, special heaters, etc.

Special test installations were built: an equivalent circuit, which allows rectifiers to be tested at the maximum current of 1000 A and maximum voltage of 160 kV (the shape of the curve for the anode-cathode potential is shown on Fig. 6); an impulse installation for 350 kV; benches for the low tension tests and others. For the overload tests the shock circuit of the high tension section of the VEI was used; this circuit was designed for testing air circuit-breakers.

The construction of high-power high-voltage rectifiers differs considerably from the construction of rectifiers that are normally used in industry and traction.

Fig. 7 shows a diagramatical section of such a rectifier (Type VR-9/3) for maximum current 900 A and maximum voltage 130 kV. The main parts of the rectifier are: the anode, which is cooled by a special cooler; the anode insulator with auxiliary inleads; the tank with a cooling jacket; the cathode; the anode high-voltage assembly, the low-voltage assembly and the cooled cathode cap.

The heat developed in the rectifier is partly carried away by the cooling liquid, and is partly dissipated in air by the cooling fins of the tank and of the cooler, and also by the insulator surface. The heat of the anode head is carried away towards the cooler surface by the mercury vapour, which is formed inside the vacuum chamber of the cooler.

The intermediate electrodes are situated between the anode and the low-voltage assembly. The low-voltage assembly consists of two grids and a filter. The excitation anodes also form a part of this assembly. On the cathode, which is filled with mercury, two quarts baffles and the slot ignitor are situated.

Although the cathode is liquid cooled, natural air cooling is also sufficient The rectifier tank is provided with a cooling jacket with a directing spiral. To increase the cooling surface one model of the rectifier was provided with a spiral tube. A cooled cathode cap is used for the following purpose: to increase

cooling, to decrease the pressure of mercury vapour and to ensure its uniformity, to improve the current distribution across the anode and grid assemblies. The cooling liquid (oil) is circulated round the cap.

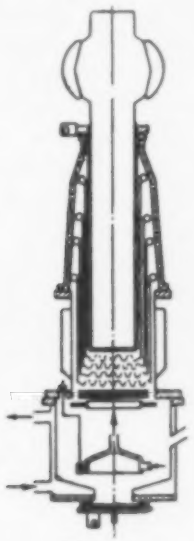

FIG. 7.

The rectifier is evacuated by an oil and a mercury pump. A high-vacuum electromagnetic tap, remote controlled electrically, is situated on the exhaust pipe. Fig. 8 shows a general view of the rectifier.

The control panel is provided with many improvements (remote control, light control), which increases the service reliability at high voltage and facilitate the operation of the installation.

The design of the control panel and some other problems are not discussed in this article, because they will be discussed separately.

Since 1952, 25 models of high-power rectifiers of different types and varieties have been constructed. These rectifiers underwent exhaustive investigations and tests. Some results of these tests are discussed later.

The electric strength of the rectifier is sufficiently high. During the static tests it withstands the effective voltage of 140-160 kV without the external divider. The use of the external divider increases the electric strength.

The peak inverse anode voltage of this rectifier is higher than that of rectifiers used in the experimental transmission installation. The results of one of the tests of the peak inverse anode voltage of a high-power rectifier, recorded

on an impulse installation, are shown on Fig. 2 (curve 3).

The density of the mercury vapour and the vapour dynamics are of great importance for the operation of the rectifier. To obtain the necessary density of mercury vapour was a very difficult problem. The investigation of the state of the mercury vapour was carried out by the probe methods developed in the gas discharge laboratories of the VEI. It has been shown that with oil cooling the density of the mercury vapour did not correspond to the temperature of the outcoming oil and that there was a difference between the temperature, corresponding to the vapour density, and the temperature of the outcoming oil. With different methods of oil cooling this temperature difference may vary from plus a few tens of degrees to minus a few degrees. For example, Fig. 9 shows curves of the variation in the temperature differences in relation to the current load of the rectifier for two different systems of cooling: the tank with a spiral tube (curve 1) and the tank with a spiral tube and a cooled cathode cap (curve 2). On comparing these curves the very strong influence of the cooled cathode cap on the vapour pressure in the rectifier becomes apparent.

Electrical tests at full current and voltage values were performed on the equivalent circuit made in the VEI for maximum current up to 1000 A and maximum voltage up to 160 kV. These tests provided very valuable information.

It was found that the occurence of backfires at the maximum back-voltage of about 135 kV and maximum current 900 A is less than one backfire every 24 hr. The rate of current decrease was 1×10^6 A/sec, the jump in the back voltage was 90 kV, and the voltage increased at a rate of 40 kV/°C.

The investigations have shown that besides loss of the control action of the grids, direct breakdown also occurred. By direct breakdown we mean such a phenomenon, when, in the pressure of a positive anode potential, a cathode spot appears on the upper grid and the current flows towards the cathode, avoiding the discharge gap the upper grid (cathode). The frequency of direct breakdown does not exceed the frequency of back-fires.

The stability of the excitation arc plays a very important role in rectifier operation. It has been found that the principal causes of the extinction of the excitation arc are: short circuiting of the tank with the cathode by mercury streams; the presence of insulating particles at the bottom of the tank; the low-quality mercury wetting considerable portions of the tank surface; and excessive oscillations of the mercury vapour pressure in the region of the excitation anodes. Different measures have been applied to avoid these disadvantages and steady arcing of the excitation arc has been achieved.

An unusual phenomenon has been observed in the high-voltage rectifiers; namely, with the positive anode potential and normal working of all excitation anodes and grids, no ignition of the main anode occurs, i.e. the ignition fails.

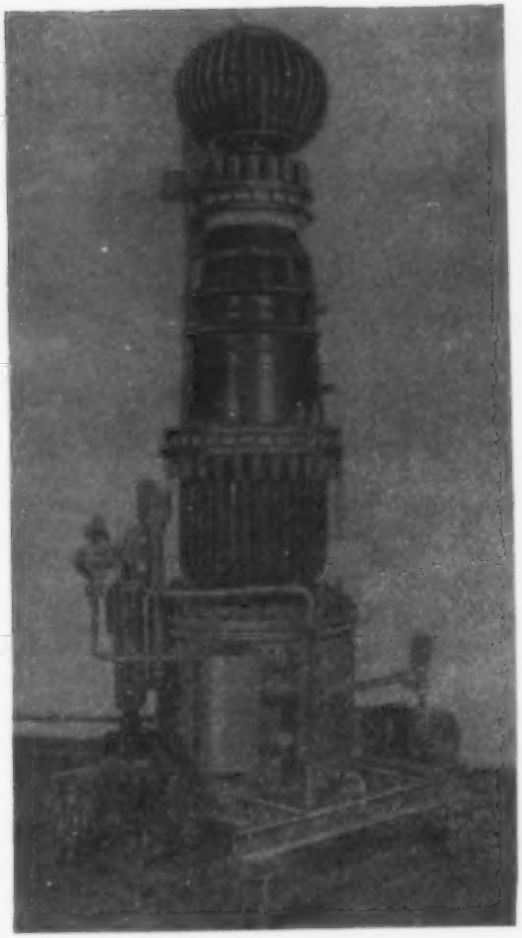

FIG. 8.

1959

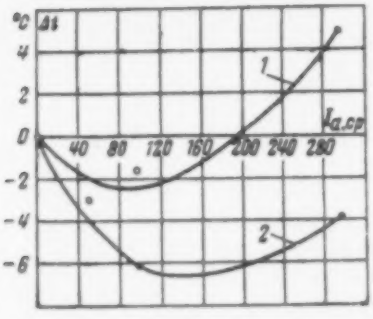

FIG. 9.

This happens only at high voltage and occurs more often when the value of the voltages increases. This phenomenon does not occur at low voltages.

The cause of the ignition failures according to our explanation is the appearance on the auxiliary electrodes of negative potential, which may be due to different causes. Thus, the problem of ignition failures is overcome by the suppression of these negative potentials.

During the development of high-power rectifiers it has been found that failures in the ignition of auxiliary electrodes may be caused by the presence of the condensed mercury vapour in the grid region, which brings about "splashes" in the vapour pressure and the cascade arcing of one of the grids. The ignition dispersion may also be connected with intermittent contacts of the auxiliary electrodes with the tank.

After modification, the failures in the auxiliary electrodes ignition ceased. The tests showed that the probability of flashover on the insulator is considerably less with the high-power rectifiers than with the rectifiers on the experimental transmission installation.

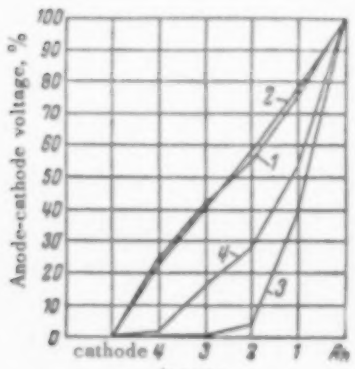

FIG. 10. Voltage distribution curves on inserts in a VR-9 valve, taken on an equivalent circuit ($U_{max.\ test.}$ = 140 kV, U_{ak} = 80 kV, I_{ar} = 280-300 A, $t_{oil\ outlet}$ = 25° C)
1 – inverter regime – jump; 2 – same regime – maximum value; 3 – rectifying regime – jump; 4 – the same, maximum value.

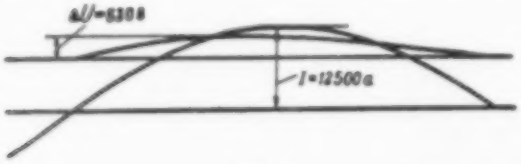

FIG. 11.

The tests showed that the potential distribution on the intermediate electrodes is very irregular owing to the influence of the remaining plasma, and maximum irregularity occurs at the beginning of deionization. The greatest potential drop takes place during the conversion period in the gap between the anode and the first insert and during the inversion period in the gap between the last intermediate electrode and the grid. After some lapse of time from the begin-

ning of deionization the potential distribution improves.

Fig. 10 shows curves of the potential distribution on the intermediate electrodes of the VR-9 high-power rectifier; they were recorded on the equivalent circuit. These curves show that during the inversion operation, in which direct potential is applied at the end of deionization, the negative potential jump is absent; the distribution of the positive potential is practically uniform both for the jump and for the maximum value. In the conversion action, the potential distribution is irregular. The maximum irregularity in distribution occurs during the jump, since in this case phenomena take place during the period of deionization. The maximum potential value is divided more uniformly than the jump value, since the maximum value is attained considerably later, after the completion of deionization.

The use of the external divider, for example, with resistances, in practice brings about a sufficiently quick equalization in potential dividing.

The overload capacity of high-voltage rectifiers differs considerably from the overload capacity of low-voltage rectifiers owing to the lower density of the mercury vapour. Tests of high-voltage rectifiers at low-voltage (220 V) show that a relatively small increase in the anode current brings about a break of the current with all its consequences (overvoltages etc). Thus, in the VR-9 high-power rectifier with a nominal value of maximum current 900A breaks occur in the current at 3500 A at an anode voltage of 220V.

Investigations of the overload capacity of the high-power rectifiers at the high voltages (50-100 kV) showed – as the authors of this article had anticipated – that the current breaks did not occur even at the currents of 15,000 A within the range of operating temperatures. The voltage arc-drop in this case reaches a value of 700-800V.

Fig. 11 shows the anode current oscillogram and the arc-drop of a high-power high-voltage rectifier recorded on the power circuit at a maximum anode voltage of about 50 kV.

The tests showed that the potential distribution along the discharge gap was rectilinear contrary to our expectations. This can probably be explained by the arc contracting to the cross-section, whose area is several times smaller than the area of the intermediate electrodes.

For power tests on high-power high-voltage rectifiers 120 MVA test plant has been installed in the Institute of Direct Current, in Moscow. Rectifiers may be tested under short-circuit conditions and on the "closed loop circuit" with a conversion and inversion group of rectifiers.

In this plant tests were made under short-circuit conditions at full current and two values of reverse voltage, 50 and 90 kV. Fig. 12 shows the shape of the reverse voltage curve.

The rate of increase of the reverse voltage at an anode voltage of 50 kV was 24 kV/degree, and 44 kV/el. degree at an anode voltage of 90 kV.

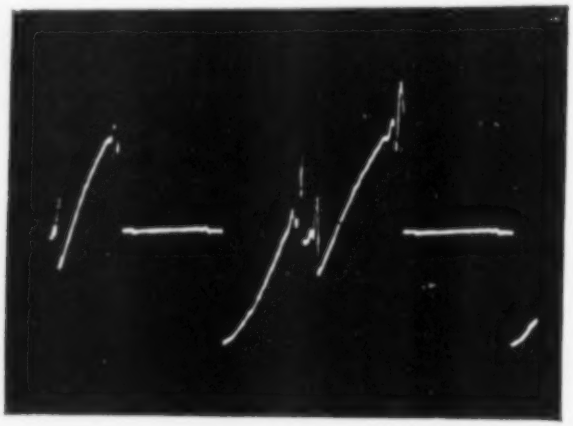

FIG. 12. Oscillogram of anode – cathode voltage on the bench with the valves working on regime 3 (U_{pr} = 77 kV, U_{obr} = 100 kV).

The results of the series of tests showed that at a current of 900 A and a reverse voltage jump of 50 kV, the rectifiers do not suffer from irregularities (back-fires, direct breakdowns, extinctions of excitation). At a current of 900 A and a reverse voltage jump of 90 kV no extinction of the excitation arc occurs in the rectifiers; the number of backfires is considerably less than one backfire in 24 hr.

If we take into consideration that rectifiers are to be series-connected into the bridge arm, we must conclude that such a performance is satisfactory. Tests of the operation of these rectifiers under more severe conditions and their further adjustment are continuing.

For the transmission line from Stalingrad HEPS to the Donbos (potential difference between poles 800 kV and line current 900 A), the VEI proposed an eight-bridge circuit. Voltage across each bridge was 100 kV. This plan has been approved by the Commission of Experts. In this circuit two rectifiers are series connected into the bridge arm.

According to data issued by the Institute of Direct Current, the normal ratings of the rectifier in this circuit are: the maximum reverse voltage 61 kV, the reverse voltage jump 34 kV, maximum current value 900 A. It is understood that under service conditions, particularly in cases of emergency, the rectifiers will operate under much heavier conditions, but these conditions will be of a transitory nature. To secure the operational reliability of the rectifiers, automatic control

and protective gear has been provided in the transmission network. A short – circuiting valve has been provided in particular.

The rational solution of the power transmission network in conjuction with automatic and special protective devices will contribute greatly to the successful operation of high-power high-voltage rectifiers and will speed up the practical realization of long distance power transmission at high direct voltages.

The results of the first series of bench tests show that the high-power rectifier developed by the VEI will be able to work singly in the bridge arm, provided rational power circuits are developed to limit currents and voltages under emergency conditions.

The rectifier design permits a great variety of modifications for different operating conditions by changing the parameters of the high- and low-voltage assemblies.

The high-power high-voltage rectifier can ensure the reliable operation of the transmission line between Stalingrad HEPS and the Donbos in the network designed for it.

The work discussed in this article has been carried out for several years in the high-voltage rectifier laboratories of the VEI in co-operation with the laboratories for gas discharge apparatus and physical research of the same institute. The rectifier models were made by the experimental electromechanical factory of the VEI.

The porcelain and ceramic parts were developed and manufactured by the porcelain factory "Izoliator" and the Institute GIEKI.

The investigations on the rectifiers and the tests on the test power installation were carried out jointly with the Institute of Direct Current.

The following persons took direct and active part in this work: N.P. Stepanov, N. P.Savin, N.M. Maslennikov, I.D. Shkolin, A.A. Pertsev, V.S. Grigor´ev, A.A. Timofeev, R.I. Grigor´eva, V.V. Bazhenov, I.V. Blond, A.A.Ivanov, E.P. Shmarina, and others.

Translated by S. Szymanski

THE PROBLEM OF THE APPROXIMATE ANALYTICAL SOLUTION OF OSCILLATIONS OF A SYNCHRONOUS MACHINE*

B.L. KONSTANTINOV

Bulgaria, Sofia

(Received 2 February 1957)

If a synchronous generator works whilst connected to the bus-bars of a constant voltage then if working conditions are changed, the differential equation of the motion of the rotor, after certain simplifications, can be written:

$$M\frac{d^2\delta}{dt^2} = P_0 - P_m \sin\delta, \tag{1}$$

where M – the inertial constant of the machine;

δ – the angle between the vectors of an axial e.m.f. and the voltage of the system;

P_0 – the power of the prime mover;

P_m – the maximum value of the power characteristic under the new conditions.

The substitution:

$$d\delta / dt = \phi(\delta)$$

lowers the order of the differential equation:

$$\frac{d\delta}{dt} = \sqrt{\frac{2P_0}{M}}\sqrt{\delta - \delta_0 \frac{P_m}{P_0}(\cos\delta_0 - \cos\delta)} \tag{2}$$

To make clear the character of the rotor motion (oscillations or continuous acceleration) it is necessary to analyse the function:

$$y = \delta - \delta_0 - \frac{P_m}{P_0}(\cos\delta_0 - \cos\delta). \tag{3}$$

*Elektrichestvo No. 5, 24-26, 1958.

If the equation $y = 0$ has no other root except δ_0 then the machine breaks out of synchronism; the presence of the two roots is evidence of the ordinary oscillatory process.

The analysis of the first and second derivative of function (3), and also of the equation $y = 0$ (Kepler's equation of the type $\delta = p\sin\delta + \alpha$), shows that for the existence of the second root the condition $P_m / P_0 > 1$ should be satisfied. In so far as this condition is not connected with the initial angle δ_0, it cannot be considered as a criterion, which determines the character of the rotor motion. In order to find an approximate criterion determining the relationship between the values P_0, δ_0 and P_m, it is necessary to make use of the condition of the preservation of the stability, which is based on the principle of the comparison of areas.

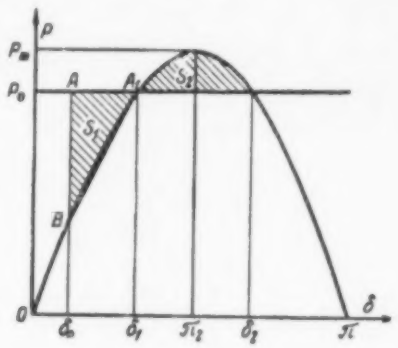

FIG. 1

If with the change of working conditions the parallel working remains undisturbed, then the area S_1 is smaller than the area S_2 (see Fig.) In further discussion, in order to make the analysis easier, we shall assume that the power characteristic under the new conditions may be represented by a parabola [1]

$$P = P_m\left[1 - \frac{4}{\pi^2}\left(\frac{\pi}{2} - \delta\right)^2\right], \tag{4}$$

which passes through the points (0,0), ($\frac{\pi}{2}$, P_m) and (π, 0). Such an approximation, which is permissible within the interval $0 < \delta < \pi$, does not alter the result substantially.

In this case:

$$S_2 = \int_{\delta_1}^{\delta_2} P_m\left[1 - \frac{4}{\pi^2}\left(\frac{\pi}{2} - \delta\right)^2\right] d\delta - P_0(\delta_2 - \delta_1),$$

and the values of δ_1 and δ_2 are found from:

$$P_0 = P_m\left[1 - \frac{4}{\pi^2}\left(\frac{\pi}{2} - \delta_{1,2}\right)^2\right],$$

i.e.

$$\delta_{1,2} = \frac{\pi}{2}\left(1 \mp \sqrt{1 - \frac{P_0}{P_m}}\right).$$

Thus, as a final result we get:

$$S_2 = \frac{2}{3}\pi P_m\left(1 - \frac{P_0}{P_m}\right)^{3/2}.$$

Without making any great mistake we may assume that the area S_1 is equal to the difference of the areas of the rectangle $\delta_0 AA_1\delta$ and trapezium $\delta_0 BA_1\delta_1$, i.e.

$$S_1 \approx P_0(\delta_1 - \delta_0) - \frac{P_0 + P_m\left[1 - \frac{4}{\pi^2}\left(\frac{\pi}{2} - \delta_0\right)^2\right]}{2}(\delta_1 - \delta).$$

Substituting the value of δ_1 obtained above, after certain rearrangements, we get:

$$S_1 \approx \frac{1}{4}\pi P_m\left(1 - \frac{P_0}{P_m}\right)^{3/2}(z^2 - 1)(z - 1),$$

where

$$z = \frac{2}{\pi}\frac{\frac{\pi}{2} - \delta_0}{\sqrt{1 - \frac{P_0}{P_m}}}.$$

Taking into account the condition $S_1 < S_2$, we get the inequality

$$(z^2 - 1)(z - 1) < \frac{8}{3},$$

which is satisfied for $Z > 1.951$.

Consequently:

$$\frac{1}{\pi}\frac{\frac{\pi}{2} - \delta_0}{\sqrt{1 - \frac{P_0}{P_m}}} < 0.9755$$

or

$$\frac{P_m}{P_0} > \frac{1}{1 - 1.051\left(\frac{1}{2} - \frac{\delta_0}{\pi}\right)^2}. \quad (5)\ *$$

It is necessary to point out that a similar result is obtained by the analysis of the solution of equation (4-58), which is given in [1, p.123]. The analysis shows that:

$$\frac{P_m}{P_0} > \frac{1}{1 - \left(\frac{1}{2} - \frac{\delta_0}{\pi}\right)^2}. \quad (6)$$

The difference between the right-hand sides of equations (5) and (6) is less than 1.7 per cent even for $\delta = 0$, i.e. in the case which is impossible in practice. By using an exact value of S_1 we may expect that this value will be equal to zero.

* If we introduce a more accurate value of S_1, the preservation of stability is also possible for a smaller value of P.

Therefore, in the further discussion we shall consider the inequality (6) as a criterion for the preservation of stability. We substitute into equation (2)

$$\delta = \frac{\pi}{2} - x \text{ and } \delta_0 = \frac{\pi}{2} - x$$

and by using equation (4), we get an approximate solution of equation (1) within the interval $0 < \delta < \pi$

$$t = \sqrt{\frac{\pi^2 M}{8P_m}} \left[\frac{\pi}{2} - \arcsin \frac{\pi^2 P_0 - 8P_m \delta}{\pi^2 P_0 - 8P_m \delta_0} \right]. \tag{7}$$

Solving (7) with respect to δ we get:

$$\delta = \delta_0 + \left(\frac{\pi}{4} \cdot \frac{P_0}{P_m} - 2\delta_0 \right) \sin^2 \left[t \sqrt{\frac{2P_m}{\pi^2 M}} \right], \tag{8}$$

from which we determine at once the initial interval of oscillations.

$$\delta_0 \leqslant \delta \leq \frac{\pi}{4} \frac{P_0}{P_m} - \delta_0,$$

and also a "half-period" of this interval.

$$T = \frac{\pi^2}{2} \sqrt{\frac{M}{2P_m}}$$

1959

It is understood that the relationship (8) and the values of δ_0 and T, that we obtained, have a meaning if the inequality (6) is satisfied.

If the inequality (6) is not satisfied then, substituting into (7) instead of angle δ the value of the limiting permissible angle δ_{lim}, we obtain the maximum permissible time of the cutting-out of the short-circuit. Obviously, the formula for this case, due to its simplicity, has a considerable advantage in comparison with the method of successive intervals.

If δ_{lim} does not exceed 60° we can by solving equation (2) make use of the expansion of cos δ into the series:

$$\cos \delta = 1 - \frac{\delta^2}{2!} + \frac{\delta^4}{4!}.$$

In this case the solution of equation (2) leads to the Abel's elliptical integral. Without discussing the solution itself we shall give only the final results. The limiting time of the cutting-out of the short-circuit is determined by the following relationship.

$$t = \left[\frac{M}{2P_m k_1 \sqrt{2a^2 + c}} \right]^{1/2} \int_0^{\varphi} \frac{d\varphi}{\sqrt{1 - k^2 \sin \varphi}}, \tag{9}$$

where

$$k = \frac{P_0}{P_m} - \delta_0 + \frac{\delta_0^3}{3};$$

a – a real root of the cubic equation $u^3 + pu + q = 0$, in which:

$$r=\frac{\delta_0}{6k_1}-3a^2;\quad q=\frac{a\cdot\delta_0+0{,}25}{6k_1}-2a^3 \text{ and } a=\frac{2-\delta_0^2}{12k_1};$$

$$c=-\frac{q}{a};\quad k^2=\frac{1}{2}\left(1-\frac{3}{2}\,\frac{a}{\sqrt{2a^2+c}}\right);$$

$$\varphi=2\operatorname{arctg}\left[\frac{\sqrt{2a^2+c}}{\dfrac{1}{\delta_{np}-\delta_0}-(a+a)}\right]^{1/2}.$$

Three real roots α, β, γ ($\alpha > \beta > \gamma$) of the cubic equation $u^3 + pu + q = 0$ correspond to the conditions of the machine oscillations. Therefore the formulae for t, k^2 and ϕ assume another form:

$$t=\left[\frac{M}{2P_m k_1(\alpha-\gamma)}\right]^{1/2}\int_0^{\varphi}\frac{d\varphi}{\sqrt{1-k^2\sin\varphi}};$$

$$k^2=\frac{\beta-\gamma}{\alpha-\gamma}\quad\text{и}\quad\varphi=\arcsin\left[\frac{\alpha-\gamma}{1-(\alpha+\gamma)(\delta-\delta_0)}\right]^{1/2}. \tag{10}$$

Let us remark that these formulae can also be used for $\delta > 60°$. Thus, for example, formula (9) gives the same results as the solution by the method of successive intervals even for $\delta = 90\text{-}100°$.

The solutions of two concrete problems, which were obtained by formulae (7) and (9), are given below; for comparison the results obtained by the method of successive intervals are also shown.

TABLE 1

References in which problems are solved	Initial conditions	Limiting time of cutting-out of the short-circuit, sec.		
		By formula 7	By formula 8	By the method of successive intervals
[2] pp. 122-127]	$S=\frac{300}{220}$; $T_j=6$ sec, $P_0=1$; $\delta_0=0{,}6026$ rad, $P_m=0{,}502$; $\delta=1{,}0943$ rad. (62.7°)	0.189	0.193	0.193**
[3 p.95]	$S_n=1.3$; $T_j=6$ sec; $P_0=0{,}9$; $\delta_0=0.422$ rad; $P_m=0{,}66$; $\delta=1.593$ rad (91.3°)	0.321	0.330	0.330

$$M=\frac{S_n T_j}{\omega_0}$$

** In the book the third decimal figure is omitted; this can be seen from Fig. 5-14

As can be seen from these data, the time calculated by formula (9) is exactly the same as that calculated by the method of successive intervals, although the angle δ is greater than 90°. This is explained by the relatively small influence of $\cos\delta$, which appears in the square root sign of equation, (2), for angles of tripping of about 90°.

It is necessary to point out that formula (9) can be successfully used in the case of the parallel operation of two stations of a comparable power under the same limitations concerning the variation of the angle δ.

Since in this case equation (1) can be written in the following form:

$$\frac{d^2(\delta+\mu)}{dt} = P_0' - P_m' \sin(\delta+\mu),$$

where

$$P_0' = \frac{1}{M_1}\left(P_{01} - \frac{E_1^2}{z_{11}}\sin\alpha_{11}\right) - \frac{1}{M_2}\left(P_{02} - \frac{E_2^2}{z_{22}}\sin\alpha_{22}\right);$$

$$P_m = \left(\frac{1}{M_1}+\frac{1}{M_2}\right)\frac{E_1E_2}{z_{12}}\frac{\cos\alpha_{12}}{\cos\mu}$$

and

$$\operatorname{tg}\mu = \frac{M_1 - M_2}{M_1 + M_2}\operatorname{tg}\alpha_{12},$$

then we have to substitute into formula (9) unity instead of M, because M_1 and M_2 appear in P_0 and P_m. For the numerical example given in [2, pp. 134-142] the limiting time of tripping the short-circuit obtained by this method was 0.278 sec. Solution by the method of successive intervals gave this time equal to 0.277 sec.

Translated by S. Szymanski

REFERENCES

1. V.A. Vyenikov and L.A. Zhukov; *Perekhodnyye protsessy v elektricheskikh sistemakh (Transient processes in electrical systems)*, Gozenergoizdat (1953).
2. P.S. Zhdanov; *Ustoichivost' elektricheskikh sistem (Stability of* electrical systems), Gozenergoizdat (1948).
3. K. Bogatev; *Parallelna rabota na elektricheskite tsentrali (Parallel operation in a power station)*, *Izd. "Nauka i Izkustvo"*, Sofia (1951).

THE INFLUENCE OF THE LAW OF THE EXCITATION CONTROL ON THE DAMPING OF OSCILLATIONS OF A SYNCHRONOUS MACHINE*

V.M. MATIUKHIN

Krzhizhanovski Power Institute, U.S.S.R. Academy of Sciences

(Received 29 June 1957)

Knowledge of the roots of a characteristic equation of a synchronous machine is important for a quantitative characterization of the degree of stability of the machine for small oscillations, and for an approximate evaluation of the speed of damping of a transient process for finite disturbances. The analysis of the roots enables us to compare different laws of control in this respect and, as far as possible, to choose the best.

We know from experience that the cause of disturbance of the stability of a synchronous generator connected with the automatic excitation control is usually the tendency of the rotor towards self-oscillation. Therefore, the roots related to the frequency and degree of damping of the rotor fundamental oscillations are of major interest.

In this article the influence of different laws of control on the damping and frequency of the machine oscillations are discussed using as an example the fourth-order system.

Differential and characteristic equations of a synchronous machine for automatic control of excitation

Assuming that the voltage of the receiving system remains constant, and also neglecting transient processes in the stator and the influence of the damping winding, we write the equations of a synchronous machine for a small disturbance in the following form:

$$Jp^2\Delta\delta + \frac{\partial P}{\partial \delta}\Delta\delta + \frac{\partial P}{\partial E_d}\Delta E_d = 0;\quad \Delta E_d(1 + T'_d p) - Cp\Delta\delta = \frac{\Delta U_e}{1 + T_1 p} = \Delta U_f;$$
$$\Delta U_e = k\Delta R_1 + (k'p + k''p^2)\Delta R_2, \tag{1}$$

where J is the mechanical constant of the rotor; P is its power; E_d the e.m.f. of the

* *Elektrichestvo*, No.5, 27 – 31 1958.

no-load run; U_c the control device output voltage; U_f the voltage on the rotor rings; T_d the time constant of the rotor winding during closing of the line on the bus-bars of the receiving system; T_1 the time constant of the exciter; R_1 and R_2 respectively: a parameter by which a basic excitation control is carried out; and a parameter which is used for stabilizing the control process (as R_1 and R_2: voltage U, the stator current I or angle δ may be used); k k' k'' control coefficients.

Constant C_1 if we neglect the ohmic resistance of the line and generator and assume $x_q = x_d$, is given by the following formula [1]:

$$C = T_{d0} U_0 \frac{x_d - x'_d}{x_d} \sin\delta,$$

where x_d and x_q are synchronous and transient reactances of the generator and the line taken together; T_{d0} the time constant of the rotor for the open stator winding. To the set of equations (1) there corresponds the characteristic equation:

$$\begin{aligned} &J\left(T_1 T'_d - \frac{\partial R_2}{\partial E_d} k''\right) p^4 + J\left(T_1 + T'_d - \frac{\partial R_2}{\partial E_d} k'\right) p^3 + \\ &+ \left[J\left(1 - \frac{\partial R_1}{\partial E_d} k\right) + T_1\left(\frac{\partial P}{\partial E_d} C + \frac{\partial P}{\partial \delta} T'_d\right) - \left(\frac{\partial P}{\partial \delta}\frac{\partial R_2}{\partial E_d} - \frac{\partial P}{\partial E_d}\frac{\partial R_2}{\partial \delta}\right) k''\right] p^2 + \\ &+ \left[\frac{\partial P}{\partial \delta}(T_1 + T'_d) + \frac{\partial P}{\partial E_d} C - \left(\frac{\partial P}{\partial \delta}\cdot\frac{\partial R_2}{\partial E_d} - \frac{\partial P}{\partial E_d}\cdot\frac{\partial R_2}{\partial \delta}\right) k'\right] p + \\ &+ \left[\frac{\partial P}{\partial \delta} - \left(\frac{\partial P}{\partial \delta}\cdot\frac{\partial R_1}{\partial E_d} - \frac{\partial P}{\partial E_d}\frac{\partial R_1}{\partial \delta}\right) k\right] = 0. \end{aligned} \tag{2}$$

1959

General analysis of the fourth-order equation

According to the Hurvitz criterion it is necessary for the stability of a fourth-order system that the coefficients of the characteristic equation should be positive

$$a_4 p^4 + a_3 p^3 + a_2 p^2 + a_1 p + a_0 = 0 \tag{3}$$

and that the following inequality should be satisfied:

$$a_1 a_2 a_3 - a_1^2 a_4 - a_3^2 a_0 > 0. \tag{4}$$

From this inequality we may draw certain conclusions.

It is obvious that the increase of a_3 can never bring a stable system into an unstable state. On the contrary, the increase of a_2 makes the inequality more marked and, consequently, should increase the margin of stability. Furthermore, it is seen that a_0 and a_4 are contained in the inequality only with a minus sign, i.e. their increase may upset the stability of the system. But we have no influence on a_0, since it depends on amplification factors, which are determined by static characteristics (static conditions of the generator voltage or conditions of normal and emergency states). Therefore the only thing we may consider is to try to make the coefficient a_4 as small as possible.

So far as values a_1 and a_3 are concerned, condition (4) shows that their increase

is possible only up to a certain limit. It is necessary to try to vary the coefficients of the characteristic equation in the desired sense by introducing into the control device derivatives of this or another quantity. The characteristic equation has four roots, of which two, usually conjugate complex roots, determine the basic motion of the rotor; let us call them conventionally "mechanical" roots. We shall call the two remaining roots, which strongly depend on time constants T_1 and T_d, "electrical" roots.

When the damping of the rotor oscillations is insignificant and the constant T_1 is not very small, the frequency of the rotor oscillations and the damping ratio may be expressed approximately by formulae (see Appendix):

$$\omega^2 \approx \frac{a_3}{2} + \sqrt{\left(\frac{a_3}{2}\right)^2 - a_0}; \tag{5}$$

$$\alpha \approx \frac{1}{2}\left(a_3 - \frac{a_1}{\omega^2}\right). \tag{6}$$

In these formulae it is assumed, for the sake of brevity, that the coefficient of the highest-degree term in equation (3) is unity. This obviously does not impair the general character of our considerations.

Although formulae (5) and (6) are valid only near the limit of stability of the system, nevertheless they permit, as can be seen from the examples given below, a correct estimate of the values of various coefficients of the equation; these values can be varied by means of the control device. From expressions (5) and (6) it follows that to increase the damping moment it is necessary to increase the value of a_2. This agrees with the deduction about the importance of the value of a_2 for the stability of the system, which is obtained from the Hurvitz criterion. The increase in a_2 means, in conformity with expression (5), an increase in the frequency of the rotor oscillations. Thus, if by the action of the control device, only the value of a_2 is increased, then the increase in damping will be accompanied by an increase in the frequency of the rotor oscillations.

From expression (6) it follows that to improve the action of damping it is also desirable to increase the value of a_3 and decrease a_1. The Hurvitz criterion does not allow such a categorical conclusion in this respect, but this criterion deals with arbitrary values of the equation coefficients, whereas in the case under consideration they are restricted by the relatively small values of electrical roots.

Investigation of the fourth order system for various methods of control

Let us first consider the excitation control of a generator by the angle and its derivatives. In this case, in the characteristic equation (2), we have to assume that:

$$R_1 = R_2 = \delta,$$

i.e.

$$\frac{\partial R_1}{\partial E_d} = \frac{\partial R_2}{\partial E_d} = 0; \quad \frac{\partial R_1}{\partial \delta} = \frac{\partial R_2}{\partial \delta} = 1.$$

Let us also denote

$$k = k_\delta; \; k' = k'_\delta; \; k'' = k''_\delta.$$

The subscripts of factors k, k', k'' indicate the quantity by means of which the

control is exerted.

The factor of control, k''_δ, by the second derivative of the angle, affects only the value of a_2; i.e. the coefficient of the second degree of p in equation (2). According to the above considerations a sufficiently large value of k''_δ will ensure good damping of the rotor oscillations. With the increase of k''_δ and a_2 the frequency of rotor oscillations will also increase, as follows from formula (5).

The control factor k_δ affects only the value of a_1, and therefore, in accordance with formula (6), it should weaken the action of damping.

For the numerical examples given below the parameters of the long range transmission line are chosen; they correspond approximately to the parameters of the preliminary project of the Kuibyshev-Moscow transmission line:

$J = 16$ sec; $T_d = 3.85$ sec; $\delta = 68°$, $E_d = 1.28$; $C = 1.08$, $x_{\text{d.gen}} = 0.5$, $x_1 = 0.8$; $x'_{\text{d.gen}} = 0.2$, $\cos \phi_n = 0.92$.

Table 1 shows the influence of the control factors k''_δ and k'_δ on the frequency of rotor oscillations and the damping ratio. The time constant of the exciter was $T_1 = 0.3$ sec and the static factor of the angle control $k_\delta = 0.5$.

TABLE 1.

k'_δ	k''_δ	$p_{1,2}$: "mechanical" roots	$p_{3,4}$: "electrical" roots
0	0	$+0.025 \pm j\,3.32$	$-0.34 \quad -3.26$
0	1	$-0.88 \pm j\,4.45$	$-0.43 \quad -1.41$
0	2	$-1.24 \pm j\,5.7$	$-0.56 \pm j\,0.234$
0	4	$-1.48 \pm j\,7.6$	$-0.32 \pm j\,0.33$
1	2	$-1.06 \pm j\,5.7$	$-0.31 \quad 1.26$

From Table 1 it follows that the second derivative of the angle control ensures good damping of the rotor oscillations. For example, for $k''_\delta = 2$ and $k' = 0$, for the frequency of oscillations $f = 5.7/2\pi = 0.9$ c/s, the amplitude of oscillations decreases in 1 sec to the value $\exp(-1.24) = 0.29$ of the initial value. The frequency of the rotor oscillations increases with the increase of k''_δ.

The introduction of the first derivative of the angle control decreases the damping ratio of the rotor oscillations, as can be expected from the general analysis. Without the first derivative of the angle control the system is unstable, and it is characteristic that this instability manifests itself in a self-oscillation of the rotor, since the "electrical" roots remain negative. If the control applied is only the second derivative control, then for a sufficiently large value of k''_δ the "electrical" roots remain a conjugate complex, and the frequency of electrical oscillations is low.

Table 2 shows the influence of the time constant T_1 for control factors

$k_\delta = 0.5$; $k'_\delta = 1$; $k''_\delta = 2$.

TABLE 2.

T_1	$p_{1,2}$ — "mechanical" roots	$p_{3,4}$ — "electrical" roots
1	$-0.17 \pm j\ 4.3$	-0.36; -0.56
0.3	$-1.06 \pm j\ 5.7$	-0.31; -1.2
0.1	$-4.03 \pm j\ 7.32$	-0.29; -1.85
0.02	-6.50; -2.40	-0.29; -41.4

From Table 2 it follows that the decrease in the value of time constant T_1 leads to the increase in damping of the rotor oscillations. For a very small value of $T_1 = 0.02$ sec the motion of the rotor becomes aperiodic. However, it does not follow from this that in a simple system we should try at all costs to obtain a very small value of T_1 since already for $T_1 = 0.3$ sec the damping is good and can be still increased by increasing the factor k''_δ. The increase in the damping ratio is accompanied by an increase in the rotor oscillations, as long as the rotor motion preserves its oscillatory character.

For the control by the stator current and by its derivatives we have to assume in the characteristic equation (2):

$$R_1 = R_2 = I,$$

i.e.

$$\frac{\partial R_1}{\partial E_d} = \frac{\partial R_2}{\partial E_d} = \frac{\partial I}{\partial E_d}; \qquad \frac{\partial R_1}{\partial \delta} = \frac{\partial R_2}{\partial \delta} = \frac{\partial I}{\partial \delta},$$

and also

$$k = k_1; \quad k' = k'_1; \quad k'' = k''_1.$$

The analysis of equation (2), for the control stability derivatives of the stator current, leads to the following conclusions:

Factors of the derivative control k'_1, and k''_1 are limited above because if they are sufficiently large, coefficients a_3 and a_4 of the characteristic equation become negative, and this means instability of the system. The main problem of getting a stable and well-damped system consists in increasing the coefficient a_2 and decreasing a_4; this problem can be solved by a proper choice of the factor of the second derivative of the stator current control.

According to the conditions of control stability and of good damping there is no need in the first derivative of the stator current control, since in this case the coefficient of p^3 decreases and the coefficient of p increases, and this is, according to formula (6), undesirable. However, the first derivative control may be used to force the exciter voltage. This general analysis of the characteristic equation (2) is confirmed by the examples given in Table 3. The evaluation of roots was performed for

$T_1 = 0.3$ sec and $k_1 = 0.5$.

TABLE 3.

k_1'	k_1''	$p_{1,2}$ – "mechanical" roots	$p_{3,4}$ – "electrical" roots
0	0	$-0.05 \pm j\ 3.32$	-0.24; -3.28
0	0.5	$-0.57 \pm j\ 3.7$	-0.25; -3.31
0	1	$-1.6 \pm j\ 4.2$	-0.26; -3.24
0	1.5	$-4.15 \pm j\ 4.4$	-0.26; -3.04
1	1	$-1.15 \pm j\ 4.65$	-0.22; -3.28

As follows from this table, the second derivative of the stator current control produces a strong damping moment of a synchronous machine, which arises when the departures from synchronous running occur. In this case, as in the case of the second derivative of the angle control, the increase in damping is accompanied by an increase in frequency of the rotor oscillations.

The addition of the first derivative of the current control weakens the damping action of the control. When the derivatives of the current are zero the system is on the verge of stability, because the damping of mechanical oscillations falls almost to zero. The "electrical" roots are separated, and

$$p_3 \approx -\frac{1}{T_d'}; \quad p_4 \approx -\frac{1}{T_1}.$$

Stabilizing the process of the control by introducing the derivatives of the stator current also has, as is known from [2], a certain disadvantage; this consists in that for a considerable variation in the parameters of a transmission line, a change in the setting of the control device may be needed in order to preserve the stability of operation. Moreover, as has already been said, the derivatives of the stator current are limited above for the sake of stability, which has significance, for example, in the excitation control by voltage.

Let us now consider voltage control and control by its two derivatives. Into the characteristic equation (2) we have to substitute:

$$R_1 = R_2 = U,$$

i.e.

$$\frac{\partial R_1}{\partial \delta} = \frac{\partial R_2}{\partial \delta} = \frac{\partial U}{\partial \delta}; \quad \frac{\partial R_1}{\partial E_d} = \frac{\partial R_2}{\partial E_d} = \frac{dU}{\partial \delta},$$

and also

$$k = -k_U; \quad k' = -k_U'; \quad k'' = -k_U''.$$

Then, on the basis of equation (2) we may draw the following conclusions.

The increase of the coefficient a_2 by introducing the second derivative of the

current control cannot produce the same effect as the second derivative of the angle or stator current control, since in this case coefficient a_4 increases simultaneously, and this has an unfavourable influence on the stability. At the same time the increase a_3 (the first derivative of voltage control) will not always produce the required effect, since the value of a_1 increases simultaneously, and this, according to formula (6), acts unfavourably on the damping of mechanical oscillations. Thus, only certain optimum values of the factors k'_U and k''_U can be obtained.

Table 4 confirms these general considerations. Roots are calculated for $T_1 = 0.3$ sec and $k_U = 20$.

TABLE 4.

k'_U	k''_U	$p_{1,2}$ — "mechanical" roots	$p_{3,4}$ — "electrical" roots
5	10	$-0.045 \pm j\ 3.7$	$-0.46 + j\ 1.26$
5	30	$-0.024 + j\ 3.77$	$-0.166 \pm j\ 0.8$
20	10	$-0.195 \pm j\ 3.56$	$-0.93 \pm j\ 1.0$
40	10	$+0.015 \pm j\ 3.72$	$-3.42;\ -0.51$

The increase in the factor of the second derivative control from 10 to 30 has decreased the already weak damping of the rotor oscillations (for $k'_U = 5$). The best result is obtained for $k'_U = 20$ and $k''_U = 10$. But even in this case the damping ratio is equal to 0.195, i.e. is considerably smaller than for the second derivative of the angle or stator current control. The increase of k'_U acts favourably only up to a certain limit; for $k'_U = 40$ the motion of a generator becomes unstable.

A radical method for the increase in damping of the rotor oscillations for the excitation control by the stator voltage consists in introducing into the means of control derivatives of the angle instead of derivatives of the voltage.

$$\frac{\partial R_1}{\partial \delta} = \frac{\partial U}{\partial \delta};\ \frac{\partial R_1}{\partial E_d} = \frac{\partial U}{\partial E_d};\ \frac{\partial R_2}{\partial \dot{\delta}} = 1;\ \frac{\partial R_2}{\partial E_d} = 0;$$

$$k = -k_U;\ k' = k'_\delta;\ k'' = k''_\delta.$$

Substituting these values into equation (2) we may draw conclusions about the favourable influence of the second derivative of the angle control.

Table 5 gives the values of roots for the case in question for $T_1 = 0.3$ sec., $k_U = 20$, $k'_\delta = 1$.

TABLE 5.

k''_δ	$p_{1,2}$ — "mechanical" roots	$p_{3,4}$ — "electrical" roots
2	$-1.27 \pm j\ 6.2$	$-0.54 \pm j\ 1.85$
4	$-1.44 \pm j\ 8.05$	$-0.36 \pm j\ 1.4$

From these data it follows that the damping of mechanical oscillations has sharply increased after the introduction of the second derivative of the angle control. The first derivative of the angle control will be significant, as in the previous cases, only for forcing excitation.

Thus, in a fourth-order system, irrespective of parameters by which the basic control is exerted, the second derivative of the angle control always ensures a good damping of the rotor oscillations.

Conclusions

1. The damping of the rotor oscillations depends upon the e.m.f.'s applied to the control device, these e.m.f.'s being proportional to the derivatives of current, voltage or angle.

2. By using the second derivative of the angle control in a fourth-order system we may ensure strong damping. The first derivative control on the contrary lowers the damping ratio of the rotor oscillations. The second derivative of the stator current control also gives strong damping for the excitation control by the stator current. However, the value of the second derivative of the stator current is limited above for the sake of stability, and this is significant for basic control by the voltage.

3. The improvement of damping, when using the second derivative of the angle and stator current control, depends on the increase in frequency of the rotor oscillations.

4. For the derivative of voltage control both derivatives should be used. However, in this case, in principle, no strong damping can be ensured. The examples given above show that in this case the damping is much weaker than in the case of the second derivative of the angle control.

Appendix

Let us consider the equation:

$$p^4 = a_3 p^3 + a_2 p^2 + a_1 p + a_0 = 0. \tag{I,1}$$

Let us assume that equation (I,1) has two conjugate complex roots with a small real part. Then we may assume:

$$p^2 \approx -\omega^2, \tag{I,2}$$

where ω is the coefficient of the imaginary parts of the root. Thus, the equation (I,1) may be written:

$$p^2 + \left(a_3 - \frac{a_1}{\omega^2}\right) p + \left(a_2 - \frac{a_0}{\omega^2}\right) = 0. \tag{I,3}$$

Let us find out on what conditions in this equation the coefficient of p, taken with the opposite sign, is equal to the sum of the real parts of the roots in question. The Viette formula gives:

$$a_3 = -(p_1 + p_2) - (p_3 + p_4); \quad a_1 = -p_1 p_2 (p_3 + p_4) - p_3 p_4 (p_1 + p_2).$$

Let p_1 and p_2 be the complex roots with which we are concerned. According to condition (I,2),

$$p_1 p_2 \approx \omega^2. \tag{I,4}$$

Using the Viette formula and condition (I,4) we get:

$$a_3 - \frac{a_1}{\omega^2} = -(p_1 + p_2) + \frac{p_3 p_4 (p_1 + p_2)}{\omega^2}. \tag{I,5}$$

Therefore, in order that the coefficient of p in equation (I,3) should give the modulus of the sum of the real parts of the complex roots, it is necessary that the product of the two other roots $p_3 p_4$ be small in comparison with ω^2. In powerful synchronous generators one of the roots connected with T_d' (say p_3) is usually small, so as a rough approximation we can write $p_3 = -1/T_d$. On the other hand, with frequency of the rotor oscillations 1 c/s, $\omega^2 \approx 36$. Therefore, if the second constant T_1 is not very small, i.e. if the root p_4 is not large, then the condition $p_3 p_4 \ll \omega^2$ is fulfilled and, consequently, near the limit of stability we shall have

$$a \approx \frac{1}{2}\left(a_3 - \frac{a_1}{\omega^2}\right),$$

where a is the damping ratio of the rotor oscillations.

Let us determine further on what conditions the free term of equation (I,3) is equal to the square of the frequency.

By the Viette formula we have:

$$a_2 = p_1 p_2 + p_3 p_4 + (p_1 + p_2)(p_3 + p_4); \qquad a_0 = p_1 p_2 p_3 p_4.$$

Therefore, for the condition assumed (I,4) we get:

$$a_2 - \frac{a_0}{\omega^2} \approx p_1 p_2 + (p_1 + p_2)(p_3 + p_4).$$

Since the sum $p_1 + p_2$ is assumed small, p_3 is of comparatively small magnitude; then again, if the constant T_1 is not too small, we get:

$$a_2 - \frac{a_0}{\omega^2} \approx p_1 p_2 = \omega^2.$$

Therefore, the frequency of the rotor oscillations is:

$$\omega^2 \approx \frac{a_2}{2} + \sqrt{\left(\frac{a_2}{2}\right)^2 - a_0}.$$

Thus the principal conditions for using equation (I,3) to find the mechanical roots p_1 and p_2 are as follows: the real part of these roots should be small in comparison with the imaginary one and every one of the two other roots should be small in comparison with ω.

After finding the mechanical roots, the "electrical" roots p_3 and p_4 can be found. The better the conditions discussed above are fulfilled, the more accurately the roots are determined. If the roots p_3 and p_4 are real, they can be easily determined exactly

by applying the Horner method for the evaluation of polynomials, after which the more accurate values of the roots p_1 and p_2 can be found.

Another method of solving the fourth order equation for widely differing roots is described in [3].

Equation (I,3) has been used in this work not so much for solving the fourth-order equation, as for a qualitative investigation of the influence of different coefficients on the damping of the rotor oscillations; and this was done in this article.

The calculation of roots in this work was carried out by one of the processes of the iteration method, discussed in [4]. Only in the case when the system was on the verge of stability were calculations made by the method discussed in this appendix. In all cases the accuracy of the solutions can be verified by the Viette formulae given here.

Translated by S. Szymanski

REFERENCES

1. V.M. Matiukhin; Uravneniia i strukturnaia skhema sinkhronnogo generatora pri avtomaticheshom regulirovanii vozbuzhdeniia (Equations and a block diagram of a synchronous generator for automatic excitation control), *Izv. Akad. Nauk SSSR, otd. tekh. nauk*, No. 9 (1952).
2. V.A. Venikov and I.V. Litkens; *Elektrichestvo*, No. 11 (1955).
3. V.S. Vyedrov; *Dinamicheskaia ustoichivost' samoleta (Dynamical stability of an aircraft)*, Oborongiz (1938).
4. E.V. Popov; *Dinamika sistem avtomaticheskogo regulirovoiniia (Dynamics of automatic control systems)* (1954).

1959

ARTIFICIAL METHODS OF OBTAINING HIGH POWER FOR THE INVESTIGATION OF ARC EXTINCTION DEVICES*

M.M. AKODIS

Sverdlovsk

(Received 24 February 1957)

The principle of designing of artificial networks† which was proposed in 1940, allows a correct reproduction of operational conditions of circuit breakers and ionic rectifiers. In these networks (Fig. 1, 2) the full voltage is applied from charged capacitors (of circuit II) to the point of junction of two series connected pieces of apparatus. Circuit I acts as a source of current. The networks designed on this principle allow an arbitrary choice of the resistance of the high-tension circuit; this enables a correct reproduction of the real conditions of operation of both circuit-breakers and rectifiers, [1 and 2].

A network for testing circuit-breakers

In testing circuit-breakers it is necessary to ensure a time of arcing not less than 1.5 - 2 half-cycles and even more. In the network in Fig.1 the time of arcing, due to the lower voltage in the circuit of the current at cut-off will be, as a rule, shorter, than in the circuit of the full voltage. In this arrangement the high-tension circuit cannot increase the time of arcing, since the arc can be restruck only in one of the two pieces of apparatus, which are series connected in the circuit of the current at cut-off. Thus this network, which has already found a wide application, does not permit the conducting of exhaustive tests of the great majority of existing circuit breakers.

To ensure the necessary time of arcing the network should be supplemented by one or more circuits III Fig.2, which are added to restrike the arc in both circuit-breakers. In most cases it is advisable to design this network in such a way that the full voltage of the circuit III, striking the arc, should be applied to circuit breakers, before the current to be cut-off reaches its zero value. This

* *Elektrichestvo* No. 5, 42-47, 1957.

† M.M. Akodis. Author's certificate No. 85, 166 of 25 March 1940, *Bulletin of inventions*, No.8, 1951.

allows restriking of the arc in both circuit breakers by using a comparatively small voltage in circuit III. After the action of the arc restriking circuits III, of which there may be 2-3 and more, has ceased, the recovery voltage from the capacitors of the circuit is applied to the circuit-breakers.

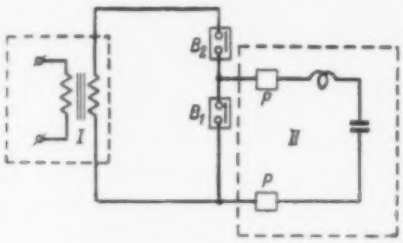

FIG.1. An artificial network without a restriking circuit. I- circuit of the current to be cut off; II- circuit of the recovery voltage; B_1 and B_2 - apparatus on test and auxiliary; P - separation and synchronizing device.

1959

To ensure reliable striking and maintaining of the arc in both circuit breakers it is necessary that the circuit III should be connected slightly before the current reaches its zero value; that is, when the conductance of the arc gaps is sufficiently high (moment of time t_1 in Fig.3). In this case the current from circuit III increases in both circuit breakers at a greater rate and is directed towards the current to be

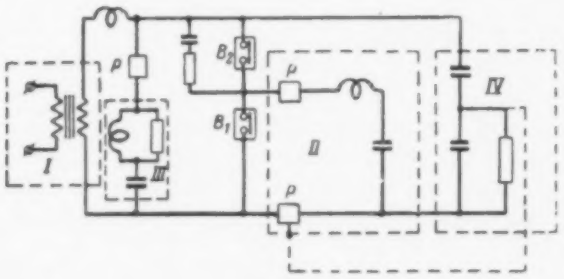

FIG.2. An artificial network with a restriking circuit. I- circuit of the current to be cut off; II- circuit of the recovery voltage; III- circuit of the arc restriking; IV- voltage divider; B_1 and B_2 apparatus on test and auxiliary; P - separation and synchronizing device.

cut-off. Due to a very quick decrease of the full current in both circuit-breakers, after circuit III has been connected, the conductance of the arc gaps, at a moment

of the zero value of the currents, will still be high, and this will ensure the flow of the pulse current i_3 (from circuit III) in the reverse direction. During the time of flow of the current i_3 in the circuit-breakers the current at cut-off reverses its direction and continues to flow through the circuit breakers, and this ensures one more half-period of arcing. Using several arc-striking circuits III, it is possible to increase the time of arcing in the low voltage circuit, through which the current to be cut-off flows, by a few half-periods. After the action of striking circuits has ceased, the circuit breakers come under the influence of the recovery voltage from the capacitors of circuit II.

By varying the extent of the influence of circuits III, we may find the critical length of the arc, for which the circuit-breaker can withstand the recovery voltage of the circuit II, and consequently we may determine the limiting rupturing capacity of the circuit breaker.

The current pulse from the arc igniting circuit should be of a sufficient duration since its quick damping may bring about the suppression of the current at cut-off off immediately after the firing pulse has stopped.

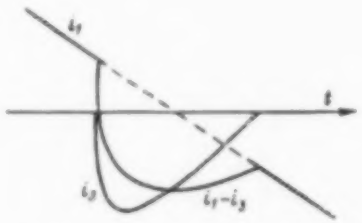

FIG.3. Current variation in the circuit breaker on test. i_1 - current at cut-off; i_2 - current pulse of the restriking circuit.

Investigations of the operation of the igniting network* have shown that normal arc igniting may be secured by means of a capacitance, which is discharged into the arc through parallel connected inductance and resistance, and by a circuit, which is designed as a chain network with inductances of the first links shunted by resistances.

The operation of such a network is illustrated by the oscillograms shown in Fig.4. Since the capacitance of the arc igniting circuit is considerable, it is necessary to separate it after discharge from the network of the cut-off current by protectors.

Another alternative, which is also possible for the operation of the network, is shown in Fig.2. At first, the recovery voltage from circuit II is applied to the

* Investigations were carried out by V.M. Rudnyi

circuit-breakers. If after this a restriking occurs in the circuit-breaker on test, then the synchronizing devices will cause circuit III to operate, and this will send a voltage sufficient for restriking the arc in the second circuit-breaker. At the end of the arcing half-period, high voltage is applied from the circuit II (or from the same circuit, which in the meantime has been recharged, or from a doubling circuit). If the circuit-breaker on test does not extinguish the arc, the process is repeated, but, if the circuit-breaker on test withstands the recovery voltage, then the experiment is finished. Such an arrangement of the network enables us to reduce the number of experiments, which are needed for determination of rupturing capacity of a circuit-breaker, but requires either a stronger insulation of the interrupted circuit, or installing of a protective reactor in this circuit.

The rupturing capacity of a modern circuit-breaker should be determined in a cycle of automatic reclosure (AR). The artificial network under consideration enables us to carry out tests on an arbitrary cycle of AR, and to do this it is sufficient only to provide a certain number of circuits II and III.

In modern circuit breakers, operating in the AR cycle, the arc extinction capacity decreases with each cut-off, therefore it is sufficient to verify the arc-extinction capacity, when applying voltage from circuit II, only for the last half-cycle of the last cut-off in the AR cycle.

1959

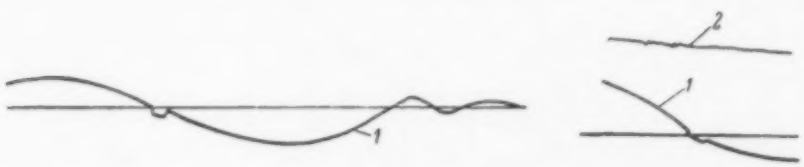

FIG.4. Oscillograms of tests of an experimental arc extinction device of a tank oil circuit-breaker for 110 kV. a - arc ignition for a current of 10.8 kA; b - arc ignition for a current of 19 kA; 1 - current i_1; 2 - recovery voltage of a frequency 17,000 c/s.

In all previous switching-off tests, our action may be restricted to securing the necessary time of arcing, fixed in advance, by means of arc igniting circuits III.

Such a design of a network allows a considerable simplification of the installation and lowering of its cost, while preserving the full validity of the tests.

Voltage recovery in the circuit-breaker on test

The circuit of the recovery voltage may be connected in different ways.

If in the networks of Figs. 1 and 2 the apparatus on test is the circuit breaker B_2 then the recovery voltage from circuit II should be opposite in polarity to that of the tripping circuit I, in so far as they act on the opposite sides of the apparatus on test. In this case the recovery voltage on the circuit breakers on test is equal

to the sum of voltages of both circuits, but only the voltage of circuit II acts on the second (protective) circuit-breaker.

If in the network under consideration the recovery voltage is applied at the mid point between the two series connected circuit-breakers, it appears as a recovery (reverse) voltage only for one piece of apparatus, (i.e. for that on test B_2), but for the second, protective B_1 it has the polarity of the arc voltage before extinction. If we change the polarity, i.e. shift by 180°, the phase of the circuit of the recovery voltage or of the circuit of the current being cut-off, then the voltage of circuit II will be equivalent to the recovery voltage for the second apparatus B_1 and to the arc voltage for the first B_2. In other words, the circuit-breaker on test and the protective one will interchange their roles. In the last case, only the voltage of circuit II will be applied to the circuit-breaker on test B_1, and the difference of the circuit voltages will be applied to the protective B_2.

The circuit of the recovery voltage II may be connected to the network either before the cut-off of the current in the circuit-breaker on test, or at the moment of its cut-off. In applying a high voltage to the circuit-breaker on test, when the current reaches its zero value, we should ensure the exact synchronization of the action of the circuits. In this case, the synchronizing network must ensure the switching on of circuit II with great precision, a few micro seconds before the current being switched off reaches its zero value. For synchronizing the action of

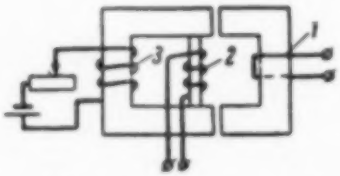

FIG.5. A peak transformer for the circuit synchronization. 1 - primary winding; 2 - secondary winding; 3 - d.c. winding.

circuits a special three-bar peak transformer may be used (Fig.5). The presence on the additional bar of a winding, shifting the voltage peak, and the presence of an air-gap in the core ensure the elimination of the influence of the strong primary current on this winding at the moment of reversal of the magnetic polarity. Investigations have shown that such a transformer, with a sufficiently small dispersal, can reproduce the voltage peak with an advance of a few microseconds.

In testing circuit breakers with a small residual conductance of the arc gap we may have a somewhat increased inductance of the recovery voltage circuit and a corresponding decrease in the capacitance of the network, which brings about a reduction of its cost. In this case the requirements concerning the accuracy of

synchronization may be considerably lowered, if the network is designed in such a way that, from the first moment after the current passes through zero, and till the rupture of the separating gap P of the circuit II, the recovery voltage of the circuit in which the current is being switched off, should be applied to the circuit-breaker on test. In this case we may considerably simplify the synchronizing device, using for the connecting of circuit II a part of the recovery voltage of circuit I [3], through the divider IV, (Fig.2).

It is necessary to take into consideration that the use of the increased inductance in the circuit of the recovery voltage requires in each particular case a verification of the absence of the influence of the arc residual conductance of the operation of the circuit-breaker.

In switching on the recovery voltage circuit, before the moment of dying out of the current in the circuit-breaker on test, the arc extinction in the auxiliary circuit-breaker and the reclosing of the circuit-breaker on test into the circuit of the full voltage may occur before the cessation of the current in the circuit-breaker on test.

In other networks, in which the exact reproduction of the inductance in the recovery voltage circuit was impossible, this procedure always brought about inadmissible distortion of the current at cut-off [4].

So far as the inductance of the network under discussion may be reproduced with a required degree of accuracy, we may in principle avoid the distortion of the current to be disconnected, when connecting the recovery voltage circuit shortly before the arc extinction in the circuit-breaker on test. At the instant of connection of circuit II, before the cut-off current has died out the capacitor of this circuit starts discharging through this circuit-breaker, which is connected into the discharge circuit, provided arcing still persists in this circuit. After one half-period of the natural oscillations of this circuit its current again assumes the zero value, and the voltage across the capacitance assumes the amplitude value of the reverse polarity.

If the circuit of the recovery voltage is switched on before the current in circuit I reaches its zero value (approximately at a time a half-period of its natural frequency oscillations earlier) and if the polarity of circuit II is so chosen, that in the circuit-breaker in the discharge circuit of circuit II the current is directed against the current which is cut-off, then the current in this circuit-breaker will die out a little earlier (moment of time t_2 in Fig.6), than in the circuit-breaker on test (moment of time t_3). Because of this, at the end of the half-period of arcing, circuits I and II become connected in series with the circuit-breaker on test which from this moment on will be under the influence of the sum of voltages of both circuits.

Such a connexion may somewhat decrease the distortion of the curve of the current at cut-off at the end of a half-period, particularly if a voltage peak occurs on the arc immediately before its extinction, which apparently is possible in

certain circuit-breakers even when heavy currents are interrupted. For this connexion it is more difficult to ensure the exact synchronization of circuits, since the switching-on of circuit II should be done 1000 - 2000 μsec before the current being interrupted reaches its zero value, nevertheless for such closing rather large variations of the moment of switching on are permissible. It is necessary to keep in

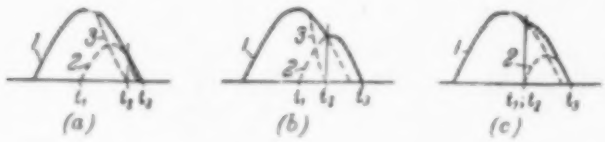

FIG.6 Graphs showing the relationship between the shape of the current at cut-off and the moment of connecting the circuit of the recovery voltage 1 - current from the circuit I, 2 - current from the circuit II, 3 - current in the auxiliary circuit-breaker after the connexion of circuit II. t_1 - connexion of the recovery voltage circuit; t_2 - the moment of arc extinction in the auxiliary apparatus; t_3 - the moment when the current at cut-off reaches zero value.

mind that an excessive advance in arc extinction in the auxiliary circuit-breaker will bring about a discontinuity in the curve of the current through the circuit-breaker, and the interruption of the current will occur with an excessive delay, (Fig. 6b).

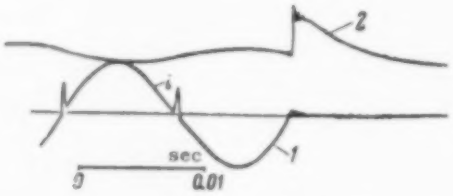

FIG.7 Oscillogram illustrating the operation of the network during the tests of an air circuit-breaker with isolating nozzles. 1 - current at cut-off; 2 - recovery voltage.

The artificial increase in the lapse of time between the moment of current dying out and the moment of its amplitude value, which occurs in this case, may in certain arc extinction devices considerably facilitate the arc extinction, and in others make it more difficult. As experiments have shown a peak transformer enables us to choose the moment, when the peak of the restriking voltage appears with a sufficient accuracy, even when the circuit of the recovery voltage is switched on long before the current reaches its zero value. If for such a connexion of circuit II we choose the voltage polarity on the capacitor in such a way, that in the circuit-breaker of the discharge circuit of circuit II both currents flow in the same

direction, then this circuit-breaker becomes the one on test, on which after the arc extinction the voltage of the required polarity will be restored. For such a choice of polarity of circuit II, which has been made by Biermans [5], the current from circuit II in the circuit-breaker on test is superimposed on the current flowing in the same direction from circuit I thus, in most cases, not decreasing but rather increasing its distortion at the end of a half-period, (Fig. 6c).

Oscillograms, shown in Fig. 7, illustrate a complete operation of the network, with a twofold arc restriking and voltage recovering. These oscillograms were recorded during tests of an air circuit-breaker for 110 kV, having a double break per phase and isolating nozzle. Before the contacts leave the nozzles the circuit-breaker does not disconnect the arc at full voltage, but breaks the arc in the low voltage circuit, because, due to a clearance between the contacts and the nozzle a certain blast occurs even before the contacts leave the nozzle. Without arc restriking circuits for a current of 4-4.5 kA and a voltage of the circuit of the current at cut-off of 8.5 kV, the network ensures a time of arcing within the limits of 0.008-0.018 sec. At this current the circuit breaker safely interrupts the full recovery voltage (71 kV for each break of the circuit-breaker), at a rate of voltage recovery 700 V/μ sec, only if the time of arcing is not less than 0.025-0.027 sec. Therefore, in the tests with an artificial network, without arc restriking circuits, the arc extinction did not as a rule occur at full voltage.

1959

By using two restriking circuits the time of arcing was increased to 0.025-0.035 sec.

The oscillogram shown in Fig. 4, illustrates the operation of a complete network during the tests of an oil circuit-breaker for 110 kV. The value of the interrupted current was 1.2 kA. By using one restriking circuit the time of arcing was brought up to 0.023 sec. During the process of arc extinction the voltage of 71 kV_{max} was applied to the connexion between two extinction devices of the same phase of a circuit-breaker; the frequency of recovery of this voltage was 17 kc/sec. The circuit-breaker did not extinguish the arc, and through it a current of an increased frequency and slowly diminishing flowed from the circuit of the recovery voltage. During the tests of one phase of this circuit-breaker in a network for a current of 10-12 kA and voltage 148 kV_{max} (two extinction devices), of which the frequency of recovery was less than 1 kc/sec, the circuit-breaker interrupted the arc in 0.017-0.024 sec, and for the low voltage the arc extinction took 0.010-0.015 sec, which predetermined the necessity of using a restriking circuit for tests of the circuit-breaker in an artificial network.

The use of the network for the testing of rectifiers

For the testing of rectifiers a network designed on the same principle as that for testing circuit-breakers may be used. As a separation device, P, it is necessary to use two rectifiers connected in parallel opposing one another. The circuit in the network of the testing current should ensure the same shape of the curve of

the current flowing through the rectifiers, as that of the current in the natural network. For this purpose it is advisable to use in the lower voltage network full-wave Fig. 8 or multiphase rectification.

The voltage of the transformer, inductance of the commutation network and parameters of other circuits should be so chosen as to ensure the required shape of the current curve, particularly during the commutation process. In the circuit of the testing current a half-wave rectification may also be used (Fig. 10), which makes this part of the installation somewhat cheaper. For full-wave and multiphase rectification the shape of the current curve in the rectifier on test is well reproduced in Fig. 11b. For half-wave rectification the correct reproduction of the conditions

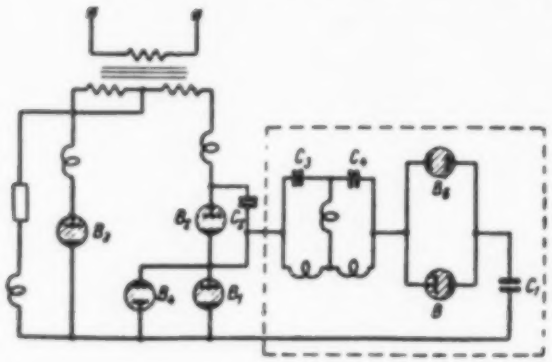

FIG. 8 Full-wave network for the testing of ionic rectifiers.

of operation under natural conditions is impossible (Fig. 11a). By a proper choice of the inductance and total voltage in the commutation circuit (voltages across arcs of rectifiers B_1, B_2, B_3), we may even in this arrangement reproduce correctly the shape of the current curve during the commutation process, but we cannot achieve this during the whole time of arcing.

It is necessary to point out that the major part of the installation cost is the cost of the high voltage circuit, therefore, a certain increase in the cost of the low voltage circuit does not substantially increase the price of the whole testing installation.

The recovery voltage appears as a reverse for the rectifier on test and direct for the protective rectifier. The peak inverse anode voltage, as a rule, recovers more quickly than the direct strength. Therefore, in testing rectifiers it is necessary to use this network by connecting the high voltage circuit before the current in the rectifier on test dies out and with the subsequent recharging of the capacitance C_1, because in this case the current in the protective rectifier stops flowing earlier than in the rectifier on test.

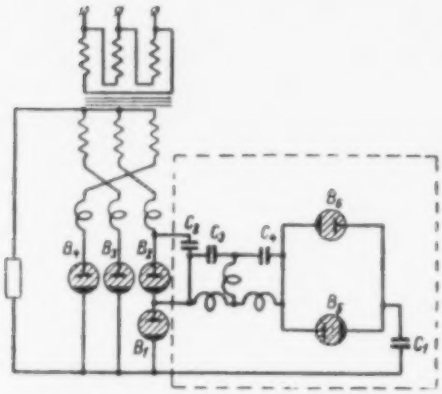

FIG. 9 Multiphase network for testing ionic rectifiers.

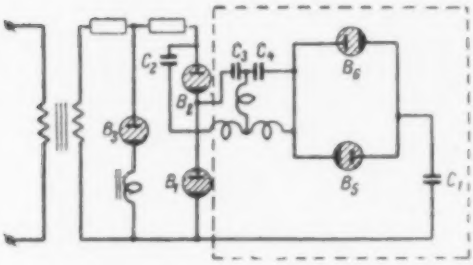

FIG. 10 Half-wave network for testing ionic rectifiers.

For the operation of a rectifier in the usual multiphase conversion network the inductance of the commutation circuit differs from the inductance of the recovery voltage circuit, which is also under the influence of the third phase of the transformer, this phase being connected during the process of the voltage recovery with the rectifier through the capacitances of the network [1]. By connecting into the network of the high voltage circuit an inductance, equal to the phase inductance, we obtain a network, which fully reproduces the real conditions of rectifier operation.

The overwhelming majority of rectifiers normally operate at small ignition angles (large commutation angles) and a peak of reverse voltage not greater than 50-60 per cent of its amplitude value. Since the arc extinction in rectifiers occurs periodically 50 times per second, therefore, for normal operation a rectifier should have a great reserve in arc extinction capacity. Because of that the inductance of the high voltage circuit may be chosen a little smaller than the inductance of the real network, allowing at the same time a somewhat increased rate of change of the

current in the circuit. In this case we may tolerate a certain increase in the angle of advance in the arc extinction in the auxiliary rectifier at the expense of an increase of a few per cent in the rate of change of the current near to its zero value. Under these conditions the capacitance C_1 may be of a moderate value for a sufficiently accurate reproduction of the rectifier operation under normal conditions.

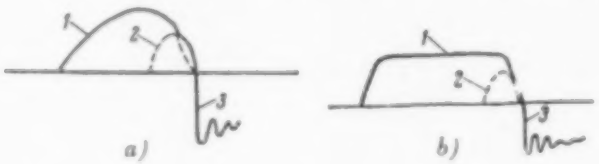

FIG.11 Current in the rectifier on test and its recovery voltage 1 - current of the low voltage circuit; 2 - current of the high voltage circuit; 3 - recovery voltage in the extinguished rectifier.

Insofar as the majority of rectifiers, and particularly high voltage power rectifiers, operate very seldom at large ignition angles and, so in these working conditions we may tolerate a certain distortion of the shape of the current curve, and during tests we may shift the moment of connecting the high voltage circuit. This enables us to ensure the necessary time of advance in the arc extinction in the auxiliary rectifier without increasing the capacitance C_1. Obviously in this case there will be no exact reproduction of conditions of the rectifier operation. The further slow increase in voltage in the rectifier (after a jump) may be ensured by a low power auxiliary transformer. When it is necessary to test a rectifier in reproducing exactly the shape of the current curve for operation at a large ignition angle, then the voltage jump, and consequently, the voltage across capacitance C_1 increases 1.7-2 times, and the cost of the capacitance C_1 increases 3-4 times. Moreover, to ensure the reliable operation of the protective rectifier B_1, for the increased rate of change of the current and under conditions without distortion in the shape of the current curve during the commutation process, it may be necessary to increase the capacitance C_1. Thus, to ensure entirely accurate testing of rectifiers for large ignition angles as well, it may be necessary to increase several times the cost of the installation this cost for high power being mainly determined by the cost of the capacitance C_1.

The addition into the network of the rectifier B_4 (Fig.8) ensures a considerable decrease in the value of the capacitance C_1, and consequently reduces the cost of the whole installation for a given advance in the arc extinction in the protective rectifier. The presence of the rectifier B_4 enables us to eliminate the influence of the current of the high voltage circuit on the shape of the curve of the current, which flows through the rectifier on test during the process of commutation, since, from the moment, when the value of the current of the high voltage circuit exceeds the instantaneous value of the low voltage circuit Fig. 11, a part of the current

$i_2 - i_1$ may flow through the rectifier B_4.

Because of this the choice of the inductance of the high voltage circuit is determined solely by the conditions of reproduction of the process of the recovery of the voltage.

As a result, the time of advance of the arc extinction in the protective rectifier B_1, when the auxiliary rectifier B_4 is present, may be more than doubled, the capacitance C_1 remaining unchanged; if, moreover, the advance in the arc extinction in the protective rectifier is kept unchanged, this capacitance may be decreased several times. For the rectifier B_4 a low power full voltage rectifier may be used, since only a small current $i_2 - i_1$ flows through it during a short time $t_3 - t_2$ (Fig. 11). For a sufficiently large value of the capacitance C_1, in a network with an auxiliary rectifier B_4, we may obtain an arbitary advance in the arc extinction in the rectifier B_1. In this case no distortion of the current flowing through the rectifier on test occurs [7].

Translated by S. Szymanski

REFERENCES

1. M.M. Akodis; *Elektrichestvo* No. 6 (1950).
2. M.M. Akodis; *Elektrichestvo* No. 5 (1953).
3. M.M. Akodis; *Elektrichestvo* No. 5 (1940).
4. M.M. Akodis; *Elektrichestvo* No. 12 (1939).
5. I. Biermans; The circuit for the testing of high voltage circuit breakers with very high rupturing capacity. *Report No. 102 of the session of the CIGRE* (1954).
6. M.M. Akodis, M.V. Bril', V.M. Rudnyi and Kh. P. Khirvonen; *Elektrichestvo* No. 7 (1954).

1959

INCREASE OF STABILITY OF A WELDING A.C. ARC *

O.G. VEGNER

Leningrad

(Received 24 September 1957)

When alternating current in a welding arc passes through a zero value the arc is extinguished and a partial deionization of the arc gap occurs. In welding a.c. installations the necessary conditions of arc restriking are ensured by the presence in the welding circuit of a reactor, due to which a phase shift of 60° and more is produced in the current and voltage in the secondary winding of the feeding transformer. Thus the moment, when current passes through its zero value, corresponds to the moment, when the instantaneous value of the secondary voltage equals to 80-90 per cent of its amplitude value. The welding reactors are usually made with an air gap in the magnetic circuit in order to avoid a certain distortion in the shape of the current curve in networks with closed magnetic circuits; this distortion manifests itself as a delay of current in passing through zero, or almost zero.

An open welding arc in air and in a medium of inert gases is very sensitive to such a shape distortion of the current curve and reacts with a sharp decrease in arcing stability. The welding arc under the flux coating is less sensitive to unfavourable distortions in the shape of current curve, but even in this case they are undesirable. The a.c. arc stability is poorer than the stability of the d.c. arc, particularly within the range of low welding currents. Nevertheless, many important branches of welding operations require the use of a.c. feeding sources, that will ensure the arc stability within a wide range of variation of welding currents, including the smallest values: 20–30 A. One of these branches is welding of aluminium in argon.

One of the main causes of the relative instability of an a.c. arc is an insufficient rate of passing of current through the zero value for sinuisoidal law of variation; this rate is still smaller for frequent distortions, which are due to the variation in the permeability of the magnetic paths of chokes, magnetic shunts and other elements, through which magnetic fluxes pass, determining the values of inductances connected in a welding circuit.

* *Elektrichestvo* No. 5, 67-70.

One of the possible ways of increasing the rate of passing of the current through zero is to increase the frequency, e.g. up to 400–500 c/s (in high-frequency welding generators). A disadvantage of this solution is the great influence of the inductance of the circuit, consisting of welding leads, and this requires the use of special conductors and rotary convertors with small power factors.

The author has found another solution in designing a static device, which ensures such a change in the current curve, that a sufficiently fast rate of passing through zero is produced. To obtain a rectangular, and in practice a trapezoidal shape of the current curve, it would be sufficient to introduce into the current circuit a reactor with a variable coefficient of self-inductance (L): very small for small current values and sharply increasing when the current reaches certain specified values.

As a reactor with an automatic variation of the coefficient of self-inductance, a saturation choke with a magnetic path, made of steel of a high permeability for a small m.m.f. and with a sharp inflection point in the magnetizing curve at saturation may be used. Such a saturation choke should be set in conditions of "forced superposed magnetization", when in the circuit of the control winding currents of higher harmonics are suppressed.

1959

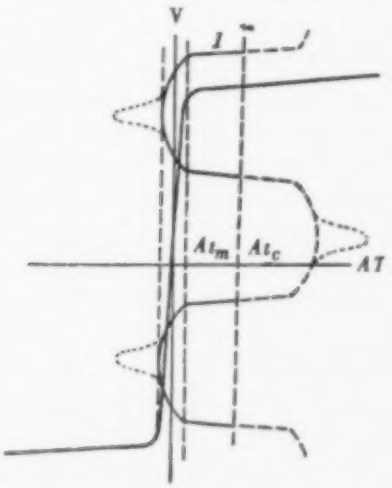

FIG. 1. Obtaining of an a.c. curve with accelerated passing through zero.

Fig. 1 shows a magnetizing curve for the steel for a magnetic path of a choke; this curve has a sharp inflection point at saturation. The control winding produces a m.m.f. At_c. The line (t), passing through the point corresponding to the m.m.f. At_c, is used as a time axis in plotting the curve of the current flowing

through the choke. It is assumed that the choke is made symmetrically; i.e. with two a.c. windings situated on separated bars of the magnetic circuit magnetized by d.c.

So long as the ampere-turns produced by the a.c. winding (At) are less than the difference $At_c - At_m$ (Fig. 1), the effective coefficient of self-inductance of the choke is comparatively small (the core is saturated) and the rate of change of current is high, but when $AT_c + At_m > At_p > At_c - At_m$, the rate of change of current is low, (the core is not saturated).

If $At_p > At_c + At_m$ then "the working point", that determines the magnetic state of the magnetic circuit of the choke, once more moves to a portion of the gentle slope of the lower branch (Fig.1) of the magnetizing curve; i.e. in the region of saturation. This manifests itself by the appearance of peaks in the current curve as shown in Fig. 1 by dotted lines.

From the above approximate and simplified discussion of the conditions of flow of the current in the choke windings, we may draw the conclusion that, in order to increase the rate of passing of the current through zero we should try to achieve the following conditions:

(a) Saturation of the magnetic circuit by the flux of the control winding should be as complete as possible; i.e. the slope of the portion of the magnetizing curve, which corresponds to the m.m.f. At_c, should be very small. From this it follows that the magnetic circuit of the choke should be made from a special steel; the following cold-rolled steels (marks in order of preference) may be used: E370, E330, E320, E310.

Experiments have shown that quite satisfactory results in obtaining a required shape of the curve of the welding circuit were obtained even without a special thermal treatment of the steel, after cutting and punching.

For a ratio of the height of the hole in the core to its width greater than two we may use the so-called wasteless punching of the core sheets, when its two legs and one yoke may be oriented along the direction of rolling of sheets, and only one yoke, which is cut together with legs, is orientated across the direction of rolling.

(b) The leakage inductance of welding transformer and of the saturation choke, which is due to magnetic fields closing through air, should be reduced to a minimum, and this should be accounted for in designing them.

It is desirable to have a welding transformer of a shell type, and the a.c. windings of the choke in a single-layer, with the smallest possible number of turns with increasing transverse dimensions of the core. Thus, in the total weight of active materials of the transformer and choke, the weight of steel should be proportionally greater, than is the case in usual welding installations.

(c) The magnitude of currents of higher harmonics, induced in the control winding of the choke, should be reduced to a minimum, by increasing, for example,

the inductance of the control circuit.

The appearance of an a.c. component of control current leads to such a situation that at the moment, when the current in the operating windings passes through zero, the current in the control winding has a much smaller value, than that, which it would have had in the absence of current in the operating windings.

A partial "demagnetization" of the choke magnetic circuit occurs at the moment, when we would like it to have its maximum saturation in order to decrease its inductance and to increase the rate at which it passes through zero.

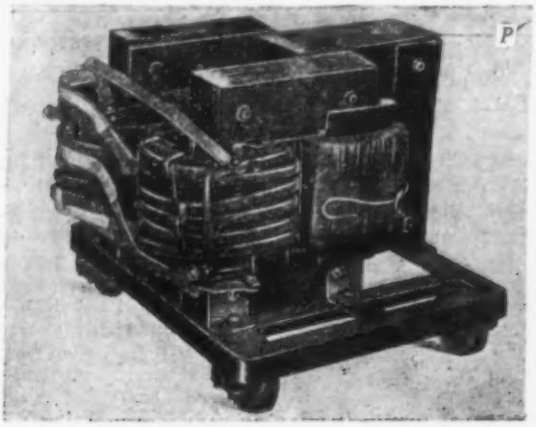

FIG. 2. A saturation choke with additional leakage stamping a/s *P*, linked with the control winding.

The author has proposed the choke design shown in Fig. 2 . It is distinguished in that the control winding surrounds not only the two cores with a.c. windings, but also an additional core, "leakage stampings" with a small air gap, which serves to increase the leakage inductance of the control winding.

A further development of this construction is the addition of an auxiliary winding, which is situated on the second, free bar of the leakage stampings and is connected in series with the control winding.

This auxiliary winding increases still more the leakage flux and the inductance of the control winding. For a relative increase of the electric strength of this arrangement it is advisable to divide the control winding and the auxiliary winding into a few sections and to connect them in pairs in series, i.e. a section of the control winding with a section of the auxiliary winding, then with the next section of the control winding and so. Then in the circuit of the control winding no voltage will appear higher than that in one of its sections.

The following design of the choke is also possible: the control winding is designed to carry a comparatively high current, but with a correspondingly reduced number of turns. The feeding of this winding may be realized by means of semi-

conductors, preferably germanium rectifiers. The suppression of higher harmonics in the control current may be done in this case by connecting into the circuit of the control winding an external choke of a sufficient inductance. Because of the small number of turns in the control winding its voltage cannot assume dangerous values.

Some results of experimental tests of saturation chokes, that ensure a quick passing of current through zero are considered below.

Fig.3a, shows an oscillogram of the current $I = 84$ A in a circuit comprising a transformer type STE-34 with the no-load voltage 60V, a choke, constructed according to Fig. 2 with a core made of cold rolled steel mark E 310, and a ballast rheostat with a voltage drop across it of $U = 18$V. The control current was equal to 0.52 A. The air gap in the magnetic circuit of the leakage stampings of the control winding was 2 mm.

The third curve in this oscillogram (not counting curves I and i_c) is the curve of the rate of change of current dI/dt. It was obtained by recording an oscillogram of the e.m.f. of the secondary winding of an instrument current transformer with an open, and, consequently, quite unsaturated magnetic circuit.

As can be seen from the oscillogram, a quite definite increase of the rate of passing of current through zero is obtained. The curve dI/dt shows the peaks at the moments when the current passes through zero. The current curve has a characteristic shape. Fig. 3b shows oscillograms of the same quantities recorded under similar conditions but for an increased gap in the magnetic circuit in the leakage stampings of the control winding; namely of from 2 to 65 mm.

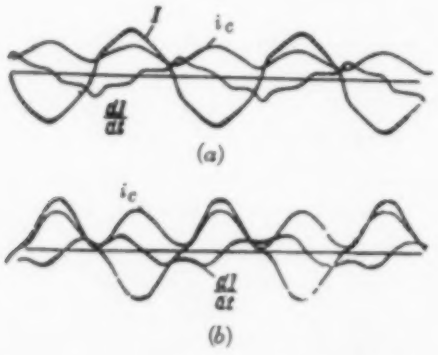

FIG. 3. Curves of the current flowing through the choke (I), of the control winding current (i_c) and of the rate of change of current dI/dt for a small gap in the leakage stampings of the control winding (curves a) and for a large gap (curves b).

The shape of curves is sharply altered: the a.c. component of the control current has so increased that at the moment of the passing of the current I through zero the instantaneous value of the magnetizing current (i_c) drops almost

to zero. The curve of the current I shows the usual distortion with delayed transition through zero. In the curve dI/dt at the moment $I = 0$ instead of peaks, which occurred in the case of a small air gap in the magnetic circuit of the leakage, troughs are present.

Further, tests were carried out in welding by chalk electrodes of 3 mm diameter for currents 120-130 A, using both a saturation choke and a choke with an air gap, type RSTE-34, of lowered voltage of no-load run of 38 V. Fig. 4 shows corresponding oscillograms.

We may note the following circumstances:

1. By using a choke type RSTE-34 and for welding at a lower voltage we have to maintain a shorter arc, than for welding by using a special saturation choke at the same voltage.

2. For the voltage of no-load run $U_0 = 38$ V welding under these conditions becomes practically impossible when using choke type RSTE-34 due to breaks of the arc even for a very small increase in its length.

3. The use of a special choke makes welding quite possible under the same conditions.

It is necessary to keep in mind that the scales of I, U, dI/dt are everywhere the same. The rate of passing of the current through zero at moments, when the voltage across the arc changes its polarity, is 2.5-3 times greater, when using the special choke, then when using the choke of the ordinary type RSTE-34. The use of the choke of the above special design proved particularly effective in an argon arc installation with a non-fusible electrode with a pulse thyratron stabilizer; this installation was designed in the VNIIESO. The improved shape of the current curve and a steeper slope of the operational portion of external characteristics allowed a quite stable process of welding with no-load running at 60V and a current of 25-30A. The accelerated passing of current through zero enables the effective use of a current pulse of very short duration produced by the thyratron stabilizer; to achieve this would be difficult when welding at low currents using an ordinary choke, which gives a nearly sinusoidal shape of the current curve. In the last case it was impossible to achieve a stable welding process with currents smaller than 50 A.

Thus,an advantage of the proposed system for a welding installation manifests itself mainly in welding with small currents. Consequently we have to expect that the main practical application of this installation will be welding with small currents in a medium of inert gases, when special conditions for a welding installation are demanded concerning the arc stability.

A disadvantage of a choke of this type is the increased expense of active materials. Nevertheless, the weight and the price of the feeding source for the arc welding are not the only important criteria, which determine its quality; the welding and exploitation properties, which affect the productivity of the welder, are more important criteria.

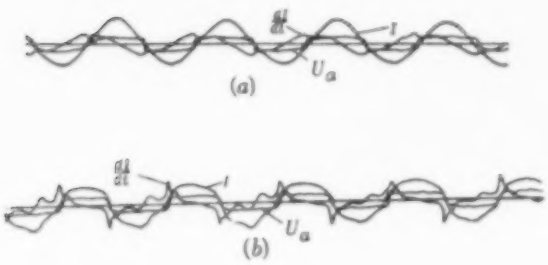

FIG. 4. Welding oscillograms for no-load running at 38 V, current 125-130A, voltage across the arc 18-20 V. Chalk electrodes of 3 mm diameter.
Curves a – when choke RSTE-34 was used;
b – when a special saturation choke was used.

The increase in the arcing stability, particularly for small currents and for such processes as the welding of aluminium, will contribute to the development of the technological uses of welding installations and to the increase in the productivity of welders work. The increased expenditure on active materials in the choke of the new construction may be justified in view of the above discussion.

Translated by S. Szymanski

PHYSICAL PROCESSES IN ELECTRICAL CERAMICS AND RATIONAL METHODS OF DEVELOPMENT *

N.P. BOGORODITSKII and I.D. FRIBERG

Leningrad

(Received 25 September 1957)

Electro-technical ceramics comprises very varied kinds of electro-technical materials: insulating, semiconductor, and magnetic materials. Common features of all ceramic materials are: the process of sintering in producing objects, and the same type of chemical bond, namely an ionic structure of crystals which form a crystalline phase of ceramics.

The division of electro-technical ceramics into three categories is not based on the physical nature of current carriers or on polarization. Technical characteristics of a material, and in the first place its conduction, serve as a criterion of classification. Many kinds of insulation ceramics with good electrical properties possess electronic conduction. Due to this physical property these materials should be classified as semiconductor . However, a sharp distinction between the insulating and semiconductor ceramics cannot be found by considering their properties, because physical processes in them often are the same.

Table 1 shows the principal categories and types of electro-technical ceramics. Later, we shall discuss the principal properties only of insulating ceramics.

Work performed during recent years has enabled us to determine the electrical properties of the most important crystalline substances which are used in modern electro-technical ceramics. From Table 2 it is seen that crystalline substances may be divided into three types on the basis of a particular way of packing the ions in the lattice [1].

The majority of compounds are characterized by close packing of the ions in the lattice and by electronic conduction. At the same time these crystalline formations are distinguished by the energy spectrum of the "forbidden" zone. The narrower the band of the forbidden zone, the greater is the influence of impurities on the electrical properties and crystalline structure, sometimes leading to their catastrophic deterioration.

* *Elektrichestvo*, No. 5, 72-78, 1958.

TABLE 1. Principal classes of electro-technical ceramics.

Category	Class of ceramic materials according to their use	Characteristic properties	Appellation of the ceramic material
Electric insulation ceramics	Ceramics for components of installations and capacitors of small capacity	Rather small permittivity ($\varepsilon < 10$)	Steatite, ultra-porcelain*, celsan ceramics, corpndum mullite, radio-porcelain*
	Capacitor ceramics for:	High value of permittivity ($\varepsilon > 10$)	
	High-frequency circuits, including thermo-compensating and separate capacitors	High value of ϵ negative value of TC ϵ	Rutile (T_i-cond T-80) ** Perovskite (T-150)
	High-frequency thermostable capacitors	Low value of TC ϵ	Titanium-zirconium (T-40, T-20)
	Low-frequency capacitors	Very high permittivity	Strontium-bismuth titanate (S.B.T.)
	Porous ceramics for:	Insulation at high temperatures	
	Insulators for electron tubes	Low value of tan δ	Porous corundum and steatite ceramics
	Bases of wire resistors	High thermal stability	Chamotte, alundum, cordierite ceramics
	Rochelle salt and piezoceramics for:	Presence of dielectric hysteresis	
	Low-frequency capacitors	Ultra-high permittivity	
	Piezo-elements	High value of piezo-electric modulus	SM-1, T-7500, T-1700, (Variconds***) Solid solutions of titanates, zirconates, stannates
	Non-linear elements	Sharp dependence of permittivity on field intensity	
Semiconductor ceramics	Semiconductor ceramics for:	High electronic conduction	
	High power radio resistors, waveguide loads, high temperature heaters	Little dependence of resistance on temperature and voltage	Ceramics on the silicon carbide base, and also containing graphite (silit† Reraks).
	Non-linear elements	Strong dependence of resistance on voltage	Ceramics with a silicon carbide base (vilit, †† NPS)
	Thermo-resistors	Strong dependence of resistance on voltage	Ceramics based on copper and cobalt-manganese reverse spinels
Magnetic ceramics	Magnetic ceramics:	High permeability with high resistivity	
	Magnetic-soft	Low value of coercive force	Nickel-zinc, manganese-zinc, magnesium and other ferrites

TABLE 1. Principal classes of electro-technical ceramics *(continued)*

Category		
Magnetic ceramics	Magnetic hard	High value of coercive force	Barium ferrites

EDITOR'S NOTES:

* Basic porcelain with barium oxide and alkali glass.

** An abbreviation for "titanium condenser".

*** An abbreviation for "variable condenser".

† *Silit* : Semiconductor heater element; a ceramic material based on heat-resistant carborundum SiC with the addition of pure silicon and carbon. Withstands temperatures up to 1500°C in electric furnaces; used for 220 V and 20 A.

†† *Vilit* : Non-linear resistances, ceramic material based on carborundum, consists of SiC with the addition of clay and carbon (graphite).

For further details see B. M. Tareev; *Elektrotekhnicheskie Materialy*, Gosenergoizdat (1955).

In our previous works mullite was included in the group of materials characterized by increased dielectric losses. Kirillova's investigations [2] have shown that an absolutely pure mullite, obtained artificially from the purest components, is characterized by high electrical properties and has its ions closely packed. Thus, it was made clear that the increased dielectric losses in mullite, which were observed earlier, are due to the presence in it of normal alkaline impurities, which contribute to the formation of alkaline aluminosilicate glass. According to the data given by Odelevska and Verebyeichik [3] this glass is distinguished by its high dielectric losses.

Cordierite and beryl are characterized by an open structure, and due to this both its own ions and those of the impurity can participate in conduction and relaxation polarization.

In experimental investigations into the conduction of ceramics we often observe a decrease in current with time, even in those cases when the applied voltage and temperature remain strictly constant. Previously the current-time relationship was expressed by the formula

$$i_\tau = \frac{U - P_\tau}{r},$$

where i_τ is the current at time τ after application of voltage to the specimen;

U is the applied voltage;

P_τ is the "inverse e.m.f. of polarization";

r is a conventional real impedance.

The expression given above was based on the assumption that in dielectrics as well as in metals volume resistance should be independent of time. Therefore,

TABLE 2. Classification of crystalline phases of electro-technical ceramics

Type of the crystalline phase	Character of ion packing; peculiarity of the atomic bond	Name of the material	Chemical formula	Character of electric conduction	Refractive index	tan δ at radio frequencies	Volume resistance (Ω cm)
						$t = 20^{\circ}C$	
I. Crystals: dielectrics with a small refractive index	Open structure (non-corresponding to conditions of a close packing, large anion numbers for small cation charges)	Cordierite Beryl β – aluminium	$2MgO.2Al_2O_3.5SiO_2$ $Al_2O_3.3BeO.6SiO_2$ $Na_2O.11Al_2O_3$	Appreciable ionic conduction	1.537 1.560 1.668	} ≤ 0.01	} $10^{13}...10^{14}$
	Close packing	Wollastonite Clinoenstatite Mullite	$CaSiO_3$ $MgSiO_3$ $3Al_2O_3.2SiO_2$		1.631 1.655 1.648	} ≤ 0.0005	} $\sim 10^{13}$
II. Crystals: dielectrics with medium and high refractive index	High transition energy of a cation into another valency state	Periclase Spinel Corundum	MgO $MgAl_2O_4$ Al_2O_3	Appreciable or high ionic conduction	1.736 1.718 1.768	} ≤ 0.0003	} $\sim 10^{13}$
	Small transition energy of a cation into another valency state	Rutile – Type of wurzite	TiO_2 Nb_2O_5 ZnO		2.616 – 2.004	} Sharp dependence on impurities	} $10^{6}...10^{14}$
III. Crystals: Rochelle salt type	Blast furnace * structure	Type of perovskite Type of perovskite Type of pyrochlore	$BaTiO_3$ $KTaO_3$ $Cd_2Nb_2O_7$	Electronic conduction	2.40 – –	} ≤ 0.01	} $10^{13}...10^{14}$

* *EDITOR'S NOTE:* Blast-furnace possibly refers to the shape of the crystal structure.

in order to avoid such a dependence, the "real impedance" was related not to the total thickness of the specimen, but only to a certain portion of it (after deduction for a thin layer of the high resistance).

In actual conditions, an initially homogeneous dielectric, due to the redistribution of electric charges at a constant voltage, is transformed into a two-layer or three-layer one, with different resistances of layer insulation. However, it is hardly expedient to consider the resistance of the insulation of these layers separately.

The real impedance of a specimen of dielectric, which determines the magnitude of the true current after the completion of electronic and ionic polarization, may be calculated by the formula

$$r_{thr} = \frac{U}{I - \Sigma I_p},$$

where ΣI_p is the sum of the currents for a retarded polarization.

In view of the fact that the determination of the polarization currents presents considerable difficulties, the resistance is in practice calculated regardless of these currents, as a quotient of the voltage divided by the current, which is measured a long time after the application of the voltage when we can neglect the polarization currents.

1959

It is possible to indicate five mechanisms of the through conduction of the ionic dielectrics, including electrical ceramics:

(1) Cation-cution conduction. The ions of one sign are mobile, namely cations. They are deposited at the cathode, are neutralized and become atoms of the substance(sometimes dendrites). However, it is possible, when the anode is made of a metal such as silver, that its ions diffuse into the dielectrics and replace the dielectric cations, which are transformed into atoms. In their turn silver ions in many cases participate in through-conduction and are also neutralized at the cathode, being simultaneously replaced by ions from the electrode.

(2) Electronic-cation conduction. Ions of one sign are mobile, namely cations, and these are separated from the electrode (anode). At the cathode the electron in its turn enters the dielectric and reforms its cation. This mechanism takes place in dielectrics with cations of a variable valency. Thus, for instance, in ceramics containing titanium, along with a purely electronic current, a process of electric reduction of titanium dioxide takes place according to the reaction

$$Ti^{+4} \rightarrow Ti^{+3} + Ag^{+1}$$

first of all silver ions migrate along the surface and imperfections of the ceramics.

(3) Electronic-anion conduction. Ions of one sign are mobile, namely anions. They are deposited on the anode, are neutralized and become atoms of the substance. However, this can occur when electrons from the cathode enter the dielectric, thus leading to the formation of F-type centres. For example, in the

ceramics containing titanium, along with the purely electronic current, the process of electric reduction of titanium dioxide occurs according to the reaction

$$Ti^{+4} + \bar{e} \rightarrow Ti^{+3}$$

(4) Cation-anion conduction. Both positive and negative ions are mobile. They are deposited on the cathode and anode respectively, are neutralized and become atoms of the substance.

(5) Purely electronic conduction. This kind of conduction is characteristic for a series of oxides of high-valency metals.

The types of conduction discussed above are often superimposed one on another. Let us remark that ionic conduction necessarily brings about irreversible changes in the substance.

In certain types of ceramics, for example in rutile, perovskite and others, ionic conduction is negligibly small in comparison with the electronic one; nevertheless it is sufficiently high, so that after a certain time, at an increased temperature and with silver electrodes, electro-chemical "ageing" of the material takes place. Electro-chemical ageing is an irreversible change in the electrical properties at a certain intensity of a constant field, which depends on the operational temperature.

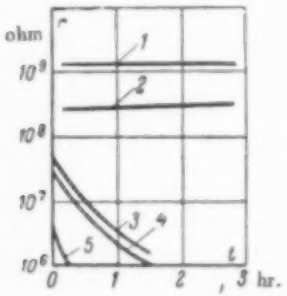

FIG. 1. Insulation resistance of disk capacitors with silver electrodes as a function of the time of application of direct voltage. θ = 400°C; U = 1000 V; thickness of the capacitor plate 0.7 mm.

(1) zirconnate ceramics; (2) stannate ceramics; (3) calcium titanate; (4) nickel titanate; (5) rutile ceramics.

As a result of the progressive decrease of the insulation resistance at increased temperatures tan δ in the ceramic material increases and breakdown occurs. The electro-chemical ageing of ceramics containing titanium is explained by the processes of reduction of titanium dioxide to the lower oxidation state under the influence of the electric field, due to the polyvalency of titanium. The electro-chemical ageing of aluminosilicate ceramics, porcelain, steatite and others possessing high ionic conduction, at increased temperatures and when silver electrodes are used, is due to the formation of dendrites, particularly of silver.

Fig. 1. shows how the resistance of the ceramics containing titanium for capacitors and certain new types of capacitor ceramics depends on the time of voltage application. From these graphs it follows that materials containing free

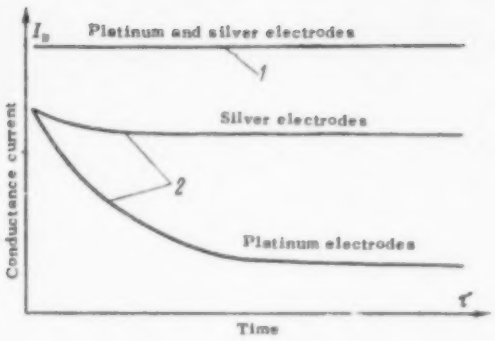

FIG. 2. Conduction current as a function of time for a constant voltage. (1) electronic conduction; (2) ionic conduction.

titanium dioxide, for example the rutile ceramics, are particularly unsuitable for use at increased temperatures. Ceramics based on chemical compounds of titanium dioxide exhibit slightly better characteristics. From this point of view, the titaniumless ceramics (e.g. zirconnate, stannate) represent another class of materials, in which the process of electro-chemical ageing is much less pronounced.

The nature of electric conduction of ceramic materials – whether electronic or ionic – has been usually determined for many years by the "Tuband" method, which requires weighing of the tested specimen and electrodes. This method is sufficiently complicated: our investigations have shown that the character of the electric conduction of ceramics can be determined much more simply by comparing experimentally-obtained relationships between current and time, when using silver, platinum or gold electrodes. This method is based on the fact that, with silver electrodes, the diffusion of silver into ceramics is observed, whereas with platinum electrodes this phenomenon is almost completely absent. Ionic conduction is present if, in the case of platinum electrodes, the current sharply drops with time; and in the case of silver electrodes, when the mechanism of electric conduction corresponds to points 1 and 2 of the above classification, the absorption is almost undetectable. The constancy of current with time with platinum and silver electrodes permits the conclusion that a purely electronic conduction is present.

Fig. 2 shows the character of the dependence of the conductance current on time at a constant voltage for ceramics with electronic and ionic conduction.

This relationship has been observed by Plashchinski on a number of ceramic materials.

The most important property of insulation ceramics is dielectric losses. We can subdivide them into three groups: losses due to polarization, losses due to the through conduction and losses caused by a heterogeneous structure.

Losses due to polarization are most important; they characterize the physical nature of the material. They may be of three kinds: of the ionic-and electronic-relaxation type, losses due to spontaneous polarization and losses at resonance

TABLE 3. Classification of dielectric losses in electro-ceramics

Basic mechanism of losses	Kind of losses	Conditions under which this kind of loss occurs
I. Dielectric losses in polarization	Ionic relaxation	1. In crystal: individual chemical compounds with an open lattice (cordierite, beryl) 2. In crystal, solid solutions of subtraction type (oxide systems $MgO-ZrO_2$; $CaO-ZrO_2$), solid solutions of the addition type, ($Si^{+4} = Al^{+3} + R^{+1}$) and in solid solutions in a state of breakdown. 3. In a vitreous phase, particularly in the presence of alkaline oxides and in the absence of alkali-earth oxides of a large ionic radius.
	Electronic relaxation	In crystals: electronic semiconductors with a disturbance of the stoichiometric composition (TiO_2, ZnO, Nb_2O5)
	Spontaneous polarization.	In crystals: of the Rochelle salt type, at temperatures below Curie-point ($BaTiO_3$, $PbTi_3O_3$, $NaNbO_3$)
	Resonance	In crystal and glasses at frequencies above 10^{10} c/s.
II. Dielectric losses due to through conduction	Losses due to the surface conduction	Contaminated surface of the object, high air humidity
	Losses due to volume conduction	High temperature of heating of the substance, capillary hygroscopicity
III. Dielectric losses due to heterogeneous structure	Ionization losses in the substance volume	In presence of enclosed porosity and at high field intensities
	Losses due to polarization and the through conduction owing to impurities	Presence of the adsorbed and absorbed humidity at open porosity, presence of semi-conducting impurities and others

in the region of ultra-high frequencies.

Fig. 3 shows the permittivity and the dielectric power factor as functions of frequency for relaxation and resonance losses according to data given by Birks [4].

The dependence of tan δ on temperature for a great majority of electro-ceramic materials is expressed by an exponential function.

TABLE 4. Permittivity temperature coefficient of crystalline compounds which are used as components of electro-technical ceramics for capacitors.

Group	Name of the compound	Chemical formula	Permittivity	Permittivity temperature coefficient, within the temperature range		Type of structure
				from – 60°C to + 20°C	from + 20°C to + 80°C	
I. Positive TCϵ	Calcium Stannate	$CaOSnO_2$	16	+ 100	+ 115	Perovskite
	Magnesium orthotitanate	$2MgOTiO_2$	16	– 10	+ 40	Spinel
	Zinc orthotitanate	$2ZnOTiO_2$	16	+ 170	+ 180	Spinel
	Nickel titanate	$NiOTiO_2$	18	+ 40	+ 70	Ilmenite
	Calcium zirconate	$CaOZrO_2$	28	+ 50	+ 65	Perovskite
	Strontium	$SrOZrO_2$	30	+ 60	+ 60	Perovskite
II. Negative TCϵ	Barium stannate	$BaOSnO_2$	~ 20	– 80	– 40	Perovskite
	Barium zirconate	$BaOZrO_2$	~ 40	– 900	– 500	Perovskite
	Zirconium titanate	ZrO_2TiO_2	~ 40	– 120	– 90	–
	Barium tetratinate	$BaO4TiO_2$	~ 40	~ 0	~ 0	–
	Titanium dioxide	TiC_2	~ 100	– 1000	– 850	Rutile
	Calcium titanite	$CaOTiO_2$	~ 150	– 2300	– 1500	Perovskite

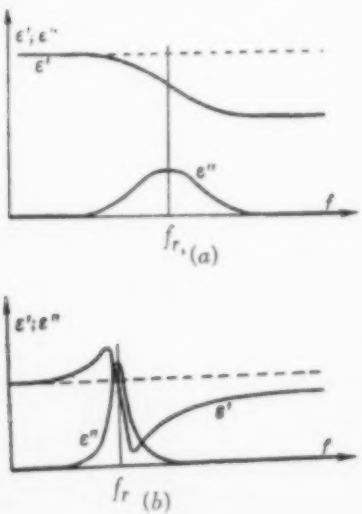

FIG. 3. Permittivity ϵ' and dielectric power factor ϵ'' as functions of temperature. (a) relaxation losses; (b) resonance losses.

TABLE 5. Ceramic materials according to GOST 5458-57.

Type of	Class	Group	Permittivity at + 20° ± 5°C	Temperature coefficient of capacity (degree^{-1} x 10^{-6})	Tangent of the dielectric loss angle, not more than				Volume resistivity (Ω) at temperature + 100± 5, not less than	Electric strength (kV/mm) not less than	Limit strength for static bending (kg/cm^2) not less than	Linear coefficient of expansion (degree^{-1} x 10^{-6}) not more than	Recommended field of application
					at temperature, (°C)			after damping					
					+20± 5	+80± 5	+100±5						
High frequency materials of permittivity more than 12	I	a	130 . . . 190	— (1.300 ± ± 200)	0.0006	0.0008	0.001	0.0008	10^{11}	6	800	12	For circuit and separation capacitors, not affecting frequency stability
		b	65 . . . 100	— (700 ± ± 100)	0.0006	0.0008	0.0012	0.0008	10^{11}	8	800	8	For the circuit, thermo-compensation and separation capacitors
	II	a	31 . . . 50	— (80 ± 30)	0.0006	0.0008	0.0010	0.0008	10^{11}	8	700	8	For capacitors of high stability
		b	17 . . . 30	— (50 ± 20)	0.0006	0.0008	0.0012	0.0008					
	III	—	12 . . . 30	+ (30 ± 20)	0.0006	0.0008	0.0012	0.0008	10^{11}	8	700	8	
High frequency materials of permittivity less than 9	IV	a	Not more than 7.5	+ (110±30)	0.001	0.0012	Not standarized	0.0012	10^{12}	20	1.400	8	For small (a) and large (b) installation components
		b	Not more than 8		0.002	0.003		0.0022	10^{12}	20	1.400	8	
		c	Not more than 7.5	+ (60±20)	0.0006	0.0008		0.0008	10^{12}	20	800	3	For high stability induction coils and high-frequency capacitors

1959

(Continued Table 5.)

	V	–	Not more than 9	+(110±30)	0.0012	0.0018		0.0015	10^{12}	20	2.000	6	For small and medium size components with high mechanical strength and thermostability
	VI	–		Not standarized			0.0012 +300°C	Not standardized	10^{12} (300°C)	Not standarized	600	6	For insulators used inside vacuum apparatus
	VII	–	Not more than 7.5	+(200±100)	0.005	0.007	Not standarized	0.006	10^{11}	18	600	6	For installation components not affecting the apparatus stability
Low frequency materials of permittivity more than 1000	VIII	a	Not less than 2.800	Not standardized	0.04	0.05	Not standarized	0.07	10^{10}	2	500	12	For low frequency and d.c. capacitors
		b	Not more than 2.000	Not standardized	0.04	0.05		0.10	10^{10}	3	500	12	For piezo-electric converters++/and low frequency capacitors
		c	Not more than 1.000	*	0.005	0.005		0.007	10^{11}	6	500	12	For low-frequency and d.c. capacitors

* Variation of permittivity of the materials of the group c, class VIII, within the range from – 60 to + 100°C, should be not more than ± 35 per cent of the permittivity at temperature + 20 ± 5°C.

** For the materials group b, class VIII, in the case when they are used in producing converters, the piezo-electric modulus d_{31} is measures, the value of which should not be less than 1.5×10^{-6}.

However, consider these dielectric losses from the point of view of the relaxation phenomena. The absence of the usual maximum of tan δ as a function of temperature can be explained by the increased number of relaxation ions with increased temperature. This was not taken into account by earlier theories of relaxation losses. On the contrary, in the relationship tan δ-frequency at a constant temperature, when the number of relaxation particles remains constant, a maximum of tan δ is possible at a certain frequency.

Table 3 gives the classification of dielectric losses in electrical engineering ceramics.

It has been said earlier that one of the important groups of insulation ceramics is that used for capacitors. In the construction of capacitors those types of ceramics are mainly used, which have a crystalline phase which exhibits electronic conduction. The high permittivity of these ceramics is explained by the presence of a strong internal electric field.

Table 4 gives characteristics of crystalline structures which are components of the crystalline phase of the capacitor ceramics.

Not long ago production of electro-ceramics materials was based mainly on experimental investigations. Theoretical conceptions have since been accumulated and allow us to establish certain laws on the basis of which electro-chemical ceramics are now developed. However, in spite of the necessity for continuously improving the electrical standards of ceramics, it is also necessary to consider the technological properties of the materials and the costs of production.

In the new specifications, GOST 5458-57, is given a sufficiently comprehensive list of ceramic materials which possess the required electrical properties and which have been tested in production. Table 5 shows the main standards for ceramic materials approved by the GOST 5458-57 specifications.

Translated by S. Szymanski

REFERENCES

1. N.P. Bogoroditskii; Dielektricheskiye poteri v radiokeramike (Dielectric losses in radio ceramics), *Dokl. nauch.-tekh. soveshchaniia po radiokeramike*, Leningrad (1955)
2. G.K. Kirollova; Elektricheskiye svoistvo mullita (Electrical properties of mullite) Zh. tekh. fiz. (1957).
3. V.I. Odelevskii and N.M. Verebyeichik; Relaksatsionnye dielektricheskiye poteri v neorganicheskikh silivatnykh steklakh (Relaxation dielectric losses in inorganic silicate glasses) *Trudy. soveshchaniia po tverdym dielektrikam.* Tomsk (1955).
4. J.B. Birks; Magnetic spectra, *J. Inst. Elect. Engng.* October (1956).

AUTOMATICALLY CONTROLLED SERIES EXCITATION FOR GENERATORS*

G.I. POLIAK

Leningrad

(Received 6 May 1957)

In automatically controlled generator excitation systems used at present, exciters with the shunt and separate excitation are used †. As far as series excitation is concerned, it is naturally useless in its pure form. Nevertheless, if it is used in conjunction with separate excitation or in special circuits, which are discussed below, it can bring about a substantial increase of stability and accuracy of control. Moreover, special circuits are extremely simple and allow us in many cases to dispense with the use of automatic voltage regulators.

Series excitation was very exhaustively investigated in 1934 by N.N. Shchedrin in the Smurov Laboratory [1]. The investigations showed that the series connexion of the series and shunt exciters of a synchronous generator is effective.

In 1943 P.S. Zhdanov [2] proposed a circuit in which the exciter of the synchronous generator is provided with two windings. One of them is series wound. The other is a separate one, fed by the difference of the standard and of the automatically controlled voltage. Such a method of excitation possesses the property of self-regulation and replaces a special automatic voltage regulator.

In 1944-1945, descriptions of electrical machine regulators acting as exciters were published; they were called rototrols. In these devices the control effect is achieved by a proper combination of series and separate excitation windings the exciter, [3-5].

In this article the properties and advantages of series excitation for automatic voltage control are discussed.

Before discussing automatic control with series excitation let us consider a d.c. generator with a direct automatic control according to the voltage deviation.

†Ionic excitation can be considered as separate excitation.

*Elektrichestvo No. 6, 10-15, 1958.

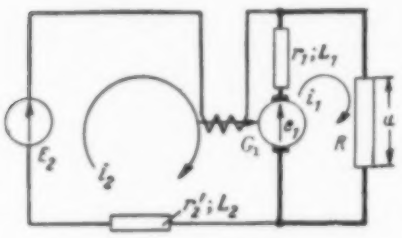

FIG. 1. Circuit of the direct automatic control according to the voltage deviation.

This automatic control circuit is shown in Fig. 1 and is characterized by the following equations (the list of notations is given at the end of this article):

$$\left.\begin{aligned}(r_1+R+pL_1)\,i_1-(r_1+pL_1)\,i_2&=e_1;\\ -(r_1+pL_1)\,i_1+[r_1+r_2'+&\\ +p\,(L_1+L_2)]\,i_2&=E_2-e_1,\end{aligned}\right\} \qquad (1)$$

where $e_1 = c_1 i_1$; c_1 is the coefficient of proportionality;

$$i_1 = \frac{u}{R}.$$

In the case of a non-linear magnetic characteristic of the generator coefficient c_1 is a variable quantity.

For steady-state conditions, the generator voltage found from equation (1) is equal to:

$$u = \frac{(r_1 + c_1)\,E_2}{\dfrac{r_1 r_2'}{R} + r_1 + c_1 + r_2'}. \qquad (2)$$

This expression shows that the generator voltage for constant parameters is determined by the setting voltage E_2 and by the load resistance R.

In this form the control circuit is unsuitable due to high quiescence and the non-linear magnetic characteristic of the generator. However, by assigning to the $r_1 r_2/R$ various appropriate positive and negative values, we may obtain the required static characteristics with a positive or negative quiescence). We may also get an astatic characteristic.

The condition imposed, $r_1 r_2/R \gtrless 0$, can be satisfied, if the co-factors r_1 and r_2' are expressed in the form of differences $r_1 = (r_1' - c_2) \gtrless 0$ or $r_2' = (r_2 - c_3) \gtrless 0$. Obviously coefficients c_2 and c_3 represent negative resistances, which may be produced by connecting into the network of series generators with resistances r_1' and r_2.

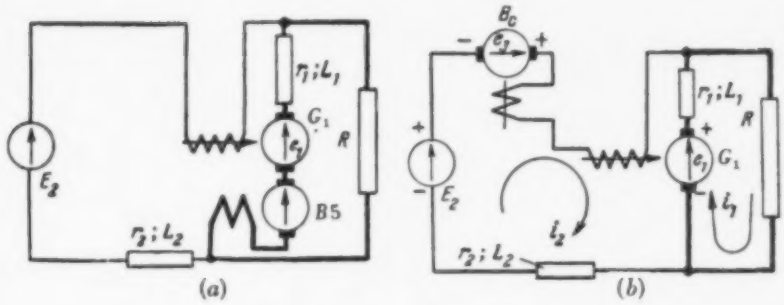

FIG. 2. Circuit of the voltage automatic control with compounding of the load current (a) and of the excitation current (b).

If the series generator B_s is connected into the armature circuit Fig. 2a then compounding of the armature current occurs which is usually performed by a series winding of the generator G_1. We shall not discuss this method of compounding as it is already well known. If a series generator B_s is connected into the excitation circuit, we then get a circuit which can be called by analogy a "circuit with compounding of the field current". This circuit, which will be called henceforth the automatically controlled series excitation circuit, is the subject of the following discussion.

1959

For compounding of the field current, expression (2), after substitution $r_2' = r_2 - c_3$ assumes this form:

$$u = \frac{(r_1 + c_1) E_2}{\frac{r_1 (r_2 - c_3)}{R} + r_1 + c_1 + r_2 - c_3}. \tag{3}$$

Obviously, this expression can also be obtained by solving equations for the network shown in Fig. 2b.

$$\left.\begin{aligned} (r_1 + R + pL_1) i_1 - (r_1 + c_1 + pL_1) i_2 = 0; \\ -(r_1 + pL_1) i_1 + [r_1 + c_1 + r_2 - c_3 + \\ + p(L_1 + L_2)] i_2 = E_2. \end{aligned}\right\} \tag{4}$$

In establishing the equations, we expressed the e.m.f. of the generator and series exciter by means of currents: i.e. it was assumed that:

$$e_1 = c_1 i_2 \text{ and } e_3 = c_3 i_2 .$$

Static properties of this control are determined by a fractional term in the denominator of equation (3).

When $(r_2 - c_3) = 0$ the control becomes astatic. When $(r_2 - c_3) > 0$ the quiescence

control characteristic will be positive, but when $r_2 - c_3 < 0$, it will be negative.

The problem of stability of automatically controlled series excitation can be explained by solving the characteristic equation of the set of equations (4):

$$L_1 L_2 p^2 + [(r_2 - c_3) L_1 + RL_1 + + (r_1 + R) L_2] p + [(r_2 - c_3)(R + r_1) + + R(r_1 + c_1)] = 0. \tag{5}$$

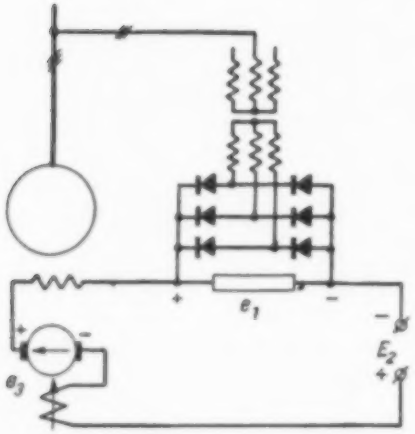

(*a*)

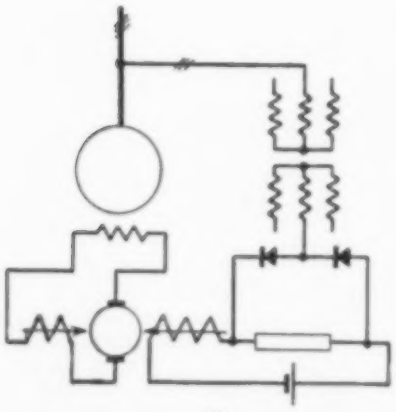

(*b*)

FIG. 3. Circuits of the voltage automatic control with the automatic series excitation.

The control is stable if the coefficients of equation (5) are positive, which is possible if the following conditions are satisfied:

$$\left.\begin{aligned} \frac{RL_1+(r_1+R)L_2}{L_1} &> -(r_2-c_3);\\ \frac{R(r_1+c_1)}{r_1+R} &> (r_2-c_3). \end{aligned}\right\} \tag{6}$$

The analysis of conditions (6) shows that control stability is ensured even for such high values of negative quiescence as are not encountered in practice.

Automatically controlled series excitation of synchronous generators can be realized in the circuit in Fig. 3a. The voltages acting in the excitation circuit are added directly Fig. 3a. Other circuits are also possible in which instead of voltages, magnetic fluxes are added, which are proportional to the voltages, or a combined system can be used with the summation of both voltages and fluxes. As an example of these systems, the circuit proposed by P.S. Zharnov, mentioned above can be given (Fig. 3b).

We shall discuss the automatically controlled series excitation on the example given in [6, p. 310] for a case of ordinary non-inertial control.

Let us write the set of the Gorev-Park equations adding to it the equation which relates the voltage under control e_s to the remaining variables. We neglect in this case the active impedances of the stator circuits.

$$pu_d + u_q + pe_d = e_n \sin\psi; \tag{7a}$$

$$-u_d + pu_q - e_d = -e_n \cos\psi; \tag{7b}$$

$$\mu pu_d + (\rho_r + p)e_d = \rho_r e_r; \tag{7c}$$

$$Kps + u_q e_d = xM_m; \tag{7d}$$

$$(e_d + hu_d)^2 + h^2 u_q^2 = e_s^2. \tag{7e}$$

In the presence of series excitation, the voltage acting in the rotor circuit is equal to:

$$e_r = k_c(E_2 - e_s) + e_c. \tag{8}$$

where k_c – is the regulation factor.

The voltage of the series exciter, when expressed in relative units, can be written in this form:

$$e_c = c_r e_d. \tag{9}$$

Let us assume that the series exciter B_s is not saturated, and, consequently, coefficient C_r, which is equal in relative units to the degree of compensasation of the resistance of the rotor circuit, is constant.

Taking into account (8) and (9) we find that the equation of the rotor circuit (7c) assumes this form:

$$\mu p u_d + (\alpha p_r + p)\, e_d = p_r k_c (E_2 - e_s), \tag{10}$$

Where $\alpha = 1 - c_r$.

Static characteristics of voltage control can be obtained from equations (7) for steady-state conditions:

$$u_q = e_n \sin\theta; \tag{11a}$$

$$u_d + e_d = e_n \cos\theta; \tag{11b}$$

$$\alpha e_d = k_c (E_2 - e_s); \tag{11c}$$

$$(e_d + h u_d)^2 + h^2 u_q^2 = e_s^2. \tag{11d}$$

From equation (11c) we find:

$$e_s = E_2 - \frac{\alpha}{k_c} e_d. \tag{12}$$

From the expression obtained, it follows that when $\alpha = 0$, i.e. in the presence of full compensation of the resistance of the rotor circuit by series excitation, the voltage control is astatic and depends neither on the magnitude and character of the load of a synchonous machine nor on the parameters of the stator circuit.

From (12) it follows further that, for considerable values of the factor k_c the influence of the instability of quantity α, which is possible due to the temperature variation of the field winding resistances, becomes less important.

When $\alpha \neq 0$, it follows from equations (11) that:

$$e_s^2 - 2\,\frac{k_c (1-h)^2 E_2 + \alpha k_c (1-h) e_n \cos\theta}{k_c^2 (1-h)^2 - \alpha^2}\, e + \\ + \frac{[\alpha e_n \cos\theta + k_c (1-h) E_2]^2 + (\alpha h e_n \sin\theta)^2}{k_c^2 (1-h)^2 - \alpha^2} = 0. \tag{13}$$

From the equation obtained, the relationship $e_s = f(\alpha)$ is plotted in Fig. 4 when $\theta = 0$ and $\theta = 90°$. In this case, the normal voltage E_2 was determined from the conditions, that, when $\theta = 0$, the quantity e_s is equal to unity for all values of α. As follows from the graphs, the values of α within the limits of from -0.05 to $+0.1$ are important in practice. For other values of α, the error in control is excessively large, therefore, a special voltage corrector would be required. In plotting the curves shown in Fig. 4, the regulation factor was assumed to be $k_c = 3.5$.

To evaluate the influence of automatically controlled series excitation on static stability, we have to change from equations (7) to equations of small

disturbances, neglecting transients in the stator:

$$\left.\begin{aligned} \Delta u_q - e_n \cos\vartheta_0 \Delta\vartheta = 0; \\ -\Delta u_d - \Delta e_d - e_n \sin\vartheta_0 \Delta\vartheta = 0; \\ \mu p \Delta u_d + (2p_r + p)\Delta e_d - p_r k_c \Delta e_s = 0; \\ e_{d0}\Delta u_q + u_{q0}\Delta e_d + K p^2 \Delta\vartheta = 0; \\ \Delta e_s = -\frac{(e_{d_0} + h u_{d_0})(\Delta e_d + h\Delta u_d) + h^2 u_{q_0}\Delta u_q}{e_{s0}}. \end{aligned}\right\} \quad (14)$$

In the presence of non-inertial voltage control according to the law $\Delta e_r = k\,\Delta e_s$, we have to put in the set of equations (14) $a = 1$ and $k_c = k$.

From the four of the stability conditions given by Hurvitz, which follow from the characteristic equation of the set of equations (14), the dominant condition is:

$$a_3 = p_r e_{d0} e_n \left\{ a\cos\vartheta_0 + \frac{k_c}{e_{s0}}(1-h)[h e_n + \right.$$
$$\left. + (1-h)\, e_{d0}\cos\vartheta_0] \right\} > 0. \quad (15)$$

1959

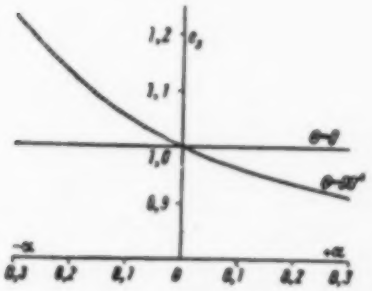

FIG. 4. Accuracy of automatic control as a function of factor a.

Fig. 5 shows curves of relationships for ordinary control ($a = 1$) and automatically controlled series excitation:

$$A_3 = \frac{a_3}{p_r e_{d0} e_n} = a\cos\vartheta_0 + \frac{k_c}{e_{s0}}(1-h)[h e_n +$$
$$+ (1-h)\, e_{d0}\cos\vartheta_0.$$

The example given in [6] is reproduced here as a case of the ordinary control ($a = 1$).

The influence of series excitation on dynamic stability can be estimated by the extent to which the field flux of a synchronous machine can be maintained and even increased in emergency processes.

Since the greatest decrease in flux is possible in the presence of a generator short-circuit, this case of emergency, in analogy to [1], is discussed below.

In investigating series excitation, Shchedrin comes to the conclusion that "the connexion of an unsaturated series exciter in series with a shunt exciter can produce an extremely powerful effect in sustaining the magnetic flux of a synchronous machine. This effect is equivalent to a ten-fold increase in the time constant of the generator excitation circuit" * [1].

Riudenberg also points out the use of series excitation in order to increase stability, [7].

To evaluate the efficiency of automatically controlled series excitation, the variation of the aperiodic component of the excitation current in the presence of the generator short-circuit was investigated [see 1].

Such an analysis permitting a simplification of the problem, is at the same time very instructive since the largest drop in flux is possible at short-circuit. So far as the character of the flux variation is concerned it is represented by the aperiodic component of the synchronous e.m.f.

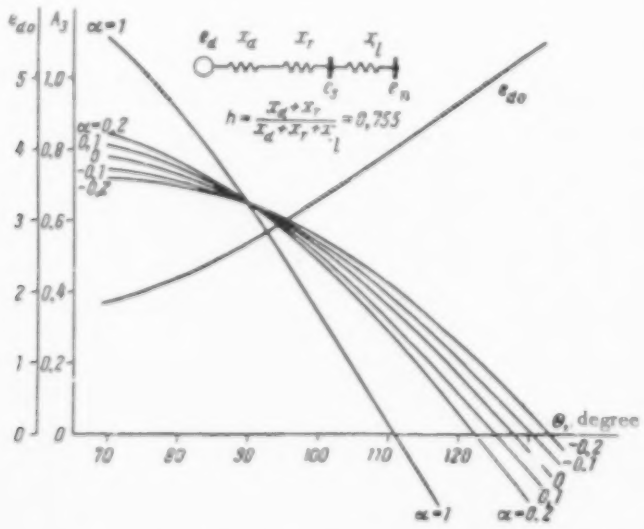

FIG. 5. Curves to determine the limiting angles.

* In the case, when the series excitation ensures 90 per cent of the rated value of the m.m.f.

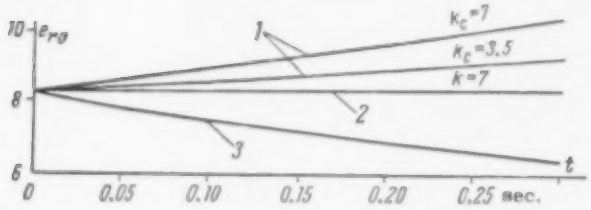

FIG. 6. The aperiodic component of the excitation current for different kinds of automatic control of excitation.
1. automatically controlled series excitation;
2. forced excitation;
3. no automatic control.

The e.m.f. e_d is determined by solving equations (7). In this case the right hand sides of equations (7a) and (7b) are made equal to zero, but the right-hand side of equation (7c) is $\rho_r - e_{r0}$ in the absence of the excitation control, and $\rho_r\, k e_{r0}$ if the non-inertial regulator is used. Here k is the regulation factor, which in this case is equal to the multiplicity of the ceiling excitation.

In the presence of automatically controlled series excitation, $e_s = 0$ and, consequently, the right hand side of equation (10) is $\rho_r\, k_c\, E_2$. The solution of equations (7) for the short-circuit of a generator on no load, i.e. for initial conditions $t = 0$, $u_{d0} = 0$, $U_{q0} = 0$, $e_d = e_{r0}$, gives the operator solutions for e_d and for the aperiodic component of its original function. See the following table with the notations:

$$\sigma = 1 - \mu = \frac{x'_d}{x_d};\quad T'_d = 2\pi f \frac{\sigma}{\rho_r}.$$

Fig. 6 shows curves plotted from the formulae given in the table. These curves were constructed for the circuit shown in Fig. 3b in this case, the excitation ceiling relating to the no-load excitation was taken as seven.

Certain of the above assumptions have been verified under laboratory conditions on d.c. and a.c. generators. In particular, experiments which have been carried out have confirmed control stability not only for small and zero quiescence but also for negative quiescence.

The circuit of the automatically controlled series excitation was tested on a model turbo-generator of the electro-dynamical d.c. NII class when an asynchronous motor of comparable power was connected. In this case, the sources of the normal and controlled voltage E_n and e_s were connected to the separate field windings of the balancing exciter, which was series connected to the armature of the series exciter. In the latter instead of series winding ordinary shunt winding was used, which was connected in parallel to the rotor winding.

Oscillograms of the starting of the motor are shown in Fig. 7.

TABLE 1.

Type of the excitation control	Operator solution $e_d(p)$	Aperiodic component e_{da}
No control	$e_{r0}\dfrac{p^3+\frac{\rho_r}{a}p^2+\frac{1}{a}p+\frac{\rho_r}{a}}{\left(p+\frac{\rho_r}{a}\right)(p^2+1)}$	$e_{r0}\left[\frac{x_d}{x'_d}e^{-\frac{t}{T'_d}}+\left(1-e^{-\frac{t}{T'_d}}\right)\right]$
For $a=1$	$e_{r0}\dfrac{p^3+\frac{k\rho_r}{a}p^2+\frac{1}{a}p+k\frac{\rho_r}{a}}{\left(p+\frac{\rho_r}{a}\right)(p^2+1)}$	$e_{r0}\left[\frac{x_d}{x'_d}e^{-\frac{t}{T'_d}}+k\left(1-e^{-\frac{t}{T'_d}}\right)\right]$
With automatically controlled series excitation for $a\neq 0$	$\dfrac{\rho_r k_c E_2(p^2+1)+ae_{d0}p\left(p^2+\frac{1}{c}\right)}{a\left(p+\alpha\frac{\rho_r}{a}\right)(p^2+1)}$	$e_{r0}\frac{x_d}{x'_d}e^{-\alpha\frac{t}{T'_d}}+\frac{k_c}{a}E_2\left(1-e^{-\alpha\frac{t}{T'_d}}\right)$
With automatically controlled series excitation for $a=0$		$e_{r0}\frac{x_d}{x'_d}+k_cE_2\frac{t}{T'_d}$

The oscillogram (Fig. 7a) is an example of the control with positive quiescence.

$$\delta = \frac{u_{xx} - u_n}{u_{xx}} = \frac{1-0.94}{1} = 0{,}06.$$

In this case, factor $k_c = 1$; currents in the windings of the balancing exciter are equal to the excitation currents on no-load when the exciter is used in the ordinary circuit of the shunt exciter.

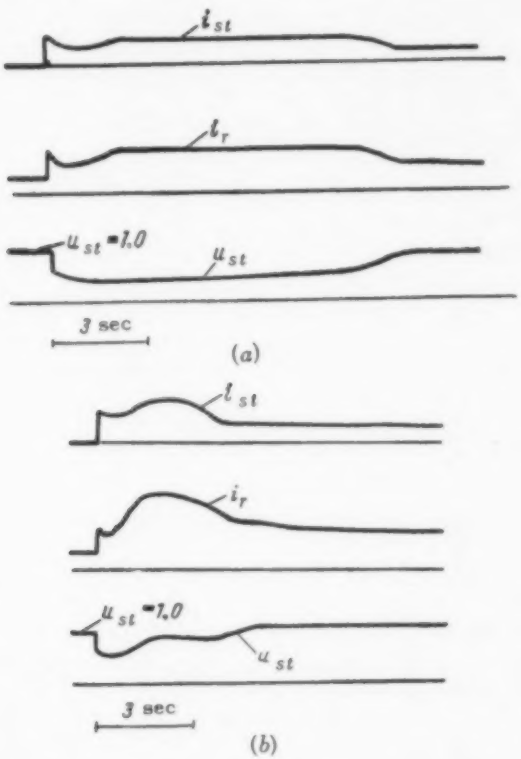

FIG. 7. Oscillograms of the starting of an asynchronous motor..

The oscillograms in (Fig. 7b) are examples of the control with negative quiescence.

$$\delta = \frac{u_{xx} - u_n}{u_{xx}} = \frac{1 - 1.1}{1} = -0.1.$$

Negative quiescence is obtained by decreasing the resistance in the excitation circuit. In this experiment $k_c = 2$.

These oscillograms confirm the stability and effectiveness of the control system discussed both for the positive and negative quiescence.

As can be seen from the oscillograms, the excitation current "follows" the stator current and can be maintained equal to or greater than the initial value of the aperiodic component. The decrease of the excitation current at the beginning of the process is explained mainly by the inductance of the shunt winding, which plays the role of the "series" winding of the exciter B_s.

The considerations given above permit the conclusion that the automatically controlled series excitation of synchronous machines is a very simple excitation automatic control system and allow us to obtain a considerably greater effect in preserving static and dynamic stability than does the use of automatic regulators acting on the shunt or separate excitation.

LIST OF LETTER NOTATIONS

R – the load resistance of a d.c. generator;
r'_1, r_1 – resistances of the armature circuit;
L_1 – inductance of the armature circuit;
r_2, r'_2 – resistances of the excitation circuit;
L_2 – inductance of the excitation circuit;
i_1 – load current of a d.c. generator;
i_2 – current of the excitation circuit of a d.c. generator;
e_1 – e.m.f. of a d.c. generator;
e_s – e.m.f. of the series exciter of a d.c. generator
E_2 – standard voltage of a d.c. generator.
u – terminal voltage of a d.c. generator.
U_d, U_q – axial and cross components of the voltage drop in the stator circuit.
e_d – e.m.f. in the axial circuit;
e_r – excitation voltage;
e_s – terminal voltage of a generator;
e_n – voltage at the receiving end of a transmission line;
θ – angle between e.m.f. e_d and voltage e_s;
ρ_r – decrement of the rotor circuit;
i_r – rotor current;
e_c – voltage of a series exciter.

Translated by S. Szymanski

REFERENCES

1. N.N. Shchedrin; *Vliianiye reguliatora Tirrillia na perekhodnoye i ustanovivsheyessia dvizheniye sinkhronnoi mashiny i nekotoryye voprosy kinetiki vozbuzhdeniia. Otchet po nauchno-issledovatelskoi rabote laboratorii vysokikh napriazhenii im Smurova (Influence of the Tirrill regulator on the transient and steady state motion of a synchronous machine and certain problems of excitation kinetics. Report on the scientific and research work of the Smurov H.T. laboratory)* (1935).
2. P.S. Zhdanov; Kompoundiravannyye skhemy vozbuzhdeniia sinkhronnykh mashin. (Compound excitation circuits of synchronous machines) *VEP*, No. 9 (1943).

3. E.L. Harder; G.E. Valentine *Trans. Amer. Inst. Elect. Engrs.* Vol. 64, 601 (1945).
4. W. Harris; *Elect. Engng.* Vol. 65, 118, No. 3 (1946).
5. A.B. Cheliustkin; Rototrol i ego primeneniye (Rototrol and its application), *Amerikanskaia tekhnika i promyshlennost*, No. 7 (1944).
6. A.A. Gorev; *Perekhodnye protsessy sinkhronnoi mashiny (Transients in a synchronous machine)*, Gosenergoizdat (1950).
7. P. Ruidberg; *Perekhodnye protsessy v elektroenergeticheskikh sistemakh (Transients in electrical power systems)*, Izd. Inostrannoi literatury (1955).

1959

NEGATIVE SEQUENCE FILTERS WITH INDEPENDENT ARMS *

A.B. VITANOV

Bulgaria, Sofia

(Received 30 April 1957)

Symmetrical component filters are now being used very widely. The most common are negative sequence filters almost all are filters with independent arms. These filters are subdivided into many classes, groups etc. and to each subdivision there are appropriate formulae. However, these classes and groups do not cover the infinite variety of filters with independent arms.

In this article an attempt is made to lay down the foundation of a single theory for all filters with independent arms and to give general formulae, the analysis of which should enable us to choose the optimum variants of filters.

Filters of negative sequence voltage

In its general form a device for distinguishing any one voltage symmetrical component consists of a voltage converter and a filter (Fig. 1).

In the voltage converter, the applied voltages $\dot{U}_{AB}$ and $\dot{U}_{BC}$ are converted into those required:

$$\left.\begin{aligned}\dot{U}_m &= k\dot{U}_{AB} + k_2\dot{U}_{BC}\,;\\ \dot{U}_n &= k_3\dot{U}_{AB} + k_4\dot{U}_{BC}\,.\end{aligned}\right| \qquad (1)$$

In a particular case, a device may be used without a converter in this case it consists only of a filter, to which voltages are applied:

$$\dot{U}_m = \dot{U}_{AB} \text{ and } \dot{U}_n = \dot{U}_{BC}\,.$$

Filters with independent arms may have two arms (Fig. 2) or one arm (Fig.3); single-arm filters are a special case of two arm filters.

* *Elektrichestvo*, No. 6, 29-32, 1958.

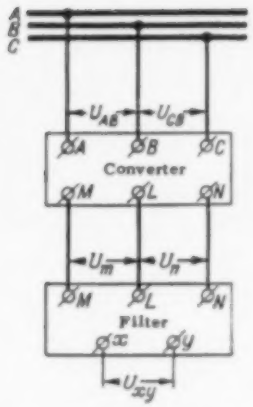

FIG. 1. Block diagram of a device for distinguishing voltage symmetrical components.

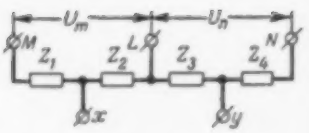

FIG. 2. A two-arm voltage filter.

Two arm filters.

In order that the circuit shown in Fig. 2 should be a filter of negative sequence voltage, it is necessary and sufficient that, when the voltage of the positive sequence U_1 is applied to the voltage converter, the potentials of the points x and y should be equal; i.e.

$$\dot{U}_x = \dot{U}_y \,. \tag{2}$$

Assuming $U_M = 0$ we get:

$$\left.\begin{aligned} \dot{U}_x &= -\frac{Z_1}{Z_1+Z_2}\dot{U}_m; \\ \dot{U}_y &= -\dot{U}_m - \frac{Z_3}{Z_3+Z_4}\dot{U}_n. \end{aligned}\right\} \tag{3}$$

Assuming in equation (1) that $\dot{U}_{AB}$ and $\dot{U}_{BC}$ are voltages of the positive sequence $\dot{U}_{AB} = U_1$ and $\dot{U}_{BC} = a^2 U_1$, we find:

$$\left.\begin{aligned} \dot{U}_{m1} &= U_1(k_1 + a^2 k_2); \\ \dot{U}_{n1} &= U_1(k_3 + a^2 k_4). \end{aligned}\right\} \tag{4}$$

Let us introduce the following substitutions:

$$\left.\begin{aligned} \xi = \frac{Z_2}{Z_1}\,; \quad \eta_1 = \frac{Z_4}{Z_3}\,; \\ n = \frac{Z_3+Z_4}{Z_1+Z_2}\,; \quad p = \frac{k_1 + a^2 k_2}{k_3 + a^2 k_4}\,. \end{aligned}\right\} \tag{5}$$

Using the relationships obtained, after a number of transformations, we get:

$$\eta_1 = -1 - \frac{1+\xi}{\xi} \cdot \frac{1}{p}. \tag{6}$$

Parameters of the negative sequence voltage filter should satisfy this condition; it is assumed below that this condition is always satisfied.

On applying to the circuit the negative sequence voltage U_2, we get at the terminals x, y the no-load voltage U_{xy}:

$$\dot{U}_{xy} = \dot{U}_{x2} - \dot{U}_{y2}. \tag{7}$$

In this case $\dot{U}_{AB} = U_2$, $\dot{U}_{BC} = aU_2$, and therefore:

$$\left.\begin{aligned} \dot{U}_{m2} &= U_2(k_1 + ak_2); \\ \dot{U}_{n2} &= U_2(k_3 + ak_4). \end{aligned}\right\} \tag{8}$$

Substituting (8) into (3) and afterwards into (7) we get:

$$\dot{U}_{xy} = j\sqrt{3}\,\frac{U_2\xi}{1+\xi}\,\frac{k_2k_3 - k_1k_4}{k_3 + a^2k_4}. \tag{9}$$

The ratio of no-load running m is defined as the ratio of the no-load voltage to the negative sequence voltage U_2:

$$m = \frac{\dot{U}_{xy}}{U_2} = j\sqrt{3}\,\frac{\xi}{1+\xi}\,\frac{k_2k_3 - k_1k_4}{k_3 + a^2k_4}. \tag{10}$$

The total impedance of the filter short-circuit Z_{sf} is the impedance measured on the secondary terminals when the primary ones are short-circuited, [1].

From the circuit shown in Fig. 2 it is seen that

$$Z_{s.f} = \frac{Z_1Z_2}{Z_1 + Z_2} + \frac{Z_3Z_4}{Z_3 + Z_4}. \tag{11}$$

Substituting (5) into (11) and taking into consideration (6) we get:

$$Z_{s.f} = \frac{\xi Z_1}{1+\xi}[1 - n\xi p^2 - n(1+\xi)p]. \tag{12}$$

If a relay is connected at the point x and y (Fig. 2), then its current, voltage and power are determined by expressions [1 and 2]:

$$\dot{I}_p = \frac{\dot{U}_{xy}}{Z_p + Z_{s.f}}; \tag{13}$$

$$\dot{U}_p = \frac{\dot{U}_{xy} Z_p}{Z_p + Z_{s.f}}; \tag{14}$$

$$\dot{S}_p = \hat{U}_p \dot{I}_p = \left| \frac{\dot{U}_{xy}}{Z_p + Z_{s.f}} \right| Z_p^*. \tag{15}$$

Here and below the conjugate values of the quantities, which are not functions of time, are denoted by a superscript *.

When U_2 = const, the relay gives maximum power when $|Z_p| = |Z_{s.f}|$. Since this corresponds to the maximum sensitivity of the filter-relay circuit, this condition is nearly always satisfied by the rewinding of the relay.

Assuming that the condition $|Z_p| = |Z_{s.f}|$ is satisfied and denoting $\phi = \phi_p - \phi_{s.f}$, where ϕ_p and $\phi_{s.f}$ are respectively angles of impedances, from (13), (14), and (15) we get the following formulae:

1959

$$\dot{I}_p = \frac{j\sqrt{3}U_2}{Z_1(1+e^{j\varphi})} \frac{1}{1+np(1+\xi-\xi p)} \frac{k_2k_3 - k_1k_4}{k_3 + a^2k_4}; \tag{16}$$

$$\dot{U}_p = \frac{j\sqrt{3}U_2}{1+e^{-j\varphi}} \frac{\xi}{1+\xi} \frac{k_2k_3 - k_1k_4}{k_3 + a^2k_4}; \tag{17}$$

$$\dot{S}_p = \frac{3U_2^2}{Z_1(1+e^{j\varphi})^2} \frac{1}{\left(1+\frac{1}{\xi^*}\right)[1+np(1+\xi-\xi p)]} \frac{(k_2k_3 - k_1k_4)^2}{k_3^2 - k_3k_4 + k_4^2}. \tag{18}$$

In determining the power consumed by the filter, we shall only take into account the power which is due to the voltage of the positive sequence [1, p. 24].

$$\dot{S}_f = \frac{\dot{U}_{m1}^2}{Z_1 + Z_2} + \frac{\dot{U}_{n1}^2}{Z_3 + Z_4}.$$

Taking into account (4), (5) and (6) we get:

$$\dot{S}_f = \frac{U_1^2}{Z_1(1+\xi)} \left[k_1^2 - k_1k_2 + k_2^2 + \right.$$
$$\left. + \frac{1}{n}(k_3^2 - k_3k_4 + k_4^2) \right]. \tag{19}$$

It is quite sufficient to use the following filter characteristics:

(1). Ratio of the maximum power on the relay to the power consumed when $U_1 = U_2$:

$$a = \left(\frac{\dot{S}_p}{\dot{S}_\varphi}\right)_{U_1=U_2} = \tag{20}$$

$$= \frac{3(k_3k_2 - k_1k_4)^2}{(1+e^{j\varphi})(k_3^2 - k_2k_4 + k_4^2)\left[k_1^2 - k_1k_2 + k_2^2 + \frac{1}{n}(k_3^2 - k_2k_4 + k_4^2)\right][1+np(1+\xi-\xi p)]}.$$

(2). The ratio of the relative unbalanced voltage, caused by the frequency deviation to the relative frequency variation:

$$\gamma_f = \frac{d\dot{U}_{nb}}{mU_1} : \frac{df}{f_0} = \frac{d\dot{U}_{nb}}{df}\frac{f_0}{mU_1}, \tag{21}$$

where $\dot{U}_{nb} = \dot{U}_{xy_1} = \dot{U}_{x_1} - \dot{U}_{y_1}$
From (3), (4) and (5) we get:

$$\dot{U}_{nb} = U_1\left[\frac{\xi}{1+\xi}(k_1 + a^2k_2) + \frac{1}{1+\eta}(k_3 + a^2k_4)\right].$$

Differentiating this equation for f:

$$\frac{d\dot{U}_{nb}}{df} = U_1\left[\frac{1}{(1+\xi)^2}\frac{d\xi}{df}(k_1 + a^2k_2) - \right.$$
$$\left. - \frac{1}{(1+\eta)^2}\frac{d\eta}{df}(k_3 + a^2k_4)\right].$$

Substituting the value of this derivative into (21) and taking into account (6) and (10) we find:

$$\gamma_f = \frac{-j}{\sqrt{3}}\left(\frac{1}{\xi}\frac{d\xi}{df} - \xi\frac{d\eta}{df}p\right)\frac{1}{1+\xi} \times$$
$$\times f_0\frac{(k_1 + a^2k_2)(k_3 + a^2k_4)}{k_3k_2 - k_1k_4}, \tag{22}$$

where the values of derivatives and quantity ξ are calculated for $f = f_0$.

The derivatives which appear in expression (22) are calculated by the formulae:

$$\left(\frac{d\xi}{df}\right)_{f=f_0} = \frac{j}{f_0}\,\frac{|X_3|Z_1 - |X_1|Z_3}{Z_1^2}\,; \tag{23}$$

$$\left(\frac{d\eta}{df}\right)_{f=f_0} = \frac{j}{f_0}\,\frac{|X_4|Z_3 - |X_3|\cdot Z_4}{Z_3^2}\,. \tag{24}$$

Substituting (23) and (24) into (22) and taking into consideration (5) and (6) we get:

$$\gamma_f = \frac{1}{Z_1(1+\xi)}\left[-|X_1| + \frac{|X_2|}{\xi} + \right.$$
$$\left. + \frac{|X_3|}{n}\left(1 + \frac{1}{p} + \frac{1}{\xi p}\right) + \frac{|X_3|}{n}\right]\frac{(k_1 + a^2k_2)(k_3 + a^2k_4)}{\sqrt{3}(k_2k_3 - k_1k_4)}\,. \tag{25}$$

Single arm filters.

The single arm filters are a particular case of the two-arm negative sequence filters; for the single-arm filters $Z = \infty$, $Z_4 = 0$. In this case ξ and η assume the following values:

$$\eta = \frac{Z_4}{Z_3} = 0; \quad \xi = -\frac{1}{1+p}\,. \tag{26}$$

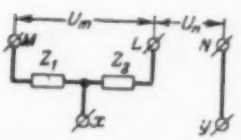

FIG. 3. A single-arm voltage filter.

For the single-arm filters $n = \infty$. If we repeat the deduction of all formulae obtained above with respect to the single-arm filters, we find that they can be obtained by the formal removing of all terms containing n (these terms are characteristic for the presence of the second arm).

Removing from expressions (10), (12), (16), (17), (18), (19), (20) and (25) all terms containing n and substituting into these expressions the quantity ξ from (25), we get for the single-arm filters the following expressions:

$$m = -j\sqrt{3}\,\frac{k_3k_2 - k_1k_4}{k_1 - a^2k_2}\,; \tag{27}$$

$$Z_{s.f} = -\frac{Z_1}{p}; \tag{28}$$

$$I_p = \frac{j\sqrt{3}U_2}{Z_1(1+e^{j\varphi})} \cdot \frac{k_2k_3 - k_1k_4}{k_3 + a^2k_4}, \tag{29}$$

$$\dot{U}_p = \frac{-j\sqrt{3}U_2}{1+e^{-j\varphi}} \cdot \frac{k_2k_3 - k_1k_4}{k_1 + a^2k_2}; \tag{30}$$

$$\dot{S}_p = -\frac{3U_2^2}{Z_1(1+e^{j\varphi})^2} \cdot \frac{(k_2k_3 - k_1k_4)^2}{(k_1 + ak_2)(k_3 + a^2k_4)}; \tag{31}$$

$$\dot{S}_\phi = \frac{U_1^2}{Z_1}(k_1 + ak_2)(k_1 + a^2k_2 + k_3 + a^2k_4); \tag{32}$$

$$a = \frac{-3(k_2k_3 - k_1k_4)^2}{(1+e^{j\varphi})^2(k_1 + ak_2)^2(k_3 + a^2k_4)[k_1 + k_3 + a^2(k_2 + k_4)]}; \tag{33}$$

$$\gamma_f = jf_0\frac{d\xi}{df} \cdot \frac{[k_1 + k_2 + a^2(k_2 + k_4)]^2}{\sqrt{3}(k_2k_3 - k_1k_4)} =$$

$$= -\frac{1}{Z_1}[X_1 + X_2(1+p)] \cdot \frac{(k_3 + a^2k_4)(k_1 + a^2k_2 + k_3 + a^2k_4)}{\sqrt{3}(k_2k_3 - k_1k_4)}. \tag{34}$$

Negative sequence current filters

In the general form a filter for distinguishing any current symmetrical component (Fig. 4) is similar to a filter for distinguishing voltage symmetrical components and consists of the same parts.

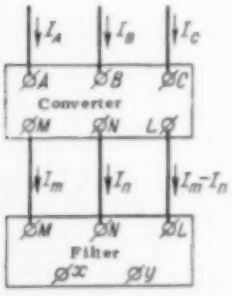

FIG. 4. Block diagram for distinguishing current symmetrical components.

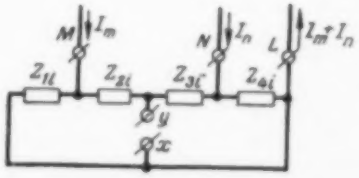

FIG. 5. A two-arm current filter.

As it known, the circuit of every current filter can be obtained from the circuit of the voltage filter by arranging a binary circuit with conjugate elements.

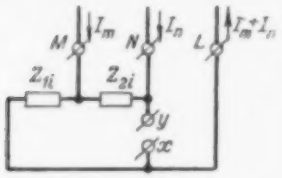

FIG. 6. A single-arm current filter.

In this way, the circuits shown in Figs 2 and 3 can be converted into general circuits of two-arm and single-arm negative sequence current filters.
In this case:

$$\left.\begin{aligned} I_m &= (k_1 + ak_2)\, I_A; \\ I_n &= (k_3 + ak_4)\, I_A \end{aligned}\right\} \tag{35}$$

and

$$Z_i = \frac{1}{Z^*}, \tag{36}$$

where Z_i is the impedance of the current filter corresponding to the impedance Z of the voltage filter.

1959

All the expressions deduced for the voltage filters therefore remain valid for the current filters, if we introduce into these expressions the following parameters:

$$Z_1 = \frac{1}{Z^*_{1i}}; \tag{37}$$

$$\xi = \frac{Z^*_{1i}}{Z^*_{2i}}; \tag{38}$$

$$n = \frac{Z^*_{1i}\, Z^*_{2i}}{Z^*_{3i}\, Z^*_{4i}} \, \frac{Z^*_{3i} + Z^*_{4i}}{Z^*_{1i} + Z^*_{2i}} \tag{39}$$

and substitute everywhere instead of U_1 the current of the positive sequence I_1, and instead of U_2 the current of the negative sequence I_2.

In analysing the results obtained we have to take into consideration the following.

For current filters:

$$m = \frac{I_{xy}}{I_2}, \tag{40}$$

where I_{xy} is the short-circuit current flowing between the short-circuited terminals x and y when negative sequence currents I_2 enter the filter.

To the short-circuit impedance of the voltage filter $Z_{s.f}$ there corresponds in the current filter, a no-load impedance $Z_{s.c}$, which is measured on secondary terminals, when the primary terminals are open:

$$Z_{c.s} = \frac{1}{Z^*_{s.f}}. \tag{41}$$

For current filters, formulae (16), (17), (18), (20) or (29), (30), (31), (33) give conjugate values of the sought quantities; i.e.

$$I_{pi} = \hat{I}_p,\ \dot{U}_{pi} = \hat{U}_p,\ \dot{S}_{pi} = \hat{S}_p,\ a_i = a^*.$$

When total impedances, which are the result of the series connexion of resistances and reactances, are present in filters, then formulae (25) and (34) for γ are not correct since the value of the derivatives $d\xi/df$ and $d\eta/df$ is changed. The new values of the derivatives are:

$$\left(\frac{d\xi_i}{df}\right)_{I=I_0} = \frac{j}{f_0}\,\frac{|X_{2i}|\,Z^*_{1i} - |X_{1i}|\,Z^*_{2i}}{Z^{*2}_{2i}}; \tag{42}$$

$$\left(\frac{d\eta_i}{df}\right)_{I=I_0} = \frac{j}{f_0}\,\frac{|X_{4i}|\,Z^*_{3i} - |X_{3i}|\,Z^*_{4i}}{Z^{*2}_{4i}}. \tag{43}$$

Substituting (42) and (43) into (22) and (34) and taking into consideration (36) and (38), after transformation we get:

for the two-arm current filter of negative sequence,

$$\gamma_{fi} = \frac{Z_1}{1+\xi}\,\{\xi\,|X_{2i}| - |X_{1i}| + \\ + n\,(\xi_p + \xi - 1)\,[\,|X_{4i}|\,(\xi p + \xi + 1) + |X_{3i}|\,\xi p]\} \times \\ \times \frac{(k_1 + a^2 k_2)\,(k_3 + a^2 k_4)}{\sqrt{3}\,(k_2 k_3 - k_1 k_4)};$$

for the single-arm current filter of negative sequence,

$$\gamma_{fi} = -\,Z_1\,[\,|X_{1i}|\,(1+p) + |X_{2i}|\,]\,\frac{(k_3 + a^2 k_4)^2}{\sqrt{3}\,(k_2 k_3 - k_1 k_4)}$$

The formulae obtained can be used to determine the characteristics of any filter with independent arms and the filter parameters and to choose the optimum filter.

Translated by S. Szymanski

REFERENCES

1. V.L. Fabrikant; *Filtry simmetricheskikh sostavliaiushchikh (Symmetrical components Filters)*, Gosenergoizdat (1950).
2. A.M. Fedoseyev; *Releinaia zashchita elektricheskikh sistem (The relay protection of electrical systems)*, Gosenergoizdat (1952).

1959

CALCULATION OF THE CHARACTERISTICS OF AN ELECTRIC DRIVE WITH FREQUENCY CONTROL BY THE EQUIVALENT RESISTANCE METHOD*

V.V. ARTAMONOV

Krasnoiarsk Polytechnic Institute

(Received 3 February 1958)

The analytical method of calculating the characteristics of an electric drive with frequency control [3] is based on the equivalent circuit of an asynchronous motor, (Fig. 1). This method is discussed in [1 and 2]. It is cumbrous and not sufficiently accurate. This is due to the complexity of the calculations of magnetic circuit saturation and of the current displacement in the rotor. In most cases this compels us to assume that the parameters of the equivalent circuit are constant.

A method is proposed which permits us to obtain more accurate results, if in calculating we take as a basis the motor characteristics given for the rated frequency of the supply.

The equivalent circuit of an asynchronous motor for variable frequency.

The equivalent circuit shown in Fig. 1 can be represented in the form of two parts; one of them reproduces only the influence of the supply current frequency, the other - only of the load.

For this purpose let us separate the resistance of the stator winding from the resistance r_1 / α .

$$\frac{r_1}{\alpha} = r_1 \frac{1-\alpha}{\alpha} + r_1. \qquad (1)$$

In this case, the equivalent circuit of an asynchronous motor for any frequency can be represented as a series connexion of an additional resistance::

$$r_d = r_1 \frac{1-\alpha}{\alpha} \qquad (2)$$

with an ordinary standard equivalent circuit (Fig. 2).
The "internal" voltage of this equivalent circuit, we shall in the following call the rated voltage.

* *Elektrichestvo* No. 6, 66-69, 1958.

$$\dot{U}_{r.p.} = \frac{\dot{U}_{1p}}{a} - I_1 r_d \tag{3}$$

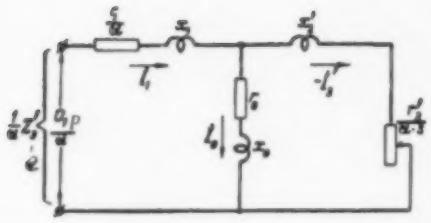

FIG. 1.

Equivalent circuit of an asynchronous motor for the supply variable frequency $U_{1.p.}$ Complex phase voltage across the stator winding at the nominal frequency; $a = f/f_n$ - current frequency parameter in the stator winding;
Z'_e – the motor equivalent impedance at a supply variable frequency; $s = \frac{a\omega_c - \omega}{a\omega_c}$ – the rotor slip;

I_1, I_2, I_0 – currents in the corresponding arms of the equivalent circuit;

$r_1, r_2, r_0, X_1, X_2, X_0$ – resistances of the arms of the equivalent circuit.

Its influence on the motor properties for a frequency differing from the normal is analogous to the influence of the voltage U_1 on the stator terminals of the motor, for the nominal frequency. Thus, for example, assuming that the parameters of the equivalent circuit are constant, we get for the driving torque of the rotor the following formula:

$$M = M_k \left(\frac{U_p}{U_n}\right)^2 \frac{2 + as_k}{\frac{\beta}{s_k} + \frac{s_k}{\beta} + as_k}, \tag{4}$$

where M_k and s_k are the critical torque and slip of the natural mechanical characteristics respectively.

Thus, the motor mechanical characteristic can be easily obtained for any supply frequency by using the known relationship between the rated voltage and the load parameter β by simple recalculation of the natural mechanical characteristic.

The latter can be given analytically or graphically.

The equivalent impedance of this part of the equivalent circuit, which remains after the separation of the resistance r_{d_1} when expressed as a function of the parameter β, represents an ordinary equivalent impedance of the motor, which corresponds to the nominal frequency:

$$Z_e = R_e + jX_e. \tag{5}$$

In this case the equivalent impedance, which also accounts for the influence of the supply frequency, is obtained on the basis of the equivalent circuit, shown in Fig. 2.

$$\frac{1}{a} Z_e' = Z_e + r_d. \tag{6}$$

Equality (6) gives the relationship between the motor characteristics, which correspond to various frequencies.

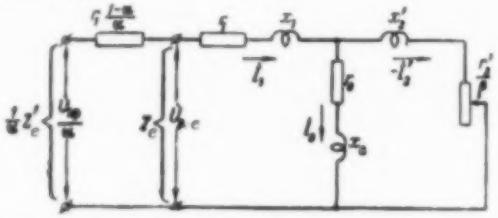

Equivalent circuit of an asynchronous motor for the supply variable frequency reduced to the nominal frequency.

$U_{r.p_1}$ – rated phase voltage across the stator winding;

$\beta = f/f_n$ – parameter of the current frequency in the rotor (load parameter);

Z_e – equivalent impedance of the motor for the supply nominal frequency.

I_1, I_2, I_0 – currents in the corresponding arms of the equivalent circuit;

r_1, r_2, r_0, X_1, X_2, X_0 – resistances of the arms of the equivalent circuit.

Active R_e and reactive X_e components of the motor equivalent impedance, corresponding to the nominal frequency, are usually determined by means of the known parameters of the equivalent circuit:

$$R_e = r_1 + \frac{\beta^2 r_0 x_2'^2 + \beta^2 z_0^2 r_2' + r_0 r_2'^2}{\beta^2 (z_0^2 + x_2'^2 + 2x_0 x_2') + \beta \cdot 2 r_0 r_2' + r_2'^2}; \tag{7}$$

$$X_e = x_1 + \frac{\beta^2 (z_0^2 x_2' + x_0 x_2'^2) + x_0 r_2'^2}{\beta^2 (z_0^2 + x_2'^2 + 2x_0 x_2') + \beta 2 r_0 r_2' + r_2'^2}. \tag{8}$$

However, if we find the equivalent impedance in this way, the method of calculation discussed now has no advantage in comparison with the existing one so far as

the accuracy and volume of calculations are concerned.

At shown above, to determine the motor properties for an arbitrary frequency it is sufficient to know the dependence of the equivalent impedance on the slip and the natural mechanical characteristic, which can be obtained experimentally. Therefore, the field of the most effective application of the method discussed is not the calculation of characteristics for an arbitrary frequency on the basis of given parameters of the equivalent circuit, but the re-evaluation of characteristics, appropriate to the nominal frequency, for any other arbitrary frequencies.

Calculation of operating characteristics

Under steady-state conditions the properties of an electric drive are determined by the families of: mechanical characteristics, characteristics of the current fed to the motors under control by the frequency converter, curves of efficiency, cos ϕ and the torque developed by the machine frequency converter. It is most convenient to represent all the above characteristics as functions of the load parameter β.

The main stage in calculating characteristics by the method discussed is the determination of the rated voltage as a function of the load parameter, when the dependence of the voltage of the supply source on the frequency is known. In spite of the fact that the rated voltage is a complicated function of the slip, frequency and stator voltage, its determination by means of the equivalent impedance is comparatively simple and, for the arbitrary values of the frequency and load parameters α and β is performed in the same way, independently of the presence or absence of the frequency converter.

In a general case, when the power of the converter is comparable to the power of the connected motors, we have:

$$U_p = \frac{E_{f.c.}}{a} \left| \frac{Z_e}{Z_e + Z_d} \right|, \tag{9}$$

where $E_{f.c.}$ = the e.m.f. of the frequency converter, which is known for any arbitrary value of the frequency;

$Z_d = R_d + jX_d$ is the additional impedance including all resistances of the stator circuit of the motor:

$$R_d = \frac{1}{a}(r_{f.c.} + r_l) + r_d; \tag{10}$$

$$X_d = x_{f.c.} + x_l, \tag{11}$$

where $r_{f.c.}$ and $X_{f.c.}$ are components of the frequency converter impedance;

r_l and X_l are corresponding components of the connecting loads:

If we can neglect the impedance of the variable frequency source and assume that the motor is connected to a grid of infinite power, then formula (9) assumes this form:

$$U_p = \frac{U_1}{a}\left|\frac{Z_e}{Z_e + r_d}\right|, \tag{12}$$

where U_1 is the voltage at the stator terminals for the nominal frequency.
After determinating the rated voltage, it is easy to find the remaining characteristics.
The stator current of the motor:

$$I = \frac{U_p}{\sqrt{3}z_e} = \frac{E f.c.}{\sqrt{3}z_\Sigma}, \tag{13}$$

where

$$z_\Sigma = \sqrt{(R_e + R_d)^2 + (X_e + X_d)^2}$$

and

$$z_e = \sqrt{R_e^2 + X_e^2}.$$

The active power taken in by the motor from the frequency converter is:

$$P_{1d} = 3I^2(R_e + r_d), \tag{14}$$

The total power of the frequency converter, neglecting steel losses and mechanical losses in the converter:

$$P_{1\Sigma} = 3I^2(R_e + R_d). \tag{15}$$

The useful power on the motor shaft:

$$P_{2d} = \frac{M\omega}{9,81} = M\frac{\omega_c}{9,81}(\alpha - \beta) \tag{16}$$

Efficiences of the motor and converter:

$$\eta_d = \frac{P_{2d}}{P_{1d}} \quad \text{si} \quad \eta_{f.c.} = \frac{P_{1d}}{P_{1\Sigma}}. \tag{17}$$

The reactive power consumed and the efficiency of the motor-converter circuit are determined in the usual way.

The calculation ends by determining the electro-magnetic torque developed by the frequency converter:

(a) for a synchronous generator:

$$M = \frac{I^2 p}{10,26}(R_e + R_d) \quad [\text{kgm}]; \tag{18}$$

(b) for an asynchronous frequency converter:

$$M = \frac{I^2 p}{1026}\left(R_e + R_d - \frac{r_1'}{c}\right) \text{ [kgm]}, \tag{19}$$

where p is the number of pole pairs of the machine;

r_1' is the active resistance of the primary winding of the asynchronous converter reduced to the secondary (load) winding; and

$c \approx 1 + \frac{X_1}{X_0}$ is the reduction factor of the asynchronous converter.

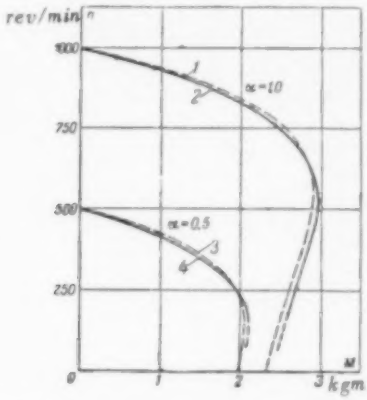

Rated (1, 3) and experimental (2, 4) mechanical characteristics of the MTK – 12-6 motor when fed by an asynchronous frequency converter of the AMK – 75 type, (Maker – AEG).

Using the method discussed the mechanical characteristics of the MTK-12-6 motor for 3.5 KW and 1000 rev/min were calculated when fed by an asynchronous frequency converter. The equivalent impedances were calculated by formulae (7) and (8). The parameters of the equivalent circuit were determined from no-load and short-circuit experiments. The natural mechanical characteristic was plotted on the basis of the catalogue data. The results of the calculations and experiments are shown in Fig. 3.

The determination of the law of the voltage variation of the frequency converter

Let us determine a law of the voltage variation of the frequency converter such that the constancy of the absolute slip of the motor rotor is ensured regardless of the variation of the supply frequency and load.

In the simplest case when the load torque is independent of the speed of rotation and is equal, for example, to the nominal torque, the above conditions of

the frequency control are ensured if $U_p = U_n = \text{const}$. In this case for all frequencies $\beta = S_n$.

Consequently by formulae (9) and (12) we get:

$$U_1 = aU_n \left| 1 + \frac{r_d}{Z_{e.n.}} \right|; \tag{20}$$

$$E_{n.s} = aU_n \left| 1 + \frac{Z_d}{Z_{e.n}} \right|, \tag{21}$$

where $Z_{e.n} = \text{const}$. is the motor equivalent impedance corresponding to the rated slip.

If the load torque varies with the frequency then, to ensure the conditions discussed of the frequency control, the following additional condition should be satisfied [4].

$$\frac{\Phi}{\Phi_n} = \sqrt{\frac{M}{M_n}}. \tag{22}$$

Since for $\beta = \text{const.}$, $U_p = \Phi$, from (22) we get:

$$U_p = U_n \sqrt{\frac{M}{M_n}}. \tag{23}$$

Thus, in a general case:

$$U_1 = aU_n \sqrt{\frac{M}{M_n}} \left| 1 + \frac{r_d}{Z_{e.n}} \right|; \tag{24}$$

$$E_{f.c.} = aU_n \sqrt{\frac{M}{M_n}} \left| 1 + \frac{Z_d}{Z_{e.n}} \right|. \tag{25}$$

In formulae (22) – (25), M is the torque developed by the motor for a speed of rotation corresponding to the value of the frequency in question.

Calculating the starting torque of the motor

Let us find the relationship between the starting torque of the motor and the frequency of the feed current: For the stalled rotor, $a = \beta$. Consequently, the starting torque of the motor can be calculated on the basis of the natural mechanical characteristic of the motor taking into account the voltage drop in the additional resistances of the stator circuit.

Thus, for example, if the motor mechanical characteristic can be expressed by equation (4) then the equation for calculating the starting torque assumes this form:

$$M_n = M_s \left(\frac{U_p}{U_n} \right)^2 \frac{2 + as_s}{\frac{a}{s_s} + \frac{s_s}{a} + as_s}. \tag{26}$$

The rated voltage is determined, as in the general case, by formulae (9) and (12), and the equivalent and additional impedances by formulae (7), (8), (10) and (11), In this case we have to replace β in formulae (7) and (8) by α.

If the natural mechanical characteristic is given in the form of a graph, as, for example, for motors with an increased starting torque, then the equivalent impedance should be determined taking into account the saturation of the magnetic system and the current displacement in the rotor.

Translated by S. Szymanski.

REFERENCES

1. A.A. Bulgakov; *Chastotnoye upravleniye asinkhronnymi elektrodvigatelyami (Frequency control of asynchronous motors).* Izd. Akad. Nauk SSSR (1955).
2. A.A. Bulgakov; *Asinkhronnyi dvigatel' pri peremennoi chastote (Asynchronous motor at a variable frequency), Trudy VEI,* 46, Gosenergoizdat, (1941).
3. V.T. Kas'yanov; *Elektrichestvo,* No. 2 (1949).
4. M.P. Kostenko; *Elektricheskie mashiny. "Spetsialnaya chast'" (Electric machines. "Special part")* Gosenergoizdat (1949).

1959

PROPERTIES AND DESIGN OF A MULTI-MOTOR DRIVE SYSTEM WITH A MECHANICAL DIFFERENTIAL*

B.M. SHKOLNIKOV and I.I. SUD

Giproneftemash Gosplana RSFSR

(Received 27 December 1957)

For many operating machines a reversible drive is needed which allows a smooth and continuous variation of the mechanism speed of rotation within a practically unlimited range. Usually the upper speed of the direct and reverse sense of rotation is given, and within the range from this maximum speed to the minimum speed, which is very near to zero, a continuous sequence of steady rotation speeds should be possible.

This kind of drive is particularly useful in mechanisms for boring oil holes [1].

In installations of this type an intermediate gear with a variable gear ratio is inserted between the driven mechanism and the driving motor. An asynchronous squirrel-cage motor can be used as a driving motor in such installations. The gear ratio can be changed either by steps, remaining constant at each step, or smoothly.

Due to operational requirements, for mechanisms driving the cutting tool a gear with a continuously varying gear ratio (from the output shaft to the driving motor) is needed, this ratio varying from zero to a certain maximum value for various directions of the output shaft.

In practice this problem can be solved by using a gear, which consists of a differential speed reducer, of which one driving shaft is driven by a controlled d.c. motor, and the other by an asynchronous squirrel-cage motor. Such a system of drive is used in the drilling automatic regulator type BAR 1-150 and is a particular case of a system, consisting of two controlled electric machines, which drive a common load; static and dynamic conditions of this system are discussed in detail in the works of Golovan and Gudkov [2-4].

The purpose of this article is to discuss the method of calculating and choosing the gear ratios of speed reducers and electrical machines for the drive shown in Fig. 1 , in addition, a comparison of this electric drive with other known

* *Elektrichestvo* No. 6, 69-74, 1958.

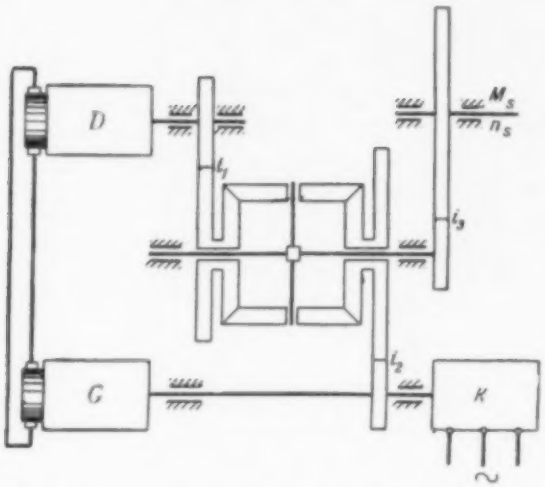

FIG.1. Kinematic diagram of an electrical differential drive.

1959

systems is given on the basis of operating experience.

In the above diagram an asynchronous motor with a squirrel-cage rotor K and a d.c. machine D drive two driving shafts of a speed reducer. At the same time, motor K drives another d.c. machine G. Machines G and D are connected as a generator-motor system. They are both separately excited. Machine K is fed from the a.c. gird.

Similar drive systems are used abroad. For example the firm "Speed Control" (U.S.A.) produces for the textile and metal machining industries many commercial types of similar mechanisms [5].

Choice of gear ratios

Let us introduce the following notations M_S, M_K, M_D - load torques on the speed reducer shaft and on shafts of machines K and D respectively; n'_S, n''_S - maximum and minimum speeds of the output shaft of the speed reducer for direct and reverse sence of rotation; i_1 - gear ratio from planet gears to machine B; i_2 - gear ratio from planet gears to machine K; i_3 - gear ratio from the output shaft to the differential shaft; n'_D and n''_D - maximum and minimum speed of rotation of machine D; Taking into account possible signs of speeds, equation $n_S = f(n_D, n_K)$ assumes this form:

$$n_S = \pm \frac{n_D}{2i_1 i_3} \mp \frac{n_K}{2i_2 i_3} . \qquad \text{A}$$

However this form of the equation makes a general solution more difficult, therefore, in the following discussion we shall write this equation in the following form:

$$n_S = \frac{n_D}{2i_1 i_3} - \frac{n_K}{2i_2 i_4}, \tag{1}$$

which is valid for the opposite sense of rotation of machines K and D under the condition that $n_D > o$. Particular cases may be accounted for by a proper choice of signs n_S, n_D and n_K.

Assuming n_K = const., we get the expression for $n_S = f(n_D,)$ which represents the equation of a straight line, passing through the given points of the co-ordinates (n_D'', n_S'') and (n_D', n_S'):

$$n_S = \frac{n_S'' - n_S'}{n_D'' - n_D'} n_D - \frac{n_S'' - n_S'}{n_D'' - n_D'} n_D' - n_S' \tag{2}$$

From (1) and (2) it follows:

$$i_1 i_3 = \frac{n_D'' - n_D'}{2(n_S'' - n_S')} \tag{3}$$

and

$$\frac{n_K}{2i_2 i_4} = \frac{n_S'' - n_S'}{n_D'' - n_D'} n_D' + n_S'. \tag{4}$$

If we neglect the efficiencies of mechanical gears, then the torques on the shafts of machines K and D can be determined from the following expressions:

$$M_K = \frac{M_S}{2i_2 i_4}; \quad M_D = \frac{M_S}{2i_1 i_3}. \tag{5}$$

In this way, for a given M_S, we can by the gradient of this line evaluate approximately the value of M_D, which determines the weight, size and cost of the machine D.

In a similar way the segment cut by this straight line on the axis n_S characterizes the power of the machine K.

In Fig. 2 relationships $n_S = f(n_D)$ are shown for the case, when the maximum speed of the output shaft is achieved for the upper (straight line 1) and for the lower (straight line 2) limits of the speed control of the machine D. The size of the machines D in both cases will be the same. In the second case, the power of the machine K (oa_2) will be greater than in the first case. We can decrease the size of the machine by decreasing the speed limits of the machine under control (straight line 3).

The choice of this or another alternative is made on the basis of the graph of

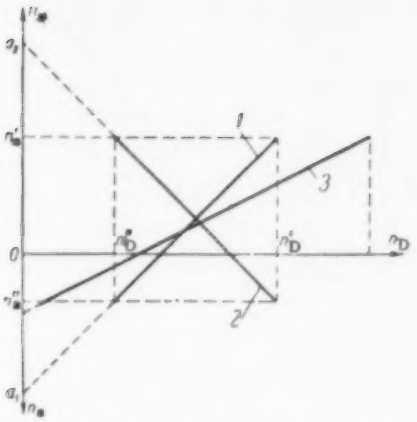

FIG.2. Speed characteristics of an electrical differential drive.

the speed variation with time of the reducer output shaft and the character of the load torque. The sense of rotation of the machine D should coincide with the operational sense of rotation of the reducer output shaft.

In the automatic drilling regulator BAR 1-150 the direct sense of rotation of the output shaft is in the direction of the lowering of the drilling column, consequently the machine D rotates in the same direction. Accordingly the motor K rotates in the direction of the raising of the column.

From the given conditions we can determine $i_1 i_3$ and $n_K / i_2 i_3$ [equations (3) and (4)]; thus, the choice of two out of the four of these quantities is arbitrary. Usually we choose n_K and i_3.

The choice of i_3 depends on considerations of design. In choosing a nominal speed of rotation of machine, that is not regulated, we have to take into account the necessity of ensuring the operation of the machine G under rated conditions and also the fact that the decrease in size of the machine K leads to the increase of the gear ratio i_3.

Reduction factor for the moments of inertia and the load torques

The usual formula for expressing the moments of inertia about one axis of rotation (2) with respect to the other axis (1) has the form:

$$J_{r\,1} = J_2 \left(\frac{\omega_2}{\omega_1}\right)^2 = J_2 \frac{1}{k_r^2}. \tag{6}$$

For the differential mechanism:

$$k_r = \frac{\omega_1}{\omega_2} = \frac{n_1}{n_2} \neq \text{const.} \tag{7}$$

In fact, from (1) we get:

$$\frac{n_1}{n_2} = \frac{n_D}{n_S} = 2i_1 i_3 + \frac{n_K}{n_S}\frac{i_1}{i_2}. \tag{8}$$

The ratio n_K/n_S varies within very wide limits and, in particular for $n_S = o$ it tends towards infinity. However, in spite of the fact that $k_1 \neq$ const., no change in the moments of inertia takes place in this case. For a differential mechanism, expression (6) is not valid.

Since a differential reducer represents a system with two degrees of freedom, the Lagrange equations of the second order, which relate to this mechanism, will have the following form:

$$\left.\begin{aligned} \frac{d}{dt}\frac{\partial A}{\partial \omega_D^*} - \frac{\partial A}{\partial \varphi_D^*} &= Q_D^*; \\ \frac{d}{dt}\frac{\partial A}{\partial \omega_K^*} - \frac{\partial A}{\partial \varphi_K^*} &= Q_K^*, \end{aligned}\right\} \tag{9}$$

where A is the kinetic energy stores in the system; Q_D^* and Q_K^* are generalized forces reduced to the differential driving pinions; ϕ_D^* and ϕ_K^* are angles of rotation of the shafts of machines D and K, reduced to the differential driving pinions; ω_D^* and ω_K^* are angular speeds of machines D and K reduced to the differential driving pinions.

If we neglect the rotation of the planet gears about their own axes, the amount of kinetic energy stored in the system is equal to:

$$A = \frac{1}{2} J_S^* (\omega_S^*)^2 + \frac{1}{2} J_D^* (\omega_D^*)^2 + \frac{1}{2} J_K^* (\omega_K^*)^2, \tag{10}$$

where J_S^*, J_D^*, J_K^* are total moments of inertia reduced to the appropriate differential shafts.

It is easy to show that the generalized forces are equal respectively to:

$$\left.\begin{aligned} Q_D^* &= \frac{1}{2} M_S^* - M_D^*; \\ Q_K^* &= -\frac{1}{2} M_S^* - M_K^*, \end{aligned}\right\} \tag{11}$$

where M_S^*, M_D^*, M_K^* are torques reduced respectively to the corresponding differential shafts.

Substituting (10) and (11) into (9), we get:

$$\left.\begin{aligned} J_D^* \frac{d\omega_D^*}{dt} - \frac{1}{4} J_s^* \frac{d\omega_K^*}{dt} = \\ = \frac{1}{2} M_s^* - M_D^* = M_{dynD}^* \\ J_K^* \frac{d\omega_K^*}{dt} - \frac{1}{4} J_s^* \frac{d\omega_K^*}{dt} = \\ = M_K^* - \frac{1}{2} M_s^* = M_{dyn\,K}^* \end{aligned}\right\} \quad (12)$$

where $\overline{J}_D^* = \frac{1}{4} J_s^* + J_D^*$;

$\overline{J}_K^* = \frac{1}{4} J_s^* + J_K^*$.

Since the angular speed ω_K^* varies little, (2-3 per cent), then $\frac{d\omega_K^*}{dt} = O$. Thus, the first of equations (12) can be written in this form †:

$$\overline{J}_D^* \frac{d\omega_D^*}{dt} = \left(\frac{1}{4} J_s^* + J_D^*\right) \frac{d\omega_D^*}{dt} = M_{dynD}^* \quad (13)$$

Thus, the moments of inertia reduced to the differential shaft are reduced to its driving pinions by dividing by the constant factor $k_r^2 = 4$. In the steady state conditions $\frac{d\omega_D^*}{dt} = O$. Therefore, $|M_D^*| = |M_K^*| = \frac{1}{2} M_s^*$, i.e. the load torques are reduced by the same reduction factor $k_r = 2$.

Choice of machine

When choosing a machine we make use of the functional block diagram of the drive shown in Fig. 3 where single lines represent mechanical connexions and double lines - electrical connexions.

Depending on the character of the load torque and the sense of rotation, machines K and D can work either as motors or as generators. When the load torque has the properties of reactance, then, with the change of the sense of rotation of the reducer output shaft, the operational character of a d.c. machine changes. Machine K, which is non-regulated always works as a motor. In the case of the potential load torque when the sense of rotation of the reducer output shaft changes, the operational conditions of a machine, that worked as a generator,

† Equation (13) was deduced independently of the authors by A.I. Driakhlov.

do not change. Machine K, which worked as a motor begins working as a generator, if a power regeneration system is provided; when working without regeneration it continues to work as a motor.

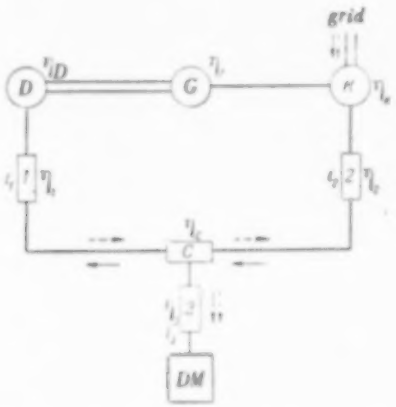

FIG. 3. Functional block diagram of an electrical differential drive. K, D and G. - electrical machines. 1 transmission from planet gears to machine D; 2 - transmission from planet gears to machine K; 3 - transmission from the output shaft to the differential shaft; C - planet gear assembly; DM - driven mechanism; η_1, η_2, η_3, η_C, η_G, η_D, η_K, - values of the efficiencies of the links on rated load.

In designing the drive mechanism we assume its normal operational conditions. In particular, in the BAR 1-150 the sense of rotation of machine D, which rotates in the sense of the lowering of the tool, coincides with the sense of the load torque, and consequently, whether the load goes up or down, this machine works as a generator. Machine K, which rotates in the sense of raising the load, can work both as a motor (forced lowering) or as a generator (regeneration) when the load goes down.

In Fig. 3, the sense of the power transfer is shown by continuous arrows for the case, when machine K works as a motor and machine D as a generator; dotted arrows indicate that both machines K and D work as motors. Formulae for calculating the torques of the machines are given in table 1.

For choosing a machine we assume in these formulae values of efficiencies, and of n_D and n_K for nominal conditions. Obviously, the second alternative of the operational conditions of machines offers a less advantageous solution from the point of view of weight and size and consequently, the price of a d.c. machine. Other possible operational conditions of drives are calculated in a similar way according to the direction of the power transfer.

Mechanical characteristic of a drive

We assume that a mechanical characteristic of machine D is linear within the

TABLE 1.

Conditions of the machine operation	Formulae for calculating torques of the machines		
	machine K	machine D	machine G
Machine K as a motor Machine D as a generator	$\frac{M_s}{2i_1i_2\eta_{i1}\eta_{i2}\eta_C}\left(i_1-i_2\eta_{i1}\eta_{i2}\eta_G\eta_D\eta_C^2\frac{n_D}{n_K}\right)$	$\frac{M_s\eta_{i1}\eta_C}{2i_1i_2\eta_{i2}}$	$\frac{M_s\eta_{i1}\eta_C\eta_G\eta_D}{2i_1i_2\eta_{i2}}\frac{n_D}{n_K}$
Machine K — as a motor Machine D — as a motor	$\frac{M_s}{2i_1i_2\eta_{i1}\eta_{i2}\eta_C\eta_D\eta_G}\left(i_2\frac{n_D}{n_K}-i_1\eta_{i1}\eta_{i2}\eta_C^2\eta_G\eta_D\right)$	$\frac{M_s}{2i_1i_2\eta_{i1}\eta_{i2}\eta_C}$	$\frac{M_s}{2i_1i_2\eta_{i1}\eta_{i2}\eta_C\eta_G\eta_D}\frac{n_D}{n_K}$

operational limits and that the speed of rotation of machine K is constant, i.e.

$$n_D = a_1 + b_1M_D \text{ and } n_k = a_2 = \text{const.} \tag{14}$$

In this case the equation of the mechanical characteristic of drive assumes this form:

$$n_s = A + BM_s. \tag{15}$$

The values of coefficients A and B for various operational conditions are given in table 2. Neglecting the variation of the efficiencies of the individual links of the system, we may assume that the drive mechanical characteristic is linear.

Speed control

Speed control of the reducer output shaft is realized, as in a usual generator-motor circuit, by varying the excitation of machines G or D. However, taking into account the presence of a.c. in the system of the non-regulated machine, in both cases the speed control can be exerted only at a constant torque. Equation 1 can be represented in this form:

$$n_s i_2 = 0.5\left(\frac{n_D}{i_1} - \frac{n_K}{i_2}\right)$$

or

$$n_s^* = 0.5\,(n_D^* - n_K^*),$$

where n_s^*, n_D^*, n_K^* - are respectively the speeds of rotation reduced to the shaft and driving gears of the differential.

If $n_D^* > n_K^*$ then $n_s^* > 0$; if $n_D^* < n_K^*$ then $n_s^* < 0$; and $n_s^* = 0$ if $n_D^* = n_K^*$. Varying the magnitude of n_D^* we can get a speed of rotation of the drive output shaft, which is variable in magnitude and direction. The direct and reverse sense of rotation of the output shaft is realized without reversing the sense of rotation of the driving motor.

Efficiency

In a general case

$$\eta_g = \frac{\text{useful power}}{\text{power taken from the grid}} = \frac{M_s \cdot n_s}{M_K \cdot n_K} \eta_K$$

where η_K - efficiency of motor K.

Substituting the values of M_K and n_D we get

$$\eta_g = \frac{an_s}{\beta n_K - \gamma - \delta M_s} \tag{16}$$

(the values of a, β, γ and δ for the conditions under consideration are given in table 2).

The efficiency of the transmission gear is proportional to n_s; the control is uneconomical and involves losses. From this point of view the control in the drive is analogous to the control of electrical machines, when the speed on no-load running remains constant.

The power N_{grid}, taken by motor K from the grid, when the load torque is applied to the gear output shaft and for a speed of rotation of the shaft equal to zero is:

$$N_{grid} = \frac{M_K n_K}{\eta_K}.$$

The values of M_K are taken from table 1, putting $\frac{n_D}{i_1} = \frac{n_K}{i_2}$

Thus, the advantages of the drive system described above are:

(1) the possibility of obtaining a speed of rotation of the driven shaft as small as we like, without decreasing the speed of rotation of the driving shaft to a value, that is undesirable from the point of view of the cooling of the motor.

(2) the possibility of reversing the sense of rotation of the driven shaft, when

TABLE 2

Machine operational conditions	Coefficients in formulae (15) and (16) for different operational conditions of the electrical machines of the drive					
	A	B	α	β	γ	δ
Machine D - as a generator Machine K - as a motor	$\frac{a_1 i_2 - a_2 i_1}{2 i_1 i_2 i_3}$	$\frac{b_1 \eta_1 \eta_C}{4 i_1^2 i_3^2 \eta_3}$	$2 i_1 i_2 i_3 \eta_2 \eta_3 \eta_C \eta_K$	i_1	$i_2 a_1 \eta_1 \eta_2 \eta_C^2 \eta_D \eta_G$	$\frac{b_1 i_2}{2 i_1 i_3 \eta_2 \eta_C \eta_C \eta_D}$
Machines D and K as motors	$\frac{a_1 i_2 - a_2 i_1}{2 i_1 i_2 i_3}$	$\frac{b_1}{4 i_1^2 i_3^2 \eta_1 \eta_3 \eta_C}$	$2 i_1 i_2 i_3 \eta_1 \eta_3 \eta_C \eta_D \eta_G \eta_K$	$- i_1 \eta_1 \eta_2 \eta_C^2 \eta_D \eta_K$	$- i_2 a_1$	$\frac{b_1 i_3}{2 i_1 i_3 \eta_1 \eta_3 \eta_C}$

the sense of rotation of electrical machines remains unaltered;

(3) the possibility of obtaining wide limits of speed variation of the driven shaft for relatively narrow limits of speed control of electrical machines.

The disadvantages of drives of this kind are: low efficiency when operating under the conditions of the control characteristics, and the comparatively complicated construction of the reducer.

Conclusions

(1) The method proposed makes it possible to choose correctly, by means of simple calculations, the proper gear ratios and electrical machines of the generator-motor system with a differential reducer.

(2) The properties discussed enable the field of rational application of this system to be determined.

Translated by S. Szymanski

REFERENCES

1. B.M. Shkolnikov and I.I. Sud; Burovoi avtomaticheskii reguliator tipa BAR 150 (Automatic boring regulator type BAR - 150) *Energeticheskii biulleten* No. 7 (1954).
2. A.T. Golovan; Rabota dvukh elektricheskikh mashint cherez mekhanicheskii differentsial, (Operation of two electric machines by a mechanical differential) *VEP*, Nos. 7-8 (1942).
3. A.T. Golovan; *Elektroprivod (Electrical drive)* Gosenergoizdat (1948).
4. V.S. Gudkov; *Elektrichestvo* No. 10 (1956).
5. Electrical differential speed drive *Machinery*, 56, No. 2 (1949).

THE UTILIZATION OF SEMICONDUCTORS IN RELAY PROTECTION*

V.L. FABRIKANT

(Received 8 October 1957)

The utilization of semiconductors permits the improvement of many aspects of relay protection. However, as the first results of developments indicate, the most substantial changes have occurred in the power consumption and overall size of individual relays and protective gear. So with a certain increase in operation speed and a decrease in accurate operation voltage, the power consumption in an impedance relay circuit can be decreased from 60 to 5 W. With the decrease in power consumption there is a reduction in the dimensions of all auxiliary devices, and the overall relay size can on the whole be reduced 3-4 times.

Such a substantial reduction in the power consumption and size of relays make it possible to decrease the dimensions of relay panels and the space reserved for them, and also to revise the construction of current and voltage metering transformers. Possibly the application of metering transformers without steel cores or gap cores will become expedient, which would eliminate distortion in secondary circuits due to metering transformer non-linearity.

The great possibilities which lie in the use of semiconductors in relay protection must be seriously applied to the development of relays and protective gear based on this principle.

It seems that at first it is most desirable to conduct research in various directions so that when the most rational principles have been exposed, all effort can be concentrated on their utilization. Some preliminary results of the developments in relays and protective gear using semiconductors can in our opinion already be appreciated.

As is known, protection comprises three types of dissimilar components:

* *Elektrichestvo* No. 7, 42-45, 1958.

1. Complex protective devices (impedance relays, power directional relays, etc.). These units use the two electrical quantities: voltage and current. Electromechanically the counter-torque is small and plays a secondary role.

2. Simple protective devices (current and voltage relays). These members use a single electrical quantity. Electromechanically, the counter-torque determines the primary parameter of operation.

3. The logical section of the circuit, (intermediate relays and time relays). This section of the circuit must ensure the transmission of a braking pulse with given combinations of the action of the complex and simple units, and the absence of a braking pulse with other combinations.

Let us consider each of these protection components separately.

The design of complex protection units

Two principles are possible for the design of these members: (1) comparison of the vectors $\dot{A}$ and $\dot{B}$ of the two electrical quantities according to absolute magnitude; (2) comparison of the vectors $\dot{A}$ and $\dot{B}$ of the two electrical quantities according to phase.

In the first case the relay must act where $|\dot{A}| \leqslant |\dot{B}|$ or $|\dot{A}| / |\dot{B}| \leqslant 1$ independently of the angle between $\dot{A}$ and $\dot{B}$. The boundary characteristic of such a relay in the complex plane $\dot{A}/\dot{B}$ will be expressed by a circle with a centre at the origin and a radius equal to unity.

If the vector $\dot{A}$ represents a voltage $\dot{U}$, and vector $\dot{B}$ is proportional to the current, a total impedance relay with setting resistance Z_y is obtained.

If vector $\dot{A}$ represents the braking current $\dot{I}_m$, and vector $\dot{B}$ is proportional to the operating current $\dot{I}_r$, a differential relay with braking is obtained.

If each of the vectors $\dot{A}$ and $\dot{B}$ is a linear function of two electrical quantities, for example, voltage and current, i.e.

$$\left.\begin{aligned}\dot{A} &= K_1\dot{U} + K_2\dot{I};\\ \dot{B} &= K_3\dot{U} + K_4\dot{I},\end{aligned}\right\} \tag{1}$$

then the quantity

$$\frac{\dot{A}}{\dot{B}} = \frac{K_1\dot{U}+K_2\dot{I}}{K_3\dot{U}+K_4\dot{I}} = \frac{K_1 Z + K_2}{K_3 Z + K_4}, \tag{2}$$

where

$$Z = \frac{\dot{U}}{\dot{I}}.$$

Expression (2) shows that $\dot{A}/\dot{B}$ is a fractional linear function of the quantity Z. As is known in this case the characteristic, having the form of a circle or straight line in the plane $\dot{A}/\dot{B}$, forms another circle or straight line in the plane Z. By a corresponding selection of coefficients K_1, K_2, K_3 and K_4, a given circle in the plane $\dot{A}/\dot{B}$ can be transformed into any given circle or straight line in plane Z. Thus, an impedance relay can be obtained with a characteristic in the complex plane in the form of a circle or a straight line.

It must be noted that the same characteristic can be obtained with different combinations of coefficients K_1, K_2, K_3, and K_4. In particular, for obtaining a characteristic in the form of a straight line which does not pass through the origin, or in the form of a circle, one of the coefficients can be taken as equal to zero; i.e. one of the quantities $\dot{A}$ or $\dot{B}$ can depend only on the current or only on the voltage.

A block diagram of any complex unit based on the comparison of absolute magnitudes is shown in Fig. 1.

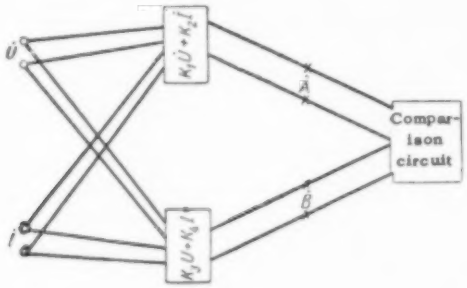

Fig. 1

The devices for obtaining the quantities $\dot{A}$ and $\dot{B}$ are extremely simple, and consist of voltage autotransformers, transreactors and intermediate current transformers. As a rule there are not more than three of these units in both devices, for example, one voltage autotransformer and two transreactors. For directional relays it is sometimes necessary to have an extra slugging circuit to provide for the action of the relay in the presence of faults near the location where it is set up.

However, the chief section, the comparison circuit, can be made up the same for all or almost all complex protective devices, which is a considerable advantage, and at the same time makes the development of this device particularly reliable.

In order to decrease the power consumption and overall size of the circuit, the secondary devices for obtaining the quantities $\dot{A}$ and $\dot{B}$ must have a small

power. Then the resulting power at the outlet will be extremely small, and a sensitive responding unit will be required to provide sufficiently high relay parameters.

It is known that in a number of countries [3, 6, 7] highly sensitive moving-coil or polarized relays with an operating power of the order of 10^{-6}W are used for this end. It seems to us, however, that a more reliable, simpler and more economical solution lies in the application of coarser relays with a semiconductor triode as a d.c. amplifier and an operating power of about 10^{-3}W. With this the responding unit can be made sufficiently reliable and quick-acting.

The final solution to the question of which of the relays indicated should be used as the responding unit can be obtained in our opinion only after comparing the best models of these relays.

Two methods different in principle for making up a comparison circuit are possible with the use of semiconductor triodes as d.c. amplifiers: (1) amplification of each of the quantities to be compared and subsequent subtraction of these amplified quantities; (2) subtraction of the quantities to be compared and subsequent amplification of this difference.

The first method appears to be inappropriate for the following reasons:

1. The amplifier is used in this case as a measuring component, and an error in the amplifier creates a similar error in the relay.

2. This deficiency is considerably heightened by the fact that the amplification factor of semiconductor triodes is variable for various specimens, and depends on the temperature and on the supply voltage. The fulfilment of temperature stabilization requiring individual adjustment and temperature testing for each specimen is not practicable.

3. The use of an amplifier as a measuring component not only fails to simplify the circuit, but complicates it somewhat.

The second method by which a semiconductor triode is used for difference amplification, i.e. in the capacity of a null-detector relay, is more expedient since a variation in the amplification characteristics results only in a change in the insensitivity zone and has comparatively little effect on the primary parameters of the relay. The more sensitive the circuit, the less the zone of insensitivity and the less the value of the change in the triode characteristics.

A possible principal circuit for the comparison of vectors $\dot{A}$ and $\dot{B}$ according to absolute magnitude with a triode amplifier as a null-detector relay is shown in Fig. 2.

With phase comparison of the vectors $\dot{A}$ and $\dot{B}$ the relay must act when

$$\psi < (\dot{A}, \dot{B}) < \psi + 180^\circ, \tag{3}$$

where ψ is a certain constant angle.

Fig. 2

The boundary line corresponding to expression (3) in the plane $\dot{A}/\dot{B}$ will be expressed as a straight line passing through the origin at an angle ψ to the positive axis of the abcissa. If the vector $\dot{A}$ represents the voltage and vector $\dot{B}$ the current, then the relay becomes a power directional relay. However, if each of the vectors $\dot{A}$ and $\dot{B}$ represents a linear function of the two electrical quantities, for example, voltage and current (1), the quantity $\dot{A}/\dot{B}$, as follows from expression (2), is a fractional linear function of Z. By selecting corresponding coefficient values it is possible to transform the straight line representing the boundary line in the plane $\dot{A}/\dot{B}$ into any circle or straight line in the plane Z.

1959

Thus, the angular comparison of quantities $\dot{A}$ and $\dot{B}$, like their comparison according to absolute magnitude, makes it possible to obtain an impedance relay with a characteristic in the complex plane in the form of a circle or a straight line.

Comparison by phase can be performed by determining the fraction of the cycle during which the signs of the compared quantities coincide. So, if the two quantities coincide in phase, their signs are similar during the whole cycle. With an increase in phase divergence, the fraction of the cycle during which the signs of the values coincide decreases, and with divergence equal to 180° it is equal to zero.

Measurement of the fraction of the cycle during which both values coincide in phase can be accomplished by various methods. One of the possible methods is shown in Fig. 3.

Quantities $\dot{A}$ and $\dot{B}$ rectified in a half-wave rectifier are fed into circuit E. The signal appears at the output of this circuit only in that case where both signals were fed into the input; i.e. if quantities $\dot{A}$ and $\dot{B}$ are positive. A responding unit is set at the output whose action depends on the time of pulse flow. In Fig. 3 a relay with a triode amplifier is used in this capacity.

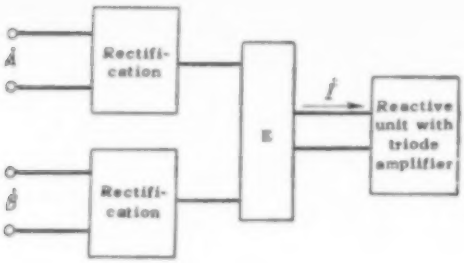

Fig. 3

In the circuit in Fig. 3 the relay with a triode amplifier is used as a measuring component. The inadequacies of such a solution were indicated above.

In the circuit in Fig. 4 [1 and 2], the same time measurement is accomplished by means of a comparison of the voltage on a charged capacitor with the voltage taken from a potentiometer. Since condensor charge and potentiometer feeding are accomplished from the same source, the sign of the voltage difference is independent of the magnitude of the supply voltage, and depends only on the charging time. A relay with a triode amplifier is used in this system as a null-detector relay. As has already been indicated, the relay with a triode amplifier as a null-detector relay must be given preference in our opinion.

In the circuit in Fig. 4, as in the circuit in Fig. 3, the time is measured during which both quantities are positive, which is fully permissible since this time amounts to half the time during which the quantities A and B have the same sign. With this there will be a delayed action of the protective gear. To increase the speed of this circuit an analagous circuit for negative values can be added.

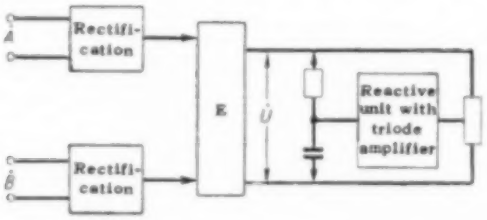

Fig. 4

The pulse principle can also be used for phase comparison, [4]. Here, one of the quantities compared is transformed into short pulses and the other into rectangular pulses, (Fig. 5). Phase comparison is accomplished by determining the sign of the quantity B at the instant when a positive pulse of quantity A appears. An overall view of the block diagram, constructed on the pulse principle is shown in Fig. 6.

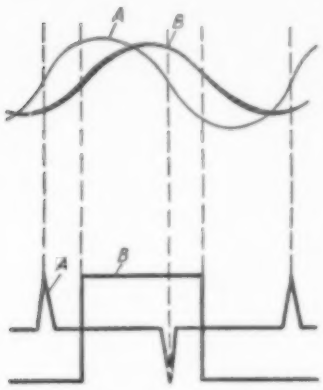

Fig. 5

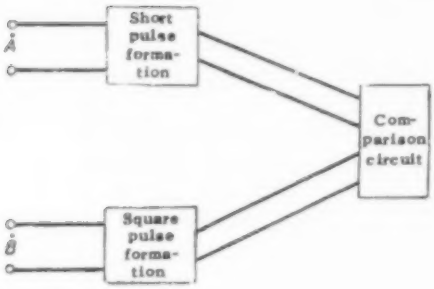

Fig. 6

In principle, the pulse circuit should be the more rapid. However, in the tests made up to now it has been necessary to delay its action in order to tune out transients. Due to this it has not yet been possible to make use of its advantages. In addition, this circuit is more complicated than the others.

It must be noted that circuits comparing absolute magnitudes and phases make it possible to produce any characteristic in the form of a straight line or a circle in a complex plane, and make it possible to have a universal comparison device. However, up to now this unit is produced more simply in an absolute magnitude comparison circuit than in a phase comparison circuit.

Considering the fact that there is not a great deal of experience with new developments, it is our opinion that work must be continued in both directions.

Design of simple devices

Simple units would be produced more simply if the effective electrical quantity were directly supplied to the responding unit which would at the same

time be used as a measuring component. In this case, the use of the responding unit as a measuring component results in a substantial simplification and also an improvement of the parameters. However, considering the essential instability at present of triode amplifier characteristics, it is our opinion that it is impossible even in this case to make use of them as measuring components in relays requiring accurate setting. In order to obtain a setting accuracy within the limits of ± 5 per cent, which is already unacceptable for many relays, the amplification factor must be constant to a degree which is at the present time impossible in practice.

The possibility of obtaining simple relays based on the principle of the comparison of the outputs from linear and non-linear components supplied from a common source was examined. As is seen from Fig. 7, with comparatively small values for a certain quantity, for example current, the non-linear component output is greater than the linear. With large values, however, the linear component output is greater. A block diagram of a simple unit based on this principle is shown in Fig. 8.

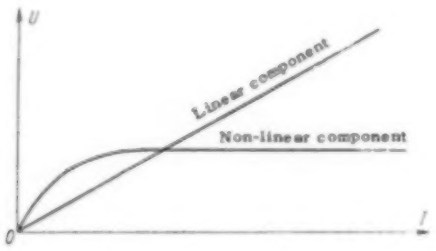

Fig. 7

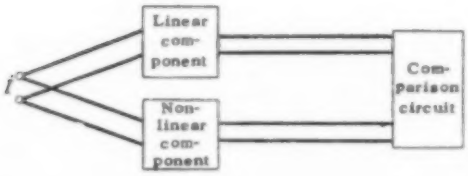

Fig. 8

As tests have shown, the power consumption of such units is greater than for corresponding electromechanical relays. Their application can be justified only for protective gear in which they simplify the complete circuit.

A certain stabilized voltage, fed from an outside source, can also be used as a non-linear component. Here, the difficulty lies in obtaining a sufficiently durable and accurate stabilizer in which capacity a Zener diode might possibly be used.

It must be noted that in the use of semiconductors as null-detector relays, complex units are obtained which are no more complex than simple units. In this connexion, a relay with braking must more frequently be applied. So, a negative sequence current relay is not apparently complicated if phase current braking is used for it. In addition, its characteristics can be improved by this.

The design of the logical section of the circuit

The functions performed by intermediate relays and time relays are reduced to a series of logical operations, for example, "or", "and" and "not", and to the introduction of time.

So, operation "or" is fulfilled by parallel connected intermediate relay contacts which are normally open, and the operation "and" by the same contacts connected in series. These operations can be carried out by the use of semiconductors, [5].

In our opinion, in the design of protection circuits it would be undesirable to seek to exclude all electromechanical relays, replacing them by semiconductors. Intermediate relays or logical semiconductor circuits must be applied depending on which of them give the best solution for the circuit as a whole.

Translated by F.J.C. Griffiths

REFERENCES

1. C. Adamson and L.M. Wedepohl; Power system protection with particular reference to the application of junction transistors to distance relays. *The Proceedings of the Institution of Electrical Engineers;* Pt. A. No. 10 (1956).
2. C. Adamson and L.M. Wedepohl; A dual-comparator mho-type distance relay utilizing transistors. *The Proceedings of the Institution of Electrical Engineers;* Pt. A. September (1956).
3. G.I. Atabekov; Application of moving-coil and polarized relays to relay protection circuits. *Elektrichestvo;* No. 7 (1956).
4. H.C. Barnes and R.H. Macpherson; Field experience-electronic mho distance relay. *Trans. Amer. Inst. elect. Engrs.*, Vol. 72, Pt. III (1953).
5. A.I. Kitov; *Elektronnye tsifrovye meshiny, (Electronic digital computers).*
6. H. Nengebauer; *Gleichstrom-Drehspulelais mit Gleichrichter fur die Seletivschutz-technik.* (D.C. moving-coil Relay and Rectifier for Selective Protective Gear). ETZ; No. 12 (1950).
7. Stark; Neuzeitliche Relaiskonstruktionen. *(Contemporary Relay Designs). Deutsche elektrotechnik,* No. 6 (1955).

CONTROLLED REACTORS FOR LONG-DISTANCE TRANSMISSION*

I.S. BRUK

(Received 29 July 1957)

At the present time the construction of large-scale hydroelectric stations and the connexion of energy systems into a single h.v. system are widespread occurrences. In this regard the development of measures for further increases in the power and distance of electrical energy transmission is of great significance. The majority of transmissions in time lose their initial "through" nature as power is drained off and other systems are connected at intermediate points. In these cases an economical solution can be obtained by the use of three-phase current; however, with long transmission distances this meets serious difficulties which are not to be overcome by only stepping up the voltage.

Economic requirements dictate the necessity of amplifying the transmitted power which flows in one circuit of a transmission line in order to compensate for the cost of the line which increases with the length. However, stability conditions prevent this. At the same time underloading the line in relation to its natural power causes an unfavourable voltage condition. Thus we encounter a serious contradiction which can be resolved only by shortening the electrical length of the line. One way or another all the means of increasing line capacity have been applied at various times.

The electrical length of a line, equal to 2π times the ratio of its geometric length to its wavelength, is directly proportional to the current frequency and $\sqrt{L_0 C_0}$. To reduce it, either its capacitive susceptance, or its inductive resistance per unit length or both must be reduced.

In actual practice, as is known, there has been an increase in the use of reactors for capacitive current compensation and capacitors to compensate for the inductive drop in voltage in the line. As shunt compensation with the aid of reactors and series compensation with the aid of capacitors are not simple

* *Elektrichestvo*, No. 7, 14-19, 1958.

conceptions, many problems arise in their application in practical conditions. Some of them, relative to the use of reactors, are considered below. The reactor power necessary for full compensation of discharge current for each thousand kilometres overhead line is slightly greater than the natural power of the line. For example, for a h.v. line with split conductors (wave resistance 300 Ω) with voltage 600 kV for a length of 2,000 km the necessary reactor power is about 2.5 GVA for one circuit. With the distribution of this power at several points to distances of 300-400 km, extremely powerful reactor groups are required with a unit power of 200-300 MVA.

The creation of powerful reactors presents a complex technical problem. A reactor possessing a linear volt-ampere characteristic should operate with a magnetic circuit containing air gaps of considerable volume in which almost all the energy of the magnetic circuit is concentrated. With a frequency of 50 c/s and power of 100 MVA the magnetic energy maximum is:

$$A_m = \frac{100\,000}{314} = 319 \text{ kW hr}$$

The air gap volume

$$\frac{A_m \, 10^{11}}{0.4 B_m^2} = \frac{319 \cdot 10^{11}}{0.4 \times 256 \times 10^6} = 311 \times 10^3 \text{ cm}^3,$$

i.e. almost 1/3 m³, corresponds to this with a maximum induction of B_m = 16,000 G.

It is obvious that the concentration of such a volume in one gap with a core diameter of the order of 0.8-1.0 m is unsuitable, and it must be distributed at several gaps according to core height. Serious difficulties (apart from obtaining a stable construction) are caused by heating due to additional losses in the copper of the winding and in the construction elements.

However, a linear volt-ampere reactor characteristic is not the best solution to the problem of increasing line capacity for long distances. For example, compensation of 50 per cent of the capacitive current with an unchanged value for the natural power reduces the electrical length of the line to half the length of a non-compensated line. With a great line length, for example 2000 km, it would be unsuitable to confine oneself to only one compensation for reactance and capacitive current. The subdivision of a long line into a number of 400-600 km sections at the ends of which voltage is maintained independently of changes in line loading, for example with the aid of synchronous compensators, imparts to it the stability characteristics of a line one section long. Here, the desired results are attained more fully the more the separate sections of the line are independent; i.e. the more stably the voltage is maintained.

The voltage can be maintained at support points with the aid of reactors possessing a sufficiently steep characteristic for the dependence of reactive current on voltage, (according to r.m.s. value); here both methods of shortening the electrical length of a line are combined in one device.

With this in mind we suggested a system of two three-phase transformer groups whose cores are premagnetized by a direct current according to the circuit shown in Fig. 1*. Varying the direct premagnetizing current makes it possible to displace the operating point on the magnetization curve, thereby altering the reactive power Q required by the reactor with a given voltage U, and simultaneously the steepness of the characteristic $Q(U)$.

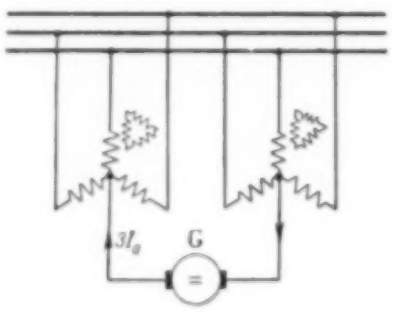

FIG. 1. Transformer premagnetization system

The increase in the power of the combined systems necessarily involves a rise in the general level of transmission voltage and an increase in the requirements made on the compensating reactors. Therefore, combining a reactor and transformer in one unit presents certain economical advantages, particularly in those cases where a consumer or source of energy is connected to the line at the location of the reactor assembly.

The characteristic of a three-phase transformer group with premagnetization

The characteristic of a reactor whose core is premagnetized by a direct current is determined only as the magnetic characteristic of the core if active losses are disregarded. If the average value for the magnetic flux (Φ_1) in the core is found, then by calculation or graph it is easy also to find the value for the m.f. constant component for a given amplitude value (Φ_m) of a sinusoidally alternating magnetic flux.

*I.S. Bruk. Author's certificate No. 75749 (1948).

With the replacement of the magnetic characteristic shown in Fig. 2 by a straight line $i = K(\Phi - \Phi_0)$, the current curve will consist of sinusoid and rectilinear sections varying in dependence on the constant displacement flux Φ_1, and the sinusoidal flux amplitude Φ_m (Fig. 3). When the reactor terminal voltage and premagnetization are so correlated that the condition $\Phi_m - \Phi_2/\Phi_0 < 1$ is fulfilled, the expression for the nth harmonic of the magnetizing current (Fig. 4) assumes the simple form:

$$\pi I_n = K\Phi_m \int_{t_1}^{\pi - t_1} (\sin t - \sin t_1) \sin nt \, dt, \tag{1}$$

from whence

$$2\pi I_1 = K\Phi_m (\pi - 2t_1 - \sin 2t_1), \tag{2}$$

and for premagnetizing current I_0

$$2\pi I_0 = K\Phi [2 \cos t_1 - \sin t_1 (\pi - 2t_1)], \tag{3}$$

where

$$\sin t_1 = \frac{1 - \Phi_1/\Phi_0}{\Phi_m/\Phi_0}. \tag{4}$$

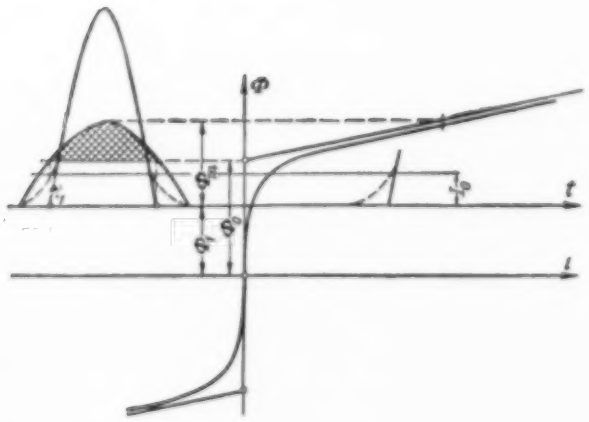

FIG. 2. Graph plotted to determine magnetizing current components

The conventional current curves shown in Fig. 3 will in reality be rounded as the dotted lines show. However, current "cut-off" is clearly indicated. On the basis of this system other phenomena are explained which are to be observed in steel circuits.

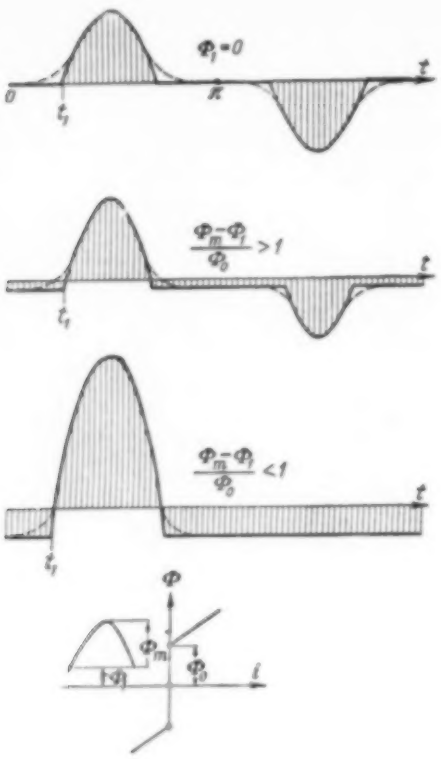

FIG. 3. Characteristic curve forms for the magnetizing current

In connecting the windings of the two three-phase groups, as shown in Fig. 1, all the even harmonics of the magnetizing current are in opposition and cannot develop in the external circuits when the transformers are identical which in actual practice is the case for large transformers. These harmonics are localized in the transformer windings and are distributed in inverse proportion to their dispersion resistance. The double frequency component grows together with the premagnetizing current. Certain data for rating the value of the second harmonic are introduced below.

The third harmonic and its uneven multiples are localized chiefly in the lower voltage delta winding. The amplitude of the third harmonic depends strongly on premagnetization. With a certain small value for the premagnetizing current, the third harmonic amplitude is at a minimum. It increases with further increase in premagnetization. These relationships can be obtained from the magnetic characteristic; they are explained by the mechanism of third harmonic formation:

its strong dependence on the "cut-off" angle t_1 which can be demonstrated by calculating the amplitude of this harmonic according to formula (1).

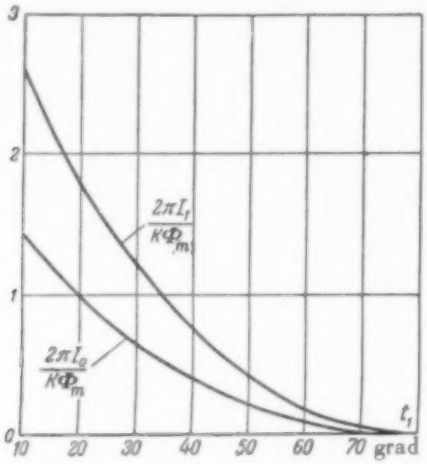

FIG. 4. Graph for determining the premagnetization current and the basic harmonic of magnetizing current

1959

The fifth and seventh current harmonics penetrate into the external circuit (into the line), and their distribution according to the separate circuits (windings) depends on the connexion of the circuit being considered with the magnetic flux of the transformer core, the reactor. Here, it is obviously necessary to consider the reactance for the given harmonic and also for the external circuit connected at the transformer terminals (line, load, etc.).

We present some of the results of the calculation for the reactive power characteristic of a reactor with premagnetization. A rectilinear magnetic characteristic with a steepness of $K = 7$ is the basis of the calculation which makes a good approximation of the actual magnetic characteristic of large transformers. Expressing all values in relative units we obtain, for example, for $\Phi_m = 0.8$ ($U = 0.8$), $I_1 = 0.23$ and $K = 7$, the "cut-off" angle $t_1 = 56°$ according to formula (2), and according to formula (3) $I_0 = 7 \times 0.8 \times 0.135/2\pi = 0.120$ or $0.120 \times \sqrt{2} = 0.170$ (r.m.s. value). Analogously for $I_1 = 0.366$, we find $t_1 = 50°$, $I_0 = 0.193$ (0.273), and for $I_1 = 0.675$ we obtain $t_1 = 40°$; $I_0 = 0.368$ (0.52).

These results agree with experimental data. The dependence of reactive power on voltage with constant premagnetization is approximately parabolic. Thus Thus, a reactor with premagnetization, if it is diverted from higher harmonics, acquires the properties of a reactor with a linear characteristic whose steepness is controlled.

It is possible to put transformer premagnetization into actual practice by various methods. One of the systems is shown in Fig. 5 for earthed neutral transformers. Here two d.c. sources are used, preferably controlled rectifiers. The d.c. source must be shunted for the passage of alternating current. The shunting resistance must be selected several times greater than the transformer winding resistance. The power of the d.c. source for premagnetization is negligible. If the losses in power transformer windings are rated at ¼ per cent for premagnetization by a ⅓ rated current, it would be sufficient to have a d.c. source of approximately 0.05 per cent of the transformer group power. In fact a greater power must be provided: double, and with a reserve according to the voltage, bearing in mind control requirements. A source having a total output of approximately 200 kW would be required for a group with an output of 180 MVA.

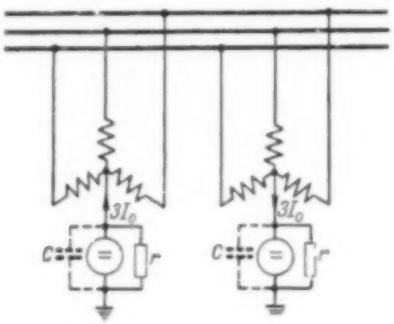

FIG. 5. One of the premagnetization circuits with earth neutral

The possibility of evenly varying the reactive power required by the reactor by varying premagnetization makes it comparatively easy to control the line voltage automatically with the object of increasing the stability, above all static stability. Here known difficulties arise in connexion with control lag. The fact is that with variation of the premagnetizing current the direct magnetic flux in the cores varies considerably more slowly since it is impeded by currents developing in the lower voltage delta winding. The time constant of this process, the true steadying time, amounts to more than 10 sec. Therefore, in order to quicken up control, forcing must be used, and the system must be constructed to avoid overshoot and swings in the complex oscillatory system which is formed by the synchronous machines at the ends of the line together with the reactors.

Results of tests

In order to determine the electromagnetic characteristics of large transformers premagnetized by a direct current, and the feasibility of prolonged transformer

operation under such conditions, tests were made on ODTG - 60000/220 transformers at the Noginsk substation, Mosenergo, * in March 1956.

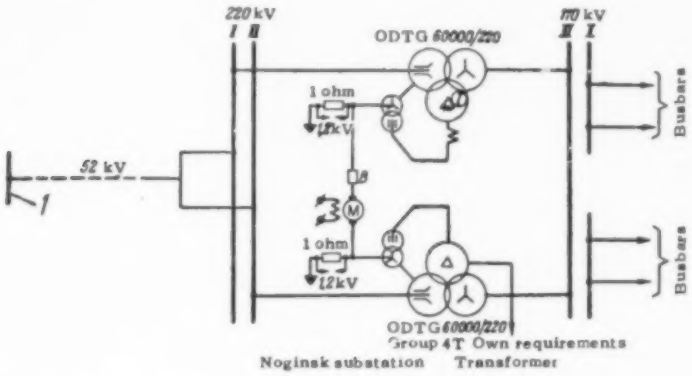

FIG. 6. Circuit for connecting transformers during tests
1 – supply substation

The following characteristics were determined:

1. The dependence of the reactive power required by the transformers on the premagnetizing direct current.

2. Voltage and current curve forms.

3. The time for the system to be steadied when making and breaking the d.c. circuit.

It was suggested that the basis of the tests should be an attempt to reveal to what extent local heating of the transformer magnetic circuit and the elements of its construction can be caused by stray losses. The tests were performed with the system shown in Fig. 6. The voltage at the busbars amounted to 110 kV and was controlled with the aid of series connected transformers. An exciter of a synchronous compensator served as the d.c. source.

The dependence of the reactive power required by the test transformers on the applied alternating voltage and the premagnetizing direct current are shown in Figs. 7 and 8 (conveniently: $U_{baz} = 115$ kV; $Q_{baz} = 360$ MVA; $I_{baz} = 472.5$ A).

From Fig. 8 it is seen that with a constant alternating voltage, the reactive power varies almost directly with direct current I_0 at an average steepness of 1.2 per cent for 1 per cent of the direct current, when $U = 0.75 - 0.9$.

* The tests were made by S.S. Vorob'ev and Iu.S. Vukolov with the participation and guidance of M.S. Libkind who carried out all the work in preparing the tests.

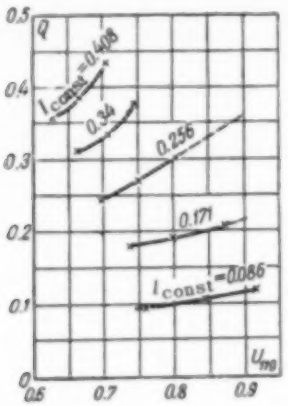

FIG. 7. Dependence of reactive power on voltage on 110 kV busbars

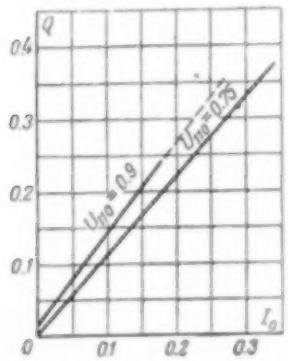

FIG. 8. Dependence of reactive power on premagnetization current

The maximum value for the reactive power Q = 156 MVA was obtained with an alternating voltage of U = 81.2 kV (0.71) and direct current of I_0 = 193 A (0.408). Here the power supplied by the d.c. source amounted to 141 kW; i.e. less than 0.1 per cent of the required reactive power.

The voltage at the supply substation during the experiments was almost unchanged. The currents which flowed in the 220 kV line contained the fifth higher harmonic.

With a premagnetizing current of I_0 = 120 A (0.256) in phase and an alternating voltage at the 110 kV busbars, a value of U = 92 kV (0.8) was obtained which corresponded to the reactive power demand Q = 108 MVA (0.3). The voltage curves at the Noginsk substation had the following harmonic composition:

Phase voltage at 220 kV busbars

$U_1 = 110$ kV; $U_2 \approx 4$ kV; $U_3 \approx 5$ kV; $U_5 = 4$ kV; $U_7 = 1$ kV; $U_9 = 6$ kV;

Phase voltage at 110 kV busbars

$U_1 = 53$ kV; $U_2 \approx 1.5$ kV; $U_3 \approx 0.5$ kV; $U_5 \approx 7$ kV; $U_7 \approx 3$ kV; $U_9 \approx 1$ kV;

Harmonic analysis of the curve for the current in the 220 kV windings gave the following results (r.m.s. values):

$$I_1 = 181 \text{ A}; \quad I_2 \approx 23 \text{ A}; \quad I_3 \approx 9 \text{ A}; \quad I_5 \approx 46 \text{ A}; \quad I_7 \approx 5 \text{ A}.$$

A current of predominately double frequency flowed in the 110 kV windings. Triple frequency currents were almost completely localized in 11 kV delta windings.

A full double frequency current applied to the 220 kV winding amounted to 150 A (r.m.s. value) in one of the operations which gives 150/120 = 1.25 A per 1 A direct current. In other conditions, other relative values for double frequency current were obtained; however, in all cases they were close to unity.

1959

It is desirable to pass a direct current through the higher voltage windings. Then a double frequency current will flow in the medium voltage windings, the r.m.s. value of which is approximately equal to the applied d.c. value. The triple frequency current is concentrated basically in the lower voltage delta windings.

Quintuple frequency currents, as has already been noted, flowed in all windings connected with external circuits. During the experiments only 220 kV windings were so affected. Therefore, the amplitude of the fifth harmonic of the current in these windings reached approximately 25 per cent of the first harmonic amplitude in one set of conditions.

As a first approximation it can be considered that 0.3-0.5 A of quintuple frequency current was generated for each ampere of premagnetizing direct current. The current flowing in the 220 kV line also contained the fifth higher harmonic. In one of the operations the relative amplitude of the fifth harmonic in the current measured at the supply substation amounted to 10 per cent.

A transient process was created by means of closing and breaking circuit-breaker V in the d.c. circuit (Fig. 6) with a previously excited generator. Direct currents established up to 160 A were tripped in phase.

Oscillographic recordings indicated that the duration of the transient process in the a.c. circuit (of the 220 kV winding), depending on the value of the supply voltage and the direct premagnetizing current, amounts to 20 to 40 sec. The direct current is established in 5-7 sec.

The heating of the magnetic circuit was observed with the aid of resistance thermometers set in the tank and in the output section of one transformer of the group.

Extended premagnetization was carried out under the conditions shown in Table 1.

TABLE 1

Voltage kV	Current A	Power MVA	Oil temperature at beginning of experiment °C	Duration of experiment, hr	Oil temperature at end of experiment °C
103	40.7	41	35...40	4	35...40
101	80.8	75	37...40	5	49...56
92	121	121	36...38	Total 4.5 hr with interval of 2.5 hr	43...46

It can be concluded from the experiments that with premagnetization by a direct current, the total losses in the transformer were slightly increased in comparison with no load losses. Measurements showed that the rate of increase of the yoke temperature was approximately the same as for oil; this is substantiated by the absence of local heating in the yoke.

The steel pressing limbs of the upper yoke were heated under the first set of conditions to 75°C, under the second to 90°, and under the third set, the limb temperature could be expected to reach 100-105°C. Rapid limb heating was conditioned by eddy currents caused by the field of magnetic circuit dispersion.

The experiments indicated the following facts:

1. The electromagnetic characteristics of the Noginsk substation transformers under conditions of premagnetization by direct current, correspond basically to the theoretical propositions and results of the experimental study made in 1954 at Hydro-electric station – 13, Mosenergo.

2. With short transformer premagnetization (10-15 min.) the reactive power required can be brought up to at least half the rated power of the two groups;

3. With prolonged premagnetization, the reactive power required by ODTG-60000/220 transformers can be brought up to approximately 25 per cent of their rated power. Further increase in premagnetization is limited by heating of the magnetic circuit steel yoke limbs.

Conclusion

Transformer premagnetization by a direct current is an economical solution to the problem of obtaining a powerful controlled reactor for long-distance a.c. transmission.

Premagnetization is also applicable to power autotransformers which, undoubtedly, will be widely used for connecting long-distance transmission with intermediary systems in the U.S.S.R.

Here it must be remembered that direct current for all practical purposes will flow in only the main section of an autotransformer winding, since the resistance of the connecting busbars is small in comparison to the resistance of the remaining part of the winding. This does not affect the electromagnetic characteristic of an autotransformer as a reactor, if the windings are distributed with sufficient evenness.

A detailed consideration of the effect of a transformer (reactor) with premagnetization on the course of transient processes during line making and breaking, and on dynamic overvoltages is beyond the scope of this paper. This effect can be roughly evaluated by comparing it with the connexion of a choke reactor premagnetized from an independent source.

1959

At the present, work is being done which is connected with the examination of these questions as well as the permissible load of multi-winding transformers and autotransformers.

Additional experimental studies must also be carried out on the interaction of the reactor and the long-distance line, as well as the constructive development of magnetic circuit parts in order to decrease additional losses and heating.

Translated by F.J.C. Griffiths

NEW METHODS OF CONNECTING STARTER-CONTROL RESISTANCES OF ASYNCHRONOUS MOTORS*

I.K. KHRUSTALEV

Siberian Metallurgical Institute

(Received 9 July 1957)

In contemporary methods of relay switch control of asynchronous motors there is a considerable array of switch connexions of rotor magnetic sets by means of which disconnexion or connexion in series of resistance steps in the engine rotor circuit take place. In this case the number of resistance steps and, consequently, the number of rheostat characteristics of the motor are equal to the number of contactors. Just as two out of 5 ..... 9 rheostat steps are usually preliminary, the number of working steps does not exceed 3 ..... 9. The presence of a relatively small number of resistance steps produces a deterioration in the performance of the starter and brake action of the motor, irregularity in its speed control and also contributes to the emergence in the system of intolerable dynamic loads. An increase in the number of steps as a result of an increased number of contactors in a magnetic set makes the starter systems of the motor less reliable and is not usually implemented.

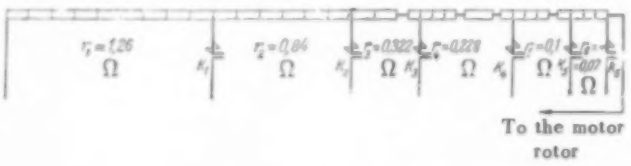

FIG. 1. Method of equipping a single-phase rheostat by means of contactor-connexion in series
K_1 ..... K_6 = contactors

It is possible to eliminate the defects of existing systems of resistance connexions in the case of switch connexions in parallel and parallel-series.

* *Electrichestvo* No. 7, 55-56, 1958.

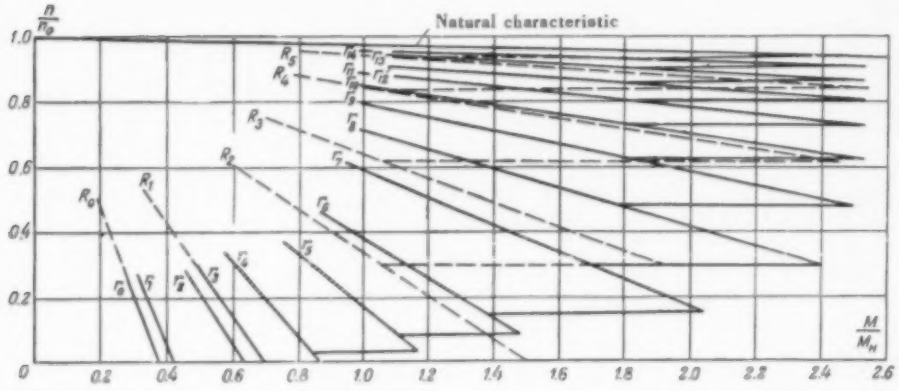

FIG. 2. A series of rheostatic and mechanical characteristics of an induction motor by means of contactor connexions in series ($R_0 \ldots R_5$) and in parallel-series ($r_0 \ldots r_{14}$)

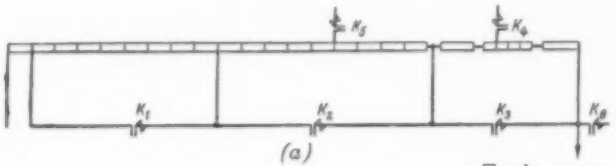

(a)

Contactor	Number of step															
	1	2	3	4	5	6	7	8	9	10	11	12	13	14	15	16
K_1	—	—	×	—	—	—	—	×	×	—	—	×	—	—	×	×
K_2	—	—	—	×	×	—	—	×	×	×	—	×	—	×	×	×
K_3	—	×	—	—	×	—	×	—	—	×	—	×	×	×	×	×
K_4	—	—	—	—	—	—	—	—	—	—	×	—	×	×	×	×
K_5	—	—	—	—	—	×	×	—	×	×	—	—	—	×	×	×
K_6	—	—	—	—	—	—	—	—	—	—	—	—	—	—	—	×

(b)

FIG. 3. Method of equipping a single-phase of resistances and a diagram of commutation of switches when connected in parallel-series. × = closed contact

Thus, by one of the methods of parallel switch connexions of a six-contactor

rotor set one can obtain 18 rheostat ratings of the motor instead of six obtained by the standard method of switch connexion.

TABLE 1

Schedule of resistances of a single-phase rheostat with switch connexion in parallel-series

Number of step	Resistance of step, Ω	Number of step	Resistance of step, Ω
1	2.82	9	0.396
2	2.52	10	0.253
3	1.70	11	0.170
4	1.56	12	0.14
5	2.26	13	0.074
6	0.902	14	0.0595
7	0.602	15	0.0416
8	0.44		

A six-step metallic rheostat has been designed and equipped for one of the coal-mines in the Karaganda coal-field. The method of complementing a single-phase rheostat is shown in Fig. 1 and a series of rheostatic mechanical characteristics of an induction winding motor is represented in Fig. 2 by dotted lines (characteristics $R_0 \ldots R_5$). By another method of connecting resistances of this rheostat and by parallel-series switch-connexion, 15 rheostat mechanical characteristics of the motor are obtained, (characteristics $r_0 \ldots\ldots r_{14}$ in Fig. 2). The method of equipping a single-phase of resistances for this instance and the diagram of switch commutation are produced in Table 1 and in Fig. 3.

Conclusion

It is possible to obtain a greater number of rheostat mechanical characteristics of a motor with a small number of contactors, resulting in an increased reliability in the motor control system, by means of metallic rheostats inserted in accordance with the resistance connexion methods which have been suggested.

TRANSIENT PROCESSES IN A MAGNETIC BOOSTER WORKING IN A RELAY SYSTEM*†

R.A. LIPMAN and I.B. NEGNEVITSKI

Moscow Institute of Energy

(Received 17 February 1958)

Transient processes in an actively loaded magnetic booster working in a relay system (non-contact magnetic relay) are examined by the authors in comparative detail in [1, 2]. It is, however, well known from practical experience that in certain cases considerable retardation in the operation and release of the relay is observed which is somewhat higher than the values determined by the formulae produced in [1].

In the work under consideration a physical explanation and a rigid mathematical analysis of the effect of delay on an example of a most elementary non-contact magnetic relay are provided. Formulae have been deduced by which it is possible to calculate the time of delay and also the total time of operation and release at initial displacement.

For simplification, the magnetization curve is assumed to be perfect. The main relay system with an external return connexion is shown in Fig. 1a, and with an internal and auxiliary feedback in Fig. 1b. In studying the effects in a non-contact magnetic relay we assume that the rectifiers are perfect and do not take into account the influence of eddy currents.

Transient processes in an ordinary magnetic booster without feedback are examined by the authors in [5] and in half-phase (high-speed) boosters in [4]. In both cases it was shown that provided the maximum amplitude of the alternating component induction B_m is less than the saturation induction B_s the indicated effect of delay in a transient process can take place. The reasons for delay in a

* *Electrichestvo* No. 7, 25-30, 1958.

† From a report on magnetic boosters in the Seminar at the Institute of Automation and Telemechanics Akad. Nauk U.S.S.R.

transient process in a relay system are of that particular nature.

In this way an essential (but not always adequate) condition for the presence of delay is as follows:

$$B_m < B_s \text{ or } E < 2E_s, \tag{1}$$

where E_s = the e.m.f. of saturation of one choking-coil, determined by the formula:

$$E_s = 4fw_\sim SB_s \times 10^{-8} * \tag{2}$$

Condition (1) is conveniently written in the form:

$$\varepsilon = \frac{E}{2E_s} < 1 \dagger \tag{3}$$

and the relative value ε called the degree of saturation [3].

When $\varepsilon < 1$ during the transient process, there is an interval of time when, for instance, an increase in the constant component of induction B_0 occurs in one core, but the absolute value of induction still does not amount to the induction of saturation. During all this time the cores are not saturated and we may assume that the current in the load remains at zero. This in fact also explains the presence of delay.

Transient processes in a relay are examined in respect of current and inductive values averaged per phase (or half-phase) on the supposition that the "natural magnetization process" takes place, and on those assumptions which are usually obtained by analysis of transient processes in magnetic boosters [1]. In addition, it is possible to assume that the static dependence of mean values of the current in the load I on the control current I_y and of the constant component of induction B_0 on the current I_y are maintained in the transient process for averaged values.

The dependence of B_0 on I_y for various ε for a magnetic booster with a feedback is shown in [5]. Below, the dependence of B_0 on I_y is produced in the relay system when $\varepsilon < 1$, which determines the course of the transient process and graphically illustrates the presence of delay.

* Here and below the mean values of e.m.f., currents, and induction will basically apply. Index (av) omitted.

† For the method with internal feedback $\varepsilon = E/E_s$

Relay system

At initial displacement the magnetic booster possesses the relay rating shown in Fig. 2a in relative units. Here the ratings of the booster without feedback and direct feedback are shown.

We shall determine in relative units the basic parameters which characterize the performance of a non-contact magnetic relay. The load current and the inductive currents in other circuits we shall refer to as the maximum load current I_{max} when $\epsilon = 1$, and the induction as the saturation induction B_s.

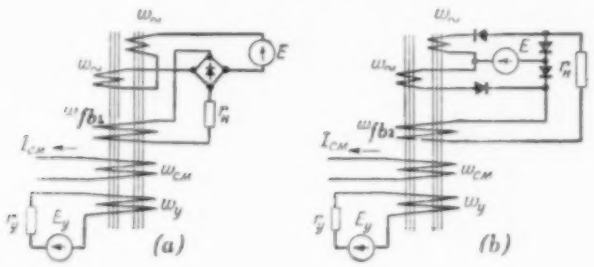

FIG. 1. Principal non-contact magnetic relay systems
a – relay with external feedback
b – relay with internal and auxiliary additional external feedback
E – e.m.f. of alternating current feed of frequency f
E_y – e.m.f. of direct current control (signal)
r_H – resistance of load
r_y – total resistance of control circuit

At full saturation the following relationship between the parameters of the system takes place:

$$I_{max} = \frac{E}{r}; \quad I^0_{max} = \frac{Er}{2E_s f} = \varepsilon. \tag{4}$$

The width of the relay rating (loop):

$$\Delta = I_{max} \frac{w_\sim}{w_y}(k_{fb} - 1);$$
$$\Delta^0 = \varepsilon(k_{fb} - 1). \tag{5}$$

The relative displacement current * =

* Anywhere below I_{cm} is the absolute volume of displacement current.

$$I^0_{cm} = I_{cm} \frac{w_{cm}}{w_\sim} \cdot \frac{r}{2E_s}. \tag{6}$$

The operating and release currents:

$$\begin{aligned} I^0_{op} &= I^0_{cm}; \\ I^0_{rel} &= I^0_{cm} - \Delta^0 = I^0_{cm} - \varepsilon (k_{fb} - 1). \end{aligned} \tag{7}$$

The reset factor of the relay:

$$k_{\text{reset}} = \frac{I_{rel}}{I_{op}} = 1 - \varepsilon \frac{k_{fb} - 1}{I^0_{cm}}. \tag{8}$$

The reserve factor is determined by the formula:

$$\begin{aligned} k_{\text{reserve}} &= \frac{I_y}{I_{op}} = \frac{I^0_y}{I^0_{op}} = \frac{E^0_y}{I^0_{cm}} = \\ &= \frac{E^0_y (1 - k_{\text{reset}})}{\varepsilon (k_{fb} - 1)}, \end{aligned} \tag{9}$$

where

$$E^0_y = \frac{E_y w_y}{r_y w_\sim I_{\max}}.$$

The initial value of the load current:

$$\begin{aligned} I_0 &= \frac{I_{cm} w_{cm}}{w_\sim} \cdot \frac{1}{k_{fb} + 1}; \\ I^0_0 &= \frac{I^0_{cm}}{k_{fb} + 1}. \end{aligned} \tag{10}$$

In these formulae r is the total resistance of the alternating current circuit.

The dependence of the constant component of induction on the control current is produced in comparative units in Fig. 2b which corresponds with the relay rating of the booster represented in Fig. 2a when $\varepsilon < 1$. This dependence can easily be represented by the curve $B_0 = B_0 (I_y)$, which is familiar for a procedure without feedback, and with a direct feedback Fig. 2b.

Section 2-3 corresponds with the performance of a relay with a negative feedback. For this section the following relationship takes place:

$$B_0^0 = \frac{B_0}{B_s} = -(1-\varepsilon) + \frac{I_y^0 - I_{cm}^0}{k_{fb}+1} \tag{11}$$

and

$$\frac{dB_0^0}{dI_y^0} = \frac{1}{k_{fb}+1}. \tag{12}$$

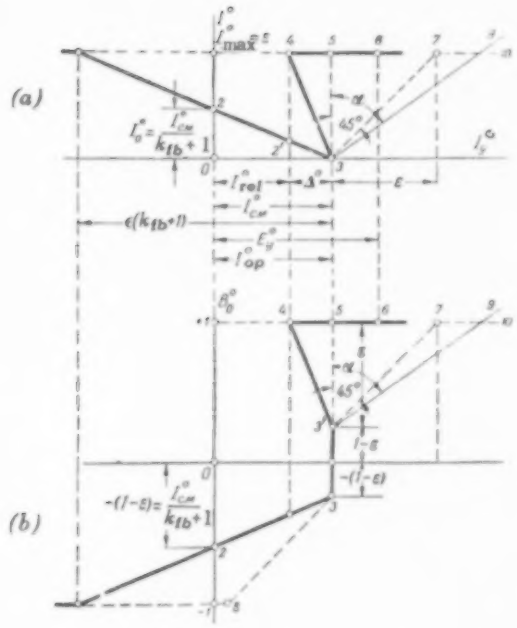

FIG. 2. a – relay rating in relative units at initial displacement, corresponding to normal open contact operation (lines 2-3-4-6); booster rating without feedback (lines 3-7-10); direct feedback (lines 3-9); b – dependence of direct component of induction on control current in relative units, corresponding to relay rating 2-3-4-6; line 8-3-3′-7-10 is the dependence of B_0^0 on I_y^0 of the booster without feedback when $\varepsilon < 1$; line 3′-9 is the direct feedback. The scales along the axes of the ordinates; $\tan\alpha = k_{\text{feedback}}$

Section 3′-4 corresponds with the region of unstable relay operation. For this section it is possible to write:

$$B_0^0 = 1 - \varepsilon + \frac{I_{cm}^0 - I_y^0}{k_{fb}-1} \tag{13}$$

and

$$\frac{dB_0^0}{di_y^0} = -\frac{1}{k_{fb} - 1} .$$

Transient process

Let us consider a transient process in a non-contact magnetic relay with instantaneous connexion of the e.m.f. of the signal E_y, assuming that the displacement circuit is fed from the source of the current. At positive displacement (Fig. 2a), the relay will have a "normal open contact".

The transient process in the control circuit is described by the following differential equation:

$$2w_y S \cdot 10^{-8} \frac{dB_0}{dt} + i_y r_y = E_y. \tag{14}$$

It is convenient to express the time in the number of frequency cycles of the supply voltage, (relative time t^0):

$$t^0 = \frac{t}{T} = tf. \tag{15}$$

The equation (14) in relative units takes the form:

$$\frac{k}{4} \cdot \frac{dB_0^0}{dt^0} + i_y^0 = E_y^0 ; \tag{16}$$

$$k = \frac{w_y^2 r}{w^2 r_y} , \tag{17}$$

where k is the power amplification factor (for mean values) of a booster without feedback.

It is evidently necessary to examine the transient process in separate stages to correspond with the various sections of the curves in Fig. 2.

The transient process is analysed in the appendix; only the final expressions for determining the duration of separate stages is produced below.

Duration of first stage (Section 2-3):

$$t_1^0 = \frac{k}{4\,(k_{fb} + 1)} \ln \frac{k_{\text{reserve}}}{k_{\text{reserve}} - 1} \tag{18}$$

Duration of the delay stage (section 3-3′):

$$t_1^0 = \frac{k\,(1-\epsilon)}{2\epsilon} \times \frac{1-k_{reset}}{(k_{fb}-1)\,(k_{reserve}-1)} \tag{19}$$

Duration of third stage (section 3′-4):

$$t_3^0 = \frac{k}{4\,(k_{fb}-1)} \ln \frac{k_{reserve}-k_{reset}}{(k_{reserve}-1)} \tag{20}$$

Towards the end of the third stage the load current reaches a steady value and in the fourth stage remains constant.

In this way the relative operating time equals:

$$t_{op}^0 = t_1^0 + t_3^0 + t_4^0 \tag{21}$$

or

$$t_{op}^0 = \frac{k}{4}\left[\frac{1}{k_{fb}+1} \ln \frac{k_{reserve}}{k_{reserve}-1} + \frac{2\,(1-\epsilon)\,(1-k_{reset})}{\epsilon\,(k_{fb}-1)\,(k_{reserve}-1)} + \right.$$
$$\left. + \frac{1}{k_{fb}-1} \ln \frac{k_{reserve}-k_{reset}}{k_{reserve}-1}\right] \tag{22}$$

1959

When disconnecting the control signal (without breaking the control circuit), the transient process in the booster continues in the following manner. The electro-motive force E_y decreases in a jump to zero which corresponds in section 6-4 with the intermittent decrease of the control current to the magnitude:

$$I_{rel}^0 = \epsilon(k_{fb}-1)\,\frac{k\,k_{reset}}{1-k_{reset}} \tag{23}$$

During this time the current in the load and the induction B_0 remain constant.

Equation (16) is actually in respect of section 4-3 and its solution in conjunction with the calculation of (13) when $E_y = 0$ and with the initial condition $i_y^0(0) = I_{rel}^0$ takes the form:

$$i_y^0 = I_{rel}^0\, e^{-\frac{t^0}{\tau_3^0}}. \tag{24}$$

At the end of section 4-3 the current i_y^0 increases to I_{cm}^0, and the current in the load decreases to zero. The duration of this stage is determined by the equality:

$$t_4^0 = \frac{k}{4\,(k_{fb}-1)} \ln \frac{1}{k_{reset}} \tag{25}$$

Section 3′-3 corresponds with the delay of variation of the control current. In solving equation (16) when $E_y = 0$ and $i_y^\circ = I_{cm}^\circ = \text{const.}$, the initial condition $B_s^\circ(0) = 1-\epsilon$ and the final condition $B_s^\circ(t_3^\circ) = -(1-\epsilon)$, we find that the time of delay =

$$t_3^\circ = \frac{k(1-\epsilon)}{2I_{cm}^\circ} = \frac{k(1-\epsilon)}{2\epsilon} \times \frac{1-k_{reset}}{k_{fb}-1} \tag{26}$$

The time of delay at the release of the relay t_3° generally differs from the time of delay t_3° on operation.

In the last section (3-2) the control current decreases from the value $i_y^\circ = I_{cm}^\circ$ to zero, and the current in the load increases to the initial value I_0, which is determined by equality (10). These variations take place in accordance with the law of exponents with the time constant τ_1° (cf. appendix). Theoretically the duration of the last stage is equal to infinity. It is not usually possible in a relay system to take into consideration the time of the increase of the current in the load in section 3-2, and then one may assume that the delay in the variation of the current of the load is not indicated and the release time of the relay:

$$t_{rel}^\circ = t_4^\circ = \frac{k}{4(k_{fb}-1)} \ln \frac{1}{k_{reset}} \tag{27}$$

Similarly expressions for determining the operating and release times of a relay can be obtained for the occasion, when the displacement winding works in accordance with the feedback winding, (a relay with a "normal closed contact"):

$$t_{rel}^\circ = \frac{k}{4} \left[\frac{1}{k_{fb}+1} \ln \frac{k_{reserve}}{k_{reset}} + \frac{2(1-\epsilon)(1-k_{reset})}{\epsilon k_{reset}(k_{fb}-1)} + \frac{1}{k_{fb}-1} \ln \frac{1}{k_{reset}} \right]; \tag{28}$$

$$t_{op}^\circ = \frac{k}{4(k_{fb}-1)} \ln \frac{k_{reserve}-k_{reset}}{k_{reserve}-1}, \tag{29}$$

where,

$$k_{reserve} = \frac{E}{E_y^\circ} \frac{I_{cm}^\circ}{I_{cm}^\circ + \Delta^\circ}; \quad k_{reset} = \frac{I_{cm}^\circ}{I_{cm}^\circ + \Delta^\circ} \tag{30}$$

In formulae (22) and (27)-(29) it is possible to calculate the operating and release times of a relay by the known reserve factor $k_{reserve}$, reset factor k_{reset}, the feedback k_{fb}, the power amplification factor without feedback k, and by the magnitude of the relative supply voltage $\epsilon = B_m/B_s$. All these quantities are usually ascertained from the static ratings of the relay. The determination of the operating and release times of a relay by means of relative coefficients, and not by the absolute values of the control and operating currents, etc. is, in our

opinion, a very convenient method for calculating and analysing the influence of various parameters on t_{op} and t_{rel}.

Results of experimental verification

A quantitative check on the theoretical results obtained has been carried out in a number of boosters designed according to the systems represented in Fig. 1. One of these boosters had the following data. Each core consisted of 18 rings of molybdenum permalloy measuring 34 × 50 mm and 0.25 mm thick. The number of winding turns: $w_{\sim} = 300$; $w_{\text{feedback 1}} = 340$; $w_y = 400$; $w_{\text{feedback 2}} = 40$. The supply frequency was 500 c/s. Saturation induction was taken to be equal to 6300 G; e.m.f. of saturation of one choking coil $E_s = 13.6$ V; the total resistance of the load circuit for the method in Fig. 1a amounted to 44 Ω, but for the method in Fig. 1b, 21 Ω; the total resistance of the control circuit in all cases was $r_y = 7\,\Omega$. The germanium rectifiers were of the DG - TS23 type.

Results of calculation and experiment for five different relay procedures are reproduced in Table 1. The duration of each stage in the transient process was determined by oscillograms. The oscillogram currents on operation and release of the relay for systems 1, 4 and 5 are shown in Fig. 3.

Three quantities for each time component of the transient process are produced in Table 1. The first column contains quantities calculated by (18), (19), (20) and (25) on the basis of the rated static characteristics for a perfect magnetization curve. The quantities given in the second column, which are calculated by those formulae, but which enter into the formulae of the coefficients k_{reserve}, k_{reset}, k_{feedback} are determined by the experimental static relay ratings of the booster. The experimental quantities are given in the third column. The variation of experimental volumes from those calculated in the second column does not exceed the limits of accurate measurement.

It is apparent from analysis of the oscillograms in Fig. 3, that the vibrators of the oscillograph in the control and load circuits are shunted by capacitances to reduce the even harmonics of current in the vibrators. With sufficiently large capacitances the variations of the stubs are practically proportional to the mean values of the current (provided the circuit resistance is considerably greater than the resistance of the vibrator). An oscillograph of momentary values of currents can produce a misrepresentation of the character of the transient process and operating and release times. In Fig. 4 oscillograms of relay operation and release are provided for comparison. They were taken in system 3 in the presence and absence of capacitance shunting the vibrator in the load circuit. An examination of oscillograms taken without shunting capacity can create the false impression that on operation of the relay, delayed variation of the load current takes place, and that on release, the load current reaches a steady value sooner than the

control current. This case is explained by the considerable difference in the laws of variation of amplitude and mean values of currents in magnetic boosters in a transient process, [5].

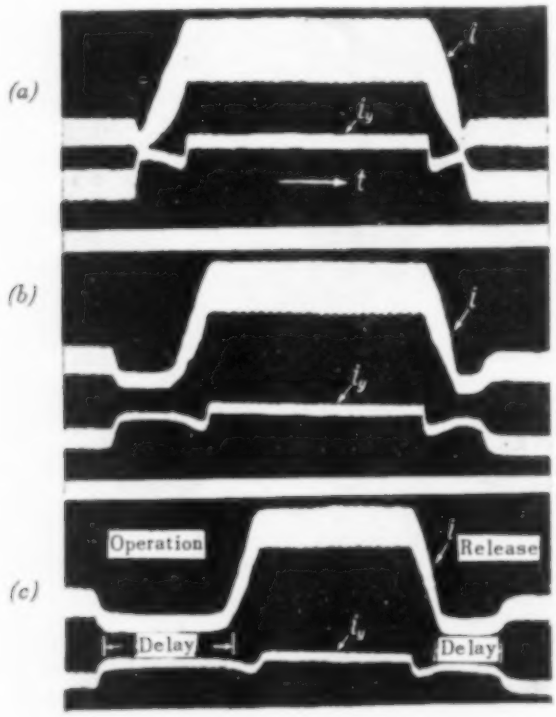

FIG. 3. Oscillograms of currents in the load i and in the control circuit i_y during relay operation and release a – system 1; b – system 4; c – system 5. The vibrators are shunted by capacitance

Conclusion

The delay effect on operation (or release) of a non-contact magnetic relay can be utilized to create non-contact time relays, which will profitably differ from similar non-contact relays, in that in the passage of time the current in the load practically does not vary.

In spite of the accepted perfection of the magnetization curve, calculated formulae for determining the operating and release times of a relay are more in conformity with experiment, if the values $k_{reserve}$, k_{reset}, Δ^0 are determined by the experimental static ratings of the relay. Without the latter, the calculation of the operating and release times by means of derived formulae produce satisfactory

results given a sufficiently accurate calculation of the static ratings. Conversely, if in devising a relay, the requisite values of $k_{reserve}$, k_{reset}, k and Δ° are given, then the calculation thereby of the operating and release times is more in conformity with experiment, provided that after the approximate calculation of the relay experimentally, the given values of $k_{reserve}$, k_{reset}, k and Δ° are ensured. This conformity of experimental and calculated values of the operating and release times is explained by the fact that the static ratings of the relay entirely determine the actual dependence of the direct component of induction on the control current and, consequently, determine the course of the transient process.

It is natural that the results obtained can also be used to solve the problem of determining the possible values of $k_{reserve}$, k_{reset}, ϵ and Δ° by means of the given operating and release times.

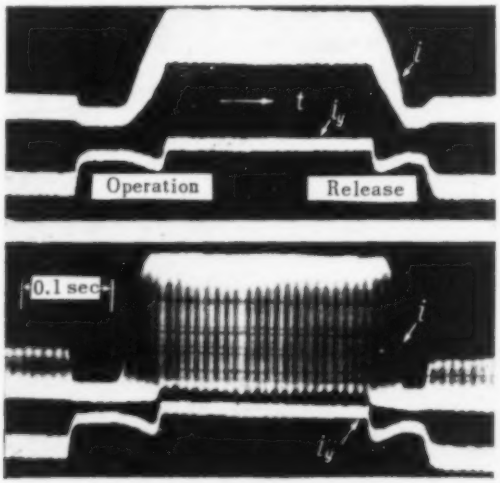

FIG. 4. Oscillograms of currents in the load i and in the control circuit i_y during relay operation and release in system 3 with the vibrator shunted by capacitance in the control circuit
a - vibrator shunted by capacitance in the load circuit
b - vibrator in load circuit not shunted by capacitance

Appendix

Let us examine the transient process on operation of the relay by separate stages in accordance with the various sections of the curves, represented in Fig. 2.

The first section, (section 2-3). Here the control current varies within

TABLE 1

Operating condition	Figure	E, V	s	I_{LM}, ma	E_y/I_y, ma	t_1, m sec			t_2, m sec			t_3, m sec			t_{op}, m sec			$t_4 = t_{rel}$, m sec		
						1	2	3	1	2	3	1	2	3	1	2	3	1	2	3
1	1, *a*	27	1	425	124	5.2	3.3	6.8	—	—	—	61	49	48	66	52	55	34	35	36
2	1, *b*	12.6	0.93	405	121	4.3	3.5	6.6	17	11	14	53	46	48	74	61	69	36	37	39
3	1, *a*	16	0.75	300	92	4.4	3.3	5.5	72	47	50	53	49	45	129	99	101	34	35	36
4	1, *b*	14.8	0.70	300	92	4.2	3.2	6.6	89	60	55	51	47	42	144	110	104	36	37	38
5	1, *b*	5	0.465	200	62	4.2	3.2	7	240	146	140	51	44	38	295	193	185	36	31	33

limits from zero to I^0_{cm}.

Taking (12) into consideration we should write equation (16) in the form:

$$\frac{k}{4(k_{fb}+1)} \cdot \frac{di^0_y}{dt^0} + i^0_y = E^0_y. \tag{I,1}$$

The solution of (I,1), with the initial condition $i^0_y(0) = 0$, is:

$$i^0_y = E^0_y\left(1 - e^{-\frac{t^0}{\tau^0_1}}\right); \quad \tau^0_1 = \frac{k}{4(k_{fb}+1)}. \tag{I,2}$$

The current in the load and direct component of induction vary in accordance with the following equations:

$$i^0 = \frac{I^0_{cm} - i^0_y}{k_{fb}+1}; \quad B^0_0 = -\left(1 - \varepsilon + \frac{I^0_{cm} - i^0_y}{(k_{fb}+1)}\right). \tag{I,3}$$

In time t_1 this stage terminates. Here the following dependences take place:

$$i^0_y(t^0_1) = I^0_{cm}; \; i^0(t^0_1) = 0; \; B^0_0(t^0_1) = -(1-\varepsilon). \tag{I,4}$$

The duration of the first stage:

$$t^0_1 = \frac{k}{4(k_{fb}+1)} \ln \frac{E^0_y}{E^0_y - I^0_{cm}} \tag{I,5}$$

or

$$t^0_1 = \frac{k}{4(k_{fb}+1)} \ln \frac{k_{reserve}}{k_{reserve} - 1}$$

The second section, (section 3 - 3′). In this stage the delay of variation of the control current takes place until the direct component of induction increases to the value: $(1-\varepsilon)$. In the second section:

$$i^0_y = I^0_{cm} = \text{const}; \; i^0 = 0. \tag{I,6}$$

Equation (16) takes the form:

$$\frac{k}{4} \cdot \frac{dB^0_0}{dt^0} = E^0_y - I^0_{cm}. \tag{I,7}$$

The solution of (I,7) with the initial condition $B^0_0(0) = -(1-\varepsilon)$, is:

$$B^0_0 = \frac{4}{k}(E^0_y - I^0_{cm})t^0 - (1-\varepsilon). \tag{I,8}$$

Induction B_3^0 at the end of the second stage increases according to linear law and reaches the value $B_3^0(t_2^0) = \xi - \varepsilon$; consequently, the duration of the second stage is as follows:

$$t_2^0 = \frac{k(1-\varepsilon)}{2(E_y^0 - I_{cm}^0)}$$
$$t_2^0 = \frac{k(1-\varepsilon)}{2\varepsilon} \cdot \frac{1 - k_{\text{reset}}}{(k_{fb}-1)(k_{\text{reserve}}-1)} \qquad \text{(I,9)}$$

The third section (section 3′-4). By taking (13) into account we may write equation (16) in the form:

$$-\frac{k}{4(k_{fb}-1)} \cdot \frac{di_y^0}{dt^0} + i_y^0 = E_y^0. \qquad \text{(I,10)}$$

The solution of (I,10), with the initial condition $i_y^0(0) = I^0$, is as follows:

$$i_y^0 = E_y^0 + (I_{cm}^0 - E_y^0)\, e^{-\frac{t^0}{\tau_3^0}};$$
$$\tau_3^0 = \frac{k}{4(k_{fb}-1)}. \qquad \text{(I,11)}$$

The current in the load and induction B_3^0 vary in accordance with the following equations:

$$i^0 = \frac{I_{cm}^0 - i_y^0}{k_{fb}-1}; \quad B_0^0 = 1 - \varepsilon + \frac{I_{cm}^0 - i_y^0}{k_{fb}-1}. \qquad \text{(I,12)}$$

We shall note than an exponential term with a positive characteristic enters into the equations of all the values. At the end of the third section a total saturation of the cores takes place:

$$B_0^0(t_3^0) = 1;\ i(t_3^0) = \varepsilon;\ i_y^0(t_3^0) = I_{cm}^0 - \varepsilon(k_{fb}-1). \qquad \text{(I,13)}$$

The duration of the third stage:

$$t_3^0 = \frac{k}{4(k_{fb}-1)} \ln \frac{I_{cm}^0 - \varepsilon(k_{fb}-1) - E_y^0}{I_{cm}^0 - E_y^0} \qquad \text{(I,14)}$$

or

$$t_3^0 = \frac{k}{4(k_{fb}-1)} \ln \frac{k_{\text{reserve}} - k_{\text{reset}}}{k_{\text{reserve}} - 1}$$

In fact, the transient process comes to an end after the third stage - the current in the load has reached a fixed value.

The fourth section (section 4-6, Fig. 2). The control current (on accepted hypotheses) reaches the fixed value $i_y^0 = I_y^0 = E_y^0$ in a jump, but the current in the load and induction B_δ^0 remain constant. The qualitative character of current and inductive variations in a transient process during relay operation and release is shown in Fig. 5.

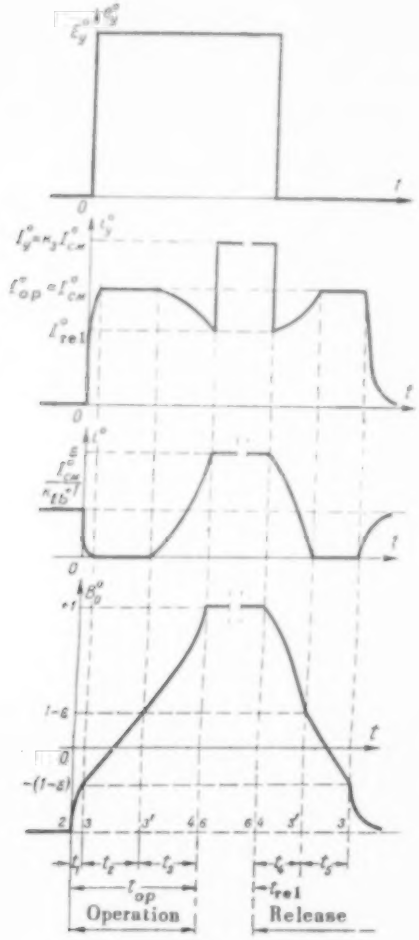

FIG. 5. Qualitative character of the variation of the direct component of induction and of the control and load currents in the transient process during relay operation and release with normally open contact

Translated by J.F. Boyland

REFERENCES

1. M.A. Rozenblat; Magnitnye usiliteli. (Magnetic amplifiers). *"Sovetskoe radio"* (1956).
2. I.B. Negnevitskii and L.L. Samurina; Experimental'noe issledovanie perekhodnykh protsessov V deskon-taktnykh magnitnykh rele (Experimental investigation of transients in contactless magnetic relays). *Elektrichestvo*, No. 9 (1953).
3. R.A. Lipman and I.B. Negnevitskii; K teorii ideal'novo drossel'novo magnitnovo usilitelya, (Theory of the ideal choke magnetic relay). *Elektrichestvo*, No. 1 (1956).
4. R.A. Lipman and I.B. Negnevitskii; k teorii odnopoluperiodnovo magnitnovo usilitelya, ch. 1. (Theory of the single half-period magnetic amplifier). *Avtomatika i Telemekhanika*, No. 4 (1957).
5. R.A. Lipman and I.B. Negnevitskii; Drossel'nyi magnitnyi usilitel. (Choke magnetic amplifier). *Elektrichestvo*, No. 6 (1958).

ABSTRACTS FROM PAPERS PUBLISHED IN ELEKTRICHESTVO No. 7, 1958

General questions of the theory of electric motors: A.N. Larionov, N.Z. Mastiaev, I.N. Orlov and D.N. Panov. (pp 1-6)

The first work on the theory of hysteresis motors was begun in the U.S.S.R. in 1950. These motors have been widely applied as their power indices have been improved. The article considers the method of operation of the motors, the character of magnetic polarity reversal and the distribution of the field in the rotor. Expressions for the electromagnetic hysteresis torque and parameters of the rotor circuit in the equivalent network are shown. Diagrams are presented showing the mechanical characteristic of a hysteresis machine; the spatial arrangement of the induction vectors B, field strength H and intensity of magnetization J at a point of the rotor during magnetic polarity reversal; the dependance of losses in the ferromagnetic material during rotary magnetic polarity reversal and magnetic polarity in the alternating field and the sine of the hysteresis angle γ on the induction of the magnetic field; the equivalent network of a hysteresis motor; the operating characteristics of an ideal hysteresis motor; experimental characteristics of a four pole hysteresis motor and rotor of a hysteresis motor with regions of different magnetic permeability. An appendix deals with the region of the hysteresis layer which is of interest.

Currents of tooth frequency in the damping winding and damping losses of a synchronous generator: P.M. Ipatov. (pp 7-10)

Damping losses in a synchronous machine can cause distortion and pulsation of the field in an air gap leading to the distortion of the shape of the e.m.f. curve of a generator. Expedient choice of the tooth division of a damping winding can considerably reduce higher harmonics in the e.m.f. curve of the generator. The author concentrates on the currents in the transverse axis of the poles and the additional losses caused by these currents.

Measurement of the strength of the electromagnetic field using the auxiliary electrode method: M.I. Sysoev. (pp 11-14)

A new method is described for the experimental investigation of the field, making it possible for high voltage installations to measure directly and simply the field strength in complex insulation, compared with the probe method or modelling of

the field in an electrolytic tank. The method consists of introducing a small auxiliary electrode at the point of the field under investigation, the electrode preferably being in the form of a sphere, washer with rounded edges, or a semi-ellipsoid made of steel, or better, refractory metals. If the voltage is increased gradually between the main electrodes then a discharge arises from the auxiliary electrode. The author shows that the rise of the discharge can be taken as the signal of the attainment of a value of strength of the main field at the point where the auxiliary electrode is inserted. This method has an accuracy of ± 5 per cent when the field is uniform. It is specially useful for apparatus insulated with compressed gas.

Compensation of the resistance in the rotor circuit of synchronous generators of electrodynamic models: V.V. Pruss-Zhukouskii and V.V. Fetisov. (pp 19-24)

A special difficulty arises when modelling synchronous machines having comparatively low inertia constants (T_j = 4-6 sec) and high time-constants, (T_{do} = 10-12 sec), e.g. for turbogenerators and synchronous compensators. It is, therefore, necessary to compensate excess resistance by means of special electrical machines or devices. The authors here consider experience with single-phase commutator generators in connexion with long distance transmission. Provided (1) the resistance to be compensated is constant in static and dynamic conditions, (2) the magnitude of the resistance can be smoothly regulated, (3) operation is stable, (4) self-excitation is absent, (5) and given the permissible magnitude of the inductive resistance in the conditions of modelling the parameters of the generator, the single phase commutator generator can ensure high stability of operation and constant compensation of resistance at a degree of compensation up to 0.75-0.85 and even higher values.

Oscillographing the electromagnetic torque in electrical d.c. machines with the aid of the Hall effect in semiconductors: O.D. Elpat'evskaia and V.A. Perchuk. (pp 31-35)

The practical use of the Hall effect became possible only after sufficient study of the electrical properties of semiconductors with great mobility and comparatively low concentration of the current carriers in which the Hall e.m.f. is several times greater than in metals. The author here considers the use of fine plates of selenide of mercury on a micaceous backing which have the advantages of flexibility and thinness compared with monocrystals. The method of producing the plates is then considered together with the method of measurement. Zero compensation is effected by an impedance between a current and a Hall outlet allowing several activators to be connected in a bank, as illustrated graphically. Two methods of reducing interference are noted; namely, increasing the sensitivity of the plates and introducing a filtering choke in the Hall circuit. Such a method of oscillographing gives sufficiently accurate results and has other advantages.

The calculation of three phase circuits with an arbitrary number of asymmetrical short-circuits and phase breaks: N.M. Gorbatov. (pp 35 and 41)

Simple methods of calculation have still to be formulated, the criterion being the number of necessary time consuming multiplication and division operations. The use of computers and the recording of intermediate results is also considered. Tables are included and an example given of the calculation of a circuit with one short-circuit and two breaks.

A special case of synthesis of circuit schemes: V.S. Davydov. (pp 45 - 50)

The problems of the construction of electrical oscillating systems with given frequency characteristics have been dealt with elsewhere and so the author limits himself to a linear electrical system in the form of a circuit scheme formed by a number of elementary oscillating contours. He proceeds to consider how with $2n$ given natural frequencies, a circuit scheme of n elementary contours can be synthesized on the condition that n frequencies are obtained in the no-load state of the circuit system and n other frequencies are obtained in the presence of a short-circuit on the output terminals of the scheme. He bases the solution of this problem on the property of continued fractions and certain aspects of electrical circuit schemes. He then considers an analogous problem of determining the reactive parameters of a circuit scheme of both the high and low frequency filter type. The method may be extended to cases with attenuation. The paper ends with an example of the synthesis of a circuit system for a three link scheme of the low frequency filter type.

Design of heaters for thermal bi-metallic elements of thermal apparatus: IA.A. Rips. (pp 51 - 55)

An effective method of protecting electrical equipment from dangerous overloads is the use of thermal protective gear, the metering device of which reacts to the temperature developing on account of the heat due to current. The most improved gear makes use of the properties of thermal bi-metal for this purpose. As regards the planning of such gear, the first stage is to create a specimen apparatus with any magnitude of nominal current and direct heating of the thermo-bimetallic element, to choose a shape and investigate the kinematic properties common to all the planned series of apparatus. A further stage is the design of the sensitive elements for all the different models within the series. Here, no difficulties arise if the direct method of heating is employed. However, in the case of indirect or combined methods of heating, the design of the heater is complicated. The author, therefore, introduces formulae for designing heaters for the case when a series of apparatus with indirect or combined heating elements is produced from a specimen with a direct heating element, and concludes with an example of the calculations.

Neutralization of the charges of static electricity on paper: V.M. Orlov and N.I. Kromiak. (pp 56-58)

Electrification of paper in printing processes etc. breaks production. The Lenin Electrotechnical Institute in Leningrad has developed a neutralizer based on the principle in P.S.H. Henry's article "Electrostatic Eliminators in the textile Industry", *Brit. J. Appl. Phys.* Suppl. pages 78-83, 2, 1953, and applied it to printing processes.

Permissible overloads of cables in fault and operating conditions: D.S. Livshitz and S.M. Messerman. (pp 59-63)

In practice the problem arises of permissible short run (30-60 min and over) overloads of cables in fault conditions. The author reviews Soviet literature on this subject and proposes a method of calculation which will reduce capital expenditure. Taking into account ageing of the insulation, it is necessary to consider the long run operation of the cables as well as fault conditions. He concludes that the choice of cable on the "30 minute maximum load" rule leads inevitably to substantial non-utilization of the section and to an unwarranted freezing of capital expenditure.

Constant wire resistances for operation in a tropical climate: B.N. Dolgov, N.P. Kharitonov, G.V. Belinskaia and V.G. Abetikov. (pp 64-65)

Since in a tropical climate the resistance of insulation must be high and the equipment resistant to humidity and fungus, five constant tropical wire resistances of the P.T. series have been developed. Their general appearance is illustrated and values of rated power of dispersion (7.5 to 75W), dimensions and the rated values of resistance (5-30,000 Ω) are tabulated. At rated load, the surface temperature is no more than 200°C above ambient. Special thermal-humidity insulation has been developed based on silicone organic polymer compounds. The results of humidity tests thereon are tabulated and are favourable. The resistances have also undergone tests for fungus resistance and electrical and mechanical strength.

Device for measuring the angle between voltage vectors and the e.m.f. of a synchronous machine: M.Z. Gurgenidze and I.K. Servingin. (pp 65-67)

Experimental investigations show that indirect measurement does not reveal the overload capacity of machines. The authors propose the plotting of an angle power characteristic for different operating conditions using oscillograph recording of variations in active power and angle θ both for slow and quick load changes. A device for measuring θ produced by the Water-power Institute of the

Academy of Sciences of the Armenian S.S.R. has been modified to overcome the distortion of the linear dependence between θ and the voltage at the output of the filter. Both schemes are illustrated diagrammatically. Tests on the operation of the modified scheme in the presence of variations of the input voltage show that these variations do not affect the operation of the scheme within the limits of 100-60 V. When θ changes abruptly the lag of the scheme does not exceed 20 m sec.

1959

HEAT RESISTANT WINDING CONDUCTORS

V.A. PREVEZENTSEV

Moscow Energy Institute*

(Received 27 February 1958)

At the present time in the U.S.S.R. and in the leading techniques of advanced countries there is a noteworthy development of conductors with enamel insulation gradually replacing winding conductors with fibrous insulation. In this direction, in the next few years we are forced to do much more, since now the total production of our enamelled conductors forms about 50 per cent of the whole output of winding conductors, while in some advanced countries it has reached 65-70 per cent. Much attention must be directed also to the production of aluminium enamelled conductors.

The pre-eminent development must be to produce high-stability enamelled conductors. For a long time the volume of production of these conductors with polyvinylacetate lacquers (Viniflesk and Metalvin) was very small in our country and did not reach more than 8-10 per cent of the total output of enamelled conductors.

The remarkable increase in the production of high-stability enamelled conductors in 1956-57 took place as a result of the inclusion of the output of conductors with polyamide-bakelite bases by the factories "Yuzhkabel" (Kharkov), "Estikabel" (Tallin) and "Kuibyshevkabel" as a result of much work carried out by NIIKP on the creation of formulae for a given lacquer and of the exploitation with the given factories of a new technology of enamelling with these lacquers.

The electro-insulating and physicomechanical properties of high-stability conductors with polyvinylacetate and polyamide-bakelite lacquers are well known to the many users of these conductors and are fairly widely described in our technical literature. It is only essential to remark that in accordance with GOST 7262-54 and with the technical conditions TUK.OMM 505.073-54 the long term

* *Elektrichestvo* No. 8, 5-11, 1958.

temperature of these conductors may not exceed 110°C. For a strictly limited time of use it is permissible to increase the working temperature.

High-stability heat-resistors enamelled conductors class B

The organization of production of high-stability enamelled conductors in accordance with the classes B,F and H of heat-resistance is of great practical importance. Abroad, great attention is given to polyamide-epoxy enamels and in general to enamels with polyurethane and polyester bases. This is borne out, in particular, by an article by the English firm Henley [1]. According to the data in this article, Fig. 1 shows the relationship between the elasticity of various enamels and the duration of their exposure to a temperature of 200°C. It is not hard to see that at such a temperature the elasticity of enamelled conductors with polyvinylacetate lacquers falls fastest of all, and that for conductors with polyurethane enamels it falls noticeably slower, and least of all with silicone enamels. In comparison with the latter enamelled conductors with polyester lacquers appear more stable. In the same place follow the results of investigations of twisted samples with a voltage (a.c.) of 1 kV and a simultaneous ambient temperature of 200°C. The polyester and silicone enamels stood up to this test for about 5000 hr the polyurethane enamels about 700 hr epoxy about 500 hr and polyvinylacetate about 100 hr.

1959

The investigatory works on the creation of high-stability enamelled conductors, in accordance with Class B heat resistance in recent times have been carried out in NIIKP in two ways: the exploitation of formulae for polyamide-epoxy lacquers and for lacquers on the basis of polyurethane resin.

For the development of polyamide-epoxy lacquers for conductor enamelling the property of epoxide resins whereby they pass into a thermoreactive condition was used, and also the property of giving, in combination with other components, lacquers of high dessication and of increased heat resistance. An enamelled conductor with insulation of polyamide-epoxy lacquers has high mechanical and electrical durability and may be used in electromechanical devices without additional protection of the enamel insulation with woven materials. In the original condition enamel conductors stand up to winding on a core of equal diameter; the enamel has good adhesion to the exterior of the wire. In the process of heat ageing at a temperature of 180°C polyamide-epoxy enamel conductors behave better than Viniflex conductors at a temperature of 150°C. Experiments at a temperature of 130°C show that over a period of 30 days polyamide-epoxy enamel films retain their elasticity at their original level.

[1] A new Henley high temperature enamelled wire. Distribution of Electricity, May 1957.

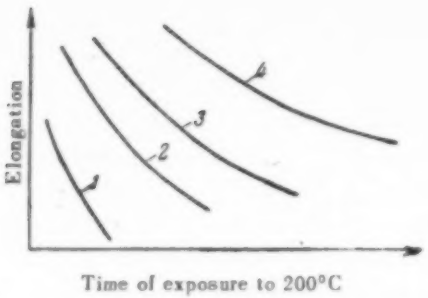

Fig. 1. Variation of elongation of enamel insulation (with stretching of the conductor) as a function of the duration of exposure to a temperature of 200°C
(1) Polyvinylacetate enamels
(2) Polyurethane enamels
(3) Silicone organic enamels
(4) Polyester enamels

The conclusions given enable one to assume that such enamel conductors may, over a protracted period, be exploited at a temperature of 130°C and for short periods at temperatures up to 150°C. This insulation has high resistance to the effects of solvents such as benzine and benzole.

A defect of enamel insulation of the first formulae for polyamide-epoxy lacquers appeared as an excessive thermoplasticity which reached 18 - 20 per cent at a temperature of 200°C. A reduction of the thermoplasticity of these materials was achieved by the introduction of polybutyltitanate. A general defect of enamelled conductors with polyamide-epoxy insulation appeared as a sharper fall in insulation resistance in conditions of high relative humidity of the air than with Viniflex enamel. Nevertheless the insulation resistance of experimental enamelled conductors remains noticeably higher than with woven insulation (Mark PBD etc.) which gives grounds for considering that the new enamel conductors are more suitable for general electromechanical apparatus.

Noticeably better results were obtained in the exploitation of a formula for polyurethane enamels. Polyurethanes appear as products of mutual reaction between diisocyanates and compounds containing hydroxyl groups. For a general picture of the reaction for the production of polyurethanes one may write the following:

$$x.\mathrm{HOROH} + x.\mathrm{OCNR'NCO} \rightarrow (\mathrm{-OROCONHR'NHCO-})_x.$$

For the preparation of polyurethanes the most suitable manner would seem to be the application of the aromatic diisocyanate – toluylenediisocyanate

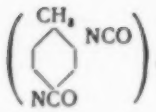 , which is produced by the reaction of toluylenediamine with

phosgene and the production of which is well known to our chemical industry.

Isocyanates seem to be remarkably chemically active substances. When they are mixed with polyesters, even at room temperatures, after a short while a reaction takes place between the two. For preparation of enamels it is essential to apply stabilized ("masked") diisocyanates, by the production of which high dessication lacquers are obtained. Stabilized diisocyanates are obtained by reactions with phenols, cresols etc. according to the equation:

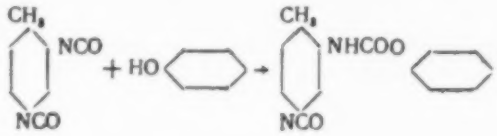

In this case one active group –NCO is blocked by the phenol and so the diisocyanate changes to monophenylurethane, losing, at ordinary temperatures, its liability to reactions. The second active group –NCO when mixed with polyesters reacts with free OH groups, as a result of which monophenylurethane becomes completely blocked and particularly inert at normal temperatures; moreover blocked diisocyanates are non-toxic.

1959

At higher temperatures (180°C and above) monophenylurethane decomposes into its original products – phenol and diisocyanate, which is also used in enamelling, so that diisocyanate goes into a deeper reaction with the second component of the lacquer – the polyester, forming insoluble enamel films.

Enamel conductors on a basis of polyurethane resin are distinguished by high elasticity. They stand up to winding on a core the diameter of which is equal to the conductor under investigation, and under these conditions neither cracking nor damage to the enamel occurs. The thermoplasticity of these conductors is noticeably lower than the demands presented in GOST 7262-54, and is found within the limits 6-7 per cent. Insulation on the basis of polyurethanes is inert to benzine and to aliphatic hydrocarbons.

Prolonged investigations of enamelled conductors under heat ageing showed the exceptional heat resistance of enamel insulation. Thus after being thermostatically maintained at 150°C for 25 days, they showed their original elasticity and could be wound on a core of equal diameter to that of the wire. At the same time, wires with insulation of Viniflex lacquer maintained their original elasticity at 150°C for only 1-2 days.

At 180°C after five days, the elasticity of enamelled wires on a base of polyurethanes remained at the same value as at the beginning. These conductors maintained a satisfactory elasticity after eleven days exposure to the same temperatures; a further reduction of elasticity took place uniformly in the course of a comparatively long time interval. Tests on protracted ageing of enamelled conductors at a temperature of 125°C show that the elasticity of the conductors is maintained without change for a period of 150 days.

The foregoing data on the heat resistance of enamelled conductors on a polyurethane basis allows one to assume that they may be used for long periods at a temperature of 130°C (Class B insulators) and for a limited period – at higher temperatures (150 - 180°C).

Measurements have shown that enamelled conductors with polyurethane base insulation are particularly noted for high electrical insulation characteristics not only in the original condition but also in an atmosphere with high relative humidity (Fig. 2).

The information obtained permits the recommendation of enamelled conductors with a base of polyurethane for application in the radio industry or the production of high-frequency apparatus where there are specially stringent demands on the electro-insulation characteristics of the conductors.

An especially valuable property of enamelled conductors on a polyurethane base appears in that they can be covered with a layer of tin (or its alloys) without preparatory dressing of the enamel and without the use of fluxes. The temperature necessary for soldering enamelled conductors is in the range 320 - 360°C, in which the higher the temperature of the tin, the shorter is the time required for soldering. Thus, at a temperature of 360°C, 2 - 3 sec are needed for soldering enamelled wires, while at 320°C, 15 - 40 sec are needed depending on the thickness of the insulation. Wires of small diameter are much more rapidly soldered at these temperatures than wires of greater gauge.

In this manner the use of polyurethane enamelled conductors noticeably facilitates the assembly of many different types of apparatus. From this point of view, polyurethane enamelled wires are particularly desirable for the preparation of high-frequency winding conductors (Litz wires). Their current carrying elements often consist of many tens or hundreds of enamelled wires whose diameter is from 0.05 - 0.10 mm the cleaning and soldering of which is very complicated and time consuming. With the use of polyurethane enamelled conductors the necessity for cleaning vanishes, and even the soldering process may be accomplished quickly and without any difficulty.

It may also be observed that these wires may be made with the enamel films dyed in various colours, which has a special significance for mass production.

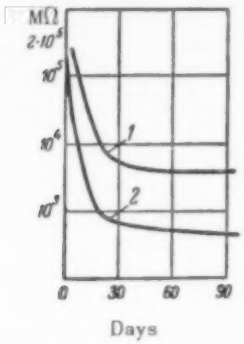

Fig. 2. Variation of insulation resistance of (1) Polyurethane and (2) Oil based enamels as a function of time of exposure to a relative humidity of 97 per cent and a temperature of 35°C (according to the Swiss firm Huber)

Enamel conductors with additional thermoplastic covering

In the production of low-power electric motors and generators and of electrical apparatus, it is often necessary that the windings of the coils be made in sections or in frames for the purpose of gluing them together without a support or other similar device. To achieve this it is essential that the wires besides their usual enamel insulation (of polyvinylacetate, oil, polyamide and other similar lacquers) should have an additional exterior thermoplastic layer, which ensures the solid adhesion of the coils one to the other if they, or other section or the spools are exposed to baking at 170-180°C for 3-5 hr. The additional coverings may be made by the use of enamels from such thermoplastic resins as polyvinylacetate, polyvinylacetal, (without hardeners) etc. with the addition of some quantity of hardening plasticizer. The prepared wires may be produced on ordinary lathes with an increase in the number of operations of 2-3. Work on the construction of such wires is successfully achieved in NIIKP and it is being introduced at the first opportunity into the factories "Mikroprovod" and "Moskabel". On investigation, a thermoplastic lacquer on a polyvinylacetate basis has shown better results.

Enamel conductors with particularly high heat resistance of the enamel insulation

At the present time there is a very great demand for enamelled conductors with yet greater resistance to heat (for extended working at 150-300°C). One of the ways for the production of such conductors has appeared until recently to be the use of Silicone compounds. As a result of combined work the VEI, NIIKP and

the cable factory "Mikroprovod" have organized the production of conductors with these lacquers (Type PETK) with diameters of 0.05 - 0.25 mm.

Frequent attempts to produce silicone lacquers for enamelling larger circular conductors and conductors with rectangular cross-sections have, until recently, not led to successful results on account of the low mechanical strength of the insulation on these wires. Moreover the wires obtained showed unsatisfactory resistance to benzene and a greatly lowered breakdown voltage after an operating temperature of 180°C. The undertaking MAP produced the silicone lacquer (Type MK-4) modified with glyptal resins. The enamelled conductors with this lacquer, as regards mechanical durability, noticeably exceed wires with similar lacquers of the VEI and for durability approach that of the wires type PEV-1; moreover, they are resistant to benzene. Nevertheless, these lacquers have less heat-resistance in comparison with VEI lacquers so that after 5 - 7 days exposure to 150°C the elasticity of the enamel insulation has noticeably decreased. The wires lose the elasticity of their insulation after 2 - 3 days at 180°C. In this way, enamelled conductors with MK-4 lacquer may be worked for limited periods at temperatures not exceeding 150 - 160°C.

Recently, fellow-workers of one of the undertakings developed the formula for this lacquer to increase its heat resistance; therefore, the new lacquer (MK-4y), suitably modified, was tested and investigated on an experimental basis for enamelled conductors. Noticeably better results were obtained with lacquers in which polyester resins were incorporated. These latter are obtained as a result of the reaction of polycondensation of double radical acids and multi-atom alcohols. Examples of such resins are the polyterephthalates (Lavsan, Mailar, Terebek, Terylene), obtained as a result of the reaction of terephthalic acid on ethyleneglycol:

$$n(HOCH_2-CH_2OH) + n(COOH\text{-}C_6H_4\text{-}COOH) \rightarrow$$

Ethylene glycol Terephthalic acid

$$HOCH_2-CH_2OOC\text{-}C_6H_4\text{-}COOCH_2-CH_2OOC\text{-}C_6H_4\text{-}COOCH_2- + 2n.H_2O$$

Polyethyleneterephthalate

A linear molecule construction determines the properties of polymers, and often its elasticity, mechanical durability etc. For the preparation of lacquers, polymers are essential which are capable of giving a spacious structure. In connexion with this, in the molecules of the polymer, substances are introduced with groups giving possibilities of side reactions (e.g. glycerine $\begin{pmatrix} CH_2OH \\ CHOH \\ CH_2OH \end{pmatrix}$), enabling the function of such a structure.

Wire, enamelled with polyester lacquers is marketed in the U.S.A. under the names "Teramel" and "Levkanex".

In the German Federal Republic polyester enamels are prepared – "Terebek F-35" and "Terebek F-45" (different viscosities) with prolonged heat-resistance at 155°C. The solvent of these lacquers is tricresol. Finally, for the production of enamelled conductors with prolonged heat resistance at 155°C, within limits, enamels with a polyester base are used, in which to increase the heat resistance about 20-25 per cent silicone resin is added.

It remains to mention that some polyester enamels give films insufficiently resistant to warmth, blows and to the action of hot solvents (while bent), which reduces the use of these products. In mechanical and electrical strength of the enamel films, polyester enamelled conductors do not give rise to high resistant conductors.

In the VEI in this direction much work has been done as a result of which a modified polyester lacquer No. 124 has been developed, and the NIIKP with the factories "Moskabel" and "Mikroprovod" have produced a technique of enamelling with these lacquers.

In Fig. 3. are shown curves of the variation of elasticity of enamelled conductors in the ageing process at temperatures of 180 and 200°C. It is apparent that the elasticity of enamelled wires after 30 days ageing at a temperature of 180°C has hardly changed:

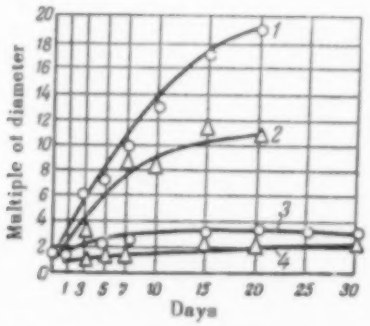

Fig. 3. Variation of elasticity of enamelled wires in lacquer No. 124 as a function of the time of exposure to temperatures of 180°C and 200°C

(1) Wire diameter 0.8 mm, temperature 200°C
(2) Wire diameter 0.44 mm, temperature 200°C
(3) Wire diameter 0.8 mm, temperature 180°C
(4) Wire diameter 0.44 mm, temperature 180°C

the enamel films fail by cracking when the conductors are wound on a core 2-3 times the wire diameter. Holding of the conductors at a temperature of 200°C noticeably reduces their elasticity.

Determination of the breakdown voltage of enamelled conductors at room temperature after they have been exposed for 1 - 20 days to a temperature of 200°C, and also indefinitely at this temperature has shown that the new insulation shows high electrical strength. The thermoplasticity of wires measured at a temperature of 200°C reaches 8.3 per cent.

It is possible that on aluminium or aluminium coated wires the heat resistance of polyester films may be increased a little as a result of the exclusion of catalytic influence of the copper during the ageing of the enamel insulation.

Fluoroplast - 4 $(\ldots - \underset{F}{\overset{F}{C}} - \underset{F}{\overset{F}{C}} \ldots)$ also appears as a desirable prime material for enamels on account of its lasting heat resistance in any case not less than 250 - 300°C. In connexion with this, great interest has been caused by the development of a formula for enamels on the basis of a suspension of the copolymers of Fluoroplast-4 leading to LF NIIKP. In the creation of such lacquers, high lacquer strength and humidity resistance of the enamel wires will be achieved. However, these enamels may exhibit reduced adhesive qualities and increased thermoplasticity.

Abroad, wires with especially high heat resistance of the insulation with a very thin layer of ceramic material are recommended, which is deposited from a solution by electrophoresis. Ceramic insulation is additionally supported by a suspension of a Fluoroplast-4 or Silicone base lacquer. Conductors with this type of insulation are recommended for protracted use at temperatures up to 300°C.

Conductors with heat resistance up to 250 - 300°C may be obtained in the same way by impregnation with oxide insulation by suspensions on a base of Fluoroplast-4 or of its copolymers, or indeed, with heat resistant silicone compounds or polyester lacquers, as is done on an experimental basis in the NIIPP and by some foreign firms. For the formation of the oxide insulation the copper conductors must first be covered with a thin layer of aluminium. Such conductors may only be used for the preparation of various coils, designed to work at particularly high temperatures, but the wires thus obtained exhibit limited elasticity (they stand up to winding on a core of 10 - 20 times the wire diameter), low electric strength (150 - 200 V) and an increased hygroscopic quality.

Very thin manganin* wires with continuous glass insulation

In recent times the factory "Mikroprovod" with special techniques has

* Manganin is a manganese-nickel-copper alloy.

prepared for small scale, high ohmic resistances of increased stability, manganin wires with diameters of 6-10 μ with continuous glass insulation. Since measurements of the dimensions of such bare manganin wires is exceedingly laborious, these wires are classified in relationship to their electrical resistance (see Table 1).

Selection and general characteristics of very thin manganin wires with continuous glass insulation

TABLE 1

Resistance of manganin wire 1 m long (Ω)	Permissible deviations of resistance (Ω)	Maximum outside diameter of the insulated wire (μ)	Breaking strength of the wire. Not less than g (grams)
15,000	± 2500	14	8
11,000	± 1500	16	10
8000	± 1500	17	12
5500	± 1000	18	14
4000	± 500	20	18

1959

Disregarding the very small thickness of the glass insulation the latter exhibits high electro-insulation properties (the absence of small points of damage, puncture voltage not less than 1000 V). Naturally, continuous glass insulation has less flexibility and much more brittleness than fibre-glass. In connexion with this, the wires remain wound on aluminium formers 25-30 mm diameter with a weight of not less than 0.5 g on one end. For 20 per cent of the total quantity a minimum weight of 0.2 g on the end is permitted.

For the determination of elasticity and strength of glass insulation the wires are tested by winding them on a core of 4 mm diameter. In general it is possible to obtain it with this sort of insulation on copper and constantan wires.

Enamelling of conductors with rectangular cross-section

In recent times, wires with rectangular cross-sections have only been made with enamelled insulation with films of Viniflex lacquer. The selection of these wires has been limited to copper about 0.5-1.95 mm thick and 2.10-8.8 mm wide. The electrical strength of the enamel insulation of the wires (175-250 V) is determined by the thickness of the film at the edges, so that for enamelling rectangular conductors with small radii of curvature, the film in these places runs, compacts and goes over to the flat part of the surface of the conductor. In fact, at the edges a high pressure of film p will be obtained according to the Laplace equation

$$p = \sigma\left(\frac{1}{r} + \frac{1}{r_1}\right),$$

where; σ is the surface tension

r, r_1 the radii defining the curvature of the surface.

In the case given $r = \infty$ and consequently,

$$p = \frac{\sigma}{r_1}.$$

The removal of the given defect may be achieved if for rectangular conductors with a thickness of 1.35 mm one takes a curved form for the edges (Fig. 4) with a radius of curvature of $r = a/2$, where a is the thickness of the copper conductor, and for wires of greater thickness one uses a radius of curvature about 0.7 - 2.0 mm (Fig. 5). The reduction in the calculated section for rectangular wires with a thickness less than 1.35 mm will be expressed by the following equation

$$\eta\,{}^{0}/_{0} = \frac{a^2 - \frac{\pi}{4}a^2 - \xi}{ab - \xi} \cdot 100$$

and for wires of greater dimensions:

$$\eta\,{}^{0}/_{0} = \frac{4r^2 - \pi r^2 - \xi}{ab - \xi} \cdot 100,$$

where ξ is the reduction of section established in the calculated tables GOST 434 - 53 and equal approximately 0.50 mm².

In principle, the value η may be further reduced, in taking an ellipsoidal form for the narrow side of the rectangular wire (Fig. 6). In this case the reduction in section as against that calculated in GOST 434 - 53 may be obtained from the equation:

$$\eta\,{}^{0}/_{0} = \frac{2aq - \frac{\pi}{2}aq - \xi}{ab - \xi} 100.$$

A given increase in the radius of curvature on the edges which is accomplished by foreign firms may increase the value of the breakdown voltage. The losses of the cross-section in a wire of small cross-section will not exceed 2 - 3 per cent. Therefore, the question relating to the change of profile of our rectangular copper and aluminium conductors must be given great attention by us.

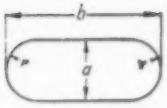

FIG. 4. "Rectangular" copper wire with semi-circular narrow sides

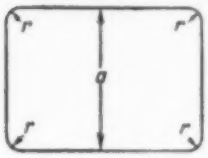

FIG. 5. "Rectangular" copper wire with increased radius of curvature at the edges

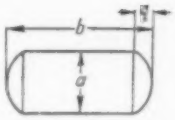

FIG. 6. "Rectangular" copper wire with semi-ellipsoidal narrow sides

The enamelling of rectangular conductors is also possible when using other enamels (Metalvin, polyamide-resol, polyester etc.). In particular, in recent times for special applications rectangular conductors of high heat resistance, which can be used for limited periods at 180 - 200°C are prepared with the use of polyester lacquers. Abroad (in Czechoslovakia, Eastern Germany etc.) for the preparation of rectangular enamelled conductors, lacquers on a polyamide-resol base are widely used. In the U.S.S.R., the production of rectangular enamelled conductors must be greatly increased rapidly since that would allow the output of wires type PBD,PDA and others to be reduced and would give new possibilities for the perfection of construction of various electrical machines.

1959

Conductors with delta-asbestos insulation

Asbestos insulation is put on and stuck to the copper wire with a final impregnation and dessication of the insulation. At the present time, glyptal lacquer is used for sticking, but for the impregnation of the insulation for a long time, only bituminous lacquer was used. The presence of the impregnating bituminous lacquer gave difficulty in soldering wound conductors, in particular for mechanized soldering of collectors since, when heated, this lacquer melted out of the conductors and fell into the baths with the solder.

Experiments to improve the properties of delta-asbestos coated wires by completing the work on the formula for bituminous impregnating lacquers (modifications to it of quick drying vegetable fats, kanifol and other resins) did not give suitable results. Therefore an investigatory work was undertaken having for its aim the explanation of the use of other impregnating lacquers. As a result of this work it has been confirmed that in use as an impregnated and sticking lacquer more or less useful results were given by water emulsified glyptal lacquers.

When using this lacquer, particular attention must be given to its quality and careful preparation in order to exclude the possibility of the appearance of separate cracks on the bends of the insulation, in particular after prolonged storage. GOST 7019 - 54 sets forth the maximum permitted heat for these

conductors at the time of use as up to 130°C. Some foreign firms allow the heating for limited periods of asbestos and delta-asbestos insulation in combination with glass-fibre to reach 200°C and even up to 250°C. Therefore the additional investigations by ourselves in these directions are undoubtedly of practical interest.

Wires with fibre-glass insulation

At the present time, a special type of conductor with fibre-glass insulation conductors type PSD has appeared, which the cable factories have produced in accordance with GOST 7019-54, which sets out the long term permissible temperature as 150°C. Past investigations show that this temperature may yet be slightly increased and raised to 160-170°C. Short term conductors may be worked at temperatures of 200-250°C.

PETSO type conductors, the long term permissible temperature of which is about 125°C, are as yet produced in limited quantity. At the present time, for the preparation of these conductors instead of enamelled ones type PET (with glyptal lacquer) conductors type PEV-1 (Viniflex or Metalvin) are used which only raised their quality.

The choice of covered conductors with fibre-glass insulation is now noticeably greater. As a sign of the organization of production of electric motors for tropical conditions manufactured in recent times may be given type PETSO-T and PSD-T (TUK OMM, 190-56). In these the thickness of the insulation is of the same order as with type PELBO.

In the cable factories conductors type PSDK are also made in which in the place of adhesive and impregnated substances Silicone lacquers are used. BTU MEP OAA 505.023-52 gives the long term temperature of these conductors as up to 180°C. For a limited period these conductors may be used at temperatures of 250-300°C.

Moreover, as a result of the needs of aviation electric machine construction, our cable factories produce conductors type PETKSO and PETKSOT for the preparation of which wire enamelled with Silicone lacquer is used adaptable also for sticking and impregnation with single layer fibre-glass insulation. Wires type PETKSOT are distinguished from wires PETKSO by some increase in the thickness of the insulation, which is reached by the use for all conductor dimensions 4 μ and with the presence of small holes in the insulation. These and other wires are designed for work for limited periods (500-2000 hr) at temperatures of up to 180°C.

Using fibre-glass 3 and 4μ thick in recent times NIIKP in co-operation with "Moskabel" have developed the construction of conductors type PSDK with a

reduced thickness of insulation. Type PSDKT is manufactured with these conductors. With the same purpose, for the needs of the aviation industry there was developed the construction of conductors type PSOT with single layer insulation with glued and impregnated fibre-glass insulation of heat resistant Silicone lacquers. In the NIIKP and MEI, experiments were carried out which showed that these conductors, particularly type PSDKT, may for a limited time (a few hundred hours) be worked at temperatures up to 300-350°C. With these experiments it was determined that the action of such a temperature does not really affect the electrical properties of fibre-glass insulation; although the latter at these temperatures does lose (especially with small diameter circular conductors) a noticeable portion of its silicone impregnated lacquer. In particular, after 100-200 hr exposure to these temperatures, it continues to stick to the wire stably and stands up to vibratory conditions (the amplitude of oscillation 2 mm at 1350 c/s).

According to the conditions of these experiments one may consider the oscillations to proceed according to the law, $s = A \sin(\omega t + \phi)$.

The acceleration of this oscillation is:

$$s'' = -A\omega^2 \sin(\omega t + \varphi).$$

If in this equation one puts the given conditions of the test, $A = 2$ mm, $\omega = (2\pi 1350)/60$, then the maximum acceleration will be:

$$s'' \approx 4g.$$

In this way, the experiments mentioned correspond to the maximum acceleration equal to $4g$, by which in the course of 16 hr of such tests there was no noticeable decomposition of the insulation and exposure of the copper conductor. In recent times on conductors type PSDKT and PSOT the provisional technical specifications TUKP 18-58 and TUPK 17-58 were confirmed.

More stable for generally high temperatures is insulation made from windings and braids of fine fibre-glass as well as with glued and impregnated heat resistant silicone lacquers. In this case especially, the thickness of the insulation is a little increased. However, the technical process of applying braid is very tedious and slow and so conductors made in this way may only be used in very special circumstances.

According to a communication from the General Electric* Co., radio apparatus has been built allowing operation at temperatures up to 500°C. All the components in it may work at red heat and without reaction to the effects of powerful radioactive radiation. The development was made at the order of the military command of the U.S.A. for general defence purposes.

* *Electronics*, October 1956.

The windings of transformers, electric motors and selsyns in this apparatus are wound from copper silver-plated conductors with insulation by a layer of heat resisting glass. Such a conductor is made with a diameter of from 0.12-1.8 mm. Test samples of the electric motors and transformers in which glass thread has been used for the external insulation have worked continuously for some hundreds of hours at temperatures of 520°C.

For the heating of conductors above 250°C, a copper wire becomes covered with a layer of copper oxide. For the preliminary experiments no particular importance was assigned to this effect. The ohmic resistance of the wire during the course of 260 hr at 300°C increased approximately 1 per cent, and after 103 hr at 400°C to 4-6 per cent. Here additional experiments are essential. It seems more dangerous, that for a very long exposure to a high temperature with periodic cooling of the conductors small pieces of detached copper start to project through the glass-fibre insulation and this latter darkens, as a result of which the insulation resistance of the winding is noticeably reduced. Attempts to prevent this by using an electroplated silver covered copper conductor did not give positive results. Evidently a thin porous layer of silver put on by electro-deposition does not give the desired protection against oxidation of the copper when the wires are exposed to high temperatures for long periods. It is possible that significantly better results may be achieved if the added layer achieves a greater thickness and additionally its penetrability can be reduced by a suitable filler. Aluminium coverings show themselves to be very resistant at temperatures of 300-400°C. However, if the copper conductor is covered with a melted layer of aluminium there is the fear that a brittle layer with higher electrical resistance may appear on the surface of the copper conductor. Better results may be attained if the aluminium envelope is put on a copper wire of large cross-section with a cold process and then the wire reduced to the desired size by drawing. When such an aluminium coated conductor is exposed to 300°C for 48 hr no change whatsoever in the ohmic resistance can be observed. Moreover, the requisite effect may be obtained if the aluminium covering is carried out not on a bare copper wire but on a wire previously covered with a thin layer of silver or nickel.

Translated by R.P. Froom

AN INVESTIGATION OF AN AUTOMATIC SYSTEM OF EXCITATION FOR LARGE TURBOGENERATORS USING SEMICONDUCTOR POWER RECTIFIERS*

IA.N. SHTRAFUN and M.S. ROSTOVTSEVA

Leningrad

(Received 31 October 1957)

The further growth of power systems in the Soviet Union has placed before the electrical industry the problem of the development of and putting into production and use of turbogenerators with powers up to 300 MW. The solution of this complicated problem of national economics has raised a series of serious scientific and technological questions, to the number of which is frequently added the development of an automatic regulating system for the excitation of turbogenerators which satisfied the demands of modern exploitation.

The desire for the utmost use of active materials and, connected with this, the application of forced draught hydrogen cooling with the hydrogen under a pressure of up to 3 atm in the body of the generator leads to a noticeable increase in the parameters of the excitation system of the generator (see Table 1).

TABLE 1

Turbogenerator power (*MW*)	Rotor current in rated conditions (*A*)	Rotor voltage in rated conditions (*V*)	Rotor voltage with forced excitation (*V*)
200	2250	400	800
300	3000	525	1000

As tests over many years have shown in use, a system of machine excitation has the greatest reliability in the case where the exciter is assembled on the same shaft as the turbogenerator. However, the given practical parameters of the

* *Elektrichestvo* No. 8. 37-41, 1958.

system of excitation exclude the possibility of such a constructive solution if a d.c. machine is used as the exciter.

The progressive increase in the production of semiconductor rectifiers gives favourable grounds for their use in the power circuits of excitation systems, and the availability of reliable sources of alternating current for supplying these rectifiers gives an especial perspective to such a system of excitation. To the total of such sources of supply may be added three-phase generators of increased-frequency alternating current (400-500 c/s) of the induction type which may be used for power circuits, and also generators with permanent magnets on the rotor for supplying the control circuit and the apparatus for automatic regulation. The absence of windings on the rotor and the need for connexion only to the stator of all the circuits substantially increases the reliability under working conditions of such arrangements. The necessity of increased-frequency a.c. generators of this type determined by constructional considerations may be expeditiously used for the reduction of the dimensions and the increase in the rapid action of the general elements of automatic excitation control, which gives the possibility of making a system compact and of small inertia.

With the aim of investigating the parameters of such a system of excitation in various conditions of use, and also of accumulating working experiments as separate elements, as well as of systems of excitation the exploitation of a new system of excitation of a turbogenerator with a power of 30 MW type TBF-30 was worked out by the whole factory "Elektrosil", prepared and handed over for operating tests in one of the electric stations LENENERGO. The technical details of the system are given in the appendix.

The main circuit of the excitation system is given in Fig. 1. A three-phase

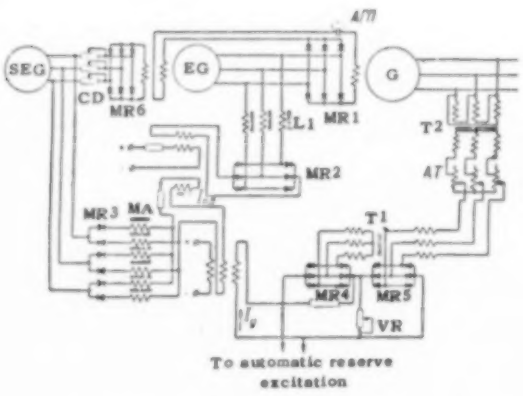

FIG. 1. Principal circuit for turbogenerator excitation

generator *EG* is used as a source of supply to the excitation system. This is of the induction type, having two excitation windings on the stator. The frequency generated is 500 c/s. The main excitation winding which is designed to make use of the compounding effect of the free current in the rotor is connected as a series self-excitation circuit. The second – auxiliary winding is connected as an independent excitation circuit. It is intended for the initial excitation of the generator and for adjustments of the circuit, and also may be used for forced excitation.

The independent excitation circuit receives a controllable supply from the high-frequency pilot exciter *SEG* through the rectifier *MR6*. The pilot exciter is itself excited by permanent magnets.

The generator and the pilot exciter are mounted on the same axle as the turbogenerator *G*.

The excitation winding of the generator gets its supply from the exciter of the generator through the Selenium Power Rectifier *MR1*.

To achieve great effectiveness in the rise of rotor voltage during the process of automatic regulation and forced excitation, the exciter of the generator is so calculated and constructed that with nominal rotor current for the turbogenerator, as a result of the consequent self-excitation, it produces a voltage at the exciter which exceeds the demands of a given condition and prepares the exciter for forced excitation. This produces a definite excess voltage at the exciter of the generator in this or another condition of the turbogenerator. The compensation of this excess of voltage is realized by switching an additional reactive load into the exciter circuit, automatically regulated in accordance with the conditions of working of the turbogenerator.

To this end power inductors *L1* are connected to the stator windings of the exciter in parallel with the output of the rectifier *MR1* with magnetization appearing in the main regulating element of the power part of the system. The automatic regulation of the turbogenerator excitation is achieved by means of a regulated fall in voltage on the stator windings of the exciter from the boost current of the power inductors. The degree of magnetization of the inductors is automatically changed by the excitation regulator.

Regulation of this kind seems effective in view of the character of generators type *BGT* which have relatively high values of reactance x_d, equal to $0.12\,\Omega$ in the given case. The necessary boost current is defined as the ratio of the excess voltage on the exciter to x_d.

Other variants of the automatic regulation of the excitation voltage of generators are possible, an analysis of which does not enter particularly, into

the scope of the present article. It is only right to observe that, for a given rate of rise of voltage, and to attain the desired excitation power with forced excitation, the transition for example to a parallel self-excitation circuit demands the use of a rheostat, the losses in which increase the active boost losses in the inductors. The need for the use of relay forced excitation in this case also appears insufficient in comparison with a system of uninterrupted regulation for all the range of excitation current almost up to the maximum value.

As a possibility the use of a combined series-parallel circuit for self-excitation with automatic regulation in the circuit of the parallel self-exciter etc. may be considered.

The automatic regulator for the excitation operates as a function of the voltage across the intermediate amplifying element which is the Magnetic Amplifier *MA*. This is provided with an external return circuit for increasing the amplification factor. The a.c. windings of the magnetic amplifier are fed by the pilot exciter.

The metering element of the regulator consists of a three-phase saturated transformer *T1* which is connected across a variable autotransformer *AT*, *T1* gets its supply from the generator voltage transformer *T2*. The primary current of the metering transformer, appearing as the magnetizing current, is non-linearly dependent on the voltage of the generator to a marked degree.

The secondary windings of the metering transformer are only used for operating the automatic excitation regulator for the reserve excitation system. The magnetizing currents of the transformer are rectified by the rectifiers *MR5*; at their output the regulating resistance *VR* is established to which are connected the main control windings of the magnetic amplifier. For effective forced excitation the reduction of the no-load current both in the inductors and in the magnetic amplifiers must be substantial. With this in view the magnetic amplifier has an additional winding as well as the normal control windings the supply to which is from the operating current. As protracted tests have shown, the circuit may conveniently be supplied by the rectified exciter current.

The current flowing through this winding causes an initial magnetization directed towards the field by the condition of the external feedback, thanks to which the no-load currents of the magnetic amplifier are reduced. Moreover, the magnetic amplifier has an external winding of opposite sense which serves for adjustment of the circuit.

The current from the output of the magnetic amplifier is fed into the main magnetizing windings of the power inductors, having a winding external to the permanent return circuit. For the reduction of the no-load current in the inductors an additional winding is provided fed through a resistance from the operating

current circuit. The direction of the m.m.f. of the additional magnetizing winding is in opposition to the direction of the m.m.f. of the normal winding of the external feedback. In this way under conditions of forced excitation the inductor current reaches a minimum value.

The process of automatic excitation regulation is achieved by use of the magnetizing current of the metering transformer as a function of the voltage of the turbogenerator, operating suitably on the magnetizing current of the power inductors.

In the event that it is necessary to maintain constant voltage and reactive power of the generator, the voltage of the measuring element is changed accordingly by the use of the variable autotransformer.

In the system of excitation relay blocking is provided which maintains the supply excitation of the generator in the event of rupture of the fuses on the high-voltage side of the voltage transformers by automatically connecting to the reserve.

Under working conditions the main direction of investigation was the determination of the following parameters of the system: the limits of voltage regulation, automatically maintained by the constants in the statistical regime; the steadiness of the regulation of excitation; the rapidity of voltage rise when the exciter worked on the excitation winding of the generator and the determination of the influence of the free rotor current under short-circuit conditions on the system.

1959

For the preliminary stage of the investigations the optimum parameters of the elements of the system were determined. In addition, in the circuits for maintenance of forced excitation after extinction of the free rotor current, the effectiveness was determined of the additional relay forced excitation, which was achieved by means of adding to the independent exciting windings an additional current the magnitude of which depended on the value of the rectified excitation voltage of the generator *EG*.

The following stage was the investigation of the system of excitation and of automatic regulation when the turbogenerator was working in the no-load condition; by changing the load on the generator from zero to the normal value; by the transference of reactive power from the turbogenerator on test to the parallel working generators and back, with the sudden application of a three-phase short circuit to the stator of the turbogenerator, working on no-load at reduced initial excitation.

For reduction of the time constant of the control circuit of the magnetic amplifiers, an additional adjustable resistance is included in this circuit, the magnitude of which influences the steepness of the characteristics $I_u = f(U_g)$.

The characteristics were taken for various values of the resistance, but with a constant value for the resistance of the rheostat; they are shown in Fig. 2.

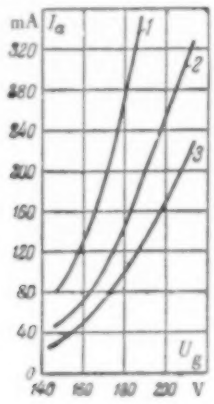

FIG. 2. Relationship of the control current of the magnetic amplifier to the generator voltage
(1) Without boost resistance. (2) and (3) Boost resistors 100 Ω and 200 Ω respectively

For reduction of the time constant of the circuits of the power inductors an additional variable resistance is included in this circuit also.

In Fig. 3 are shown the characteristics of a magnetic amplifier in its operation on the magnetization windings of the power inductors. The necessity for transference from no-load to normal power of the generator, the changing of the magnetizing regime of the power inductors and of the magnetic amplifier defines the regulation of the system which does not exceed 2 - 2½ per cent.

According to the results of the experiments performed on the elements of the automatic excitation regulator the parameters of the resistances in the magnetic amplifier and inductor circuits were chosen and these were left unaltered during the subsequent tests.

To define the effectiveness of the additional forced excitation of the exciter by means of the action on the independent winding as a function of the rectified voltage of the exciter, the regime of forced excitation was tested with operation of the exciter on a resistance equivalent to the resistance of the rotor winding.

The results of the regime of forced excitation without the additional effect of the independent excitation on the windings are given in Table 2.

In as much as with the extinction of the free rotor current of the turbogenerator there takes place some reduction in the effectiveness of the consequent self-

excitation, so the effect was determined of the simultaneous action of the supplementary relay forced excitation.

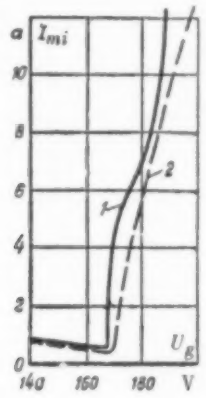

FIG. 3. Relationship between the output current of the magnetic amplifier (magnetizing current of the inductor) and the generator voltage
(1) Without a resistor in the magnetizing circuit. (2) With a resistor 10Ω. (Twice the resistance of the magnetizing winding)

TABLE 2

State	Magnetizing current in the inductors (A)	Equivalent load current (A)	Voltage on the equivalent load (V)
Initial	5.0	925	50
Forced excitation	0.8	3450	191

This forcing was achieved with the help of the feeding of the rectified excitation voltage to the independent winding of the excitation through a limiting resistor fixed at about 35 per cent of the additional m.m.f. of the excitation of the exciter in relation to the m.m.f. of the turbogenerator in its nominal running conditions. The results of the tests are given in Table 3, and the given working oscillogram in Fig. 4.

The rapidity of growth of the voltage on the equivalent resistance with the presence of additional forced excitation is 96 V/sec, and with forced excitation

with additional operation on the independent winding, this speed equals 192 V/sec. The voltage on the independent winding appeared as given after 0.24 sec. Since the actual time of operation of the relay arrangement does not exceed 0.08 sec, this speed of growth of voltage of excitation in the second state is determined taking into account this time.

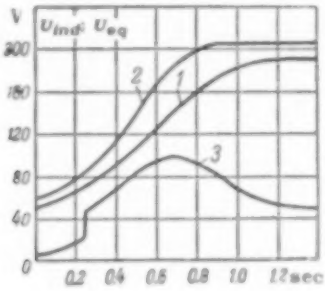

FIG. 4. Relationship between the voltage on the independent excitation winding of the exciter of the generator (U_{ind}) and on the resistance, equivalent to the resistance of the excitation winding of the generator (U_{eq}) and time with forced excitation.

(1) U_{eq} with the absence of additional forced excitation. (2) and (3) U_{eq} and U_{ind} with forced excitation with the additional effect on the independent winding

TABLE 3

State	Magnetizing current of inductors (A)	Voltage on independent excitation winding (V)	Equivalent load current (A)	Voltage on equivalent load (V)
Initial	4.5	6.7	1080	60.0
Forced excitation		100	3800	207

From the data given, it is seen that the additional action on the independent excitation winding, simultaneously with the increase in the rate of growth of the excitation, increases the maximum of excitation also.

The system of automatic regulation tested in a closed system worked as stably under no-load conditions as with the normal load on the turbogenerator

without the use of the stabilizing transformer provided for the system of reserve excitation.

In the process of operation there takes place a transfer of reactive power from the turbogenerator on test to parallel working and back; the transfer proceeds evenly from almost full shedding of the reactive load of the turbogenerator on test to the limit of permissible load according to the conditions of operation.

For the testing of a system of series excitation with the appearance of free current in the rotor, a short circuit was suddenly applied to the output of the turbogenerator, with the generator voltage reduced to 2000 V. The change in generator stator current and voltage on the exciter are shown in Fig. 5.

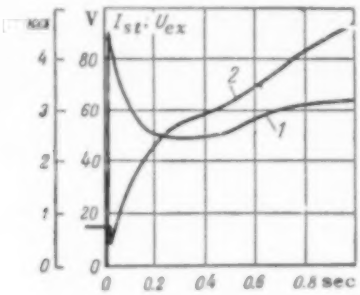

FIG. 5. A short-circuited generator
(1) Stator current (2) Exciter voltage

The speed of rise of voltage was determined graphically according to the stator voltage of the exciter and was found to be 128 V/sec which, in relation to the initial voltage (15 V) gives an 8.5 : 1 change in voltage in one second. If this parameter is calculated in relation to the generator voltage (6500 V) and the stator voltage of the exciter (100 V) running in normal conditions before the short circuit on the generator output a rate of change of voltage of almost 4 : 1 is found on the exciter.

Conclusions

A system of excitation built according to the parameters obtained above fully satisfies the given demands and guarantees the necessary statistical characteristics, in particular the range of regulation of voltage and reactive power of a generator with a low statism*. The process of regulation takes place stably. From tests of forced excitation on the equivalent resistance, the parameters of

* Statism is the deviation of the controlled quantity at nominal load from its value at no load expressed as a percentage (of its value at no load).

the system are found by the rapidity of voltage build-up. The effectiveness of the additional action is verified by the help of relay circuits on the excitation winding independent from its rectified voltage.

Such an additional action is expedient, since it gives the possibility, in the event of forced excitation being necessary of obtaining stable forced excitation at the required level even after extinction of the free rotor current. Having obtained with this the additional saturation of the magnetic system of the exciter it leads in addition to the improvement of commutation of the rectifiers by means of the reduction of the reactiveness of the source of supply, and also guarantees a noticeable increase in the excitation maximum.

Experiments with suddenly applied three-phase short circuits with small initial excitation on a generator on no-load determined the rate of voltage build-up with the action of the free rotor current, stressing the expediency of series self-excitation for the exciter.

The experiments carried out give reason to conceive the development of the system as a project for large turbogenerators.

Translated by R.P. Froom

Appendix

Technical data of the arrangements.

1. Generator – Factory "Elektrosil", Type TVF-30-2; 30 MW, 3440 A; 6.3 kV; $\cos\phi = 0.8$; Nominal rotor current 1450 A; rotor resistance 0.0455 Ω.

2. Exciter – (for the turbogenerator), high-frequency generator. Type VGT-350-500 from the factory "Elektrosil"; 275 kVA; 110 V; 500 c/s; 1450 A; 3000 rev/min; Induction type, winding – delta connexion.

3. High-frequency pilot exciter – Type GSP-4.5, from the factory NIIEP; 118 A; 3.6 kW; 220 V; 3000 rev/min; 400 c/s; Permanent magnet excitation.

4. Automatic panel Type EPA-502 from the factory "Elektrosil"; with an assembled automatic regulator for the main and reserve excitation systems, with Selenium rectifiers type VS-59, rectifying the pilot exciter current, and with high-voltage Selenium rectifiers type TVS-100 for the feedbacks of the power inductors.

5. High power rectifier panel type PVS from the factory "Elektrosil" with high-voltage Selenium rectifiers type TVS-100 connected as a three phase bridge circuit with 150 parallel branches and 4 series branches in each arm; nominal rectified current 1500 A; nominal voltage 100 V; forced air draught cooling.

6. Power inductor panel type DS-1 from the factory "Elektrosil" 600 A; 500 c/s; power of the single-phase inductor.

1959

THE EXCITATION OF SYNCHRONOUS MOTORS OF NORMAL CONSTRUCTION BY THE APPLICATION OF MECHANICAL RECTIFIERS*

N.S. SIUNOV, B.K. GAVRILOV and V.N. BREEV

Uralian 'Kirov' Polytechnic Institute

(Received 4 March 1958)

The problem of the replacement of the electromechanical exciter of synchronous machines by mechanical rectifiers is of great importance to low-and medium-power installations. Owing to the application of mechanical rectifiers [1] the construction is simplified and the cost of the plant is significantly decreased, (especially in the low-power range). The main cause of the inadequate introduction of mechanical rectifiers is the bad switching of current in these devices. Questions on the sparkless switching of the mechanical rectifiers of synchronous generators were most successfully resolved by Tamantsev [1]. In his proposed circuit a mechanical rectifier obtains its supply from an auxiliary winding situated in the recesses of the stator of the generator. The installation was provided with three single-phase current transformers, the secondary windings of which were shunted by small active resistors inserted into the circuit of the mechanical rectifier. Tamantsev's circuit enables us to obtain sparkless commutation of a mechanical rectifier and practically constant voltage for a synchronous generator with changes of load from zero to the nominal value.

As the experimental researches of Artanov showed [2], the circuit under consideration provides sparkless commutation in the motor only with an even load. Hence the pressing problem of the subsequent development of a circuit for synchronous motors with mechanical rectifiers, providing also satisfactory commutation of current with sudden loads. For this purpose one may employ a triple-wound transformer by means of which the supply is drawn via a mechanical rectifier to the circuit of the winding for starting the synchronous motor. Also, the synchronous motor is of normal construction as the manufacture of a supplementary

* *Elektrichestvo* No. 8, 46-49, 1958.

winding on the stator is not required. As is known [3] triple-wound transformers in circuits for exciting synchronous generators were employed in one factory as far back as in 1947. The circuit for switching in the synchronous motor with a mechanical rectifier and triple-wound transformer is illustrated in Fig. 1.

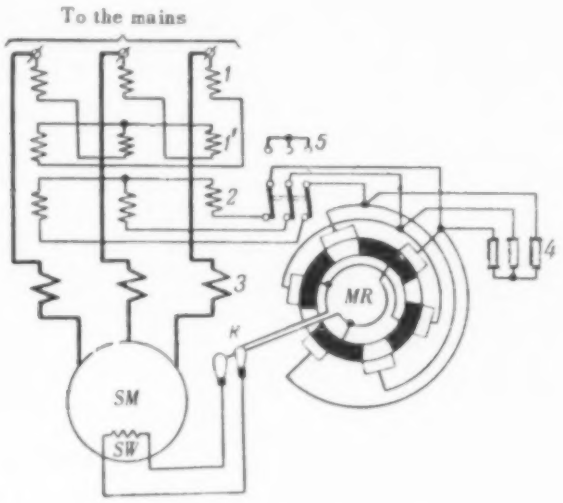

FIG. 1. Circuit of the switching of a synchronous motor with a mechanical rectifier and a triple-wound transformer

The three-phase regulating transformer has three windings. The primary winding *1-1'*, coupled "zigzag" is inserted in parallel with the stator winding of motor *SM*; winding *2* is supplied via the mechanical rectifier excitation winding *SW* of the motor. The series winding *3*, around which flows the full current of the stator, provides supplementary regulation of the current for exciting the synchronous motor with a change of its load. For changing the rate of the effect of current winding *3*, a transformer is provided with a movable magnetic shunt (Fig. 2).

On the same shaft with the motor is the mechanical rectifier *MR*, the width of an idle segment of which is equal to half of the width of a working segment. For improving the conditions of excitation, the brushes of the rectifier are shunted by the active resistors *4*. Change-over switch *5* locks the brushes during the starting period of the motor; after attaining hyper-synchronous speed, excitation is produced with the aid of a mechanical rectifier. As the load of the motor is increased, so the excitation current is automatically increased. The motor will work all the time with leading current and a practically hardly varying power factor.

As pointed out by Tamantsev, for flashless commutation during changes of

working conditions from no load to full load, it is necessary to provide automatically for a constant position of the voltage vector on the rectifier brushes relative to the no load e.m.f. vector. In so far as the most essential factor for the practical application of the mechanical rectifier is the satisfactory commutation of current, so in the first instance, we shall consider the problem of rectifier operation in the circuit with the triple-wound regulating transformer.

The equivalent circuit of the commutator circuits is illustrated in Fig. 3

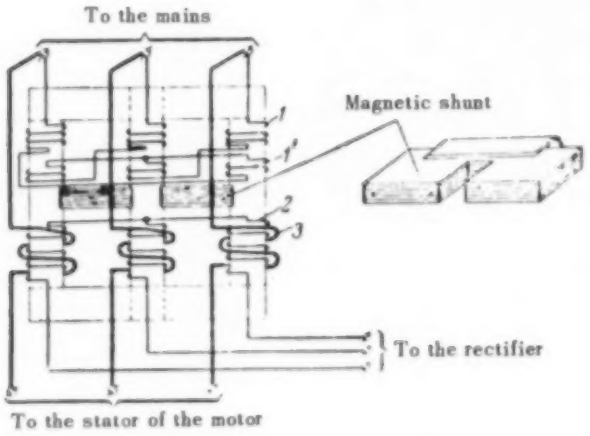

FIG. 2. Triple-wound transformer with a magnetic shunt

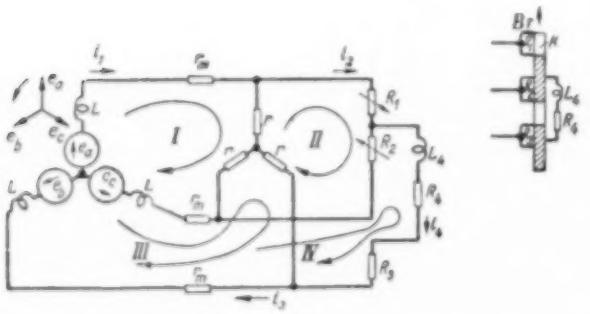

FIG. 3. Equivalent circuit of the commutator circuits

The direction of motion of the commutator in Fig. 3 is indicated by an arrow.

With the width of the brush equal to the width of an idle segment and equal to 60°, the period of commutation $T = 1/6f = 1/300$ sec. Since the picture of the commutation with motion of the commutator is periodically repeated, it is enough to consider the process for time equal to the period of commutation. The problem

comes to the determination of the current in one of the brushes, as the current of a second brush is equal to the difference between the current of the winding for the excitation and the unknown value of the current. The value of the rectified current is assumed known and is practically constant. Taking into consideration that the resistance r_m of the secondary winding of the transformer is notably less than the resistance of the shunting brush, we may take it further that $r_m = 0$.

As a result of tracing circuits I and II we obtain the equation:

$$2L\frac{di_1}{dt}+2ri_1-2ri_2-L\frac{di_3}{dt}-ri_3-ri_4=e_a-e_c; \tag{1}$$

$$-2ri_1+(R_1+R_2+2r)\,i_2+ri_3-R_2i_4=0, \tag{2}$$

where e_a and e_c are the resulting phase e.m.f. of the transformer; i_1, i_2, i_3 and i_4 is the current in the contours of the equivalent circuit; L is the equivalent inductance of a phase of the transformer device; r is the resistance shunting the brushes; R_1 and R_2 are the resistances of the brush contacts, dependent on time. Resolving equations (1) and (2) together, after simple conversion we obtain

$$\begin{aligned}&\frac{L}{r}(R_1+R_2+2r)\frac{di_2}{dt}+\\&+\left[\frac{L}{r}\frac{d}{dt}(R_1+R_2)+R_1+R_2\right]i_2-\\&-\left(\frac{L}{r}\frac{dR_2}{dt}+R_2\right)i_4=e_a-e_c.\end{aligned} \tag{3}$$

We accept that resistances R_1 and R_2 depend only on the area of contact of the brushes with the working segments and, consequently, their dependence on time has the form:

$$R_1=\frac{T}{t}R;\quad R_2=\frac{T}{T-t}R,$$

where R is the resistance of a brush contact when a brush is completely situated on a working segment.

Having substituted in equation (3) the values R_1, R_2, dR_1/dt, dR_2/dt and having separated all the terms in the coefficient with derived current according to time, we obtain:

$$\frac{di_2}{dt}+\frac{RT^2[(2L+rT)t-rt^2-LT]}{Lt(T-t)[RT^2+2rt(T-t)]}i_2= \tag{4}$$

$$= \frac{RT\,[r\,(T-t)+L]\,t}{L\,(T-t)\,[2rt\,(T-t)+RT^2]} + \frac{r\,(e_a-e_c)\,(T-t)\,t}{L\,[RT^2+2rt\,(T-t)]}.$$

Having produced integration and taking into consideration that $r \gg R$, we find the equation for determining the current i_2:

$$i_2 = \frac{t\,(T-t)\left(\frac{t}{T-t}\right)^{-\frac{RT}{2L}}}{2rt\,(T-t)+T^2R} \left\{ \int_0^t \left[\frac{RT\,[r\,(T-t)+L]}{L\,(T-t)^2} + \right. \right. \tag{5}$$

$$\left. \left. + \frac{r}{L}(e_a-e_c) \right] \left(\frac{t}{T-t}\right)^{\frac{RT}{2L}} dt \right\}.$$

For satisfactory working of the mechanical rectifier it is necessary to provide sufficient resistance for the brush contact, low equivalent inductance of the transformer device and a strictly fixed position of the brush cross-arm. One may join the first two conditions and in addition reduce to a formula in the following way. The transitory currents in the closed circuit, the operating segment – adjacent phase brushes – the external circuit, excited by the commutation processes will in practice damp during the period of commutation $T = 1/6f$, if the time constant of this circuit $T_{s.k}$ is 3 times less than the period of commutation, that is

$$T_{s.k} \leq \frac{1}{3} T = \frac{1}{18f}. \tag{6}$$

The time constant T_y of the external part of the circuit from brush to brush in consequence of the practically clear active resistance of the brush contact may be considered greater than the time $T_{s.k}$, calculated in formula (6). Experiment shows that with a relatively large transitory fall of voltage in the brush contact of the order of 1.2 V and with effective line voltage on the brushes not exceeding 30-32 V the time constant T_y may be 3-4 times greater than $T_{s.k}$. In these conditions, with the correct setting of the brush cross-arm, the commutation of current flows satisfactorily.

In Fig. 4 are represented the calculated graphs of the change of current $i_2 = f(t)$ under the running brush for various values of the initial phase ψ with $e_a - e_c = 173 \sin(\omega t + \psi)$ V. The parameters of the circuit: $R = 0.1\ \Omega$, $r = 5\ \Omega$, and $L = 0.00833$ H, or brought to the voltage of the circuit and expressed in relative units, $R' = 1.15$, $r' = 57.5$ and $L' = 33.4$. From the graphs of Fig. 4 it is evident that flashless commutation of the current of a mechanical rectifier, connected according to the proposed circuit, is possible with the resulting e.m.f. of

the first phase within the limits of from 15 to 30°.

The character of the change of the commutation current i_2 for a synchronous motor of 15 kW, 1500 rev/min, 220 V is represented on the oscillogram, (Fig. 5).

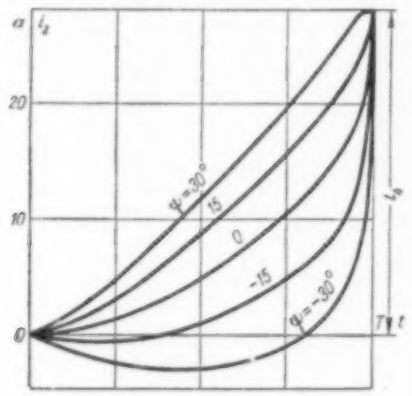

FIG. 4. Calculated graphs of the current under the running brush for various values of the initial phase ψ

1959

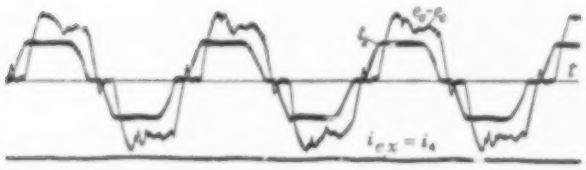

FIG. 5. Oscillogram of the change of commutation current

During experimental research on the synchronous motor with a mechanical rectifier its work was checked both with a smooth and with a sudden change of load.

With a smooth change of load in the range from idle running to nominal value the excitation current increased automatically, ensuring the operation of the motor with a given power factor. Numerous tests showed that during change of load of the motor in all ranges, commutation of current was satisfactory. As is clear from the oscillogram (Fig. 5), the rectified current i_4 is practically constant. The curve of current commutation has a trapezoidal form. At the beginning and end of the process the commutation of current does not exceed the arranged value, which testifies to the smooth running of the process. As the load of the motor increases simultaneously with the stator current, the excitation current winding is also increasing. (Fig. 6). The power factor of the motor with leading current in all

ranges of load change remains constant in practice. The motor without sparking on the brushes of the rectifier works wholly satisfactorily up to 110 per cent of the rated load.

With sudden changes of load from zero to 70 per cent of the rated value the motor works soundly with practically sparkless commutation of current, (Fig. 7).

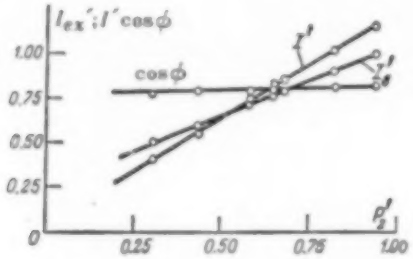

FIG. 6. The dependence of the stator current I', the current of excitation I'_B and $\cos\phi$ on the load P_2 on the motor shaft, (all values in the relative units)

FIG. 7

The limits indicated above of the permitted change of the initial phase ψ of the resulting e.m.f. $(e_a - e_c)$ at the input to the commutator circuits testify to the possibility of a considerable displacement of the brush cross-arm, relative to its optimum position and to the possibility of a certain disharmony over the phase of the voltage system, applied to the brushes of the rectifier with an interior angle of the machine θ, which has considerable significance for reliable and steady work of the synchronous motor with a mechanical rectifier.

As investigations showed on a 15 kW motor which were carried out in the Electrical Machines Laboratory of the Uralian Polytechnic Institute, the displacement of a brush cross-arm by 8 - 10° does not result in a disturbance of the satisfactory commutation of current. Analogous results were also obtained from tests in industrial conditions of a synchronized 300 kW induction motor, the rotor circuit of which was supplied by current via a mechanical rectifier.

The possibility of a certain disharmony of work of a rectifier on the interior angle of the machine together with the possibility of the combination of the windings of a triple-wound transformer by a "zigzag" connexion, permits us to break

the strict ratio of the parameters, adopted for generators in Tamantsev's system (1). With the operation of the machine by a motor this is still possible because there is no necessity to calculate the conditions of the machine for a wide range of changes of the power factor.

Conclusions

1. The excitation of synchronous motors of normal performance and of low and medium power may be accomplished with the aid of mechanical rectifiers attached to the output of a three-phase triple-wound transformer with a regulable magnetic shunt.

2. The proposed circuit provides an automatic increase of the excitation current with an increase of the load of the motor.

3. The commutation of the current of the mechanical rectifier is as satisfactory with slow as with sudden changes of load.

Translated by David Rex-Taylor

REFERENCES

1. S.G. Tamantsev; The synchronous generator with self-excitation from a mechanical rectifier. *Elektrichestvo* 3 (1952).
2. S.G. Artanov; *Issledovanie sinkhronnogo dvigatelya s mekhanicheskim vypryamitelyem (Investigation of the synchronous motor with a mechanical rectifier) Dissertatsia* NII MEP, (1954).
3. E.Yu. Movshin; The synchronous generator with excitation from selenium rectifiers in circuit with a triple-wound transformer. *Elektrichestvo* 7 (1947).

1959

DIRECTIONAL PROTECTION FROM SHORT-CIRCUITS TO EARTH*

T.V. STEPNOV

(Received 5 July 1957)

In the design of protection gear for short-circuits to earth acting on transient process currents in a compensated network complications arise in the selection of settings on long out-going lines having a considerable natural capacitive current. As follows from a curve which has been previously published [1], when the earth-fault point is 7-12 km from the station bus-bars, the magnitude of the transient process current is reduced 3-5 times. This effect must be considered in the selection of the setting of protection gear.

The possibility of increasing the sensitivity of protection gear is limited by the presence of natural transient process currents in all faultless lines. In a network then, with a sustained capacitive current of 60-120 A, on outgoing lines with a natural capacitive current of more than 10 A the setting current can be less than the maximum possible natural transient process current which arises in the presence of a short-circuit to earth outside the given line, causing incorrect operation of protection gear. The maximum natural transient process current develops in faultless lines in the presence of short-circuits to earth at or near the station bus-bars. Strengthening of protection gear with the aim of increasing its selectivity leads to failures in cases of distant faults on the protected line.

Achieving the desired tuning out of natural currents and increasing protection sensitivity require a more detailed study of transient processes in unfaulted lines generally, and in "long distance lines" in particular. In this case, the term "long distance lines" is taken to mean lines with a sustained natural capacitive current of 10 per cent and more of the total capacitive current of the whole network, and with a distance of 7-12 km to the most distant points.

Information is presented below on working tests for an analysis of the operation of a previously described [1] directional protection gear in the light of the

* *Electrichestvo*, No. 8, 75-79, 1958.

above-mentioned conditions. Current oscillographs were made in the network in the presence of artificial short-circuits to earth at various points. The latter, as a rule, were made across a spark gap. Each short-circuit lasted 0.7 - 1.2 sec. Here breakdown of the gap was repeated after 0.1 - 0.16 sec.

A simplified 3-line circuit of the station and network with an indication of the earth-fault points is shown in Fig. 1. The parameters of its elements and the conditions in which the experiments were made are given in Table 1, and characteristic oscillographs are shown in Fig. 2.

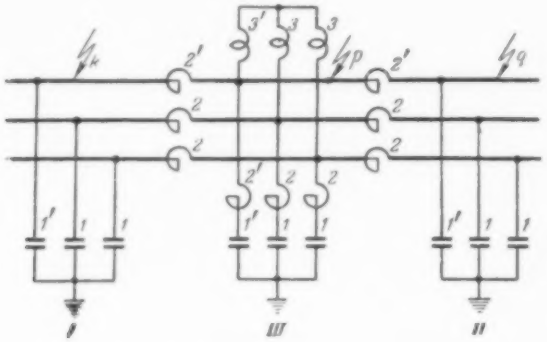

FIG. 1. Simplified circuit of station and network

I, II, III - outgoing lines

1 – capacitance of unfaulted phases of the line; *1'* – capacitance of earthed phase of the line; *2* – section and line reactors of unfaulted phases; *2'* – same for earthed phase; *3* – inductances of unfaulted phases of generating sources; *3'* – same for earthed phase.

Curve 7 is for the station where all the lines are equipped with reactors, and as a result, it corresponds in frequency and form with two other curves for long distance lines with approximately similar parameters.

In Fig. 3 a simplified equivalent circuit is given which is more suitable for analysis of the passage of currents in line II. In it the current directions in the earthed and unfaulted phases in the first half-cycle after the occurrence of a short-circuit to earth are shown under the action of which a resultant current develops in the secondary winding of the zero-sequence current transformer. Thus, this resultant current which is shown on the oscillographs is a superposition of the currents in the two unfaulted phases on the current in the faulty (earthed) phase.

The frequency and form of these currents are determined by the circuit which is formed in dependence on the location of the fault point. So when a short-circuit occurs at point *q* (Fig. 3), the following circuits are formed: for the earthed

TABLE 1

Line number in Fig. 1	Natural current of line, A	Length of cable, km, from bus-bars to		Cross-section of cable up to first reactor mm²	Type of reactor		Power of generating sources, MW		Fault point in Fig. 1	Curve number in Fig. 2
		Most distant point	First reactor		Line	Section	Generators	Transformers		
I	10.6	8.2	5.1	2×50	None	RB-1000-10	26	10	*q*	3
							10	25	*q*	6
							10	25	*k*	9
III	2	1.9	0.15	150	RB-600-6	same	26	10	*q*	4
II	14.6	5.6	1.8	2×120	None	same	26	10	*q*	1
							26	10	*k*	2
III	10.3	7.0	4.3	120	RB-600-6	2500a	108	40	*p*	7
I	6.6	6.4	2.7	70	None	None	0	27.5	*k*	10

phase q – earth – o – capacitance $1'-q$, the principal inductances (reactor and generating source windings) being absent in it; for the unfaulted phases q – earth – o – capacitance 1 – reactor 2 – generating source windings 3 and $3'$ – reactor $2'-q$. All the principal inductances (the 2 reactors and the 2 windings of the different generating source phases) are connected in series in this circuit.

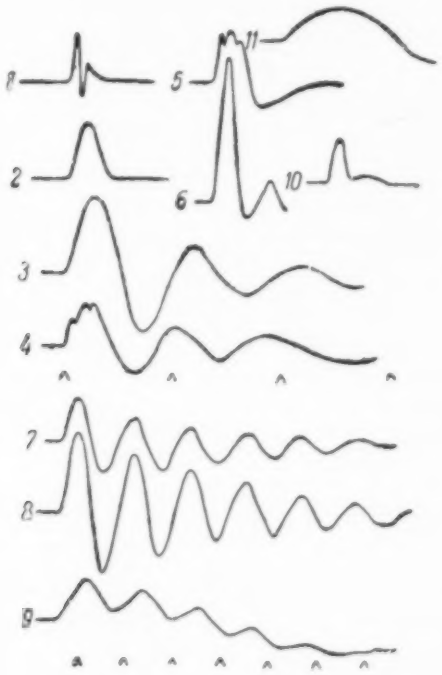

FIG. 2. Current and voltage oscillograms for various short-circuit to earth conditions

When a short-circuit occurs at point p, reactor $2'$ switches from the unfaulted phase circuit. In this case the inductances of the faulty and unfaulted phase circuits differ little in magnitude. When a short-circuit occurs at point k, an extra reactor is connected to the common branch for both circuits ($p-2'$ – earth – o). The passage of currents in line 1 can be seen from Fig. 3 if the letters k and q are interchanged.

In considering the oscillograms, the sharp difference in the currents for the same line when a short-circuit occurs at different points is most noticeable (curves 1 and 2, 3, 5 and 6, Fig. 2). In curve 1 the frequency is considerably higher than in curve 2 since the earthed phased circuit current is predominant in the former where in this case the reactor is absent, whereas two reactors are connected in series to the unfaulted phase circuits. The current in the latter

circuit (smaller both in frequency and in magnitude) is guessed according to the completion of the curve, (see dotted line on curve 1).

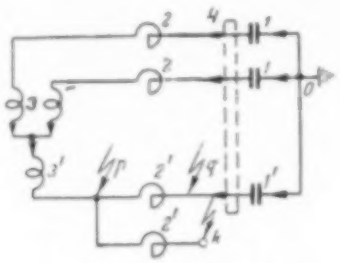

FIG. 3. Simplified equivalent circuit of test unfaulted line II, Fig. 1
1 – capacitance of unfaulted phases; *2* and *3* – reactors and total inductance of generating sources of unfaulted phases; *1′*, *2′* and *3′* – same for faulty (earthed) phase; *4* – position of zero-sequence current transformers in the secondary winding of which the current oscillograms were taken

The current frequency is considerably lower in curve 2 since the earthed and unfaulted phase circuits include the same reactor; i.e., the inductances of both circuits differ little in magnitude and therefore the current frequencies differ little. Due to this, frequency divergence is not found in curve 2. The reactor connected to the common branch also affects the general reduction of frequency in this case.

Superposition of currents of dissimilar frequency is also clearly seen in curve 5. This occurs as the result of a considerable difference in the inductance of the earthed and unfaulted phases when a short-circuit occurs at point *k*, (line *I*, Fig. 1).

Frequency divergence of the earthed and unfaulted phase circuits is not found either in curve 3 or in curve 6, since when a short-circuit occurs at point *q*, the difference in the inductance of the earthed and unfaulted phases is not great.

However, curves 3 and 6, which are both for line *I* (Fig. 1), differ both in form and in current frequency when a short-circuit occurs at the same point *q*. As is seen from Table 1, this frequency divergence must occur due to the difference in the characteristics of the generating sources.

Curve 3 was taken during a predominance of generator (operating) power, whereas when curve 6 was taken there was a predominance of transformer power, other conditions being equal.

The same applies to curves 4 and 10.

As is seen from Table 1, the network line corresponding to curve 4 is considerably shorter and has a smaller capacitance. However, the frequency of its current is lower than in the line corresponding to curve 10. This is explained by the fact that curve 10 shows the natural current of the transient process in the unfaulted line supplied from a substation having no reactors and using only transformers as generating sources. Curve 4 is for an extremely short line; however, the presence of line and section reactors levels off the current form and lowers the frequency. This is an illustration of the considerable effect of reactor inductance on the frequency of the natural current of the line. The gradient of this curve (A/mm) is reduced approximately 10 times.

Simultaneously with the taking of oscillograms on "long distance lines", oscillograms were taken for the current at the earth-fault point and for the voltage at the secondary terminals of the voltage zero-sequence filter connected to the bus-bar section of line III, Fig. 1.

Curve 7, Fig. 2, is typical for the natural current of an unfaulted long distance line supplied from a station with reactor-equipped lines during a considerable predominance of power developed by operating generators (see Table 1), in the case of a short-circuit at the station bus-bars. Curves 8 and 9 were taken at the same time as curve 7 (curve 8 for the current at the earth-fault point, and curve 9 for the voltage at the terminals of the zero sequence voltage filter).

1959

In the experiments, the first half-cycle of transient voltage exceeded the steady voltage by 1.5 - 1.7 times.

Curve 11 (Fig. 2) shows the current when a short-circuit occurs in the cable network at a distance of 12 km from the substation. It has a frequency of the order of 250 c/s, whereas when a short-circuit occurs at the substation bus-bars the current frequency at the fault point amounts to 1600 c/s.

Analysis of the oscillogram curves shows the most typical and all the remaining curves for a cable network of 6 kV with a capacitive current of 60 - 120 A permits the following conclusions:

1. When a short-circuit to earth occurs at or near the station bus-bars the frequency of the transient process current at the earth-fault point is determined by the frequency of the longest lines, (compare curves 7 and 8).

2. In a generator voltage network (for short-circuit conditions as in section 1) with lines fully equipped with reactors, the frequency of the transient process current at the earth-fault point and in the long distance lines lies within the narrow limits of 400 - 600 c/s.

3. In networks supplied from transformer substations (for short-circuit conditions as in section 1), without reactors, the frequency of the transient process

currents is higher and lies within the limits of 1000-1800 c/s.

4. When a short-circuit occurs at a distant point on the cable, the frequency of oscillations in all cases is lowered to 200-250 c/s, and the current as a rule is aperiodic.

5. From curves 7 and 8 it follows that the transient processes in long distance lines correspond in practice (excluding amplitude) with the transient processes at the earth-fault point. At the secondary terminals of the zero-sequence voltage filter a voltage is developed (curve 9) which corresponds to the transient process in a "long distance unfaulted line" with sufficient accuracy for all practical purposes.

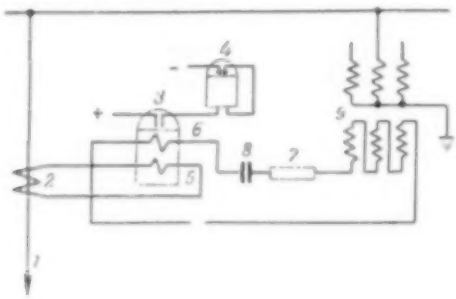

FIG. 4. Protection circuit
1 – protected line; *2* – zero-sequence current transformer; *3* – relay of type ET-521; *4* – signal relays; *5* – current (operating) winding; *6* – braking winding (additional); *7* – resistance; *8* – capacitance; *9* – zero-sequence voltage filter

The coincidence of these processes permitted the utilization of zero-sequence voltage for relay (type ET-521) braking in the presence of a short-circuit to earth outside the protected line. For this, relay *3*, Fig. 4, was provided with an additional braking winding *6* which was connected to the zero-sequence voltage filter *9* in such a manner that when a short-circuit to earth occurred outside the line, the additional winding created a demagnetizing effect and weakened the magnetic flux of operating winding *5*. It is necessary that the currents in both windings should be accurately displaced 180° in phase and coincide both in curve form and in magnitude. Therefore, capacitance *8*, which also locks a current with a frequency of 50 c/s, is connected to the circuit of winding *6*.

In addition to capacitance *8*, the current phase in the braking winding is also affected by the e.m.f. of the mutual inductance which is induced by the current of the operating winding *5*, so that during the braking process, i.e. when a short-circuit occurs outside the protected line, the e.m.f. of the mutual inductance and

the self-inductance in the braking winding circuit are calculated, approximating the inductance of this circuit to zero. This occurs because the self-inductance factor of the braking winding circuit and the mutual inductance factor of the braking and operating windings are approximate in magnitude owing to appropriate parameter selection. Therefore, when a short-circuit occurs outside the protected line a capacitive current similar to the natural capacitive current in the protected line is developed in the braking winding circuit.

Due to the small difference in magnitude of the self-inductance and mutual inductance factors, the inductance of the braking winding circuit will also remain approximately zero and when short-circuit conditions vary causing a variation in the frequency and form of the natural current in the unfaulted line. The current in the braking winding in this case, remaining capacitive as before, will correspond in frequency and form to the altered natural current in the unfaulted line since the voltage at the terminals of the zero-sequence voltage filter also varies in accordance with the new conditions.

This is proven by the curves for the currents in the operating and braking windings and for the voltage supplied to the braking winding shown in Fig. 5 for the same relay in different short-circuit conditions outside the protected line and on two different lines.

1959

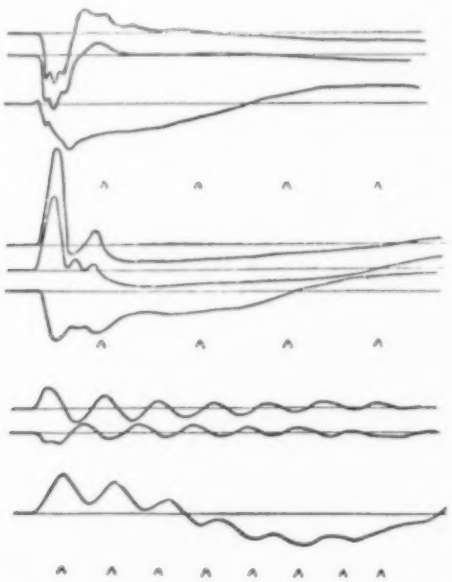

FIG. 5. Oscillograms of currents in braking and operating windings and of voltages at terminals of a zero-sequence voltage filter

In each of the three groups of curves in Fig. 5 the upper curve describes the current in the operating winding, the middle curve the current in the braking winding, and the lower curve the voltage at the terminals of the secondary winding of the zero-sequence voltage filter. The voltage filter on the primary side is connected to the bus-bar section of the test line.

The first two groups of curves are for line I which is connected to the station, a simplified diagram of which is given in Fig. 1: the upper group for the case of a short-circuit at point k, and the middle group for cases of a short-circuit at point q; the lower group is for line III, Fig. 1, for the case of a short-circuit at point p.

From what has been said it is seen that the relay in question can be applied on long distance lines of various networks without special changes in their parameters.

The relay should have the initial setting in order to compensate for a certain variance in magnitude of the currents in the braking and operating windings, (in different conditions). This setting, being determined by the condition of the longest line (according to Fig. 3, p.64 [1] without considering the natural current), is sufficient to compensate for the indicated variance of the processes.

When a considerable section of the line is tripped and when a short-circuit occurs outside the line, the braking current begins to predominate; however, incorrect operation is excluded by the presence of the same initial setting.

When a distant short-circuit occurs outside the line in question, the natural current in the given line is reduced; however, due to frequency reduction in this case, the braking current is also reduced.

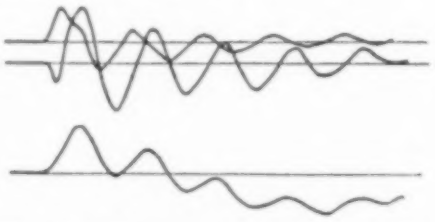

FIG. 6. Oscillograms of currents in relay when incorrectly connected

Curves are shown in Fig. 6 for the currents in the operating (upper curves) and the braking (mean curve) windings in the presence of an incorrect connexion of the leads of the operating winding, (the leads were crossed). This case reproduces a short-circuit at a distant point on the protected line. As is seen from the curves, the braking winding, increasing the sensitivity of the protection gear, came into operation.

The parameters of the relay circuit shown in Fig. 4 were selected for the most part by experiment.

Each coil of relay ET-520/0.2 consists of two windings of 250 turns connected by a PE-0.35 conductor. The lower winding of one coil is connected in series to the upper winding of the second coil, and vice versa. Thus, entirely separate windings (of 500 turns each) are obtained for a relay of 0.2 A.

With such a winding connexion the relay does not operate in the presence of counter-currents of 2.5 A in the braking and operating windings. The capacitor capacitance in the zero-sequence filter circuit amounts to 2 uF at 180 V and 3.3 uF at 100 V. The resistance in both cases amounts to 50 Ω.

At present, four such directional relays have been installed in the network. Here, there have only been two cases of incorrect operation but 12 cases of correct action.

The cases of incorrect operation were caused by two- and three-phase short-circuits to earth near the station bus-bars. They did not cause complications for the staff on duty since the fault was tripped with maximum protection. However, it must be remembered that in these cases incorrect operation of protection from short-circuits to earth is always possible; so, during a three-phase short-circuit to earth the protection gear operated incorrectly on 6 connexions which previously had not done so. Incorrect operation is eliminated in the presence of multi-phase short-circuits at distant points.

In the presence of a short-circuit to earth on 3 phases, due to their asychronization in phase, three transient process current pulses develop one after the other in the unfaulted lines causing incorrect operation of the protection gear.

In conclusion it must be noted that the operation of a network of 6 kV with almost total compensation of capacitive current (a simple metering device which has been developed has been installed in the stations allowing compensation control as required without any disturbances), over a number of years has shown positive results.

Such a type of fault as intermittent short-circuiting to earth has disappeared in practice since the current at the earth-fault point (including considerable higher harmonics), does not exceed 7-8 A.

Two forms of short-circuit to earth have remained: stable and transitory self-eliminating short-circuits, the latter in 1956 accounting for 75 per cent of the total number of short-circuits to earth. The number of short-circuits in cables has been halved.

The application of protection gear acting on transient process currents with the utilization of the given directional protection gear in networks of 6-10 kV is

expedient, and also because, due to its quick action, directions are fixed automatically in the presence of transitory self-eliminating short-circuits to earth. The latter frequently precede stable short-circuits to earth.

Translated by F.J. Griffiths

REFERENCES

1. V.E. Darchenko and T.V. Stepnov; Zashita ot zamykanii na zemlyu v kompensirovannykh setiakh. (Protection from Short-Circuits to Earth in Compensated Networks). *Elektrichestvo*, No. 2, 1958
2. F.A. Likhachev; *Vybor, ustanovka i eksplutatsiia dugogasiashchikh apparatov. (The Selection, Setting and Operation of Arc-quenching Apparatus)*, Gosenergoizdat, 1955.

ABSTRACTS OF PAPERS PUBLISHED IN ELEKTRICHESTVO NO. 8, 1958

High-molecular compounds in power engineering: K.A. Andrianov. (pp 1 - 4)

Many of the most important characteristics of electrical engineering equipment, for example, weight, dimensions and reliability in service, are determined mainly by the quality of materials, especially insulating material. The author argues at length for the advantages of high-molecular compounds, artificial fibres and plastics over non-thermostable electrical insulation and envisages an increase in the use of synthetic high-molecular compounds like phenolformaldehyde resins, silicone organic polymers and polyester resins in conjunction with fibre glass, asbestos and mica. The basic criterion for choosing from the great variety of polymers is thermal stability. He gives examples of the fields of application of high molecular compounds and tabulates the elasticity of polymers and the losses in weight (as a percentage) of polymers after 24 hr at different temperatures °C.

1959

Plastic masses in power engineering: V.V. Baranovskii and Ia. L. Shugal. (pp 12 - 16)

The author considers the increasing use of plastics in electrical engineering. He tabulates certain electrical properties of plastic insulation; laminated plastics (genitex, tekstolite and glass textolite and organic and silicone-organic bonding); mounding plastics, (organic fillers and non-organic fillers with organic and silicone organic bondings) finally cast plastics. Photographs are shown of moulded components of the phenolformaldehyde type, arc-resistant moulded contactor chambers, and dry mining explosion proof transformer and its winding made of heat-resistant plastics, a mobile telescopic platform for repairing high-voltage lines without disconnecting them and miscellaneous insulating components of laminated plastics.

The author then reviews plans for developing these materials. Plastic masses to sustain over 200 - 220°C are envisaged. For obtaining glass textolites (suitable for service in tropical conditions), investigations are to be made into special types of glass cloth and special compositions of stekol. Cast plastics are to be investigated. Methods of radiation of hard rays and ultra-sound and the use of thermo-reactive bonds are to be investigated. The article closes with remarks on the organization of research, (mentioning the possibility of test stations in India or Viet Nam).

The electrical properties of artificial and synthetic fibres: P.A. Polonik. (pp 17-21)

This article examines (1), specific resistance as a property directly connected with the dispersion of the station electrical charges arising on the fibre and (2), electric susceptibility as the tendency for the fibre to generate and accumulate charges in defined conditions. The author concentrates on the effect of humidity on the specific resistance and electric susceptibility of fibre. He considers the method of measuring specific resistance and tabulates the results. He then proceeds with the method of investigating electric susceptibility. He concludes that all artificial synthetic fibres can be electrified, the charge depending on the relative humidity of the air and the speed of the movement of the fibre. There is no connexion between the specific resistance and the electric susceptibility of a fibre, but specific resistance and the rate of dispersion of the charges are completely interrelated. Only viscous and acetate fibre can be worked without considerable interference from static electricity when $\phi = 65\%$. To work synthetic fibres it is necessary to hold them 20-30 hr in conditions of $\phi = 75\%$ and more or to apply ionization of the air to neutralize the charges.

Synthetic polymers and micaceous insulation: L.A. Epshtein and A.I. Petrashko. (pp 21-27)

Synthetic polymers (alkide) resins, in particular, glypthal, are now being successfully used in the production of micanites. A new stage has been marked in the development of mica bonds by oil and bitumen-oil varnishes used in stator winding insulation of high-voltage machines and the slot insulation of low-voltage machines of humidity resistance design. But to reduce the consumption of vegetable oil required for food purposes the VEI developed new synthetic organic and silicone organic polymers of the TGF and TGF-8 types. The Stalin electromechanical works in Kharkov has developed epoxy resins. Also, silicone organic resins and varnishes with glass-mica materials have been developed to operate at 250-300°C for limited periods. The author then considers the properties of glass-mica-tape, flexible heat resistant micanite, flexible heat-resistant glass micanite, heat-resistant moulding mica, heat-resistant glass-micafolium, micanite, flexible heat resistant glass S-mica, moulding S-mica, glass S-mica tape.

The use of mica, glass-mica and S-mica materials in silicone organic varnishes increases heat resistance and prolongs the life of the equipment.

Varnish polymers in electrical insulation: K.I. Zabyrina and M.B. Fromberg. (pp 28-37)

Special interest is centred on replacing vegetable oils by new synthetic materials based on different polyesters, epoxy resins, melamineformaldehyde resins polyurethanes, polyamines, polyvinylacetal and other synthetic film-forming

substances. These substances are then discussed in turn with tables of the electrical properties of certain varnishes and their compositions

Certain questions of the theory of the autodyne electrical machine: O.B. Benedikt. (pp 43-46)

It is desirable to create electrical machines combining the advantages of single armature converters (low weight, high efficiency and cos ϕ) with the good regulating features of motor-generators for direct current. To explain the method of operation of an autodyne the author considers the operation of a single armature converter without stator windings and the m.m.f. caused thereby. The theory expounded has been experimentally verified on specimens and models in the MIIT and NII ME P and the results of the investigations coincide with the results of the calculations. He presents an oscillogram showing that on a sudden increase in load current from 56 to 152 A the voltage remained practically constant. The effect of internal torques, assumed absent in the theory, is offset by the use of an amplifier or by a system of additional windings as illustrated.

Development of polyphase transformers and generator-transformers: R.S. Klimov. (pp 50-54)

For d.c. high-voltage transmission the publication of the rectified voltage (e.g., to values corresponding to a 24 phase scheme) can be reduced and the form of the current improved in generators by supplying several of a number of converters connected in series via phase-shifting transformers. The author describes three types of multi-phase transformer. Firstly, the method of a multi-phase transformer with a closed or other winding and the supply of the individual three phase (or single phase) transformers via phase-shifting transformers, the output of which amounts to 5-10% of the main transformers. Secondly, for a 48 phase transformer it is necessary to have three single phase transformers with a tertiary winding connected in star on each core (as illustrated) assuming the equality of the primary and secondary m.m.f. on every core. Thirdly, the author uses normal single- or three-phase transformers supplied direct from the stator coils of hydro- or turbogenerators the e.m.f. of which are shifted in relation to one another. The secondary windings are connected in the closed multi-phase winding. This principle underlying the third method has been extended to turbogenerators in the U.S.A. The author considers it expedient to divide the winding of each phase of a generator into two or more parts.

Currents and torques of asynchronous and synchronous machines when changing speed: L.G. Mamikoniants. (pp 54-63)

It is important to determine the conditions in which static characteristics can be used instead of dynamic and the method of deriving dynamic characteristics not

only for induction motors but also for synchronous motors, especially in connexion with self-synchronization, re-synchronization and modelling. The author introduces formulae of currents and torques common to synchronous and asynchronous machines for an arbitrary known law of rotor movement. It is shown that in the presence of uniform acceleration the integrals entering the formulae can be found with the aid of known tables of special functions. The author concludes that it is necessary to take into account the effect of speed changes on currents or torques as a function of slip to analyse the processes (synchronization, swings), when the slip is relatively small or changes sign. For large machines the calculation of speed changes is as a rule necessary for lesser acceleration than for very small machines. These conclusions are qualitatively true for any laws of rotor motion.

Determination of the discharge voltage along column and garland insulators: A.M. Zalesskii. (pp 64 - 68)

The use of protective rings as armatures equalizing the voltage are very valuable for protecting insulators from corona and, in some cases, for increasing the discharge voltage of insulators. The use of protective armatures on the Kuibyshev G.E.S. to Moscow transmission line reduces the length of the garlands by 20%. The author proposes a method of calculating the effect of protective rings on the distribution of voltage in columns and garlands of insulators and determining the dimensions and distribution of the protective rings. The curve of the puncture voltage between the bar and the surface is used to determine the discharge voltage in the case of garlands of insulators of the "plate" type. In the case of columns of insulators of the rod or bar type, however, the discharge voltage is calculated from the voltage applied to the upper insulator and the puncture voltage between the ring and the flange of the upper insulator.

Control of frequency and output with the additional action of the first product of deviation: S.V. Usov, G.M. Pavlov and P.L. Shirshov. (pp 69 - 74)

The problem of maintaining frequency in the power system even by one station has yet to be settled for hydro-electric stations. The author introduces formulae to determine the structural scheme of the regulator which should have elements to reveal and measure the deviation of the frequency from 50 c/s, and the deviation of output from the desired value, an "executive" element for increasing the sensitivity of the regulator between the executive and metering elements and an intermediate amplifier for each group. Such a frequency regulator has been developed by the Leningrad Polytechnic Institute and produced and installed by the Leningrad Power Supply (Lepe´nergo). The scheme and construction of the regulator is shown in Fig. 1. The author then investigates frequency and power regulation and concludes that the qualitative regulation can only be obtained by

agreeing the parameters of secondary and tertiary regulators on condition that they operate jointly. Additional action of the first product effectively stabilizes the regulation process and in conjunction with a reduction in the constant T_u (time constant of the isodrome) can speed up the regulation process and maintain stability. An increased speed of regulation up to 40-50 MW/min obtained when testing two hydro-electric groups was the limit. He considers that with a correct choice of T_u and the amplification factor using the first derivative, loading speed can be raised to 80-100 MW/min as required in large power systems.

The Umov electromagnetic vector in the field of a transmission line: L.B. Slepian. (pp 79-81)

The Umov electromagnetic vector is a special value of the Umov vector which gives the density of any form of power flux and is determined by the relationship

$$U = vE_{\omega}$$

where U – the Umov vector;
V – the rate of power transfer;
E_{ω} – the volumetrical density of the power transferred.

1959

The author considers how to establish the values of the rate of transfer of electromagnetic energy and the density of the transferred electromagnetic energy at all points of an electromagnetic field and whether the magnitudes derived equal the Poynting vector, (for the field around a power transmission line). He calculates that such an equality does exist although the Soviet editor points out that the article is controversial and in particular the author's assertion that the rate of power transfer along a line is in all cases equal to the speed of propagation of the free electromagnetic wave has yet to be substantiated.

The operation of carrier ducts of differential phase protection on long distance transmission lines: Mas Shi-Khe, Se Bo-En, Van Chzhu-Chun, Li Tsin-Cen and V.G. Kagan. (pp 82-85)

The Chinese People's Republic met with difficulties in installing PVZ-K carrier differential-phase protective gear on 220 kV lines 250-260 km in length. The simplest solution was the use of a double frequency variant of the duct and the scheme of double frequency receiver-sender was evolved, as illustrated in the text. The use of two frequencies is not always practicable however, and differential-phase protection is impossible on lines with branches.

SURFACE EFFECT IN SOLID FERROMAGNETIC BODIES TAKING NON-LINEARITY INTO ACCOUNT*

M.A. PANASENKOV

(Received 25 April 1958)

A great deal of attention is paid to the surface effect in ferromagnetic bodies. A considerable number of national and foreign works deal with this question. Soviet studies have made a large contribution to this field of science.

In 1913 Arkad'ev first introduced the concept of complex magnetic permeability. This was very useful for many investigations and calculations taking hysteresis loss into account, [1]. Fine steel plates and wires were the main object of Arkad'ev's investigations. A considerable part of the investigations made by him assumed constant complex magnetic permeability of the medium.

Neiman investigated electromagnetic processes in ferromagnetic bodies taking into account a variable magnetic permeability and hysteresis loss. On the basis of these investigations he proposed simple methods of calculating the electrical resistance of ferromagnetic material and the magnetic resistance of magnetic circuits. Larger solid bodies were the object of his investigations, [2].

The author of the present article selected relatively solid bodies as the object of his investigations, for example, ferromagnetic armatures of electrical machines (electromagnetic braking and induction motors), calendar shafts, cylinders of large dimensions and other units.

The presence of the air-gap, edge effect, unsatisfactory measurement of the temperature of the rotating armatures and a number of other factors interfere with the investigation of the basic characteristics in solid armatures of electrical machines. A solid steel ring was therefore investigated which excluded a number of the factors that could be subsequently taken into account more simply and with greater accuracy in individual cases. Fig. 1 shows an element of a solid steel ring of rectangular cross-section. The relationships of the dimensions of the

* *Elektrichestvo* No. 9, 1-7, 1958.

ring are such that for solving the problem, use can be made of the equations of the electromagnetic field for a flat wave in rectangular co-ordinates:

$$-\frac{d\dot{H}}{dz} = \dot{\delta} = \gamma \dot{E}, \tag{1}$$

$$\frac{d\dot{E}}{dz} = -j\omega\dot{\mu}\dot{H}, \tag{2}$$

where H and E are the effective values of the voltages of the magnetic and electrical fields;

δ is the effective value of current density;

γ and $\dot{\mu}$ are the specific electrical conductance and the complex magnetic permeability of the steel of the specimen under investigation;

ω is the angle frequency of the eddy currents;

z is a co-ordinate.

The introduction into the equations of the electromagnetic field of complex magnetic permeability $\dot{\mu}$, as is known, is linked with the substitution of the effective non-sinusoidal periodic functions of the induction B and strength H of the magnetic field by equivalent sinusoids. As a rule, non-linearity I of the $b(h)$ kind is taken into account for complex magnetic permeability. That is, the non-linearity of the instantaneous values of induction b from the instantaneous values of the strength of the magnetic field h. This non-linearity, caused by hysteresis, leads to distortion (skewing) of the shape of the curves and itself determines the hysteresis losses. However, the main ferromagnetic characteristic is non-linearity II of the $B(H)$ type, (non-linearity expressing the basic magnetization curve). The latter non-linearity, caused by a different degree of saturation, generally leads to a non-sinusoidal state of the curves $B(t)$ and $H(t)$. Here, in weak and medium fields up to a maximum of magnetic permeability μ, the curve $B(t)$ has a pointed shape and a large amplitude factor, whereas the curve $H(t)$ is flattened and has a smaller amplitude factor. In powerful fields after the maximum of μ, the reverse phenomenon takes place. Besides taking into account non-linearity I it is also necessary to take non-linearity II into account. Here, the additional losses will also be taken into account which characterize this non-linearity and, apparently, the magnetic viscosity, in so far as the latter is caused by non-linearity II.

The total argument ψ of this complex permeability is a function of frequency. It can be represented in the form of two components:

$$\psi = \psi_1 + 2\psi_{II}, \tag{3}$$

where ψ_1 is the argument caused by non-linearity I and taking hysteresis losses into account;

ψ_{11} is the argument caused by non-linearity II and taking the additional losses into account which characterize this non-linearity.

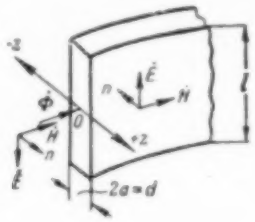

FIG. 1. Penetration of an electromagnetic wave into a steel ring
l, width of ring; $d = 2a$, thickness of ring. Z, co-ordinate; Φ, magnetic flux; E and H, strengths of the electrical and magnetic fields; n, vector of the direction of the electromagnetic wave

The argument ψ_1, equal to the hysteresis loss angle determined by static or quasi-static hysteresis loops, is only a function of the magnetic properties of the material. Argument ψ_{11} is a function of the process; that is, it is a function of all the parameters characterizing the electromagnetic process: $\psi_{11}(\omega, d, \mu, \gamma, \beta)$, where d is the thickness of the ring and β the angle between the induction and strength of the magnetic field, Argument ψ_{11} exists independently of the argument ψ_1. For example, in ferromagnetic bodies without hysteresis $\psi_1 = 0$, but argument $\psi_{11} \neq 0$, in so far as the basic non-linearity $B(H)$ is real. To determine argument ψ_{11}, it is necessary to solve the problem on the assumption that there is no hysteresis. It is, therefore, necessary to know the angle β.

Determination of the angle β

Fig. 2 shows the most characteristic (with two recurvatures) sections of the main d.c. magnetization curve. The curve $\mu(H)$ is also given there and the volume density of magnetic energy BH is plotted as a function of H. It is characteristic that from a certain value, the dependence of BH on H is practically a straight line and in a number of cases, this simplifies the calculations [3].

Assume a process where with a change of frequency within wide limits, the effective primary current of the ring I_1 is fixed. Here, the corresponding field strength H_1 will also be fixed. If the surface effect manifests itself sharply then H_1 will be the strength on the surface of the ring, but when $\omega \to 0$, H_1 will coincide with the average value according to the cross-section of the ring. Take a certain arbitrary point (4) of the $B(H)$ curve, Fig. 2. Here H_1 has a corresponding value of magnetic induction B_1 and an appropriate value of the volume density of

magnetic energy B_1H_2, being a rectangle with the sides B_1 and H_2 in a system of co-ordinates (B, H). In the case of the quasi-static (i.e. slowly changing field), when the d.c. and a.c. magnetization curves coincide, the specific energy B_1H_1 is simultaneously both the effective and the average value according to the cross-section of the ring. Similarly, the corresponding value of the energy B_mH_m will be the amplitude and maximum value simultaneously. The connexion between these magnitudes is determined by the relationship;

$$B_1H_1 = \frac{B_mH_m}{2}, \tag{4}$$

true both for the linear and non-linear dependence $B(H)$. If the dependence $B(H)$ should vary along the straight line 0-4, then the magnetic permeability would be substantially constant and equal to $\mu_1 = B_1/H_1$ for any values of H at any point of the ring cross-section. Here B and H would vary according to the sinusoidal law with the amplitudes $\sqrt{2}B_1$ and $\sqrt{2}H_1$, whereas the value of $\sqrt{2}B_1$ would lie along the straight line 0-4. At the point of intersection of the straight line 0-4 with the actual curve $B(H)$, the values B_1 and H_1 correspond to the effective values of the equivalent sinusoids for the actual curve, whereas $\sqrt{2}B_1$ and $\sqrt{2}H_1$ correspond to the amplitudes of these equivalent sinusoids. The amplitudes of the equivalent sinusoids are not as a rule severally equal to the actual amplitudes of B_m and H_m, but their products (i.e. the amplitude values of the energy), should be equal to one another, in so far as one and the same effective value of the volume density of magnetic energy corresponds to them: $B_mH_m = \sqrt{2}B_1 \times \sqrt{2}H_1 = 2B_1H_1$.

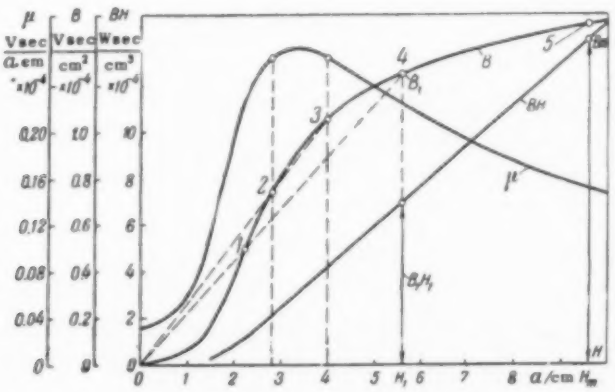

FIG. 2. Magnetic permeability μ, volume density of energy BH and induction B in relation to strength H, (direct current)

The method of determining the actual amplitudes B_m and H_m is derived from this. Given the value of H_1, we find the corresponding induction B_1 from the curve $B(H)$, and from the dependence $BH(H)$, the corresponding value of energy B_1H_1 and its doubled value B_mH_m, (Fig. 2). Induction B_m and strength H_m corresponds to this value of energy from curve BH at point (5).

Represent the amplitudes H_m and B_m in vector form, (Fig. 3). Their projections to the horizontal axis will correspond to their actual values. These vectors in relation to the horizontal axis, are then displaced through different angles ψ_H and ψ_B, the difference of which gives the angle β which characterizes the shift between H_m and B_m. The angles are analytically determined from the following relationships:

$$\cos\psi_H = \frac{H_1}{H_m} = \frac{1}{k_H}, \tag{5}$$

$$\cos\psi_B = \frac{B_1}{B_m} = \frac{1}{k_B}, \tag{6}$$

$$\beta = \psi_H - \psi_B, \tag{7}$$

where k_H and k_B are the amplitude factors.

After denoting the orthogonal components from B_m to the direction H_m by $B_s = B_m \sin\beta$ and $B_c = B_m \cos\beta$, but the orthogonal components from H_m to direction B_m by $H_s = H_m \sin\beta$ and $H_c = H_m \cos\beta$, respectively, we shall have:

$$\tan\beta = \frac{B_s}{B_c} = \frac{H_s}{H_c}, \tag{8}$$

whence we have a relationship similar to the expression for magnetic losses:

$$B_cH_c \tan\beta = B_1H_1 \sin 2\beta = B_1H_1 \cos\theta. \tag{9}$$

Here,

$$\theta = \frac{\pi}{2} - 2\beta.$$

The right-hand side of (9) is the actual part of the complex $H_1^2\mu$, where

$$\mu = \mu_1 e^{-j\theta} \tag{10}$$

is the complex magnetic permeability which must be introduced into (2) in order to find the solution for the argument ψ_B. However, the equation to determine ψ_B

can be obtained from the general solution by substituting θ into the corresponding equation of the argument ψ.

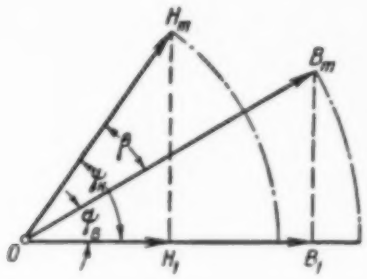

FIG. 3

Steel ring as a single-phase transformer with a short-circuited secondary turn

The solution of equations (1) and (2) in the presence of complex magnetic permeability $\mu = \mu_1 e^{-j\psi}$, taking into account the non-linearity of the magnetic characteristic of the material, gives:

$$\dot{H} = \dot{c}_1 e^{\dot{k}z_a} + \dot{c}_2 e^{-\dot{k}z_a} \tag{11}$$

and

$$\dot{\delta} = -\frac{\dot{k}}{a}(\dot{c}_1 e^{\dot{k}z_a} - \dot{c}_2 e^{-\dot{k}z_a}), \tag{12}$$

where

$$\dot{k} = a\sqrt{j\omega\dot{\mu}\gamma} = k_1 + jk_2, \tag{13}$$

$$k_1 = k\cos\left(\frac{\pi}{4} - \frac{\psi}{2}\right), \tag{14}$$

$$k_2 = k\sin\left(\frac{\pi}{4} - \frac{\psi}{2}\right), \tag{15}$$

$$k = a\sqrt{\omega\mu_1\gamma}, \tag{16}$$

$Z_a = Z/a$; $a = d/2$ is half the thickness of the ring.

Where $Z_a = 0$ the current density in the middle of the ring cross-section is zero and the constant integrations c_1 and c_2, as follows from (12), are equal one

to another. Here, we have from (11):

$$\dot{H} = 2\dot{c} \cosh kz_a. \tag{17}$$

When $Z_a = 1$, we obtain the strength of the magnetic field on the surface of the ring:

$$\dot{H}_1 = 2\dot{c} \cosh \dot{k}. \tag{18}$$

Having excluded the constant $\dot{c}$ from (17) and (18), we shall have:

$$\dot{H} = H_1 \frac{\cosh \dot{k} z_a}{\cosh \dot{k}}, \tag{19}$$

$$\dot{\delta} = -\frac{\dot{H}_1 \dot{k}}{a} \frac{\sinh \dot{k} z_a}{\cosh \dot{k}}, \tag{20}$$

$$\dot{E} = -\frac{\dot{H}_1 \dot{k}}{\gamma a} \frac{\sinh \dot{k} z_a}{\cosh \dot{k}}. \tag{21}$$

Integrating (20) according to the square $radz_a$, where r is the length of the average magnetic path, we shall find the total current, equivalent to the eddy currents in the ring:

$$\dot{I}_e = ra \int_0^1 \dot{\delta} dz_a = -r\dot{H}_1 \frac{\cosh \dot{k} - 1}{\cosh \dot{k}} = r\dot{H}_0 - r\dot{H}_1, \tag{22}$$

Where $\dot{H}_0$ is the strength of the magnetic field in the middle of the ring cross-section, being obtained from (19) where $Z_a = 0$.

The values of the magnetizing forces are determined by the respective relationships:

$$r\dot{H}_1 = \dot{I}_1 w_1, \tag{23}$$

$$r\dot{H}_0 = \dot{I}_0 w_1, \tag{24}$$

the substitution of which into (22) gives

$$\dot{I}_1 w_1 + \dot{I}_e w_1 = \dot{I}_0 w_1, \tag{25}$$

whereas we have the value of the primary current

$$\dot{I}_1 = \dot{I}_0 - \dot{I}'_e = \dot{I}_0 + \dot{I}_{1e}. \tag{26}$$

Here $\dot{I}'_e = \dot{I}_e w_2 w_1$, is the eddy current applied to the turns of the primary winding of the ring w_1.

The number of the turns of the secondary winding $w_2 = 1$.

Analogously to the transformer, the primary current of the ring $\dot{I}_1$ has two components. One of them $\dot{I}_0$ goes to create the magnetic flux and the other $\dot{I}_{1e}$ compensates the demagnetizing action of the eddy current (the load current), $\dot{I}'_e$. The equivalent network and vector diagram will have the same form as in the case of the transformer on load.

Determination of resistance. Having taken the integral from strength $\dot{E}_1$ on the surface of the ring from the contour l_E which embraces the cross-section of the ring, we find the secondary e.m.f. $\dot{E}_2 = \dot{E}_1 l_E$. After multiplying it by the number of turns of the primary winding we obtain the applied e.m.f.

$$\dot{E}_1 = \dot{E}'_2 = - w_1 l_E \frac{\dot{H}_1 \dot{k}}{\gamma a} \tanh \dot{k}. \tag{27}$$

The components of the primary current are:

$$\dot{I}_{1e} = (- \dot{I}'_e) = \frac{r\dot{H}_1}{w_1} \frac{\cosh \dot{k} - 1}{\cosh \dot{k}}; \tag{28}$$

$$\dot{I}_0 = \frac{r\dot{H}_1}{w_1} \frac{1}{\cosh \dot{k}}. \tag{29}$$

The resistances applied to the eddy current are:

$$Z'_e = \frac{- \dot{E}'_2}{\dot{I}_{1e}} = r'_c \frac{\dot{k} \sinh \dot{k}}{\cosh \dot{k} - 1} = r'_e + jx'_e;$$

$$r'_c = \frac{l_E w_1^2}{\gamma r a} \tag{30}$$

$$r'_e = r'_c \frac{k_1 \sinh k_1 + k_2 \sin k_2}{\cosh k_1 - \cos k_2} \tag{31}$$

$$x'_e = r'_c \frac{k_2 \sinh k_1 - k_1 \sin k_2}{\cosh k_1 - \cos k_2}. \tag{32}$$

The resistances applied to the magnetization current are:

$$Z'_0 = \frac{- \dot{E}_1}{\dot{I}_0} = r'_c \dot{k} \sinh \dot{k} = r'_0 + jx'_0; \tag{33}$$

$$r'_0 = r'_c (k_1 \tanh k_1 - k_2 \tan k_2) \cosh k_1 \cos k_2; \tag{34}$$

$$x'_0 = r'_c (k_2 \tanh k_1 + k_1 \tan k_2) \cosh k_1 \cdot \cos k_2. \tag{35}$$

The equivalent resistance is:

$$Z_e = \frac{U_1}{I_1} = Z_1 + \frac{Z_0' Z_e'}{Z_0' + Z_e'} = Z_1 + Z'; \tag{36}$$

$$Z' = \frac{-E_1}{I_1} = r_c' k \tanh k = r' + jx'; \tag{37}$$

$$r' = r_c' \frac{k_1 \sinh 2k_1 - k_2 \sin 2k_2}{\cosh 2k_1 + \cos 2k_2}; \tag{38}$$

$$x' = r_c' \frac{k_2 \sinh 2k_1 + k_1 \sin 2k_2}{\cosh 2k_1 + \cos 2k_2}; \tag{39}$$

where Z', r' and x' are the full, active and reactive resistances which are applied to the current in the turns of the primary winding;

Z_1 is the full resistance of the primary winding;

U_1 is the voltage applied to the primary winding.

Argument ψ_B. Dividing equality (27) by $-j\omega w_1$, we find the expression for the magnetic flux:

$$\dot{\Phi} = l_E a \dot{H}_1 \mu_1 k_p (\sin \psi_1 - j \cos \psi_1) = l_E a_k \dot{H}_1 \mu_1 e^{-j\left(\frac{\pi}{2} - \psi_1\right)} \tag{40}$$

where

$$\sin \psi_1 = \frac{x'}{Z'} = \frac{k_2 \sinh 2k_1 + k_1 \sin 2k_2}{k\sqrt{\sinh^2 k_1 + \sin^2 2k_2}}; \tag{41}$$

$$\cos \psi_1 = \frac{r'}{Z'} = \frac{k_1 \sinh 2k_1 - k_2 \sin 2k_2}{k\sqrt{\sinh^2 2k_1 + \sin^2 2k_2}}; \tag{42}$$

$$a_k = ak_d = \frac{a}{k} \sqrt{\frac{\cosh 2k_1 - \cos 2k_2}{\cosh 2k_1 + \cos 2k_2}}; \tag{43}$$

$$k_d = \frac{1}{k} \sqrt{\frac{\cosh 2k_1 - \cos 2k_2}{\cosh 2k_1 + \cos 2k_2}}. \tag{44}$$

Here ψ_1 is the phase angle between $\dot{E}_1'$ and $\dot{I}_1$;

a_k is the equivalent depth of penetration of the alternating magnetic flux in the ferromagnetic body; that is, the depth to which the magnetic induction B_1 is distributed uniformly;

k_d is the demagnetization factor characterizing the decrease of the flux owing to the demagnetizing action of the eddy currents.

From the expression for the module of the magnetic flux

$$\Phi = S_k B_1 = S k_s B_1 \tag{45}$$

a connexion is derived between the a.c. and d.c. induction:

$$B_k = \frac{\Phi}{S} = \frac{S_k}{S} B_1 = k_s B_1, \tag{46}$$

where $S_k = L_E a_k$ and $S = 2al$ are the equivalent and actual cross-sections of the ring; L is its width; $k_s = k_E k_d$

In the general case, the coefficient $k_E = l_E/2l$ is a variable magnitude, but when $l \gg d$ it is approximately 1 and its effect is insignificant. Here, induction B_k for a given induction B_1 will only be a function of the coefficient k_d ($k_E \approx 1$). When $\omega = 0$, $k_d = 1$ and $B_k = B_1$. When ω increases, induction B_k diminishes with a decrease of k_d. Having substituted θ into argument ψ in (46) in accordance with (6), we shall have:

$$\cos \psi_{Bk} = \frac{B_{k1}}{B_{km}} = \frac{k_{d1} B_1}{k_{dm} B_m} = \frac{k_{d1}}{k_{dm}} \cos \psi_B, \tag{47}$$

where

$$\left.\begin{aligned} k_{d1} &= \frac{1}{k} \sqrt{\frac{\cosh 2k_3 - \cos 2k_4}{\cosh 2k_3 + \cos 2k_4}}; \\ k_3 &= k \cos \beta; \quad k_4 = k \sin \beta; \end{aligned}\right\} \tag{48}$$

$$\left.\begin{aligned} k_{dm} &= \frac{1}{k_m} \sqrt{\frac{\cosh 2k_{m3} - \cos 2k_{m4}}{\cosh 2k_{m3} + \cos 2k_{m4}}}; \\ k_{m3} &= k_m \cos \beta; \quad k_{m4} = k_m \sin \beta; \\ k_m &= a \sqrt{\omega \mu_m \gamma}. \end{aligned}\right\} \tag{49}$$

Having determined the tangent of the secondary angle ψ_2 by the relationship of (32) to (31) and substituted ψ in the latter by θ and ψ_B by ψ_{Bk}, we obtain an analogous equation to determine the argument ψ_u

$$\tan \psi_u = \frac{k_5 \sinh k_5 - k_6 \sin k_6}{k_5 \sinh k_5 + k_6 \sin k_6}, \tag{50}$$

where

$$k_5 = k \cos \beta_k; \quad k_6 = k \sin \beta_k; \quad \beta_k = \psi_H - \psi_{Bk}.$$

When there is no surface effect ($k < 0.5$), $k_d = k_{dl} = k_{dm} = 1$, $\psi_{Bk} = \psi_B$ $\psi_u = 0$; $\psi_2 = 0$; $\psi_1 = \frac{\pi}{2} - \psi_1$. When the surface effect is sharp ($k > 3$) the coefficients

$k_{d_1} = 1/k = k_d$ and $k_{dm} = 1/k_m$ do not depend on the angle β. In this case, we have from (47), in accordance with (4):

$$\cos \psi_{Bk} = \frac{B_1}{B_m} \sqrt{\frac{\mu_m}{\mu_1}} = \sqrt{\frac{B_1 H_1}{B_m H_m}} = \frac{1}{\sqrt{2}} \tag{51}$$

and, consequently, $\psi_{Bk} = \pi/4$. Here, from (50) and (41), respectively, we obtain $\tan \psi_n = \tan \beta_k$ and $\sin \psi_1 = \sin \left(\frac{\pi}{4} - \frac{\psi}{2} \right)$, whence it follows:

$$\psi_{II} = \beta_k = \psi_H - \psi_{Bk} = \psi_H - \frac{\pi}{4}; \tag{52}$$

$$\begin{aligned} \psi_1 = (\psi_2) &= \frac{\pi}{4} - \left[\psi_{II} + \frac{\psi_1}{2} \right] = \\ &= \frac{\pi}{2} - \left[\psi_H + \frac{\psi_1}{2} \right]. \end{aligned} \tag{53}$$

Comparing (50) with (52) it follows that in (50), argument ψ_n depends on the coefficient k, and therefore is a function of all the parameters determining k. In (52) ψ_n only depends on the magnetic properties of the steel and on the degree of non-linearity of the magnetic characteristic. When μ is constant the arguments $\beta = \beta_k = 0$. Here, from (50 and (52), it follows that $\psi_n = 0$ for any manifestation of surface effect. This again proves that the argument ψ_n actually takes into account the non-linearity of the magnetic characteristic caused by the basic magnetization curve. On the magnetization curve there is a characteristic point at which $\beta = \beta_k = \psi_n = 0$. For example, in Fig. 2, this is point (2), the magnetic permeability at which μ_1 equals the magnetic permeability μ_m at point (3) with double magnetic energy in accordance with (4). At this point when there is a sharp surface effect, the angle ψ_1 is only determined by the difference $\pi/4 - \psi_1/2$, which can easily be verified by tests.

Fig. 4 shows the curves of the dependence of the individual arguments on H_1 for sheet steel, the magnetization curves of which are shown in Fig. 2 and below in Fig. 6. The curves of Fig. 4 enable us to establish that the arguments β and $\beta_k = \psi_n$ have clearly expressed negative minima, practically coinciding with the maximum ψ_1. In powerful fields (see Fig. 7), the arguments ψ_H and ψ_B and, consequently, β and $\beta_k = \psi_n$, are practically constant magnitudes, approximately equal to 57°, 22°, 33° and 12°. The argument ψ_1 in powerful and weak fields is negligibly small compared with ψ_H and, therefore, in accordance with (5), ψ_H has a decisive value for weak and powerful fields. When the surface effect is sharp, the phase angle ψ_1 in accordance with (53) does not depend on frequency, which also confirms the tests carried out at 50 and 500 c/s, (Fig. 5).

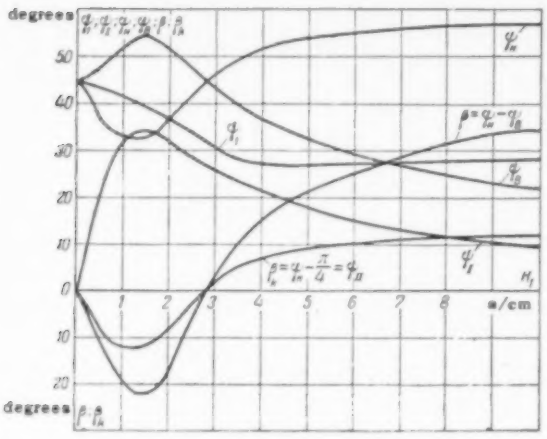

FIG. 4. The arguments in relation to the effective values of strength H_1

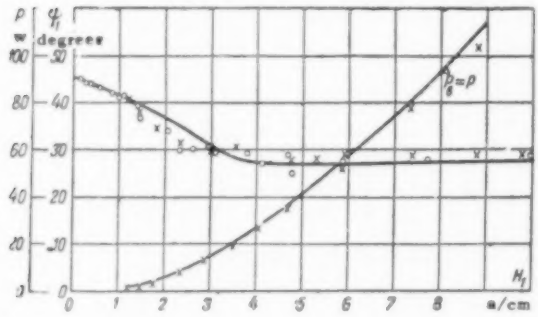

FIG. 5. Curves of the losses in the steel P and the angle of shaft ψ_1 between the current and the e.m.f. as a function of strength H_1.
o, test values at 50 c/s; ×, the same at 500 c/s

On passing from weak fields, the angle ψ_1 decreases from 45° to approximately 27° (when $H_1 = 4$) and then with a decrease of ψ_1, in accordance with (53) slowly increases to 33° when ψ_H increases to 57°, (see Fig. 7). Thus, when the surface effect is sharp, tan ψ_1 is always less than unity and only in very weak fields when $H \to 0$, tan $\psi_1 \to 1$. When the surface effect is poor, tan ψ_1 = cot ψ_1 and any values depending on the angle ψ_1 can be taken.

Determination of the losses in the steel

The losses in the steel are the sum of the electrical losses from eddy currents $P_e = I_e^2 r_e'$ (taking the hysteresis effect into account), and the magnetic

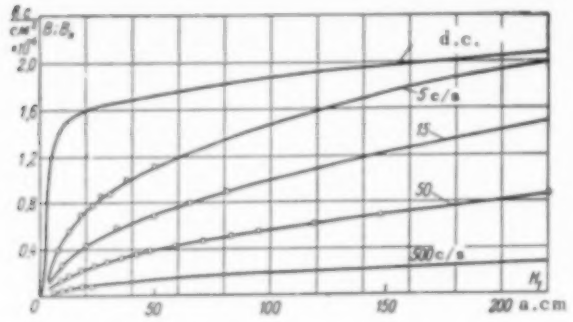

FIG. 6. A.C. magnetization curves at different frequencies ($\varphi 20 = 0.225 \times 10^{-4}$ Ωcm), compared with test data. Upper curve experimental. ○ – test points

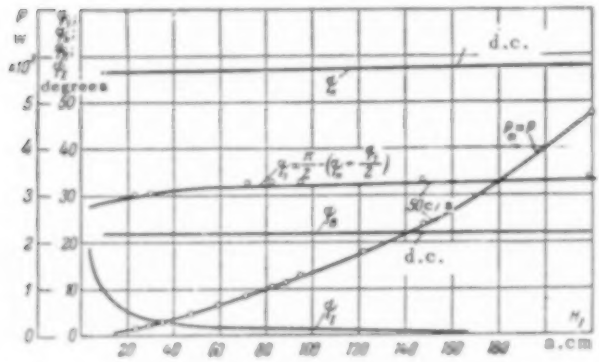

FIG. 7. Angles ψ and losses in the steel as a function of strength H_1. ○ – test points

losses caused by the magnetization current $P_0 = I_0^2 r_0'$, (taking the effect of eddy currents into account). The sum of these losses is

$$P = I_1^2 r' = E_1' I_1 \cos \psi_1 = \\ = \omega \Phi F \cos \psi_1 = \omega V_k B_1 H_1 \cos \psi_1, \tag{54}$$

where $F = rH_1$ is the magnetizing force;

$V_k = l_E a_k r$ is the equivalent volume of the ring.

Equation (54) can also be obtained with the aid of the Umov-Poynting vector. The special feature of equation (54) is that it generalizes in a simple and profitable form the total losses in the steel. For example when there is no surface effect ($k < 0.5$) and when the eddy current $I_e' = 0$, the electrical losses $P_e = 0$ and

the magnetic losses P_0 equal the hysteresis losses, ($\Psi_n = 0$):

$$P = P_0 = \omega V B_1 H_1 \sin \psi_1 = \\ = \omega V \frac{B_m H_m}{2} \sin \psi_1. \tag{55}$$

Here,

$$\left.\begin{array}{l} r_e' = 2r_c' \\ x_e = 0 \end{array}\right| \left.\begin{array}{l} r_0' = r' = r_c' k^2 \sin \psi_1; \\ x_0' = x' = r_c' k^2 \cos \psi_1. \end{array}\right| \tag{56}$$

where $l_E = 2l(k_E - 1)$ and $V = 2abr$ is the actual volume of the ring, ($k_d = 1$).

In another limiting case when the surface effect is sharp ($k > 3$), when $l_e' = l_1$, $l_0 \approx 0$ (which corresponds to short circuit conditions of the transformer), the magnetic losses $P_0 \approx 0$ and the total losses equal the electrical losses from eddy currents:

$$P = P_e = \omega V_k B_1 H_1 \sin \left(\psi_H + \frac{\psi_1}{2}\right) \text{ [w]}. \tag{57}$$

In this case,

$$\left.\begin{array}{l} r_0' \to \infty, \\ x_0' \to \infty, \end{array}\right| \left.\begin{array}{l} r_e' = r' = r_c' k \sin \left(\psi_H + \frac{\psi_1}{2}\right); \\ x_e' = x' = r_c' k \cos \left(\psi_H + \frac{\psi_1}{2}\right). \end{array}\right| \tag{58}$$

Unlike (55), with a charge of ω in (57) the depth $a_k = a/k$ varies and, consequently, the equivalent volume

$$V_k = l_E a_k \tau = V \frac{k_E}{k} \text{ [cm}^3\text{]}. \tag{59}$$

The coefficient k_E, when the surface is sharp, can be determined with sufficient accuracy by the approximate formula

$$k_E = 1 + 0.65 \frac{d}{l}, \tag{60}$$

where the numerical coefficient 0.65 takes into account the curvature of the current path at the angles of the cross-section of the model, (when the surface effect is sharp).

A sharp manifestation of the surface effect has frequently to be dealt with in practice: for example, in the case of high frequency hardening of components,

heating different installations and applications (calender shafts and cylinders etc.), and when investigating electrical machines with solid rotors and so on. Therefore, equations (57) and (58) are of practical interest owing to their simplicity. In so far as ψ_H and ψ_1 are functions of the magnetic properties of the material, so in accordance with curves ψ_H and $\psi_1 = f(H_1)$ (Figs. 4 and 7), it is easy to trace the effect of the arguments ψ_H and ψ_1 on the course of the process, for example, on the magnitude of the losses (57) when H changes from zero to the most powerful fields. In weak and powerful fields, where $\psi_1 \approx 0$, the argument ψ_H is the basic magnitude characterizing the process when ω is constant, for it also characterizes non-linearity II when $k > 3$. When $H \to 0$, the angle $\psi_H \to 45°$, which corresponds to the condition $\mu = \text{const}$. From the relationship:

$$\cos \psi_H = \frac{H_1}{H_m} = \frac{B_m}{2B_1} = \sqrt{\frac{\mu_m}{2\mu_1}} \tag{61}$$

it follows that in the case of powerful saturation, when $B_1 \to B_m$, the angle $\psi_H \to 60°$, but in so far as $B_1 \neq B_m$, so $\psi_H < 60°$. It also follows from (61) that beyond the limits of technical saturation when μ_1 and $\mu_m \to \mu_0$, the magnetic permeability of the air, $\psi_H \to 45°$. Thus, when H changes from zero to infinity, the changes of the angle ψ_H can be schematically represented in the form of the following chain: $45° - \psi_{H\,\min} - 45° - \psi_{H\,\max} - 45°$. It is analogous for ψ_B: $45° - \psi_{B\,\max} - 45° - \psi_{B\,\min} - 45°$. Consequently, the vectors B_m and H_m (Fig. 3), now converge and now diverge. The character of the divergence of these vectors beyond the characteristic point is inductive, but before the characteristic point, it is capacitive. However, in real conditions the capacitive divergence is smoothed out by the angle ψ_1 and the divergence of these vectors in all fields acquires an inductive character since the algebraic sum $(\psi_H + \psi_1/2$ is always positive, (Fig. 4).

The truth of the relationships (57) and (58) is the simplest to verify in tests on fields where $\psi_1 = 0$ and, consequently, where there is no error due to the angle ψ_1 because of inaccurate calculation with hysteresis loops. Experience fully confirms the truth of the definition of the angle ψ_H from (5).

The order of calculation. Using a value of H_1 given by the d.c. magnetization curve, first H_m and B_1. From (5) calculate ψ_H. From the curve $\psi_1 = f(H_1)$ for H_1, find ψ_1. Using (16), determine k. Here $\mu_1 = B_1/H_1$ is measured in (V.c/a.cm); B_1 in V.c/cm² or in *Vb*/cm², H_1 in a/cm; the specific conductance:

$$\gamma = \frac{1}{\rho} = \frac{1}{\rho_{20}[1 + \alpha_{20}(t - 20)]} \left[\frac{1}{\Omega\,\text{cm}}\right],$$

ρ 20 and α 20 are the specific resistance of the ferromagnetic body and its temperature coefficient at 20°C.

From (60) find k_E and from (59) V_k. Then from (57) and (58) determine the losses and resistances.

Experimental verification is carried out on a solid steel ring of rectangular cross-section which guarantees a sharp manifestation of the surface effect. The average diameter of the ring $D_c = 24$ cm; $r = \pi D_c = 75.5$ cm; $l = 8.7$ cm; $d = 2a = 1.5$ cm. Tests have been carried out using the E'pshtein apparatus with two windings (each with 440 turns), with a temperature of the steel at 20°C. The specific resistance of the steel at 20°C $\rho_{20} = 0.225 \times 10^{-4}$ Ω cm. The fundamental magnetization curve is shown in Figs. 2 and 6 (upper). Comparison of the results of the calculation with test results is given in Figs. 5, 6 and 7. The angle ψ_1 in weak fields has been measured with the aid of an electronic-ray oscillograph. The curves $B_k = f(H_1)$ are calculated from (46), taking (60) into account.

Conclusions

The coincidence of the calculations with the test results testifies to the accuracy of the theoretical conclusions, taking into account the non-linearity of the magnetic characteristic. The formulae have been verified within the range of induction from 20 to 20,500 G at frequencies from 5 to 500 c/s. Overstatement of the losses by calculation (5-6 per cent), is only observed in medium fields in the region of maximum values of μ. In weak and powerful fields (Fig. 7), the results of the calculation practically coincide in full with the tests. Formula (46) enables a.c. magnetization curves to be plotted for different frequencies from the d.c. magnetization curve. It has been established that the phase angle between I_1 and E_1' when the surface effect is sharp does not depend on frequency. Its maximum value 45° and, consequently, the tangent of this angle will never be greater than unity, (when the surface effect is sharp). The division of the total current by I_e' and I_0 and the total resistance by Z_e' and Z_0' results in the equivalent circuit of the transformer. The method eases the transition to the analysis of the operation of an induction motor with a solid steel rotor such that when investigating induction motors of normal design, an equivalent circuit of a transformer is used as the starting point.

Translated by O. Blunn

REFERENCES

1. V.K. Arkad'ev; *E'lektromagnitnye protsessi v metallakh, (Electro-magnetic Processes in Metals).* pt. II United Scientific and Technical Press (1936).
2. L.R. Neiman; Poverkhnostnyi e'effekt v ferromagnitnykh provodakh i magnitnykh tsepiakh. (Surface Effect in Ferromagnetic Conductors and Magnetic Circuits). *Elekt. I.* (1950).

3. M.A. Panasenkov; *Teoriia metodika rascheta i e'ksperimental'nye issledovaniia e'lektromagnitnykh tormozov, (Theory, Method of Calculation and Experimental Investigation of Electro-magnetic Braking).* Dissertation. ME'I. Jan. (1955).

AN EXPERIMENTAL TURBOGENERATOR WITH INTERNAL HYDROGEN COOLING OF STATOR AND ROTOR WINDINGS AT A PRESSURE OF THREE ATM*

L. Ia. STANISLAVSKII

(Received 2 April 1958)

In 1958 the Khar'kov turbogenerator works will produce the first two mark TGV-200 turbogenerators of 200 MW power which will come into regular production in 1959. Simultaneously, the plant is being prepared for the production of mark TGV-300 turbogenerators of 300 MW power. These generators will have internal hydrogen cooling of stator and rotor windings at increased pressure, and a number of other special design features.†

The mark TVO-30 experimental turbogenerator of 30 MW, 10-5 kV and 3000 rev/min, which in design is a prototype of the 200-300 MW turbogenerators, was planned as part of the preparation of the factory for the production of these large machines and was built in 1957. The generator was carefully tested with air and with hydrogen cooling on a specially constructed test stand at the works. After December 1957, detailed testing of this generator was continued in conditions of normal operation at one of the Mosenergo power stations.

Design of generator

The mark TVO-30 generator was planned and built to the overall dimensions of the mark TGV-25 turbogenerator in batch production, retaining its actual dimensions and assembly. The following new design features have been used in the experimental generator: the stator and rotor windings are internally cooled by hydrogen at a pressure up to 3 atm, eliminating the temperature drop in the winding insulation which occurs in machines having surface cooling of windings; the stator core, in contrast to usual machines, has axial ventilation only; a

* *Electrichestvo* No. 9, 30-34, 1958.

† L. Ia. Stanislavskii; Turbogenatory ot 30 do 300 MW zavoda KhETZ (Turbogenerators of 30 to 300 MW built by the Khar'kov Turbogenerator Works), Electrichestvo, No. 3, 1958.

compressor is set inside the generator to build up the required pressure of gas; a new disk oil seal is used for the first time with piston rings between the housing and the seal plain bearings, making it possible to eliminate the diaphragm made of cable plastic or rubber which were unsatisfactory in operation.

The generator is excited by a turbine of 30 MW power. In order to test the generator thoroughly over a wide range of currents in the windings, its rated continuous output was taken as 50 MVA at $\cos \phi = 0.6$.

The generator bearings were situated in the external shields in which the disk oil seals were located. Since oil consumption in the body of the stator does not exceed 1 L/min when the hydrogen pressure is within the limits of 0.05 to 3 atm, vacuum purification of oil is not required, and therefore oil purification apparatus is unnecessary. The calculated excess of oil pressure over gas pressure in the stator casing is 0.3 - 0.5 atm. These values are substantiated by experimental data. The temperature of the babbit in the seal was 48 - 50°C with a total oil consumption of 50 l/min. The system developed for decreasing the load on the seals provides for a slight variation in oil consumption through the seals when the hydrogen pressure alters.

Cold rolled electrical steel was used for the stator core. The latter is cooled by the gas flowing through the axial channels in the teeth and back of the stator sections. There are no radial channels in the core. The stator sections are attached in the usual manner: with clamp bolts and non-magnetic steel retaining rings.

The stator winding is of the basket type. The design of the bars in the stator winding is new. Each bar consists of two series of transposed glass-insulated conductors. Stainless non-magnetic steel tubes carry the hydrogen which cools the bars are placed between the vertical series of conductors. The tubes have a specific resistance of 0.8 $\Omega\,mm^2/m$ and a magnetic permeability of not more than 1.5 in the presence of a field strength of 200 oersted. The hydrogen enters the ducts through silicone rubber caps from the turbine side and passes out through similar caps on the contact ring side. These caps serve as insulation between the bar heads. The ducts are insulated from one another and from the winding conductors by glass strip.

The greater portion of the winding bars have the usual compounded mica insulation in asphalt varnishes. A certain number of experimental bars of this type were inserted in the stator in order to gain experience in the manufacture and use of bars with silicone rubber insulation. These bars were developed in co-operation with the Lenin All-Union Electrical Engineering Institute (VEI). They were made from the same conductors and tubes, which were also compounded, but were insulated with glass mica in silicone-organic varnishes. Each bar was

doubly insulated, baked and mounded in special pressure dies covering both the slotted and the front section of the winding.

The forging and also the banding rings, bushes and wedges of the mark TGV-25 generator were used in the rotor. The rotor winding turns consist of two U-shaped copper conductors forming the channel for the passage of the hydrogen coolant. The gas enters the hollow conductors from each side of the rotor and passes into the middle section of the latter through holes in the conductors and rotor wedges. The manufacture and applying of coils having such conductors differs little from usual practice. It was not necessary to cut up the coils in order to insert them into the slots. Accuracy in the matching of holes for the passage of gas in the coils and wedges was ensured with the aid of special appliances and conductors. Glass-textolite packing was used as the inter-turn insulation. Compressed sections of glass cloth in silicone-organic varnishes were used for the insulation under the bandings.

Forty-six thermocouples were installed for temperature measurement in various sections of the winding and sides of the rotor, as well as twelve thermo-anemometer pick-ups for measuring gas speed and consumption. Securing and insulating the pick-ups and thermocouples situated in the rotor, and, particularly, the withdrawal of the conductors presented a complex problem. A delicate operation was required in drilling blind holes 35 mm in diameter and 1500 mm in depth situated parallel to the central bore of the rotor occupied by the current conductor. One hundred and eight conductors were drawn through these holes to the terminal block connected to the slip ring. The production and arrangement of the pick-ups were carried out in co-operation with the Scientific Research Institute of the Electrical Industry.

A compressor with forward inclined blades was used to reduce the distance between the bearing axes, which is necessary in order to increase the vibration resistance of the rotor. This compressor, with overall radial dimensions determined by the position of the front sections of the stator winding, made it possible to obtain the required head of hydrogen.

In co-operation with the turbine department of the Khar'kov Aviation Institute, the compressor was examined on a specially constructed stand. By means of a suitable selection of diffuser blade pitch in the compressor, the zone of vibrationless operation was enlarged. At the same time a zone of noiseless operation was ensured by selecting the optimum clearances between the blades of the compressor flywheel and the diffuser. The disks and blades of the compressor flywheel were made of steel. Four vertical gas coolers were used for cooling the gas. In order to obtain a considerable rise in the rotor current and in order to use batch production contact rings, two pairs of contact rings with standard brush holders

and two pairs of current-carrying bolts were installed in the rotor.

The generator is excited from a triple-phase current grid through ionic rectifiers with grid control. A d.c. motor-generator was used as a reserve group.

Experimental operations

When producing bars for generators with internal cooling the penetration of a compound into the ventilation tubes must be eliminated. After a number of experiments the introduction of a filler into the tubes and its removal after the end of the bar production process was found to be desirable.

The observance of requirements for tube strength and elasticity is important in order to obtain high-quality bars of uniform shape.

Lengthy experiments were carried out on the determination of the thermal parameters of the bars for a correct determination of their temperature. Here, the dependence of aerodynamic resistance on the velocity of the gas was established, making possible an exact determination of gas consumption and, consequently, of gas overheating. During internal hydrogen cooling the excess of the temperature of the stator copper is determined almost entirely by the heating of the gas, which is:

$$\Delta t = \frac{N}{C_p G},$$

where N is the losses in the stator copper, kW; C_p is the specific heat of the gas, kW. sec/kg. deg; and G is the gas consumption, kg/sec.

The gas consumption can be determined according to the formula

$$G = F \sqrt{\frac{2g\gamma_{cp}\lambda H}{1.5 + \zeta \frac{l}{d}}},$$

where F is the total area of the cross-section of the ventilation ducts, m²; γ_{av} is the specific weight of the gas in the mean cross-section of a bar, kg/m³; ΔN is the applied pressure mm hyd. col.; l is the tube length, m; d is the hydraulic diameter of a tube, m; ζ is the coefficient of friction of the gas in the tubes, $\zeta = \frac{0.3636}{Re^{0.25}}$ (Re– Reynolds number).

The results obtained are substantiated by experimental data with an accuracy up to 1°C.

As a result of these experiments, it was established that temperature drop

from the walls of the tube to the gas when Re= 4500 - 25,000 (which corresponds to the whole possible range of turbogenerator operating conditions) amounts to 2.3°C, and 5.3°C considering the temperature drop in the duct and conductor insulation.

Dielectric losses for the bars with compound mica insulation coincided fully with the normal values for standard bars. The experimental bars with silicone rubber insulation had a dielectric loss angle tangent of 0.020 - 0.049 increasing within the limits 0.022 - 0.027 on a voltage increase from 0.5 U_n to 1.5 U_n. The electrical strength of this insulation is approximately the same as that of bars having the usual mica insulation.

It was interesting to determine the losses in the active steel of the stator and to determine its heating, since the stator core was made for the first time without radial ventilation channels, and had an active length of 2700 mm. Specific losses during induction of 10,000 G were equal to 1.24 W/kg, (1.26 W/kg according to calculations).

No less interesting were the tests of the electrical strength of the stator winding insulation, since the bar heads, where the silicone rubber caps separate the cooling ducts (which are under full voltage) of one bar from the other, are not insulated. Tests with a voltage of $2U_n + 3$kV = 24 kV confirmed the adequate reliability of these caps. There were no breakdowns or flashovers in the bar heads.

1959

Testing the generator*

Factory tests of the generator were made on a reinforced concrete stand faced with iron plates allowing two turbogenerators of 300 - 500 MW each to be set up simultaneously. An oil supply system with an oil line pressure up to 5 atm, a water supply system, a gas supply station and a control panel for the regulation of hydrogen pressure from 0.03 to 4 atm were set up. During the course of sealing and the tuning of the generator at hydrogen pressures up to 3 atm, individual points of gas leakage were found and eliminated (it was necessary to seale the stator surface and the external shields), the reinforcement of the external shields was strengthened along the horizontal joint, and other gas leakage points were found and eliminated, (fine flanges, gas coolant reinforcement, etc.).

In addition to the thermocouples inserted in the rotor the following were also inserted in the active sections of the generator for the ensuing thermal tests in

* The factory tests were made with the participation of the All-Union Scientific Research Institute of Electric Power and the Scientific Research Institute of the Electrical Industry; the tests at the Mosenergo power station were made with the participation of the works and the Scientific Research Institute of the Electrical Industry.

the process of manufacture of the generator: resistance thermometers and thermocouples for measuring the temperature of the stator windings and steel; thermocouples for measuring the temperature of the babbit in the oil seal; resistance thermometers and mercury thermometers for measuring the temperature of gas, water and oil. Thermal tests were made on the stand only in no-load conditions and during triple-phase short-circuit operation of the generator. Tests were made at the power station in conditions of the parallel operation of the generator with the Mosenergo system.

The temperature rises of the rotor and stator windings are shown in Tables 1 and 2 according to data from tests at the power station. These tests were carried out at rated generator voltage and at rated rotation speed.

TABLE 1

Mean excess of rotor winding temperature, °C
(by the method of measuring the winding resistance)

Output of generator MVA	Rotor current A	Hydrogen pressure atm				
		0.05	0.5	1	2	3
31.25	910	36	26	20.5	14	10.5
50	1320	–	62	43.5	28.5	20
62.5	1460	–	–	53	34.5	24.5
67	1580	–	–	–	40	29

TABLE 2

Maximum local excess of temperature in stator slot, °C
(measured by resistance thermometer placed between bars)

Output of generator MVA	Stator current A	Hydrogen pressure atm				
		0.05	0.5	1	2	3
31.25	1720	54	37	28	19	14
50	2750	–	–	57	40	29.5
62.5	3440	–	–	–	63	43
67	3680	–	–	–	–	49

The thermocouples placed in the rotor made it possible to determine both the maximum local temperature and the temperature distribution along the length of and around the rotor. Here, it was found that around the rotor there is a slight variation in temperature. In the coil nearest the large tooth of the rotor the temperature is 8°C less than in the coil farthest removed from it.

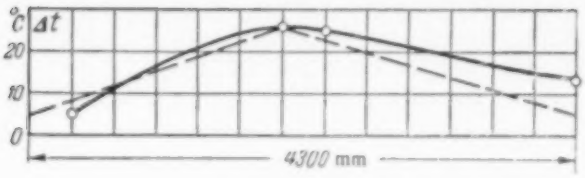

FIG. 1. Distribution of temperature rise along the conductor for the hottest coil in the rotor winding. Rotor current 907 A, hydrogen pressure 3 atm
—— experimental
– – – calculation

The distribution of temperature rise of the copper along the length of the rotor over the temperature of the cold gas is shown in Fig. 1. These results are somewhat better than the calculated results, according to which the maximum temperature of the winding at the mid-point of the rotor is approximately 1.85 times greater than the mean temperature of the winding. With the elimination of cold gas preheating when being supplied from the compressor (which does occur in the experimental generator), and the adoption of other measures, the ratio of maximum to mean temperature will be lowered to 1.6.

1959

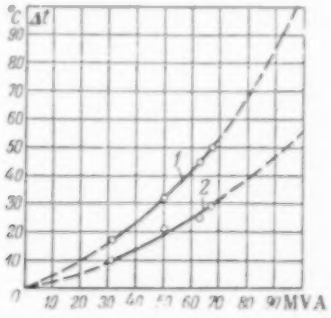

FIG. 2. Maximum temperature rise in stator slot (1), and mean temperature rise in rotor winding (2) over temperature of cold gas during variation in generator load. Hydrogen pressure 3 atm

The application of internal rotor winding cooling combined with an increase in gas pressure to 3 atm was very effective. As is known, the mean temperature rise in the presence of a load of 37.5 MVA amounts to 90°C in the rotors of mark TGV-25 or TV2-30-2 turbogenerators with the usual surface hydrogen cooling. In the test rotor of the TVO-30 generator which has the same active dimensions, the mean temperature rise in the presence of similar loading and a pressure of 3 atm was only 13°C (Fig. 2), and during double loading and a gas pressure of

3 atm the mean temperature rise was only 34°C. The temperature distribution along the length of the stator bars is shown in Fig. 3. Assuming linear dependence of the temperature of a bar on its length, it is easy to determine the maximum bar temperature from the readings of the hottest resistance thermometer. In the presence of a load of 50 MVA the maximum rise of the bar temperature over the temperature of the cold gas is only 39°C. Thus, the permissible load of the generator according to the heating conditions of the stator winding (the temperature rise at the hottest point is equal to 65°C) is 68 MVA. The dependence of the rise of the stator winding temperature on the hydrogen pressure is shown in Fig. 4.

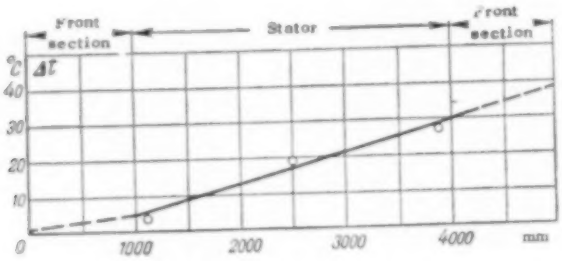

FIG. 3. Distribution of the temperature rise in rotor slot over temperature of cold gas along the length of the winding in the presence of a load of 50 MVA. Hydrogen pressure 3 atm

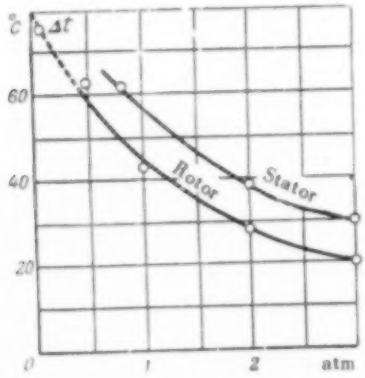

FIG. 4. Dependence of maximum temperature rise of the winding in the stator slot and the mean temperature rise of the rotor winding over the temperature of the cold gas during variation of hydrogen pressure. Load 50 MVA, rotor current 1320 A

The temperature rise of the remaining sections of the generator (the steel in the stator, bearings, seal, etc.) lay within the limits of normal values. Vibration

of the generator bearings was within the limits of 0.02-0.04 mm, the vibration in the axial direction amounting to 0.02 mm.

During operation of the turbogenerator the hydrogen consumption (relative to normal pressure) at the various pressures was as follows:

TABLE 3

Hydrogen pressure in the generator, atm	Hydrogen consumption m^3/day
0.05	0.8*
0.5	0.8*
1	1.8
2	4.5
3	7.0

* Gas leakage is absent in practice. These values are an estimate of hydrogen consumption after taking tests and cleaning the drier.

1959

Let us now dwell briefly on our experience in loading and mounting the TVO-30 generator.

Arrangement of the bearings in the shields of the body of the stator made it possible to load the machine as assembled, i.e. with installed rotor, coolers, internal and external shields, oil seals and outlets. The generator was assembled and tested at the factory during hydrogen cooling. The total weight of the generator as assembled was approximately 85 tons. A standard flatcar of 100 tons load capacity which had previously carried only turbogenerator stators was used for its transportation (Fig. 5). In order to avoid axial displacements of the rotor during its transportation the half-sleeve of the rotor was fastened to the external shield of the generator, by a number of screws of sufficient cross-section. The erection of the generator at the power station including trial starting, connexion into the grid and conversion to hydrogen cooling was accomplished in 14 days, instead of the usual 3-4 months necessary for mounting turbogenerators sent from the plant in a dismantled state.

Conclusion

1. Tests of the mark TVO-30 turbogenerator with internal hydrogen cooling of stator and rotor windings showed that it can develop twice the output of the 25-30 MW series of generator with the same overall dimensions. This corresponds to previously made calculations.

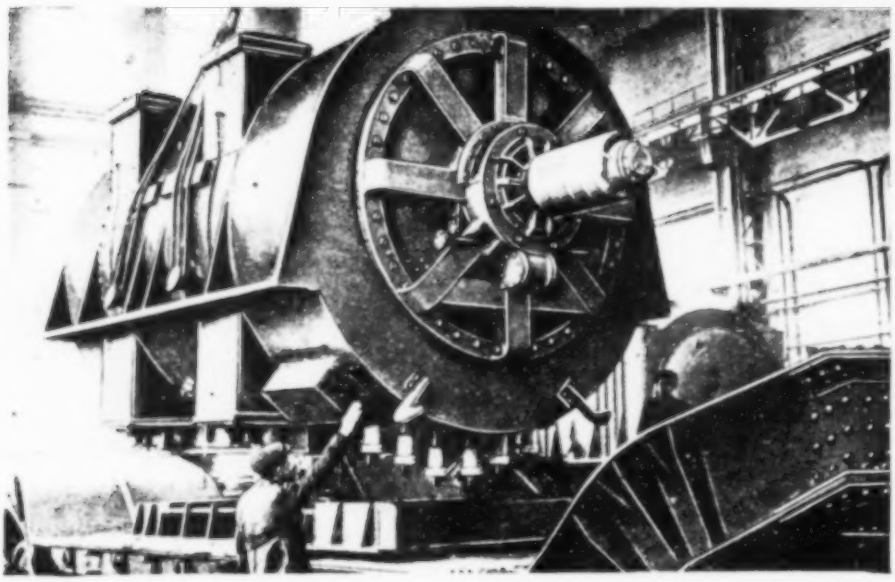

FIG. 5. Loading mark TVO-30 turbogenerator on railway flatcar

2. In manufacturing the generator a number of engineering problems were solved related to the regulation of the production of turbogenerators with internal cooling of windings, and additional requirements were made clear for the design of machines when increasing gas pressure up to 3 atm.

3. The possibility and economic expediency of transporting turbogenerators which have been assembled and tested at the works and also the possibility of mounting them rapidly on site were demonstrated.

Translated by F.J. Griffiths

CALCULATION OF THE REDUCTION OF VOLTAGE ON THE TERMINALS OF HIGH-POWER CURRENT COLLECTORS WITH STRONG ACTUATING CURRENTS*

G.M. KASPRZHAK

(Received 7 January 1958)

The calculation of the voltage loss in factory circuits supplying high-power current collectors with strong actuating currents (squirrel-cage motors and welding transformers), is usually undertaken with maximum actuating current using the well-known formula of approximation [1]:

$$\Delta U = klL(r_n \cos\varphi + x_n \sin\varphi), \tag{1}$$

where r_n and x_n = the active and inductive resistance 1 km of the line Ω/km;
L = length of line km;
I = load current A;
$\cos\phi$ = power factor;
k = coefficient depending on the number of phases and equal to 2 or $\sqrt{3}$.

As can be seen from Fig. 1, such a calculation may give a most inaccurate and minimized result. In the example illustrated the inaccuracy amounts to 20/30 per cent when starting a squirrel-cage induction motor or when short circuiting the secondary circuit of a welding transformer supplied from a relatively weak low-power circuit; in other cases (c.f. appendix) it can amount to 100 per cent and above.

The error in calculation is explained by two factors. The first is that the power factor in activating circuits is very low (not more than 0.15 - 0.2) and as a result of this [2] the formula of approximation (1) is insufficient for calculations. The second factor is that the maximum reduction of voltage on the terminals of current collectors depends, as we know, not only on the strength of the load

* *Elektrichestvo* No. 9, 39-42, 1958.

current but also on the angle of phase displacement between the load current and the short circuit current of the line. In the process of starting, the load current slowly decreases and the angle of phase displacement decreases rapidly. Consequently *the maximum voltage loss will be not in the short circuit but in another circuit* determined in the first instance by the angle of phase displacement.

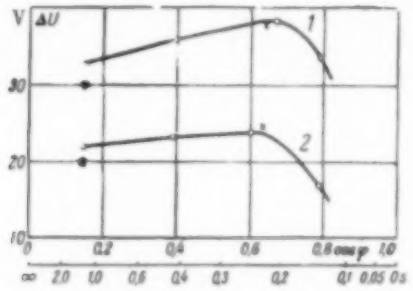

FIG. 1: The reduction of voltage on the terminals of current collectors when starting shown in relation to cos ϕ (for welding transformers), and to slip (for induction motors)
1 = for welding transformers type STE-34; 2 = for squirrel-cage induction motors with 28 kW output;
○ = test data; ● = data from calculations by equation (1);
X = data from calculations by the vector diagram

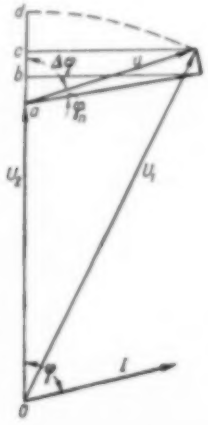

FIG. 2: Vector diagram
I = load current; U_1 = voltage at beginning of line; U_2 = voltage at end of line; u = voltage drop in the line

From the vector diagram shown in Fig. 2 it will be seen that with low power factors and considerable voltage drops in the conductors, the amount of voltage

loss as computed from equation (1) (segment *ac*), can be appreciably different from the true value of that quantity, (segment *ad*). Consequently, when determining the maximum voltage loss in starting an induction motor and when welding, it is essential to state the mathematical relationships more precisely, (2). It will also be seen from the vector diagram Fig. 2 that the greatest voltage loss at a given current and consequently, with a given triangle of the voltage drop of a circuit, attains its maximum value when there is no phase displacement between the load current and the line current in the presence of a short circuit; that is, when $\Delta\phi = \phi - \phi_n = 0$.

This deduction, however, is true only when the load current is constant. In fact, it will decrease somewhat as soon as the motor is started. Consequently, conditions corresponding to the maximum voltage loss do not exactly fit the specification $\Delta\phi = 0$.

Let us determine analytically the conditions of maximum voltage loss having first of all studied the character of the change in the load current I of induction motors and welding transformers, and also the drop in voltage in the lines supplying them in systems from short circuit (starting) to no-load states. With this in mind, assume that the relation of current to load can be determined for medium and high power motors and transformers by a simplified equivalent network Fig. 3, in which, changing the system of operation from short circuit to rated load, we can disregard the conductivity of a parallel circuit of the equivalent network that is, ignore the no-load current. We know [5] that the relation of the current of a series circuit in the equivalent network I_n to the angle ψ between U_2 and I_n is as follows:

$$I_n = I'_{nk} \sin\psi = I_{nk} \frac{\sin\psi}{\sin\psi_k}, \tag{2a}$$

Where I'_{nk} and I_{nk} are the current of the theoretical and the actual short circuit of the series circuit of the equivalent network; ψ_k = the angle of displacement between U_2 and I_{nk}

Consequently for high loads we obtain, with sufficient accuracy:

$$I \approx I_k \frac{\sin\psi}{\sin\psi_k} \approx I_k \frac{\sin\varphi}{\sin\varphi_k}, \tag{2b}$$

where I_k is the current of the actual short circuit, ϕ and ϕ_k = the angle of phase displacement between the voltage and the current in the primary circuit in normal conditions and in the presence of a short circuit.

The angle ϕ_k can be determined for squirrel-cage induction motors from the

parameters of the equivalent network of induction motors and consequently from the size of the critical slip of the machine S_k, such as

$$\cos \varphi_k \approx \cot \varphi_k \approx S_k^{\bullet}. \tag{3a}$$

For welding transformers the value of cos ϕ_k cannot be directly calculated from rating plate or catalogue data. Proceeding from data from the "Elektrik" factory the following approximate values of cos ϕ_k can be recommended for transformers made in our own country: for low-power transformers type STE-24, STAN-0, and STAN-1, cos ϕ_k = 0.2; for medium power transformers type TSD-500, cos ϕ_k = 0.15; for high-power transformers type TSD-1000, cos ϕ_k = 0.1.

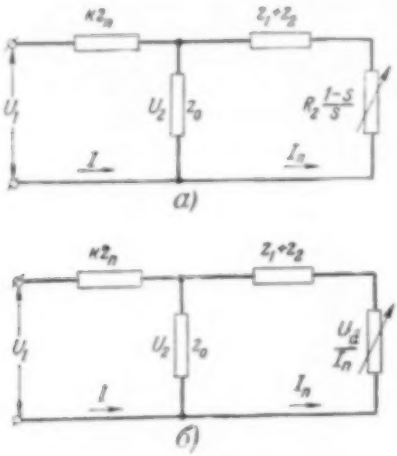

FIG. 3: Equivalent network of an induction motor (a) and of a welding transformer (b)

Z_0, Z_1, Z_2, R_2, $\frac{U_d}{I_n}$,= overall and active resistance of the equivalent network; kZ_n = total impedance of the line

Having determined current I let us determine the voltage drop in the line, the resistance of one conductor of which equals Z_n:

$$u = kI_k \frac{\sin \varphi}{\sin \varphi_k} z_n, \tag{3b}$$

Where $kI_k z_n / \sin \phi_k = u_k$ is the fall in voltage in a line in the presence of an ideal short circuit.

• The method of determining S_k is stated, for example in [4].

Thus,

$$u = u_k \sin \varphi \tag{4a}$$

or, in relative units,

$$\varepsilon = \frac{u}{U_2} = \varepsilon_k \sin \varphi. \tag{4b}$$

To calculate the voltage loss we shall use exact relationships where the unknown value of ΔU is defined, not as the sum of the distances ab and bc, but as $ab + bc + cd$ Fig. 2, i.e., by calculating the transverse components of the voltage drop in the conductors. The expression is given a more convenient form if, for the initial value, we take the voltage drop in the conductors for a given current and angle of $\Delta\phi$, but express the initial and calculated values in relative units. Here, we obtain the mathematical formula introduced in [2]:

$$\delta = \sqrt{1 + 2\varepsilon \cos \Delta\varphi + \varepsilon^2} - 1, \tag{5a}$$

Where $\delta = \Delta U / U_2$: the voltage loss in relative units: $\Delta\phi = \phi - \phi_n$: the angle of phase displacement between U_2 and u.

1959

Substituting in equation (5) the expression for ϵ from (4b) and changing the parameter $\Delta\phi$ for its value, we obtain:

$$\delta = \sqrt{1 + 2\varepsilon_k \sin \varphi \cos (\varphi - \varphi_n) + \varepsilon_k^2 \sin^2 \varphi} - 1, \tag{5b}$$

where $\epsilon_k = U_k / U_2$: the voltage drop in the system in the presence of short circuit current I_k.*

Let us determine the conditions under which the quantity δ attains its maximum value. After differentiation and a series of conversions we obtain:

$$\cot 2\varphi_k = \frac{\varepsilon_k}{2 \cos \varphi_n} - \tan \varphi_n. \tag{6a}$$

Thus, in the examples we have considered when the load current varies with angle ψ according to the sine rule the maximum voltage loss occurs not when $\phi = \phi_n$, but when the relationship between the angles ϕ and ϕ_n is determined by equation (6a). As can be seen from this formula, the relation between the

* With a considerable voltage drop on the terminals of current collectors, the quantity ϵ_k, estimated from the catalogue value of the short circuit current I_k, must be corrected, [1 and 6].

parameters ϕ and ϕ_n is determined also by the amount of the relative voltage drop in the system ϵ_k with a short-circuit current I_k. However, in practice the function $\delta = f(\cos \phi)$ has no strongly expressed maximum. Consequently, the conditions where the voltage loss attains a maximum value can be determined approximately, disregarding the first term of the right-hand side of equation (6a); i.e., by the formula:

$$\cot 2\phi_k = -\tan \phi_n \tag{6b}$$

or, simpler still, by the following equality:

$$\varphi_s = 45^\circ + \frac{\varphi_n}{2}. \tag{7}$$

The relationships $\cos \phi = f(\tan \phi_n)$ for different values of ϵ_k are shown graphically in Fig. 4.

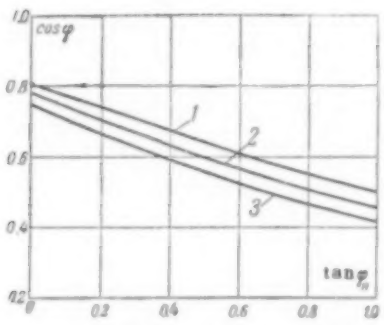

FIG. 4: Diagram to determine the conditions corresponding to maximum voltage loss
(1) $\epsilon_k = 0.6$; (2) $\epsilon_k = 0.4$; (3) $\epsilon_k = 0.2$

Here, it is essential to note that usually $\tan \phi_n < 0.5$. As a result, the maximum voltage loss in low-voltage distributing systems occurs when $\cos \phi = 0.5 \ldots 0.8$, i.e., far beyond the limits of starting conditions.

For cases frequently encountered in practice, when factory circuits are purely an active resistance, i.e. $\tan \phi_n \approx 0$, *the maximum voltage loss when starting an induction motor will occur when the slip is approximately critical.* Actually, in this case $\phi_k = 45^\circ$, but with considerable slip $\tan \phi \approx \tan \psi = s_k/s$, whence $s = s_k \tan \psi$. When $\tan \psi = \tan \psi_k = \tan 45^\circ = 1$ the unknown slip $s = s_k$.

When supplying a welding transformer from an analogous network, the maximum voltage reduction will be in the operating, and not the starting conditions; i.e. when the arc voltage $U_d \neq 0$. Actually, in this case, in accordance with the

equivalent network shown Fig. 3b

$$\cos \phi = \cos \psi = \frac{U_d}{U_s}$$

whence

$$U_d = \cos \psi . U_s.$$

when

$$\tan \psi = \tan \psi_k = \tan 45°, \cos \psi_k = 0.707$$

and, consequently, the arc voltage corresponding to the maximum voltage loss is $0.707 U_s$.

Thus, with automatic welding (U_d up to 45 V) the maximum voltage loss occurs in practice in the presence of operating currents, and with manual welding ($U_d \approx 25$ V), when the arc is relatively low; i.e., with currents lower than operating strength, [5]. As the inductance of the supply system increases, so the conditions corresponding to maximum voltage loss will tend towards an increase in current: i.e. towards the short circuit system. Thus, for example, when starting a high-voltage induction motor directly and the line between the supply source and the motor is a purely inductive resistance [6], the maximum fall in voltage will occur in conditions close to starting conditions.

1959

And so, knowing the conditions which correspond to the maximum fall in voltage on the terminals of the current collectors, and having used an accurate formula to calculate its value, we can calculate the voltage loss in electrical networks when supplied by high output squirrel-cage induction motors and welding transformers. It is not possible, however, to obtain a simple mathematical formula. Therefore, using in turn equation (6a) and (5b) we can plot a family of universal calculation curves. As is to be expected, the functions $d_{\max} = f(\epsilon_k)$ with the given $\tan \phi_n$ are expressed by straight lines.

The approximate expression with which to determine the maximum voltage loss when starting high-power current collectors may be obtained by substituting the conditions for the maximum (7) into equation (5b). Here after conversion we obtain:

$$\delta_{\max} = \sqrt{\left(1 + \varepsilon_k \left(\frac{1}{2} + \varepsilon_k\right)(1 + \sin \varphi_n\right)} - 1. \qquad (8)$$

We can obtain an even more simple mathematical formula by assuming that with a given value of ϵ_k the relative voltage loss $d_{\max}$ increases in proportion to the value of $\tan \phi_n = x_n / r_n$ according to the sine rule. Then, when $\tan \phi_n \leqslant 1$:

$$\delta_{max} = \varepsilon_k \left[\frac{1}{2} + \frac{1}{3} \sin\left(\frac{\pi}{2} \cdot \frac{x_n}{r_n} \right) \right]. \quad (9)$$

As has been shown by checking, equations (8) and (9) give sufficiently accurate results and they may be recommended for practical calculations.

It can be deduced from Fig. 5 and the mathematical formulae (8) and (9) that when $\tan \phi_n = 0$, $d_{max} = 0.5\ \epsilon_k$; when $\tan \phi_n = 1$, $d_{max} = 0.707\ \epsilon_k$; when $\tan \phi_n = \infty$, $d_{max} = \epsilon_k$.

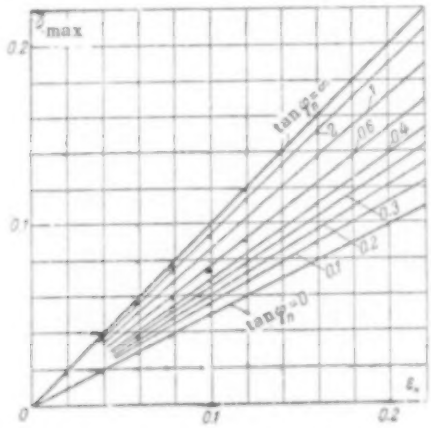

FIG. 5: Curves to determine maximum voltage loss

The relationships we have obtained may be used for approximate calculations. It can be seen from these relationships that with the standard method of calculating the voltage loss, the largest error is admitted in the case of a circuit with purely active resistance. When calculating the voltage loss in a line which only has inductive resistance, the method suggested in this article does not give greater accuracy in the calculations. In the appendix will be found examples of calculations confirming the need to use the suggested methods when calculating the voltage loss in low voltage factory circuits.

Appendix

As confirmation of the necessity to state the calculation of the voltage loss in conductors with large starting currents more precisely, we compare the results of a calculation by the standard method and by the method proposed. The calculations are shown in the table which may also be used as a model to study the sequence of the calculations of the voltage loss on the terminals of current collectors with large starting currents.

Initial data for the calculation:

Example 1: A squirrel-cage induction motor of 28 kW power (U_n = 380 V; I_n = 53.2 A; I_k = 265 A; $\cos\psi_k$ = 0.151) connected to an overhead line 52 m long with a copper conductor section 6 mm² (r_n = 3.06 Ω/kM; x_n = 0.37 Ω/kM).

Example 2: A welding transformer (U_n = 220 V; I_n = 345 A; I_k = 520 A; $\cos\phi_k$ = 0.08) connected to a copper cable 188 m long section of a cable strand 70 mm²; r_n = 0.26 Ω/kM; x_n = 0.06 Ω/kM).

TABLE 1

Calculated value	Basis for calculation (equation diagram)	Example 1	Example 2
Voltage drop:			
In a theoretical short circuit	$\varepsilon_k = \frac{kI_k z_n L}{U_2 \sin\varphi_k}$	$\frac{\sqrt{3}\cdot 265\cdot 3{,}1\cdot 0{,}052}{380\cdot 0{,}99} = 0{,}196$	$\frac{2\cdot 520\cdot 0{,}289\cdot 0{,}188}{220\cdot 0{,}997} = 0{,}248$
In an actual short circuit	$\varepsilon_k' = \frac{kI_k z_n L}{U_2}$	$\frac{\sqrt{3}\cdot 265\cdot 3{,}1\cdot 0{,}052}{380} = 0{,}194$	$\frac{2\cdot 520\cdot 0{,}289\cdot 0{,}188}{220} = 0{,}247$
Critical power factor ($\cos\phi_k$):			
Exact value	$\cot 2\varphi_k = \frac{1}{2\cos\varphi_n} - \tan\varphi_n$	0,60	0,66
Approximate value	$\cot 2\varphi_k \approx -\tan\varphi_n$	0,66	0,62
Maximum voltage loss:			
Exact value	Graphs $\delta_{max} = f(\varepsilon_k; \lg f_n)$ (Fig. 5)	0,112	0,157
Approximate value	$\varepsilon'_{max} = \varepsilon'_k\left[\frac{1}{2} + \frac{1}{\pi}\sin\left(\frac{\pi}{2}\cdot\frac{x_n}{r_n}\right)\right]$	$0{,}194\left[\frac{1}{2} + \frac{1}{\pi}\times\right.$ $\left.\times\sin(90°\cdot\frac{0{,}37}{3{,}06})\right] = 0{,}125$	$0{,}247\left[\frac{1}{2} + \frac{1}{\pi}\times\right.$ $\left.\times\sin(90°\cdot\frac{0{,}06}{0{,}26})\right] = 0{,}172$
Voltage loss in short circuit			
Exact value	$\delta'_k = \sqrt{1 + 2\varepsilon'_k\cos\Delta\varphi + \varepsilon'^2_k} - 1$	$\sqrt{1+2\cdot 0{,}194\cdot 0{,}27+0{,}194^2} - 1 = 0{,}072$	$\sqrt{1+2\cdot 0{,}247\cdot 0{,}303+0{,}247^2} - 1 = 0{,}105$
Approximate value	$\delta'_k = \frac{kI_k L}{U_2}(r_n\cos\varphi + x_n\sin\varphi)$	$\frac{\sqrt{3}\cdot 265\cdot 0{,}052}{380}(3{,}06\cdot 0{,}151 + 0{,}37\cdot 0{,}99) = 0{,}052$	$\frac{2\cdot 520\cdot 0{,}188}{220}(0{,}26\cdot 0{,}08 + 0{,}06\cdot 0{,}997) = 0{,}072$
Error in calculation	$\frac{\delta_{max}}{\delta'_k}\cdot 100\%$	$\frac{0{,}112}{0{,}052}\cdot 100 = 215\%$	$\frac{0{,}157}{0{,}072}\cdot 100 = 218\%$

REFERENCES

1. V.N. Voronov and N.N. Lovtskii; *Proektirovanie silovovo elektrooborudovaniia promyshlennykh predpriiatii. (Designing the power equipment of industrial enterprises).* Gosenergoizdat (1950).
2. G.M. Kasprzhak; *Ob utochnenii rascheta poteri napriazheniia v provodakh. (More precise calculations of the voltage loss in conductors).* All-Union Correspondence Polytechnical Institute (1958).
3. G.M. Kasprzhak; *Individual'naia kompensatsiia reaktivnoi moshchnosti svarochnykh transformatorov. (The individual compensation of the reactive power of welding*

transformers). All-Union Institute of Scientific and Technical Information, Academy of Sciences U.S.S.R. (1958).

4. P.N. Solodovnikov; *O kriticheskom skol'zhenii asinkhronnykh dvigatelei. (The critical slip of induction motors).* VEP No. 11 (1956).
5. B.E. Paton and V.K. Lebyedyev; *Elementy raschetov tsepei i apparatov peremennovo toka dlia dugovoi svarki. (Elements for calculating a.c. circuits and apparatus for arc welding).* Publishing House of the Academy of Sciences of the Ukr. S.S.R. (1953).
6. I.A. Syromiatnikov; *Rezhimy raboty asinkhronnykh elektrodvigatelei. (The operating conditions of induction motors).* Gosenergoizdat (1955).

DIELECTRIC LOSSES IN CONDENSER PAPER*

V.T. RENNE, N.N. KALIAZINA and M.N. MOROZOVA

Kalinin Polytechnical Institute, Leningrad

(Received 13 December 1957)

Every year more uses are found in electrical engineering for paper condensers and in this connexion the manufacture of condenser paper in the U.S.S.R. is continuously increasing. At the same time there has been an improvement in its quality to correspond with the growth of demand for this dielectric from the point of view of the condenser industry in our country.

Furthermore, until recently such an important index of quality as the angle of dielectric loss could not be found in the All-Union State Standard on condenser paper, although in certain types of paper condensers, especially power ones, operating on alternating voltage, the magnitude of the losses in the dielectric determines the overheating of the condenser in operating conditions and the limiting value of its reactive power. In this connexion in recent years a series of investigations into dielectric losses in condenser paper have been carried out in the dielectric research laboratory of Leningrad Polytechnical Institute during which period contact was established with scientific research organizations of the paper industry (Central Paper Scientific Research Institute, Ukranian Paper Scientific Research Institute) and with the Chair of Cellulose Chemistry at Leningrad Technological Institute.

Methods of measuring the loss angle of the dry paper condensers described in foreign journals [1], are comparatively complicated, time consuming and difficult to utilize in the method of paper production, where it would be essential to be able to measure the loss angle of paper in connexion with the introduction of standards for this characteristic in the All-Union State Standard. We have, therefore, developed a special method of measuring the loss angle by means of a simplified system of electrodes, [2]. The method requires a paper specimen to be vacuum dried and eliminates the possibility of ionization developing in the

Elektrichestvo No. 9, 47-52, 1958.

test specimen. It was developed in the Ukranian Scientific Paper Research Institute and with certain modifications has been included in a new and recently approved edition of the All-Union State Standard on condenser paper. Use of this method enables us not only to establish the preliminary standard in the tan δ of paper, but also to obtain certain facts about the dependence of the loss angle of condenser paper on various factors in order to devise means of improving this fundamental characteristic.

It is known that one can successfully use the simplest equivalent sequence method [3] to calculate the electrical properties of condenser paper by means of the familiar characteristics of cellulose, (i.e. the substances forming the fibre walls), and by means of the characteristics of the substances filling the pores of the paper. Using this method for the case of dry non-impregnated condenser paper [4] we may obtain an expression which connects the loss angle of paper with the dielectric permeability of cellulose ($\varepsilon_k \approx 6.5$), its angle of dielectric loss ($\tan\delta_k \approx 60\text{-}70 \times 10^{-4}$ at a frequency of 50 c/s and at a temperature of 20°C) and its density $\gamma_k = 1.5\text{-}1.55$ g/cm³):

$$\tan\delta = \frac{\tan\delta_K}{1 + \dfrac{\varepsilon_K(\gamma_K - \gamma)}{\gamma}},$$

where γ – density (volumetric weight), of test paper determined experimentally.

Thus, the loss angle of condenser paper must primarily depend on its density, which determines the intensity of the calendering process. Our rational paper industry manufactures two main kinds of condenser paper: KON-I, – normally compressed, and KON-II – highly compressed. According to the All-Union State Standard the density of paper KON-I must be between 0.97 and 1.03 g/cm³ irrespective of its thickness; the density of paper KON-II in small thicknesses can vary between 1.14 and 1.23 g/cm³ and in large thicknesses (12-15 μ) amounts to 1.18 – 1.26 g/cm³.

Experimental data concerning the influence of the degree of compression of paper on the size of its loss angle [5] are compared in Fig. 1 with the results of calculations with the formula introduced, (for calculation it is assumed that $\tan\delta_k = 65 \times 10^{-4}$ and $\gamma_k = 1.53$ g/cm³). The conformity of experimental with calculated data has proved to be adequately satisfactory, especially at a density of the order of 1 g/cm³ and above. Using this same data, [5] the dependence is shown in Fig. 2 of the loss angle on temperature for raw uncalendered paper, removed from the paper machine (1), for normally calendered paper (2) and for highly calendered paper (3). The density of the specimens amounted to 0.82, 1.0 and 1.22 g/cm³, respectively.

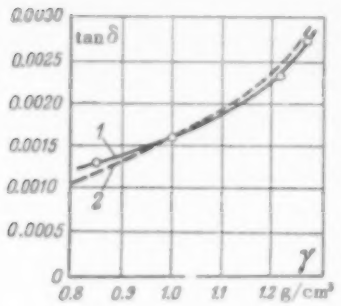

FIG. 1. Dependence of the loss angle on the density of paper, (50 c/s)
1 – experiment
2 – calculation

An increase in the density of paper, causing an increase in the tangent of the loss angle, at the same time leads to an increase in its electrical strength. Therefore paper KON-II is mainly used with direct current or with alternating current of low voltage, when its increased losses are not a special danger. Obviously it would be extremely desirable to produce such a paper Kon II, which would by conserving its electrical strength, reduce losses to the level of paper KON-I. In the new edition of the All-Union State Standard the following permissible maximum values of the tangent of the loss angle have been stipulated: for paper KON-II not greater than 0.002, but for paper KON-I not greater than 0.0017. These figures are appropriate for a frequency of 50 c/s and a temperature of 60°C, [range of minimum losses in the curve $\tan\delta = f(t)$].

It can be seen from the formula introduced that with a given density of paper, its loss angle can be reduced primarily because of the decrease in the magnitude of $\tan\delta_k$; i.e. the loss angle of the substance producing the paper's fibre wall in which there is inevitably an appreciable amount of organic ingredients and a certain amount of inorganic impurities (ashes) besides cellulose. One can primarily refer to the number of organic ingredients as "hemi-celluloses" (hexosans, pentroans and poly-uronic acids) and also lignin; the composition of the ashes includes silica, alumina, calcium oxide and magnesium oxide, and also the oxides of other metals (moreover, chlorides and sulphates are to be found in the ashes).

The contents of these substances obviously depend on the type of raw fibre from which the paper is manufactured; one might therefore assume beforehand that the value of $\tan\delta_k$, and consequently also the magnitude of dielectric losses in the paper can vary with the type of raw fibre. Experiment confirms this supposition. The data produced in Fig. 3 show that one can obtain a marked

difference in the size of the loss angle of paper not only between such extremely diversified types of raw material as linen, rag and wood sulphate cellulose, but even for one type of material – wood sulphate cellulose. The kind of conifer from which cellulose is manufactured – fir and pine – can be of substantial importance. It is interesting to note that rag paper, in which the cellulose content proper (Alpha-cellulose) is greater than that in sulphate cellulose paper (i.e. the impurity content is less), provides not a lower but, on the contrary, a higher value of the loss angle than paper made from sulphate wood cellulose.

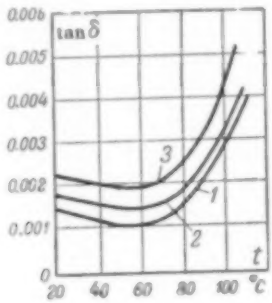

FIG. 2. Dependence of the loss angle on temperature, (50 c/s)
1 – uncalendered specimen of paper;
2 – paper KON-I;
3 – paper KON-II

In the U.S.S.R. and also abroad sulphate cellulose derived from pine wood is used as the basic raw material for the manufacture of condenser paper. Naturally the question arises: at what cost can one attain a reduction of the loss angle of paper in these conditions?

For an explanation of this, work has been carried out in the U.S.A. to study the influence which the cleansing of sulphate cellulose from non-cellulose ingredients has on the size of the loss angle of paper, [6]. The fundamental results of this work are shown in Fig. 4. The removal of inorganic substances and small amounts of foreign matter soluble in water and in organic solvents as well as lignin produces only a slight reduction of losses. When the hemi-cellulose content (mainly pentosans) was further reduced the losses began to decrease appreciably and reached a minimum with a certain optimum content of pentosans; a further elimination of pentosans was then accompanied by an increase of tan δ, whereupon the paper which had been prepared from almost pure alpha-cellulose showed a higher value of losses than in the case of the initial uncleansed sulphate cellulose. One should note that according to the data of this work the initial content of hemi-cellulose (pentosans) amounted to approximately 17 per

cent in the American wood sulphate cellulose; minimum losses were reached with a residual content of pentosans of the order of 11 - 12 per cent.

Using cellulose with a decreased pentosan content, the Americans have produced a new kind of paper with reduced losses; the industrial use of such paper in the manufacture of power condensers has enabled losses in condensers to be reduced to 30 per cent and the reactive power of single condensers to be increased from 15 k var initially to 25, and eventually to 50 k var, [7].

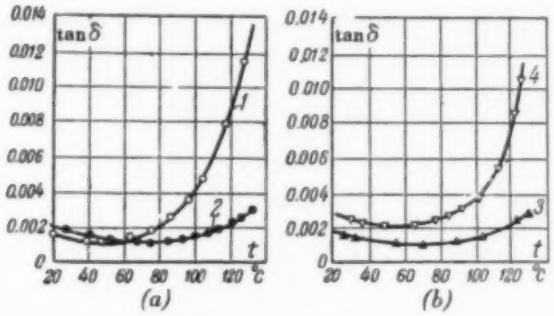

FIG. 3. Influence of type of raw fibre on the loss angle of condenser paper, (50 c/s)
1 – rag paper;
2 – sulphate-cellular paper;
3 – sulphate paper from pine cellulose;
4 – sulphate paper from fir cellulose

Analysis of national pine sulphate cellulose shows that the content of pentosan amounts to 11 - 12 per cent; i.e. without any further treatment it already lies within the limits of those values which were recognized in the U.S.A. as optimum from the point of view of obtaining minimum losses. Therefore, the purification of our cellulose for the purpose of reducing the hemi-cellulose content (pentosan) would not have to produce a decrease of tan δ. In fact, testing of experimental mouldings of purified cellulose produced in the Krasnogorodsk paper factory has shown that losses increase when the pentosan content in national KN type sulphate cellulose is reduced, (Fig. 5).

It was interesting to explain to what extent the residual lignin contained in KN cellulose and used in the production of national condenser paper can lead to a deterioration of its loss angle. For this purpose we measured the losses of that lignin which we obtained from the Central Scientific Research Institute of Paper in the form of powder and examined in the form of disks, cold-pressed at a pressure of 520 kg/cm^2. In view of the fact that it was impossible to make a direct comparison of the results of testing these disks with paper tests, for comparison, an experiment has been carried out with disks pressed out of

low-molecular powdered cellulose (hydrate-cellulose), in these very same conditions, with a degree of polymerization of less than 200. The results obtained are shown in Fig. 6. In the range of temperatures of up to 80°C, losses were greater in lignin than in cellulose, but at higher temperatures the low-molecular cellulose produced a sharp increase in losses. These data indicate that the removal of lignin by purification of KN cellulose can produce a certain decrease of losses, but scarcely very great, as the lignin content in this cellulose is not very large – of the order of 3-4 per cent. Furthermore, there is reason to

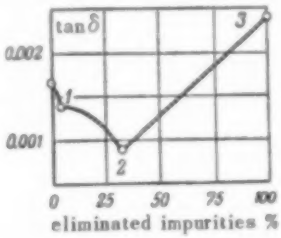

FIG. 4. Dependence of the loss angle on the degree of purification of paper from non-cellulose components, (60 c/s)

1 – without substances, extractable by solvents, of tannin lignin and ash; 2 – without part of the pentosan, (up to optimum); 3 – residual alpha-cellulose after every impurity has been removed

assume that a small residual content of lignin can even be useful with regard to an increase in the thermal stability of paper. In particular, it is known that rag paper, containing a sharply reduced quantity of residual lignin, (less than 0.5 per cent, has an appreciably lowered thermal stability in comparison with sulphate cellulose paper. It is, therefore, necessary to approach the question of reducing the content of residual lignin in KN cellulose very carefully.

In the American work a special attention has been paid to the question of the influence of ashes and their composition on the size of the loss angle of paper. Moreover, there were reasons for supposing that even small changes in the composition of ash can have a considerable influence on the size of tan δ. Particularly, in one English work [8], it was shown that the presence of positively charged ions of monovalent metals in paper can substantially increase its conductivity. If the ash is analysed, we shall find in it metals in the form of oxides, However, before the specimen of paper is burnt to determine its ash content, metals can be found both in the paper and in another state, in particular, in the form of positively charged ions (cations) attached to the cellulose because of cation exchange reaction. In this connexion we have experimented with a solution

of ash specimens of sulphate-cellulose condenser paper (solution is effected by treatment in a centi-normal solution of hydro-chloric acid with subsequent careful washing in distilled water), and we have also experimented with specially prepared specimens of paper, saturated after dissolving with various metallic cations, by producing a cation exchange reaction. These specimens were also carefully washed to remove that part of the metallic cations which had not become attached to the cellulose in the cation exchange. The quantity of connected cations was comparatively small and proved to be proportional to the atomic weight of the metal applied; for example, when saturated with magnesium the increase in weight of the sample amounted to about 0.05 per cent. The residual ash content of the specimens amounted to approximately 0.03 - 0.04 per cent. A spectrum analysis of the residual ash showed that it mainly consisted of compounds of silicon, aluminium and iron.

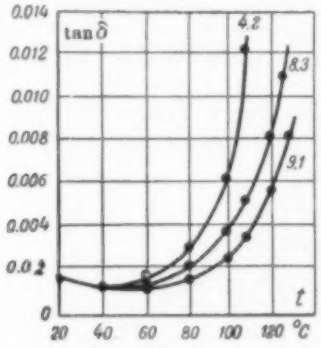

FIG. 5. The influence of a reduction of the pentosan content on the loss angle of experimental mouldings (50 c/s). The figures show the percentage content of pentosan

Measurements which were taken showed that the specific resistance of paper specimens appreciably decreases in comparison with decalcified (dissolved) samples, when cations of monovalent metal, such as sodium, are introduced into the paper; when cations of bivalent metals are introduced into paper, such as magnesium, there is little change in its specific resistance, (Fig. 7). In accordance with this, the loss angle of the specimens containing cations of monovalent metals sharply increases with temperature (Fig. 8), whereas the shape of the curve of the dependence tan δ on the temperature, representing the decalcified sample, remains practically unchanged, when cations of bivalent metals – magnesium, calcium, barium – are introduced. It is interesting to note that the deterioration of losses in paper is greater, the smaller the radius of the ion, when monovalent ions are introduced into it. Thus, losses of lithium, having the

smallest ionic radius and to a lesser extent sodium and even less potassium, increase most of all; in this respect we have an interesting analogy with the behaviour of monovalent ions in inorganic glass, [9]. Evidently, in both cases the detrimental effect of monovalent ions is associated with their increased mobility.

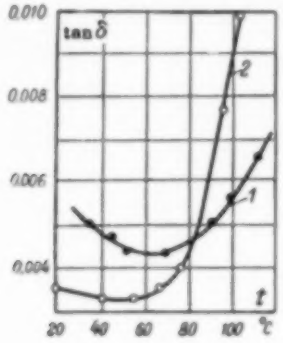

FIG. 6. Results of measuring losses (50 c/s) in lignin (1) and hydrate-cellulose (2)

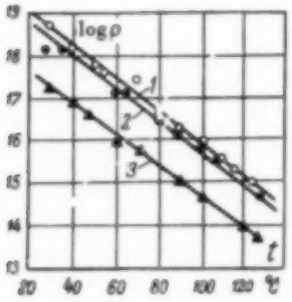

FIG. 7. Influence of cations on specific resistance of paper. 1 – decalcified sample; 2 – specimen, saturated with cations of bivalent magnesium; 3 – specimen, saturated with cations monovalent sodium

The influence of different types of ions on losses in paper at temperatures lower than zero is shown in Fig. 9. The minimum value of the dipole maximum of losses is seen in the case of the decalcified specimen. The introduction of metallic cations increases the dipole maximum all the more, the greater the radius of the ion and the higher its valency. Thus, in this temperature range the influence of bivalent ions on the amount of the losses is greater than the influence of monovalent ions in contrast to the range of temperatures above zero.

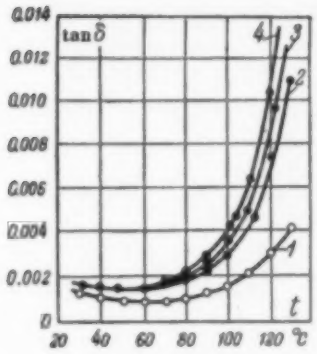

FIG. 8. Influence of cations on the loss angle of paper, (50 c/s)

1 – decalcified specimen; this particular curve agrees with curves for specimens saturated with bivalent cations of Ba^{++}, Ca^{++}, Mg^{++}; 2 – saturation of K^{+}; 3 – saturation of Na^{+}; 4 – saturation of Li^{+}

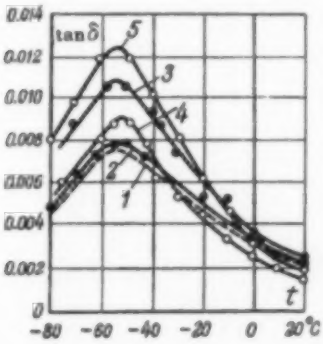

FIG. 9. Influence of cations on the loss angle of paper at low temperatures (1000 c/s)

1 – decalcified sample; 2 – saturated Na^{+}; 3 – saturated K^{+}; 4 – saturated Mg^{++}; 5 – saturated Ca^{++}

A study of the influence of metallic cations on the dielectric characteristics of condenser paper has enabled us to clarify the problem of selecting a system to purify the water used in processing this kind of paper. The introduction of a water-purifier at the "Kommunar" factory had, at first glance, a peculiar effect: paper, produced in purified water with its hardness sharply reduced, had appreciably worsened electrical characteristics compared with those groups of paper, which were previously produced in hard river water, (Fig. 10). Research into this

problem showed that the sodium-cationic filter used in the water-purifying system introduced into the purified water cations of sodium, which passed from the water into the paper and worsened its dielectric properties. While retaining a little hardness in the water (ensuring an accelerated flow process compared with the use of hard river water), the removal of the sodium-cationic filter in the new water-purifying system enabled us to ensure that the electrical properties of the paper are no less than when river water is used.

These facts show that in solving the problem of reducing losses in paper one should pay attention not only to its organic composition but also to the volume of inorganic ingredients it contains, for which in the case in question the absolute content of ash in the paper is not so important as the ash's composition, in particular the presence of cations of monovalent metals.

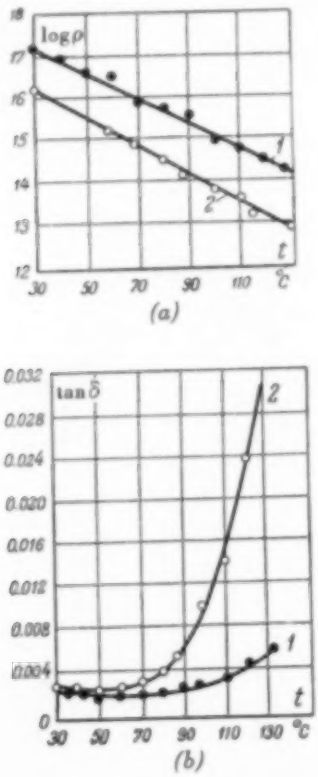

FIG. 10. Influence of the quality of the water used for production on the dielectric characteristics of condenser paper
A – specific electrical resistance; b – loss angle; 1 – river water; 2 – purified water (sodium-cationic filter in water-purification system)

In accordance with the prescription for boiling alkali, sulphate cellulose inevitably contains sodium, whose content practically remains constant in the process of pulverization and discharge of the paper, if additional portions of sodium cannot pass from the water used for production purposes into the paper in a defective water-purifying system. The possibility of eliminating sodium from raw cellulose to improve the characteristics of paper is an interesting proposition.

In the Moscow branch of the Central Scientific Paper Research Institute experiments have been carried out on the decalcification of paper by an electro-dialysis method, [10]. The results of our measurements of the loss angle made on experimental mouldings from finely ground cellulose are given in Fig. 11. The data obtained show that electrodialysis is of short duration, which lowers the ash content to 0.12 per cent and practically rids the cellulose of its sodium content, appreciably reduces the loss angle; further decalcification ensuring a reduction of the residual ash content three times, but practically without changing the sodium content, does not reduce tan δ.

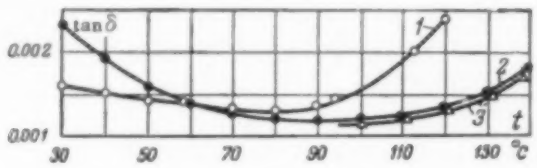

FIG. 11. Dependence of the loss angle on temperature for experimental mouldings of sulphate cellulose, purified by electro-dialysis

1 – raw cellulose, (ash content 0.53 per cent, sodium content 0.0590 per cent of weight of dry cellulose); 2 – cellulose after electro-dialysis of short duration, (ash content 0.12 per cent, sodium content 0.0017 per cent); 3 – cellulose after prolonged electro-dialysis, (ash content 0.04 per cent, sodium content 0.0013 per cent)

It is evident that the practical use of the electrodialysis method for eliminating the sodium contained in cellulose could assist the manufacture of paper with reduced losses.

Figure 3 shows a comparison of losses in paper prepared from different raw materials, a marked difference having been established between rag and sulphate cellular papers. In the light of data shown here regarding the influence of small changes in the composition of the ash on the dielectric characteristics of paper, one can imagine that the difference in the curves in Fig. 3 is caused not only by different raw material (from the point of view of the different organic composition), but also by a possible difference in the composition of the ash. To verify this supposition measurements were taken of the loss angle of specimens of rag and

sulphate cellular paper, similar to that for which results of testing are shown in Fig. 3, but only after they had been subjected to a process of preliminary solution in hydrochloric acid and careful washing. Results which were obtained showed that, although the familiar difference between paper of different raw materials still subsisted, it did prove to be considerably less marked compared with that which had been observed before the samples were decalcified. This example confirms that the composition of ash exerts a great influence on the dielectric characteristics of paper.

Conclusions

1. The loss angle of condenser paper in a dried condition is an important criterion of its quality.

2. Purification of national sulphate cellulose in order to reduce its content of pentosans does not improve the paper's quality in so far as the reduction of its loss angle is concerned, but, on the contrary, leads to its increase.

3. An important factor, influencing the size of the loss angle of paper, is the composition of its ash; monovalent metals, in particular sodium, have a particularly detrimental effect.

4. A reduction of the loss angle of paper can be ensured by reducing the percentage of sodium using the electrodialysis method.

5. The use of sodium-cationic filters in systems for purifying the process water in the manufacture of electro-insulating types of paper should not be entertained.

Translated by J.F. Boyland

REFERENCES

1. H. Endicott; *Gen. El. Rev.* P. 28, No. 9 (1949).
2. V.T. Renne and N.N. Kaliazina; *Trud. LPI im. Kalinina (Works of the Kalinin Polytechnical Institute, Leningrad)* p. 343, No. 184 (1956).
3. V.T. Renne; *Raschet dielektricheskoi pronitsaemosti propitannoi bumagi. (Calculation of the dielectric permeability of impregnated paper). Elektrichestvo,* No. 1 (1949).
4. V.T. Renne; *Electrical Condensers.* Gosenergoizdat p. 303 (1952).
5. L.N. Kuligina; *Sbornik nauchno-issledovatel'skikh rabot studentov elektromekhanicheskovo fakul'teta LPI (Collection of the scientific research works of the students of the electromechanical faculty of Leningrad Polytechnical Institute)* p. 31 (1956).
6. H. Miller and R. Hopkins; *Gen. El. Rev.* P. 20, No. 12 (1947).
7. *El. World,* p. 241, No. 4 (1956).
8. H. Church; *J. Soc. Chem Ind.* p. 221. No. 7 (1947).

9. G.I. Skanavi; *Fizika dielektrikov, (Physics of Dielectrics)*, Gostekhteore tizdat, p. 423 (1949).
10. S Kh. Kitaevai and V.V. Korolev; *Bumazhnaia promyshlennost' (Paper Production)*, p. 4, No. 6 (1957).

1959

ABSTRACTS FROM PAPERS PUBLISHED IN ELEKTRICHESTVO No. 9, 1958

Development of practical methods for designing low-frequency semiconductor amplifiers. I.L. Kaganov: (pp 8 - 15)

The author examines the methods of determining the operating conditions of (1) cascades of preliminary current amplification with RC and (2) current amplifiers with transformer coupling. As regards category (1), the formulae introduced are in respect of a voltage and current feedback scheme with different triodes and load resistances. As regards category (2), the author examines the choice of the coefficient of transformation *n*. He considers the case when the impedances cannot be agreed at the input and output to the cascade and proceeds to determine the resulting coefficient of amplification and the lower and upper limits of frequency.

Electrostatic field of a split phase. A.I. Darevskii: (pp 16 - 19)

Bi-polar co-ordinates are used and the Laplace equation directly solved for plane-parallel fields caused either by similarly charged double cylinders, or conducting double cylinders in a uniform field, or by two cylinders and an axis similarly charged and arranged at the points of an isosceles triangle.

Transformation method of circle representation and its use in solving electrostatic problems in a plane. G.N. Aleksandrov: (pp 20 - 23)

A field created by a linear charge *q* arranged in parallel to an axis of a conducting circular cylinder and outside it, can be found by superposing the fields of three linear charges without a conducting cylinder. The author's method implies the calculation of the distribution of field strength on the surface of split conductors.

Angular characteristic of a power directional device with phase sensitivity. Iu.G. Nazarov: (pp 24 - 30)

The angular characteristic represents the dependence of the average value of the voltage at the output of the scheme over a period on the angle between the current and voltage. The author examines distortions in the angular characteristic

caused by (1), currents and voltages containing harmonics of the upper and lower frequencies and an aperiodic component and (2), by changes in the impedances of the rectifiers. In the event of impermissible distortions of the angular characteristic the author recommends the use of band filters which can be made sufficiently compact for detector-type relays.

A study of the heating of series A and AO 0.6 to 100 kW squirrel cage induction motors during continuous duty. P.A. Suiskii (pp 35 - 38)

Investigations have shown average values of the coefficients of heating losses can differ greatly from actual values. The author proposes formulae to determine the thermal parameters based on the regularities of a class of motors and the results of tests of a number of models. The method of equivalent heating losses is used to calculate the average temperature rises of the windings, illustrated in Appendix II. Apendix I shows the formulae for determining the air speed on different sections of the air conductor.

Industrial tests of a cable-bucket excavator with a new motor-drive system. V.P. Shafranov, A.I. Shishkov, V.D. Fursov and G.P. Petrenko: (pp 41 - 46)

1959

The 1946 model with relay-contactor control and asynchronous drive did not ensure smooth starting and stopping, reliable operation and the required shape of the mechanical characteristic. In 1955 Novokramatorsk engineering works produced the E:Sh-4/40 excavators with drive mechanisms on the generator-motor system with a three-winding generator, but the cost was too high and the machines were unnecessarily powerful. In 1956 new electrical equipment was developed and in 1957 five excavators were built with the new system of asynchronous motor drive. The article then proceeds to discuss the most important results of tests on the drive mechanisms of one of these models. The use of powerful controlled saturation chokes in the circuit of the turning motor, the use of an inductive resistance in the rotor circuit of the main winch driving motor and the use of single phase braking of this motor has improved the technical and operating indices of the machine. In specified conditions the operating cycle of the excavator is 40 - 50 sec, its productivity 200 - 210 m^3/hr, the maximum volume of work per shift 1800 - 2000 m^3 and its specific power consumption 1 - 1.1 kW hr/m^3.

Portable electrical equipment and safety. M.R. Naifel' d: (pp 52 - 54)

Portable electrical equipment includes, electrical tools and production apparatus, domestic and laboratory appliances, children's toys and any electrical equipment connected to the mains by a flexible conductor and plug. The author states that the best guarantee of safety is the reliable construction and good insulation of the live parts of the equipment itself and the cables plugs and sockets. He

reviews home and foreign practice and calls for a revision of the regulations governing this class of electrical equipment taking into account the different conditions in, for instance, schools, theatres, factories and homes.

The formation of static electricity charges and means of their neutralization. V.N. Egorov: (pp 55 - 58)

A special piece of laboratory equipment is described and shown for determining the effect of factors causing the surface density of static electricity charges. The conditions causing the electrification of the materials in industrial conditions are reproduced on the apparatus. This consists of three driving and three driven rollers which move continuous tapes made of dielectric material. Each pair of rollers, as in industrial conditions, is made of metal, rubber, oak or organic glass. It is at the same time possible to measure the potential on tapes of three different materials with the same parameters (speed, tension, humidity, air temperature). Metering is effected by electro-static voltmeters both with the aid of a lamellar probe set up parallel to the surface of the belt and with the aid of foil brushes directly in contact with the surfaces of the moving tapes. The author then discusses his investigations with illustrations and tables of results and concludes that the speed of the tape in relation to the humidity of the air and the specific tension of the tape hardly affects the degree of neutralization and that temperature changes within the limits of 13 - 20°C do not really affect the process of de-electrification of the products. Soiling of the surfaces making contact likewise has little effect.

For neutralization of the static electricity charges he proposes new equipment. The surface of the grinding or driving organs rubbing the tape during operation should be intermittent strips made of material having a different permittivity, for example, rubber and plexiglass or of metal and plexiglass. The width of the strip on the rollers, with intermittent strips of different materials, should be inversely proportional to the potentials forming on the tape if the rollers are as a whole made of corresponding homogeneous materials. In this case, in the presence of friction at adjacent points of the products being electrified, charges arise which are the same in magnitude but opposite in sign. These are mutually compensated in the process of the passage of the product over the guiding or driving organ.

Calculating the power losses in a long line using the r.m.s. current. T.B. Zaslavskaia (pp 58 - 59)

The author seeks to simplify the calculation of power losses in transmission lines by using the r.m.s. current method described in the text. Results are accurate within 2 - 4 per cent.

Electrical multiplication and division and its application to measurement and control. B.Sh. Bungin: (pp 60-62)

The author considers a method of obtaining the product or ratio of two or more electrical magnitudes based on the conversion of values into logarithms with subsequent addition or subtraction. As summing devices, use may be made of electrical machine or magnetic amplifiers with several control windings.

In the case of control using a logarithm of a function ϕ the absolute error ϵ corresponds in the whole range to an identical relative control error δ of the same function ϕ:

$$Y = \ln \varphi;$$
$$Y \pm \varepsilon = \ln \varphi \pm \varepsilon = \ln \varphi + \ln (1 \pm \delta) = \ln [(1 \pm \delta) \varphi].$$

If the absolute error ϵ of the function $Y = \ln \phi$ is a constant magnitude, then the relative error δ of the function ϕ is also constant.

Thus, logarithmic control of a magnitude can admit a lesser value of the coefficient of amplification of the system (for the desired relative error), or obtain a lesser relative error for small values of ϕ than in a system of control using the value of the function ϕ itself.

1959

Measuring power by the equal temperature method. V.S. Popov: (pp 63-66)

The author's method is the direct measurement of the difference in power in the heaters of thermal converters or heating resistances; here the characteristics of each pair of converters or heating elements should be similar but the form of these characteristics can be quite arbitrary. The Electromechanical Institute of the Academy of Science has made a number of measurements of power with the aid of heating resistances. Here special equalizing heating resistances were developed consisting of two nichrome or constantan heaters, each of which was set in a glass insulation tube and a tungsten or platinum spiral mounted round the heater. Measurement of power by the equal temperature method is applicable to the measurement of power in the range of sound frequencies with an accuracy of hundredths of parts of a per cent, measurement and registration of power in a wide range of frequencies and the accurate measurement of power when the coefficient of power is low.

EDDY CURRENTS IN SYNCHRONOUS AND ASYNCHRONOUS MACHINES WITH UNLAMINATED ROTORS*

I.M. POSTNIKOV

Kiev

(Received 17 April 1958)

In synchronous machines with unlaminated rotors it is very important to know the losses, caused in the rotor by higher harmonics of the m.m.f. of the armature, and also losses due to the fundamental harmonic during asynchronous running. These losses are sometimes called surface losses, since it is assumed that eddy currents only penetrate the rotor surface to a small depth. In fact, the depth of penetration depends on the frequency and magnetic properties of the rotor material, and may be very considerable.

The methods, which are widely used for calculating eddy currents, in many important cases give considerably different results and lead to exagerations. For example, in one recent work [1], we find an erroneous determination of the induction of the rotor surface due to eddy currents, and in consequence a greatly exaggerated value of losses was obtained. The application of the usual formulae to machines with a small air gap or for various materials and frequencies also leads to incorrect results. The reasons why the formulae of individual authors lead to widely divergent answers, are explained by a different evaluation of the screening effect and variable permeability.

As will be shown later, it is possible to obtain a method of calculating losses due to eddy currents, by which all the main factors that influence the magnitude of these losses are accounted for. The method discussed in this article may also serve for designing electromagnetic couplings, brakes, high-frequency heating etc.

We shall first analyse the phenomena connected with propagation with respect to the rotor surface of any one single sinusoidal wave of the armature m.m.f. of the order ν_1. The result is obtained by the summation of all possible harmonics (we assume that the superposition of results due to individual harmonics is admissible).

* *Elektrichestvo* No. 10, 7–14, 1958.

When the sinusoidal current flows in a three phase stator winding with an integral number of slots per pole and phase, a series of space waves of the order ν_1 is induced in the stator; these waves move in various directions; $\nu_1 = 6k + 1$, i.e. is equal to 1,5,7,11 and so on, ($k = 0, \pm 1, \pm 2, \pm 3$ etc.) During synchronous running, the fifth harmonic rotates in the opposite direction to the fundamental wave, the seventh harmonic rotates in the same direction as the fundamental wave. Therefore, the fifth and seventh harmonics during synchronous running induce harmonics in the rotor, the order of which is $\nu = \nu_1 - 1 = \pm 6$.

In a similar way, the 11th and 13th harmonics induce the 12th order harmonic and so on. Harmonics ν_1 which are multiples of 3, are absent. For the slip $s \neq 0$, $\nu = \nu_1 - (1 + s_1)$.

For windings with a fractional number of slots per pole and phase

$$q = b + \frac{c}{d} = \frac{bd + c}{d} = \frac{N}{d};$$

the order of the stator harmonics [2] for the six-zone windings is

$$\nu_1 = \frac{6k}{d} + 1$$

where k is any arbitrary integer, positive or negative, including zero; for the three-zone windings $\nu_1 = \frac{3k}{d} + 1$. In this case the fractional values of the m.m.f. order ν_1 appear in the stator, and $\nu = \nu_1 - 1$ in the rotor. Moreover, harmonic ripples appear, the order of which is $\nu_1 = k\frac{Z_1}{p} + 1$; since $\nu = \nu_1 - (1 + s\,\nu_1)$ then

for S = 0

$$\nu = k\frac{Z_1}{p}$$

where Z_1 is the number of the stator slots;

p is the number of pole pairs;

k is any arbitrary positive or negative integer.

when $k = \pm 1$, we have two fundamental ripple harmonics: direct and reverse. Both these harmonics induce in the rotor rotating at a synchronous speed a harmonic of the order of frequency $\nu = \frac{Z_1}{p}$

The fundamental harmonic $\nu_1 = 1$ during a synchronous running determines, in the rotor, the slip frequency $\nu = s$.

For a non-sinusoidal current, every current harmonic of the i-th time order produces its own series of space harmonics.

The frequency in the rotor will be $\nu_1 = i\,\nu$

Calculation of losses

In order to calculate the losses, it is necessary to determine the resultant induction in the rotor produced by a propagating wave of the stator m.m.f. of the order of ν_1. If we denote a co-ordinate that rotates together with the wave in question by X, then the amplitude of the m.m.f. wave $F_{\nu\, im}$ is equal to the integral of the linear load $A_{\nu\, im} \sin \frac{\pi}{\tau \nu_1} x$ at the middle of the pole spacing $\frac{\tau_{\nu 1}}{2}$

$$F_{\nu im} = \int_0^{\frac{\tau_{\nu 1}}{2}} A_{\nu im} \sin \frac{\pi}{\tau_{\nu 1}} x \; dx = \frac{\tau_{\nu 1}}{\pi} A_{\nu im}. \tag{1}$$

The rotating wave of the linear load of the order of ν_1 can be represented in this form:

$$A_{\nu i} = A_{\nu im}\, e^{j\left(\frac{\pi \nu_1}{\tau} x' - \omega_i t\right)} = A_{\nu im}\, e^{j\frac{\pi \nu_1}{\tau} x}, \tag{2}$$

where $\tau_{\nu 1} = \frac{\tau}{\nu_1}$;

$\omega_i = \omega_1 \nu_i$ is the angular frequency of the supply current (or angular frequency of rotation of the wave of the excitation current in the case of d.c. excitation).

The m.m.f. wave of the order of ν_1 induces in the rotor a corresponding m.m.f. due to induced currents of frequency

$$\omega_\nu = \omega_1 \nu i, \tag{3}$$

where νi – multiple of the frequency ω_1.
For $i = 1$, $\nu = [\nu_1 (1 - s) \pm 1]$; for $s = o$, $\nu = \nu_1 - 1$; for $\nu_1 = 1$, $\nu = s$,
(for a non-sinusoidal current $\nu_1 = i\,\nu$ for the current harmonic of the order of ν; further we assume $i = 1$, i.e. we assume a sinusoidal current).

The resultant field in the gap on the rotor surface and inside its body can be determined by solving Maxwell's differential equations for vectors of the magnetic field strength $H = \frac{B}{\mu}$, of the electric field $E = S'\rho$, and of the current density s μ if the permeability μ remains constant, i.e.

$$\text{rot}\, \dot{H} = \dot{s} = \frac{\dot{E}}{\rho}; \tag{4}$$

$$\text{rot}\, \dot{E} = -\frac{\partial \dot{B}}{\partial t} = -\mu \frac{\partial \dot{H}}{\partial t}. \tag{5}$$

In the majority of cases we can neglect the curvature of the rotor surface and consider it as a plane x-z (z is the direction of the rotor axis). The radial direction corresponds to y, ($y = o$ at the surface of the stator circle, $y = -\delta$ on the rotor

Constants α and α_1 are determined by substituting equation (10) into (8), i.e.

$$-\left(\frac{\pi\nu_1}{\tau}\right)^2+\alpha^2-\alpha_1^2+2j\alpha\alpha_1=-j\omega_\nu\frac{\mu}{\rho}, \tag{19}$$

where we get the set:

$$\left.\begin{aligned}\alpha^2-\alpha_1^2-\left(\frac{\pi\nu_1}{\tau}\right)^2&=0;\\ 2\alpha\alpha_1&=-\frac{\omega_\nu\mu}{\rho}.\end{aligned}\right\} \tag{20}$$

Solving (20) we get:

$$\left.\begin{aligned}\alpha&=\frac{1}{\sqrt{2}}\frac{\pi\nu_1}{\tau}\sqrt{1+\sqrt{1+\left(\frac{\omega_\nu\mu}{\rho}\cdot\frac{\tau^2}{\pi^2\nu_1^2}\right)^2}};\\ \alpha_1&=\frac{1}{\sqrt{2}}\frac{\pi\nu_1}{\tau}\sqrt{-1+\sqrt{1+\left(\frac{\omega_\nu\mu}{\rho}\cdot\frac{\tau^2}{\pi^2\nu_1^2}\right)^2}}.\end{aligned}\right\} \tag{21}$$

Except for very high values of ν_1, very low frequencies ν_ν and small values of μ, which have no practical significance, the quantity $\left(\frac{\omega_\nu\mu}{\rho}\cdot\frac{\tau^2}{\pi^2\nu_1^2}\right)^2$ is considerably greater than unity, and consequently

$$\alpha=\alpha_1=\sqrt{\frac{\mu\omega_\nu}{2\rho}}=\frac{1}{\Delta_\nu}, \tag{22}$$

where the quantity, which is the reciprocal of the conventional depth of penetration, is given by:

$$\Delta_\nu=\sqrt{\frac{2\rho}{\mu\omega_\nu}}. \tag{23}$$

In this case equations (17) and (18) assume the following form:

$$H_x=\frac{B_{\nu 0}\tau}{j\mu\pi\nu_1\Delta_\nu}(1+j)e^{\frac{y+\delta}{\Delta_\nu}}e^{j\left(\frac{\pi\nu_1}{\tau}x+\frac{y+\delta}{\Delta_\nu}\right)}; \tag{24}$$

$$H_y=\frac{B_{\nu 0}}{\mu}e^{\frac{y+\delta}{\Delta_\nu}}e^{j\left(\frac{\pi\nu_1}{\tau}x+\frac{y+\delta}{\Delta_\nu}\right)}. \tag{25}$$

Determination of constants C_1 and C_2 and induction on the rotor surface $B_{\nu 0}$.

1. Normal components of the induction on the surface of separation should vary continuously.

The tangential components of the magnetic field strength vary continuously in the

surface, in the rotor centre we can assume $y = -\infty$). We assume that the rotor surface is smooth since the influence of slots in cylindrical rotors or of interpole spaces in salient pole rotors is to a certain degree compensated by the losses on the slot walls, on the metal wedges or on the radial surfaces of the poles shoes. Moreover, we neglect at first the influence of frontal parts, i.e. we assume that all currents flow in the axial direction, and, consequently, we have:

$$E_x = E_y = 0, \quad E_z = E, \quad \frac{\partial E}{\partial z} = \frac{\partial^2 E}{\partial z^2} = 0.$$

Under these conditions, applying the operation:

$$\text{rot rot } \dot{E} = -\nabla^2 \dot{E},$$

for the solenoidal vector E from (4) and (5) we get:

$$\frac{\partial^2 \dot{E}}{\partial x^2} + \frac{\partial^2 \dot{E}}{\partial y^2} = \frac{\mu}{\rho} \frac{\partial \dot{E}}{\partial t}. \tag{6}$$

Similar equations are obtained for vectors H and s.

For the region of the air gap the right-hand side of equation (6) is zero. The solution of equation (6) for cases when E is a periodic function of x of the form:

$$f(x) = \cos \frac{\pi \nu_1}{\tau} x; \quad f(x) = \sin \frac{\pi \nu_1}{\tau} x,$$

or in a complex form, $\exp\left(-j \frac{\pi \nu_1}{\tau} x,\right)$ it is:

$$E = \varphi(y) e^{j \frac{\pi \nu_1}{\tau} x} =$$
$$= \left(C_1 e^{-j \frac{\pi \nu_1}{\tau} y} + C_2 e^{j \frac{\pi \nu_1}{\tau} y}\right) e^{j \frac{\pi \nu_1}{\tau} x}. \tag{7}$$

For the rotor body, equation (6) for a field varying sinusoidally with time $E = E(x, y) \cdot \exp(-j \omega_\nu t)$ is of this form:

$$\frac{\partial^2 E}{\partial x^2} + \frac{\partial^2 E}{\partial y^2} = -j\omega, \frac{\mu}{\rho} E. \tag{8}$$

This equation is satisfied by the function

$$E = (C_3 e^{\beta y} + C_4 e^{-\beta y}) e^{j \frac{\pi \nu_1}{\tau} x}, \tag{9}$$

where $\beta = \alpha + j a_1$ is a complex number, which is determined by substituting (9) into (8).

Since, for $y = -\infty$, $E = o$, then the second solution $C_4 \exp(-\beta y)$ has no meaning and should be made equal to zero.

Putting on the rotor surface $y = -\delta$ and assuming the value of the E on the surface $E_{\nu 0} = -B_{\nu 0} U_\nu$, where $B_{\nu 0}$ and U_ν are the induction and the wave tangential speed on the surface, we get

$$E = E_{w0} e^{j\beta(y+\delta)} e^{-j\frac{\pi v_1}{\tau}x} =$$

$$= B_{w0} v_w e^{j\beta(y+\delta)} e^{-j\frac{\pi v_1}{\tau}x}; \tag{10}$$

$$v_w = \frac{\omega_w \tau}{\pi v_1}; \tag{11}$$

$$C_3 = -\frac{\omega_w B_{w0} \tau}{\pi v_1}. \tag{12}$$

Equations for the magnetic field strength H in the gap and inside the rotor body can be obtained from (7) and (10) by using equation (5). For a field varying sinusoidally with time, the equation assumes the form:

$$\text{rot}\, \dot{E} = -\mu \frac{\partial \dot{H}}{\partial t} = j\omega_w \mu \dot{H};$$

$$\text{rot}_x \dot{E} = \frac{\partial E_z}{\partial y} - \frac{\partial E_y}{\partial z} = \frac{\partial E}{\partial y} \quad \text{(since } \frac{\partial E_y}{\partial z} \text{ is by assumption zero, } E_z = E\text{)}$$

$$\text{rot}_y \dot{E} = \frac{\partial E_x}{\partial z} - \frac{\partial E_z}{\partial x} = -\frac{\partial E}{\partial x} \quad \text{(since } \frac{\partial E_x}{\partial z} \text{ is by assumption zero).}$$

Therefore:

$$H_x = \frac{1}{j\omega_w \mu} \frac{\partial E}{\partial y}; \tag{13}$$

$$H_y = -\frac{1}{j\omega_w \mu} \frac{\partial E}{\partial x}. \tag{14}$$

Taking partial derivatives of (7) and (10) we get for the region of the air gap:

$$H_x = -\frac{\pi v_1}{j\omega_w \mu_0 \tau}\left(C_1 e^{-\frac{\pi v_1}{\tau}y} - C_2 e^{\frac{\pi v_1}{\tau}y}\right) e^{j\frac{\pi v_1}{\tau}x}; \tag{15}$$

$$H_y = -\frac{\pi v_1}{\omega_w \mu_0 \tau}\left(C_1 e^{-\frac{\pi v_1}{\tau}y} + C_2 e^{\frac{\pi v_1}{\tau}y}\right) e^{j\frac{\pi v_1}{\tau}x}, \tag{16}$$

and for the region of the rotor body:

$$H_x = \frac{1}{j\omega_w \mu} \cdot \frac{\partial E}{\partial y} =$$

$$= -\frac{B_{w0}\tau}{j\mu\pi v_1}(\alpha + j\alpha_1) e^{(\alpha+j\alpha_1)(y+\delta)} e^{j\frac{\pi v_1}{\tau}x}; \tag{17}$$

$$H_y = \frac{B_{w0}}{\mu} e^{(\alpha+j\alpha_1)(y+\delta)} e^{j\frac{\pi v_1}{\tau}x}. \tag{18}$$

absence of surface currents (we consider the rotor currents as distributed inside the rotor body, and not confined to the surface).

The first condition causes equation (25), for $y = -\delta$, multipled by μ to become:

$$-\frac{\pi\nu_1}{\omega_\nu\tau}\left(C_1 e^{\frac{\pi\nu_1\delta}{\tau}}+C_2 e^{-\frac{\pi\nu_1\delta}{\tau}}\right)=B_{\nu 0}. \tag{26}$$

The second condition causes equation (24), for $y = -\delta$, to be equivalent to equation (15) for $y = -\delta$, i.e.

$$-\frac{\pi\nu_1}{j\omega_\nu\mu_0\tau}\left(C_1 e^{\frac{\pi\nu_1\delta}{\tau}}-C_2 e^{-\frac{\pi\nu_1\delta}{\tau}}\right)=-\frac{B_{\nu 0}\tau}{j\pi\mu\nu_1\Delta_\nu}(1+j). \tag{27}$$

From these two conditions we get:

$$C_1=-\frac{1}{2}\frac{B_{\nu 0}\omega_\nu\tau}{\pi\nu_1}\left[1-\frac{\tau(1+j)}{\pi\mu'\nu_1\Delta_\nu}\right]e^{-\frac{\pi\nu_1\delta}{\tau}}; \tag{28}$$

$$C_2=-\frac{1}{2}\frac{B_{\nu 0}\omega_\nu\tau}{\pi\nu_1}\left[1+\frac{\tau(1+j)}{\pi\mu'\nu_1\Delta_\nu}\right]e^{\frac{\pi\nu_1\delta}{\tau}}, \tag{29}$$

where $\mu_1=\frac{\mu}{\mu_0}$ is the relative permeability of the rotor material.

1959

The third condition is that on the rotor surface i.e. for $y = 0$, according to the law of the total current the tangential component H_x of the field strength from equation (15) should be equal to the linear load $A_{\nu 1m}$ (we neglect the field strength in the stator steel).

$$-\frac{\pi\nu_1}{j\omega_\nu\mu_0\tau}(C_1-C_2)=A_{\nu 1m}. \tag{30}$$

Substituting the values of the constants C_1 and C_2 obtained in this way, we get the value of the induction on the surface:

$$B_{\nu 0}=\frac{\mu_0 A_{\nu 1m}}{\sinh\frac{\pi\nu_1}{\tau}\delta+(1+j)\frac{\tau}{\nu_1\mu'\pi\Delta_\nu}\operatorname{ch}\frac{\pi\nu_1}{\tau}\delta}, \tag{31}$$

or

$$B_{\nu 0}=\frac{\mu_0 A_{\nu 1m}}{\sqrt{\left(\sinh\frac{\pi\nu_1}{\tau}\delta+\frac{\tau}{\mu'\nu_1\pi\Delta_\nu}\operatorname{ch}\frac{\pi\nu_1}{\tau}\delta\right)^2+\left(\frac{\tau}{\mu'\nu_1\pi\Delta_\nu}\operatorname{ch}\frac{\pi\nu_1}{\tau}\delta\right)^2}} \tag{32}$$

In the absence of currents in the rotor, we would have:

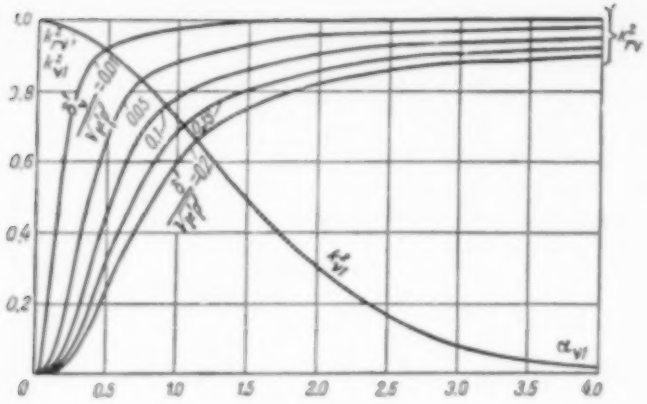

FIG. 1.

$$B_{v0} = \frac{\mu_0 A_{v1m}}{\sinh \frac{\pi \nu_1}{\tau} \delta}, \tag{33}$$

and for small values of $\frac{\pi \nu_1}{\tau} \delta$, when we can put:

$$\sinh \frac{\pi \nu_1}{\tau} \delta \approx \frac{\pi \nu_1}{\tau} \delta,$$

we have:

$$B_{v0} = \frac{\mu_0 A_{v1m} \tau}{\pi \nu_1 \delta} = \frac{\mu_0 F_{v1m}}{\delta}. \tag{34}$$

It is expedient to introduce two factors:

$$k_{v1} = \frac{\alpha_{v1}}{\sinh \alpha_{v1}}; \tag{35}$$

$$k_{rv} = \frac{1}{\sqrt{\left(1 + \frac{\tau}{\Delta_v \mu' \nu_1 \pi \operatorname{th} \alpha_{v1}}\right)^2 + \left(\frac{\tau}{\Delta_v \mu' \nu_1 \pi \operatorname{th} \alpha_{v1}}\right)^2}}, \tag{36}$$

where

$$\alpha_{v1} = \frac{\pi \nu_1 \delta}{\tau}.$$

The first factor accounts for the field attenuation due to the finite gap magnitude, and the second one – the back influence of the rotor currents, i.e. it is equal to the field attenuation factor or to the reaction factor of the rotor currents (Fig. 1). Thus, we obtain the expression for the induction on the surface in this form:

$$B_{v0} = \frac{\mu_0 F_{v1m}}{\delta} k_{v1} k_{rv}. \tag{37}$$

Losses per unit area of the unlaminated rotor due to the harmonic of the order of ν are:

$$w_\nu = \frac{B_{\nu 0}^2 \tau^2 f_1^{1,5} \nu^{1,5}}{\nu_1^2 \sqrt{\pi \mu \rho}} \left[\frac{W}{cM^2}\right]. \tag{38}$$

This expression can be obtained from equations (10) and (24) as the real part of the Umov – Poynting vector:

$$w_\nu = \frac{1}{2} \operatorname{Re} \left| \dot{H} \dot{E}^* \right| = \frac{1}{2} H_{z0} E_0. \tag{38a}$$

The imaginary part becomes equal to the real part and is equal to the mean value of the reactive power per unit of the reactor surface. Substituting the value of B_{ν_0} into (38) we get:

$$w_\nu = \frac{\mu_0^2 F_{\nu 1 m}^2 k_{\nu 1}^2 k_{r\nu}^2 \tau^2 f_1^{1,5} \nu^{1,5}}{\delta^2 \nu_1^2 \sqrt{\pi \mu_0 \mu' \rho}} \cdot \left[\frac{W}{cM^2}\right]. \tag{39}$$

The amplitude of the m.m.f. of the stator harmonic of the order of ν_1 can be expressed by means of the m.m.f. of the fundamental wave F_1 in the form:

$$F_{\nu 1 m} = \frac{1}{\nu_1} F_{1m} \frac{k_{w\nu 1}}{k_{w1}}, \tag{40}$$

where

$$F_{1m} = \frac{\sqrt{2}\, m}{\pi p} w I_1 \, k_{w1} = \frac{\sqrt{2}\, A_1 \tau k_{w1}}{\pi}, \tag{41}$$

$A_1 = \dfrac{F_1 \pi}{\sqrt{2} \tau k_{w1}}$ is the active value of the linear load of the fundamental wave.

Hence, substituting (40) and (41) into (39) we get:

$$w_\nu = \frac{2 \mu_0^2 A_1^2 \tau^4 c f_1^{1,5}}{\pi^2 \sqrt{\pi \mu_0 \rho_{Cu}}\, \delta^2 \sqrt{\mu' \rho'}} \left(\frac{k_{w\nu 1}}{\nu_1^2}\right)^2 k_{\nu 1}^2 k_{r\nu}^2 \nu^{1,5} \left[\frac{W}{cM^2}\right], \tag{42}$$

where $\rho' = \dfrac{\rho}{\rho_{Cu}}$; for steel $\rho = 6\text{-}10$.

Taking the sum for all values of ν_1 and ν and multiplying it by the rotor area, we obtain total losses:

$$P_{\nu R} = 4.5 \times 10^{-8} \left(\frac{f_1}{50}\right)^{1,5} \frac{A_1^2 \tau^4 S_R}{\delta^2 \sqrt{\mu' \rho'}} \varphi [W], \tag{43}$$

where $S_R = 2 p \tau l$ – the rotor area

$\rho_{Cu} = 1.6 \times 10^{-6}$ ohm.cm.

$$\varphi = \sum_{\nu 1} \left(\frac{k_{w\nu 1}}{\nu_1^2} \right)^2 k_{\nu 1}^2 k_{r\nu}^2 \nu^{1.5} . \tag{44}$$

For the range of frequencies and values of $\sqrt{\mu' \rho'}$, for which we can assume $k^2_{\nu 1} \approx 1$, and the screening factor $k^2_{r\nu} \approx 1$ we have:

$$\varphi = \varphi_1 = \sum_{\nu_1} \left(\frac{k_{w\nu 1}}{\nu_1^2} \right)^2 \nu^{1.5} , \tag{45}$$

ϕ and ϕ_1 as functions of the winding pitch y, expressed in fractions of τ, for windings with an integral number of slots per pole and phase, are represented for higher space harmonics, $\nu = \nu_1 - 1$, in Fig. 2. In this case,

$$k_{w\nu 1} = k_{y\nu 1} \cdot k_{p\nu 1}; \quad k_{y\nu 1} = \sin \nu_1 \frac{\pi}{2} y; \quad k_{p\nu 1} = \frac{\sin 30^\circ}{q \sin \frac{30^\circ}{q} \nu_1} .$$

For six-zone windings, with a fractional number of slots per pole and phase $k_{y\nu 1} = \sin \nu_1 \frac{\pi}{2} y$, the distribution factor when d is even is:

$$k_{p\nu 1} = \frac{\sin 30^\circ}{N \left(\cos \frac{30^\circ}{N} \right) y_w \nu_1 d} ;$$

when d is odd we have to substitute into the denominator $\sin \frac{30^\circ}{N}$ instead of $\frac{30^\circ}{N}$.

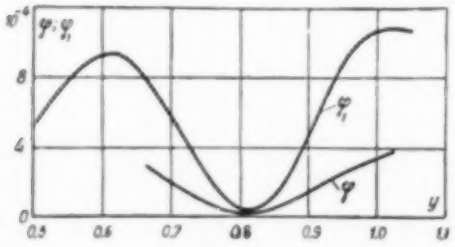

FIG. 2.

Here $N = bd + c$ – numerator of an improper fraction for q;

$y_w = \frac{1 + Ngm}{d}$ is the difference of the numbers of the adjacent rays of the slot star;

g – is the smallest integer ($g > 1$) which makes y_w an integer;

m – is the number of phases.

According to the method discussed in [3] we assume that the factor $k^2_{r\nu}$ is the

same for all harmonics and is equal to $k_d \simeq 0.5-0.6$, the value of $\sqrt{\mu' \rho'}$ being included in the constant k_0. With this method of calculation we may get wrong results if the value of $\sqrt{\mu' \rho'}$ varies. Indeed, from (42) it follows that, for $k^2_{r\nu}$ = const., the losses when $\sqrt{\mu' \rho'}$ decreases. However, with the decrease of $\sqrt{\mu' \rho'}$, due to the screening effect, the factor $k^2_{r\nu}$ might decrease still faster, and the losses will decrease. If we substitute into (36) the value of the depth of penetration Δ_ν (formula (23)) we get:

$$k^2_{r\nu} = \frac{1}{\left(1 + \frac{\delta'_\nu}{\sqrt{\mu' \rho'} \cdot \alpha_{\nu 1} \operatorname{th} \alpha_{\nu 1}}\right)^2 + \left(\frac{\delta'_\nu}{\sqrt{\mu' \rho'} \alpha_{\nu 1} \operatorname{th} \alpha_{\nu 1}}\right)^2}, \tag{46}$$

where $\delta'_\nu = \sqrt{\frac{\mu_0 \omega_1 \nu}{2 \rho_{Cu}}}\, \delta.$

For $\rho = \rho_{Cu} = 1.6 \times 10^{-6}$ ohm.cm., $f_1 = 50$ c/s. we get:

$$\delta'_\nu = \sqrt{\nu} \cdot \delta. \tag{47}$$

Graphs of $k^2_{r\nu}$ and $k^2_{r\nu} k^2_{\nu 1}$ as functions of $\alpha_{\nu 1}$ for various values of $\frac{\delta'_\nu}{\sqrt{\mu' \rho'}}$ are shown respectively in Figs. 1 and 3.

1959

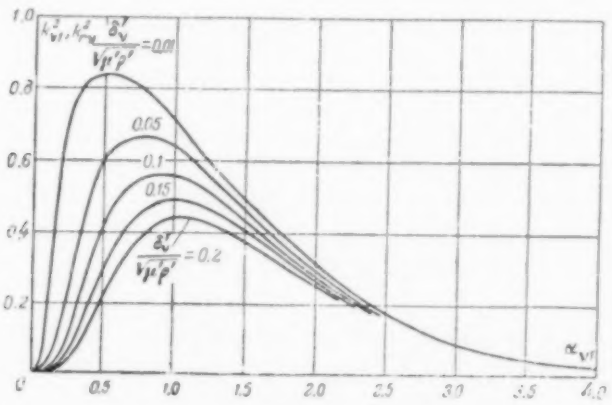

FIG. 3.

Instead of (42) we get

$$w_\nu = \frac{2\mu_0^2}{\sqrt{\pi \mu_0 \rho_{Cu}}} \frac{A_1^2 \tau^2}{\delta} \cdot f_1^{1.5} \left(\frac{k_{\nu 1}}{\nu_1}\right)^2 \varphi_{x_\nu \nu}, \tag{48}$$

where $\phi_{x\nu}$ is a function of: the space order ν_1 of the constant $x_\nu = \frac{\sqrt{\nu}\,\delta}{\sqrt{\mu' \rho'}}$ and the frequency in the rotor ν, (Fig. 4):

Taking into consideration (40) and (41) we get:

$$\varphi_{x\nu} = \frac{x_\nu}{\left(\sinh\alpha_{\nu 1} + \frac{x_\nu \operatorname{ch}\alpha_{\nu 1}}{\alpha_{\nu 1}}\right)^2 + \left(\frac{x_\nu \operatorname{ch}\alpha_{\nu 1}}{\alpha_{\nu 1}}\right)^2}. \tag{48a}$$

Taking into consideration (40) and (41) we get:

$$w_\nu = \frac{(\pi\mu_0 f_1)^{1.5}}{\sqrt{\rho_{Cu}}} \cdot \frac{F_{1m}^2}{\delta} \cdot \psi(\nu,\mu) = 2{,}17 \cdot 10^{-6} \frac{F_{1m}^2}{\delta} \cdot \psi(\nu,\mu),$$

where

$$\psi(\nu,\mu) = \left(\frac{k_{\alpha\nu 1}}{k_{\alpha 1 \nu_1}}\right)^2 \varphi_{x\nu} \sqrt{\nu}.$$

For small values of $\alpha_{\nu 1}$ it is more convenient to express the function $\phi_{x\nu}$ in this form:

$$\varphi_{x\nu} = \frac{\alpha_{\nu 1}^2}{x_\nu \cosh^2\alpha_{\nu 1}\left[1 + \left(1 + \frac{\alpha_{\nu 1} \operatorname{th}\alpha_{\nu 1}}{x_\nu}\right)^2\right]}. \tag{49}$$

As can be seen, when the values of $\sqrt{\mu'\rho'}$, $\alpha_{\nu 1}$ and δ'_ν vary, $\phi_{x\nu}$ assumes a certain maximum value $\phi_{x\nu max}$ which is determined from the equation $\partial\phi_{x\nu}/\partial x_\nu = 0$, and in this case $X_\nu = \alpha_{\nu 1}\operatorname{tank}\alpha_{\nu 1}/\sqrt{2}$. Substituting this value of X_ν into (49) we get:

$$\phi_{x\nu max} \approx 0.2 \text{ (Fig. 4).}$$

We can express the formulae for losses per unit area, (42) and (48), for small values of $\alpha_{\nu 1}$ in a more convenient form:

$$\varphi_{x\nu} = \frac{\sqrt{\mu'\rho'}\,\pi^2\delta^2\nu_1^2}{\cosh\alpha_{\nu 1}\sqrt{\nu}\,\delta\tau^2\left[1 + \left(1 + \frac{\alpha_{\nu 1}\operatorname{th}\alpha_{\nu 1}}{x_\nu}\right)^2\right]}. \tag{50}$$

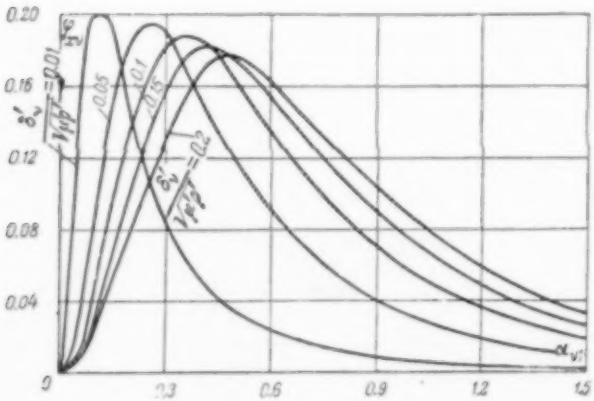

FIG. 4.

Substituting the last expression into (48) we get

$$w_\nu = \frac{1}{\sqrt{2}} \frac{(\mu_0 \omega_1)^{1.5}}{\sqrt{\rho_{Cu}}} A_1^2 C_{\mu\nu}, \tag{51}$$

where

$$C_{\mu\nu} = C'_{\mu\nu} k^2_{w\nu_1} \sqrt{\mu'\rho'} \sqrt{\nu}; \tag{51a}$$

$$C'_{\mu\nu} = \frac{1}{\cosh^2 \frac{\pi\delta\nu_1}{\tau} \left[1 + \left(1 + \frac{\alpha_{\nu 1} \operatorname{th} \alpha_{\nu 1} \sqrt{\mu'\rho'}}{\sqrt{\nu}\,\delta} \right)^2 \right]}. \tag{52}$$

The graph of $C'_{\mu\nu}$ as a function of $\alpha_{\nu 1}$ is shown in Fig. 5.

The factor $C_{\mu\nu}$ takes into account: the order of the space harmonic ν_1, the frequency ν of the harmonic induced in the rotor, the distribution factor $k_{w\nu 1}$, the properties of the rotor material ($\sqrt{\mu'\rho'}$) and the ratio $\frac{\delta}{\tau}$. Under these conditions, the losses depend on the product of the square of the linear load by $C_{\mu\nu}$ and by the constant value of the factor $1/(\mu_0 \omega_1)^{1.5-0.5}_{\rho Cu}$; Here, ω_1 is equal to $2\pi\phi_1$ for fields excited by multiphase currents, and for fields excited by d.c. currents it is equal to the angular speed of rotation of the wave of the excitation field $\omega_{rot} = 2\pi\phi_{rot}$.

1959

Summary losses will be:

$$P_{\nu R} = \frac{1}{\sqrt{2}} \frac{(\mu_0 \omega_1)^{1.5}}{\sqrt{\rho_{Cu}}} A_1^2 S_R \sum_\nu C_{\mu\nu} \approx$$
$$\approx 4{,}34 \cdot 10^{-6} A_1^2 \, 2p\tau l \sum_\nu C_{\mu\nu} \, [\mathrm{W}]. \tag{53}$$

The formulae obtained are universal for all kinds of losses due to eddy currents. In particular they allow the determination of parameters r_2 and x_2 of an unlaminated rotor for the fundamental wave when the frequency in the rotor is $\nu = s$.

In fact, neglecting the magnetizing current, we get:

$$P_\nu = \frac{(\mu_0 \omega_1)^{1.5}}{\sqrt{2\rho_{Cu}}} A_1^2 2p\tau l C_{\mu\nu} = m I_1^2 r'_2. \tag{54}$$

Hence, taking into account that $\nu = s$, $\nu_1 = 1$, $A_1 = \frac{m w_1 I_1}{p\tau}$ we find the resistance reduced to the stator:

$$r'_2 = \frac{(\mu_0 \omega_1)^{1.5} (2\rho_{Cu})^{-0.5} A_1^2 2p\tau l C_{\mu\nu}}{m I_1^2} =$$

$$= \sqrt{2}\,\frac{(\mu_0\omega_1)^{1.5}}{\sqrt{\rho_{Cu}}}\,\frac{lm\,w_1^2 k_{w1}^2 \sqrt{\mu'\rho'}\,\sqrt{s}}{p\tau\left[1+\left(1+\frac{\pi^2\delta\sqrt{\mu'\rho'}}{\tau^2\sqrt{s}}\right)^2\right]}, \tag{55}$$

and in this case $k_{w\nu 1} = k_{w1}$; $\cos h\, \alpha_{\nu 1} \approx 1$.

It was shown earlier that for $\alpha = \alpha_1$ losses per unit area are equal to the mean value of the power of the magnetic field inside the rotor body, therefore the resistance is equal to the internal reactance:

$$r_2' = r_{2i}' = X_{2i}.$$

To account for the influence of frontal parts, variation of μ with the depth of penetration and hysteresis losses [4 and 8] we introduce the factors:

$$r_2' = a_r k_\Delta r_{2i}', \quad x_2' = a_x k_\Delta x_{2i}', \tag{56}$$

where

$$a_r \approx 1.4, \quad a_x \approx 0.85.$$

Factor a_r should also be substituted for the evaluation of losses by formula (53). The influence of the frontal parts is approximately accounted for by multiplying r_{2i}' x_{2i}' by the factor

$$k_\Delta \approx 1 + \frac{2}{\pi}\cdot\frac{\tau}{l}. \tag{57}$$

The usual formula for r_2' [8] was obtained in this form:

$$r_2' = a_r k_\Delta \frac{l}{\tau p}\, 2m\,(w_1 k_{w1})^2 \sqrt{\frac{\mu_0\omega_1\rho}{2}}\cdot\sqrt{\mu' s}.$$

On comparing this formula with (55) and in connexion with (56) and (57) we see that it differs by the factor $k_{2s} = \dfrac{2}{1+\left(1+\frac{\pi^2\delta\sqrt{\mu'\rho'}}{\tau^2\sqrt{s}}\right)^2}$; for large values of s, $k_{2s} \approx 1$.

The influence of the transverse slotting of the surface can be accounted for by introducing the increased value of ρ' equal to $\rho\frac{u}{l}$, where u is the perimeter of the slotted surface along the length; l is the rotor active length.

For the longitudinal slotting or when the slots are not deep we may use the decreased value of $\rho'' = \rho'\frac{\pi D_R}{u'}$ where u' is the perimeter of the slotted surface measured on the circumference.

Formulae (42) to (53) can be used for an approximate calculation of losses on the

laminated rotor surface or on the surface of the stator circle by introducing increased values of δ'_r.

$$\rho'_r = \rho' \left(1 + \frac{\tau}{\pi \nu_1 \Delta_1} \right), \tag{58}$$

where Δ_1 – thickness of the lamina.
For calculating losses due to the ripple harmonics induced by the armature current, we may use formula (42), after summing the losses due to harmonics $\nu_1 = k \frac{Z_1}{p} + 1$; for this purpose we can assume that $k_{wv} \approx k_{wl}$ is approximately equal to unity.

For the first two harmonics ($k = \pm 1$) we may approximately assume that

$$\left(\frac{\tau}{\nu_1}\right)^4 \approx \left(\frac{\tau p}{Z_1}\right)^4 = \left(\frac{t_1}{2}\right)^4,$$

where $t_1 = \frac{2p\tau}{Z_1}$ – is the pitch of the slot. In this case, according to (42), for the two ripple harmonics of the first order we get:

$$w_{z1} = \frac{2\mu_0 A_1^2 f_1^4 / f_1^{1.5} \left(\frac{Z_1}{p}\right)^{1.5} k_{v1}^2 k_{rv}^2}{8\pi^2 \sqrt{\pi \mu_0 \rho_{Cu}}\, b^2 \sqrt{\mu' \rho'}} \quad [W/cm^3] \tag{59}$$

1959

In summing the series for all harmonics we get approximately twice the value of (59), i.e. for $\rho_{Cu} = 1.6 \times 10^{-6}$ ohm.cm; $\mu_0 = 0.4\ \pi \times 10^{-8}\ H/cm$;

$$w_z \approx 1.13 \times 10^{-8} \frac{A_1^2 f_1^4 \left(\frac{Z_1}{p}\right)^{1.5}}{b^2 \sqrt{\mu' \rho'}} \left(\frac{f_1}{50}\right)^{1.5} k_{rv}^2 k_{v1}^2. \tag{60}$$

It is seen from (60) that for the correct ratio $\frac{t_1}{\delta}$, these losses are considerably smaller than the losses due to the space harmonics.

The influence of the value $\sqrt{\mu' \rho'}$.

As can be seen from (48) there is a value of $\sqrt{\mu' \rho'}$ for which, when a frequency ν_1 a space order ν_1 and ratio $\frac{\delta}{\tau}$ are given, maximum losses occur. The value of μ' is a function of the field strength and depends on the saturation of the steel. The problem of a proper choice of μ' when calculating eddy currents has been investigated in detail in a number of works.

For purposes of approximation, we may assume a certain effective value of μ'. To calculate losses due to higher harmonics in rotors made of mild steel we may assume $\sqrt{\mu' \rho'} = 100$, because of the comparatively small field strength of these harmonics and with regard to the saturation due to the fundamental field.

For a copper surface, $\sqrt{\mu' \rho'} = 1$. For strong saturations which can occur owing to the fundamental wave at the asynchronous start, the value of $\sqrt{\mu' \rho'}$ can amount to 30 or less. The influence of $\sqrt{\mu' \rho'}$ on losses for the given values of ν_1, ν and $\frac{\delta}{\tau}$ can be determined from (49) and (50).

Application of formulae (39) to (52) for calculating losses for non-sinusoidal current.

The formulae can be supplied for any current harmonic of the order i. For this purpose it is sufficient to substitute $A_i = k_i A_1$ instead of A_1, where k_i is the ratio of the amplitude of the i^{th} current harmonic to the amplitude of the fundamental wave, and to substitute $i\nu$ instead of ν. Total losses will be found by the summation of losses due to the time harmonics of all orders.

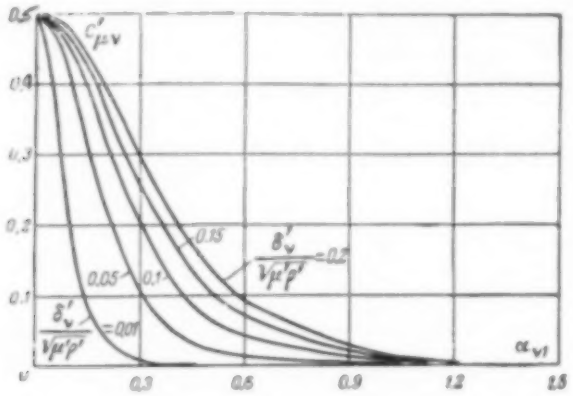

FIG. 5.

EXAMPLE

Data of the turbogenerator of 37, 500 kVA power, 3000 rev/min; $r = 137\,cm$, $t_1 = 5.09$ cm; $k_{w1} = 0.9$, $Z_1 = 54$; $A_1 = 814\ A/cm$; $\delta = 3.3 cm.$; $\gamma = 0.78$.
By formula (43) we calculate losses due to higher harmonics:

$$\Sigma w_\nu = 1.4 \cdot 4.5 \cdot 10^{-9} \frac{814^2 \cdot 137^4}{3.3^2 \cdot 100} 0.4 \cdot 10^{-4} = 0.545 \frac{W}{cM^2}.$$

The coefficient 1.4 is introduced to account for the hysteresis losses (R-4) Function $\phi = 0.4 \times 10^{-4}$ is taken from Fig. 2 with the response accounted for. By the method given in [6] neglecting hysteresis losses we get $\Sigma w_\nu = 1.48$ W/cm^3. As can be seen, the first method gives too small a value for losses, the second one – too big a value.

Losses due to the ripple harmonics for the example in question by formula (6)

and for $\alpha_\nu = 1.4$ are:

$$w_z = 1.4 \cdot 1.3 \cdot 10^{-8} \frac{814^2 \cdot 5.09^2 \cdot 0.02 \cdot 54^{1.5}}{3.3^2 \cdot 100} = 0\,051 \ \frac{W}{cM^3};$$

here $k_{r\nu}^2 k_{s1}^2 = 0{,}02$ (Fig. 3) for

$$\alpha_{s1} = \frac{\pi \nu_1 \delta}{\tau} = \frac{\pi Z_1 \delta}{p\tau} = \frac{2\pi\delta}{t_1} = \frac{2\pi \cdot 3.3}{5.09} = 4{,}06. \qquad (N)$$

As can be seen these losses in our case are considerably smaller than those losses due to higher harmonics.

Translated by S. Szymanski.

REFERENCES

1. G. Barello; *Rev. gen. elect. No. 11 (1955).*
2. T.G. Soroker and Iu. V. Mordvinov; *Sostavlenie skhem i raschet obmotochnykh koeffitsientov obmotok peremennogo toka (Circuit design and calculation of the distribution factors of a.c. windings), VEP,* No. 2 (1955).
3. A.E. Alekseyev and M.P. Kostenko; *Turbogeneratory (Turbogenerators),* Gosenergizdat (1939).
4. L.P. Neiman; *Poverkhnostnyi effekt v ferromagnitnykh telakh (Surface effect in ferromagnetic bodies),* Gosenergizdat (1949).
5. I.A. Syromiatnikov; *Rezhim raboty sinkhronnykh dvigatelei (Operational conditions of synchronous motors),* Gosenergizdat (1952).
6. R. Rikhter; *Elektricheskiye mashiny t.I i II (Electrical machines, vols. I and II),* Gosenergizdat (1936).
7. W.I. Gibbs; *JIEE,* No. 46 (1948).
8. I.M. Postnikov; *Proyektirovanie elektricheskikh mashin (Designing electrical machines),* Gostekhizdat U.S.S.R (1952).

1959

COMPENSATION OF CAPACITIVE CURRENTS IN DIFFERENTIAL PHASE CARRIER PROTECTION OF TRANSMISSION LINES *

E.D. SAPIR

All-Union Scientific and Research Institute of Electroenergetics

(Received 9 September 1957)

Capacitive susceptance in long distance transmission lines makes differential phase carrier protective gear difficult to use on transmission lines [1].

In the case of external short-circuits, this susceptance can cause at the end of the line a flow of currents which differ from one another in magnitude and direction; when two phases are in operation on the line and also when there is a short-circuit on one of the circuits of a double circuit line, a phase shift between currents can occur at the place where a protective gear is located. This can cause faulty operation of the protective gear; in order to prevent this [1 and 2], it was necessary to introduce compensation for the capacitive currents in the differential phase protective gear of the DFZ–400M type on 400 kV lines. The use of this compensation is also necessary in the protective gear of the DFZ–2 type which is widely used in the U.S.S.R. on 220 kV lines with a length over 300 km, [1].

The principles of compensation for line capacitive currents and the design of compensation devices of the DFZ–400 M and DFZ–2 types † for protection are discussed below.

General principles of compensation

In a differential phase protective gear, devices for compensating line capacitive currents can be used in the manipulator with a carrier transmitter and in the current starting device.

In the first device as a general rule, the compensation of capacitive currents of the positive and negative sequences is required, and in the second device of the negative and zero sequences.

In the current starting device, the compensation device is used in those cases when, due to capacitive susceptance during external short-circuits, currents flow at the ends of the line and these differ considerably in magnitude; under these conditions there is a possibility that the protective device will operate wrongly, being triggered at one end of the line only.

† Ing. G.G. Iakubson participated in working out several of the problems discussed in this article.

* *Elektrichestvo* No. 10, 14–20, 1958.

The possibility of the faulty operation of the protective gear under the influence of capacitive currents due to a short-circuit in one of the parallel circuits can be seen by considering Fig. 1, where the line is represented as an equivalent T-network.

When the negative sequence voltages on busbars m and n are equal at both ends of the undamaged line currents $I_{2c}/2$ * flow (I_{2c} is the line capacitive current), which correspond, so far as phase relations are concerned, to the currents flowing during a short-circuit in the protected zone. In this case the probability of the incorrect operation is particularly high in the DFZ–400M protective gear because its starting device responds at short-circuits to negative sequence voltage in the middle of the protected line and consequently, should operate in this case as a rule.

The compensating devices which are discussed below equalize currents in the half-sets of the protective gear at the line ends in magnitude and make them opposite in phase in the cases of: external short-circuits, during two-phase operation of the line and during normal symmetrical conditions of operation irrespective of the magnitude of capacitive susceptance.

In a general case, when the devices discussed are used at both ends of the line, they are connected to the voltage of that phase sequence, the capacitive current which should be compensated.

1959

In this case, the compensation current $\dot{I}_k$ is determined by the expression

$$\dot{I}_k = \dot{U} Y_k, \tag{1}$$

where U is the voltage of the corresponding phase sequence at the point where the protective gear is installed;
Y_k is the compensation device admittance.

In the case of a uniform line, which can be represented by a symmetrical equivalent T-circuit or by a symmetrical four-pole, the admittance Y_k will be equal for both half-sets of the protective gear.

Denoting by $\dot{I}_m$, $\dot{I}_n'$, $\dot{U}_n$ the currents and voltages at the line ends and taking into account that in the presence of an external short-circuit at the substation busbars n, the secondary current of the instrument current transformer of this substation is in the opposite direction to that of the primary current, we can write:

$$\dot{I}_m - \dot{U}_m Y_x = -(-\dot{I}_n - \dot{U}_n Y_x), \tag{2}$$

hence

$$Y_x = \frac{\dot{I}_m - \dot{I}_n}{\dot{U}_m + \dot{U}_n}. \tag{3}$$

* According to custom in the U.S.S.R., complex quantities are denoted by a dot over the symbol.

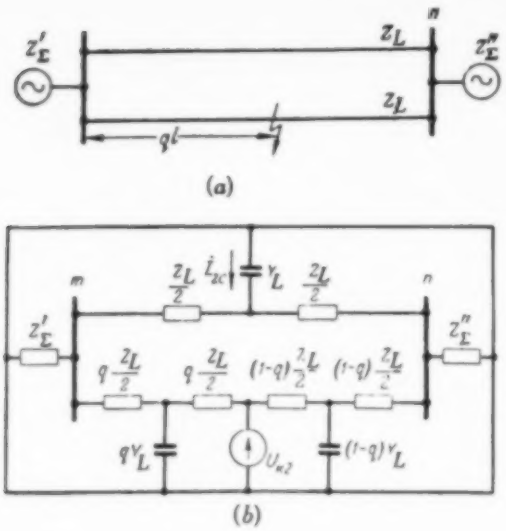

FIG. 1. Equivalent circuit (*b*) for calculating the negative sequence components during short-circuits on one of the parallel circuits (*a*). Circuit capacitive susceptances are accounted for.

Replacing the line by a four-pole and determining the relationship between voltages and currents at the output

$$(\dot{U}_m, \dot{I}_m)$$

and output

$$(\dot{U}_n, \dot{I}_n)$$

by means of expressions:

$$\left.\begin{aligned} \dot{U}_m &= A\dot{U}_n + B\dot{I}_n \\ \dot{I}_m &= C\dot{U}_n + D\dot{I}_n, \end{aligned}\right\} \qquad (4)$$

and due to the fact that for a uniform line $A = D$ and $A^2 - BC = 1$, by dividing we get the expression for the determination of Y_k through the four-pole coefficients:

$$Y_k = \frac{A-1}{B}. \qquad (5)$$

Substituting into expression (5) the values of coefficients A and B we may

assume with an accuracy sufficient for practical calculations, that

$$Y_{\pi} = j\frac{bl}{2}, \tag{6}$$

where b is the capacitive susceptance of the appropriate phase sequence per 1 km of lines;

l is the length of the line, km.

The error in this case for the 400 kV line for the positive and negative sequences is 1.2–2.3 per cent and for the zero sequence it is 2 and 6 per cent. The first figure relates to the line of 250 km length, but the second one to 500 km length. The values of susceptances b_1 for the positive and negative sequences and b_0 for the zero sequence for lines of 220 and 400 kV are given in Table 1.

TABLE 1.

Line voltage, kV	220	400
$b_1, \frac{1}{\Omega\,\text{km}}$	$2.7.10^{-6}$	$3.95.10^{-6}$
$b_0, \frac{1}{\Omega\,\text{km}}$	$1.9.10^{-6}$	$2.72.10^{-6}$

1959

The equivalent T-circuit of a non-uniform line, when, for example, the capacitance of the series compensation device is present at one end of the line, is asymmetrical Fig. 2; admittances Y_{km} and Y_{kn} at the end of this line will be different.

Assuming

$$Y_{kn} = \frac{A-1}{B}$$

and substituting this value of Y_{kn} into equation (2) we get:

$$Y_{km} = \frac{D-1}{B}.$$

Since the parameters of the elements of the equivalent T-circuit of the line are known in any case, the four-pole coefficients A, B and D, which are needed for the determination of Y_{km} and Y_{kn}, are most easily found from expressions:

$$\left.\begin{aligned} A &= 1 + Z_{1T}Y_T; \\ B &= Z_{1T} + Z_{11T} + Z_{1T}Z_{11T}Y_T; \\ D &= 1 + Z_{11T}Y_T. \end{aligned}\right\} \tag{7}$$

For determination of the parameters of the circuit in Fig. 2b, we may assume for practical calculations that $Y_T = jbl$, and for a uniform line $Z_{lT} = Z_{llT} = Z_l/2$, where Z_l is the total line impedance neglecting its capacitive susceptance.

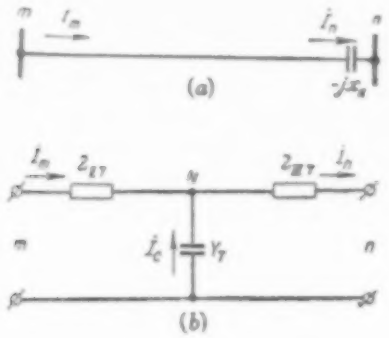

FIG. 2. Circuit of the line with series compensation (*a*) and its equivalent T-circuit (*b*)

$$Z_{lT} = \frac{Z_L}{2};\ Z_{llT} = \frac{Z_L}{2} - jx_s;\ Y_T = jbl.$$

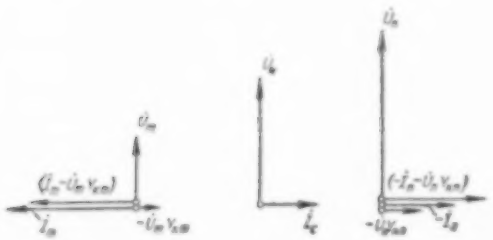

FIG. 3. Vector diagrams of the negative or zero sequences in the presence of an external short-circuit at the busbars of the substation *n* (Fig. 2a) with the compensation of the line capacitive currents accounted for

$$-(\dot{U}_m Y_{km} + \dot{U}_n Y_{kn}) = -(I_{km} + I_{kn}) = I_C;$$
$$I_m - \dot{U}_m Y_{km} = -(-I_n - \dot{U}_n Y_{kn}).$$

If we neglect the active resistance of the line, then in the case of an external short-circuit, the compensation current will in practice coincide in phase with the secondary current of the current transformers or will be of the opposite phase. In

the case of an asymmetrical short-circuit at the substation busbars *n* Fig. 2a, the negative and zero sequence components coincide in phase with the secondary current at substation *n* and are in antiphase with the current in substation *m*. The sum of currents of the compensation devices at both ends of the line is equal to the capacitive line current of the corresponding phase sequence. The vector diagrams shown in Fig. 3 illustrate this position.

It is necessary to point out that the phase shift compensation between the currents at the end of the line, when it operates in two phases, is only possible, if the voltage transformer is connected directly to the line, since in this case the symmetrical components on the busbars cannot characterize voltages applied to the line capacitive susceptance. For correct operation of the compensation devices it is necessary that, simultaneously with the cutting-off of the line phase, the voltage should be disconnected on both sides from the same phase of the voltage transformer. In this case, the voltage symmetrical components applied to the compensation devices will correspond to the voltage applied at the end of the line to its capacitive elements.

In principle, the compensation of the total capacitive current I_c can be realized only in one of the half-sets of the protective gear. However, the compensation device should be connected not only for voltage but also for the current of the corresponding phase sequence. If compensation is realized, for example, only on the side of the substation *m* Fig. 2a then the compensation current is:

$$\dot{I}_{Km} = -\dot{I}_C = \dot{U}_N Y_T = (\dot{U}_m - \dot{I}_m Z_{lT})\, Y_T \,. \qquad (8)$$

So far as the manipulator of the high-frequency transmitter is concerned, it is possible in many cases to realize the compensation only on one side of the line, neglecting the component $-I_m\, Z_{lT}\, Y_T$; this is due to the fact that for this device, unlike for the starting device, no equality of the values of the currents at the line ends is needed. The reason is that in the case considered of a short-circuit on one of the parallel circuits or during two-phase operation of the line, when only low power is transmitted and currents are comparatively small, we may neglect the component $-I_m\, Z_{lT}\, Y_T$.

Particular properties of compensation for capacitive currents of the zero sequence

The analysis carried out by the author showed that the method of compensation discussed, when applied to currents of the zero sequence, gives good results for single or two-circuit lines only for short-circuits outside the line.

For short-circuits on one of the parallel circuits, compensation is realized in many cases with considerable error due to mutual induction between circuits, and this should be taken into account for the zero sequence current starting device of the differential phase protective gear concerned.

The usual equivalent circuits [3 and 4] for calculating zero sequence currents

in the case of short-circuits on one of the circuits of a double circuit line do not give a clear idea about the influence of the mutual induction between circuits on the operation of the compensation devices. This can be done more conveniently if, assuming the short-circuit currents to be known, we replace the e.m.f. of the mutual induction by impedances, on which the voltage drops are equal in magnitude and opposite in phase to these e.m.f.

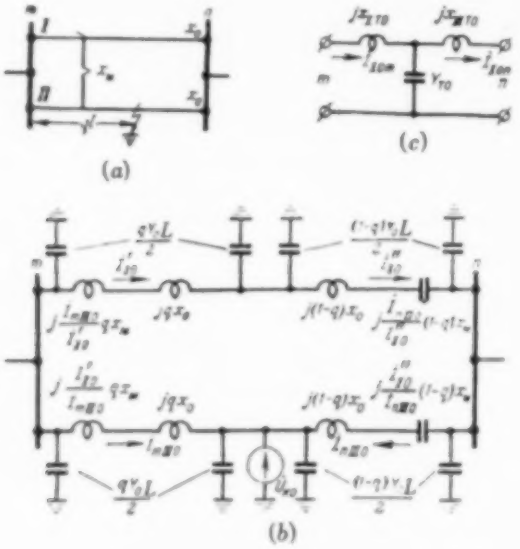

FIG. 4. Equivalent circuit (*b*) of the zero sequence of a double circuit line (*a*) for a fault on one of the circuits; the circuit explains the influence of the mutual induction between the circuits on the accuracy of the compensation of the line capacitive currents in the carrier protective gear; equivalent T-circuit of the undamaged line (*c*).

Such an equivalent circuit, in which the capacitive susceptance of the zero sequence is accounted for, is shown in Fig. 4b, where the lines to the left and right from the place of fault are replaced by an equivalent π-circuit, and active resistances of the network are neglected.

On the section to the right of the fault, where the currents in the lines flow in different directions, and the ratios of the current vectors

$$\dot{I}_{nIIo} \mid \dot{I}''_{Io} \text{ and } \dot{I}''_{IIo} \mid \dot{I}_{nIIo}$$

are negative, the e.m.f. of the mutual induction are replaced by inductive reactances.

The circuit shown in Fig. 4b is an approximate one. We can obtain a more accurate result by dividing sections of the line to the left and right from the fault into smaller sections and representing each section by an equivalent π-circuit, in which impedances are introduced that correspond to the mutual-induction e.m.f. of everyone of these sections.

However, calculations show that the circuit shown in Fig. 4b gives a result that is sufficiently accurate in practice.

In Fig. 4c an equivalent T-circuit of the unfaulted circuit *I* is shown; the circuit shown in Fig. 4b is reduced after transformations to the above equivalent circuit.

The parameters of the circuit shown in Fig. 4c are approximately equal to:

$$\left.\begin{aligned} x_{IT0} &= \frac{x_0}{2} + \frac{q}{2}(2-q)\frac{I_{mII\,0}}{I'_{1\,0}}x_M + \\ &\quad + \frac{(1-q)^2}{2}\frac{I_{nII\,0}}{I''_{1\,0}}x_M; \\ x_{IIT0} &= \frac{x_0}{2} + \frac{q^2}{2}\frac{I_{mII\,0}}{I'_{1\,0}}x_M + \frac{1-q^2}{2}\frac{I_{nII\,0}}{I''_{1\,0}}x_M; \\ Y_{T0} &= jb_0 l. \end{aligned}\right\} \tag{9}$$

In the case of a short-circuit outside a double circuit line, i.e. when $q = 1$ or $q = 0$, and when

$$\frac{I_{mII\,0}}{I'_{1\,0}} = \frac{I_{nII\,0}}{I''_{1\,0}} = 1,$$

then

$$x_{IT0} = x_{IIT0} = \frac{x_0 + x_M}{2}. \tag{10}$$

Thus, for short-circuits outside the double circuit line Fig. 4a each chain can be considered as a line, having a symmetrical equivalent T-circuit; for short-circuits on one of the chains, however, the undamaged chain can be, in a general case, represented with respect to the zero sequence currents by an asymmetrical equivalent T-circuit. Parameters X_{IT_0} and X_{IIT_0} of this equivalent circuit depend both on the location of the short-circuit and on the ratios of currents in the faulty and undamaged circuits.

In the first section of this article it was shown that for a uniform and a non-uniform line, which can be represented by a symmetrical and asymmetrical equivalent T-circuit respectively, the compensation admittances have different values. Since for a uniform line it is necessary to assume that

$$Y_{0km} = Y_{0kn} = j\frac{b_0 l}{2},$$

the exact compensation of capacitive currents of the zero sequence will be realized only for short-circuits outside the parallel circuits, but, for a fault on one of the circuits, the compensation will be realized with a certain error, which will depend on parameters X_{IT_0} and X_{IIT_0} of the circuit shown in Fig. 4c. For example, for $X_{IIT_0} = 0$, which will occur when

$$\frac{I_{nII\,0}}{I''_{1\,0}} x_M = -\frac{1}{1-q^2}\left(x_0 + q^2 \frac{I_{mII\,0}}{I'_{10}} x_M\right),$$

the coefficient D of the equivalent four-pole of the line is equal to unity, and an exact compensation will take place for $Y_{okm} = 0$ and $Y_{okn} = j\,b_0 l$. When the admittances Y_{okm} and Y_{okn} are both equal to half of the capacitive susceptance of the line zero sequence, the under-compensated capacitive current ΔI_{ok}, according to Fig. 4c for $X_{IIT_0} = 0$, will be determined by the voltage drop across the reactance X_{IT_0} and will be equal to:

$$\Delta \dot{I}_{0k} = \dot{I}_{1\,0m} j x_{1T0} j \frac{b_0 l}{2} = -\dot{I}_{1\,0m} x_{1T0} \frac{b_0 l}{2}. \qquad (11)$$

In the limit, when $I_{Iom}\, X_{IT_0} \gg (\dot{I}_{Iom} + \dot{I}_{IIom})\, X_{om\Sigma}$, where $X_{om\Sigma}$ is the resultant reactance of the system zero sequence at the side of the substation busbars m, the current ΔI_{ok} will be nearly equal to 50 per cent of the line capacitive current.

In spite of the error, the compensation device improves the conditions of operation of the current starting device of the zero sequence, because in the presence of this device currents flowing at the ends of the line in the half-sets of the differential phase protective gear will in all cases differ less from one another, than currents in the primary circuit. Because of this the compensation device of the zero sequence currents can be recommended for very long double circuit lines.

However, taking into account that the influence of the error will be less for heavy operational currents of the starting device, it is necessary, as far as possible, to increase the operational current of the starting device from the zero sequence components at the expense of sensitivity to the components of the negative sequence currents. In the protective gears DFZ–400 M and DFZ–2 the realization of the latter condition is facilitated by the fact that for asymmetrical earth faults, both these current symmetrical components are added in the relay windings of the starting device.

For example, in the protective gear type DFZ–400 M of the 400 kV transmission line Kuibyshev HEPS–Moscow it was possible to dispense with a compensation device of the zero sequence capacitive currents because it was possible to allow the operational currents of the starting device from this sequence

to be much larger than the capacitive current of the protected line.

Design of the compensation device

In Fig. 5, a block circuit diagram of the compensation device for capacitive currents in the manipulator of the high-frequency transmitter is shown; this arrangement is used in the protective gear type DFZ–400 M on the 400 kV lines. From 1956 this device is used in the protective gear type DFZ–2 on one of the 220 kV lines 250 km long for the compensation of the phase shift between the currents at the line ends, when the line operates on two phases in the single phase automatic, reclosure cycle.

The method of compensation adopted consists in applying e.m.f. $\dot{E}_{1s}$ and $\dot{E}_{2s}$ from the active-capacitive filters of the positive and negative sequence voltages to the manipulator; voltages

$$\dot{E}_{1s} \text{ and } \dot{E}_{2s}$$

are respectively equal to the corresponding components of the e.m.f.

$$\dot{E}_{1T} \text{ and } \dot{E}_{2T}$$

of the combined filter

$$\dot{I}_1 + k\,\dot{I}_2\,,$$

these components being reduced to the secondary winding of the intermediate transformer TM (Fig. 5).

When the voltage filters are connected as shown in Fig. 5 e.m.f.

$$\dot{E}_{1s}\,,\ \dot{E}_{2s}$$

are determined by the expressions [5]:

$$\left.\begin{aligned} \dot{E}_{1s} &= 1.5\sqrt{3}\dot{U}_{1b}e^{j30^\circ}n_{ky1};\\ \dot{E}_{2s} &= 1.5\sqrt{3}\dot{U}_{2c}e^{j30^\circ}n_{ky2}, \end{aligned}\right\} \tag{12}$$

where $\dot{U}_{1b}$ and $\dot{U}_{2c}$ are secondary voltages of the positive and negative sequences of phases B and C;

n_{ky1} and n_{ky2} are transformation ratios of the compensation device transformers TKY_1 and TKY_2 respectively.

Since in the combined filters of the protective gear of the DFZ–400 M and DFZ–2 types symmetrical components of phase a currents are separated, we can write [6]:

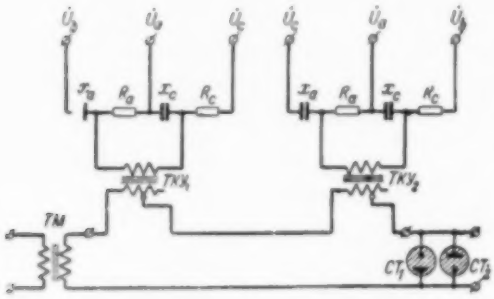

FIG. 5. Circuit showing the arrangement for compensation of the line capacitive currents for the manipulator of the carrier transmitter with the combined current filter

$$\dot{I}_1 + k\,\dot{I}_2.$$

$$\dot{E}_{1T} = \frac{2R\dot{I}_{1ka}}{k+1}\,n_{TM}; \quad E_{2T} = \frac{2kRI_{2ka}}{k+1}\,n_{TM}, \tag{13}$$

where $\dot{I}_{1ka}$ and $\dot{I}_{2ka}$ are secondary compensation currents of the positive and negative sequences;

k is the factor of the filter $\dot{I}_1 + k\dot{I}_2$;

R is the resistance of the filter $\dot{I}_1 + k\dot{I}_2$;

n_{TM} is the transformation ratio of the intermediate transformer TM.

By using these formulae it is not difficult to show that $\dot{E}_{1S}$ and $\dot{E}_{1T}$ as well as

$$\dot{E}_{2S} \text{ and } \dot{E}_{2T}$$

are respectively in phase opposition.

The unknown transformation ratios n_{ky_1} and n_{ky_2} can be determined from equalities

$$\dot{E}_{1S} = \dot{E}_{1T} \text{ and } \dot{E}_{2S} = \dot{E}_{2T},$$

if we take into account that

$$\left|\frac{\dot{I}_{1ka}}{\dot{U}_{1b}e^{j30^\circ}}\right| = \left|\frac{\dot{I}_{2ka}}{\dot{U}_{2c}e^{j30^\circ}}\right| = y_k,$$

where y_k – admittance factor of the compensation of the positive and negative sequences, which is reduced to the secondary side of the current and voltage instrument transformers.

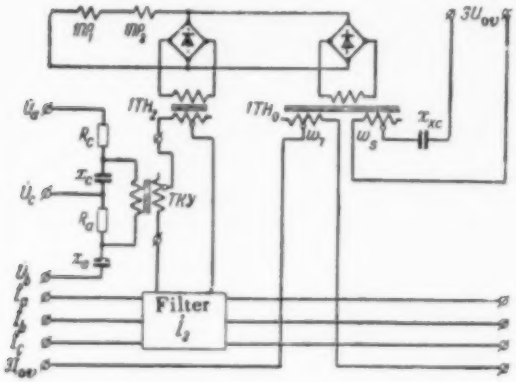

FIG. 6. Principal circuit of a starting device for negative and zero sequence current of the protective gear DFZ–2 with compensation devices for line capacitive currents.

1959

Fig. 6 shows the principal circuit of the starting device of the negative and zero sequences of the protective gear type DFZ–2 with the arrangements for compensation of capacitive currents. The use of these arrangements, as was stated earlier, can prove necessary when the protective gear is used on 220 kV lines more than 300 km long.

The arrangement for compensation of the negative sequence capacitive current in the starting device of the DFZ–2 gear is similar to the device for compensation of the current of the same sequence in the manipulator of the high-frequency transmitter. The connexion of the voltage circuits to the filter of the compensation device according to Fig. 6, is made, however, in such a way, that the voltage vector at the output has the same direction as the vector

$$\dot{U}_{2b}\, e^{j30^\circ}.$$

Such a connexion is made because the negative sequence filter of the starting device of the DFZ–2 gear, unlike the filter of the manipulator of the carrier transmitter, separates the phase c current.

A distinguishing feature of the compensation of the negative sequence current in the starting device is the connexion of the secondary winding of the intermediate transformer to the primary winding of the saturation transformer $1TH_2$. This connexion allows the elimination of the influence of impedance of the magnetizing branch of the transformer $1TH_2$ on the correctness of the compensation. This

follows from the equivalent circuit of the starting device if we take into account that the impedance of the magnetizing branch of the transformer $1TH_1$, even before its saturation, is quite commensurable with the load impedance.

The compensation of the zero sequence capacitive currents in the starting device of the DFZ–2 gear can be realized by means of a winding w_s shown in Fig. 6 which should be added to the transformer $1TH_0$.

This winding is connected through a capacitor to the zero sequence voltage.

The ratio of the number of turns of the windings W_T and W_s of the transformer ITH_0 is chosen on the basis of the condition that the m.m.f. of the winding W_T, induced by the compensated component of the line capacitive current is equal in magnitude to the m.m.f. of the winding W_s and opposite in phase, i.e. the following equality holds good:

$$3\dot{I}_{0ks}w_T = j\frac{3\dot{U}_{0v}}{x_{KC}}w_s,$$

where $\dot{I}_{0kv}$ and $\dot{U}_{0v}$ is the secondary compensation current and the zero sequence voltage;

X_{KC} is the capacitor reactance in the winding circuit.

Taking into consideration that

$$\left|\frac{\dot{I}_{0v}}{j\dot{U}_{0s}}\right| = y_{0k},$$

where Y_{0k} is the susceptance factor of the zero sequence compensation, reduced to the secondary side of the instrument current and voltage transformer; we get an expression for W_s:

$$w_s = y_{0k}x_{KC}w_T. \tag{14}$$

Conclusions

1. By using special devices for compensating capacitive currents in differential phase carrier protective gear, we can eliminate the influence of these currents on the correct working of the gear.

2. Due to the influence of mutual induction the compensation of the zero sequence capacitive currents during a fault on one of the parallel circuit of the line can be realized only with a substantial error. Nevertheless, the use of compensation devices for currents of this sequence is expedient on double circuit lines, since the presence of these devices improves conditions for the working of protective gear in all cases.

3. When compensation devices are used at both ends of the line they are connected only to the voltage of that phase sequence, the capacitive current of which they have to compensate; this ensures sufficient simplicity for the circuits of the devices used.

4. When the compensation of the total line capacitive current takes place at only one end of the line, the compensation device should be connected to both the voltage and current of the corresponding phase sequence. However, in the manipulator in the carrier transmitter, in this case, as a rule, the device could be connected only to the voltage.

5. Experience in the working of compensation devices for line capacitive currents shows that their application satisfactorily solves the problem of the use of differential phase carrier protective gear on 220 and 400 kV lines of very great length.

Translated by S. Szymanski

REFERENCES

1. E.D. Sapir, *Elektrichestvo* No. 3 (1956).
2. V.M. Yermolenko and S.Ia. Petrov, *Kompensatsia vliianiia yemkostnoi provodimosti linii elektroperedachi. (Compensation of the influence of the capacitive susceptance of transmission lines).* Biulletin' Teploelektroproyekta, No. 2 (1955).
3. S.A. Ulianov, *Korotkiye zamykaniia v elektricheskikh sistemakh. (Short-circuits in electrical systems),* Gosenergoizdat (1952).
4. K.F. Wagner and R.D. Evans, *Metod simmetricheskikh sostavhiaiushchikh. (Method of symmetrical components).* ONTI (1936).
5. A.M. Fedoseyev, *Releinaia zashchita elektricheskikh sistem. (Relay protection of electrical systems).* Gosenergoizdat (1952).
6. *Rukovodiashchiye ukazaniia po naladke, proverke i ekspluatatsii releinoi chasti differentsialno – faznoi vysokochastotnoi zashchity* tipa DFZ–2. *(Instructions for adjusting, verifying and operating the relay part of the differential phase carrier protective gear of the DFZ–2 type).* Gosenergoizdat (1957).

1959

THE PROBLEM OF A CIRCUIT FOR A RECTIFYING SEMICONDUCTOR SET ON ELECTRIC ROLLING STOCK OF A.C. SINGLE-PHASE – D.C. TRACTION*

V.A. GOLOVANOV

Moscow

(Received 25 April 1958)

The progress in constructing powerful semiconductor rectifiers (germanium, silicon) made during recent years, permits their use on electric rolling stock for a single-phase a.c.–d.c. traction; this problem can be considered now as a practical problem. Besides many well known advantages [1] the use of semiconductor rectifiers on rolling stock opens up the possibility of choosing a more rational circuit for the rectifying set, which enables the weight of the main transformer and the power losses to be reduced. In this article, problems connected with this property of rolling stock equipped with a semiconductor rectifying set are discussed. The importance of making these problems clear is due to the fact that the choice of this or that solution leads to substantially different technical requirements for the performance of a semiconductor rectifier, and the choice determines the construction of the electrical equipment of the rolling stock and its power indices.

The choice of the rectifying circuit on rolling stock with static rectifiers is determined in the final result by the value of the efficiency and the possibility of effective cooling of the rectifiers.

We shall discuss in detail the problem of efficiency and consider the efficiency of a rectifying set neglecting transformer losses and power expenditure for its own needs. We shall first consider the well known circuits of a single-phase rectifying set with a centre tap in the transformer secondary circuit, and the bridge circuit.

It is known that the total number of rectifiers in a rectifying set for an m-phase network, when each arm contains a parallel branches, each branch having s series connected rectifiers, is given by the expression

* *Elektrichestvo* No. 10, 53-57, 1958.

$$N = masq,$$

where $q = 1$, or $q = 2$ depending upon whether a starpoint or a bridge circuit are used respectively.

The efficiency of any rectifying set can be expressed by the following approximate expression:

$$\eta = \frac{U_d I_d}{U_a I_d + N U_a \frac{I_d}{ma}} = \frac{1}{1 + sq \frac{U_a}{U_d}},$$

where U_d is the rectified voltage; and U_a the direct voltage drop in a rectifying element.

This expression shows that in each rectifying set connected by a bridge-circuit or the star point method, the efficiency drops with decreasing U_d. Such a drop in efficiency occurs, for example, when an electric locomotive or an electric multiple-unit is moving at lower step speeds at a voltage $U_d < U_{dr}$. Only at higher step speeds when $U_d = U_{dr}$ does the efficiency of the set reach its possible maximum value for a given circuit. The above is valid both for circuits with semiconductor and mercury rectifiers.

1959

If we compare circuits with a star point and a bridge circuit we find that with mercury rectifiers the efficiency is higher in the first case. This is due to the fact that a mercury rectifier can withstand a sufficiently high reverse voltage U_o. In practice, in mercury rectifying circuits for any arbitrary value of U_{dr}, only one rectifier is connected into an arm, ($s = 1$).

The situation is different in the case of a semiconductor rectifying set. Due to a relatively low value of U_o of an element, it is necessary to connect into an arm as many elements as are required in accordance with the reverse arm voltage.

In the case of a bridge circuit, this voltage value is half as large as that with a star point circuit, but the number of arms is double. As a result, for a semiconductor set, the value of sq remains constant when we pass from one circuit to another and, consequently, the efficiency of a semiconductor rectifying set does not depend on the type of circuit used. Therefore, the only expedient circuit for semiconductor rectifiers is the bridge circuit.

The method of connecting of germanium and silicon rectifiers in the widely known circuits has two other specific disadvantages.

The series connexion in an arm of several rectifiers requires a parallel connexion of an ohmic resistance to every rectifier, or, as an alternative, it leads to the increase in the number of the elements in the arm by one or two rectifiers, thus increasing the reserve of strength of the set. Both measures lower the efficiency of the set. Moreover, the failure of a certain number of elements in

such a set leads to the breakdown of the whole set.

The above disadvantages can be excluded by using rectifying set circuits designed on new principles, compared with those used for circuits devised previously. Here, use is made of the specific properties of semiconductor rectifiers and the special operational conditions of a rectifying set on rolling stock. Fig.1 shows this principle circuit, [2].

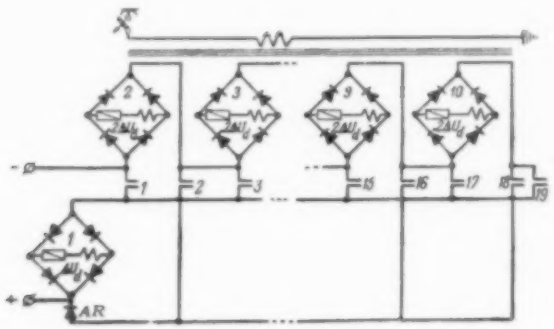

FIG.1 Circuit of a semiconductor rectifying set based on the principle of dividing it into separate sections.

The circuit is obtained by dividing the main transformer secondary winding into a number of independent main sections with a comparatively low voltage $2\Delta U$, and one auxiliary section with a voltage[1] ΔU. The magnitude of ΔU is determined by the voltage jump which is admissible when speed is changed from one step to another. A bridge circuit is connected to every transformer section, and into each arm of the bridge circuit one element is inserted. Every transformer section together with the bridge connected to it forms a rectifying section with a rectified voltage $2\Delta U_d$.

Collecting the number of such rectifying sections into a successive circuit we can increase or decrease by steps the voltage applied to the traction motors. The transition from one step to another is done by means of a special changeover switch, which consists of an additional rectifier AR and an additional rectifying section with a voltage of the order ΔU_d. The closing of each contactor shown in the circuit, Fig. 1, corresponds to a definite speed step. Nineteen contactors ensure nineteen speed steps. On transition from one step to another the two adjacent contactors are always closed: 1 and 2, or 2 and 3 or 3 and 4 and so on.

[1] The number of main sections can be arbitrary and is determined by the number of speed steps necessary for the rolling stock.

The circuit shown in Fig. 1 has several valuable advantages by which it differs favourably from the known rectifying circuits. This circuit does not require the connexion of shunting ohmic resistances since the reverse voltage of every rectifier is fixed. During the process of starting, the efficiency of the rectifying set remains approximately constant for all steps. Thus, all speed steps in this circuit can be used for continuous running. The circuit allows the same rectifying set to feed the auxiliary circuits with practically any arbitrary direct voltage, independent of the voltage applied to the traction motors. The reliability is increased since the failure of a certain number of elements causes the blowing of a fuze in the corresponding sections, and the total rectified voltage drops by a small amount equal to the section voltage. This circuit uses a method of rectified voltage regulation which basically differs from methods used in the known circuits; due to this, the circuit has no intermediate reactors and facilitates the operation of the switchgear.

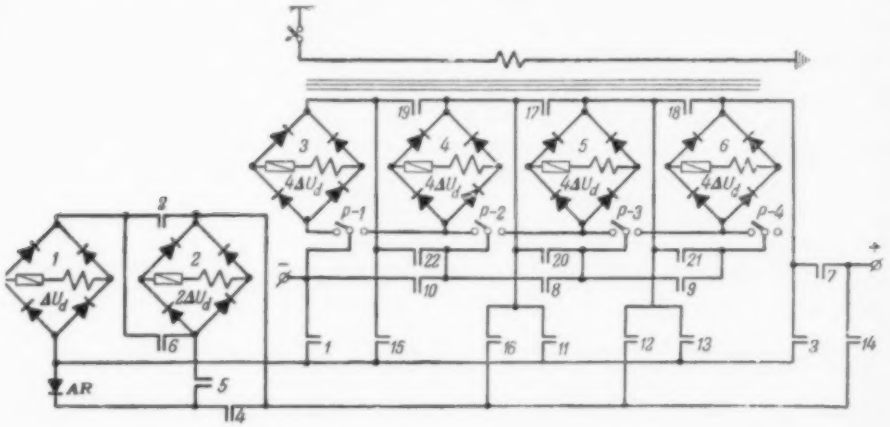

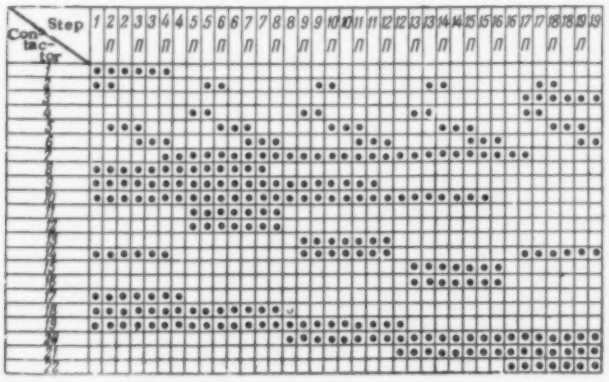

FIG.2 Circuit of a semiconductor rectifying set which allows a parallel-series switching-over of sections during the process of the rectified voltage regulation.

However, the use of semiconductor rectifiers gives us the possibility of devising a still better circuit for a rectifying set (Fig. 2), based on the method[1] proposed by the author; this method consists in the parallel-series switching-over of the rectifying set sections during the process of voltage regulation [3].

As in the circuit in Fig. 1, in this method of voltage regulation, the transformer secondary winding is subdivided into several main sections with the voltage $4\Delta U$. But, instead of one we have two auxiliary sections: one with a voltage $2\Delta U$ and another with a voltage ΔU. The number of main sections depends on the number of speed steps required.

The circuit operates in the following way. The first three steps are obtained by a combined connexion of the auxiliary sections 1 and 2 by means of contactors 1, 14, 2, 4, 5 and 6. By closing contactors 1, 14 and 2 we get the first step with a rectified voltage ΔU_d. By connecting contactor 5 of section 1 in parallel, section 2 is supplied with a voltage greater than ΔU_d, and the load from section 1 is transferred to section 2. Thus, the circuit of stage 2 is obtained with the rectified voltage $2\Delta U_d$. Then sections 1 and 2 are connected in series by closing contactor 6, and the circuit of stage 3 is formed with the voltage $3\Delta U_d$. For switching over to stage 4, the whole set of the parallel connected main sections 3-6 is switched to the parallel series connected sections 1 and 2; this is done by closing contactor 7, and sections 3-6 take over the total load. In this way the fourth stage circuit is connected up and the rectified voltage is $4\Delta U_d$. The switching over to stage 5 begins with connecting the rectifier AR in parallel to contactor 17 by means of contactors 4, 11 and 12; after this it is possible to switch off contactor 17.

By analogy with the procedure for the first three steps, contactors 2, 5 and 6 are operated. As a result, circuits for steps five, six and seven are connected up with the rectified voltages $5\Delta U_d$, $6\Delta U_d$, $7\Delta U_d$; in this case sections 5-6 are left idle, and the whole load is borne by sections 3-4 connected in parallel. Further switching over is performed in a similar way to that already described.

The throw-over single pole disconnectors P_1 to P_4 normally remain in the position shown on the diagram. If it is required for any reason whatsoever to switch off one of the main sections, then the disconnector of the corresponding section is set in a position opposite to that shown on the diagram, and the circuit continues its operation without change. True, in this case the total rectified voltage decreases by $4\Delta U_d$.

The circuit, in which series-parallel switching over of sections is used, has, – in comparison with circuits used up to this time, – all the advantages already enumerated for the circuit in Fig. 1. Moreover, it offers certain additional advantages.

[1] Author's certificate No. 108782 of 13 April 1957.

Semiconductor rectifiers are characterized by their small over-load capacity. This property contrasts with the conditions of electric rolling stock operation, which is characterized by considerable abrupt load changes, which last 0.5-15 min; these load variations occur frequently on electric multiple-units.

Considerable difficulties arise in this respect in the case of rolling stock fitted with semiconductor rectifiers, ordinary rectifying circuits, and to some extent the circuits shown in Fig. 1.

Due to the parallel connexion of the sections, the circuit proposed by the author eases the operating conditions for the semiconductor rectifying set at the time when they are most difficult; namely, during the starting period.

The drop in the value of the rectifier current, in comparison with the rated current, which is due to the parallel connexion of sections, results in a smaller voltage drop in the rectifier, and consequently reduces losses. This means that in a set designed according to the circuit shown in Fig. 2, the efficiency for the lower voltage steps will be even slightly greater than that for the higher steps. This property of the circuit makes it particularly suitable for electric rolling stock multiple-units and for electric shunting locomotives. Finally, the circuit ensures a fuller use of a rectifying set since for all speed steps the greater part of its equipment is utilized.

1959

The choice of a circuit for a rectifying set is closely connected with the choice and parameters of semiconductor rectifiers. In the case of silicon rectifiers, which can withstand a comparatively high admissible reverse voltage, the use of the circuit shown in Fig. 3 is recommended. If we choose germanium rectifiers with a low value of reverse voltage, we have to alter somewhat the circuit in Fig. 2 in such a way that, instead of each of the main sections, two permanently series connected sections are used with a rectified voltage of the order $2\Delta U_d$. The properties of the circuits described show that on electric rolling stock, rectifying elements with a rather small admissible reverse voltage can be used. At the same time it is necessary to bear in mind that, in order to keep the efficiency of the set within the admissible limits, we cannot assume the value of the rectifier reverse voltage to be arbitrarily small.

Thus, the problem of constructing a reliable and economic semiconductor rectifying element for traction purposes is closely connected with the choice of circuit for the rectifying set.

Conclusions

1. The use of semiconductor rectifying sets offers an effective means for improvement of rolling stock for a.c. single-phase – d.c. traction systems.

2. The most rational circuit from the point of view of design and economy is a circuit, which allows parallel-series switching over of sections during the

process of rectified voltage regulation.

3. This circuit enables us to lower the requirements formulated for semiconductor rectifiers designed for operation on electric rolling stock.

Appendix

Let us consider a possible example of the use of the circuit proposed. For comparison, we take a circuit of an English electric multiple-unit with germanium rectifiers (Fig. 3), [4]. In this circuit $m = 2$, $a = 6$; $s = 50$; $q = 1$; $U_{dr} = 1500$ V; $I_{dr} = 500$ A. The circuit allows 21 speed steps, of which 1, 5, 9, 13, 17, 21 are steps which can be used for continuous running due to the symmetrical connexion of intermediate reactors in these steps. Assuming that the change-over from one step to another occurs when the rectified voltage varies by equal jumps of ΔU_d, let us consider the variation of efficiency in steps for a constant value of the rectified current I_{dr} in accordance with the expression:

$$\eta_n = \frac{1}{1 + sq \dfrac{U_a}{U_{dr}} \cdot \dfrac{21}{n}},$$

where n is the number of the steps.

In accordance with a typical volt-ampere characteristic of a germanium rectifying element [1] we assume for the rated conditions that $U_a = 0.6$ V. The results of calculations of the efficiency are given in Fig. 4.

If we assume that during the period of starting the electric coach, the current consumed by the traction motors is double their steady-state current, and the start itself lasts about 25 sec, then in the circuit in Fig. 3 each element of the rectifying set has to withstand a double load for this interval of time.

If we adjust our circuit shown in Fig. 2 to the operating conditions for the English electric multiple-unit, this will bring about the following results. Circuit on Fig. 2 should ensure under-rated conditions for higher speed steps, the voltage $U_{dr} = 1500$ V, and, consequently, the rated rectified voltage in every one of the main sections will be 316 V, and in the two auxiliary sections 158 and 78 V. Obviously, the reverse voltages per single element should be equal in both circuits 3 and 2. Let us find the order of magnitude of this value. It is quite reasonable to assume that in the circuit Fig. 3 the no-load voltage on the phase of the transformer secondary winding is approximately 2000 V. Therefore, the reverse voltage supplied to the rectifying element in the circuit is approximately 120 V. Consequently, we have to connect into the arm of the main section bridge (Fig. 2) five elements in series, and into the arms of the auxiliary sections three and two elements respectively. The number of parallel branches in each arm of all the sections is six, as in the circuit in Fig. 3.

The efficiency of the rectifying set, designed according to the circuit in Fig. 2, was calculated by the formula:

$$\eta_n = \frac{1}{1 + \frac{q}{U_{dn}} \sum U_{ai}\, s_i},$$

where U_{dn} is the rectified voltage of the n^{th} step; i the number of sections in the rectifying set.

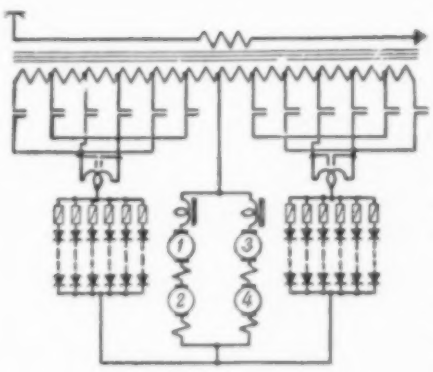

FIG.3 The principal power circuit of an English rolling stock multiple-unit with germanium rectifiers.

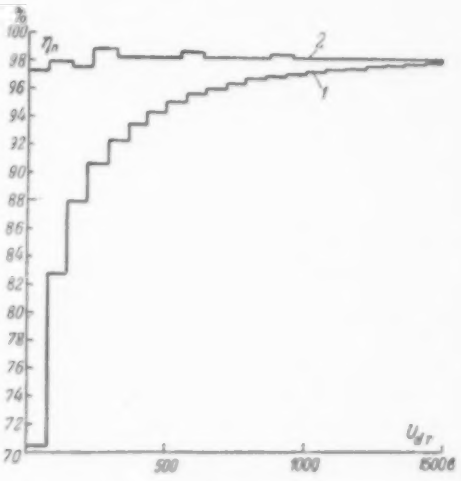

FIG.4 Efficiency of a rectifying set as a function of the rectified voltage. 1 - diagram of an English electric rolling stock multiple-unit with germanium rectifiers, 2 - diagram of parallel series switching-over of sections of a rectifying set.

For the calculation, it was taken into account that U_a for elements of parallel connected sections decreases according to the volt-ampere characteristic, [1]. The results of the calculations are shown in Fig. 4.

By examining the variations of the current throwing in the separate sections of the circuit of Fig. 2 on starting, we arrive at its values shown in the table. From this we see that the current is twice the rated value in section 5 – starting from step nine, in section 6 – starting from step twelve, in section 3 – starting from step thirteen and in section 4 – starting from step sixteen. The current throwing lasts for a much shorter time, and, consequently, starting conditions are made

easier for the whole set.

TABLE 1. Ratio of the section load of a rectifying set at the start I_{start}/I_{dn}

Sections	Steps																	
	1	2	3	4	5	6	7	8	9	10	11	12	13	14	15	16	17	18	19
1	2	—	2	—	2	—	2	—	2	—	2	—	2	—	2	—	2	—	2
2	—	2	2	—	—	2	2	—	—	2	2	—	—	2	2	—	—	2	2
3	—	—	—	0,5	1	1	1	1	1	1	1	1	2	2	2	2	2	2	2
4	—	—	—	0,5	1	1	1	1	1	1	1	1	—	—	—	2	2	2	2
5	—	—	—	0,5	—	—	—	1	2	2	2	2	2	2	2	2	2	2	2
6	—	—	—	0,5	—	—	—	1	—	—	—	2	2	2	2	2	2	2	2

Translated by S. Szymanski

REFERENCES

1. V.A. Golovanov; Primeneniye poluprovodnikovykh vypriamite-lei v ustroistvakh elektrichskoi tiagi (Use of semiconductor rectifiers in electric traction installations). *Biulleten tekhniko-ekonomicheskoi informatsii*, No. 4, Transzheldorizdat (1957).
2. V.E. Rozenfel'd and E.V. Chebotarev; Ustroistvo dlia Bezreostatnogo regulirovaniia napria-zheniia pitaniia tiagovykh dvigatelei (Device for voltage regulation without a rheostat for feeding traction motors). *Biulleten izobretenii*, No. 5 (1954).
3. V.A. Golovanov; Sposob pere-kliucheniia sektsii poluprovodnikovogo vypriamitelnogo agregata na elektropodvizhnom sostave odnofazno-postoiannogo toka (The method of switching-over of sections of a semiconductor rectifying set on electric rolling stock of an a.c. single-phase – d.c. traction system). *Biulleten izobretenii*, No. 10 (1957).
4. J.D. Watt; Redresseurs au germanium pour le service de la traction. Nouveau mode de conversion de l'energie mis au point par la BTH a l'usage des chemin de fer electrifies. *Bull. de l'Association Internationale du Congres des Chemins de fer. La traction Electrique dans les chemins de fer*, IX, No. 2 (1958).

PROBLEMS OF LIQUID COOLING IN ELECTRICAL EQUIPMENT*

O.B. BRON and D.S. ITENBERG

Leningrad

(Received 30 January 1958)

Fundamental considerations

Nowadays one cannot imagine an electrical machine without artificial cooling. In most machines this is an air ventilation system. Large turbogenerators are, however, water-cooled, the water being passed through the hollow conductors of the windings.

Electrical switchgear is a different matter. As a rule forced cooling is not applied here, the method being limited to the natural air cooling of the conductors. This can be explained by the complex design of the apparatus, by the large dimensions of the distribution gear and also by the fact that the loss of power in the equipment most commonly used is relatively small, and it is possible to make reliable and simple apparatus of acceptable size with natural air cooling. However, in recent years, a demand has grown for special apparatus which required us to use water cooling for the conductors.

First, it is necessary to mention high-frequency contactors. The development of high-frequency tempering of machine elements and the melting of metal needed the automation of processes; this can be achieved by using contactor devices.

Electromagnetic contactors were needed in systems for currents up to 1000 A, for voltages up to 1600 V, and for frequencies up to 10 kc/s. The commonly used contactors cannot satisfy these conditions.

It was necessary to work out a new, special series of high-frequency contactors. The question of cooling the live parts presented the major difficulty during the design. With natural cooling the presence of the surface effect in case of large currents and frequencies up to 10 kc/s made it necessary to build the apparatus with very large dimensions.

The application of water cooling resulted in a remarkable reduction in size and in the amount of non-ferrous metals used in high-frequency contactors, as well as making possible the replacement of a whole series of contactors designed for

* *Elektrichestvo* No.10. 65-70 1958.

current ratings of from 100 to 1000 A by a single piece of apparatus. We found that the dimensions of a water-cooled high-frequency contactor for currents up to 1000 A are smaller than for a contactor with natural air cooling for 100 A.

Water cooling was first used for small circuit-breakers with current ratings from 6 to 25 kA for ship equipment., for the chemical industry, and in several other fields.

The use of water cooling enabled the current ratings to be increased 4 to 5 times compared with naturally air-cooled equipment.

Very small alterations were required here in the design of the existing systems.

Finally, water cooling was used for making high-speed automatic mechanisms. This permitted a considerable decrease in the mass of the moving conductors, and consequently shortened the duration of the tripping processes, which essentially improves the characteristics of these devices.

The application of water cooling makes it possible to build high-speed automatic machines for currents of 5 to 10 kΩ, which was difficult and sometimes impossible by using natural air cooling.

The results of the work carried out in the factory "Elektrosila" in connexion with the water cooling of electrical equipment are published in this article.

Water and air cooling

Different views have been expressed on the artificial cooling of electrical equipment. Those who oppose water cooling consider that:

1. Water cooling results in considerable design and operating difficulties;

2. In the tripped position of the equipment there is imperfect insulation between the live conductors, since the open contacts are inter-connected by a column of cooling water;

3. The live conductors are connected to earth by the cooling water;

4. In the case of direct current, leakage through the cooling water causes an electrolytic transfer of metal from one part to another, which can put the apparatus out of order.

5. Condensation might appear when cold water is passed to the conductors. The falling drops of water can cause sparking between the conductors.

6. The water pipes can block up and then the water cooling system fails.

The opponents of liquid-cooled equipment draw the conclusion from these considerations that water cooling should not be used.

Undoubtedly, the application of liquid cooling makes the design and operation of equipment more complicated, and it should be employed only where it promises considerable advantages. In a number of cases examined below these

advantages are so great that they compensate both for the complication in operation and for necessary alterations in design.

The considerations of leakage of current through water, the electrolytic corrosion of parts of the equipment, and the imperfect insulation of the devices when water-cooling is used are greatly minimized to-day. There are simple and reliable methods of increasing the specific resistance of the water so that it can be considered practically as a dielectric (for details see below).

The application of a closed water-cooling water system, similar to that used in mercury rectifiers, removes all objections in connexion with the sweating and blocking of the pipes.

When artificial cooling of electrical equipment is chosen, a comparison should be made between water and air cooling [2].

Air at speed of 50 m/sec can remove 140 cal of heat from a surface of 1 m^2 during one hour if the temperature difference is $\Delta r = 1$ °C. Water at a speed of 2 m/sec subjected to the same conditions can remove 20 times more heat, i.e. 2800 cal.

Through an opening 1 cm^2 during one hour at a temperature difference of $\Delta r = 1$ °C it is possible to remove:

With air at a speed of v = 50 m/sec – 5 cal

With water at a speed of v = 2 m/sec – 700 cal

The heat capacity of water is 3500 times larger than the heat capacity of a monatomic gas atmospheric pressure.

Comparing water and oil cooling, it is necessary to mention the following:

The heat capacity of water is 2.5 times larger than the heat capacity of transformer oil. In the case of water cooling as opposed to oil cooling there is no danger of fire.

The viscosity of oil in the range up to 50 °C is greater than the viscosity of water a few dozens of times. The circulation of oil coolant therefore requires larger diameter tubes and a higher pressure head than water circulation.

All the previous points suggest the application of water cooling. A disadvantage of this method is the low specific resistance of tap water. This suggested the use of distilled water in a closed cooling cycle, so that the distilled water could be cooled by the tap water in a special heat exchanger.

The specific resistance of freshly distilled water is almost 40 times greater than the resistance of natural (ground) water. However, the resistance of distilled water decreases in service conditions. The water is contaminated by substances set free by the rubberized hoses, greasy bearings, stuffing boxes, pumps and so on. In given service conditions[3] after three months, the specific resistance of distilled water falls from 60 to 10 kΩ cm. But even with this decrease in specific resistance, distilled water enables us to obtain reliable

operation of cooling systems for electrical equipment.

Let us determine the magnitude of the leakage currents through the water, if specific resistance is $\rho = 10$ kΩcm. When the contacts of the apparatus are open, and at a voltage of 500 V, the diameter of the water column is 10 mm, its length is 250 mm and the leakage current will be 1.6 mA. Such a leakage does not have practical importance, and is not a danger to life. According to the rules for accident prevention, the permissible leakage current through insulations is from 20 to 50 mA; i.e. dozens of times greater than that obtained by us.

A leakage current to earth through a column of water in a pipe 10 mm in diameter and 1500 mm long is 0.27 mA; that is it is negligibly small.

Water as dielectric

The above considerations and calculations provided every reason for relying on water cooling, after taking into account the objections mentioned. However, the situation improved due to the fact that we turned to processes developed by the chemical industry for the refining of water.

The conduction of all electrolytes, including water, is dependant on the existence of ions in them. At present, there are filters capable of absorbing the ions [5]. In the simplest cases they are a device schematically shown in Fig. 1, actually used for our experiments. Insulator tube (1) is a cation filter filled with active sulphocarbon capable of holding the positive ions. Tube (2) filled with phenolformaldehide, an amino-resin, or mark EDZ-10P resin, is an anion filter which holds back the negative ions.

Fig. 1. Schematic diagram of the filter equipment for the chemical refining of water.
1. Cationite (filled with sulfocarbon).
2. Anionite (filled with resin).

After passing the water of the Leningrad water system through the anion and cation filters, its specific resistance was increased 100 times, and reached 10^4 Ω cm. According to the technical literature, it can be increased to 2.5×10^6 Ω cm. For comparison, we show the values of the usual specific resistance of water from different sources in kΩcm.

Tap water from Moscow	3.8
Tap water from Leningrad	10
Distilled water from distillery (freshly prepared)	60
Distilled water after three months use	10
Tap water from Leningrad after chemical refining.	1000

Ion filters in the flow system of water cooling virtually make the water a

dielectric, and eliminate all problems of leakage of the current through the water, of electrolysis of the conductors, of the reduction of the resistance of the insulation and so on.

The application of chemically-cleaned water makes it possible to decrease a hundredfold the leakage current in the water, considered above, and to bring it down to a negligible value of 16μ A.

The resistance of the water column in this case reaches 31 MΩ.

High-frequency contactors

With development of high-frequency melting and tempering of metals even before the war, the problem of manufacturing contactors capable of operating at frequencies of up to 3 kc/s, with voltages of 500 to 1500 V and currents of 100 to 1000 A. It was possible to satisfy these requirements only by developing a new series of high-frequency contactors.

Considerable difficulties were caused by the dimensions of the conductors of the contactors which were greatly heated owing to surface effect. It was possible to use several relays connected in parallel and to greatly increase the dimensions of the conductors in this way. This led to a general increase in the size of the contactors and to the irrational use of non-ferrous metals, since copper was practically not used in the contacts and busbars. It was possible to achieve a notable decrease in the dimensions of the equipment and in the quantity of non-ferrous metals by water-cooled hollow conductors and contacts.

1959

Fig. 2 shows a photograph and a schematic diagram of a contactor of a disconnector (without arc extinction equipment).

Here the inmovable contacts 1, and the moving contact 2 are made of hollow bus-bars of rectangular cross-section. The pulling magnet system 3 can close and open the contacts. The water flows along the pipes 4, 5, 6 and 7, passes through the contacts, cools them, and leaves the system. In the whole mechanism only pipes 5 and 6 which supply the water to the moving contact have to be flexible.

The dimensions of the contactor described are suitable for 100 A. However, using water cooling, they can operate reliably at currents of over 1000 A, and a frequency of 10 kc/s. The impedance of the contacts together with the resistance of all the live parts is 36×10^{-4} Ω. In case of a current of 1000 A, the power loss is 360 W. In order to dissipate this energy on overheaters 20 °C it is necessary to use 15 l/hr of water.

The contactor described has no arc extinction equipment, and it can therefore only be operated as a disconnector. In normal operations, when the contactor has to switch off currents at a high frequency, it is equipped with an arc extinction system as shown in Fig. 3. In this system the brass plates of the arc extinction grid (1) are mounted in the narrow slot of an asbestos-cement chamber (2). In the form of a nozzle the chamber is closed on all sides, except for the narrow slot,

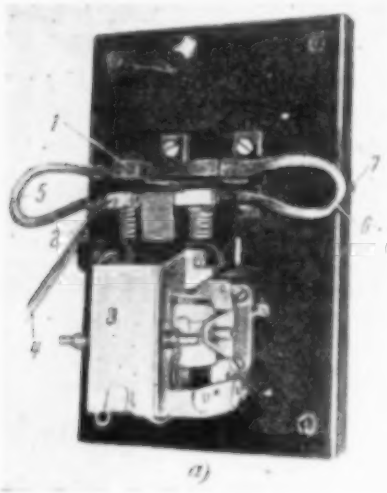

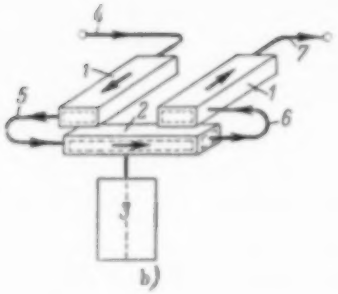

Fig. 2. High-frequency relay switch with water cooled contacts.
(a) general layout,
(b) the schematic diagram of the equipment.

into which the grid plates are inserted.

When the moving arc extinction contact (6) parts from the non-moving contact (3), the arc rises between them. The magnetic field of the coil (4) forces the arc to move to the sides of the grid, and conducts it to the internal edge of the plates. Arriving at the edge of the plates, the arc closes the outlet for the hot gases from the chamber. Pressure rises in the chamber which drives the arc into the grid. After entering the grid, the arc is extinguished at the very first passage of the current through zero.

In case of high frequency, this process is accompanied with generation of a small amount of heat [5].

The high-frequency contactor developed with water-cooled contacts, with the arc extinction equipment described has overall dimension of 360 x 250 mm. It can be operated with currents up to 1000 A, with voltages up to 15000 V and with

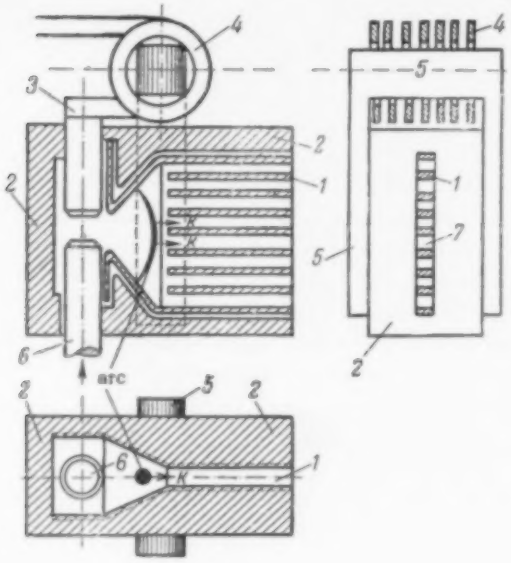

Fig. 3. Arc extinction equipment combined with high-frequency contactor.
1. the plate of the arc extinction grid; 2. extinction chamber; 3. non-moving contacts; 4. arc extinction coil; 5. magnet; 6. moving arc extinction contact; 7. the slot of the arc extinction chamber;

frequencies up to 10 kc/s. Only the main contacts are cooled by the water in the contactor. In the case of currents up to 150 A, liquid cooling is unnecessary; for currents between 150 and 750 A, it is necessary to water cool only the non-moving contacts; in case of currents higher than 750 A, the non-moving contacts as well as the bridge connecting them must be water-cooled.

The water flows to the contactors through hollow bus-bars made of copper tubes.

For comparison, we show the dimensions of the "K" series high-frequency contactors with natural air cooling. In case of a current of 100 A the dimensions are 330 x 38 mm; at 200 A 330 x 410 mm; at 400 A 330 x 600 mm; at 750 A 330 x 815 mm. Thus, dimensions of the water cooling contacter described are smaller than the 100 A contactor of the K series, and its current rating is higher than the rating of the largest in the series.

Automatic circuit breakers

In automatic circuit-breakers, water cooling of the contacts and bus-bars was introduced during the development of a class of this equipment for current ratings up to 25 kA. Such equipment was necessary for the chemical industry and for ship

equipment. The basis of development was the AS class of circuit-breakers of the "Elektrosila" factory. They are produced in standard design with the following ratings:

AS- 5	...	800 A
AS-15	...	1500 A
AS-25	...	2500 A

To increase the current ratings of this apparatus, their main non-moving contacts were water-cooled. The main contact system of such a circuit-breaker is shown in Fig. 4. The water through pipes (1) enters into the slots (2) and from here into the non-moving contact (3). It floods the body of the contact by pipe (4), goes into the insulator pipe (5) and from it enters the other non-moving contact (6). There it flows through pipe (7) and comes out into the hollow bus-bars (8) which carry off the water.

The application of water cooling permitted an increase in current rating, of circuit-breakers by a factor of 4. The current ratings, at which the automatic circuit-breakers of the AS series operate reliably, are shown in Table 1.

TABLE 1

Type	Current rating kA	
	Natural air cooling	Water cooling
AS-15	1.5	6.0
AS-25	2.5	10.0

Using four water-cooled circuit-breakers type AS-15, or two of the type AS-25 connected in parallel, we can get an automatic circuit-breaker for 20-24 kA. It has roughly the same dimensions as a three-phase circuit-breaker for 1500 A, but without water cooling.

The essential feature of the system described is that both circuit-breaker feeder bus-bars are water-cooled. This is convenient strictly from assembly considerations; there is no need for special water passing pipes, as the bus-bars act as such and the whole water-cooling system is concealed in the distributive equipment. Furthermore, this makes it possible, in some cases, to decrease the cross-section of the bus-bars, and to achieve a certain amount of economy in use of copper.

However, where there is no need to reduce the cross-section of the bus-bars for higher efficiency conditions there is an economy in reducing their temperature and consequently the power losses.

A further advantage of the system described is that it does not require the manufacture of new mechanisms but greatly increases the field of application of those already in existence (after equipping with water-cooling). The conversion of natural air cooled into water-cooled apparatus does not cause big modifications

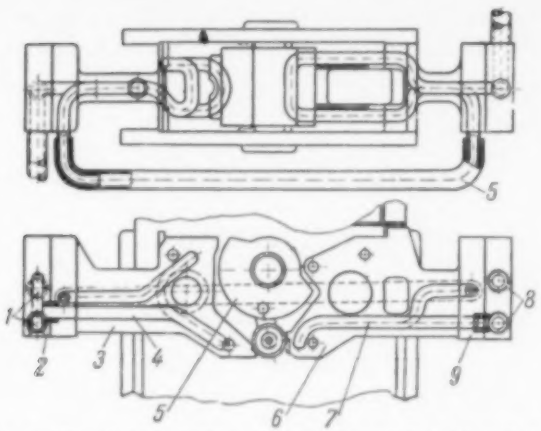

Fig. 4. The contact system of the water cooled AS series of automatic circuit-breaker.

in the design of the gear. The copper contact of an AS-25 circuit-breaker is shown in Fig. 5. On casting, holes are left in it; copper tubes are placed in them in which the water will flow.

In the circuit-breaker AS-15 apparatus at a current rating of 6 kA, the losses per pole amount to 720 W, and the water-flow through it with a temperature rise of 5° C is equal to 125 l/hr. If the pipe has a diameter of 10 mm and a cross-section of 0.8 cm², the speed of the cooling water will be 0.43/m/sec. Under these conditions the pressure drop on one pole of the equipment is 0.15 atm.

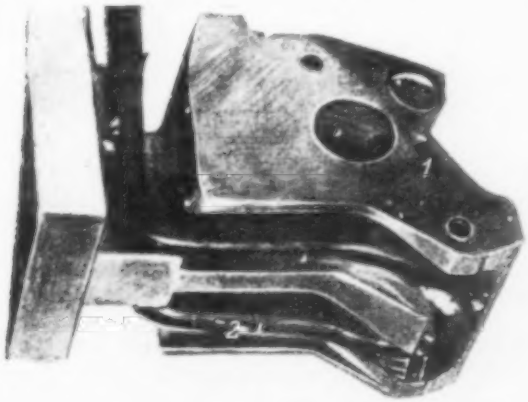

Fig. 5. Copper casting of contact (1) including the copper tube (2) for water cooling.

The maximium permissible current for the equipment in the described system is determined by the overheating of the moving main contacts, which are made in the form of rollers without water-cooling. These rollers, with a current of 6 kA

and water-cooled non-moving contacts, reach maximum permissible temperatures of 85° C.

If the design of the apparatus permitted the water-cooling of the moving contacts, the current ratings of the circuit-breaker could be increased to a much higher value. The overall dimensions of the two-pole water-cooled automatic circuit breaker for a current rating of 20 kA at 440 V are 640 x 558 x 354 mm. When we talk about water cooling, we have in mind a more or less complete project consisting of a number of such pieces of equipment, and in such cases the effect is especially great.

Long term application

Besides equipment with high current ratings and high-frequency contactors, water-cooling is expeditiously used in high-speed automatic circuit-breakers.

In the latter case, it is necessary to remember that there already exists a closed water cooling system in mercury rectifiers protected by high-speed circuit-breakers.

Therefore, the integration of high-speed circuit-breakers into this system does not involve technical difficulties and heavy expenditure.

In modern turbo-generators with a power of 200-300 MW and over, water cooling of the stator will be used. In such a case, it is obviously worth while continuing this system, and including water cooling of the bus-bars and the generator circuit-breakers.

This results both in a decrease of the dimensions of the circuit-breakers and bus-bars and in an increase in efficiency, owing to decreased copper losses, since the temperature of the live parts is decreased.

REFERENCES

1. R.S. Kuznetsov; *Elektricheskie apparaty raspredelitelnykh ustroistv nizkogo napryazhenie (Electrical equipment of low voltage distribution plant).* Gosenergoizda (1956).
2. E. Wiedemann; *Grenzleistungs - Turbogeneratoren, (Maximum voltage turbogenerators).* ETZ-A: 20, p.744 (1955).
3. P.A. Ostryakov; and I.V. Zaryanov. *Teploctvodyashchie ustanovki moshchnykh radiostantsii. (Heat dissipation equipment of large radio stations).* Svyazizdat, (1954).
4. M.S. Shkrob; *Vodopodgotovka (Water preparation).* Moscow (1952).
5. O.B. Bron and A.P. Makhonin; *Gashenie vysokochastotnoi v kontaktorakh (High-frequency arc extinction in contactors).* Symposium "Elektrosila" No.13, (1955).

ABSTRACTS FROM PAPERS PUBLISHED IN ELEKTRICHESTVO NO.10, 1958

Calculation of transient processes in linear systems: P.A. Jonkin. (pp 1-6).

The author expounds two approximate methods of calculating transient processes based on the use of integrals with a variable upper limit of a formula of right angles or of a formula of trapezoids. A table of results shows that integration based on the trapezoid formula gives practically the same result as the usual analytical method, whereas integration based on the right angle formula results in error. Such error is not considered to disturb the general character of the transient process curves and in any case can be considerably reduced by reducing the interval r. The magnitude of r is not known when beginning the calculations and the author recommends a preliminary approximate calculation by the method of successive ordinates using the right angle formula and then, after choosing r, to make the calculation more precisely by the same method using the trapezoid formula. Certain values of r may be assumed for the purpose of the calculations. The method can be used to investigate transient processes described by differential equations of high orders and also to calculate circuits with non-linear elements.

1959

Galvanic effect of a.c. electrified railways, on single-conductor circuits: M.I. Mikhailov and L.D. Razumov. (pp 20-25)

A practical method is proposed for calculating the interference currents arising, for instance, in telegraph or distance feed circuits due to the difference in the potentials of the earth points. The maximum difference in the potentials depends on the position of the earth connexion in relation to the permanent way and several typical examples are considered. He argues that the conditions for setting single-conductor lines of communication close to the track involves consideration of the magnetic as well as the galvanic effects. The formula introduced were verified experimentally on a section of the electrified line from Ozherel to Pavelets. Considerable discrepancies were found between the calculated and measured results, but the calculations are approximately right.

Permanent magnets of the oxide anisothrope type: S.A. Medvedev. (pp 25-30)

The reduction in weight and size of electrical equipment has become very

desirable. The physics of magnetic phenomena, in particular the investigation of the processes of magnetization and magnetic polarity reversal cannot only now explain the majority of observed phenomena but investigations are also directed to the creation of new materials for permanent magnets. Success has been achieved in applying the theory to the development of pressed finely dispersed powders of different magnetic materials. The author briefly expounds this theory and considers the technology of production of oxide permanent magnets, their properties and their field of application.

Constructing the characteristics of a d.c. drive with reactor control: P.B. Resenbauli and I.N. Selivokhin. (pp 31 - 33)

The recent development of small crystals power rectifier has made it possible to produce a d.c.motor with reactor control ensuring sufficiently firm mechanical characteristics and a wide range of speed control. The author proposes a graphical-analytical method of plotting the mechanical characteristics of a d.c. motor which has been developed for a scheme of reactor feedback control. The method is based upon the determination of the relationship between the current and voltage on the armature of the motor by joint graphical-analytical solution of the feedback equations and of the characteristics of the simultaneous magnetization of the reactor material. The method is illustrated by diagrams and an example of the mathematical calculations is given.

How the armature reaction influences the operation of d.c. motors with permanent magnets: Iu. S. Zakharov. (pp 34 - 35)

The development of quality magneto-hard metals has paved the way for the use of permanent magnets as the excitation of electrical machines. In the case of d.c. motors, temperature stability and efficiency have been raised thereby and in some instances weight and size have been reduced. Difficulties have been encountered, however, in their technology of production and mathematical calculation. The author qualitatively describes the phenomena arising on the reversal of a d.c. motor with a permanent magnet. Here the de-magnetization of the machine is considered in the usual three sections. He argues that the usual methods of ageing permanent magnets do not give the desired results. For excitation, magnets are necessary which not only have a high coercive force but also a high residual inductance and a high covexity factor of the de-magnetization curve.

Equivalence of dynamic braking and starting an induction motor: V.R. Shippillo. (pp 36 - 37)

He states the equations to determine the slip of the induction motor on starting and during dynamic braking and demonstrates the analogy of braking and starting

conditions and the similarity of the characteristics if the currents are equivalent. He supports this by showing the results of tests on an R55 S 12 induction motor. He then establishes a qualitative and quantitative connexion between the dynamic braking conditions and the motor conditions of an induction machine. A simple method of calculating the characteristics of an induction motor in dynamic braking conditions is then given and illustrated graphically.

A high-speed magnetic amplifier for telemechanics: V.R. Kulikov. (pp 38 - 42)

High-speed magnetic amplifiers may be used in place of relay-contactor units in systems of telecontrol, (line, distribution, etc.). There are good prospects for the use of magnetic elements in tele-control equipment on sinusoidal current where there is no generator unit and the distributor is set in motion directly by a.c. impulses with a frequency of 50 c/s or 25 switch-covers per second. A simple approximate method is considered for designing a magnetic amplifier in the presence of considerable load inductance. Appendix I deals with the action of a magnetic amplifier as an impulse voltage amplifier. Here it is demonstrated that load inductance does not affect the method of operation of the amplifier. Appendix II deals with the determination of the fundamental relationships and Appendix III considers the relationship between the volume of copper and ferromagnetic material in the core.

1959

Synchronous condensers for long-distance transmission systems: A.I. Vazhnov, E.V. Tolvinskaia, I.A. Gordon, D.A. Zavalishin and I.A. Glebov. (pp 43 - 47)

The method of installing synchronous condensers at intermediate points of a transmission line to increase stability is illustrated diagramatically. Increased effectiveness can be achieved by automatic control of excitation and compensation of the inductive resistance of the condensers with the aid of the capacitance which is connected in series in the circuit of the stator of the machine. Modified damping windings have been developed to overcome the difficulty of self-excitation by the machine. The calculations show that non-compensated synchronous condensers for prolonged service in normal conditions with lagging current can be based on the largest machines in current production, (75 MVA). In the case of leading current the condenser should operate with negative excitation currents. In the case of capacitive compensation it is necessary to develop certain rotor units, especially for the special damping windings of the visible (phaner) pole condenser. The insulation of the damping cores also needs to be investigated in order to prevent the possible burning of the pole terminal steel. Compensated condensers may also be made with non-visible poles. Compensated condensers operate with both leading and lagging current. Forced excitation of non-compensated synchronous condensers requires the ceiling excitation voltages to be raised.

Transients when rocking the wheels of an electric train: B.P. Petrov. (pp 48-52)

The phenomena of skidding of wheels often arise when operating electrical rolling stock and trains. The driver reduces the skidding by braking or pouring sand under the wheels. It is expedient to automate these processes. The author considers the transient processes arising in the presence of skiddings and curtailment of skidding by braking in the case of d.c. motors with series excitation. For this purpose he compares and solves initial equations which differ from those of Bader, (El. Bahnen; 11, 12, 1939), Minova and Trakhtman. The initial equations for graphical-analytical solution are compared on the usual assumptions. Here the equations are non-linear and in some cases Bashkirov's method of secants can be employed. Introducing a few additional assumptions he proceeds to analyse the processes arising on skidding and then when braking.

Protecting a.c. machines from internal faults in the stator windings: M.F. Shishkin. (pp 57-58)

Owing to the complexity of conventional differential protection this equipment is not usually installed on low output machines, for example, on generators for rural power stations. The author considers a simple and reliable protection against internal short circuits in the stator windings which can be used instead of differential protection. The method of operation of this protection is illustrated diagramatically and is based on the use of a magnetic coupling between the end connexions of the stator winding and a special protective coil. Tests have shown that such protection operates selectively in the presence of all types of internal and external short circuits except when the fault of an equal number of turns occurs in different phases of the stator winding.

Use of a method for testing the individual arc-extinguishing elements in high-voltage circuit-breakers: V.V. Kaplan and V.M. Nashatyr'. (pp 59-64)

The author discusses the theoretical and experimental basis for the widespread use of the method of testing the individual arc-extinguishing elements of high-voltage circuit-breakers in spite of the considerable development of synthetic schemes. He considers the effect of the static character of the arc-extinction process and the distribution of the recovery voltage on the operation of the circuit breaker. The results of experiments are then given, which partly corroborate his analysis of the operation of circuit-breakers with the enlistment of the theory of probabilities. He concludes that the breaking capacity of a circuit-breaker with several arc-extinguishing elements can be satisfactorily determined by summing the minimum values which have been determined for it with the same values of current for the individual elements provided that: (1) the elements of the circuit-breaker are identical in construction and have no noticeable direct effect on each

other in the sense of interaction on the intensity of the oil or gas blowing and so on; (2) the individual elements of the circuit-breaker are not connected up with low-ohmic shunting resistances or large capacitances.

Moving-coil oscillographs with frame type galvanometers: L.A. Biber and Iu. E'l'kind. (pp 70-71)

Moving-coil oscillographs have now been developed with frequencies of natural oscillations from 1.25 to 10,000 c/s and correspondingly with a current constant 8×10^{-3} - 9×10^{-1} Am/mm. Low frequency multi-channel frame-type galvonometers (up to 300-600 c/s) have magnetic damping; in the case of higher frequencies, liquid damping is employed. This apparatus is then described and their advantages are discussed: high sensitivity, simultaneous oscillographing of electrical and non-electrical magnitudes and their value in over damping conditions.

Where and why it is expedient to use 330 kV: N.N. Krachkovskii. (pp 72-76)

In connexion with the introduction of 500 kV in place of 400 kV for long distance transmission there is a large gap between the carrying capacities of 220 and 500 kV lines. The author supposes that there is a sufficiently wide range of distances and transmitted powers within which 330 kV could make considerable savings. He compares transmission of 220, 330 and 500 kV over 100, 200, 400, 600, 800 and 1000 km and determines the relationship of capital and operating costs to the power transmitted. The results are tabulated. He concludes that there are good reasons for adopting 330 kV transmission.

Measuring the torque of induction motors: E.A. Ivanov. (pp 77-79)

A method is proposed for determining the relationship $M = f(s)$ in transient states. An inductive coil with a straight core of electrical sheet steel is used as activator. The amplitude values of the current induced in the coil-activator are proportional to the torque of the motor and the periodicity of this curve determines the value of the slip corresponding to the ordinates of the current. The method has been verified by comparison with two methods of measurement: (1) with the aid of a tensometric and (2) a capacitive coil-activator.

Studying the sparking of traction motors by means of photo-electric indicators: A.M. Trushkov. (pp 80-82)

The results of tests are given for switching experiments on traction motors carried out recently by the Novocherkask electric traction works on the Belovo-Novokyznets Tomsk section of the line with the aid of a photo-electric indicator of the variable sparking type, Mark II-1, produced by the Railway Scientific Research Institute. This indicator has a different averaging and amplifying system and a special

system of guidance to the source of the sparks. The author considers the scaling of the apparatus and takes the line density of sparking per unit length of the brush as the standard for evaluating the sparking intensity. The method of "sparkless zones" was employed to tune and regulate the additional poles of the traction machines. Typical oscillograms are shown of the mean magnitudes of the intensity of sparking of the brushes.

The increase of sparking at the beginning and its decrease at the end of the tests is attributed to temperature. The indicator has also been set up on an actual electric train and a part of the oscillogram shows how the intensity of sparking varied with the different operating conditions of the motor. The use of the photo-electric indicator is considered to be an improved method of evaluating the degree of sparking.

SHORT-CIRCUITS, ASYNCHRONOUS DRIVE AND TURBOGENERATOR RESYNCHRONIZATION*†

N.A. POLIAK

Teploe'lektroproekt

(Received 18 June 1958)

The decelerating action of a sudden short-circuit on the rotor of a synchronous generator has already long been known, [4]. The decelerating action is connected on the one hand with considerable power losses from short-circuit currents in the resistances in the stator circuit, and on the other hand with both the alternating electromagnetic torque on the generator shaft and with the power losses in the rotor circuits caused by the aperiodic component of the stator current, [3].

Until recently this decelerating action was not considered when rating the dynamic stability of parallel synchronous generators. Only a few years ago, in connexion with studies on long distance transmission line systems [1] and experiments carried out on electrodynamic models, the conclusion was reached that consideration of the decelerating action of a sudden short-circuit can make a substantial difference to the results of calculations in certain conditions.

In spite of the decelerating action of a sudden short-circuit, in the majority of cases a power surplus (torque) exists on the turbogenerator shaft until the short-circuit is tripped. This results in the fact that after the short-circuit is tripped, the rotor speed is greater than the speed appropriate to the line frequency. Under such conditions an asynchronous electromagnetic torque develops on the generator shaft, the force of which depends on the characteristics of the synchronous machine and on the parameters of the external circuit. The asynchronous torque acts favourably on the transient electromechanical process: the amplitude of the first rotor oscillation is somewhat decreased and the following are dampened.

Due to the change in speed, the turbine speed-control comes into action

* *Elektrichestvo* No. 11, 18-24, 1958.

† From works by the author in the relay protection and stability department of the Teploe'lektroproekt.

altering the torque developed by the turbine. Certain conditions, for example during cascade tripping of the short-circuit, this can also have a favourable effect.

The sudden short-circuit abruptly increases the current in the excitation winding of the generator, and results in an increase in the electromagnetic decelerating torque on the exciter shaft. Rapid excitation forcing strengthens this effect somewhat. If the exciter is on the main shaft of the generator, the shaft is decelerated additionally, which also acts favourably on the transient process.

The greater the short-circuit current, the power losses connected with it (particularly in the rotor circuits), and the greater the asynchronous torque of the generator in the presence of slight slipping, the more favourable is the effect of these circumstances on the transient electromagnetic process during short-circuits in the network.

In this connexion, turbogenerators have extremely favourable characteristics which explains why in present-day electrical systems, where large thermal power stations are not connected to hydroelectric stations by particularly long transmission lines, cases of disturbance to the dynamic stability in parallel operation are exceptionally rare.

Large thermal power stations are usually connected to power-consuming centres by several transmission lines of relatively short length (100-200 km), but reasonably high voltage, (110-220 kV). This provides: (a) stable electrical connexion, i.e. a sufficiently large synchronizing torque between stations, (b) comparativily large short-circuit currents, and (c) considerable asynchronous torque on the turbogenerator shaft in transient conditions. Furthermore, modern high-speed relays and automatic devices, excitation forcing during short-circuits and high-speed and sufficiently powerful circuit-breakers are also of great value.

A theoretical-calculation study, the initial data and results of which are presented as follows, was made to determine the quantitative effect of the aforementioned conditions, and to explain those of them which are essential for the rating of dynamic stability in parallel turbogenerator operation, and also for rating the conditions of turbogenerator asynchronous drive and resynchronization. *

Rating circuit and initial data

The simplest system was considered with three parallel lines of 220 kV connected to a receiving system having a total turbogenerator and synchronous equalizer power of about 4000 MVA, (Fig. 1). Transmission distance was 200 km.

* The calculations were made by A.F. Tsukerman, a colleague at the Teploe'lektroproekt.

The voltage after reactance of the receiving system was taken as constant in magnitude and phase. This meant that the mechanical inertia constant of the rotors of the synchronous machines in the receiving system was considered to be infinitely great.

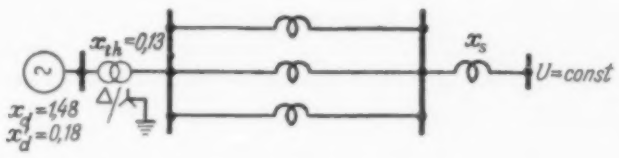

FIG. 1. Transmission circuit

The total power of the turbogenerators in the thermal station was examined within the limits of 150-600 MVA, (Table 1). In all cases, it was assumed that in normal operation prior to short-circuiting, the voltage at the outputs and the active and reactive loads of all the turbogenerators were as rated. Local demands, the station's own consumption and the power losses in the step-up transformers were not taken into consideration.

TABLE 1

Transmission parameters

Total turbogenerator power of station in MVA	x_s	In normal operation with three circuits			In post-fault operation with two circuits			
		x_l	Σx	θ, el.grad	x_l	Σx	θ, el. grad	K^{st}
150	0.050	0.075	0.255	53	0.112	0.292	55	2.40
250	0.033	0.125	0.338	58	0.187	0.400	61	1.89
400	0.133	0.200	0.463	66	0.300	0.563	74	1.45
450	0.150	0.225	0.505	69	0.337	0.617	78	1.35
500	0.166	0.250	0.546	71	0.375	0.671	—	1.26
600	0.200	0.300	0.630	77	0.450	0.780	—	1.11

The parameters 150 MVA, $\cos\phi = 0.9$, of the bipolar turbogenerator made by the S.M. Kirov'Elektrosila' factory were taken as the ratings. This selection was made because experimental data was available for this machine concerning rotor circuit parameters for different slidings which permitted a sufficiently accurate determination of the torques in the presence of short-circuits.

The exciters in the turbogenerators made by the electric machine building factories of the Soviet Union ensure sufficiently rapid double forcing of excitation voltage during short-circuits in the network. With such forcing and short-circuits immediately after the step-up transformer or in the line the constancy of the longitudinal component of the e.m.f. is almost guaranteed after the transient reactance of the generator. The introduction of this condition made possible a considerable

simplification and speeding-up of the calculations; with the same objects in mind line capacitance and resistance before and after short-circuiting were not considered.

The greater the power transmitted in normal operation, the greater the reactances of lines and receiving system in fractions of units relative to the total rated apparent power of the turbogenerators, and the greater the angle of displacement between the vector of the rotor e.m.f. and the vector of the receiving system voltage (Table 1). The size of the static limit of transmission power K'_{st} from the condition of the equality of values for E'_d in normal and fault conditions is extremely great. Thus, the electrical transmission under consideration, even with extremely heavy circuit loads, has good static characteristics. In addition, it is apparent that in order to avoid passage into the artificial stability zone, the load on the circuit during post-fault operation should not exceed 225 MVA.

Short-circuits and dynamic stability of parallel operation

All types of short-circuit were considered, both at the beginning and at the end of one of the three circuits. It was decided that the fault line would be cut off from the high-speed series differential line protection at both ends at once in 0.20 sec, or in cascade in 0.20 sec at the fault end, and 0.80 sec at the opposite end of the line.

The rating of the dynamic stability was made for maximum power transmitted on the three lines under normal conditions of operation whereby the turbogenerators in the first half-cycle after the short-circuit is broken do not drop out of synchronization. The band of powers, limited by "stable" and "unstable" results, the "rating fork", was 25 MVA.

Two series of calculations were made: one according to the universally used (standard) method [6], i.e. without calculating the aperiodic component of the stator current, the power loss in the stator winding during short-circuiting, the asynchronous torque after the short-circuit is tripped and the action of the turbine speed control, and the other with the calculation of all these factors, (precision calculation).

For the calculation of the decelerating action of a sudden short circuit in rating the dynamic stability of synchronous machines operating in parallel, we adopted the method using the "equivalent load of the synchronous machine" during a three-phase short-circuit. Since it is applied to the turbogenerator shaft throughout the duration of the three-phase short-circuit, the equivalent load is practically speaking a sufficiently accurate reflection of the results of the decelerating action up to the moment when the short-circuit is tripped. The value of the equivalent load depends on the distance of the short-circuit from the turbogenerator outlets and on its duration, (Fig. 2). In the presence of a three-phase short-circuit near the station busbars, the equivalent load is considerable.

For example, in the presence of a three-phase short-circuit after a step-up transformer with a reactance of $X_{tr} = 0.13$, and with a short-circuit duration of 0.20 sec, the equivalent load amounts to approximately 60 MVA relative to a turbogenerator of 150 MVA, cos $\phi = 0.90$. Thus, as opposed to the widely held idea that a sudden three-phase short-circuit of short duration near the station busbars results in complete generator unloading, in the given case the equivalent load of the turbine is 40 per cent of the rated load before the short-circuit is broken. If a three-phase short-circuit should occur immediately at the turbogenerator outlets, the equivalent load for a duration of 0.20 sec could not be 60 but 300 MVA, i.e. the rated power of the turbine would be doubled, and the machine would begin to decelerate.

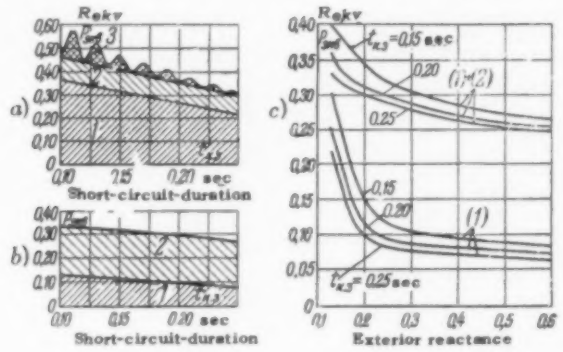

FIG. 2. Equivalent turbogenerator load with three-phase short-circuit dependant on duration of short-circuit and exterior reactance.

a – short-circuit immediately after step-up transformer; *b* – short-circuit on 220 kV line (exterior reactance $x_{tr} + x_1 = 0.30$); *c* – short-circuits at different points on the 220 kV line. 1 – component due to power losses in rotor circuits; 2. component due to power losses in the stator circuit, (including the step-up transformers and transmission line); 3 – component due to the alternating electromagnetic torque.

In the case of distant and also of asymmetrical short-circuits, the equivalent load is considerably less. In order to simplify the calculations for asymmetrical short-circuits, we included in the equivalent load only the losses in the rotor circuits caused by the aperiodic component of the positive sequence current, and by the losses from the periodic component of the negative sequence current.

In all cases precision calculations result in greater values for permissible transmission loads, (Table 2). The more powerful the type of short-circuit under consideration is, the greater the difference. With simultaneous tripping of the fault line at both ends in 0.20 sec the difference amounts to: approximately

5 per cent in the presence of a single-phase earthing fault, with two-phase short-circuiting approximately 10 per cent, in the presence of a two-phase earth fault approximately 20 per cent smaller value, but in the presence of a three-phase short-circuit approximately 100 per cent when the fault is at the beginning of the line, and approximately 80 per cent when the fault is at the end. Thus, it is impossible to consider a three-phase short-circuit close to the stator outlets without a calculation of the equivalent load. In all cases, short-circuits at the beginning of the line are essentially less powerful than the same type of short-circuits at the end of the line.

As is known, transmission capacity is determined by the conditions of normal and post-fault operation, by dynamic stability and by the multiple of the static limit of transmitted power in post-fault operation. In order to avoid transmission passage to the artificial stability zone in post-fault operation, the load for the three lines in normal operation according to Table 1 should not exceed 450 MVA. Under such conditions transmission is dynamically stable even with three-phase short-circuiting at the beginning of the line (450 MVA), and is almost stable with short-circuiting at the end of the line (400 MVA). The necessary conditions are: tripping of the fault line at both ends at once in 0.20 sec, automatic control and sufficiently effective turbogenerator excitation forcing which in all calculations were considered as constant values for the series component of the turbogenerator e.m.f. after transient reactance. The static power limit multiple in post fault operation also remains reasonably high. In this it is seen that the transmission load in post-fault operation is the same as in normal operation. When the short-circuit is tripped more slowly and also in cascade, conditions are less favourable.

In precision calculations the equivalent load during short-circuit conditions plays an extremely important role. The calculation of the asynchronous turbogenerator torque after the short-circuit has been tripped and the remaining circumstances, including the action of the turbine speed control, are of secondary importance.

If it is not required that the transmission load in post-fault operation remain the same as in normal operation, then when the fault line is tripped simultaneously, part of the turbogenerators can be tripped, and this makes possible transmission in normal operation of 450 MVA on three circuits (Fig. 1) and when the short-circuit is tripped less rapidly.

Precision calculations, particularly the rating of the equivalent load during short-circuiting in more complex transmission systems and lines than the system shown in Fig. 1, would complicate calculations considerably and increase the volume of calculating operations. On the other hand, initial rated data are usually not so accurate as to make such complications expedient.

However, in those cases where it is a question of calculating the dynamic stability for a specific transmission system, for example, calculations made before tests or calculations necessary for detailed analysis of abnormal conditions

occurring in an electrical system, particularly if it is a question of three-phase short-circuits, the complete calculation of the equivalent load of turbogenerators and of other factors becomes necessary.

Loss of synchronization, asynchronous drive, resynchronization and synchronous swings

When the short-circuit is tripped with insufficient rapidity, the turbogenerators in the thermal station fall out of synchronization and change to an asynchronous mode of operation in relation to the generators in the receiving system. In this the turbogenerators continue to operate with full excitation as opposed to asynchronous operation caused by excitation losses [5]. After a certain time turbogenerators can be drawn back into synchronization once again.

The whole process whereby turbogenerators fall out of synchronization and are subsequently drawn back into synchronization can be conventionally divided into three stages according to time: (1) loss of synchronization and acceleration of the turbogenerator rotors, (2) rotor deceleration and (3) resynchronization and synchronous operation (Fig. 3).

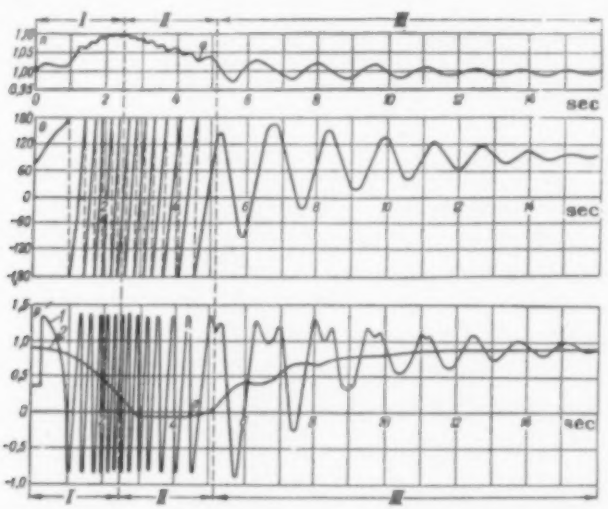

FIG. 3. Relative speed n of a turbogenerator, angular displacement of rotor θ electromagnetic power of turbogenerator (1), and power developed by turbine (2) during asynchronous drive.
a – resumption, of steam inflow into turbine; I – loss of synchronization and rotor acceleration; II – rotor deceleration; III – resynchronization and synchronous swings.

The first stage begins with the dynamic disturbance of the normal mode of operation. The electromagnetic power (load) of the turbogenerator, after

momentarily rising to the maximum value, rapidly diminishes, passes through zero and then fluctuates within considerable limits. In the conditions under consideration the average load for each cycle of asynchronous drive is small, the equilibrium of torques on the shaft of the turbogenerators is disrupted, the rotor speed increases and the turbine speed control comes into action beginning to shut off the steam inflow. The difference between the average turbogenerator electromagnetic power and the power developed by the turbine gradually decreases and disappears after a certain time. The rotor speed at this moment is at a maximum. With this the first stage ends, its duration being basically determined by the rate at which steam inflow into the turbine is decreased.

When a turbogenerator which is operating at the rated load is cut off from the system, 1 – 3 sec is required from the moment when it is cut off until the steam inflow into the turbine has been completely stopped. These values are smaller for steam condensation turbines of the usual type, and larger for turbines with intermediate steam superheating if the steam bypass into the condenser does not come into action. Since loss of synchronization is not accompanied by the instantaneous drop of the full load, slightly more time elapses before the steam inflow is completely cut off. In order to limit the duration of the first stage, and connected with this (and what is still more important) in order to decrease the duration of the second stage, it is important that the steam inflow into the turbine be decreased as quickly as possible.

During the second stage the deceleration of the turbogenerator rotors is caused by the action of the following three factors: (1) by the average power losses for each cycle of asynchronous drive in stator circuit resistances depending on the resistance of the transmission lines*, the characteristics of the system of turbogenerator automatic excitation control and the parameters of the external network; (2) by the asynchronous decelerating torque on the turbogenerator shaft, the dimensions of which depend on the generator characteristics and the parameters of the external network; (3) by turbine rotor vane friction in the steam medium after full stoppage of steam inflow, though there is a vacuum in the turbine condenser; we evaluated this decelerating torque at 5 per cent of the rated torque of the steam turbine.

If conditions are such that resynchronization can occur, it is performed at a speed approximately 2 per cent higher than synchronous speed.

In Table 3, the duration of the second stage in different conditions is shown. Since the cross-section of 110 kV lines is about half that for 220 kV lines, and the reactance per unit line length in both cases is practically the same, other

* The resistance of the transmission lines was also considered in calculations for asynchronous operation.

TABLE 2

Maximum permissible transmission loads for dynamic stability conditions with different types of short-circuit on the line.

Conditions for tripping fault circuit	Type and location of short-circuit		Permissible loads MVA		k'_{st}
			Standard method of calculation without considering resistance	Precision calculation	
Simultaneous tripping at both ends	Three-phase	At beginning of line	225	450	1.35
		At end of line	225	400	1.45
	Two-phase earth fault	At beginning of line	425	500	1.26
		At end of line	400	475	1.30
	Two-phase	At beginning of line	525	> 600	–
		At end of line	525	575	1.14
	Single-phase earth fault	At beginning of line	575	> 600	–
		At end of line	575	> 600	–
Cascade tripping	Three-phase	At beginning of line	150	325	1.65
		At end of line	< 150	200	2.11
	Two-phase earth fault	At beginning of line	375	450	1.35
		At end of line	300	350	1.56
	Two-phase	At beginning of line	475	525	1.20
		At end of line	425	450	1.35
	Single-phase earth fault	At beginning of line	550	600	%
		At end of line	525	550	1.17

before tests or calculations necessary for detailed analysis of abnormal conditions

things being equal, the power losses in 110 kV lines are greater, and this somewhat decreases the turbogenerator deceleration time.

TABLE 3

Turbogenerator rotor deceleration time

Power transmitted on line MVA	Deceleration time, sec		
	Generators have automatic excitation control		Generator field quenched
	220 kV lines	110 kV lines	220 kV lines
150	1.9	1.6	2.3
250	2.3	1.8	3.2
400	2.8	2.0	4.6
500	3.1	2.1	5.4

When applied to the conditions of the system described in Fig. 1, resynchronization for the two circuits remaining in operation is practicable even if the total power of the thermal station turbogenerators amounts to 500 MVA, i.e. almost 15 per cent of the receiving system power. This exceeds the power which can be transmitted with two circuits in long distance operation.

Retarding the action of the turbine speed control when steam inflow is resumed at the end of the second stage facilitates the conditions of resynchronization. However, the delay should not continue to the stoppage of steam inflow at the beginning of the loss of synchronization, since this lengthens the first stage and can in unfavourable conditions result in an excessive increase in the rotor speed, and the operation of the turbine automatic safety device. Partial steam inflow stoppage at the end of the first stage or too early steam inflow resumption during the second stage can make the conditions of resynchronization difficult. The less the residual statism* of the turbine speed control, other things being equal, the more favourable the resynchronization conditions; in our calculations statism* was equal to 4 per cent of the rated speed.

Artificial delaying of steam inflow into the turbine by means of secondary speed control until the rotor speed in the process of decelerating is almost reduced to the speed appropriate to the frequency of the network facilitates the conditions of resynchronization.

* "Statism" in Russian technical literature is defined as "the deviation of the controlled magnitude at rated load from its value on no load, expressed as a percentage, (of its value on no load). Editor's note.

With considerable loads on transmission lines automatic turbogenerator excitation control is a necessary condition for resynchronization in practice.

In actual conditions, where the constant mechanical inertia of the turbogenerator rotors and synchronous compensators of the receiving system has a decisive significance, the frequency in the receiving system with asynchronous turbogenerator drive in a large station does not remain constant, and resynchronization conditions are more difficult than those indicated here.

On the other hand, the consumption of power at the generator voltage, including devices requiring power for the station's own use, and also the presence of consumers feeding on the same station with separate h.v. lines result in the fact that with asynchronous operation there is not as considerable a power loss as in the case considered above. The increase in the turbogenerator rotor speed is less, the first and second stages are shorter and resynchronization takes place more rapidly.

Conditions of turbogenerator operation

In asynchronous operation the currents in the turbogenerator winding are higher than rated, and the electromagnetic power is alternately positive and negative, i.e. a torque with an alterating sign acts on the shaft of the aggregate; in the solid mass, (the "body"), of the rotor there are additional losses from slip frequency currents. Data are given in Table 4 concerning the conditions when the turbogenerator rotor speed amounts to 106 per cent of the rated speed. This value can be conventionally considered as the average rate of turbogenerator rotor speed before resynchronization.

1959

The less the system of turbogenerator excitation is inert but the more effectively automatic excitation control operates, the greater the values for average stator and rotor currents and the amplitude of their fluctuations, (second terms in Table 4). In spite of the fact that the currents are great, it can be considered that asynchronous drive for about 10 sec does not cause an excessive increase in the temperature of conductors and their insulation in present-day turbogenerators with air or the usual (not internal) hydrogen cooling. This does not include, however, the new type of turbogenerator now being made with hydrogen or liquid internal cooling of the winding in which current densities are considerably higher than in turbogenerators of usual construction.

Additional losses in the solid mass of the rotor and excitation winding are not so great as to cause their excessive heating during the above-mentioned 10 sec on the condition that the maximum slip, i.e. the difference in the rotor speeds in the thermal station turbogenerators and the receiving system generators, does not exceed 10 per cent of the rated speed of rotation. In this, of course, it is seen that rotor steel banding (end-bells), of sufficient thickness is built on to the body to ensure safety at increased speed, thus eliminating the possibility of

TABLE 4

Stator and rotor currents and variation in turbogenerator electromagnetic power in asynchronous operation (in relative units)

Power transmitted on line, MVA	Generators have automatic excitation control			Generator field quenched
	Stator current	Excitation current	Limits of variation in electromagnetic power	Stator current
150	3.27 ± 2.00	1.66 ± 1.18	± 2.04	1.84
250	2.56 ± 1.62	1.44 ± 0.96	± 1.62	1.48
400	1.93 ± 1.26	1.21 ± 0.74	± 1.26	1.16
500	1.66 ± 1.10	1.12 ± 0.65	± 1.05	1.02

of any local heating of the solid masses, teeth and banding.

Voltage fluctuations in the electrical system

Asynchronous drive of turbogenerators in the station under consideration, depending on the synchronous machines of the receiving systems, is accompanied by active and reactive current fluctuations, and in connexion with this by voltage fluctuations at different points in the network, (Table 5).

TABLE 5

Voltages (in fractions of rated voltage) at the turbogenerator outlets and the end of line during asynchronous drive.

Power transmitted on line, MVA	Generators have automatic excitation control		Generator field quenched	
	Voltage at generator outlets	Voltage at end of line	Voltage at generator outlets	Voltage at end of line
150	0.78 ± 0.22	0.82 ± 0.11	0.39	0.90
250	0.77 ± 0.23	0.77 ± 0.15	0.33	0.87
400	0.76 ± 0.24	0.72 ± 0.18	0.26	0.83
500	0.76 ± 0.24	0.69 ± 0.20	0.22	0.81

The greater the total power of the turbogenerators in the station that have dropped out of synchronization, the lower the average voltage level during asynchronous drive both at the output from the turbogenerator and at the receiving

end of the transmission line. If in the system there are separate long distance transmission lines from hydroelectric stations operating as a rule with relatively small static stability reserves, then when the thermal station generators drop out of synchronization whose power amounts to a considerable portion of the power of the system, the voltage fluctuations at the end of the line can reflect unfavourably on the operation of long distance transmission from hydroelectric stations.

With the same values in relative units for the total exterior reactances, but with a lesser receiving system reactance than shown in Table 1, i.e. with greater power in the system, the voltage deviations from normal at the receiving end of the transmission line is proportionately smaller than shown in Table 5.

It would seem that after falling out of synchronization when the quenching device is tripped, the turbogenerators are no longer excited, (the field is quenched). This would eliminate voltage fluctuations during asynchronous drive, but in addition it would lower the voltage sharply at the output from the turbogenerator. Stator current fluctuations would for all practical purposes vanish, the average turbogenerator load for each asynchronous drive cycle would be decreased and this in its turn would lead to a slight increase in the duration of rotor deceleration. However, practically speaking, field quenching would be possible only in the case where the thermal station falling out of synchronization did not have local consumers, and the station's own consumption could be fed from another source independently of the common network. Since the actual conditions of operation of thermal stations do not allow this, field quenching of the station turbogenerators which have fallen out of synchronization cannot be applied in practice.

1959

Conclusion

The dynamic stability of parallel turbogenerator operation during short-circuits in the network is always higher than the rated stability obtained by the usual standard method, the maximum difference occurring in the case of powerful short-circuits at points relatively close electrically to the turbogenerator outlets. The chief cause of this lies in the fact that in standard calculations allowance is not made for the electromagnetic torques on the turbogenerator shaft caused by the aperiodic stator current component which occurs at the instant of short-circuiting or of another abrupt change in conditions.

Thermal station turbogenerator resynchronization after loss of synchronization, depending on other generator stations in the system, is feasible in conditions close to those considered here even in the case where the total power of the station turbogenerators dropping out of synchronization somewhat exceeds the power which in continuous operation can be transmitted on the remaining lines.

The question of asynchronous drive and resynchronization of turbogenerators with internal hydrogen or liquid cooling is receiving further consideration.

REFERENCES

1. E. Ia. Kazovskii; Energeticheskie sovtnosheniya pri vnezapnom korothom zemykarii sinkhronnoi mashiny. (Power relationships during sudden synchronous machine short-circuit). *Elektrichestvo;* No. 7 (1954).
2. M.P. Kostenko; Issledovanie problem avtomaticheskogo upravleniya elektroenergeticheskimi sistemami s primeneniem metodon elektrostinemicheskoyo modelirovaniya, A study of the problems of automatic control of electrical power systems using electrodynamic modelling methods). Sessions of Academy of Sciences, U.S.S.R., on scientific problems of industrial automatization 15-20 Oct., 1956. Complex automatization of production processes. *Izd. Akad. Nauk U.S.S.R.* (1957).
3. R.A. Lyuter; Raschet momentov urashcheniya sinkhronnykh mashin pri korotkikh zamykaniyakh. (Calculation of the torque of synchronous machines during short-circuits). *Symposium No. 7 "Electrosila" factory.* Gosenergoizdat pp 29-40 (1950).
4. R. Riudenberg; Toki korotkogo zamykaniya v praktike eksplyatatsii krupnykh elektricheskikh stantsii. *(Short-circuit currents in the practical operation of large power stations).* Translated from the German. Gostekhizdat (1930).
5. I.A. Syromyatnikov; Rezhimy raboty sinkhronnykh generatorov. *(Conditions of synchronous generator operation).* Gosenergoizdat. (1952).
6. P.S. Zhdanov; Ustoichivost' elektricheskikh sistem. *(Stability of electrical systems).* Gosenergoizdat. (1948).

A SYNTHETIC METHOD OF TESTING HIGH-VOLTAGE CIRCUIT-BREAKERS*

V.V. KAPLAN, V.M. NASHATYR' and V.L. IVANOV

(Received 20 January 1958)

INTRODUCTION

Testing in an automatic reclosure cycle is of great value in rating the switching capacity of h.v. circuit-breakers in addition to checking the breaking and making capacity. Such tests should be made for all types of circuit-breakers designated for operation in these conditions. However, circuit-breakers are actually tested in an automatic reclosure cycle only in isolated cases directly on the line as there are no laboratory circuits permitting such tests with sufficiently great short-circuit powers. In connexion with this, the creation of a synthetic circuit for testing circuit-breakers in an automatic reclosure cycle is extremely significant.

In 1957 in the Gorev High-voltage Engineering Laboratory of the Leningrad Polytechnic Institute (TVN LPI) a circuit was developed on the basis of an oscillatory circuit and put into practice which allowed synthetic testing of high-speed circuit-breakers operating in a single automatic reclosure cycle, (breaking-making-breaking).

The conditions for setting up equivalent synthetic circuit-breaker testing in an automatic reclosure cycle can be formulated on the basis of the demands made on a synthetic method of testing making and breaking capacity, [1 and 2]. The following conditions form the basis of synthetic testing in an automatic reclosure cycle:

1. Only those circuit-breakers are tested in an automatic reclosure cycle which have previously undergone successful testing in a breaking cycle, and consequently perform arc quenching dependably in breaking a given current with recovery voltage at full value. Therefore, in testing in an automatic reclosure cycle, the first operation (breaking) can be performed at a decreased voltage, but naturally, at the given value for the breaking current. However, the same time must

* *Elektrichestvo* No. 11, 29-35, 1958.

be allowed for arc burning in the circuit-breaker as for breaking at full voltage. Generally, the arc burning time in the circuit-breaker must be artificially extended if it is prematurely quenched in the decreased voltage circuit.

2. The second operation of the automatic reclosure cycle (making) must be performed synthetically with the provision of complete equivalent testing conditions. The approach of the circuit-breaker contacts must occur with a voltage value corresponding to the rated line voltage. During the spark-over between the circuit-breaker contacts a making current must cross the arc gap which is of the same amplitude and curve form as in the line; an accordance must also be reached between the current derivatives in the initial instants of its flow. In addition, with the spark-over between the contacts a current impulse must cross the circuit-breaker corresponding to the capacitive discharge of the dropout lines in the system.

3. In actual conditions of circuit-breaker operation in a high-speed automatic reclosure cycle, a short-circuit current passes through the metal short-circuit contacts of the circuit-breaker for approximately 0.05 - 0.06 sec or slightly longer, from the moment of short-circuit contact to the moment when the contacts again diverge. Separate checking of circuit-breaker contact system stability with large currents (with lowered voltage), and also full preliminary testing of making capacity (at high voltage) make it unnecessary for the short-circuit current to flow while testing the switching capacity of a circuit-breaker with metal closed contacts. This results in a notable simplification in testing, since with the use of an oscillatory circuit, a great number of capacitors are required to ensure the prolonged passage of the undamped short-circuit current.

Essentially the same condition is used in the standard method of testing breaking capacity. In these tests, the duration of the "metal short-circuit", (namely, the interval of time during which the breaking current flows in the test circuit, but there is a metal contact between circuit-breaker contacts), must be reduced to zero since in actual conditions it amounts to 0.05-0.06 sec.

4. The third operation of the automatic reclosure cycle (breaking) must also be made synthetically providing for the equivalent reproduction of circuit-breaker operation on a real line. For this, from the instant preceeding current zero passage for approximately 300 - 600 μsec until zero current value, exactly to the instant when the formation of an arc quenching cycle is possible, the circuit-breaker must be in circuit where the voltage, inductance and capacitance, and the determined voltage recovery rate have the same values as in the line. With these conditions the same current to zero approach rate is ensured as in the actual line, and also voltage recovery conditions in the circuit-breaker are fully reproduced.

5. The current amplitude with each successive operation must differ little from its value in the preceeding operation, reproducing the corresponding

conditions in the actual line where the short-circuit current is little damped during the automatic reclosure cycle in the circuit-breaker.

6. Circuit-breakers on the line can operate both in a single-phase and in a three-phase automatic reclosure system with different types of short-circuit, and therefore different correlations are generally possible between the values for the voltages applied to one terminal of the circuit-breaker when making and breaking.

It is highly desirable that the test circuit in which tests are made on one circuit-breaker terminal, also makes it possible to obtain different correlations between making voltage and recovery voltage. It is at least necessary that the recovery voltage (line frequency component) should not be notably lower than the making voltage.

Principal circuit of test apparatus (Fig. 1)

Two oscillatory circuits were used in the apparatus adjusted to line frequency, one $C_0 - l_0 - L_0$ provides for the first operation of the automatic reclosure cycle (breaking), and the second $C_1 - L_1$ functions as the circuit source of the making and the breaking current for the last two operations of the automatic reclosure cycle (making, breaking).

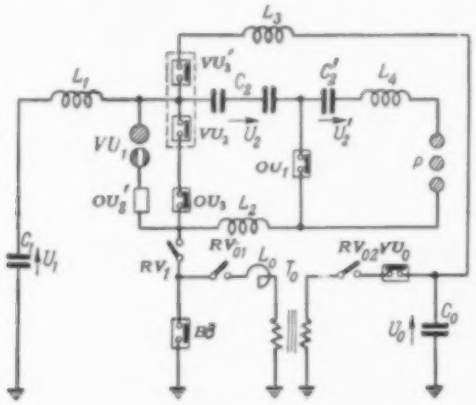

FIG. 1. Principal circuit of apparatus for the synthetic testing of circuit-breakers in an automatic reclosure cycle.

One oscillatory circuit $C_2 - L_2$ is used as the h.v. circuit in the last two operations adjusted to an increased frequency, somewhat higher than line frequency.

The circuit operates in the following manner. Initially switch RV_1 is open, and switches RV_{01} and RV_{02} are closed. The experiment begins with the closing of

switching device VU_0. The breaking current i_0 passes through the circuit-breaker being tested B. Immediately the contacts of B, operating in the automatic reclosure cycle, diverge. After one half-cycle of current flow, the arc is quenched by the test circuit-breaker. Thus, the first operation (breaking) of the cycle (breaking-making-breaking) is carried out. As was indicated above, this operation is performed at a decreased voltage, and it is expedient to use a step-down transformer I_0 in the first oscillatory circuit which makes it possible to obtain the given current i_0 with a smaller reactive power of battery C_0.

After arc quenching in B, switches RV_{01} and RV_{02} are first opened, and then RV_1 is closed which connects the test circuit-breaker to the circuit providing for the second part of the cycle (making-breaking).

Corresponding to the characteristics of the test circuit-breaker, the B contacts begin to draw together a certain time after arc quenching (making operation). The voltage $U_c = U_1 + U_2$ is applied to the B contacts in the series circuit $C_1 - L_1 - C_2 - L_2$ which is selected as equal to the making voltage for the circuit-breaker under study, (Fig. 2). At a certain position of the B contacts a spark-over passes between them, (connexion of circuit-breaker to short-circuit). An increased frequency current i_1' flows in this circuit (Fig. 2) which is conditioned by the parameters of both circuits. The parameters are selected by calculation so that the derivative of the making current is in the initial moments of flow equal to its value for the line frequency making current at a given short-circuit power.

A short time (300 - 500 μsec) after the beginning of the flow of current i_1' (Fig. 2), switching device VU_1 comes into operation. It closes the line frequency oscillatory circuit $C_1 - L_1$, and a line frequency making current i_1 of a given amplitude passes through B.* With a corresponding selection of circuit parameters and times for the operation of VU_1, passage from the series connexion of the oscillatory circuits to their parallel connexion does not result in a complete break in the making current curve at that moment, (the current derivative does not vary more than 10 - 15 per cent).

After the first zero passage the increased frequency current is broken by device OU_1, and after the first zero passage the line frequency current is broken by OU_2. Metal shorting of the contacts of test circuit-breaker B occurs during making current i_1 flow and right up to the instant of its first zero passage.

In such a manner the second operation of the test cycle (making) takes place. In the developed circuit of the testing apparatus special capacitances are provided reproducing the discharge through the test circuit-breaker of the dropout line capacitances in the system. As is seen from what has been said,

* After operation of VU_1 in the circuit C_2-L, the current continues at a higher frequency i_1.

circuit-breaker testing for a given operation is accomplished in complete equivalent conditions since circuit-breaker making at full voltage is ensured and making current curve form and amplitude are reproduced, including the current derivative in the first instants of its flow. To correspond with these conditions provision is made in the circuit for the short-circuit current not to flow through the contacts for a large part of the time t_1 of metal short-circuiting. (Fig. 2).

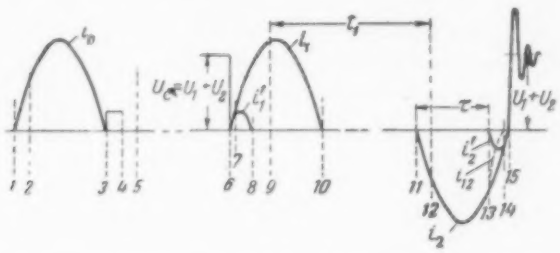

FIG. 2. Curves for currents and voltages with synthetic circuit-breaker testing in an automatic reclosure cycle.
1 – close VU_0; 2 – B contacts divergence; 3 – arc quenching in B; 4 – open RV_{01} and RV_{02}; 5 – close RV_1; 6 – spark-over between B contacts; 7 – close VU_1; 8 – open OU_1; 9 – metal shorting of B contacts; 10 – open OU_2; 11 – close VU_2; 12 – B contacts diverge; 13 – operation of P; 14 – open OU_3; 15 – tripping of B.

In the short interval before the B contact divergence in the third operation (repeated breaking) of the automatic reclosure cycle short-circuiting of the switching devices VU_2 and VU_2' occurs. Two oscillatory circuits adjusted to line frequency are connected in parallel to the test circuit-breaker and breaking device OU_3: $C_1 - L_1$ and $C_0 - L_3$. As a result the current in B and OU_3 will be equal to the sum of the currents in the two circuits, and the total current with an appropriate selection of parameters of test circuit $C_0 - L_3$ will have the same value as the making current in the preceeding operation.

After the divergence of B contacts, breaking current i_2 of a given amplitude flows through the arc formed. Almost simultaneously with B, the contacts of breaking device OU_3 break, and through it current $i_{12} = i_2$ flows for the first time.

An interval τ after current i_2 began to flow (Fig. 2) shift circuit P (Fig. 1) comes into operation, and an increased frequency current i_2' begins to flow in h.v. circuit $C_2 - C_3 - L_4 - L_3$ and the current difference through breaking device OU_3 is $i_{12} = i_2 - i_2'$. Current i_{12} passes through zero in 300-600 μsec before the current B does so, and the arc in OU_3 is quenched. The increased frequency current shorted through B flows in the series circuit formed from the two circuits $C_1 - L_1$ and $C_2 - C_2' - L_4 - L_2$ so that its derivative is the same as the line frequency current After arc quenching in B, the voltage $U_0' = U_1 + U_2 + U_2'$ recovers at its contacts.

The inductance L_4 and the voltage U_2' are selected according to the condition

of equality of making and breaking current derivatives:

$$\frac{U_c}{L_c} = \frac{U_1 + U_2}{L_1 + L_2} = \frac{U_0'}{L_0} = \frac{U_1 + U_2 + U_2'}{L_1 + L_2 + L_4},$$

where U_c, U_0' are respectively the making and recovery voltages;

L_c, L_0 are respectively the making and breaking circuit inductances.

It is obvious that the voltage U_2' can be selected at such a rating as to compensate for the damping of voltage U_2 in the making operation. If, for example, the making voltage must be equal to the recovery voltage, inductance L_4 is not connected and battery C_2' is contacted only to compensate for the damping of the charging voltage from battery C_2.

Thus, the third operation (repeat breaking) is performed in complete equivalent conditions, since even in the 300-600 μsec before current zero passage the test circuit-breaker is in a circuit where the voltage $U_1 + U_2 + U_2'$, the inductance $L_1 + L_2 + L_4$ and the capacitance determining the voltage recovery rate have the same values as in the actual line.

The circuit in Fig. 1 is extremely economical, since battery C_0 is used simultaneously as current source in the first breaking operation, and to compensate for current loss in the repeat breaking operation, while batteries C_1 and C_2 are used simultaneously for the two latter operations of the automatic reclosure cycle.

As experiments have shown, in testing a circuit-breaker during arc burning for one half-cycle of line frequency full compensation for current and voltage damping in the automatic reclosure circuit requires about 1.5 times more capacitors than for synthetic circuit-breaker testing for breaking capacity.

The circuit in Fig. 1 also permits circuit-breaker testing during arc burning for more than one half-cycle. In that case the frequency of circuit $C_0 - L_3$ will differ from the line frequency. A current flows through B in the latter breaking operation which, in the absence of losses, has the character of an oscillation beat, but with losses and appropriate selection of the test contour $C_0 - L_3$ parameters, it is practically undamped for several half-cycles, [3]. The shift circuit P comes into operation immediately before the last zero passage of the current in the test circuit-breaker. If the arc in B is permanently quenched, the circuit for artificially prolonging arc burning is switched on to it in parallel [3].

The breaking current in the first operation (breaking) can also be undamped when a test circuit has been connected in parallel to B in the same way as is done in the last operation, (circuit $C_0 - L_3$). However, in many cases the damping character of this current appears to be permissible, and in order to reproduce its effect on circuit-breaker operation in an automatic reclosure cycle the current amplitude must be slightly raised.

In testing circuit-breakers during arc burning of more than one half-cycle,

contact divergence in breaking device OU_3 is performed only after the beginning of the last breaking current half-cycle in order to avoid premature quenching.

Developed circuit (Fig. 3)

The circuit includes additional synchronizing apparatus for carrying out synthetic tests in the last two operations of the automatic reclosure cycle. Before the experiment is begun, switch RK is closed,* and ignition capacitances C_{i4} and C_{i3} are discharged through resistor R_3 ($R_3 \gg R_1$) to voltage $U_1 + U_2$.

With a spark-over between the contacts, capacitance C_{i4} is discharged through B (making operation) in the circuit C_{i4}, r, C_{i5}, R_1, IV, reproducing the capacitive discharge of the dropout lines to the circuit-breaker when it is connected to the short-circuit. The discharge circuit of this capacitance corresponds to an impulse generator circuit, and with the selection of the necessary parameters a given current impulse wave form can be produced.

Simultaneously with capacitance C_{i4} discharge, the voltage in resistor R_1 is increased leading to the operation of tri-electrode discharger P_5. Battery C_{i3} is discharged to resistor R_3, and its voltage is applied to the central electrode and sphere of switching device VU_1, (discharger of VEI construction). Discharge occurs between electrode and sphere. Arc formation is accompanied by considerable gas generation from the tube of gas-generating material set into the sphere. The gas ejected shortens the gap between the spheres, and switching device VU_1 closes. The duration of this process is 300 - 500 μsec from the instant of spark-over between the B contacts. The operation of discharger P_5 spheres does not result in a change in the impulse form of the current through the circuit-breaker, as the capacitance C_{i6} is substantially smaller than C_{i5}.

In the repeat breaking operation, the displacement of the instant when the increased and frequency current begins to flow relative to the beginning of line frequency current flow is controlled with the aid of a shift circuit consisting of a voltage transformer TN (Fig. 3) or a shunt-inductor connected to the B circuit, a synchronization circuit, an ignition circuit and dischargers P_3 and P_4 with devices for their operation.

The four electrode construction of discharger P_3 is due to its unusual mode of operation. The discharger must not function in the making operation during transient voltage recovery in breaking device OU_1 when the limit of this voltage is $2U_2$. Together with this in the repeat breaking operation the discharger on receiving the corresponding command to function must be in a circuit where capacitor battery C_2 voltage U_2 acts.* Finally, it must be seen that in the making operation when OU_1 contacts are closed the discharger is subject to the same voltage $U_1 + U_2$, relative to ground as is IV.

* To avoid premature operation discharger P_3 during charging of capacitance C_{i4}

† More accurately, voltage $U_2 + U_2'$; however voltage U_2' is applied to discharger P_3 even before the circuit begins to operate.

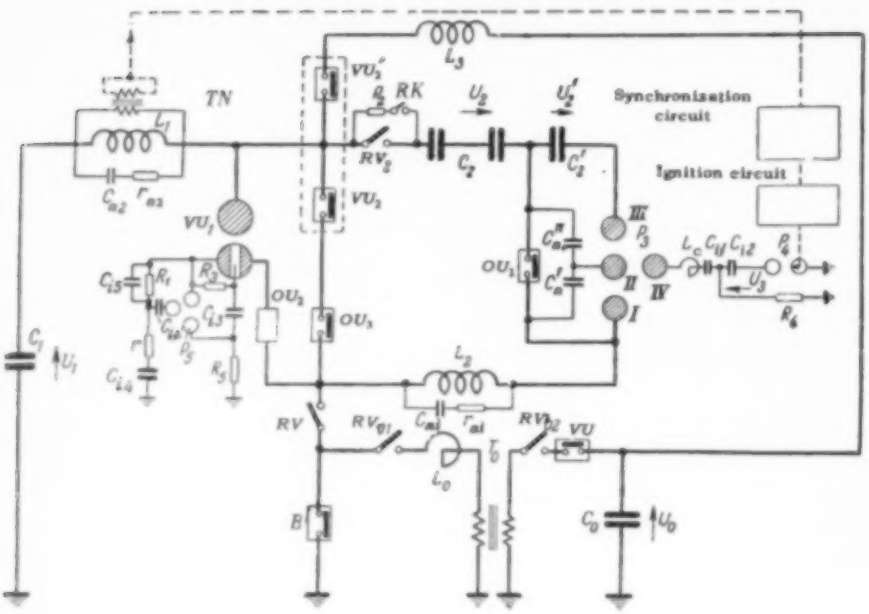

FIG. 3. Developed circuit of the testing apparatus.

This circuit for discharger P_3 makes it possible to satisfy the requirements previously indicated. The voltage recovered at OU_1 is distributed between two equal capacitances C_b' and C_b'', and therefore at each of them it does not exceed U_3. The discharge gaps *I-II* and *II-III* are selected by calculation so that they cannot operate at this voltage. When the impulse from the synchronization circuit is later received three-electrode discharger P_4 operates, and a voltage $[(\frac{U_3}{2} + U_3') + U_3]$ is applied between spheres *II-IV*, where U_3 is the charging voltage of capacitor C_{i_2}. With this a discharge takes place between spheres *II* and *IV*.

It must be noted that the arrangement of a small inductance coil L_c makes it possible to reduce the voltage U_3 somewhat, since after the operation of P_4 the voltage on spheres *II-IV* is in oscillatory operation. As a consequence, gap *II-III* is crossed since capacitance C_b' begins to be charged by capacitor battery C_{i_2} through capacitance C_{i_1} and inductance L_c. After this gap *I-II* also comes into operation after being subjected to the intense excitation of discharge gaps *II-IV* and *II-III*. Operation between spheres I-II is facilitated also by the circumstance that capacitance C_b' is charged during oscillatory operation, and the voltage on it can exceed $U_3 + U_3'$. The use of the fourth sphere makes it possible to withdraw it from the remaining spheres to such a distance as to prevent the operation of discharger P_3 on the voltage applied to *IV* in the making operation.

Controlled capacitances and resistances C_{b1}-C_{b4} and r_{b1}-r_{b4} are connected in parallel to reactors L_1, L_2, L_3 and L_4 in order to control the voltage recovery rate.

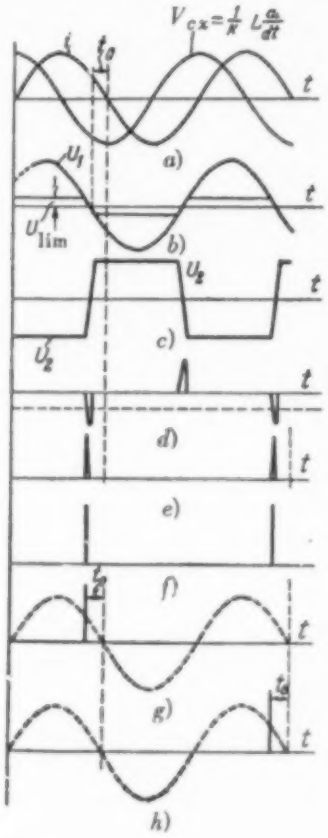

FIG. 4. Curves showing the method of operation of the synchronizing device.

The methods of operation of the synchronization circuit are explained graphically in Fig. 4. A voltage U_{cx} is supplied to the input of the circuit which is proportional to the breaking current i derivative (Fig. 4a). With the use of a phase bridge this voltage is shifted to a given angle after which the output bridge voltage U_1 is limited to the value U_{lim} (Fig. 4b). The voltage obtained is then boosted to U_2 and is supplied to a differentiating circuit, (Fig. 4c). As a result of the last two operations a voltage is obtained which is close in form to square pulses.

Therefore, in the instants after differentiation preceeding i current zero

passage for a given interval t_0 impulses of sufficiently short duration are developed (Fig. 4d) and amplified (Fig. 4e). The pulses are then supplied to a trigger mechanism developing powerful positive pulses of great steepness (Fig. 4f) which are transmitted through a special meter to the ignition circuit input (Fig. 3) immediately before one of the uneven zero passages of current i, (Fig. 4g and h). In order to produce a pulse before one of the even current zero passages, it is sufficient to vary the polarity of the input voltage U_{cx} of the synchronization circuit.

The circuit provides for great accuracy in synchronization, since its input voltage in the final analysis repeats the breaking current curve form, and the instant when the impulse is produced changes together with the variation in the i current curve form.

Results of tests

The synthetic circuit for testing circuit-breakers in an automatic reclosure cycle was put into practice in the laboratory of the TVN LPI where an air-blast circuit-breaker was tested.

Oscillograph characteristics are shown in Fig. 5 and 6 which were obtained by the use of vibrator and electron oscillographs, (Figs. 5b and 6b). In Fig. 5 an experiment is recorded for the testing of a circuit-breaker in the circuit shown in Fig. 3 without compensation for current and voltage losses, (circuit C_0-L_1 and battery C_2'); Fig. 6 records a circuit-breaker test using the complete circuit. The dotted curve on the oscillograph in Fig. 6 shows the current which in actual conditions flows through the metal shorted contacts of the circuit-breaker between the making and repeat breaking operations.

As is seen from the oscillograph (Fig. 5), without compensation for current and voltage damping the breaking current amplitude by the third operation of the automatic reclosure cycle is close to 25 per cent less than the making current amplitude. The recovery voltage is lowered by approximately the same percentage in comparison to the making voltage. As is known, damping of this order occurs with circuit-breaker testing in an automatic reclosure cycle in breaking capacity laboratories with impact generators in a full power circuit.

In circuit-breaker testing according to the circuit in Fig. 3 with the use of compensating circuits, current and voltage damping is completely eliminated, (Fig. 6); the amplitudes of all three currents and also the making and recovery voltages have similar values.

Electron-beam oscillographs show that the synchronizing devices developed make it possible to adjust the testing apparatus with great accuracy. Passage from series circuit connexion to parallel connexion in the making operation, and reverse passage in the repeat breaking operation occur without any substantial

change in the making and breaking current derivative, and the passage instants are within the limits mentioned above (t' and t'' in Figs. 5b and 6b).

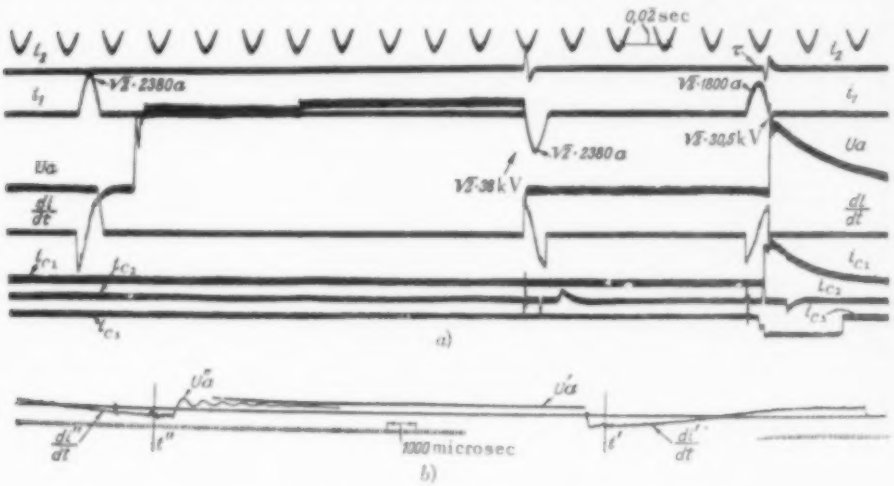

FIG. 5. Electromagnetic (*a*) and electronic (*b*) oscillograms of air-blast circuit-breaker tests in an automatic reclosure cycle in a circuit without compensation for current and voltage damping.

di/dt is the making current (*i*) derivative or breaking current (i''); i_2 is the h.v. circuit current; i_{c1}, i_{c2} and i_{c3} are secondary curves; i_{c3} indicates the instant of discharger P_4 operation (Fig. 3), i_{c2} the impulses developed by the synchronization circuit (Fig. 4d), and i_{c3} indicates the instants of impulse-meter and ignition circuit operation, (Figs. 3 and 4).

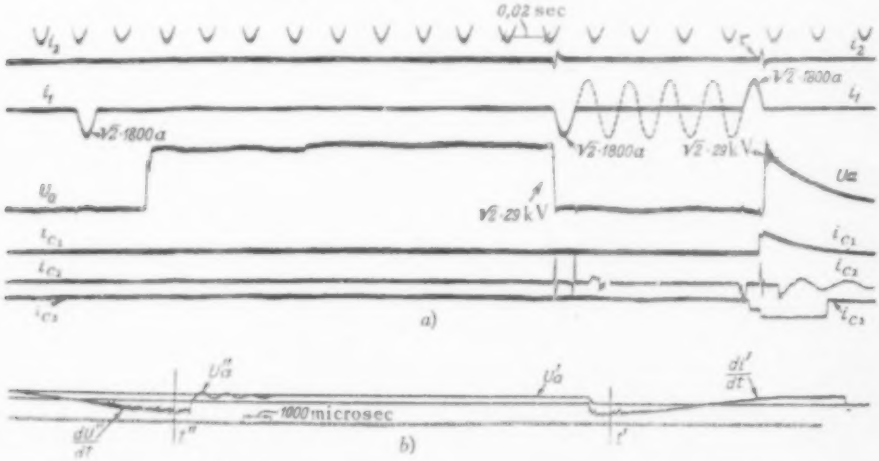

FIG. 6. Electromagnetic (*a*) and electronic (*b*) oscillograms of air-blast circuit-breaker tests in an automatic reclosure cycle. Letter designations are the same as in Fig. 5.

Conclusions

The circuit developed makes possible the solution of the extremely complex problem of a synthetic method of testing: equivalent condition testing of circuit-breakers operating in an automatic reclosure cycle. The circuit makes it possible to reproduce any correlation between making and recovery voltage.

Translated by F.J.C. Griffiths

REFERENCES

1. A.A. Gorev, V.V. Kaplan and V.M. Nashatyr'; Doukhchastotnyi kolebatel'nyi kontur dyla ispytaniya sverkhmoshchnykh vysokovol'tnykh vyklyuchetelei na otklyuchayushcohuyu sposobnost'. (Dual-frequency oscillatory circuit for testing high-power h.v. circuit-breakers for breaking capacity). *Elektrichestvo*, No. 6, (1951).
2. V.V. Kaplan and V.M. Nashatyr'; Metod issledovaniya v klynchaynshthei sposobnosti moshchnykh oyklyuchatelei vysokogo napryazheniya. (Method of studying the making capacity of powerful h.v. circuit-breakers). VEP, No. 2, (1957).
3. V.V. Kaplan and V.M. Nashatyr'; Issledovaniya otklyuchayushchei sposobnosti i nadezhnosti vnytrennei isolyatsii (Studies on the breaking capacity and reliability of the inner insulation of the MG-110 circuit-breaker). *Elektrichestvo*, No. 7, (1957).

THE ENERGY PROPERTIES OF AN ASYNCHRONOUS MOTOR WITH A SYSTEM OF IMPULSE SPEED REGULATION*

L.L. ROTKOP

ODESSA

In the present work an analysis is made of the energy characteristics of an asynchronous motor with impulse speed regulation by the use of feed-back signals indicating speed in order to attain steady mechanical characteristics (a relay system for automatic speed regulation working on the 'on-off' principle). Fig. 1 shows in block schematic form, the circuit of such a system.

The principle of operation of the circuit is as follows, [1–7]. With the application of a voltage to the motor its speed begins to increase and at a certain value of speed n_1 the input to the relay element reaches the pick-up value of the relay x_2 (n_1). When this happens the relay operates and the voltage U_1 at the output of the amplifier is reduced to a very small quantity, (if an amplifier-contactor arrangement is used, the voltage U_1 is reduced to zero). The speed of the motor falls, and at a certain speed n_2 the input to the relay falls to the release value, x_2 (n_2). The relay restores and the voltage U_1 at the output of the amplifier increases to its maximum. The speed of the motor again begins to rise to the value n_1 and so on. In this way the speed of the motor oscillates between the values n_1 and n_2 with a mean value $n_{av} = \frac{1}{2}(n_1 + n_2)$; the value n_{av} depends on the conditions of the speed arrangements in question. In place of the amplifier and relay element, a contact or a contact-less apparatus may be used. The permissible loading on the shaft of the motor over all ranges of the regulated speed is determined by the magnitude of the losses in the motor.

Over the normal range of operation of the motor in the system shown in Fig. 1, a self-oscillating regime is set up. In this, the period of oscillation consists of the periods of acceleration and deceleration of the motor.

To determine the losses in the motor it is sufficient to find the power loss per cycle. The motor losses during the time of deceleration are zero (the motor is switched off), or if a contact-less control system is used, practically zero. The

* *Elektrichestvo* No. 11, 38-42, 1958.

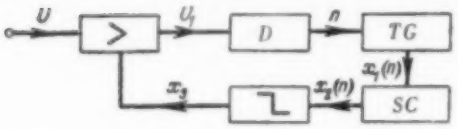

FIG. 1. Block schematic diagram of a system of control with impulse regulation of speed.
D – Asynchronous motor. *TG* – Tachogenerator. *SC* – Speed control.

motor losses during the period of acceleration from speed n_2 to n_1 will be:-

$$\Delta A_u = \int_0^{t_p} (k + v)\, dt = kt_p + \int_0^{t_p} 3I_2'^2 (r_1 + r_2')\, dt, \tag{1}$$

Where k, v are the permanent and variable losses in the machine.
t_u is the time of acceleration of the machine.
r_1 is the resistance per phase of the stator of the motor.
I_2', r_2' is the current and resistance of the rotor applied to the stator.

From the equations of the dynamics of transmission:

$$dt = -\frac{J\omega_0\, ds}{M - M_s}, \tag{2}$$

The losses in the motor, ignoring mechanical losses are:

$$3I_2'^2 r_2' = 9.81\, M\omega_0\, s. \tag{3}$$

Substituting (2) and (3) in (1) we get the losses per cycle.

$$\Delta A_u = kt_p + \frac{J\omega_0^2}{2}\left(1 + \frac{r_1}{r_2'}\right)\frac{M}{M - M_s}(s_2^2 - s_1^2)\, 9.81. \tag{4}$$

In deducing equation (4), it is assumed that the difference between the speeds n_2 and n_1 is fairly small so that the torque of the motor, the statistical torque and the phase resistance of the rotor may all be reckoned as constant during the time of acceleration.

Moreover, in equation (4), the losses from transient current components are not taken into account. These may reach fairly high values if the rotating motor is switched on; however, inasmuch as in impulse speed regulation the motor adapts itself by increasing the nominal slip, the transient components of the current are rapidly damped.

In using a contact control system, the masses of the system must be fairly large in accordance with the conditions of stability so that the number of times the motor is switched on does not exceed 200-300/hr, [1]. In this the time of acceleration of the motor appears a little greater than the transient components of the current and consequently the losses from its action can be ignored.

In using contact-less apparatus for control, the frequency of auto-oscillation of the system may be noticeably increased. In this case the voltage applied to the machine on switching on reaches a steady value in a time equal to the delay in the amplifier and relay. In this case the transient components of the current are fairly small and may be ignored.

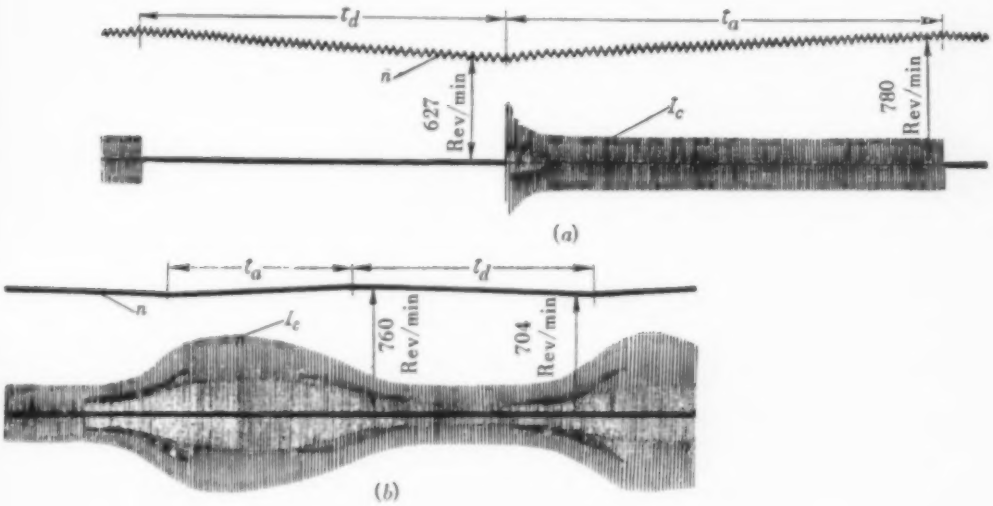

FIG. 2. Oscillograms of stator current I and speed n of an asynchronous motor AOS 51-4 in a relay system of speed regulation.
a – Using a contact apparatus for control, (contactor and relay); b – using a contact-less apparatus for control (magnetic amplifier and magnetic contact-less relay)

In Fig. 2 oscillograms of stator current and speed are shown for an asynchronous motor type AOS 51-4 in a relay system of speed regulation using contact control apparatus (contactor and relay) and also contact-less apparatus, (magnetic amplifier and magnetic contact-less relay). The oscillograms in Fig. 2 underline the validity of the assumptions made above.

The power loss per cycle will be:-

$$\Delta P_{\text{ц}} = \frac{\Delta A_{\text{ц}}}{t_p + t_d} = k\,\frac{M_s}{M} + M_s \omega_0 \left(1 + \frac{r_1}{r_2'}\right) s_{\text{av}} 9{,}81, \qquad (5)$$

where:- $t_a = \frac{J\omega_0}{M - M_s}(S_2 - S_1)$ – time of acceleration

$t_d = \frac{J\omega_0}{M_s}(S_2 - S_1)$ – time of deceleration. $(M = 0)$

$S_{av} = \frac{S_2 + S_1}{2}$ – average slip.

The power loss in the normal regime is:-

$$\Delta L_{nor} = k + M_{nor}\omega_0 s_{nor}\left(1 + \frac{r_1}{r_{2\,nor}'}\right) 9.81. \tag{6}$$

The permissible moment of load capacity of the machine for a different mean speed may be obtained from equations (5) and (6) using the relationship $\Delta L_{nor} = \Delta L_{nor} k_m$:

$$M_{sper} = A\frac{1 + z}{1 + \frac{A}{M}z} k_m, \tag{7}$$

where

$$z = \frac{k}{v}; \quad A = M_{nor}\frac{s_{nor}}{s_{av}} \cdot \frac{1 + \frac{r_1}{r_{2nor}'}}{1 + \frac{r_1}{r_2'}};$$

k_m – coefficient taking into account the deterioration of ventilation caused by a decrease in speed.

Comparison of equations (5) and (6) shows that with impulse speed regulation, the variable losses are increased and the constant losses are reduced in comparison with normal conditions. For a given mean speed, both the constant and the variable losses increase with increasing load. The reason for this is that during the period in the cycle the motor is switched off, the constant losses are zero, so that if the relative time of switching off is $t_a/t_a + t_d$ the load of the motor is increased or decreased by this ratio.

As a consequence of this, the characteristics of the energy properties with impulse speed regulation are different from the characteristics of other types of regulating systems in which the permanent losses are not usually dependent on the load.

Equation (7) has the form:

(a) For motors with normal performance, $(r_2' = r_{2nor}' = \text{const.})$

$$M_{sper} = M_n \frac{s_{nor}}{s_{av}} \frac{1+\alpha}{1+\frac{M_{nor}}{M}\cdot\frac{s_{nor}}{s_{av}}\alpha} k_m. \quad (8)$$

(*b*) For motors with increased slip, type AOS ($r_2' = r_{2nor}' = \text{const.}$)

$$M_{sper} = M_{nor} \frac{s_{nor}}{s_{av}} \cdot \frac{1+\alpha}{1+\frac{s_{nor}}{s_{av}}\frac{1-e^{-s_{nor}/0.2}}{1-e^{-s_{av}/0.2}}\alpha} k_m \quad (9)$$

where:

$$M = M_n(1-e^{-s/0.2}) \text{ [Л. 4].}$$

(*c*) For motors with phase rotors, the magnitude A in equetion (7) is defined by the formuln:

$$A = M_{nor}\frac{s_{nor}}{s_{av}}\left(1+\frac{r_{per}'}{r_{2nor}'}\right), \quad (10))$$

where: r_{per}' – is the additional resistance in the rotor circuit applied to the stator.

If simultaneously with the change in condition of the given system of speed control the rotor resistance is changed in accordance with the relationship

$$r_{per} = r_2\left(\frac{s_{av}}{s_{nor}} - 1\right),$$

then:

$$M_{s\,nor} = M_{nor}\, k_m. \quad (11)$$

(*d*) For motors with Shenfer rotors, with longitudinal slots and copper rings:-

$$M_{sper} = M_{nor\,sh}\frac{s_{nor\,sh}}{s_{av}}{}^{*}B\frac{1+\alpha}{1+\frac{M_{nor\,sh}Bas_{nor\,sh}}{M_n(1-e^{-s_{av}/0.4})s_{av}}}$$

in which

$$M = M_n(1-e^{-s/0.4}) \text{ [Л. 4];}$$

$$r_2' = k_1 r_{2nor}'\sqrt{s} \text{ [Л. 5]; } r_{2nor}' \approx r_1,$$

* Sh has been used for Shenfer

where, $s_{\text{nor sh}}$, $M_{\text{nor sh}}$, and M are nominal slip, nominal and permissible moments after changing the factory rotor.

$$B = \frac{(k_1\sqrt{0.2}+1)\sqrt{s_{\text{av}}}}{(r_1\sqrt{s_{\text{av}}}+1)\sqrt{0.2}}.$$

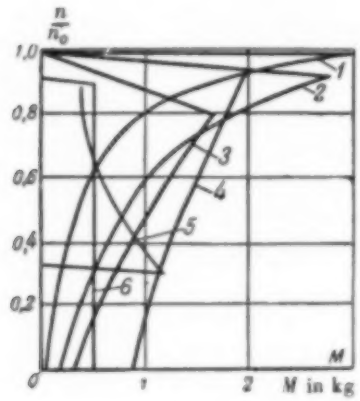

FIG. 3. Relationships between permissible moment and motor speed for motors of various performance. 1. Motor AO 51-4 2. Motor AOS 51-4 3. Motor AO 51-4 with Shenfer rotor. 4. Motor AK 51-4 5. D.C. motor, output 0.55 kW, speed 450-1450 rev/min 6. Motor PNZ 17.5. Output 0.8 kW, 1450 rev/min.

In Fig. 3, curves are plotted from equations (8), (9), (11) and (12) showing the relationship $M_{\text{s per}} = f(n_{\text{av}}/n_0)$ for motors of different design but of identical dimensions and weight, (80-84 kg). The values of the coefficient k_m for motors AO and AOS were taken from [6].

For the purpose of comparison, curves of the relationship $M_{\text{s per}} = f(n/n_0)$ for d.c. motors are also shown. The speed of the motors was changed by varying the supply voltage and the excitation current.

In both cases, motors were chosen with similar dimensions and weight, (80 kg).

In Fig. 4 are shown the mechanical characteristics $n_{\text{av}} = f(M)$ obtained experimentally and the relationships $M_{\text{s per}} = f(n_{\text{av}})$ plotted in accordance with experimental results and with equation (12) for an unventilated motor of 3 kW output, $n_a = 750$ rev/min, enclosed design ($(k_m = 1)$, with a Shenfer rotor using a system of speed control similar to Fig. 1, with a contact-less device for control (a magnetic amplifier and a magnetic contact-less relay). In practice, the

permissible temperature of the steel rotor was assumed to be 95° *C*. The curves in Fig. 4 show a degree of accuracy sufficient for practical calculations of the equations given above for the calculation of the permissible load of the motor for impulse systems of speed regulation.

From a comparison of the curves in Fig. 3, the following deductions can be drawn:-

(1) Motors of normal type are little suited to impulse speed control. From the viewpoint of the most suitable system for speed regulation over the whole of the range of regulation, one should choose a motor with increased nominal slip, of the AOS type with Shenfer rotor, enclosed and with a phase rotor. For low output motors up to 20 kW it is better to use a motor of the AOS type or with a Shenfer rotor as it is simpler and more reliable. For higher output units one may recommend the use of motors with phase rotors.

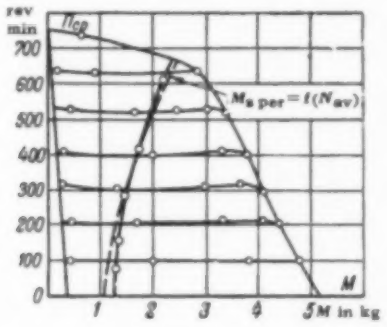

FIG. 4. — Mechanical characteristics and the relationships $M_{s\,per} = f(n_{av})$ for motors of 3kW output, $n_0 = 750$ rev/min, enclosed type, with Shenfer rotor and a speed control system similar to that in Fig. 1. with a contact-less control relay.

———— Experimental results.
---------- Calculated from Equation 12.

(2) For the regulation of speed with constant torque, the dimensions and weight of asynchronous motors with squirrel-cage rotors and of d.c. motors are approximately equal. For speed regulation in mechanisms where the torque is proportional to the speed ($M_s = N + Sn^d$) the dimensions and weight of the variable current motor are less than those for the d.c. motor.

(3) Over a sufficiently wide range of regulation when a d.c. motor-generator system is used, the dimensions of the impulse speed regulation equipment with an asynchronous motor is always less than that of the motor-generator system.

Consequently the installation costs of impulse speed regulation are considerably less than for a motor-generator system.

The coefficient of useful operation (c.u.o.) of a motor in a system of impulse speed regulation may be found from the expression:-

$$\frac{\eta_p}{\eta_{nor}} = \frac{P_p (P_{nor} + \Delta P_{nor})}{P_{nor}(P_p + \Delta P_q)}$$

or, substituting the values ΔP_{cyc}, ΔP_{nor} from equations (5) and (6) according to the formulae

$$\eta_p = \frac{n_{av}}{n_{nor}} \cdot \frac{as_{nor}\left(1 + \frac{r_1}{r_{2nor}'}\right) + \left(1 + s_{av}\frac{r_1}{r_{2nor}'}\right)}{\frac{M_{nor}}{M} as_{nor}\left(1 + \frac{r_1}{r_{2nor}'}\right) + \left(1 + s_{av}\frac{r_1}{r_2'}\right)} \eta_{nor} \qquad (13)$$

where: η_{reg}, $P_{reg} = 9.81\, M_s\, \omega_0\, (1 - s_{av})$ – the efficiency and output on the shaft of the motor when operating on the regulated characteristic.

η_{nor}, $P_{nor} = 9.81\, M_{nor}\, \omega_0\, (1 - s_{nor})$ – the same in nominal conditions. Equation (13) may be simplified if a contactor is used as an amplifier for the drive of an AOS type metor ($r_2' = r_{2nor}' = \text{const}$; $r_{2nor}' \simeq r_1$), since the first terms of the numerator and denominator are much smaller than the second terms, and so one may ignore them.

$$\eta_p = \eta_{nor} \frac{n_{av}}{n_{nor}} \frac{1 + s_{nor}}{1 + s_{av}}; \qquad (14)$$

For a motor with a Shenfer rotor:-

$$\eta_p = \eta_{nor\,sh} \frac{n_{av}}{n_{nor}} \cdot \frac{k_1 + \sqrt{s_{nor\,sh}}}{k_1 + \sqrt{s_{av}}} \approx \eta_{nor\,sh} \frac{n_{av}}{n_{nor\,sh}}. \qquad (15)$$

If a contact-less device (magnetic amplifier) is used in the main circuit of the motor, in equation (13) the magnitude r_1 will comprise the total resistance of the stator winding and of the amplifier. In this case the value of the efficiency is slightly reduced and for an AOS type motor equation (13) may be represented in the form, ($r_2' = r_{1\,nor}' = \text{const}$): $r_{1\,nor}' \simeq r_{1d}$)

$$\eta_p = \eta_{nor} \frac{n_{av}}{n_{nor}} \cdot \frac{1 + s_{nor} \dfrac{r_{1d} + r_{amp}}{r_{1d}}}{1 + s_{av} \dfrac{r_{1d} + r_y}{r_{1d}}}, \tag{16}$$

Where: r_{1d} – is the resistance per phase of the stator winding of the motor.

r_{amp} – is the resistance per phase of the amplifier.

Equations (13) – (15) show that the efficiency of a motor in a system of impulse speed control at any given speed is independent of the load on the shaft. This is in consequence of the particular power characteristics shown above for impulse regulation.

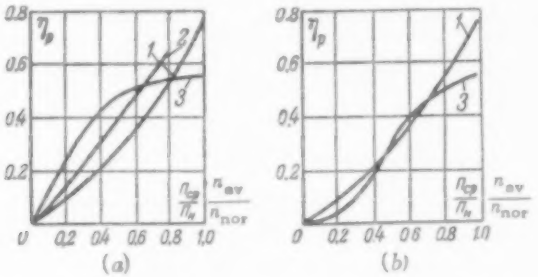

FIG. 5. Relationship between efficiency of the motor η_{reg} and speed n_{av} of the machine with (a) M_s = const. and (b) $M_s = Sn$.

1. Motor, AOS 51-4 type. 2. Motor, AO 51-4 type with Shenfer rotor. 3. Motor PNZ – 17.5 in a motor-generator system.

Fig. 5a shows the characteristics $\eta_{reg} = f(n_{av}/n_{nor})$ for an AOS 51-4 motor plotted according to equation (14), a motor AO 51-4 with a Shenfer rotor plotted according to equation (15) and a motor PNZ 17.5 with M_s = const. in a motor-generator system. The systems of impulse regulation with M_s = const. have a lower efficiency than those with direct current.

Fig. 5b shows curves of the efficiency for the same machines with speed regulation of the mechanism when $M_s = Sn$. If the torque of the transmission mechanism is proportional to the speed to a power higher than the first, the efficiency of the impulse system may show a larger value than that of the motor-generator system.

In Fig. 6 the curves are drawn showing $\eta_{reg} = f(n_{av})$ as obtained by experiment and by calculation from equation (16) for an AOS 51-4 motor with a speed control system as in Fig. 1, using a magnetic amplifier in the main circuit and a

magnetic contact-less relay in the control circuit, [7]. The curves in Fig. 6 show that the equations given above are accurate enough for demonstrative calculations of the efficiency of a system using impulse speed control.

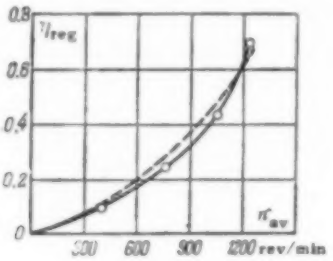

FIG. 6. Curves of the relationship between efficiency. η_{reg} and speed n_{av} of an AOS 51-4 motor in a system of speed control similar to Fig. 1.

———— Experimental results.

---------- According to equation (16).

For comparison of the power characteristics of the different systems of regulation, it is essential to make the comparison according to the integral characteristics of the regulating cycle, [3]. If, in the range of regulation D and the number of steps m, each speed step is accomplished in the same time interval, then the efficiency of the regulating cycle may be obtained from the equation, [3]:

$$\eta_{u.p} = \frac{\sum_{1}^{m} P_{pq}}{\sum_{1}^{m} (P_{pq} + \Delta P_{uq})}, \tag{17}$$

Where, P_{pq}; ΔP_{cyc} – are the useful power and loss of power at the qth. regulating step.

Since $$P_{pq} = \frac{M_{cq} n_{cp.q}}{975}; \quad P_{pq} + \Delta P_{uq} = \frac{P_{pq}}{\eta_{pq}}$$

and if the difference in speed for the two selected steps is equal when $m = 1$, $n_{av} = n_{nor}$, then for $m \to \infty$ for an AOS type motor:

$$\eta_{u.p} = \frac{\left(1 - \frac{D-1}{2D}\right)\eta_{nor}}{1 + s_{nor} + \frac{n_{nor}}{n_0}\cdot\frac{D-1}{2D}} \approx \eta_{nor}\frac{D+1}{3D-1}. \tag{18}$$

This, the equations introduced above enable us to analyse the power characteristics of a system with impulse regulation of speed approximately but quite fully.

Translated by F.P. Froom

REFERENCES

1. N.N. Krechtovich; Elektroprivod s impul'snym upravleniem skorostyu asinkhronnogo dvigatelja. Electrical transmission with impulse control of the speed of an asynchronous motor). *Elektrichestvo:* No. 3 (1956).
2. E.P. Sarkisyan; Impul'snyisposob upravlenija elektroprivodom s asinkhronnymi dvigateljami (An impulse system of control for electrical transmission with asynchronous motors) Dissertation.
3. A.T. Golovan; *Elektroprivod (Electrical Transmission).* Gosenergoizdat (1948).
4. V.V. Gorskii; Aproksimirovanie mekhanicheskoj kharakteristiki asinkhronnykh dvigatelyei. (An approximation of the mechanical characteristics of an asynchronous motor). *Elektrichestvo;* No. 3 (1957).
5. A.G. Ivakhnenko; *Avtomaticheskoye reguliravanie skorosti asinkhronnykh dvigateljei nebol'shoi moshchnosti. (Automatic regulation of speed for low-output asynchronous motors). Annals Akad. Nauk S.S.S.R.* (1953).
6. V.I. Vasin; *O regulirvanai i skorosti korotkozamknutykh asinkhronnykh dvigateljei. (On the speed regulation of squirrel-cage asynchronous motors).* VEP No. 9 (1956).
7. L.L. Rotkop; *Impul'sny metod regulirovanja skorosti asinkhronnogo dvigatelia c primeneniem beskontaktnoi apparatury upravleniya. (An impulse method of speed regulation for an asynchronous motor by the use of a contact-less control apparatus).* VEP. No. 1 (1958).

1959

ON THE CONDITIONS OF THE FORMATION OF FLASHOVER OR ARCING ON TO THE FRAMEWORK OF TRACTION MOTORS*

A.S. KURBASOV

All-Union Scientific-Research Institute of Rail Transport

(Received 2nd August, 1957)

As a result of investigations carried out by various authors [1-4], it has been established that with d.c. high-voltage machines (among which are traction motors usually utilized on electrified railways), the principal cause of flashover or arcing on to the framework are the conducting bridges between adjacent commutator segments caused by fragments from the brushes or by formations of carbon dust. In [4] it was shown that single flashes from shortings, having a high initial resistance (the appearance of such bridges is most probable in operating conditions), easily occur when the maximum intersegmental voltage is greater than 33-34 V; this after all is the ignition voltage of a flash.

To determine the maximum current of a single flash I_m for a specific machine, the following simple expression is recommended:

$$I_m = \frac{U_m - U_d}{z},$$

where U_m is the maximum intersegmental voltage; U_d is the voltage necessary for maintaining the flash, equal to 26-28 V for copper commutator segments; and z is the total resistance of the part of the winding connected to two adjacent commutator segments.

Reference [4] is a continuation of the study of the conditions of the passage of a single flash on to adjacent commutator segments, that in the end must lead to flashover and the study of the conditions of arcing of a single flash on to the framework of a traction motor. Appropriate experiments have been conducted by the author, the results of which are presented here.

* *Elektrichestvo* No. 11, 55-58, 1958.

For conducting the experiments to investigate the conditions of the arcing of a single flash on to adjacent commutator segments, an experimental installation, described in [4], was completed with one circuit having defined parameters, (Fig.1). Vectors of the e.m.f. in circuits I and II had a similar direction that sufficiently well suits the co-ordination in time of the intersegmental voltages for two adjacent pairs of commutator segments. Owing to the presence in the circuit of a thyratron, the circuit of transformer T_1 was connected up when the value of the network voltage was zero.

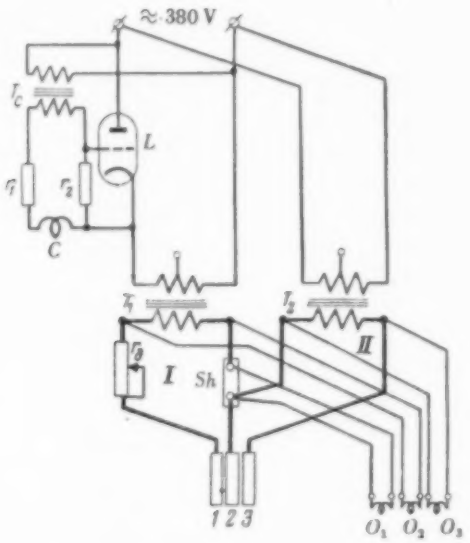

FIG. 1. Circuit of the installation for determining the conditions of the formation of flashover from flashes between two neighbouring commutator segments. T_1, T_2, T_c – transformers; L – thyratron; sh – shunt; r_1, r_2, r_d – resistors; C – choke; 1, 2, 3 – commutator segments; O_1 O_2, O_3 – oscillograph oscillators; I and II – circuits of the scheme.

On conducting the experiments a single flash was induced with the aid of shortings on to commutator segments 1 and 2 (circuit I); the current of this flash was regulated by resistor r_d and was registered by oscillator O_1 of the oscillograph. The presence of arcing on to commutator segments 2 and 3 (circuit II) was determined by oscillator O_2.

On the commutator segments of some traction motors the effect was verified of the change of the maximum voltage of circuit II in the conditions of the arcing of a single flash on to the adjacent commutator segments. It was established that

by changing the maximum voltage of circuit II from 35-60 V with one and the same commutator division (for segments of one and the same motor), for the formation of a flash to commutator segments 2 and 3 it was necessary to have one and the same current for the starting flash. Clearly, in order to obtain the arcing of a flash it is necessary that its flame links adjacent commutator segments. Conditions for the breakdown of the gap in the conditions under examination are probably lightened at a voltage on the commutator segments (2 and 3), which considerably exceeds what is possible on usual d.c. machines.

Thus, it was discovered that the maximum current of a flash in circuit I, inducing a flash to the adjacent pair of commutator segments, is solely dependent on the magnitude of the commutator division [$I_m = f(\beta_{com})$]. This dependence reflects the conditions of the transition of a single flash into a flashover which is ultimately an electric arc shorting either a considerable part of the commutator segments or all the commutator segments situated between brushes of unlike polarity. Experiments were conducted with a voltage on circuit II equal to 37-39 V; the speed of the air being blown past the commutator segments amounted to 15 m/sec. Below is established the effect of a change of this speed on the magnitude of the current I_m inducing arcing on to an adjacent pair of commutator segments.

In Fig. 2 are represented the characteristic oscillograms of the experiments connected with the investigation of the conditions of the passage of a single flash on to a neighbouring pair of commutator segments.

On the right-hand oscillogram (Fig. 2b) is registered by oscillator O_3 a flash on to commutator segments 2 and 3, indicated by a characteristic change of voltage on these segments. With the corresponding experiment for the left-hand oscillograms, there was no arcing of a flash on to the adjacent commutator segments.

Fig. 3 shows the experimental dependence $I_m = f(\beta_{com})$; Fig. 4 shows a curve making it possible to judge how the current I_m required for the formation of a flash on to segments 2 and 3, varies depending on the speed of the air v blowing on the commutator segments. From this curve it follows that in the zone of speeds exceeding 12 m/sec, I_m varies insignificantly, (these speeds are typical for the ordinary duties of traction motors). From the above relationship $I_m = f(\beta_{com})$, one may conclude that for railway traction motors in which there may arise powerful single flashes with a maximum current of up to 2000 A, the passage of these flashes on to adjacent commutator segments is inevitable; for auxiliary machines, in which the maximum current of a flash amounts to 40-100 A, the subsequent development of a single flash is difficult. These conclusions are well confirmed by experiments in the operation of the machines referred to.

A single flash – apart from the flashover, the electrodes of which are the commutator segments – may lead to a breakdown of the gap between the commutator

and the framework; that is, it may lead to "arcing". Careful research into the conditions of the incidence of arcing, involves a considerable complication of the

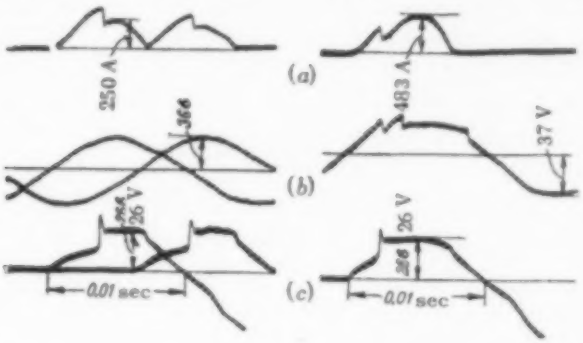

FIG. 2. Characteristic oscillograms of tests for determining the current of single flashes producing arcing on to adjacent pairs of commutator segments.
a) current of the initial single flashes; *b)* voltage on the commutator segments, to which the initial flash must pass; *c)* voltage of the initial single flash.

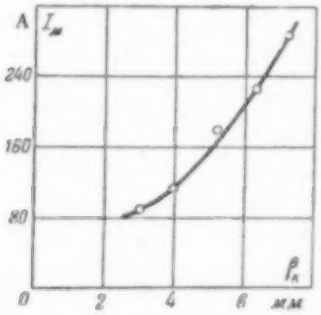

FIG. 3. The dependence of the maximum current of a flash, inducing arcing on to an adjacent pair of commutator segments, on the size of the commutator division.

original experimental plant, as in this case it is necessary to reconstruct near the commutator segments an electric field and a field of the speed of the blowing air exactly the same as in real traction motors. To produce an installation appropriate in full measure to the stated conditions was impossible even though the difficulties connected with such an accomplishment can quite be overcome. In connexion with what has been explained, experiments were carried out for investigating the conditions of arcing of single flashes on to the section of the framework situated

over the commutator and on to the bearing guard, without blowing air on the commutator segments.

The arcing of a single flash on to the part of the framework situated over the commutator is most probable, as in this direction stream powerfully ionized gases from a single flash, owing to the powerful flow of convection; arcing on to the bearing guard also seems possible in so far as it is nearer than other components of the framework, being situated near the commutator. The individual parts of the framework on to which arcing is assumed, were made of aluminium segments and coated with the varnish normally used for painting the internal walls of the traction motor frame.

The electrical circuit of the installation for investigating the conditions of arcing of single flashes on to the framework is shown in Fig. 5. This circuit makes it possible to vary the voltage U_{com} between the commutator segments and plate A from zero to 5 kV. By the matching of resistors r_1 and r_2, the inducements are eliminated in oscillator O_2 by which is registered the presence of arcing of the single flash on to the plate, which acts as a part of the framework of a traction motor.

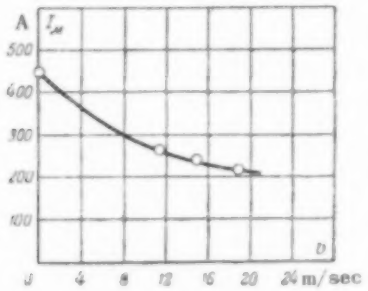

FIG. 4. The variation of the maximum current of a flash inducing arcing on to an adjacent pair of commutator segments, dependent on the speed of the air blowing on them with a constant value of commutator division.

In the experiments flashes were formed on the commutator segments by a short from a fragment of a brush with different values of voltage U_{com} (1, 2 and 3 kV) and different distances l between commutator segments and plate A. A characteristic oscillogram of a flash which produced arcing on to plate A is shown in Fig. 6.

After a large number of tests, the dependence was plotted of the maximum current of a flash – inducing a flashover on to the framework with voltages of 1, 2 and 3 kV – on the shortest distance between the commutator segments and the plate

acting as a section of the framework. This dependence is shown in Fig. 7. From an examination of Fig. 7, it follows that the variation of voltage U_{com} within the indicated limits has but small influence on the conditions of the arcing of a single flash on to the framework. Arcings were registered only when the flame of the flash touched or came very close to the plate acting as a section of the framework. It follows clearly that a breakdown from flashes with minor intensities can only be expected with voltages U_{com} measuring dozens of kV.

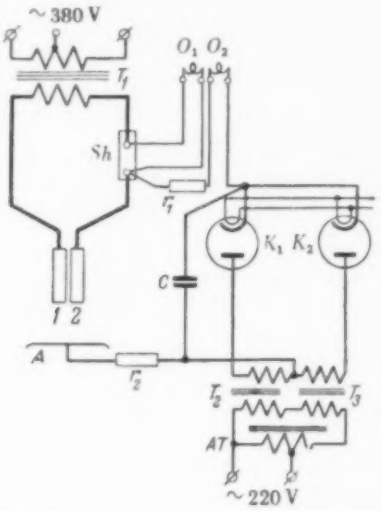

FIG. 5. Circuit of the installation for determining the conditions of the arcing of a single flash on to the framework of a traction motor.
AT – autotransformer; T_1T_2, T_3 – transformers; K_1, K_2 – kenotrons; r_1, r_2 – resistors; C – capacitor; sh – shunt; 1, 2 – commutator segments; A – screen acting as the machine frame; O_1, O_2 – oscillograph oscillators.

From the dependencies obtained, it follows that traction motors have such design dimensions and winding parameters that arcing of single flash on to the framework is fully possible. Thus, the traction motor DPE-400 I_m = 1800 A, has a minimum distance from the commutator to the part of the framework situated over the commutator of 140 mm.

A rather unexpected result was obtained when investigating the conditions of arcing of a single flash on to the bearing guard. Several dozen tests were arranged with various distances between the plate acting as the bearing guard, and the commutator segments, for flashes with different intensities, and yet arcing was not registered even with l = 35 mm, I_m = 1800 A and U_{com} = 3 kV. From these

tests it follows that the arcing of a single flash on to the bearing guard is difficult. When carrying out more careful investigations in this direction, the field of the speed of the air blowing on the commutator has to be taken into account.

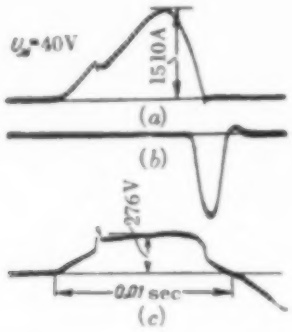

FIG. 6. Characteristic oscillograms of tests for determining the current of a single flash, inducing arcing on to the framework. *a* – current of a single flash; *b* – current of oscillator O_2, recording the arcing of a single flash on to the framework; *c* – voltage of a single flash.

From the results of the investigations carried out, it is possible to answer the following questions:

(1) Whether a single flash occurs in a given machine;
(2) If a single flash occurs, then what its intensity is;
(3) Whether a single flash of a given intensity will lead to flashover or arcing.

Consequently it is possible to select parameters of a d.c. machine with which flashover or arcings caused by short-circuits are impossible.

It follows from the dependencies introduced above, that the prevention of the development of a single flash into a flashover or arcing is rather difficult in the case of powerful machines having a possibly great intensity of single flashes. This would involve either an inordinate increase of the dimensions of the commutator (increase of the commutator division), or a considerable complication of the winding, (introduction into the section of the armature of an additional resistance, fitted near the risers of the commutator). For preventing flashovers and arcings it is necessary to take measures to stop the rise of the single flash. Certain possible measures as well as avenues for further investigation in this direction are set out in [4].

The basic mathematical criterion, determining the possibility of the appearance of the single flash, is necessarily considered to be the maximum permissible

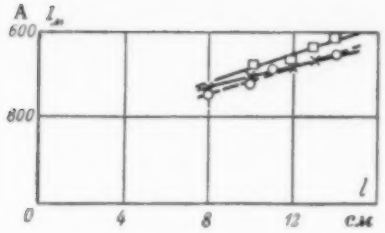

FIG. 7. Dependence of the maximum current of a single flash causing arcing on to the framework, on the shortest distance to the part of the d.c. machine frame situated over the commutator, with various values of voltage between the commutator and the framework.
○– U_{com} = 3 kV; □– U_{com} = 2 kV; ×– U_{com} = 1 kV.

intersegmental voltage, equal in the case of the existing design of commutators, to 33-34 V.

Translated by David Rex-Taylor

1959

REFERENCES

1. A.B. Ioffe; Potentsialnye usloviya na kollektore i puti ikh oblegcheniya. (Potential conditions on a commutator and the means to their alleviation). *Elektrichestvo*, No. 1 (1954).
2. M.D. Nakhodkin and V.S. Khvostov; *K voprosu o prirode krugovogo ognya na kollektore visokovol'tnykh mashin postoyannogo toka. (On the question of the nature of flashover on to commutators of high-voltage machines).* V.E.P., No. 4 (1956).
3. B.S. Sukhorukikh; *Issledovanie svoist dugi na kollektore i primenenie dugovikh kharakteristik pri analize protsessa vozniknoveniya i razvitiya krugovogo ognya v tyagovikh dvigatelyakh. (Investigation of the characteristics of arcing on a commutator and the application of arcing characteristics for the analysis of the process of the rise and development of flashover in traction motors).* Dissertatsia TsNII, MPS (1956).
4. A.S. Kurbasov; *Issledovanie uslovii vozniknoveniya i razvitiya vspyshek na kollektorakh tyagovykh elektrodvigatelei. (Investigation of the conditions of the rise and development of flashes on the commutators of electric traction motors).* Vestnik Vsesoyuznogo Nauchno-issledovatel'skogo instituta zheleznodorozhnogo transporta, No. 2, (1957).

ABSTRACTS FROM PAPERS PUBLISHED IN ELEKTRICHESTVO No. 11, 1958.

Experimental study of power system performance characteristics: S.A. Sovalov, S.I. Leznov and M.I. Smirnov. (pp 1 - 7).

The author sets out the main results of experimental investigations made in the summer of 1957 in the Inter-connected Power System Centre into the variations of frequency in a power system in the presence of control and automatic control and the character of the total load variations as well as the experimental determination of the total (frequency) statism (statism is defined as the division of the controlled magnitude on rated load from its value on no-load expressed as a percentage of its value on no-load) of the power system, the slope of the static load characteristic, the initial speed of change of the frequency in the presence of a sudden disturbance of the active power balance with an equivalent mechanical inertia constant. The results are valuable for questions of frequency regulation and for analysing normal and fault power system conditions.

Economic evaluation of energy losses by comparison of various schemes for the construction of power installations: D.S. Stepanov. (pp 7 - 10).

Only correct estimation of the power losses to be expected in planned power systems and in existing installations enables the most economic choice to be made, for instance, of conductor cross-sections, and transformer powers, distribution network voltage, transmission voltage, the position of substations and condenser stations and so on. Here he adds the recurrent cost of the power losses on full load of the system to the once and for all capital cost of erection. The article represents a strictly economic appraisal of the methods of evaluating the cost of power transmission.

Unbalanced bridge circuits for measuring corona losses: N.P. Emelianov and L.I. Tsepliaev. (pp 11 - 14).

When measuring corona losses the main difficulty is the extremely low power coefficient of the circuit to be measured. In order to improve the power coefficient the line charging current is now compensated in the U.S.S.R. by four arm bridge schemes. A calibrated high-voltage condenser is used for one arm and the corona producing line is used for another high-voltage arm. The phase displacement difference for the high-voltage arms should equal the phase displacement difference

for the low-voltage arms. Assuming there is no leakage in the calibrated condenser and the experimental line before corona, elements should be used for the low-voltage arms which give the same phase shift; i.e. capacitances or resistances. In practice, owing to the leakage of the calibrated condenser for compensation of the bridge in the pre-corona condition of the line, it is necessary additionally to introduce (1) resistances into the arms in the scheme with capacitances in the low-voltage arms and (2) capacitances into the scheme with resistances. When corona arises on the line the bridge is not compensated and becomes unbalanced. The author treats the problem mathematically. In certain conditions he recommends the connexion of a current winding of a wattmeter in the bridge diagonal and a voltage winding at a voltage proportional to line voltage.

Constructing locus diagrams for an induction motor with a saturable reactor: F.N. Zuikov and A.I. Khozhainov. (pp 14 - 18).

Saturable reactors are now used as the power elements of automatic control and regulation systems of cranes, winches, pumps and so on. Investigation of these systems is carried out by graphical-analytical methods. The author investigates the locus of an induction motor with a saturable reactor in the stator circuit when the currents and voltages are sinusoidal in all operating conditions. The author relates the inductive resistance of the reactor to the inductive resistance of the stator and then on the basis of the equivalent network shown in the text and taken from Kostenko's work 'Electrical Machines' 1949 he derives the total equivalent resistance of the main circuit. He introduces a circular diagram of an induction motor for different values of resistance when the equivalent inductive resistance of the reactor in the stator circuit is constant. Other diagrams show the curve and ellipses of simultaneous steel magnetization, the relationship between the equivalent inductive resistance of the choke and the slip for different values of magnetization current (const.), current circles for two limiting values of the equivalent inductive resistance of the reactor when the magnetization current is constant and comparative experimental and calculated relationships between the active current component and of ϕ s for different values of magnetization current (const.).

Several basic circuits for the autodyne: O.V. Benedikt. (pp 24 - 29).

The author considers certain feedback circuits for an autodyne and typical properties and fields of application of autodynes. He assumes the autodyne has a slipping stator excitation winding as this is not important in principle. After showing an example of a feed-back circuit he considers three cases when static conditions are disturbed: a change in the speed of the armature, in the voltage and in the voltage level. Unlike the motor-generator, the autodyne is a source of stabilized voltage. The relationship due to hysteresis between the voltage and the voltage level is then shown diagrammatically for test autodynes A2-B, A-3B and A-6B which have windings compensating the influence of friction on the

torque. The autodyne is considered in circuits as a power converter, and as an automatic regulator of other equipment. The different circuits are shown diagrammatically. Rotor over-excitation of the autodyne is also discussed.

Coefficient of commensurability at feeding an induction motor from the synchronous generator: Ia. B. Kadymov and M.M. Rasulov. (pp 35-38).

The operating conditions of a synchronous generator operating in an autonomous system are determined by the relationship between the power of the generator and the motor connected thereto. If the power of a short-circuited motor is commensurate with the generator power, then the power at the generator terminals can decrease to values at which the stable operation of the remaining consumers becomes impossible and the motor will not start. In order therefore to start the motor reliably, it is necessary to choose the right power relationship of the motor and generator. This relationship (the coefficient of commensurability or the relationship between the reactances of the generator and motor), is then established and the author considers the value of a system of automatic control of excitation of synchronous generators for increasing the coefficient of commensurability. The method of determining this coefficient is then examined for the case when the parameters of the machines are familiar and when different methods of regulating excitation are employed. Two examples of the calculations are given.

Inverter duty of type RMNB-500 × 6 rectifiers: L.S. Fleishman and M.V. Gel'man. (pp 43-46).

Recuperative braking on electric railways requires the conversion of one or several rectifiers to inverter duty when there are no other d.c. consumers. The unstable operation of the rectifier on inverter duty can cause a break in recuperation. Until recently the RMNB-500 × 6 rectifiers have been defective on inverter duty. The article considers the causes of instability of an inverter which have been investigated in the mercury arc rectifier laboratory of the Ural electrical apparatus works and gives the results of tests after taking special steps to improve the reliability of inverters. The author considers three inverter schemes: (1), with two reverse (inverse) stars and balancing reactor, (2), with a three phase bridge scheme and (3), with a six-phase zig-zag. The value of synthetic schemes is discussed. Shunting circuit valves and a cathode reactor were installed with an inductivity of 50-100 mH, which improved reliability considerably.

Transients in a motor drive with reactor control of the winch in a multi-scoop drag: L.F. Shkliarskii. (pp 47-50).

A previous article by the author "Automation of the Electrical Drive of a Multi-scoop Drag", Elektrichestvo, 1, 1957, considered the calculation of the static mechanical characteristics of the winch of multi-scoop dredges with an additional resistance in the rotor circuit of the induction motor and a saturable choke (reactor) connected asymmetrically in two phases of the rotor. The present article

follows on with an analysis of the transient processes arising in such drives. In view of the complexity of transient phenomena the author considers a simple and practical method of calculating these transient processes is desirable. The method is based on the use of the static characteristics which can be derived from the catalogue data of the motor and reactor. Laboratory investigations show that the error in the calculations is not over 10 per cent.

Motor-generator drive with a rotary and magnetic amplifier: A.V. Basharin. I.N. Vinogradov. A.I. Vychkov. and J.B. Byval'kevich. (pp 51-55)

To improve and develop reverse d.c. drive, rotating machine (rotary) amplifiers, semiconductor rectifiers and recently magnetic amplifiers have been employed. The quality of such systems was first measured by the degree to which the current diagram was filled. Originally the current diagram was considered to be rectangular. Then other shapes (e.g. triangular shape) were recognized to be optimum in certain cases. Later it was established that when the time of the transient processes had to be a minimum or when the system of drive had to be most productive, the "coefficient of current diagram filling" can characterize the quality factor of the control system. The present article acquaints the reader with the system of drive developed by the Faculty of Industrial Electrification of the Lenin Institute of Electrical Engineering in Leningrad. The system is based on the use of magnetic amplifiers and symmetrical semiconductor ceramic non-linear resistances. This system conforms to the best static and dynamic characteristics plotted from the maximum coefficient of current diagram filling according to the system developed by the TsKB "Elektroprivod" with matched cut-offs. The Lenin Institute system however needs to use a minimum of contact apparatus for starting, reversing and braking (without creep speeds).

Ferrites with a rectangular hysteresis loop: L.J. Robkin. B.Sh. E'pshtein and Ia. G. Koblents. (pp 59-68).

Such materials have been widely used in the memory apparatus of digital computers and "answer" computers, automatic control apparatus, magnetic amplifiers, non-linear elements for multiplying frequency, communications apparatus and so on. The paper is intended to acquaint a wide circle of engineers with the methods of production, the application and the main parameters and characteristics of certain Russian ferrites with a relative residual induction > 0.85.

Protective relaying on the basis of the "Hall effect." V.K. Sirotko. (pp 69-71).

The "e.m.f. Hall pick-up" employed in the Electromechanical Institute of the Academy of Science U.S.S.R. is shown. The design of the apparatus is considered and its method of operation. Calculations and experiments have shown that the executive relay device based on the "Hall effect" and having approximately the same sensitivity as the best inductance relays has a minimum power consumption on operation of 10^{-4} ... 10^{-5} W. To evaluate the speed of operation of the relays

1959

and study their behaviour during transient processes in long distance transmission lines, a short-circuit was imitated both inside and outside the operating zone of the relay. No incorrect operation of the relay was recorded. The operating time of the relays in the presence of short circuits within the protected zone did not exceed 10 msec.

A telemechanical system using magnetic elements with rectangular hysteresis loops: V.A. Tutevich. (pp 72-73).

There are good prospects for the development of contactless elements especially magnetic elements with rectangular hysteresis loops which can operate from an a.c. network and thereby facilitate the construction of simple telemechanical systems. Such magnetic elements embody the cyclical and continuity principles based on the division of ducts using a distributive unit and the synchronization of the transmitting and receiving points of the telecontrol system. The system can either signal the state of eight objects, (the operating time of three of them being fixed by a scheme made from filamentless thyratrons), or, control five objects, (three signals being used here for calculating the products by filamentless thyratron counters), or finally, control only two objects, (six signals being used for operating three differential filamentless thyratron counters). Continuous registration of indications is effected. The transmitting and receiving commutators are synchronized. The system can be used for transmitting orders as well as for indication and counting.

A quick method of appraising the danger of electrical sparking: P.A. Fetisov. (pp 74-78).

There is a large number of explosive mixtures of gas and air which need to be calculated to produce appropriate spark-proof equipment. These calculations take an exceptionally large amount of time. The new quick method is based on (1) the relationship obtained between the probability of ignition when the ignition current varies, (2) the fact that each mixture has a definite point in relation to other mixtures which determines its capacity to ignite from an electric spark and, (3) the curves of the probability of explosion of mixtures investigated by the author are practically parallel. His method is explained and illustrated by diagrams and test results are tabulated. The new method is quicker and explosion-proof characteristics can be plotted in the voltage range up to 60 V and with an inductance of 1 H at one or two experimental points. The difference between the results achieved by the old metnod is 4-5.5 per cent. The article was written with the requirements of the chemical industry in mind.

An over-voltage recorder for 6-10 kV networks: V.D. Iurenkov and G.A. Dorf. (pp 78-82).

This recorder has been developed in the All-Union Scientific Research Institute of Electrical Engineering for measuring the atmospheric and internal over-voltages

in 6 - 10 kV networks. It comprises capacitance limiters, a three phase spherical discharger and a three phase recorder of operation, all connected in series, (see figure in the text). When a voltage wave passes to the discharger with an amplitude greater than the setting value, there is a cascade breakdown of the discharger sparkgap and of the paper of the operation recorder. A hole is left on the paper strip showing the discharge. The moment of operation of the apparatus is determined with an accuracy of up to ± 15 min on moving the strip. The measurement of voltage impulses of a few microseconds is considered in connexion with radiation. When a capacitor and resistance were connected in the apparatus, faulty operation was overcome.

THE ELECTRICAL PROPERTIES OF COMPRESSED AIR IN AN AIR-BLAST CIRCUIT-BREAKER*

E.M. TSEIROV

(Received 15 May 1958)

One of the factors which limits the working capacity of an air-blast circuit-breaker considerably is the low electrical strength of the contact gap in its quenching chamber in spite of the comparatively high pressure and, consequently, the high electrical strength of the compressed air in it.

A distinction should be made between the two forms of electrical strength of the contact gap in quenching chambers: *static and dynamic*. Static strength is described as the minimum magnitude of the discharge voltage between the open contacts of the chamber during no-load operation (without breaking the current). Dynamic strength is described as the gradually increasing minimum discharge voltage between the contacts after the current has been broken in the chamber. It can be shown that the static and on the whole the dynamic electrical strength of the contact gap of a quenching chamber depends not only on the air pressure, but also on the construction of the chamber, the arrangement of its contact system and so on. The discharge voltage gradient (electrical strength) varies substantially both along the axis of and across the contact gap. Therefore, it is necessary to differentiate between the overall *integral* electrical strength and the *local* electrical strength of the gap which is characteristic for a given point on it.

Observation of the electrical properties of air in the contact gap of a chamber result in the conclusion that the electrical strength of moving air is always less than that of still air, other conditions being equal. This is most simply seen in a jet flowing from a compressed air tank.

The results of measurements of the puncture voltage at various points in an air jet flowing through a glass nozzle are presented in the form of curves in Fig. 1. The measurements were made with the use of a probe consisting of two hemispheres 4 mm in diameter fastened to thin but sturdy electrodes; the clearance between the hemispheres was 1.0 mm. In the course of the experiment the line frequency voltage applied to the electrodes of the probe was slowly raised until

* *Elektrichestvo*, No. 12, 1-9, 1958.

a spark-over occurred. The effect of the probe on the accuracy of measurements was apparently small, since changing its position in the jet did not affect the result.

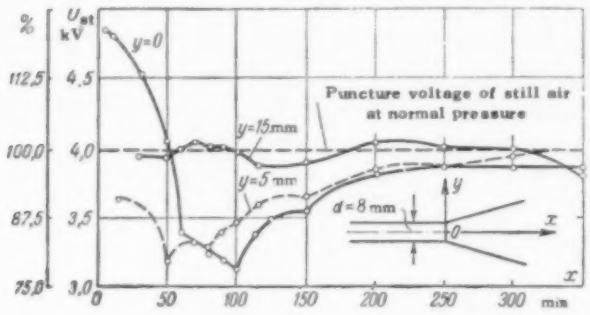

FIG. 1. Local electrical strength of a free air jet flowing through a nozzle of diameter $d = 8$ mm at a pressure $p = 3.5$ atm.

Regarding the magnitude of the discharge voltage which is determined directly by the probe and which is related, of course, to the length of the discharge gap, we have the following information: in immediate proximity to the outlet section of the nozzle ($x \approx 0$; $y \approx 0$) the puncture voltage is equal to 4.8 kV (puncture voltage gradient 48 kV/cm); along the jet stream it drops rapidly, and at a distance of approximately 50 mm from the nozzle it becomes equal to the electrical strength of still air at normal pressure which in this case was 4.0 kV. On further movement of the probe the puncture voltages continue to drop, reaching 3.14 kV at $x = 100$ mm, i.e. falling almost 1 kV below the electrical strength of air at normal pressure. After passing this minimum value the curve for the electrical strength rises slowly to approximate the electrical strength of air at normal pressure.

These results were obtained with an air pressure of 3.5 atm in the tank supplying the nozzle. Numerous similar experiments with other original pressures always led to identical results in practice. Thus, we arrive at the conclusion that in a free air jet there are areas with a substantially reduced electrical strength which is less than that of still air at normal pressure.

The curve for $y = 5$ mm shows a minimum value for the puncture voltage at approximately the same position as when $y = 0$. At a distance of 15 mm from the axis, the puncture voltages do not differ in practice from the voltages for still air at normal pressure.

There is nothing paradoxical, naturally, in the results obtained since it is well known that a gas jet flowing from a nozzle at sonic speed expands so strongly

that for a certain time the pressure within it becomes less than that of the surrounding space; this is marked in particular by a reduction in electrical strength.

The case in question is of importance to us in that it clearly demonstrates the fallacy in considering a moving gas as a homogeneous medium possessing certain mean parameters, and, consequently, corresponding mean electrical properties. In studying the operation of quenching chambers in air-blast circuit-breakers consideration must be made, evidently, of the possible presence of zones of substantially reduced electrical strength in the contact gap area. In this connexion investigations of the electrical strength of standard quenching chambers are of great interest.

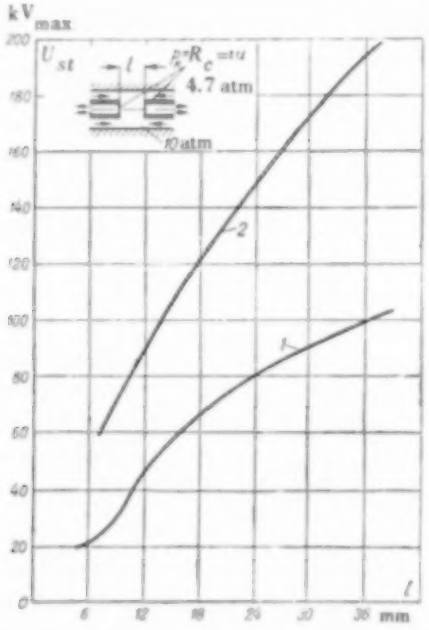

FIG. 2. Integral electrical strength of the contact gap in a standard quenching chamber.
1 — usual compressed air flow, p_0 = 10 atm; 2 — exhaust outlets closed, p_0 = 4.7 atm.

Curve *1* in Fig. 2 characterizes the electrical strength of the contact gap in an ordinary quenching chamber equipped with simple hollow cylindrical contacts as is shown in the diagram in the same figure. The curve for the electrical strength was made in natural conditions, i.e. on an ordinary circuit-breaker during no-load operation.

With fully opened contacts when the length of the contact gap reached 35-36 mm (internal diameter of contacts 32 mm), the minimum puncture voltage reached 100 kV max; here the air pressure directly at the contact intake was 4.7 atm, but 10-11 atm in the chamber itself, (Fig. 2).

If the flow of compressed air from the quenching chamber is prevented, keeping all other conditions the same, then in the presence of a constant pressure in the chamber equal to 4.7 atm (i.e. the same as in the preceding case at the contact intake) the rise in the electrical strength on increasing the length of the contact gap will be described by curve 2, (Fig. 2). If the total length of the contact gap is 35 mm, the minimum puncture voltage according to this curve is 185 kV max. Thus, in spite of the fact that in the first case the mean air pressure in the contact gap was certainly higher since in the chamber itself the pressure was maintained at 10 atm, its electrical strength was substantially (1.8 times) lower.

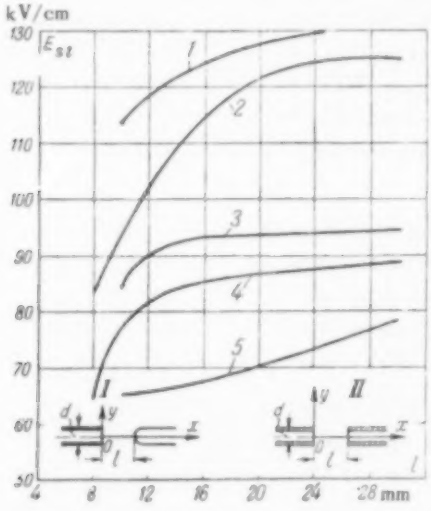

FIG. 3. Local electrical strength of contact gaps. 1 – electrical strength at point ($x = l^{-3}$; $y = 0$) with contact system *I*; 2 – same at point ($x = l/2$; $y = 0$); 3 – same at point ($x = 2$; $y = 0$); 4 – electrical strength at point ($x = l/2$; $y = 0$) with contact system *II*; 5 – same at point ($x = 2$, $y = 0$). $d = 19$ mm; $p_0 = 4.0$ atm.

Fig. 3 shows the results of measurements of the local electrical strength of contact gaps for system *I* where one of the contacts in the chamber is hollow and the other solid (unilateral blast), and for system *II* where both contacts in the chamber are hollow (bilateral blast). The measurements were made in the presence of strictly constant pressure in conditions where the effect of the walls or

other extraneous factors was eliminated in actual practice. In this series of experiments the pressure in the chamber itself was maintained at 4 atm; the internal diameter of the contacts d was in both cases 19 mm. The measurements were made on the axis of the stream (longitudinal axis of the contact system $y = 0$) half-way between the contacts ($x = l/2$) and 2 mm from the plane passing across the contact faces. The contact distance l was varied within the limits of 8 - 30 mm (0.42 - 1.58) of the internal diameter of the hollow contact).

From curve *1*, Fig. 3 it is seen that with an increase in the distance l between the contacts, the local electrical strength of the air near the face of the fixed contact rises evenly; when $l = 25$ mm it is 130 kV/cm. This curve is obviously higher than all the others, i.e. the electrical strength of the air stream in immediate proximity to the face of the fixed contact is greater than in the contact gap.

Curve *2* shows a similar dependence for the point exactly half-way between the contacts. When the length of the contact gap is small, the electrical strength of the air at this point is also comparatively small. For example, when $l = 8$ mm we have $E_{st} = 84$ kV/cm. With an increase in l the electrical strength rises with extreme rapidity, reaching 125 kV/cm when $l = 25$ mm, i.e. the maximum value for the given case. Further increase in the length of the contact gap no longer has any effect.

Curve *3* gives the same dependence for the point at the hollow contact intake. The character of the curve shows that beginning from the determined limit the electrical strength depends little on l. Actually, when $l = 10$ mm $E_{st} = 84$ kV/cm, and even when $l = 15$ mm the electrical strength in actual practice reaches its maximum value of 93 - 95 kV/cm, and from then on no longer depends on l.

If values for local electrical strength E_{st} are compared say for $l = 25$ mm, the following figures are obtained at the fixed contact, half-way between the contacts and at the hollow contact intake: 130, 125 and 94.5 kV/cm.

The lower two curves are for system *II*, i.e. bilateral blast. Curve *4* shows that at the point $x = l/2$ the electrical strength of the air depends greatly on the quantity l; when $l = 8$ mm, $E_{st} = 64$ kV/cm, and when $l = 30$ mm, $E_{st} = 89$ kV/cm. The electrical strength at the hollow contact intake (curve *5*) depends on l to a lesser degree. So, when $l = 10$ mm, $E_{st} = 65$ kV/cm, and when $l = 30$ mm, $E_{st} = 78$ kV/cm. Curve *5* for the electrical strength is substantially lower than curve *4*. Thus minimum electrical strength is observed in the zone near the intake holes of the hollow contacts.

Comparing on the one hand curves *1*, *2* and *3* and on the other hand, curves *4* and *5*, we see that the values for the electrical strength in the latter (i.e. in a bilateral blast) are considerably less than in the former (i.e. in a unilateral blast),

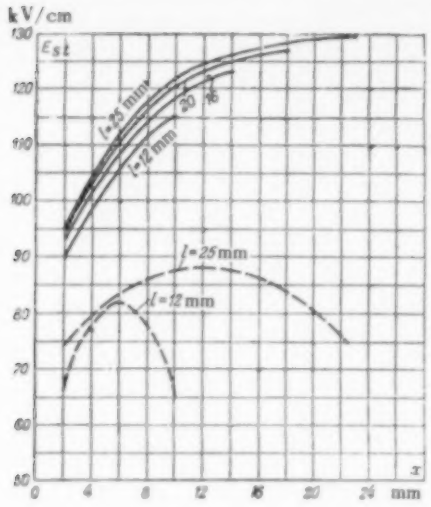

FIG. 4. Local electrical strength along the contact gap axis for various values of l

Four upper curves – unilateral blast; two lower curves – bilateral blast;
d = 19 mm; p_0 = 4.0 atm.

1959

other conditions being equal.

The local electrical strength along the axis of the contact gap for various lengths of l is presented in Fig. 4. The four upper curves which are for a unilateral blast show very clearly that the electrical strength is distributed with extreme irregularity along the contact gap. On altering the length of the contact gap l the character of the irregularity remains unchanged, but the absolute values for the electrical strength decrease with a decrease in l.

The two lower broken curves represent the distribution of electrical strength along the axis of the contact gap with two hollow contacts (bilateral blast) in the same external conditions. The form of the curves is conditional; only those points determining the minimum and maximum values for the electrical strength are reliable. The curves show that the electrical strength is distributed with irregularity along the axis of the gap, and what with a decrease in l its absolute value falls.

The distribution of air flow speeds in the contact gaps in question which is measured with a special thermoanemometer is shown for a unilateral blast in Fig. 5 and for a bilateral blast in Fig. 6. The shape of these curves is well in keeping with the character of the variation of the electrical strength in the contact gap. According to Fig. 5 the maximum speed is observed immediately at the

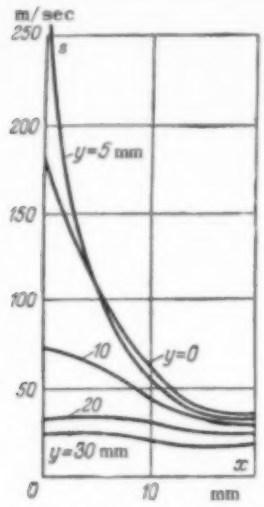

FIG. 5. Distribution of the air flow speeds s along the contact gap with a unilateral blast. Contact system *I* (Fig. 3).
d = 19 mm; l = 25 mm; p_0 = 4.0 atm.

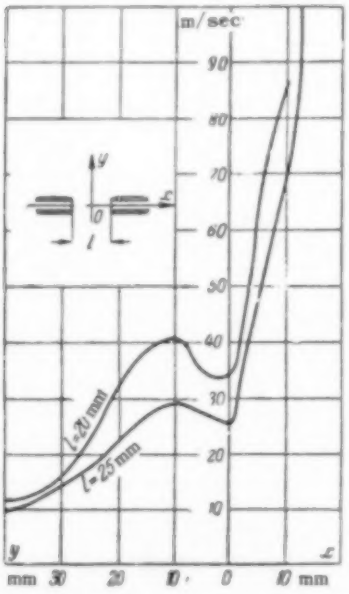

FIG. 6. Distribution of air flow speeds s along the x and y axes of the stream in the presence of a bilateral blast.
d = 19 mm; p_0 = 4.0 atm.

hollow contact intake where, of course, there is the least pressure and consequently the least electrical strength. On the other hand, in immediate proximity to the fixed contact the flow speed is small, the pressure higher and the electrical strength of the air at a maximum.

The speed distribution curves were measured, as is seen from Fig. 5, not only on the axis of the stream but also parallel to it for $y = 5$, 10, 20 and 30 mm. The further from the axis the measurements are made, the less the speed: the curves for $y = 10$, 20 and 30 are lower than for $y = 0$.

Fig. 6 represents the flow speed distribution along the transverse and longitudinal axes of the stream formed by the two hollow contacts. Along the y axis the speeds are in general relatively small. At the origin, i.e. at the centre of the stream, the flow speed barely reaches 25-33 m/sec.

Along the x axis, moving towards the intake section of the contacts, the speed increases quite rapidly, reaching 88-100 m/sec. In Table 1 data are presented allowing a comparison to be made between the values for the flow speeds and electrical strength on the longitudinal axis of the stream in both contact arrangements, ($d = 19$ mm). In the given conditions the contact arrangement with two hollow contacts has lower values for the air flow speeds and electrical strength.

1959

TABLE 1

Type of blast	l, mm	Point with minimum speed		Point with maximum speed	
		Speed, m/sec	Electrical strength, kV/cm	Speed, m/sec	Electrical strength, kV/cm
Unilateral	20	22	127.5	190	94.0
	25	34	130.0	190	94.5
Bilateral	20	33	87.0	87	70.0
	25	25	88.0	100	74.0

Both the presence of high flow speeds in the contact gap of the chamber and as high as possible an electrical strength of the air in the chamber are important for successful quenching of an electrical arc. Therefore, the arrangement with two hollow contacts must yield, apparently, to the arrangement with one hollow contact.

However, the known positive qualities of the bilateral blast compelled us to

study this system more closely.

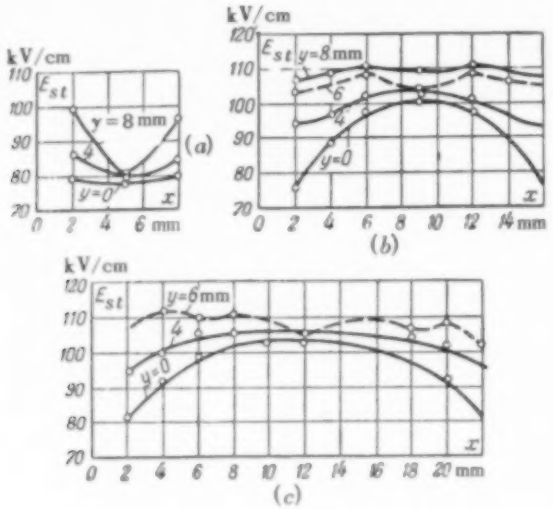

FIG. 7. Local electrical strength of the contact gap with bilateral blast. Contact system II, (Fig. 3).
d = 19 mm; p_0 = 4.0 atm.
(a) – l = 10 mm; (b) – l = 19 mm; (c) – l = 25 mm.

It has been pointed out that the state of the local electrical strength at various points on the contact gap is substantially affected by the length of the gap itself. The curves in Fig. 7 are of interest in this connexion. Here are shown three families of curves characterizing the local electrical strength of the contact gap measured both along the longitudinal axis of the stream x, and also at various other points. When l = 10 mm, the values for the local electrical strength on the axis of symmetry (y = 0) depend little on the point of measurement: the curve for the electrical strength is deflected downwards only slightly. With a rise in y the dependence of the electrical strength on x increases. All three curves are deflected downwards, i.e. the electrical strength at the mid-point of the gap is less than it is close to the contacts themselves.

With an increase in the length of the contact gap l to 19 mm, the character of the curves alters sharply. The curve for the electrical strength on the x axis becomes convex; now at the mid-point of the contact gap E_{st} = 90 kV/cm, and at the contact faces E_{st} = 74 kV/cm. In immediate proximity to the x axis when y = 4 mm, the character of the curve remains as before but the absolute values for the electrical strength rise. The curves for the electrical strength when y = 6 mm and y = 8 mm have an unusual form. It is characteristic that at certain points the electrical strength on the line y = 6 mm drops even lower than on the line y = 0.

Further increase in l gives a smoother curve and raises the local electrical strength noticeably, particularly at points distant from the contacts. For example, when $l = 25$ mm, on the x axis ($y = 0$) we get $E_{st} = 81$ kV/cm at points when $x = 2$ mm or $x = (l - 2)$ mm, but when $x = l/2$ we get $E_{st} = 103$ kV/cm. It is easily seen that the lowest electrical strength is as a rule observed on the x axis of the stream ($y = 0$) throughout its length, the minimum values being found in immediate proximity to the contacts.

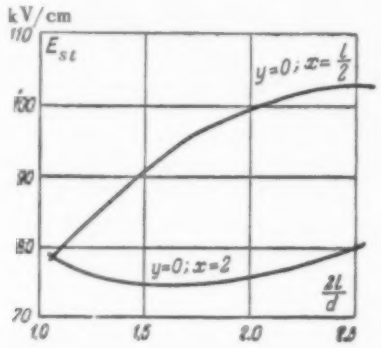

FIG. 8. Dependence of the local electrical strength of the contact gap on the value of the dimensionless parameter $2l/d$.

The area of the cross-section of the openings through which the air flows from the contact gap is equal to $2\pi d^2/4$; the lateral surface of the cylinder through which the air passes to these openings is πdl. Consequently, if it is required that a given lateral surface does not limit the air flow to the contact openings the relation $l = d/2$ must at least be maintained between them. Taking this contact gap length per unit, we plot the dependence of the local electrical strength of the latter on the dimensionless parameter $2l/d$, (Fig. 8). The electrical strength at the contact intake has little dependence on the parameter $2l/d$ within the limits of the given data. But when $2l/d = 1$ and when $2l/d = 2.5$ it remains almost unchanged. However, the electrical strength at the point $x = l/2$ shows quite a strong dependence on this parameter.

Thus, an increase in the length of the contact gap should raise its integral electrical strength not only because of this factor, but also as a result of the rise in the value for the local electrical strength.

In Fig. 9 curves are shown for the rise in the electrical strength of the air at the contact intake along the radius of the latter for various contact-gap lengths l. From the curves it is apparent that with an increase in the radius R and, moving away from the centre, the electrical strength rises smoothly. When the contact gap

l = 14 mm and more ($d = 2R$ = 19 mm), the electrical strength no longer depends on its length in actual practice.

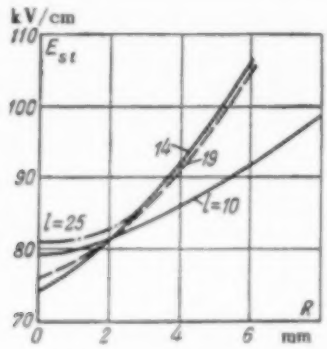

FIG. 9. Relation of the local electrical strength along the radius of contact intake.

In summarizing all this information on the distribution of local electrical strength in this type of contact gap, it is perhaps possible to conclude that the geometric path of an electrical discharge in the gap follows chiefly along the longitudinal axis, passing then to the contact walls according to radius.

Direct experiments on the contact gaps of a standard quenching chamber with a bilateral blast clearly showed that in every case the spark-over does not pass between the faces of the contacts, but between their internal surfaces. The tendency of both the integral and, naturally, the local electrical strength of the given contact gap to rise was the result of its particular construction whereby one of the hollow contacts was equipped with a diaphragm as is shown in the drawing in Fig. 10. The results of measurements of the local electrical strength in this type of arrangement are shown in the form of curves in the same figure. The measurements were made at different points on the x axis of the stream.

The comparison of these curves with the corresponding characteristics in Fig. 3 (curves *3* and *4*) show first of all that the values for the local electrical strength at the intake to the hollow (not equipped with a diaphragm) contact (curve x = 2, Fig. 3) have risen somewhat in comparison with the data given previously (curve *5*). For example then, when l = 30 mm, we get 96 kV/cm against the previous 78 kV/cm, i.e. a rise in the electrical strength of 1.2 times. The electrical strength of the air in the diaphragm-equipped contact, i.e. at the point x = 2, rose with particular strength to reach 118 kV/cm when l = 30 mm, i.e. it increased 1.5 times. A similar substantial increase in the electrical strength was noted at the point $l/2$, equalling 117 kV/cm against 94 kV/cm, i.e. it rose 1.25 times. Thus, diaphragming one of the hollow contacts raises the electrical

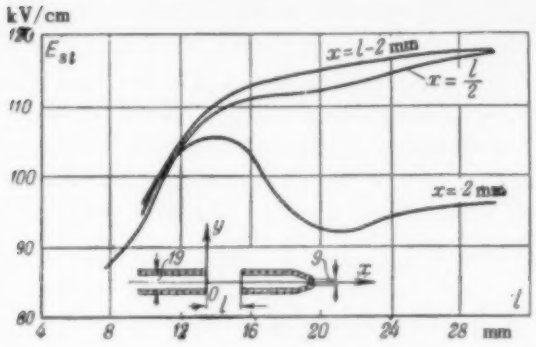

FIG. 10. Dependence of the local electrical strength of the contact gap on l for the case where one of the hollow contacts is equipped with a diaphragm.
$d = 19$ mm; $p_0 = 4.0$ atm.

strength of the contact gap substantially, approximating it to that in a unilateral blast arrangement.

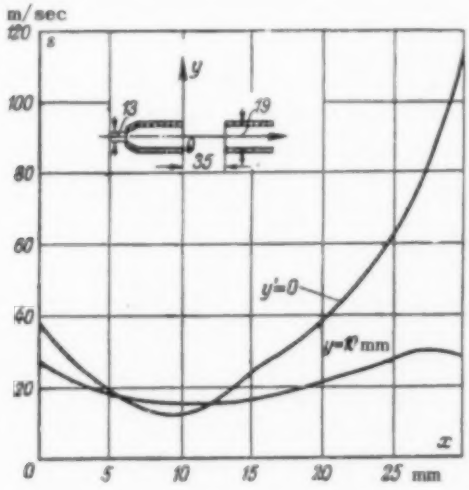

FIG. 11. Distribution of the flow speeds along the contact gap with one of the two hollow contacts equipped with a diaphragm.
$d = 19$ mm; $p_0 = 4.0$ atm.

The flow speed distribution in the gap in question is shown in Fig. 11. Here the speeds were measured exactly on the x-axis of the stream ($y = 0$) and along it at a distance of $y = 10$ mm. It is easily seen that in the given arrangement the

points with a minimum flow speed are displaced in a direction towards the diaphragm-equipped contact.

The integral electrical strength of the contact gaps should apparently be determined proceeding from the minimum values for the local electrical strength. If we consider the information in Fig. 3, when $l = 25$ mm the minimum electrical strength for a unilateral blast is equal to 94.5 kV/cm, and consequently the overall integral electrical strength amounts to approximately $94.5 \times 2.5 = 236$ kV.

In exactly the same way the minimum electrical strength for a bilateral blast amounts to 74 kV/cm, and correspondingly, the integral electrical strength is $74 \times 2.5 = 185$ kV. However, direct measurements of the integral electrical strength, as can be seen from Fig. 2, show that it is substantially smaller even in conditions of considerably higher air pressure. This unfavourable circumstance is related to the fact that in practice the electrical field is itself unevenly distributed along the contact gap. The highest gradients are found in the areas immediately adjacent to the contacts. Consequently, the gradient of the electrical field applied to the contact gap will be highest at the hollow contact, and the electrical strength will be lowest. The overall electrical strength of the contact gap is sharply reduced. Here the bilateral blast is also operating in the least favourable conditions.

Studying the electrical properties of contact gaps in quenching chambers is completely pointless if it is not accompanied by a study of their breaking capacity. Therefore, this side of the problem is considered below.

The investigations described, explaining in some degree the causes of the low overall electrical strength of a contact gap, do not permit a numerical evaluation to be made of the latter.

In order to bridge this gap an experimental determination of the static integral electrical strength of a contact gap was made on a standard quenching chamber of a 110 kV, 4000 MVA circuit-breaker equipped with a bilateral blast, (Fig. 12). It consists of two quenching elements. Its moving contacts *1* are actually simple cylindrical tubes which carry off the arcing products into the atmosphere. The fixed contacts *2*, which are also hollow, are equipped with diaphragms as is seen in the figure. In the course of the tests three types of fixed contact were used: (1) simple tubes without diaphragms, (2) diaphragms as shown in Fig. 12, and (3) with a special grid diaphragm (see below).

The measurements of the static electrical strength (minimum discharge voltage) were made entirely in natural conditions, i.e. on a standard form of circuit-breaker actuated by its pneumatic system. The air pressure in the tank was raised to 16 atm before beginning the experiment. The internal diameter of the hollow contacts was 32 mm; the airline supplying the quenching chamber was

90 mm in cross-section.

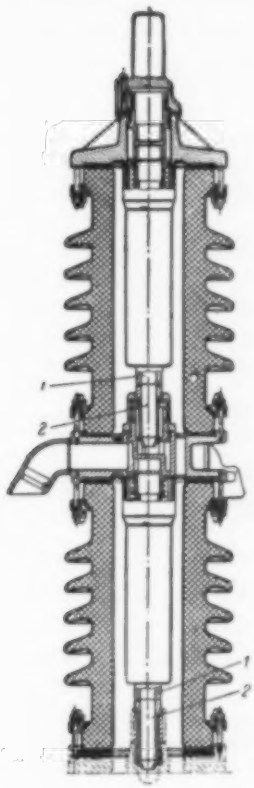

FIG. 12. Cross-section of the standard quenching chamber of a 110 kV circuit-breaker with a bilateral blast.
1 – moving contacts; 2 – fixed contacts.

Fig. 13 shows the relations of the rise in the static integral electrical strength of the contact gaps in the course of the motion of the moving contacts of the quenching chamber. They pertain to its upper element. Both the time which has passed from the beginning of contact separation and the path covered by the moving contact during this time are shown on the abcissa.

On full contact separation, equal to 32 mm, the minimum puncture voltage determined by many experiments was equal to 90 kV according to curve *1*. If consideration is made of the fact that the air pressure in the chamber during those experiments reached 12 atm, the result obtained is not encouraging.

Curve *2* shows that if the fixed contact is equipped with a diaphragm the

electrical strength of the gap rises considerably, reaching 160 kV max on full separation of the contacts. It increased even more when the fixed contact was equipped with a new grid diaphragm, i.e. when many fine choking openings were used instead of a single one (diagram and curve *3*).

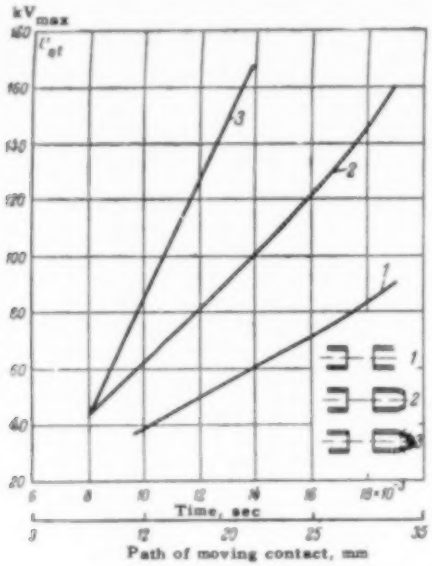

FIG. 13. Dependence of the electrical strength of the upper contact gap of a quenching chamber (Fig. 12) on time and gap length. Pressure in the circuit-breaker tank 16 atm; diameter of air supply line 90 mm.
1 – contact gap with ordinary hollow contacts in the form of smooth tubes 32 mm in diameter; 2 – same except that the fixed contact has a conical diaphragm with an outlet of 15 mm; 3 – same, except that the diaphragm has many fine openings.

Only those contact devices which to a varying degree find practical application have been described above. Generally speaking, there are other means of substantially raising electrical strength, but they fail to meet even the minimum requirements for breaking capacity.

It must be said here and now that diaphragming one of the hollow contacts in a bilateral blast system raises the capacity of the chamber to withstand the recovery voltage amplitude, but at the same time it reduces its capacity to withstand the higher frequency of this same voltage. However, the rational application of diaphragms will make it possible to obtain a more ideal combination of both these and other properties in practice.

Between those limits of recovery voltage frequency which are at the present accepted in world practice, a limited degree of the application of diaphragms to one of the contacts has a strong effect on the breaking capacity of quenching chambers in actual practice. The application of the grid diaphragm will increase its potentialities even more.

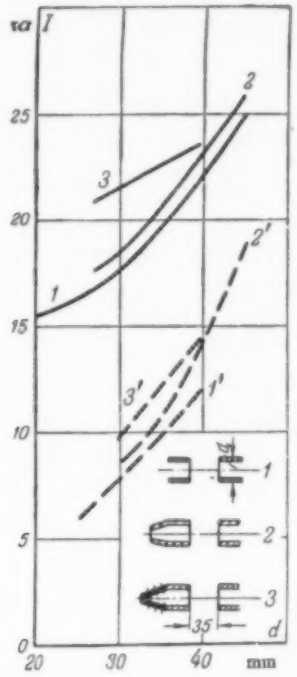

FIG. 14. Dependence of the breaking current of a 110 kV air-blast circuit-breaker on the internal diameter of the contacts. The quenching chamber has two elements. Air pressure 20 atm; total length of the contact gap $l = 35$ mm; airline diameter 90 mm. The continuous curves correspond to the amplitude of the recovery voltage $U_r = 180\ kV_{max}$ with frequency $f_0 = 800$ c/s, and the broken curves for $U_r = 220\ kV_{max}$ and $f_0 = 3000$ c/s.

For an illustration of this, Fig. 14 shows the results of an investigation of a standard industrial type of 110 kV air-blast circuit-breaker having a quenching chamber with two elements in series. The quenching chamber was equipped with three contact systems in the course of the tests: (1) ordinary hollow contacts as in system *1* (Fig. 14), (2) exactly the same contacts, one of which was equipped with a diaphragm as in system *2*, and (3) the same contacts, but with a grid diaphragm as in system *3*.

The curves represent the lower limit of the short-circuit currents which are broken in the given conditions. They were obtained by numerous and repeated experiments. The breaking current did not have an aperiodic component. In the conditions described, at least for internal diameters of the contacts up to 40 mm inclusive, the application of diaphragms somewhat increased the potentialities of the circuit-breaker. Its limiting breaking power when $d = 40$ mm was 4200 MVA with the application of contact system *1*, 4500 MVA with system *2* and 4700 with system *3*.

However unassuming this result may seem, it does show that the diaphragming of contacts, substantially raising the electrical strength of the contact gap (as has been indicated above), not only does not limit the breaking capacity but even increases it somewhat.

In the case where the diameter of the hollow contacts of the chamber in question is increased to 45 mm, its breaking power on application of system *2* was raised to 4900 MVA which could not be reached on application of system *1* due to failure to break the corresponding currents in the presence of a natural oscillation frequency of $f_0 = 3000$ c/s.

Diaphragming has a particularly favourable effect on raising the breaking capacity in the presence of relatively small breaking currents and smaller hollow contact diameters. For example, when $d = 30$ mm, changing from system *1* to system *3* makes it possible to raise the power of the circuit-breaker from 3000 to 3800 MVA, i.e. 25 per cent.

We also reach basically the same conclusions in the case of circuit-breakers of other voltage classes.

Diaphragm application made it possible to raise the breaking power of a 154 kV air-blast circuit-breakers from 4000 to 6000 MVA without actually altering the construction either of the quenching chamber or, in effect, of the contact system, and retaining the number of its elements (three) unchanged.

So that an opinion may be formed regarding the capacitive current (no-load line) breaking capacity of a quenching chamber having a diaphragm-equipped contact system, we present the results of tests of a 400 kV, 10,000 MVA air-blast circuit-breaker. Table 2 contains the basic findings from these experiments which concern us. The circuit-breaker had seven elements connected in series and the pressure of the air in its tanks was maintained at 20 atm. The internal diameter both of the moving and of the fixed contacts was 32 mm; the fixed contact was equipped with a diaphragm in the shape of a convergent cone, as has already been described, with an outlet diameter of 15 mm.

The information in Table 2 shows conclusively that the contact system is

capable of withstanding an extremely high voltage developing in the circuit-breaker on breaking no-load lines. This is perhaps its most important advantage in comparison with the usual system of two simple hollow contacts.

TABLE 2

Broken capacitive current, A	Voltage sustained by chamber 0.01 sec after the current is broken, kV	Multiple of overvoltage in relation to $U_p = \frac{420}{\sqrt{3}} = 243$ kV
470	432	1.78
550	475	1.96
620	456	1.88
570	755	3.11
560*	434*	1.78*
400	567	2.34
590	745	3.07
570	896	3.69
695	695	2.86
695	670	2.78
650	756	3.12
568	820	3.38

* In this experiment there was a repeat ignition.

1959

Conclusions

1. The electrical strength of moving compressed air is lower than that of still air, other conditions being equal.

2. The formation in the compressed air stream of areas with substantially lowered pressure in comparison with mean gas-dynamic values is a cause of the reduction of its electrical strength.

3. The electrical strength of the compressed air in the contact gap of a quenching chamber depends essentially on the position of the point of measurement, varying both along its longitudinal axis and also in other directions.

4. This fact necessitates that a distinction be made between the local electrical strength of a gap at a given point and its overall (integral) electrical strength.

5. The integral electrical strength of contact gap, which is a deciding factor determining the working capacity of the quenching chamber, in the final analysis determines the value of its minimum local electrical strength to a considerable extent.

6. The characteristics of a contact gap should be improved not only by raising its integral electrical strength but also by raising its local electrical strength.

7. A contact system with one contact hollow and the other solid has

substantially higher values for electrical strength than a contact system with two hollow contacts, other conditions being equal.

8. The disadvantage of a contact system with two contacts hollow can to a certain degree be alleviated by diaphragming one hollow contact.

9. Diaphragm application, raising the electrical strength of a contact system with two hollow contacts, improves its capacity for breaking short-circuit currents and particularly for withstanding the high voltages applied to the circuit-breaker on breaking long distance no-load lines.

10. Study of the electrical strength of the contact gaps in quenching chambers of air-blast circuit-breakers shows that the different properties of compressed air are utilized in them to a very small degree. In this connexion unremitting and careful work is necessary to rectify this deficiency and increase the potentialities of modern air-blast circuit-breakers.

The author wishes to thank engineers Katkov and Kuligin of the Lenin high-voltage department of the VEI who have given him great assistance in this work.

Translated by F.J. Griffiths

THE OCCURRENCE OF SUB-HARMONIC RESONANCE IN UNBALANCED CONDITIONS*

M.G. PORTNOI

(Received 31 May, 1958)

In recent times several works [Ref. 1 – 4] have appeared describing experiments on sub-harmonic resonance in electrical systems. In these works its appearance was investigated on 400 kV lines with capacitative and inductive compensation, on which it was assumed that the magnetizing characteristic of the compensating reactors is approximated with sufficient accuracy by the equation:-

$$i = a\psi + \beta\psi^3. \tag{1}$$

The sub-harmonic resonance is observed in a number of other cases, one of which is described in the present article.

When one phase of a 110 kV line 67 km long was disconnected the voltage transformers connected at each end of the disconnected phase were faulted. Investigations carried out jointly by VNIIE and 'Moldavenergokombinat'† showed that sub-harmonic resonance arose with the disconnexion of one phase of the line and the current in the voltage transformer grew to some 15 times greater in comparison with the normal magnetizing current, (Fig. 1a).

When this case was analysed it was ascertained that the magnetization curve of the voltage transformer is very far from the curve of the equation described in (1) above.

As a result the method did not permit the theme to be developed by the techniques described in [1 – 4] in the references.

It was desirable to substitute a method suitable for any given form of the magnetization curve. One of these methods was the use of a mathematical model,

* *Elektrichestvo*, 12, 18 - 22, 1958.

† V.M. Popov, G.T. Fomichev, N.B. Glagoleva, M.P. Savitskaia and the author took part in the investigations.

described in detail in many works, for example in the work by Korn, [5]. The investigation was undertaken with the help of this method.

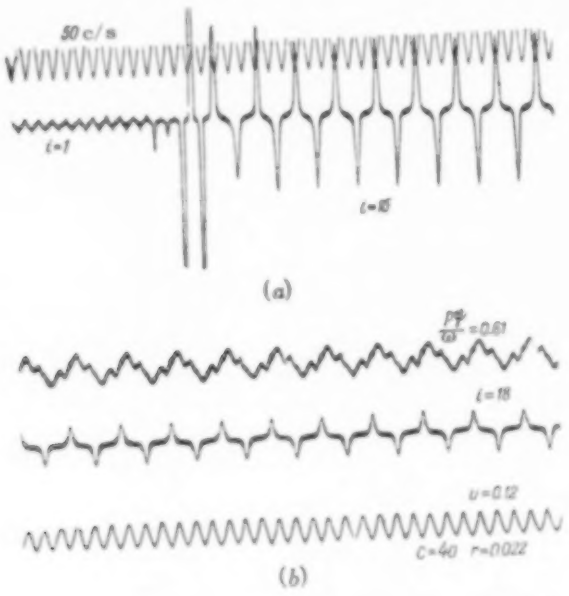

FIG. 1. Oscillograms of the sub-harmonic current in the voltage transformer on disconnexion of one phase of the line.
(a) Traced under actual conditions. (b) Traced on the mathematical model.

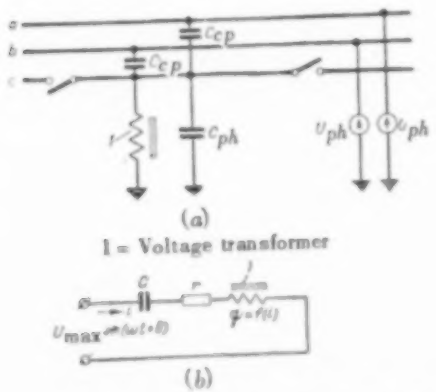

FIG. 2. Equivalent networks for a line. (a) With one phase disconnected. (b) Equivalent network.
($V_{max} = 2V_{ph} \times C_{ip}/C$; $C = 2C_{ip} + C_{ph}$).

To set up the differential equations let us examine the equivalent network for the line in unbalanced conditions.

Fig. 2a shows the equivalent circuit for the line after one phase has been disconnected. Let the two sources of e.m.f. in the diagram be replaced by one equivalent source, and the three capacitances be replaced by one equivalent capacitance, (Fig. 2b). Such a transformation is independent of frequency and so both circuits will give one and the same differential equation,

$$\frac{d\psi}{dt} + ir + \frac{1}{C}\int i\,dt = V_{\max}\sin(\omega t + \theta), \tag{2}$$

which is fundamental to the following analysis.

To set up the magnitudes entering into equation (2) on a structural model we will express them in relative units, taking the basic nominal parameters of the voltage transformer. $v_b = 98\,\text{kV}$; $i_b = 0.167\,\text{A}$; $\omega_b = 314$.

After differentiating equation (2) and solving it with regard to the higher derivatives and substituting the symbol p for d/dt we get:

$$p^2\psi = \omega\, V_{\max}\cos(\omega t + \theta) - \frac{\omega^2}{C}i - \omega r p i. \tag{3}$$

Let the non-linear relationship $i = f(\Psi)$ in Fig. 3 be assigned.

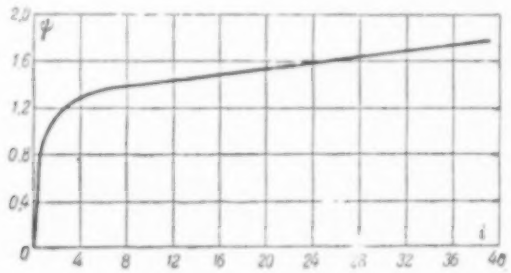

FIG. 3. Magnetizing curve of the voltage transformer.

A circuit fitting equation (3) was selected from among the elements of the mathematical model type I.P.T-5.* The model works with sufficient accuracy at frequencies not above 5 c/s, and so the input voltage had a frequency of 1 c/s and was derived from a special low frequency generator. The value of the initial interlinkage is set up at the input of the non-linear block *NB* as shown in Fig. 4.

* Y. Luginskii and Savitskaya took part in the work on the model.

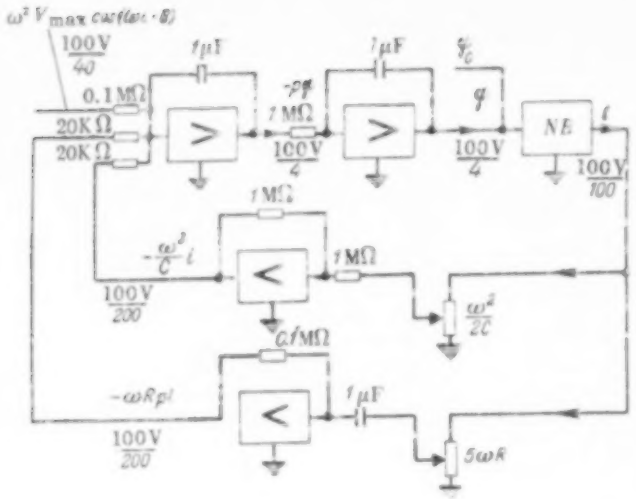

FIG. 4. Structural schematic of the mathematical model

Fig. 1 shows oscillograms of the sub-harmonic oscillations taken during tests on the power system and on a mathematical model with almost the same circuit parameters as the power system. Comparison of the oscillograms shows that the mathematical model that satisfies equation (3) gives results that coincide fairly well with the test.

The formation of sub-harmonic oscillations in the circuit in question (Fig. 2a) occurs as follows.

With the disconnexion of one of the phases, the voltage on the disconnected phase increases for a short time as a result of the cross distribution of voltage between the capacitances and the re-striking of an arc in the circuit-breaker. Subsequently, the arc in the circuit-breaker is quenched and the damped free-oscillation current appears in the circuit, the form of which is slightly distorted by the additional voltage of the circuit.

As a result of the non-linearity of the inductance, the frequency of free oscillation is reduced as the amplitude is reduced. This reduction of frequency with attenuation is clearly shown on the oscillogram reproduced in Fig. 5.

After this, the frequency of free oscillation remains at a fraction of the frequency of the additional voltage, the damping of the free oscillations may cease, so that they will be maintained by energy derived from the source of supply. In this way the free oscillations are transformed into sub-harmonic oscillations.

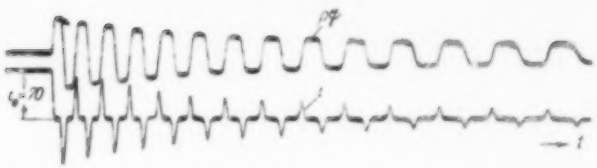

FIG. 5. Oscillogram of the open circuit damping current when:-
$C = 40$: $r = 0.0064$: $i_0 = 70$.

Let us consider the relationship between the magnitude of the sub-harmonic currents and the circuit parameters.

In the case under consideration the shape of the curve of the sub-harmonics differs insignificantly from the form of the curve of the free oscillating current. These circumstances determined by the order of the magnitudes of the circuit (a small value of applied voltage and a relatively large resistance) enables one to employ an approximate method to determine the amplitude of the sub-harmonic current.

The effect of the resistance on the magnitude of the current may be ignored, which is quite acceptable.

1959

In the process of damping the free oscillations (Fig. 5) the frequency of the real oscillations of the system is varied from the maximum value ω_{max} of the assumed magnitude of the original current i_0 to the minimum value $\omega_{min} = \frac{1}{\sqrt{L_{Lin} C}}$, in which is assumed the inductance of the transformer appropriate to the linear portion of its magnetization curve. The relationship of the real frequency of the system to the amplitude of the current may be written in the following form

$$\omega = \frac{1}{\sqrt{L_{Ass}(i_m) C}}, \tag{4}$$

where $L_{Ass}(i_m)$ = the inductance determining the frequency of free oscillations.

On the other hand one may get the frequency of free oscillation in a system without damping [7] as a result of the solution of the differential equation:-

$$\frac{d\psi}{dt} + \frac{1}{C}\int i\,dt = 0. \tag{5}$$

After differentiation, eliminating t and integrating we get:

$$\frac{\dot{\psi}^2}{2} + \frac{1}{C} \int_0^{\psi_m} i \, d\psi = 0, \tag{6}$$

Whence:-

$$\dot{\psi} = \frac{d\psi}{dt} = \sqrt{-\frac{2}{C} \int_0^{\psi_m} i \, d\psi}$$

and

$$T = \frac{2\pi}{\omega} = 2\pi \sqrt{L_{Ass} C} = 4\sqrt{C} \int_{\psi_m}^{0} \frac{d\psi}{\sqrt{-2 \int_{\psi_m}^{\psi} i \, d\psi}}. \tag{7}$$

Furthermore, as a result of combining (4) and (7) we get:-

$$L_{Ass} = \frac{4}{\pi^2} \left[\int_{\psi_m}^{0} \frac{d\psi}{\sqrt{-2 \int_{\psi_m}^{\psi} i \, d\psi}} \right]^2. \tag{8}$$

Using equation (8) and the magnetization curve it is possible to construct the curve $L_{Ass} = f(i_m)$ (see Appendix).

Equally possibly, this curve may be more easily plotted from experimental data with oscillograms of the damped free oscillations.

Using the relationship $L_{Ass} = f(i_m)$ (Fig. 6) one may determine the sub-harmonic oscillatory current for any given value of capacitance. For this, at the given sub-harmonic frequency $\omega = 1/3$ and capacitance C the inductance is determined $L_{Ass} = 9/C$ and from the curve $L_{Ass} = f(i_m)$, i_m is determined.

Fig. 7 shows the dependence of the amplitude of the sub-harmonic current on the capacitance (or length of line) obtained by the given method (curve 1) and with the help of the mathematical model (crosses) according to the circuit shown in Fig. 4. The two curves practically coincide.

From Curve 1, it is evident that the longer the line, the greater the amplitude of the sub-harmonic current. The inductance of the voltage transformer, taken from the linear portion of the magnetization curve determines the minimum length of line with which it is possible for sub-harmonics to arise.

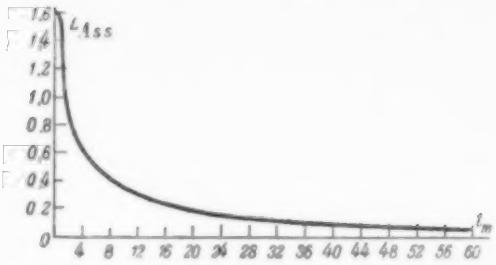

FIG. 6. Relationship of the inductance L_{Ass} to the amplitude of the current of free oscillations.

The curve $i_m = f(C)$ determined from the mathematical model (crosses) is chosen for two supply voltages: $U_m = 0.05$ and $U_m = 0.15$, but in the latter case resonance will only occur when $C > 10$, and if $C < 10$, resonance will occur at the fundamental frequency (curve 2).

With the aid of the mathematical model, the limiting values of the resistance were determined for the two values of voltage at which sub-harmonic resonance may exist, (Curves 3 and 4). The analogous relationship for resonance at the fundamental frequency is shown in curve 5.

1959

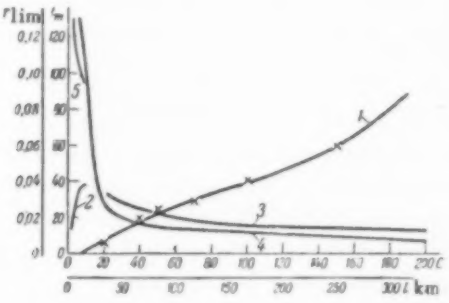

FIG. 7. Relationship of the amplitude of the sub-harmonic oscillation current and the limiting resistance to the length of line. 1. Relationship $i_m = f(l)$ for voltages 0.05 and 0.15. 2. The same with resonance at the fundamental frequency and a voltage of 0.15. 3. The relationship $r_{lim} = f(l)$ for a voltage 0.15. 4. The same for a voltage 0.05. 5. The same for resonance at the fundamental frequency.

Fig. 8 shows the relationship of the limiting value of the resistance to the supply voltage for one value of capacitance.

The resistance of a NKF-110 voltage transformer is about 6000 Ω. The equivalent voltage in the equivalent circuit for a 110 kV line is about

0.15 V*. Thus, the appearance of dangerous resonances on 110 kV lines may be observed in those cases where the line is less than 100 km long and has two voltage transformers connected to it (one at each end) or when the line is less than 50 km long and has one voltage transformer connected to it.

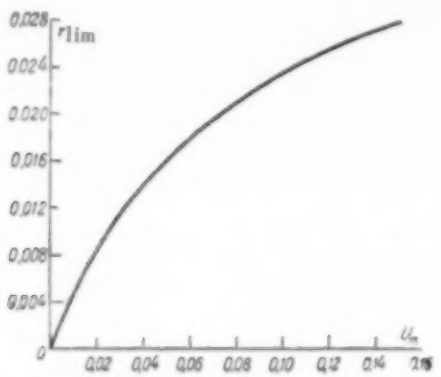

FIG. 8. Relationship between the limiting active resistance and the supply voltage when capacitance $C = 2\mu$.

To obviate the appearance of sub-harmonic resonance on 110 kV lines when unbalanced conditions occur it is sufficient to connect a resistance of 4 Ω, calculated for a prolonged flow of current of 0.2 A to the high-voltage side of the voltage transformer. The connexion of such a resistance does not in practice lead to error in the operation of the voltage transformer.

It only remains to observe that these methods are only necessary in cases of single phase automatic reclosure with automatic transfer to unbalanced conditions. If there is no automatic transfer to unbalanced conditions it is sufficient to disconnect the voltage transformers before a phase is disconnected and to reconnect them again afterwards if they are necessary.

Appendix

Determination of the relationship between the inductance of the voltage transformer and the amplitude of the open-circuit current. Determine the inductance from equation (8). For this, divide the magnetization curve of the transformer into sections, for each of which take a linear relationship $\psi = f(i)$: for $0 < \psi < \psi_1$ and $0 < i < i_1$ $\psi = \gamma_1 i$,

* The values of phase and interphase capacitances were taken from the work by Mel'nikov, [6].

$$i = \frac{\psi}{\gamma_1};\ \text{for}\ \psi_1 < \psi < \psi_2\ \text{и}\ i_1 < i < i_2\ \psi = \gamma_2 i + \psi_{10},\ i =$$

$$= \frac{\psi - \psi_{10}}{\gamma_2};\ \text{for}\ \psi_2 < \psi < \psi_3\ \text{и}\ i_2 < i < i_3\ \psi = \gamma_3 i + \psi_{20},\ i =$$

$$= \frac{\psi - \psi_{20}}{\gamma_3}\ \text{and so on}$$

Determine the relationship $L_{Ass} = f(i_m)$ for $i_3 < i_m < i_3$.

The integral which enters the right-hand side of equation (7) may be calculated by means of step changes from one limit right through to the other. As as result:-

$$\sqrt{L_{Ass}} = \frac{2}{\pi}\left[\int_{\psi_m}^{\psi_2} \frac{d\psi}{\sqrt{-2\int_{\psi_m}^{\psi} \frac{\psi - \psi_{20}}{\gamma_3}\,d\psi}} + \right.$$

$$+ \int_{\psi_2}^{\psi_1} \frac{d\psi}{\sqrt{-2\left(\int_{\psi_m}^{\psi_2} \frac{\psi - \psi_{20}}{\gamma_3}\,d\psi + \int_{\psi_2}^{\psi} \frac{\psi - \psi_{10}}{\gamma_2}\,d\psi\right)}} +$$

$$\left. + \int_{\psi_1}^{0} \frac{d\psi}{\sqrt{-2\left(\int_{\psi_m}^{\psi_2} \frac{\psi - \psi_{20}}{\gamma_3}\,d\psi + \int_{\psi_2}^{\psi_1} \frac{\psi - \psi_{10}}{\gamma_2}\,d\psi + \int_{\psi_1}^{\psi} \frac{\psi}{\gamma}\,d\psi\right)}}\right] =$$

$$= \frac{2}{\pi}\left[\sqrt{\gamma_3}\left(\sin^{-1}\frac{\psi_2 - 2\psi_{20}}{\psi_m - 2\psi_{20}} - \frac{\pi}{2}\right) + \right.$$

$$\left. + \sqrt{\gamma_2}\left(\sin^{-1}\frac{\psi_1 - 2\psi_{20}}{a_1} - \sin^{-1}\frac{\psi_2 - 2\psi_{10}}{a_1}\right) - \sqrt{\gamma_1}\sin^{-1}\frac{\psi_1}{a_2}\right]$$

Where:-

$$a_1 = \frac{\gamma_2}{\gamma_3}\left[(\psi_m - 2\psi_{20})^2 - (\psi_2 - 2\psi_{20})^2\right] + (\psi_2 - 2\psi_{10})^2,$$

$$a_2 = \frac{\gamma_1}{\gamma_2}\left[(\psi_m - 2\psi_{20})^2 - (\psi_2 - 2\psi_{20})^2\right] +$$

$$+ \frac{\gamma_2}{\gamma_3}\left[(\psi_2 - 2\psi_{10})^2 (\psi_1 - 2\psi_{10})^2\right] + \psi_1^2.$$

Using equation (C) and the magnetization curve one may plot the relationship

$L_{Ass} = f(i_m)$.

Translated by R.P. Froom

REFERENCES

1. S.S. Shur; *Delenie chastoty v prosteishei tsepi so stal'yu, (The division of frequency in very simple circuits with iron). Elektrichestvo,* 11 (1954).
2. L.F. Dmokhovskaya and V.I. Levitov; *Subgarmonicheskie kolebaniya v prosteishikh shkemakh i dal'nikh elektroperedachakh (Sub-harmonic oscillations in very simple circuits and in long distance transmission lines). Elektrichestvo*; 11, (1955).
3. M.S. Liebkind; *Subgarmonicheskie kolebaniya v prostoi posledovatel'noi tsepi. (Sub-harmonic oscillations in a simple sequence circuit). Izv. Akad. Nauk. SSSR,* 9 (1953).
4. A.I. Dolginov; *Rezonans v elektricheskikh tsepyakh i sistemakh. (Resonance in electrical circuits and systems).* Gosenergoizdat (1957).
5. G. and T. Korn; *Elektronnye modeliruyushchie ustroistva. (Electronic modelling devices).* Foreign Literature Publishing House), Izd. Irvostran. Literature (1955).
6. N.A. Mel'nikov; *Raschety rezhimov raboty setei elektricheskikh sistem. (Calculations of the operating conditions of networks in electrical systems).* Gosenergoizdat (1950).
7. R. Rudenberg; *Perekhodnye protsessy v elektroenergicheskikh sistemakh. (Transient processes in electrical power systems).* Izd. Inostran Literature, (Foreign Literature Publishing House), (1955).

EXPERIMENTAL INVESTIGATION OF DEFORMATIONS AND VIBRATIONS OF THE STATOR WINDINGS*

M.F. IUDOV

(Received 3 January 1958)

1959

Introduction

The determination of electrodynamic stresses in the windings of electrical machines by an analytical method is a difficult and painstaking problem, since it is necessary in calculations to take into account the influence of the curvature of conductors of the frontal parts, of the adjacent steel parts of the stator and also of the current in the rotor winding. For a rough estimate of the electro-dynamic stresses we can use simplified formulae, [1 and 2]. However, even if we know these stresses it is practically impossible to determine with sufficient accuracy the deformations of the stator winding produced by them. This is due to the fact that, owing to the lack of sufficient knowledge of mechanical properties of the insulation, we cannot determine the value of its reaction nor the reactions of the elements holding the stator winding. Therefore, along with further studies of the mechanical stresses in the stator windings more attention is being paid in recent time to their experimental investigation, [3]. In the present article some results of the experimental investigation of deformations and vibrations of the stator windings of hydro-electric generators and high-voltage electrical motors are given; these investigations were carried out by the author in the VNIIE MES.

Methods of experimental investigations

The VNIIE has recently carried out research work to design the necessary apparatus and to establish methods of investigation of the results of the action of electrodynamic stresses on windings of generators and synchronous motors. In the first stage, the deformation of the surface layers of the insulation and displacement (vibration) of the frontal parts of the winding were measured with respect to the clamping flange of the active steel and the stator body. In the first place the bars, situated on the boundary of the phase zone (extreme bars in each phase) were

* *Elektrichestvo*, No. 12, 39-43, 1958.

examined, since the largest electrodynamic forces act on them, [1-3].

Deformations and vibrations were measured by the wire strain gauges and tensometric amplifying devices of two types: IDD-3 [4], developed by the ORGRES, and UD-3 [5], developed by the Laboratory for the investigation of stresses of the Machine Research Institute of the Academy of Sciences, U.S.S.R. To measure the winding vibrations of the electrical motor type MS-395-AV 8/28 a high-speed cine-camera was used.

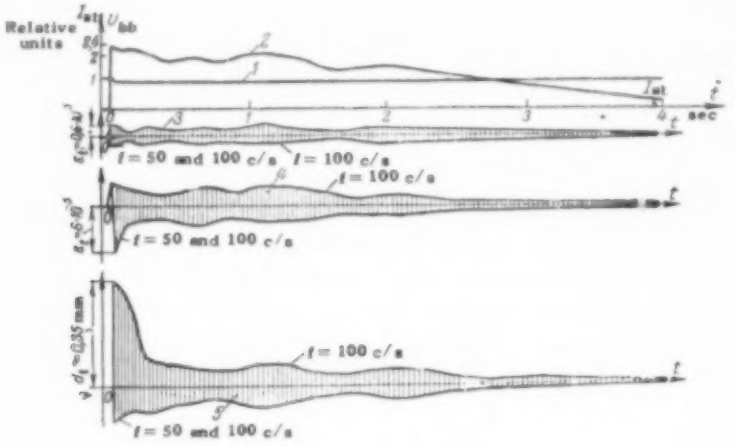

FIG. 1. Switching-in to the grid of a generator type SV (1160/180)–72 by the method of self-synchronization

1 – busbar voltage 154 kV; 2 – stator current; 3 – relative extension of insulation of the frontal part of the stator winding at the slot outlet; 4 – the same as curve 3 but in the middle of the straight portion of the frontal connexion; 5 – mutual displacements of the head of the frontal connexion and the clamping plate of the active steel in a tangential direction, (on the stator circumference).

In the references certain data are given concerning permissible and breaking deformations of normal mica isolations and of the varnish films used for its manufacture, for loads of constant sign [6]. But, unfortunately, the necessary data on the permissible variable sign deformations of the compound insulation of the stator windings are absent. Therefore, in evaluating the experimental results, a comparison was made of deformations and vibrations of the stator windings, which were recorded under various operational conditions of generators. As permissible values of deformations such magnitudes were taken as occur under conditions to which the machine could be subjected (for instance, a sudden short-circuit on the machine terminals), or under conditions which frequently occur in machine operation and do not cause damage to the machine. In particular, the deformations and vibrations of the generator windings were compared with the deformations and

vibrations of the windings of the high-voltage electrical motors which are frequently restarted.

Results of the investigations of the generators

On the basis of an analysis of oscillograms of the operation of generators with increased values of the stator current, we can conclude that deformations and vibrations usually vary with a frequency of 100 c/s, but, due to the influence of the aperiodic component of the current, components of deformations and vibrations are observed which vary with a frequency of 50 c/s (Figs. 1 and 2).

The deformations and vibrations which arise are approximately proportional to the square of the stator current.

The increased amplitudes of the heads of the frontal parts as well as the deformation of the insulation which occurs under transient conditions, are of a short duration, and, after the decrease of current in the stator winding, they decrease sharply. No permanent deformations of the insulation and displacements of the frontal parts of the stator were recorded.

1959

From an analysis of oscillograms obtained we can draw the conclusion that practically no substantial retardation in the value of the amplitudes of deformations and vibrations of the frontal parts of windings, due to the stator current, was recorded; and this applies to the first current half-period after the connexion of the generator to the grid and also to the whole period, when the increased current is flowing.

This indicates that the frequency of the free oscillations of the frontal parts of the windings is higher than the frequency of variations of the disturbing electrodynamic forces. Therefore, in calculating the results of the action of the electrodynamic forces on the windings, the shock value of the stator current should be taken, and we cannot neglect the supertransient component.

All the generators and motors tested had double-layer chain stator windings with continuous compound insulation. The working conditions of the generators, on which the winding deformations were measured, are given in Table 1 and their rated data in Table 2.

The results of tests of the hydro-electric generators types SV (1160/180)—72 and AT-I-W-72 are discussed below. These generators were most thoroughly tested. Thus, to measure deformations 50 strain gauges were attached on frontal parts of each of these generators.

As can be seen from Table 1, the maximum insulation deformation was recorded during asynchronous running with excitation and was equal to 2.1×10^{-4} of relative units (the relative extension of insulation is given), when the amplitude

TABLE 1

Multiples of the stator currents, amplitudes of maximum vibrations and of relative extensions of the frontal parts of the stator winding

Operating conditions	Stator current I/I rat.		Amplitude of vibrations, μ		Amplitude of relative extension $\times 10^{-5}$					
	Type of generator				Generator type AT-1-W-72			Generator type SV $\frac{1160}{180}$ - 72		
	AT-1-W-72	SV $\frac{1160}{180}$ - 72	AT-1-W-72	SV $\frac{1160}{180}$ - 72	Point 1 L		Point 11 L	Point 37 L		Point 41 L
					Calculated	Experimental	Experimental	Calculated	Experimental	Experimental
Normal starting	0	0	0	70	0	0	0	0	0	0
Parallel operation.	0.95	1.1	5	15	—	0	0	—	0	0
Exact synchronization.	0.36 (δ=7°)	0.9 (δ=21°)	80	200	—	0.6	—	—	—	0.5
Self-synchronization.	2.1	2.5	80	350	4.4	0.6	0.7	10.8	10	3.5
Dropping of the normal load	0.95	1.1	60	290	—	0,15	—	—	0	0
Asynchronous running with excitation.	—	4.4	—	460	—	—	—	34	21	3.3
Sudden three-phase short-circuit.	2.6	2.8	50	440	5	—	0.8	13.6	7	—
Sudden two-phase short-circuit with an earthed neutral.	1.8	2.4	170	300	3.2	—	1.5	10	6.1	—
Sudden two-phase short-circuit with a non-earthed neutral.	2.1	2	125	360	4.4	—	2.1	7	7.2	—

N.B: All short-circuits occurred behind the step-up transformer.

of the stator current beats was equal to 4.4 times its rated value. This deformation varied with a frequency of 100 c/s.

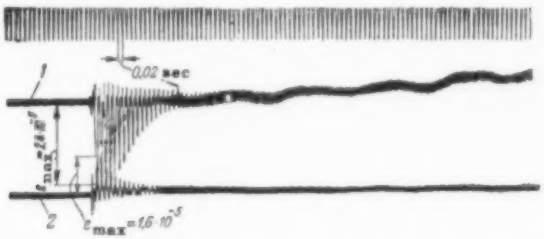

FIG. 2. Deformation of the insulation of the frontal part of the bar of a generator type SV (1030/120)–68 when switching-in to the grid by the method of self-synchronization.
1 – in the middle of the frontal part; 2 – on the straight portion near the bend.

Approximately equal deformations occurred in the presence of a short-circuit behind the step-up transformer for the rated value of the open-circuit current and the switching-in of the generator to the grid by the method of self-synchronization; this result is quite understandable, since the maximum current values are approximately equal under these conditions. Deformation of the insulation of the frontal parts was practically absent during normal starting, parallel operation with the grid, switching-in of the generator to the grid by the method of accurate synchronization and during a sudden decrease of the load.

If we compare the insulation deformations along the frontal part under the same conditions and with the same stator current, we find that the maximum deformation was recorded on the straight portion of the frontal connexion and at the part which projects from the slot. The relative extensions of the insulation of the frontal part of the bar, located on the slot top is greater than the relative extension of the insulation of the bar in the frontal part, situated at the slot bottom, a result which can be explained by the more rigid fastening of the lower layer of the winding.

The maximum amplitude of vibrations of the frontal part head was: during asynchronous running with excitation - 460 μ, for a sudden three-phase short-circuit behind the step-up transformer – 440 μ; for switching-in to the grid by the method of self-synchronization – 350 μ; for an exact synchronization – 200 μ; for the 100 per cent load drop – 290 μ; on starting – 70 μ and for the parallel operation with the grid – 15 μ.

Table 3 shows the results of the analysis of deformations and vibrations of the frontal parts for all cases of switching-in of a generator type SV (1160/180)–72

Maximum electrodynamic forces, bending moments, stresses in copper and vibrations of heads of the frontal parts of the stator windings, of generators

Type and rated values	Operating conditions	$X''_{st.g.} + X_t$ (relative units)*	I/I_{rat}		Number of slots per pole and phase	Length of the frontal parts, mm	Current on the side of the coil in or the bar for the rated load A	Trued modulus of elasticity of the frontal parts of a coil or a bar, cm^3	Electrodynamic force kg/cm		Max. bending moment kg/cm		Stress in copper of the frontal part of the section kg/cm²		Displacement (vibration) of heads of frontal parts with respect to the plate of active steel, μ
			Calculated	Experimental				Calculated	Calculated	Experimental	Calculated	Experimental	Calculated	Experimental	Experimental
SV 1160/180-72, 90,000 kVA, 3765 A, 13,8 kV, 83.3 rev/min, factory "Elektrosila", Bar winding	Short-circuit beyond the step-up transformer		2.57	2.8	$2\frac{1}{4}$	420	$1\times1887,5$	1.02	1	60	60	60	440
	Switching-in to the grid by method of self-synchronization	0.24÷0.15		2.5					1	60	60	85	350
	Short-circuit on the generator terminals	0.24	4.15	—					2.8	170	165	—	—
AT-1-W-72, 90.000 kVA, 3765A, 13.8 kV, 83.3 rev/min. Firm GEC coil winding	Short-circuit beyond the step-up transformer	0.23÷0.13	2.78	2.6	$2\frac{3}{4}$	420	$\frac{4\times3765}{9}$	0.48	1.3	17	35	7	50
	Switching-in to the grid by method of self-synchronization	0.23÷0.13		2.1					1.3	17	35	6	60
	Short-circuit on the generator terminals	0.23	4.35	—					3.3	41	86	—	—
SV (1250/170)-96; 68, 750 kVA, 2280 A, 13.8 kV, 62.5 rev/min factory "Elektrosila" coil winding.	Short-circuit beyond the step-up transformer	0.23÷0.14	2.36	—	$2\frac{7}{16}$	317	3×380	0.42	0.4	5	12	—	—
	Short-circuit on the generator terminals.	0.28	3.53	—					0.93	12	26.3	—	—
SV (1030/120)-68, 50,000 kVA, 2750 A, 10 kV, 88.2 rev/min factory "Elektrosila". Bar winding.	Short-circuit beyond the step-up transformer	0.24÷0.04	3.58	—	$2\frac{10}{17}$	380	1×1375	0.3	1.8	23	78	—	—
	Switching-in to the grid by method of self-synchronization		3.58	2.5					1.8	23	78	24	—
	Short-circuit on the generator terminals	0.24	4.2	—					3	37	124	—	—
VGS (325/135)-14, 18, 750 kVA, 1030A, 10.5 kV 428 rev/min KHETZ, coil winding.	Switching-in to the grid by method of self-synchronization.	0.21÷0.07	3.3	3.4	4	370	$\frac{1030}{7}$	0.34	1.6	12	35	38	380

N.B: X'' st.g. — supertransient reactance of the generator;
X_t — inductance of the step-up transformer.

to the grid by the method of self-synchronization. As can be seen from Table 3 the probability of the maximum deformation and vibration of the frontal part is insignificant. This scattering of the values of deformations and vibrations is explained by the influence of the aperiodic component of the stator current.

TABLE 3

Maximum values of vibrations and deformations of the frontal parts of the stator winding when switching-in to the grid a generator type SV (1160/180) – 72 by the method of self-synchronization.

Stator current, A		Amplitude of vibrations of the frontal part head, μ	Deformation of insulation of the frontal part; relative units $\times 10^{-5}$	
$i_{a.m.}$	I''		Point 41 L	Point 37 L
—	—	180	—	—
16 800	8 900	180	0.7	—
12 800	9 000	120	—	3.3
10 800	8 600	170	—	2.9
11 400	9 500	350	3.5	—
13 100	9 000	260	0.6	—
9 000	8 300	280	0.6	—
9 000	8 000	220	0.8	—
14 100	8 600	230	1.1	—
12 800	8 800	200	0 4	2.6
10 800	8 600	210	0.9	6
—	—	200	1.5	10
9 600	8 500	100	1.5	2.1
9 000	6 900	90	1	2.1
12 800	8 300	130	0.7	2.1
16 000	8 300	100	1.6	3.6
12 800	8 600	80	1.5	4.1
—	—	140	—	2.9
		4.7*	3.7*	4.7*

* Ratio of the maximum value to the rated value.

From Table 1 it can be seen that deformations and vibrations of the frontal part of the generator type SV (1160/180) – 72 are greater than those of the generator type AT-I-W–72. It can be explained by a better mounting and assembling of the stator active steel and a better quality of binding of the winding frontal parts in the generator type AT-I-W–72.

Tables 1 and 2 show the calculated values of the maximum relative extensions of the copper of the winding frontal parts, which are caused by electrodynamic forces, acting in the plane of minimum rigidity. As can be seen from these tables, the values calculated give deformations of the same order of magnitude or slightly greater than the experimental values.

It has already been said that deformations were measured in the insulation

surface of the frontal part. Laboratory investigations have shown that, for bending of the winding bar in the plane of minimum rigidity, deformations on the surface of the individual wires are smaller than the deformations of the insulation; moreover, the nearer to the surface the greater is the insulation deformation.

Let us assume that the maximum deformation on the copper surface is equal to the maximum insulation deformation; in this case, as can be seen from Table 2, the maximum stress in the copper, corresponding to the maximum insulation deformation, recorded when the generator type SV (1160/180) – 72 was switched in to the grid by the method of self-synchronization, should not exceed 85 kg/cm². But, in calculating the influence in the windings of electrodynamic forces, factories accept stresses in copper of 600 - 800 kg/cm² as permissible values. Preliminary investigations of the mechanical and electrical properties of the new continuous compound insulation for the bars of the stator winding, which was tested under a voltage of 6 kV, gave the following results.

After 1.2×10^8 vibration cycles with a frequency 100 c/s and with a double vibration amplitude of the middle of the bar of 2.5 - 3 mm; during which deformations, of a double amplitude from 4×10^{-4} to 5×10^{-3} relative units were recorded on the insulation surface, no lowering of the insulation puncture voltage was recorded. The bars were 900 mm long, and a bending moment of constant magnitude acted on their middle portion which was 340 mm long.

Tests of electrical motors

On starting electrical motors, the character of the deformations and vibrations of the frontal parts of the stator winding was the same as that which occurs in generators switched in to the grid by the method of self-synchronization, only the duration of these deformations is considerably shorter, (Fig. 3). Deformations of windings were investigated on eight high-voltage synchronous motors in which the construction and mounting of the frontal parts are the same as in the hydrogenerators tested.

The maximum deformation of the insulation of the frontal part, equal to 3×10^{-4} was registered on starting an electrical motor made by Metro-Vickers, of 2600 kVA, 6.6 kV, 228 A, 1000 rev/min. Vibrations of the frontal part head (at the projecting part 340 mm long) were 450 μ. With an electrical motor type MS - 395 - AV - 8/28, 3500 kVA, 6.6 kV, 306 A, 214 rev/min, the maximum insulation deformation was 1.3×10^{-4} and the vibrations of the frontal part head (at the projecting part 310 mm long) were 0.24 μ.

The tensometric method and high speed cine-photography gave the same values of the vibrations.

All electrical motors which were tested had been in service for a long time,

many of them having been restarted two or three times a day. Nothing abnormal during starting, operation or overhaul of these motors was recorded.

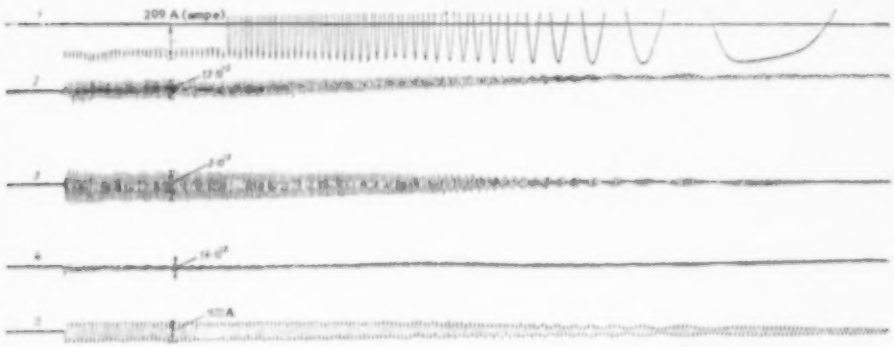

FIG. 3. Starting of an electrical motor type MS-395-AV-8/28 directly from the grid
1 – rotor current; 2–4 deformations (relative extensions) of the insulation of the frontal part on the wide side of the coil; 5 – stator current.

Conclusion

1. Investigations show the usefulness of supplementing a mathematical analysis by experimental data, which allows us to collect more complete and concrete information about the character and magnitude of deformations of windings of the generators in various operating conditions.

2. For investigation of these deformations and vibrations tensometric apparatus can be used. Besides strain gauges it is advisable to use high-speed cine-cameras. Further improvement of methods and apparatus for the research in question is needed.

3. Deformations of insulation and vibrations of the frontal parts of the stator windings, which are recorded in various operating conditions of hydro-electric generators, are insignificant: they are smaller than or of the same order as those which occur during the starting of synchronous motors directly from the grid.

4. Taking into account the individual properties of the mechanical properties of the insulation it is advisable to continue work in collecting experimental data on deformations of the hydro-electric generators windings and to extend analogous research on turbo-generators.

5. It is necessary to carry out special investigations on the mechanical properties of insulation and of bars, and to establish criteria specifying the permissible deformations of windings.

Appendix

Table 2 gives the values of the maximum electrodynamic forces calculated for 1 cm of length; of bending moments and stresses in the copper of the frontal parts of the stator winding for the three-phase short-circuits on the terminals behind the step-up transformer of hydro-electric generators; it also gives the experimental values of the maximum vibrations of the frontal part heads and the maximum stresses in the copper calculated from the insulation deformations.

In calculating the electrodynamic forces only the influence of currents in the conductors of the phase in question and of those of the adjacent phases was considered; the influence of currents in conductors located in another layer of the winding was ignored.

To determine the stresses, the frontal part was considered as a beam freely supported at its two ends, and loaded with a uniformly distributed load equal to the electrodynamic force. The span of the beam was taken as equal to the distance between two adjacent distance spacers. In the generator type SV (1160/180)-72 on the bars, where deformations were measured, the distance spacers between the two adjacent frontal parts were of insufficient thickness, and in certain places were absent. In this case, in calculating the maximum stresses in the copper, the span of the beam was taken as equal to the maximum distance between the two adjacent spacers which closely adjoined the adjacent frontal parts.

The voltage before the short-circuit was taken as equal to the rated voltage. The reactance of transformers was taken as equal to that in existing installations and is given in relative units, reduced to the rated power of the generator.

Translated by S. Szymanski

REFERENCES

1. M.P. Kostenko; *Elektricheskiye mashiny (spetsialnaia chast). (Electrical machines, special section).* Gosenergoizdat (1940).
2. E. Weber; *Veroffentlichen aus dem Siemens-Konzern*, Vol. VIII, part 3, 166 (1930).
3. J.B. Young and D.H. Tompsett; *Proc. I.E.E.* vol. 102, part A, 101-120, No. 2 (1955). Further discussion on the article, vol. 102, part A, No. 6, 856-859, 1956 and vol. 103, 449-452, No. 10 (1956).
4. *Eksperimentalnoe izuchenie mekhanicheskikh usilii v gidrogeneratorakh.* Sbornik trudov kursov-sovyeshchaniia pod redaksiyei Iu. M. Elkinda. *(Experimental investigation of mechanical stresses in hydro-generators.* Symposium of works of courses and conference under the editorship of Iu. M. Elkind). Gosenergoizdat (1957).
5. *Izmerenie napriazhenii v detaliakh mashin.* Sbornik rabot pod redaksiyei N.I. Prigorovskogo. *(Measurements of stresses in machine elements,* symposium of works under the editorship of N.I. Prigorowskii). Mashgiz G N T I Moscow Leningrad (1955).

6. Iu. I. Skanavi; *Sviaz' mezhdu mekhanicheskimi svoistvanu' statornoi obmotki nepreryvnoi izoliatsii turbo-igidrogeneratarov i ee probivnym napriazheniem.* Sbornik "Elektricheskaia Izoliatsiia". *(Relationship between mechanical properties of the continuous insulation of the stator windings of turbo and hydro-electric generators and its puncture voltage).* Symposium "Electric Insulation", part II, NKM, U.S.S.R (1938).

7. I.A. Syromiatnikov; *Rezhimy raboty sinkhronnykh generatov. (Operational conditions of synchronous generators.)* Gosenergoizdat (1952).

8. L.G. Mamikoniants; *Toki i momenty vrashcheniia, voznikaiushchie v sinkhronnoi mashine pri vkliuchenii ee sposobom samosinkhronizatsii. (Currents and driving torques occurring in a synchronous machine, when switched on by the method of self-synchronization).* Trud. Ts N I E L M E S, part IV, Gosenergoizdat (1956).

9. I. Biermans; *A.f.E.*, vol. IX, issue 7, 326 - 334 (1920).

10. N.A. Kozyrev; *Kontrol' sostoianiia izolatsii elektricheskikh mashin po ee mekhanicheskim kharakteristikam. (Control of the state of the insulation of electric machines on the basis of its mechanical characteristics).* Electric stations, No. 2 (1957).

11. A. Ia Berger; *Turbogeneratory peremennogo toka. (A.C. turbo-generators),* part I, United Scientific and Technical Press (1935).

1959

CALCULATION OF LOSSES IN THE SLIDING CONTACT OF ELECTRIC MACHINERY*

P.S. LIVSHITS

(Received 21 April 1958)

The formulation of a proven method of calculating losses in the sliding contact of electrical machines is an extremely important problem in modern electrical machine design. The different aspects of this problem have been studied in a considerable amount of research. However, because of insufficient knowledge of the properties of electrical brush materials none of the work carried out has been able to produce a conclusive result. Every calculation has been completed by recommendations propounding the use of approximate data, the basis of which has not usually been quoted. Such is the exposition of the question of losses in an electrical sliding contact given in the technical literature at present available, [1-3].

The methodical study of the properties of electrical brush materials [4-6], has enabled us to establish that the numerical values of the technical characteristics of these materials can be distributed according to the standard rule (or not far short of it), that each characteristic of each type of material has its own nominal (the most probable) value and that their volt-ampere and frictional characteristics can be described by means of the following formulae:

$$2\Delta U = A + Bj; \tag{1}$$

$$\mu = C - Dv, \tag{2}$$

where $2\Delta U$ – Intermediate drop in voltage in a pair of electrical brushes of different polarity V;

A – a free term in the equation of the volt-ampere characteristic†,

* *Elektrichestvo* No. 7, 55-58, 1958.

† Detailed information on the magnitudes of A, B, C and D can be found in [6]. Their numerical values for a number of types of electrical brush material also appear in the appendix to this article.

B – angular coefficient of the equation of the volt-ampere characteristic;

J – current density (apparent) in an electrical brush, A/cm²

μ – coefficient of friction of electrical brushes on the sliding surface of a (ring) commutator;

C – a free term in the equation of the frictional characteristic;

D – angular coefficient of the equation of the frictional characteristic;

v – peripheral speed of the sliding surface of the (ring) commutator, m/sec.

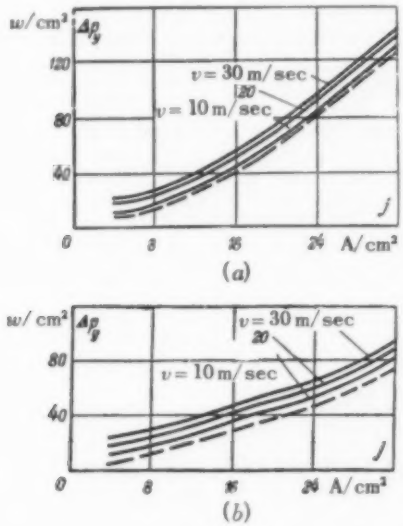

FIG. 1. Curves of dependence of specific losses in the sliding contact of electrical machines on current density. *a* – EG-4 type of electrical brush material; *b* – the same for the MGS-7 type; ------ specific electrical losses; ——— total (electrical and mechanical) specific losses with various v.

The utilization of new information which has been obtained about the properties of electrical brush materials enables one to come near to the calculation of losses in a sliding contact with more foundation than previously. As is known, these losses generally accumulate from mechanical losses in friction ΔP_m; electrical losses dependent on the intermediate drop in voltage, ΔP_e and losses dependent on sparking, ΔP_s. Just as the third kind of losses in machinery working normally need not occur, it is customary to confine oneself to the

determination of volumes ΔP_m and ΔP_e, in the corresponding calculations, and the expression for ascertaining losses is utilized in the following way:

$$\Delta P = \Delta P_m + \Delta P_e. \tag{3}$$

Each of the terms which comprise the last expression are in their turn determined by means of the well-known formulae:

$$\Delta P_m = 9.81 qF\mu v; \tag{4}$$

$$\Delta P_e = 2\Delta U I, \tag{5}$$

where q – individual pressure (apparent) on electrical brushes kg/cm²

F – area of the cross-section (apparent) of every electrical brush, cm²;

I – current, passing through sliding contact, A.

Taking into consideration the special features of the constructional formation of the elements of the brush-commutator nodes of electrical machines by which the relationship between the area of all electric brushes of both polarities F and the magnitudes of j and I is presented in the following form:

$$F = \frac{2I}{j}, \tag{6}$$

we find the loss which refers to a unit of the area of a sliding contact produced by electrical brushes of both polarities. After conversion it is possible to obtain from formulae (1)-(6) an expression for specific losses in the following form:

$$\Delta P_{sp} = \frac{\Delta P}{\frac{1}{2}F} = 2 \cdot 9\,81 qv\,(C - Dv) + \\ + j\,(A + Bj) \quad [w/cm^2]. \tag{7}$$

By substituting in the last formula the values of A, B, C and D it is possible to calculate the volume of the specific losses for the majority of cases encountered in practice where a sliding contact is employed.

Results of calculations obtained for electric brushes of types EG-4 and MGS-7 are represented in Fig. 1. The figure produced gives an entirely definite picture of the role of separate components in the overall specific losses and of the influence exerted by the operating conditions of sliding contact elements (speed, current density) on the character of the variation of these losses.

By using formula (7) we can also solve the problem of expediently selecting the area of a sliding contact, i.e. the total area of the brushes in a machine when the current load is given.

By examining formula (7) and Fig. 1, it can seem at first sight, that just as specific losses vary in proportion to the current density, so a reduction of total losses can be reached by selecting the low value of this density. In actual fact such a deduction proves to be inaccurate. In order to throw light upon this question from a correct point of view, it is essential to transform formula (7), having solved this in reference to total losses:

$$\Delta P = [2 \times 9.81 qv(C - Dv) + j(A + Bj)] \frac{I}{j} [w]. \tag{8}$$

By analysing the last formula it is possible to discover that certain optimum current densities exist, at which the losses in a sliding contact will be at a minimum, for the different values A, B, C and D, i.e. for the different types of electrical brush materials.

For an illustration of such a case let us determine the losses in the sliding contact of an electrical machine for any given current, e.g. $I = 100$ A. The results of appropriate calculations for electrical brush types EG-4, EG-14, M-3 and MGS-7 are shown in Fig. 3. It is evident from the figure that electrical losses continuously increase with the growth of current density in a sliding contact. As for the overall losses, they drop initially, reach a minimum, and only then begin to increase.

The nature of the variation of total losses which has been described is explained by the fact that a reduction of the necessary sectional area of electrical brushes and also, in conjunction with that, a reduction of the losses which depend on mechanical friction, occurs in accordance with the degree of increase in current density at a given I. While the reduction ΔP_m is more rapid than the growth of ΔP_e, total losses decrease. When the indicated relationship varies the total losses begin to increase and the appropriate curves take on a U-like form.

The regularity of the variation of total losses, strictly speaking, depends on the relationship of the volumes A, B, C and D (see formulae (1) and (2)). The influence of the term B is particularly important. In the case where $B > 0.02$, i.e. when the volt-ampere characteristic has a large gradient, the curves of total losses have a more or less clearly expressed minimum. If, however, $B < 0.02$, the growth of electrical losses cannot compensate for the diminution of mechanical losses and the graphs of total losses assume the shape described in Fig. 3*a*, *b* and *c*. The constructions shown here concern electrical brush materials of types MG-2, MGS and MG-6 in which the angular coefficient values of the volt-ampere

characteristic equation prove to be: $B = 0.01$; 0.008 and 0.01 respectively. In these instances it is no longer possible to observe the minimum points of the total losses. A similar effect also takes place for materials of the types MG, MG-4 and MGS-6.

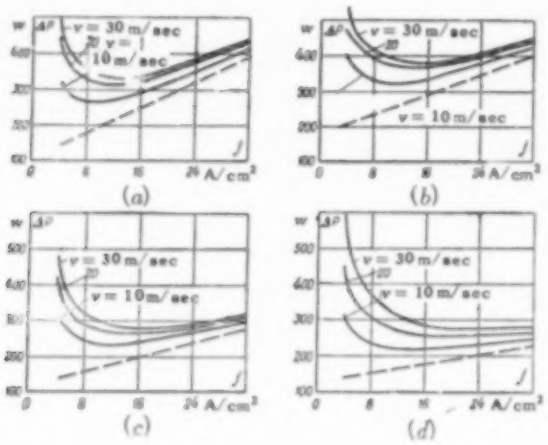

FIG. 2. Curves of dependence of total losses in the sliding contact of an electrical machine of a given output on current density.

a – EG-4 type of electrical brush material; *b* – EG-14 type; *c* – M-3 type; *d* – MGS-7 type. ------ electrical losses; ——— total (electrical and mechanical) losses with various v.

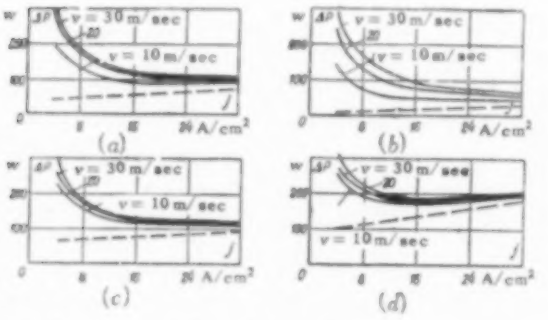

FIG. 3. Curves of dependence of total losses in the sliding contact of an electrical machine of a given output on current density.

a – MG-2 type of electrical brush material; *b* – MG-S type; *c* – MG-6 type; *d* – MGS-5 type. ------ electrical losses; ——— total (electrical and mechanical) losses with various v.

One more possible abnormality in the arrangement of curves of total losses is shown in Fig. 3*c* and *d*. Here a variation in the sequence of the arrangement of curves is implied, where the line representing $v = 30$ m/sec is lower than the line representing $v = 20$ m/sec. Such a case depends on the gradient angle of frictional characteristics. It arises in cases where $D < 0.005$ (materials of types EG-8, MG, MG-6 and MGS-5

The question of the minimum points of curves of total losses in a sliding contact of electrical machines has a practical value. The position of these can determine the nominal current density for each type of electrical brush, for only on this condition it is possible to talk about complete and expedient utilization of the potentialities of electrical brush materials.

Up to the present time no physical basis of the conception of a "nominal current density in the sliding contact of electrical machines" has existed. The values of appropriate magnitudes quoted in literature have been derived from the All-Union State Standard on brushes for electrical machines, [7], where they were established in 1943. It is natural that these values reflect the standard of utilization of electrical brush materials attained up to that time.

1959

The new data set forth in this work has enabled us to contribute a definite physical significance to the idea of a nominal current density. By nominal current density in the sliding contact of electrical machines it is suggested that one should mean that current density at which the curve of total losses at a certain speed v will have its minimum value. The results of calculations of current density values, subject to the condition formulated where $v = 20$ m/sec, are shown in Table 1.

It follows from the table that for the "ferrous" (non-metal) types of electrical brush materials the nominal current density varies between 11 and 15 A/cm^2. For the "non-ferrous" (containing metal) types these increase to between 15 and 20 A/cm^2.

The results which have been obtained give a basis for a certain stepping-up of the current densities in the sliding contact of electrical machines in comparison with those which are standardized, GOST 2332-43. Such a recommendation primarily concerns machines having a small number of brushes operating in parallel.

TABLE 1

Type of electric brush materials	Current density according to All-Union state standard 2332-43 A/cm²	Nominal current density, determined from the condition of the minimum of total losses A/cm²
G-3	10...11	15
G-8	11	15
EG-2A	10	12
EG-4	12	12
EG-8	10	11
EG-14	10...11	14
M-1	15	18
M-3	12	16
M-6	15	16
M-20	12	15
MG	20	—
MG-2	20	—
MG-4	15	—
MG-6	18	—
MGS	20	—
MGS-5	15	16
MGS-6	15	—

Total loss curves for MG, MG-2, MG-4, MG-6, MGS and MGS-6 do not have a minimum.

TABLE 2

Values of volumes A, B, C and D in formulae for calculating the volt-ampere and frictional characteristics of electric brush materials.

Type of electric brush materials	A	B	C	D
G-3	1.20	0.05	0.23	0.005
G-8	1.00	0.08	0.20	0.002
EG-2A	1.50	0.10	0.21	0.003
EG-4	1.10	0.09	0.20	0.003
EG-8	1.90	0.07	0.21	0.005
EG-14	1.80	0.07	0.23	0.004
M-1	1.30	0.03	0.23	0.004
M-3	1.20	0.05	0.20	0.003
M-6	0.80	0.04	0.20	0.003
M-20	1.20	0.04	0.19	0.003
MG	0.16	0.007	0.22	0.005
MG-2	0.40	0.01	0.22	0.004
MG-4	0.50	0.02	0.21	0.004
MG-6	0.62	0.01	0.22	0.005
MG-5	0.04	0.008	0.18	0.002
MGS-5	0.90	0.03	0.21	0.005
MGS-6	1.20	0.02	0.17	0.001
MGS-7	1.30	0.03	0.17	0.001

Appendix

Instructions for the choice of brushes*

Type	Type of m/c
G 1, G 2, G 3, EG 4	Normal generators and motors of 110, 220 and 440 V
MG 2	Generators to 6 - 12 V
M 1, M 3, M 6, M 20, M 22	Generators and motors 25 - 60 V
EG 2, EG 6, EG 8, EG 10	Motors for rolling mills
G 3, EG 4	Generators for electrical welding
EG 2, EG 6, EG 8, EG 10	Traction motors
EG 2, EG 4, EG 8, EG 14, EG 83	Turbogenerators d.c.
G 3	Exciters of synchronous generators and motors
G 3, EG 4	Hydro-electric generator exciters
EG 4, EG 83	Turbogenerator exciters
MG, MG 2, M 1	Induction motors
G 3, MG 2	Synchronous generators and motors
EG 14, EG 83	Turbogenerators 3000 rpm

NB

G = Graphite
M = Copper
E = Electro-graphited
S = Silver

* Electrotechnical Handbook.

Translated by J.F. Boyland

REFERENCES

1. M.A. Shatelen, V.F. Mitkevich and V.A. Tolvinskii; *Spravochnaia kniga dlia elektrotekhikov (Handbook of Electric technology)* Vol. 5, pp. 84 - 86, 90 and 100 - 101 (1934).
2. M.P. Kostenko; *Elektricheskie mashiny (Electrical Machines)* pp. 135 - 136, Gosenergizdat (1949).
3. V.A. Tolvinskii; *Elektricheskie mashiny postoiannovo toka (Direct Current Electrical Machines)* pp. 381 - 382 and 394 - 395. Gosenergizdat (1956).
4. P.S. Livshits; *Tekhnicheskie kharakteristiki elektroshchetochnykh materialov, opredelennye statisticheskimi metodami. (Technical Characteristics of Electrical Brush Materials, Determined by Statistical Methods)* No. 5, VEP (1956).
5. P.S. Livshits; *Primenenie metodov matematicheskoi statistiki k izucheniiu svoistv metallokeramicheskikh kompozitsii. (Application of Mathematical Statistics' Methods to the study of the properties of Metallic-ceramic Compositions).* Sbornik "Poroshkovsia Metallurgia, 4, (1956).
6. P.S. Livshits; *Vol't-ampernye i friktsionnye kharakteristiki elektroshchetochnykh materialov (Volt-ampere and Frictional Characteristics of Electrical Brush Materials)* VEP, No. 2, (1958).

7. GOST 2332-43. *Shchetki dlia elektricheskikh mashin (Brushes for Electrical Machines)* Standartgiz, (1955).

ABSTRACTS FROM PAPERS PUBLISHED IN ELEKTRICHESTVO NO. 12, 1958

Determination of the recovery voltage form in transforming installations: N.M. Maslennikov. (pp 9 - 13)

The author presents a new and simple method of determining the shape of the recovery voltage curve in d.c. converter installations. The frequency and damping of the recovery voltage can be quickly determined in simple installations. Where the installations are more complex, it is advisable to use an oscillograph and a low powered equivalent circuit in which oscillations are excited. The results produced by the method have coincided well with experimental data. Damping oscillations due to losses in larger power installations were not taken into account. Five examples of the calculations are given and seven diagrams of circuits and oscillograms.

1959

Electrical arc in longitudinal slits: O.B. Bron and L.A. Rodshtein. (pp 14 - 18)

Arc-extinction devices with narrow longitudinal slots are widely used in high- and low-voltage switchgear. The author considers new processes which have not yet been discussed and states more precisely and generally the results which have already been obtained. He considers the arc in a slot with flat parallel walls and in a ribbed slot. The results of the calculations point to the advantage of arc-extinction chambers with ribbed slots over slots with flat parallel walls. The author asserts that earlier works incorrectly used the photographic method of determining the speed of the arc in longitudinal slots. By making a cut in the walls of the slot they unsuspectingly raised the average longitudinal voltage gradient in the arc. This was discovered as the method of probes has been used for this investigation and not the photographic method.

Resonance transformer: A.A. Kosovskii. (pp 22 - 26)

High-voltage testing at line frequency of the insulation of objects such as hydro-electric generators and cables with great electrical capacitance involves difficulties due to the great reactive power required. It is therefore advisable to utilize the resonance between the capacitance of the test object and the inductance of the testing device, using the inductance of the resonance transformer without applying additional chokes (reactors). The author describes the design of this

transformer. It is characterized by its little weight, low consumption of current from the network, convenient tuning to resonance and by the sinusoidal shape of the secondary voltage.

Investigation of electrical circuits with non-linear inductance: S.P. Pivovarov. (pp 27 - 29)

When regulating and stabilizing voltage in relay, non-linear bridge starting and counting schemes etc, electrical circuits are employed which contain reactive coils with a ferromagnetic core, autotransformers and transformers, (i.e. elements with non-linear characteristics), the inductance of which depends on the amount of current. The author proposes a method of calculating the current and voltages of the basic and of the third harmonics.

Voltage regulation in low-voltage networks: N.K. Arkhipov. (pp 30 - 33)

A distribution transformer is a possible means of regulating voltage. The electrical industry is producing two types of distributor transformer with an output of from 20 to 560 MVA and automatic voltage regulation on load. The author considers the conditions in which these transformers can be applied with single and multi-step control. The degree of regulation in multi-step regulators determines the degree of accuracy of operation of the sensitive element (relay). The greater the accuracy, the less should be the degree of regulation. The author argues that a decrease of the degree of regulation is more economical, especially in metal. He uses a transformer with a 5 per cent degree of regulation to examine these questions and considers that the range of insensitivity of the switching device should be greater than the degree of regulation for stable operation. After considering such transformers he recommends the application of distribution transformers with two stage automatic voltage regulation, (5 per cent each stage) where practicable, and distribution transformers with multi-stage regulation (a larger number of finer stages). Transformer works should therefore produce 35 and 110 kV transformers of all dimensions with regulatable voltage on load and also additional-voltage transformers for 6 - 35 kV and low voltage.

A criterion of synchronous machine stability: I.D. Urusov. (pp 34 - 38)

The author considers that the usual methods of investigating rotor stability in the presence of small changes of angle θ using linearized equations ignore certain important physical factors which makes it difficult to evaluate their effect on stability and to investigate the process qualitatively. He therefore proposes a criterion of stability and a method of finding the roots of the characteristic equation which is directly based on the use of the "moment frequency characteristic" of a salient pole synchronous machine. This machine is provided (in order to improve

its damping properties, in addition to damping windings), with a stabilizing device called the "swing damping block" in which the first and second derivatives of angle θ are realized. An example of the calculations is given.

Investigation into the heating of series *A* and *OA* induction motors with a capacity ranging from 0.6 - 100 kW at the intermittent-duty conditions of their operations: P.A. Suiskii. (pp 44 - 45)

Average established temperature rises in the windings of induction motors are analysed by the method of "equivalent heating losses" for the case when the motors are being operated intermittently whereas the existing regulations in GOST 7217 - 54 provide for the use of the "resistance method" during half the subsequent period of operation. Average equivalent heating losses can be found from the relationship

$$P_{e.a} = P_{m1a} + k_{st\,a} P_{st\,a} + k_{m2a} P_{m2a} + k_{d\,a} P_{d\,a},$$

where P_{m1a} . $P_{st\,a}$, $P_{m\,2\,a}$ and $P_{d.a}$ are the average heating losses in the stator winding, in the stator steel, in the rotor and the additional losses on load $\mathbb{V}$; $k_{st.a}$, $k_{2.a}$ and $k_{d.a}$ are the average heating loss factors. Formulae are also introduced for determining these coefficients. Examples of calculations carried out on motors are given. The difference in the results of the two methods is ± 5 per cent.

1959

Change in load characteristics of magnetic amplifiers: V.S. Vysochanskii. (pp 49 - 51)

The author points to the disadvantages of magnetic amplifiers and the choice between expensive magnetic materials (permalloy, supermalloy, mumetal and so on) and special circuits to overcome there difficulties. The existing materials and circuits only partly overcome these difficulties. He therefore proposes a scheme for connexion of a magnetic amplifier on load with a standard voltage in the circuit and usual electro-technical steel which overcomes these difficulties completely. This scheme is represented diagrammatically. The scheme enables the load current of the amplifier to be equated to zero in any desired zone of change of input signals. The input current of the amplifier can pass through the load only after it attains a definite value because of the counter action of the standard voltage in the load circuit. In the presence of control signals outside the operating zone of the amplifier, all the current of the load windings is closed through a ballast resistance. In order to prevent the passage of the current through the load resistance when the voltage on the ballast resistance is less than the standard voltage, a semiconductor rectifier is connected in the load circuit. The author discusses the tests made on this device and its construction.

Maximum output of energy by induction motors when feeding the network: V.S. Mogilnikov. (pp 52-55).

When there is a short circuit in the network or a sudden voltage drop for other reasons, the induction motors are temporarily converted into a generating system and supply power to the network owing to the partial power decrease of the rotating rotor mass and mechanism. On the fault section, the power generated by the induction motors is added to the power which can be supplied from the network during the short circuit with the result that certain elements in the system are more stressed. The author sets out the conditions in which induction motors can supply maximum power to the network and proposes a formula for determining this power by a simplified method. Tests results on 'Ural' type motors are tabulated. An example of the calculation is given. He concludes that the power supplied to the network by induction motors decreases when the inductive resistance of the stator is increased. If the resistance of the stator circuit is increased, the power supplied first increases and then decreases. In the case of standard small and medium motors, the maximum power supplied is on average equal to the kinetic energy of the motor rotor at synchronous speed independently of the power of all the rotating masses of the drive.

Improved characteristics of arc-type steel furnaces: N.V. Okorokov. (pp 58-61)

A large number of works deal with the application of circular diagrams and operating characteristics to determine the optimum electrical conditions of an arc-type steel smelting furnace but these do not take into account one source of inaccuracy. Usually an equivalent network is used for the phase of the furnace, according to which, the usual resistance of the phase is merely the arc resistance, R_a. Therefore in the presence of a short-circuit of the arc, the useful resistance of the furnace R_u and the resistance of the arc are zero $R_u = R_a = 0$. Likewise the active power introduced into the furnace is zero.

$$P_u = P_a = 0$$

Accordingly, diagrams are shown for the circular diagram of one phase and the operating characteristics, both of which take the heat losses of the furnace into account and are true for a symmetrical circuit. In effect, the larger part of the electrode is inside the furnace and an active power is produced there which must be included in the active furnace power P_u, but the resistance of this section of the electrode r_e must be regarded as part of the useful resistance of the furnace R_u:

$$R_u = R_a + r_e$$

The equivalent network for one phase changes and the furnace power P_u equals the sum of the arc power P_a and the power produced in the resistance r_e:

$$P_u = P_a + I^2 r_e$$

Thus R_u can vary from infinity on no load to r_e (but not to zero) in the presence of a short circuit of the arc. The ramifications of this refinement are considered mathematically and diagrammatically and tests on ore reduction furnaces (iron smelting, carbides etc) are considered.

Method of studying power distribution in ore-refining furnaces: B.M. Strunskii. (pp 62-66)

The author reviews the existing differences of opinion on how to determine the amount and distribution of power in the hearth of an electrical ore-reduction furnace. He concentrates his attention on electrical schemes of the hearths of ferrosilicium and carbide furnaces and describes an experimental method of determining the distribution of power in the hearth. The tests made to verify this method are also described. He shows the scheme of a furnace when the position of the electrode is normal and the load is 20,000 A. When the electrode is raised to a high position and the load is reduced he shows the new scheme that would be necessary. The arcs burn between the side surface of the electrode and the hearth walls independently of the position of the electrode. There is no arc between the face of the electrode and the melt. When the electrode is in a lower position and the load is raised, the electrode sinks into the melt.

Measures for reducing the currents branching off into ground: A.S. Skuratov. (pp 67-71)

A survey is made of measures to be taken to reduce stray earth currents in underground metal equipment. The problem of protecting underground equipment from corrosion is not tackled. The author points to the increase of stray currents accompanying the increased length of railway lines in the presence of supply at one end and considers decentralized supply, parallel operation of substations, normalized voltage drop in the rails and increased transient resistance of the rails-earth (by insulation e.g. bitumin, water repellent earth covering), but finds none of these measures satisfactory. The author then advocates the two-conductor contact network for tramlines and the Underground with doubled supply voltage. He considers the pros and cons of this system and compares the capital and operating cost and power losses of single and double conductor contact networks. The conclusion is drawn that it is worthwhile to lay an experimental two conductor contact network and to see if any great operating difficulties arise.

Automatic arrangement for mutual reservation of low-voltage power supply sources: I.I. Zhigachev. (pp 71 - 76)

Present day trends favour the extensive use of automatic reclosure. Continuity of supply is improved by automatic mutual reservation of two supply sources. The author describes certain schemes developed with a two-end automatic reclosure device. The schemes are applicable to any configurations of a network with sources operating separately at a different power. The different schemes are said to be simple and the apparatus can be employed on existing gear. The schemes are represented diagrammatically.

Hysteresis coupling for frequency stabilization: A.N. Larionov and V.G. Morozov. (pp 76 - 78)

The results are given of tests on asynchronous and hysteresis couplings without windings for stabilizing the frequency of a low-power synchronous generator excited by permanent magnets. The problem was to stabilize frequency at an output of 300 VA with an accuracy of ± 0.5 per cent, when the speed of the drive varied ± 5 per cent and in the presence of a possible 30 per cent load reduction. In fact the use of a resonance frequency stabilizer obtained frequency stability of ± 0.2 per cent. Compared with the d.c. generator-converter system, the hysteresis coupling method is 20 per cent lighter in weight and has a higher efficiency (70 per cent compared with 40 per cent). The hysteresis coupling system can be used for an output of 500 VA, in the presence of a 30 - 40 per cent load reduction and at speeds over 600 rev/min.

1959